Varietal Thiols and Precursors: Biogenesis, Reactivity, and Impact of Winemaking Practices

Xingchen Wang

A thesis submitted for the degree of Doctor of Philosophy

Department of Wine Science

School of Agriculture, Food and Wine

The University of Adelaide

Adelaide, Australia

September 2022

“Where there is no wine, there is no love.”

Euripides

TABLE OF CONTENTS

THESIS SUMMARY

Over one thousand volatile compounds have been identified in wine and these arise from different chemical classes, varietal thiols are of one group which is particularly important given their substantial sensory impact on certain wine varieties. As such, furthering the understanding of thiol biogenesis through the analysis of known precursors and exploration of new ones, and reactivity of thiols based on factors related to viticulture, winemaking, and wine storage, is crucial to the manipulation of varietal thiols in wine and thus overall wine sensory profile. Additionally, exploring of other sulfur-containing volatile compounds in wine is one of the aims of the project, which could contribute to the appreciation of wine aroma complexity as a result of this important class of molecules.

A review of the literature (**Chapter 1**) summarises the production and manipulation of varietal thiols in wine, including 3-sulfanylhexan-1-ol (3-SH), 3-sulfanylhexyl acetate (3-SHA), 4-methyl-4-sulfanylpentan-2-one (4-MSP), and 4-methyl-4-sulfanylpentan-2-ol (4-MSPOH), and considers the impact on non-volatile L-glutathione and L-cysteine conjugated precursors in grapes from viticultural and winemaking practices. Specialised analytical methods for studying such compounds are necessary given their chemical reactivity. The review also identified research gaps, namely knowledge regarding potential new precursors and reactivity of varietal thiols, given that the concentrations of varietal thiols in wine could not be adequately accounted for by the utilisation of known precursors. Impacts of some winemaking practices on the concentrations of thiol precursors in grape materials and varietal thiols in the resultant wines were proposed. The review highlighted the possibility of sulfur-containing volatile compounds awaiting discovery in wine, including grapefruit mercaptan and blackcurrant mercaptan, which are key contributors to the aroma of grapefruit and blackcurrant, respectively.

Chapter 2 (prepared in manuscript format) reports a preliminary study aiming to identify new precursors to 4-MSP and 3-SH. 4-MSP can be released from its L-glutathionylated or L-cysteinylated conjugate (i.e., GSH-4-MSP and Cys-4-MSP) with mesityl oxide (MO) assumed to be their precursor but not been identified in grapes. It was hypothesised in **Chapter 1** that one route could involve MO produced by soil bacteria near grapevine roots, with subsequent uptake and transformation of MO into 4-MSP precursors. To verify this, a feeding experiment was conducted by applying deuterium labelled MO to grape leaves and

bunches of potted grapevines. Analysis of the grape tissues by HPLC-MS/MS showed the presence of deuterium labelled GSH-4-MSP or Cys-4-MSP, indicating that MO is the precursor of GSH-4-MSP and Cys-4-MSP in grapevines. However, further experiments should explore the existence of MO in vineyard soil as well as soil bacteria strains that could potentially yield MO. Additionally, this chapter studied the presence of a potential 3-SH precursor, namely the *N*-malonylcysteine conjugated 3-SH (MalCys-3-SH), in Sauvignon blanc juice extracts. The extracts were screened after optimising MS parameters using an authentic MalCys-3-SH standard based on a published HPLC-MS/MS method for thiol precursors. Although MalCys-3-SH was not identified at this stage, it cannot be concluded with the small sample set that this or other precursors are not present in juice. A greater number of grape samples should be analysed in the future, jointly with MS experiments that look for the loss of specific fragments associated with L-glutathione, for example.

The research publication presented in **Chapter 3** explores the reactivity of varietal thiols, particularly 3-SH. The recent identification of *cis*-2-methyl-4-propyl-1,3-oxathiane (*cis*-2-MPO) in wine was speculated to be the product of 3-SH reacting with acetaldehyde. In a continuation of this work, the evolution profile of *cis*-2-MPO during alcoholic fermentation was studied, revealing moderate to strong Pearson correlations with 3-SHA and acetaldehyde. Yeast strains significantly affected *cis*-2-MPO production during fermentation, but resulted in similar concentrations in the resultant wines. The instability of *cis*-2-MPO was illustrated by the continuous decline in a commercial Sauvignon blanc wine spiked with *cis*-2-MPO which was stored for one-year under various conditions (pH, temperature, presence of acetaldehyde or SO_2). In this case, *cis*-2-MPO appeared to be preserved by lower pH, acetaldehyde addition, and 4 °C storage temperature.

The research publication in **Chapter 4** was based on the hypothesis that enantiomers of *cis*-2-MPO were produced from the corresponding 3-SH enantiomers upon their reaction with acetaldehyde. To verify this, a validated stable isotope dilution assay (SIDA) using gas chromatography coupled to mass spectrometry (GC-MS) with a chiral GC column stationary phase was developed and utilised to analyse wine samples. Chemical formation of *cis*-2-MPO from the co-spiking of 3-SH and acetaldehyde standards in a commercial wine was verified and used to confirm enantiomer elution order. *cis*-2-MPO was revealed to consist of (2*R*,4*S*)-2-MPO and (2*S*,4*R*)-2-MPO in wine, which had strong Pearson correlations with (3*S*)-3-SH and (3*R*)-3-SH, respectively, upon analysing the thiol enantiomers. Additionally, one enantiomer of *cis*-2,4,4,6-tetramethyl-1,3-oxathiane (*cis*-TMO), derived from the reaction of 4-MSPOH and

acetaldehyde, was identified and quantified in a few white wine samples (≤ 28 ng/L). Although presenting below the odour detection threshold (14.9 µg/L) determined in this work, its presence demonstrated a pathway for the production of 1,3-oxathianes from acetaldehyde and varietal thiols bearing a 1,3-sulfanylalkanol substitution in their structures.

Chapter 5 (prepared in manuscript format) reports the preliminary method development to resolve 4-MSPOH enantiomers and identify the proposed sulfur-containing volatile compounds in wine. Bearing a chiral centre, 4-MSPOH can conceivably consist of two enantiomers. However, the identification of a single *cis*-TMO enantiomer (**Chapter 3**) implied that only a single 4-MSPOH enantiomer might be present in wine. To examine this, an assessment of two chiral stationary phases (CSPs), column temperature, eluent composition, and mobile phase flow rate were performed to separate 4-MSPOH enantiomers by adapting a method involving thiol derivatisation and HPLC-MS/MS analysis with a CSP. Base line separation of 4-MSPOH enantiomers was not achieved with the columns on hand, but the method was adequate to verify the hypothesis, and different wine samples were screened. 4-MSPOH was not identified at this stage and further method optimisation using alternative CSPs along with analysing additional wines with a more sensitive instrument may provide more conclusive results. **Chapter 5** also studied the potential presence of grapefruit mercaptan (GFM) and blackcurrant mercaptan (BCM) using a published HPLC-MS/MS method after thiol derivatisation. Calibration of BCM was undertaken and a selection of wines was analysed, but BCM was not detected. Further work with a broader set of wines is required to provide evidence about the presence and concentration of BCM. In contrast, GFM appears to be unstable under light or protic conditions and the degradation product was investigated, although additional study is required to verify its identity.

Research manuscripts in **Chapter 6** and **Chapter 7** highlight the effect of a novel grape crushing technique, known as accentuated cut edges (ACE), on the release of thiol precursors and varietal thiols in Shiraz and Sauvignon blanc during winemaking. Other practices, including water dilution and skin contact time for Shiraz, and yeast strain and lactic acid bacteria for Sauvignon blanc, were also evaluated. Concentrations of thiol precursors in Shiraz grape must and varietal thiols in Shiraz wine were not significantly affected by ACE (**Chapter 6**, research publication). Nonetheless, as best as it can be ascertained, this was the first time that thiol precursors were identified in Shiraz grape must. Sauvignon blanc and Pinot noir wines made with ACE or conventional crushing on a commercial scale were also analysed, giving preliminary insight into the potential of ACE for increasing concentrations of varietal

thiols in Sauvignon blanc, but causing a decrease of 3-SH in Pinot noir. The impact of ACE on varietal thiols may depend on grape variety was highlighted, which was pursued further with fermentation trials involving ACE and Sauvignon blanc (**Chapter 7**, research publication). Varietal thiols and their precursors in the Sauvignon blanc trials were markedly increased by ACE. However, the potential for browning of white wine was raised given the higher amounts of total phenolics and hydroxycinnamates in ACE treatments. The impact of crushing method, yeast strain, and malolactic fermentation on other volatile compounds was evaluated for the Sauvignon blanc fermentations. Interactions with other winemaking parameters were observed and discussed in **Chapter 6** and **Chapter 7**. The overall sensory quality of the Shiraz and Sauvignon blanc wines was assessed with a rate-all-that-apply (RATA) methodology, revealing that the grape crushing method and other winemaking practices could modify the wine sensory profiles, with ACE playing a relatively minor role, as outlined in the respective chapters.

DECLARATION

I certify that this work contains no material which has been accepted for the award of any other degree or diploma in my name, in any university or other tertiary institution and, to the best of my knowledge and belief, contains no material previously published or written by another person, except where due reference has been made in the text. In addition, I certify that no part of this work will, in the future, be used in a submission in my name, for any other degree or diploma in any university or other tertiary institution without the prior approval of the University of Adelaide and where applicable, any partner institution responsible for the joint award of this degree.

The author acknowledges that copyright of published works contained within the thesis resides with the copyright holder(s) of those works.

I give my permission for the digital version of my thesis to be made available on the web, via the University's digital research repository, the Library Search and also through web search engines, unless permission has been granted by the University to restrict access for a period of time.

Xingchen Wang Date:

06/09/2022

PUBLICATIONS

This thesis is a collection of unsubmitted manuscripts and papers that were published in Journal of Agricultural and Food Chemistry (JAFC) and Food Chemistry during the author's candidature. The impact factor of JAFC (Q1) was 5.895 in 2021. The impact factor of Food Chemistry (Q1) was 9.231 in 2021.

The text and figures in the chapters were organised in different formats according to the requirements of the journals. A Statement of Authorship, signed by all manuscript authors and listing individual contributions to the work, is included at the beginning of each chapter.

The thesis is based on the following refereed publications.

Chapter 3. Wang, X., Chen, L., Capone, D.L., Roland, A. & Jeffery, D.W. (2020). Evolution and correlation of *cis*-2-methyl-4-propyl-1,3-oxathiane, varietal thiols, and acetaldehyde during fermentation of Sauvignon blanc juice. *Journal of Agricultural and Food Chemistry*, 68(32), 8676-8687.

Chapter 4. Wang, X., Capone, D.L., Roland, A. & Jeffery, D.W. (2021). Chiral analysis of *cis*-2-methyl-4-propyl-1,3-oxathiane and identification of *cis*-2,4,4,6-tetramethyl-1,3-oxathiane in wine. *Food Chemistry*, 357, 129406.

Chapter 6. Wang, X., Capone, D.L., Kang, W., Roland, A. & Jeffery, D.W. (2022). Impact of accentuated cut edges (ACE) technique on volatile and sensory profiles of Shiraz wines. *Food Chemistry*, 372, 131222.

Chapter 7. Wang, X., Capone, D.L., Roland, A. & Jeffery, D.W. (2023). Impact of accentuated cut edges, yeast strain, and malolactic fermentation on chemical and sensory profiles of Sauvignon blanc wine. *Food Chemistry*, *400*, 134051.

An additional related publication co-authored by the candidate is listed in the appendix.

Kang, W., Bindon, K.A., Wang, X., Muhlack, R.A., Smith, P.A., Niimi, J., Bastian, S.E.P. (2020). Chemical and sensory impacts of accentuated cut edges (ACE) grape must polyphenol extraction technique on Shiraz wines. *Foods*, 9, 1027.

CONFERENCES

1. **In Vino Analytica Scientia 2022, 3rd to 7th July 2022, Neustadt an der Weinstraβe, Germany.**

   Poster presentation entitled "Evaluation of 'accentuated cut edges' technique on the release of varietal thiols and their precursors in Shiraz and Sauvignon blanc wine production".

2. **18th Australian Wine Industry Technical Conference (AWITC), 26th to 29th June 2022, Adelaide, SA.**

   Poster presentation entitled "ACE your Shiraz or Sauvignon blanc wine aroma".

3. **Macrowine 2021, 23rd to 30th June 2021, Online.**

   Oral and poster presentation entitled "Alternative fate of varietal thiols in wine: Identification, formation, and enantiomeric distribution of novel 1,3-oxathianes".

4. **Crush 2021, The Grape and Wine Science Symposium, 16th June 2021, Adelaide, SA.**

   Oral presentation titled "Discovery of novel volatile compounds in wines to explain the loss of key odorants–polyfunctional thiols".

5. **2020 School of Agriculture, Food and Wine Postgraduate Symposium, 29th to 30th September 2020, Adelaide, SA.**

   Oral presentation titled "Exploring the fate of 3-SH in wine".

6. **17th AWITC, 21st to 24th July 2019, Adelaide, SA.**

   Poster presentation titled "Fate of tropical odorants in wine: Identification and stability of 2-methyl-4-propyl-1,3-oxathiane".

PANEL OF SUPERVISORS

Principal supervisor:

Associate Professor David W. Jeffery

https://orcid.org/0000-0002-7054-0374

School of Agriculture, Food and Wine

The University of Adelaide

Co-supervisor:

Dr. Dimitra L. Capone

https://orcid.org/0000-0003-4424-0746

School of Agriculture, Food and Wine

The University of Adelaide

External supervisor:

Dr. Aurélie Roland

https://orcid.org/0000-0003-2673-3969

SPO, Univ Montpellier, INRAE, Institut Agro, France

Independent advisor:

Dr. Paul K. Boss

https://orcid.org/0000-0003-0356-9342

Commonwealth Scientific and Industrial Research Organisation (CSIRO) – Agriculture and Food, Australia

ACKNOWLEDGEMENTS

First and foremost, I would like to express my sincere gratitude to my supervisors Associate Professor David Jeffery, Dr. Dimitra Capone, and Dr. Aurélie Roland for your unwavering support, consistent guidance, and invaluable advice in all aspects of my academic research and daily life. Thank you all for teaching me the value of hard work, critical thinking, and being consistent, and I could not be luckier to have you all as my supervisors. Besides, Dave, your good sense of humour sprinkles our daily life with so much joy and makes this journey so much more enjoyable.

An immense thank you to my independent advisor Dr. Paul Boss (Commonwealth Scientific and Industrial Research Organisation, CSIRO) for your generous support and valuable advice to this project. I would especially like to thank Sue Maffei (CSIRO) for her enormous help with instrument operations and generosity for sharing her expertise in HPLC-MS/MS. I am extremely grateful to so many wine experts from the AWRI and South Australian wine industry for their generosity in the support of this project.

I would like to thank all my colleagues from the Department of Wine Science for all your help, encouragement, and support. Particularly, to my friends, Dr. Carolyn Puglisi, Claire Armstrong, Hugh Holds, Lishi Cai, Dr. Liang Chen, Dr. Lukas Danner, Nick Van Holst, Dr. Pietro Previtali, Dr. Renata Ristic, Ross Sanders, Dr. Ruchira Ranaweera, and Dr. Wenyu Kang, it has been a great pleasure to work with you all.

I am honoured to be granted with the China Scholarship Council and Adelaide University China Fee Scholarship (201806300066). I wish to acknowledge the financial support from the Wine Australia Supplementary Scholarship (WA Ph1803) and travel bursary.

To my beloved, beautiful, and inspiring partner, Zhuoya Yue. I am eternally grateful for your love, support, encouragement, accompany, and for making me a better person. I thank my parents and my partner's parents for their consistent support, caring, and understanding to allow me to pursue my dream.

THESIS STRUCTURE

The thesis contains chapters that are prepared as publications and manuscripts. As depicted below, it starts with a review of literature that was prepared in the first six months of candidature followed by six original research chapters comprising two manuscripts and four publications. The last chapter contains conclusions and future perspectives of the project.

Chapter	Content
Chapter 1: Literature review	A review of literature relevant to varietal thiols and precursors, their biogenesis, reactivity, viticultural and oenological impact, and instrumental analysis; Identification of research gaps.
Chapter 2 New thiol precursors study	HPLC-MS/MS methods development and wine samples screening for identification of precursors of 3-SH and 4-MSP.
Chapter 3 *cis*-2-MPO study in wine	Evolution profile of *cis*-2-methyl-4-propyl-1,3-oxathiane (*cis*-2-MPO) during fermentation and correlation with varietal thiols and acetaldehyde; stability study during wine storage.
Chapter 4 Chiral study of 3-SH and *cis*-2-MPO; novel 1,3-oxathiane identification	Chiral GC-MS method development for *cis*-2-MPO enantiomers analysis and chiral relationship study between *cis*-2-MPO and 3-SH enantiomers; identification of *cis*-2,4,4,6-tetramethyl-1,3-oxathiane in wine.
Chapter 5 Chiral study of 4-MSPOH and new sulfur-containing volatile compound	Preliminary HPLC-MS/MS methods development for 4-MSPOH enantiomers resolution and preliminary study for the identification of grapefruit mercaptan and blackcurrant mercaptan in wine.
Chapter 6 Oenological impact on varietal thiols in Shiraz	Volatile chemical and sensory profiles of Shiraz wine to evaluate the impact of accentuated cut edges technique, duration of maceration, and water dilution of grape must.
Chapter 7 Oenological impact on varietal thiols in Sauvignon blanc	Volatile chemical and sensory profiles of Sauvignon blanc wine to evaluate the impact of accentuated cut edges technique, yeast strain, and malolactic fermentation.
Chapter 8 Conclusions and future perspectives	Conclusive observations are made and opportunities for future research are proposed.

CHAPTER 1

Literature Review & Research Questions and Aims

The literature review in this chapter covers the literature up to April 2019. Any literature beyond this date have been incorporated into Chapters 2 to 8 as appropriate.

Introduction

Sauvignon blanc wine is characterised by 'grapefruit', 'passionfruit', 'boxwood', and 'broom'-like aroma attributes, which are contributed by a number of potent aroma compounds known as varietal (or polyfunctional) thiols. These compounds are released enzymatically during fermentation from their odourless precursors in grapes. However, research has shown that much higher concentrations of precursors are metabolised during alcoholic fermentation than varietal thiols are released and precursor consumption could not adequately explain thiol concentrations in wines. Therefore, exploring the existence of potential new precursors, novel fate of varietal thiols, and impact of winemaking practices will provide fundamental knowledge that aids in the enhancement or preservation of varietal thiols in wine.

1.1 Varietal thiols and their precursors

1.1.1 Varietal thiols

Varietal thiols are a cluster of grape-originated sulfur-containing volatile compounds in wines, with typical concentrations ranging from nanogram per litre to low microgram per litre. Despite this, they are considered to substantially impact wine sensory characteristics, given their extremely low odour detection thresholds (ODT, Table 1). Among the identified varietal thiols in wine, the most studied ones include 3-sulfanylhexan-1-ol (3-SH), 3-sulfanylhexyl acetate (3-SHA), and 4-methyl-4-sulfanylpentan-2-one (4-MSP). Some less studied varietal thiols are 4-methyl-4-sulfanylpentan-2-ol (4-MSPOH, 'citrus zest'[1]), 3-sulfanylpentan-1-ol, 3-sulfanylheptan-1-ol, and 2-methyl-3-sulfanylbutan-1-ol (Table 1). Focusing on the aroma descriptions, 3-SH contributes 'grapefruit' and 'passionfruit'-like aromas whereas 3-SHA exhibits 'passionfruit' and 'boxwood'-like notes. 4-MSP is reminiscent of 'boxwood' or 'broom'-like notes, but it also correlates well with 'blackcurrant' notes in some Languedoc (French) red wines. Specifically, the 'blackcurrant' note in such wines may be enhanced by high levels of 3-SH (11487 ng/L) and 3-SHA (154 ng/L) with the presence of 4-MSP.[2] For the most studied 3-SH and 3-SHA, their racemic ODTs have been reported to be 60 ng/L and 4.2 ng/L in a model wine matrix containing 12 % v/v alcohol and 5 g/L tartaric acid, respectively;[1] however, the chiral centre at the C-3 position of 3-SH yields enantiomers of 3-SH and 3-SHA, with the 3-dimensional difference in their chemical structures causing different perception thresholds and sensory characters. Explicitly, the ODTs for (3*R*)-3-SH and (3*S*)-3-SH were determined to be 50 ng/L and 60 ng/L, respectively; and for (3*R*)-3-SHA and (3*S*)-3-SHA were 9 ng/L and 2.5

ng/L, respectively (Table 1).[3] Further research pointed out that both enantiomers of 3-SH and 3-SHA were not present as racemic mixtures in wines, which showed that the 3*R*/3*S* ratios of 3-SH and 3-SHA were around 50/50 and 30/70 in dry wines, respectively, but the 3*R*/3*S* ratio for 3-SH in some noble rot wines was around 30/70.[3-4] Subsequently, the impact of different enantiomeric ratios of 3-SH and 3-SHA on wine sensory characters was investigated, showing that a higher proportion of the (3*R*)-enantiomer over the (3*S*)-enantiomer for both 3-SH and 3-SHA in a neutral white wine could enhance the overall 'fruity', 'tropical', and 'confectionery' notes, whereas a higher ratio of the (3*S*)-form of 3-SH and 3-SHA could enhance the 'cooked green vegetal' and 'cat urine' notes.[5]

With consideration of their occurrence, varietal thiols were first identified in Sauvignon blanc wine that is characterised by aromas of 'tropical fruits', 'grapefruit', and 'passionfruit'. Further studies revealed the wide presence of varietal thiols, with them being identified and quantified in other varietal wines, including Gewürztraminer, Riesling, Muscat, Pinot gris, Sylvaner, Pinot blanc, Petit manseng, Semillon, Chardonnay,[1,6-7] Carmenere, Merlot, and Cabernet Sauvignon,[8-9] although usually in less abundance (Table 1).

Table 1. *Structures, thresholds, and descriptors of varietal thiols and contents in wine.*

Name	ODT (ng/L)[a]	Descriptors	Concentration range, variety[b]	
(3*R*)-3-Sulfanylhexan-1-ol 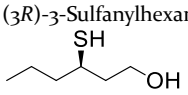	50[3]	Grapefruit, citrus peel[3]	122–18681, Sauvignon blanc (NZ) 1526–7080, Sauvignon blanc 4048–5969, Botrytised Semillon 168–5077, Chardonnay 828–4468, Petit Manseng 1336–3278, Gewurztraminer	423–1053, Colombard 312–1042, Pinot Gris 407–970, Riesling 124–898, Muscat 88.5–248, Pinot Blanc 58.4–146, Sylvaner
(3*S*)-3-Sulfanylhexan-1-ol 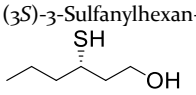	60[3]	Passionfruit[3]		
(3*R*)-3-Sulfanylhexyl acetate 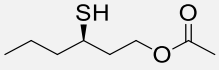	9[3]	Passionfruit[3]	24–2507, Sauvignon blanc (NZ) 21–516, Sauvignon blanc 2.1–205, Chardonnay n.d.–101, Petit Manseng	21–63, Colombard n.d.–51, Pinot Gris n.d.–6.4, Riesling 0.5–5.7, Gewurztraminer
(3*S*)-3-Sulfanylhexyl acetate 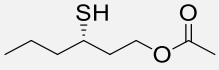	2.5[3]	Boxwood[3]		
4-Methyl-4-sulfanylpentan-2-one 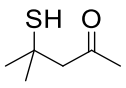	0.8[1]	Boxwood, broom[1]	7–97, Muscat ~80, Sauvignon blanc (LV) n.d.–~70, Verdejo 0–50, Sauvignon blanc (NZ) 8.5–40, Botrytised Semillon 5.5–19, Sauvignon blanc	n.d.–15, Gewurztraminer n.d.–7.6, Riesling n.d.–1.9, Pinot Gris 0.7–1.1, Pinot Blanc 0.13–0.95, Chardonnay 0.3–0.5, Sylvaner
4-Methyl-4-sulfanylpentan-2-ol 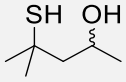	55[1]	Citrus zest[1]	1–111, Sauvignon blanc 2.2–86, Muscat n.d.–13, Semillon (botrytised)	2.4–11.2, Gewurztraminer n.d.–3.3, Riesling n.d.–0.2, Pinot gris

Table 1. Contd.

Name	ODT (ng/L)[a]	Descriptors	Concentration range, variety[b]
3-Sulfanylpentan-1-ol 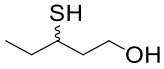	950[10]	Citrus, sulfur[10]	141–375, Botrytised Sauvignon blanc 93–291, Botrytised Semillon
3-Sulfanylheptan-1-ol 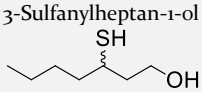	35[10]	Grapefruit[10]	95–263, Botrytised Sauvignon blanc 34–118, Botrytised Semillon
2-Methyl-3-sulfanylbutan-1-ol 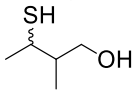	Not determined	Raw onion, sweet[10]	50–185, Botrytised Sauvignon blanc 67–134, Botrytised Semillon

[a] ODT, odour detection thresholds, they were measured in hydroalcoholic solution. [b] Typical concentration ranges of 3-SH and 3-SHA instead of their enantiomers, n.d. not detected, NZ: New Zealand, LV: Loire Valley. The combined data of Sauvignon blanc from New Zealand were from Jouanneau[11] and Lund, et al.[12]. Other Sauvignon blanc typical concentrations are from Benkwitz, et al.[13], Chardonnay is from Capone, et al.[7], Verdejo is from Belda, et al.[14], and the remainders are from Tominaga, et al.[1].

1.1.2 Non-volatile precursors of varietal thiols

L-Glutathione (GSH) is a nucleophilic biological thiol extensively present in plant cells (56–372 µmol/L and 46–333 µmol/L in grape berries and must, respectively[15]) that engages in maintaining redox homeostasis, detoxification, and sulfur metabolism in living tissues.[16-19] GSH combines with reactive electrophiles *in planta* as a result of detoxification mechanisms. One such electrophile is (*E*)-2-hexenal, which is one of the degraded products of unsaturated fatty acids catalysed by lipoxygenase and grape hydroperoxide-lyase. (*E*)-2-Hexenal can come either from endogenous (e.g., under *Botrytis cinerea* stress[20]) or exogenous (plant-plant communication[21]) stimuli and is toxic to plant cells by depolarising plasma membrane potential and increasing cytosolic calcium fluxes.[21] The condensation reaction between GSH and (*E*)-2-hexenal forms 3-*S*-glutathionylhexanal (GSH-3-SHal, Table 2) as an intermediate. This was firstly rationalised by a spiking experiment using deuterium labelled standard, where d_8-(*E*)-2-hexenal was spiked into grape berries and the corresponding d_8-GSH-3-SHal and d_8-3-*S*-glutathionylhexan-1-ol (d_8-GSH-3-SH) were detected in the subsequent crushed grape juice.[22] However, the natural existence of GSH-3-SHal was not reported until Thibon, et al.[23] identified it in Sauvignon blanc juice and quantification of this precursor form was subsequently achieved when Clark and Deed[24] reported 0.008–0.62 µmol/L of GSH-3-SHal in Sauvignon blanc juice (Table 2). Together with the identification of natural GSH-3-SHal, GSH-3-SH-SO_3 (Table 2), the bisulfite adduct that is formed from the aldehyde and bisulfite that is typically added to grapes, juices, and musts, was reported in Sauvignon blanc juice.[23]

Table 2. *Structures and concentrations of precursors in different grapes varieties.*

Name	Structure	Grape variety, concentration range[a]
GSH-3-SHal	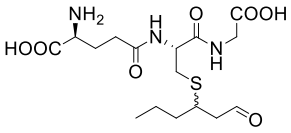	Sauvignon blanc: (0.008–0.62 µmol/L) 3.2–252[24] Catarratto BC: 635–10672 during ripening and 8096 at harvest[25] Grillo: 2644–7294 during ripening and 2644 at harvest[25]
GSH-3-SH-SO_3	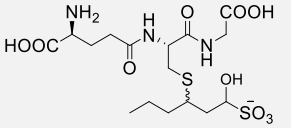	Sauvignon blanc: Identified but not quantified[23]
GSH-3-SH	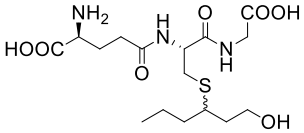	Verdejo: 649[14]; Sauvignon blanc: 40–116,[26] 8–16 µg/kg,[27] 1.35–24.8 µg/kg[28] Grechetto: 3.8–4.5[28]; Catarratto BC: 119–475 during ripening and 216 at harvest[25]; Grillo: 436–479 during ripening and 460 at harvest[25] **(*S*)-form**:[29] In Riesling, Sauvignon blanc, Chardonnay, and Pinot grigio wines: 52–392 **(*R*)-form**:[29] In Riesling, Sauvignon blanc, Chardonnay, and Pinot grigio wines: 22–175
CysGly-3-SH	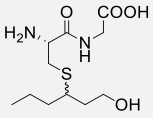	Sauvignon blanc: 10–28.5,[30] 0.4–1.6[26]
GluCys-3-SH	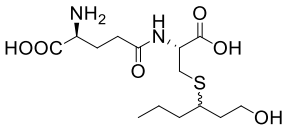	Sauvignon blanc: 3.3–36.1[31]
Cys-3-SH	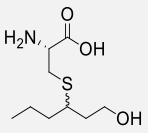	Verdejo: 44[14]; Sauvignon blanc: 27.7–54.7,[6] 4–15,[26] 1–6 µg/kg,[27] 2.2–4.4 µg/kg[28] Grechetto: 6.4–7.4[32]; Catarratto BC: 15.5–50.8 during ripening and 19 at harvest[25]; Grillo: 25.5–30.8 during ripening and 27.3 at harvest[25] **(*S*)-form**:[29] In Riesling, Sauvignon blanc, Chardonnay, and Pinot grigio wines: 4–41 **(*R*)-form**:[29] In Riesling, Sauvignon blanc, Chardonnay, and Pinot grigio wines: 3–16
GSH-4-MSP	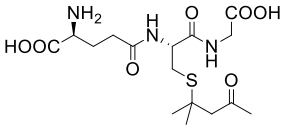	Sauvignon blanc: ~5[33], 0.028–4.304[34], 0.13–0.32 µg/kg[28], 0.3 µg/kg[27] Grechetto: 1.5–2.3[32] Riesling: 0.551–1.835[34] Gewurztraminer: 0.101–0.182[34]
Cys-4-MSP	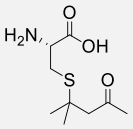	Sauvignon blanc: 15.2[35], 2.583–6.223[34], 1–4 µg/kg[27], 0.76–2.99 µg/kg[28] Melon B: 1.067–3.823[34]; Grechetto: 1.1–1.8[32]; Gewurztraminer: 0.539–0.815[34] Malvasia: 0.8[35]; Verdejo: 0.1[14]
CysGly-4-MSP	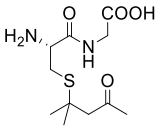	SB: < limit of quantification[31]
GluCys-4-MSP	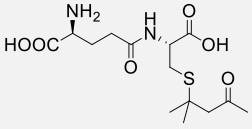	SB: < limit of quantification[31]

[a] Concentrations are given as total stereoisomers unless otherwise specified. Unit is µg/L unless specified otherwise. The unit has been converted into µg/L from nmol/L in reference[34] by timing 405.298 for the original concentration of GSH-4-MSP and 219.121 for the original concentration of Cys-4-MSP.

GSH and L-cysteine (Cys) based precursors of 3-SH and 4-MSP are the most widely

studied precursors. 3-*S*-Cysteinylhexan-1-ol (Cys-3-SH, Table 2) is the first identified precursor of 3-SH in Sauvignon blanc juice, based on the detection of free 3-SH in a volatile-free juice after the application of a crude enzyme preparation exhibiting β-lyase activity.[36] Reported in different grape varieties, the highest concentration of Cys-3-SH can be up to 55 μg/L in a Sauvignon blanc juice (Table 2).[29] 3-*S*-Glutathionylhexan-1-ol (GSH-3-SH) was the second identified precursor of 3-SH in Sauvignon blanc and Gros Manseng juice,[37] with the concentration in different grape juices reported to be up to 731 μg/L (Table 2). Comparatively, the concentration of GSH-3-SH was generally higher than that of the Cys-3-SH (Table 2),[29,38] although the opposite results were also revealed.[32,35,39] Such contrary observations might be due to the differences in juice preparation methods.[22]

In the case of 4-MSP precursors, 4-*S*-cysteinyl-4-methylpentan-2-one (Cys-4-MSP) and 4-*S*-glutathionyl-4-methylpentan-2-one (GSH-4-MSP) were identified in grape juice by Tominaga, et al.[36] and Fedrizzi, et al.[33], respectively, with concentrations in different grape juices being between 0.1–6.2 μg/L for Cys-4-MSP and 0.1–4.3 μg/L for GSH-4-MSP (Table 2). Different to what was reported for that of 3-SH precursors, the concentration of Cys-4-MSP in grape juice was reported to be slightly more abundant than GSH-4-MSP, which may imply a somewhat different formation pathway, although this remains to be investigated.

The remaining four precursors in Table 2, namely the dipeptide conjugates of 4-MSP and 3-SH, which are present at the lowest concentrations compared to the other identified precursors, are the intermediates between the glutathionylated and cysteinylated precursors.[26,30-31] The concentrations of L-cysteinylglycine-3-SH (CysGly-3-SH) and γ-L-glutamyl-L-cysteine-3-SH (GluCys-3-SH) are more abundant than those of L-cysteinylglycine-4-MSP (CysGly-4-MSP) and γ-L-glutamyl-L-cysteine-4-MSP (GluCys-4-MSP), with results for both CysGly-4-MSP and GluCys-4-MSP in Sauvignon blanc grape juice are too low to be formally identified.[31]

Due to the chiral carbon centre at C-3 of the GSH substituted hexan-1-ol, 3-SH precursors are present in juices and wines as a mixture of diastereomers. Stereochemical studies could help further the understanding of the relationship between these diastereomers and the corresponding enantiomers of 3-SH, given the knowledge that a single diastereomer of GSH-3-SH could yield the corresponding single enantiomer of 3-SH (via a single diastereomer of Cys-3-SH).[40-41] So far, however, a strong link between the stereochemical profiles of 3-SH precursors in juices and 3-SH/3-SHA in the corresponding wines has not been forthcoming in a limited number of fermentation experiments.[26]

With respect to the diastereomer concentrations, (*S*)- and (*R*)-GSH-3-SH (with the relative stereochemistry referring to the carbon of the alkyl chain bearing the sulfur atom) were quantified in different grape varieties from 52 to 556 μg/L and 22 to 175 μg/L, respectively[29] (Table 2), with *S*/*R* ratios ranging from 3/1 to 7/1.[26,29] The concentrations of (*S*)- and (*R*)-Cys-3-SH ranged between 2–41 μg/L and 3–16 μg/L, respectively, with *S*/*R* ratios ranging from 2.1/1 to 3/1.[26,29] Furthermore, (*S*)-Cys-3-SH was reported to be even more predominant (*S*/*R*=7/3) when grape berries were affected by *Botrytis cinerea*.[42] The elution order of the well resolved CysGly-3-SH diastereomers was assigned based on the analogy with the elution order of GSH-3-SH and Cys-3-SH diastereomers in the same method, with *S*/*R* ratios of CysGly-3-SH diastereomers being either between 72.8/18.2 to 78.2-11.8[30] or approximately 1/1[26] whereas the method used for identification of GluCys-3-SH in grape must partially resolved the diastereomers of GluCys-3-SH,[31] and an average diastereomeric ratio of 7/3 was estimated. However, an open question was left from the study in terms of the assignment of the elution order of the GluCys-3-SH diastereomers.[31]

Other compounds arising from bisulfite addition to (*E*)-2-hexenal have been proposed as potential precursors (Figure 1),[43] but there is doubt about whether these compounds could yield free thiols (e.g., by enzymatic reduction of the sulfonate[44]) since they have neither been shown to do so in the ensuing years after they were first reported nor they have been identified in grape materials.

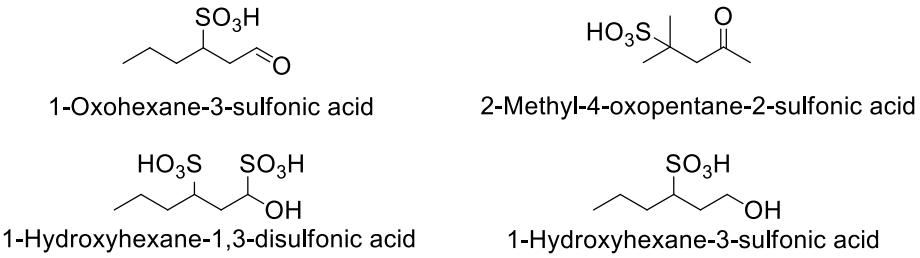

Figure 1. *Structures of four proposed precursors of varietal thiols.*[43]

1.2 Formation and degradation pathways of precursors

Although 3-SH has been reported in grape berries as the free volatile compound (at ~100 ng/L),[6] the major known pathway to the formation of varietal thiols such as 3-SH and 4-MSP requires enzymatic steps facilitated by microorganisms during winemaking (especially fermentation).[45-46] This releases the thiols from their non-volatile GSH or Cys conjugates, which themselves are formed in the grape berry. The formation and degradation pathway of

precursors to 3-SH is summarised in Scheme 1 based on current knowledge, to exemplify the processes. Step a illustrates the formation of GSH-3-SHal from condensation of GSH and (*E*)-2-hexenal (a reactive electrophile arising from oxidative degradation of linolenic acid by lipoxygenase and hydroperoxide lyase enzymes[47]), presumably catalysed by L-glutathione *S*-transferase (GST)[48] and to a lesser extent by chemical reaction.[24] The conversion rate from the substrates to GSH-3-SHal in grape juice has never been determined, although a GSH-3-SHal (3 mg/L) was produced from a model grape juice containing 100 mg/L GSH and 5 mg/L (*E*)-2-hexenal during 3-day storage as a result of chemical reactions.[24] Step b in Scheme 1 outlines the potential interconversion between GSH-3-SHal and GSH-3-SH-SO_3, with GSH-3-SH-SO_3 returning to GSH-3-SHal when SO_2 diminishes.[23] In both Sauvignon blanc juice and model grape juice, the conversion rates of GSH-3-SHal and GSH-3-SH-SO_3 into free 3-SH are around 0.4 % in the presence of 20 mg/L of free SO_2, or 8 % for GSH-3-SHal and 0.5 % for GSH-3-SH-SO_3 without the addition of SO_2.[23]

GSH-3-SHal is enzymatically reduced into GSH-3-SH (step c, Scheme 1) presumably by alcohol dehydrogenase or aldo-keto reductase.[49-50] The release of 3-SH from GSH-3-SH involves multiple enzymatic steps as outlined in Scheme 1, with conversion rates from GSH-3-SH to 3-SH determined to be 3 % and 4.4 % in synthetic medium and Sauvignon blanc juice, respectively.[40,51] Much lower conversion rates (0.5 %[52], 1.05 %[53]) have also been observed in model grape juice fermentation.

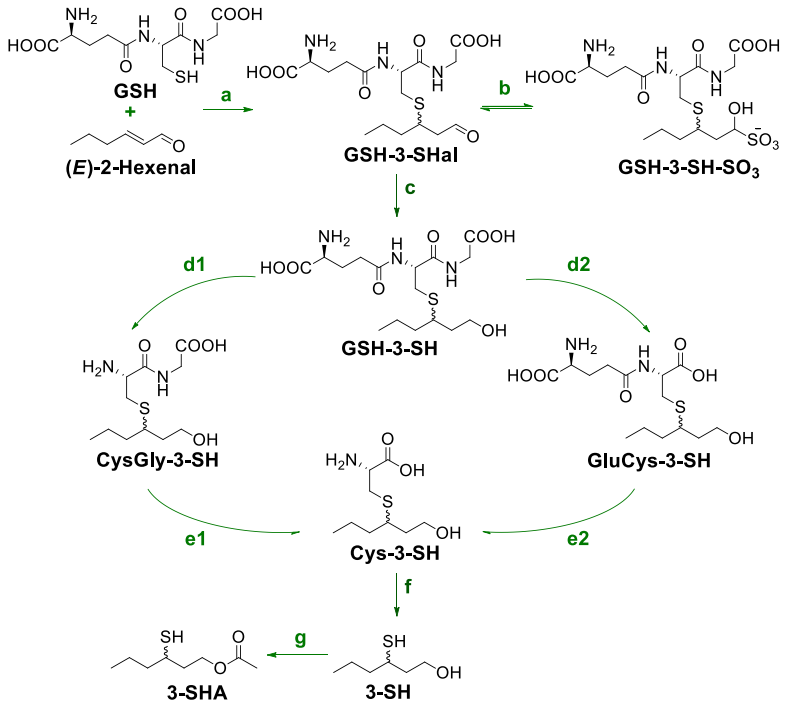

Scheme 1. *The biochemical formation mechanism of 3-SH and 3-SHA.*[24,30-31,44] *Steps: a,*

conjugation of GSH and (E)-2-hexenal catalysed by GST or from chemical reaction; b, interconversion between GSH-3-SHal and GSH-3-SH-SO_3 in the presence of bisulfite; c, enzymatic aldehyde reduction by alcohol dehydrogenase or aldo-keto reductase; d1, degradation of GSH-3-SH to CysGly-3-SH catalysed by γ-glutamyl-transpeptidase; d2, degradation of GSH-3-SH to GluCys-3-SH catalysed by phytochelatin synthase or carboxypeptidase; e1, degradation of CysGly-3-SH to Cys-3-SH catalysed by carboxypeptidase; e2, degradation of GluCys-3-SH to Cys-3-SH via an uncertain pathway; f, release of 3-SH from Cys-3-SH catalysed by yeast carbon-sulfur lyase; g, acetylation of the alcohol in 3-SH catalysed by alcohol acetyltransferase or other potential enzymes.

GSH-3-SH is degraded into Cys-3-SH, possibly through CysGly-3-SH (step d1 & d2, Scheme 1) or likely via GluCys-3-SH (step e1 & e2, Scheme 1) as an intermediate,[30-31] although some of the pathways were not passable under certain conditions.[54] Step d1 has been investigated by applying γ-glutamyl-transpeptidase (GGT) to ascertain the presence of GSH-3-SH via its conversion to CysGly-3-SH (and Cys-3-SH)[37] and 70 % yield has been achieved in the production of synthetic CysGly-3-SH under optimised conditions.[30] Such a biochemical pathway is further supported by the determination of GGT activity in grapes.[48] Subsequently, CysGly-3-SH is degraded into Cys-3-SH catalysed by carboxypeptidases[55] (step e1, Scheme 1), with a conversion rate of 54 % measured in Sauvignon blanc must with the aid of deuterated CysGly-3-SH.[54] GluCys-3-SH has been identified very recently in Sauvignon blanc must[31] and step d2 (Scheme 1) is presumably catalysed by phytochelatin synthase or carboxypeptidase.[17] However, the enzyme involved in catalysing step e2 remains unclear. GluCys-3-SH is less abundant than CysGly-3-SH and the conversion rate for GluCys-3-SH into 3-SH was 0.24 %.[54]

Cleavage of Cys-3-SH to release free 3-SH is catalysed by yeast β-lyase during AF (step f, Scheme 1).[36,56] Generally, the conversion rate from Cys-3-SH to 3-SH is approximately 1 % (<1 %[57], 1 %[41]), except when gene modified *Saccharomyces cerevisiae* yeasts are used in experiments (14 %[40], >10 %[58]). Despite the lower conversion yields of Cys-3-SH to 3-SH than that of GSH-3-SH discussed above, experiments that compared the efficiency of producing 3-SH from either precursor illustrated that Cys-3-SH is more easily transformed into 3-SH compared to GSH-3-SH.[52,59] Step g in Scheme 1 presents the acetylation of 3-SH to form its *O*-acetate, mainly catalysed by alcohol acetyltransferase during AF.[60] Generally, up to approximately 10 % of 3-SH could be acetylated, with studies showing 6.6–11.8 % in Sauvignon blanc juice fermentation[23] or 3 % in a model grape juice fermentation by a strain of selected

wild yeast.[53]

In consideration of pathways associated with 3-SH, Scheme 2 proposes formation of 4-MSP and the degradation pathway of its precursors, although multiple steps of the pathway require further study. Mesityl oxide (i.e., 4-methyl-3-penten-2-one) is likely to be the precursor of 4-MSP in wine and this was verified by the result that d_{10}-4-MSP was detected after AF of Melon B. must spiked with 1.0 mg/L of d_{10}-mesityl oxide.[61] However, with the identification of GSH-4-MSP in grapes,[33] it could be hypothesised that mesityl oxide is first combined by GSH in grapes to yield GSH-4-MSP, as shown in step a (Scheme 2), before being further catalysed to release the free 4-MSP. Despite this, the origin and function of mesityl oxide in grape berries is still a mystery, although its existence has been reported in a number of aged red wines produced in France, Italy, Spain, and Poland that underwent semi-quantitative anlaysis.[62] Another study reported the presence of mesityl oxide at the surface of grape leaf;[63] although those results may need to be interpreted with caution as the grape leaf samples were extracted with acetone that could be a source of the formation of mesityl oxide.

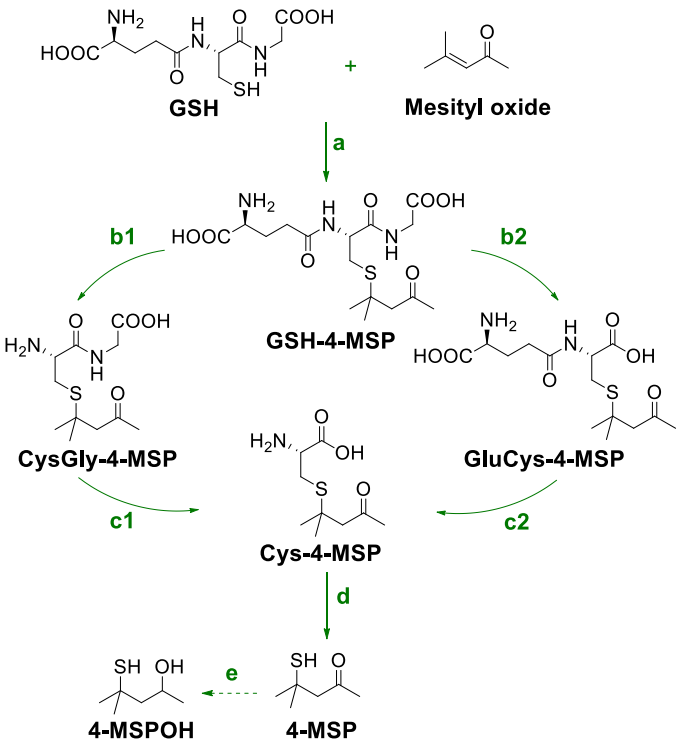

Scheme 2. *Proposed biochemical formation and degradation pathways of 4-MSP.*[31,61] *Steps: a, conjugation of GSH and mesityl oxide by GST; b1, degradation of GSH-4-MSP catalysed by γ-glutamyl-transpeptidase; b2, degradation of GSH-4-MSP catalysed by phytochelatin synthase or carboxypeptidase; c1, degradation of CysGly-4-MSP catalysed by carboxypeptidase; c2, degradation of GluCys-4-MSP through an unclear pathway; d, release of 4-MSP from Cys-4-MSP*

catalysed by yeast β-lyase; e, reduction of 4-MSP to yield 4-MSPOH presumably by aldo-keto reductase.

Presenting 'peppermint', 'flowery', and 'sweet'-like aromas,[64] mesityl oxide in grape and wine can be proposed to originate in different ways (Scheme 3). Firstly, open-chain carotenes were shown to produce unsaturated ketones after an oxidation process,[65] and mesityl oxide was presumed to be released from carotenes,[66] although detailed degradation stages were not resolved. As one of the carotenes, lycopene was shown to yield acetone at 60 °C or 100 °C with O_2,[67] but this would not be applicable to wine production. However, with lycopene and aldolase in grapes,[68-69] it may be hypothesised that lycopene produces mesityl oxide via enzymatic processes (step a in Scheme 3). Self-condensation of acetone to produce diacetone alcohol (step b) can occur through chemical synthesis,[70] but such a reaction has not been reported in grape yet. Nonetheless, diacetone alcohol was detected in grape,[71] which may potentially be derived from an enzymatic condensation reaction of acetone, with class I aldolase being a prospective enzyme catalysing the reaction. Then mesityl oxide could potentially be formed from the dehydration of diacetone alcohol, which may be proposed to be processed by either spontaneous dehydration or catalysed by dehydrase activity from uncharacterised enzymes (step c). Secondly, an assumption could be proposed that soil bacteria (e.g., *Collimonas pratensis*) secrete mesityl oxide (step d) as a result of interaction with other microorganisms or plant root,[72] with subsequent transportation into the vine (step e).[73] Thirdly, a number of authors believe mesityl oxide derives from fatty acids,[64,74-75] as shown in step f1. However, it was proposed that, either spontaneous decarboxylation or catalysed by acetoacetate decarboxylase, acetone could potentially be produced from the metabolism of acetoacetate that originated from the excess acetyl-CoA from fatty acid degradation,[76] thus there also remains the possibility that mesityl oxide is produced following the steps of step f2 to step b then step c. Fourthly, mesityl oxide is a relatively common solvent and could pre-exist in paint or ink and subsequently react with H_2S in food (or GSH and Cys) to form 4-MSP (or precursors), as is the case with a food taint.[77-78] Finally, in contrast to step f, mesityl oxide was suggested to be the oxidative cleavage product of terpenoids in an *Anabaena cylindrica* medium (step g) and fatty acids were not found as the likely source in the study.[66]

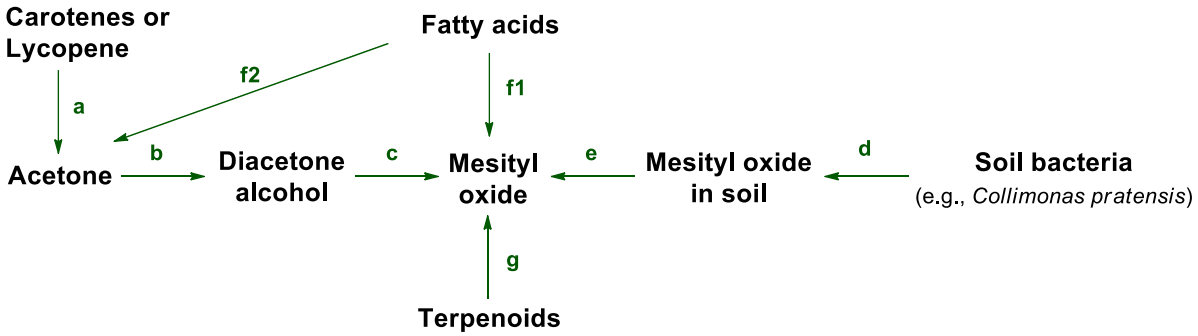

Scheme 3. *Postulated origins for mesityl oxide in grape berries. Steps: a, enzymatic degradation of open-chain carotenes or lycopene into acetone; b, self-condensation of acetone to form diacetone alcohol; c, dehydration to form mesityl oxide presumably proceeded by either spontaneous dehydration or catalysed by some uncharacterised enzyme; d, soil bacteria secrete mesityl oxide into soil; e, potential absorption of mesityl oxide by plant root; f1, degradation from fatty acids; f2, acetone produced from the metabolism of acetoacetate (from fatty acid degradation) by either spontaneous decarboxylation or catalysis by acetoacetate decarboxylase; g, enzymatic degradation of terpenoids.*

Despite the unknown source of mesityl oxide, the degradation of GSH-4-MSP to 4-MSP could potentially be similar to that of GSH-3-SH. In a model grape juice fermentation, only 0.33 % of GSH-4-MSP is consumed to produce 4-MSP.[54] In the same study, Bonnaffoux, et al.[54] showed that 6 % and 1 % of CysGly-4-MSP was converted into Cys-4-MSP and 4-MSP, respectively, whereas only 0.05 % of GluCys-4-MSP was consumed to release 4-MSP, although the two dipeptide precursors are not formally identified in grapes. In contrast though, a hypothetical explanation for the greater abundance of Cys-4-MSP compared to GSH-4-MSP, as mentioned in Section 1.1.2, might be due to the sample preparation method, which involved crushing berries under vacuum instead of air. Alternatively, it could be caused by a limited amount of GSH-4-MSP being formed in berries, which mostly degrades to Cys-4-MSP and no more mesityl oxide is available to react with GSH during crushing. On the other hand, when considering that GSH-4-MSP was not metabolised to Cys-4-MSP during fermentation by yeast,[54] it may be related to specificity of enzymes in the yeast strains used in the study that cannot catalyse step b1, b2, c1, or c2 in Scheme 2. The precursor Cys-4-MSP is enzymatically catalysed by β-lyase to release 4-MSP (Step d)[79] and the conversion yield is generally under 1 %,[58,80-82] but could be as high as 10 % when using a gene-modified yeast strain that overexpresses β-lyase.[80] Lastly, part of 4-MSP could potentially be reduced to 4-MSPOH during AF (Step e, Scheme 2), although the cysteine conjugate of 4-MSPOH has been identified in

Sauvignon blanc juice[36]and could also be a source of 4-MSPOH.

Table 3 summarises some of the conversion yields of precursors into downstream intermediates or thiols in either grape juice fermentation or model grape juice fermentation. Although these conversion yields have been discussed above, the table provides much more detailed information in terms of fermentation media and yeast strains.

Table 3. *Conversion yields of precursors in releasing varietal thiols in grape juice and model grape juice.*

Precursor	Product	Conversion yield	Yeast strains/Enzymes	Medium	Ref
GSH-3-SHal	3-SH	0.4 %–0.45 %	X5	Sauvignon blanc juice containing 20 mg/L SO_2	
		0.78 %–0.86 % without SO_2	X5	Model grape juice	23
		0.39 %–0.42 % with 20 mg/L SO_2	X5	Model grape juice	
GSH-3-SH-SO_3	3-SH	0.38 %–0.42 %	X5	Sauvignon blanc juice containing 20 mg/L SO_2	
		0.48 %–0.51 % without SO_2	X5	Model grape juice	23
		0.38 % with 20mg/L SO_2	X5	Model grape juice	
GSH-3-SH	3-SH	4.4 %	VIN13	Sauvignon blanc juice	51
		3 %	VIN13 (overexpress *E. coli TNA A in* VIN 13)	Model grape juice	40
		1.05 %	Lab selected wild yeast BY4742	Model grape juice	53
		0.5 %	Vl3	Model grape juice	52
		0.19 %	Esperide	Sauvignon blanc juice	54
	CysGly-3-SH	70 %	GGT from equine kidney (type VI, Sigma-Aldrich)	Optimised Tris-HCl buffer	30
	GluCys-3-SH	7 %	Esperide	Sauvignon blanc juice	54
	Cys-3-SH	9 %	Esperide	Sauvignon blanc juice	54
CysGly-3-SH	Cys-3-SH	54 %	Esperide	Sauvignon blanc juice	54
	3-SH	0.17 %	Esperide	Sauvignon blanc juice	54
GluCys-3-SH	3-SH	0.24 %	Esperide	Sauvignon blanc juice	54
Cys-3-SH	3-SH	0.48–0.81 %	Commercial strains ES1 and ES2, lab strain BY4743	Sauvignon blanc must	57
		1 %	AWRI 1655	SCD liquid media	41
		14 %	VIN13 (overexpress *E. coli TNA A in* VIN 13)	Model grape juice	40
		>10 %	VIN13 (overexpress *E. coli TNA A in* VIN 13)	Model grape juice	58
3-SH	3-SHA	6.6 %–11.8 %	X5	Sauvignon blanc juice	23
GSH-4-MSP	4-MSP	0.33 %	Esperide	Sauvignon blanc juice	54
CysGly-4-MSP	Cys-4-MSP	6 %	Esperide	Sauvignon blanc juice	54
	4-MSP	1 %	Esperide	Sauvignon blanc juice	54
GluCys-4-MSP	4-MSP	0.05 %	Esperide	Sauvignon blanc juice	54
Cys-4-MSP	4-MSP	2.3 %	VIN13 (overexpress *E. coli TNA A in* VIN 13)	Model grape juice	58
		34 %, 67 %	F15 (overexpress *IRC7*)	Model grape juice	80

SCD liquid media: 6.7 g/L yeast nitrogen base, 6 % glucose.

1.3 Reactivity of thiols

Reactivity refers to the reactions or potential reactions between thiols and other constitutes in wine that could cause the decline of thiols in wine. Thus, this could be a key aspect of varietal thiol research, given their extremely low ODTs (Table 1), whereby even minor changes in their concentrations could potentially induce substantial influence on wine aroma. As reported, concentrations of both 4-MSP and 3-SHA could decrease during storage:[83] for instance, the concentration of 3-SHA in South African Sauvignon blanc wines dropped from 98 ng/L to 63 ng/L after 7-months of storage at 15 °C in the dark[83] and similar losses of 3-SHA were also observed for New Zealand Sauvignon blanc.[84] The evolution of 3-SH during storage is controversial, where some research reported that the concentration of 3-SH either kept steady or dropped marginally during early stage of storage before a significant increase,[83-84] whereas others reported that 3-SH dropped 34 % in a 3-month storage before bottling and 53 % decrease in one year of bottle storage.[85] Also, two Cabernet Sauvignon red wines in 1996 and 1998 vintages lost 78 % and 73 % of 3-SH after a 390-day and 360-day barrel aging, respectively.[86]

Except for the volatilisation, thiols could be bound by quinones (originates from phenolics), whose formation is catalysed by copper and iron,[87-90] which could explain the major loss of thiols in wine,[91] and acetate hydrolysis could also partly explain the loss of 3-SHA.[84] Furthermore, disulfides (i.e., oxidised thiols),[92] or the potential existence of polysulfides (although not identified in wine in the study),[93] or mixed disulfide/polysulfide[94] forms of 3-SH and 3-SHA could be responsible for some losses, and yet other reactions of thiols could explain their disappearance. Recently, *cis*-2-methyl-4-propyl-1,3-oxathiane was identified in wine and proposed to arise from a combination of acetaldehyde and 3-SH. This oxathiane presents a 'fruity' note accompanied with 'green', and slightly 'burnt' aromas,[95] and has been determined in some commercial wines with the concentrations of up to 460 ng/L (Figure 2),[96] which could explain a partial loss of 3-SH to a commensurate extent (i.e., up to about 390 ng/L of 3-SH). Using this inspiration, another four varietal thiols bearing 1,3-sulfanylalkanol substitution in their structures (similar to that of 3-SH) can be proposed to undergo such reactions to yield the corresponding 1,3-oxathianes (Figure 2).

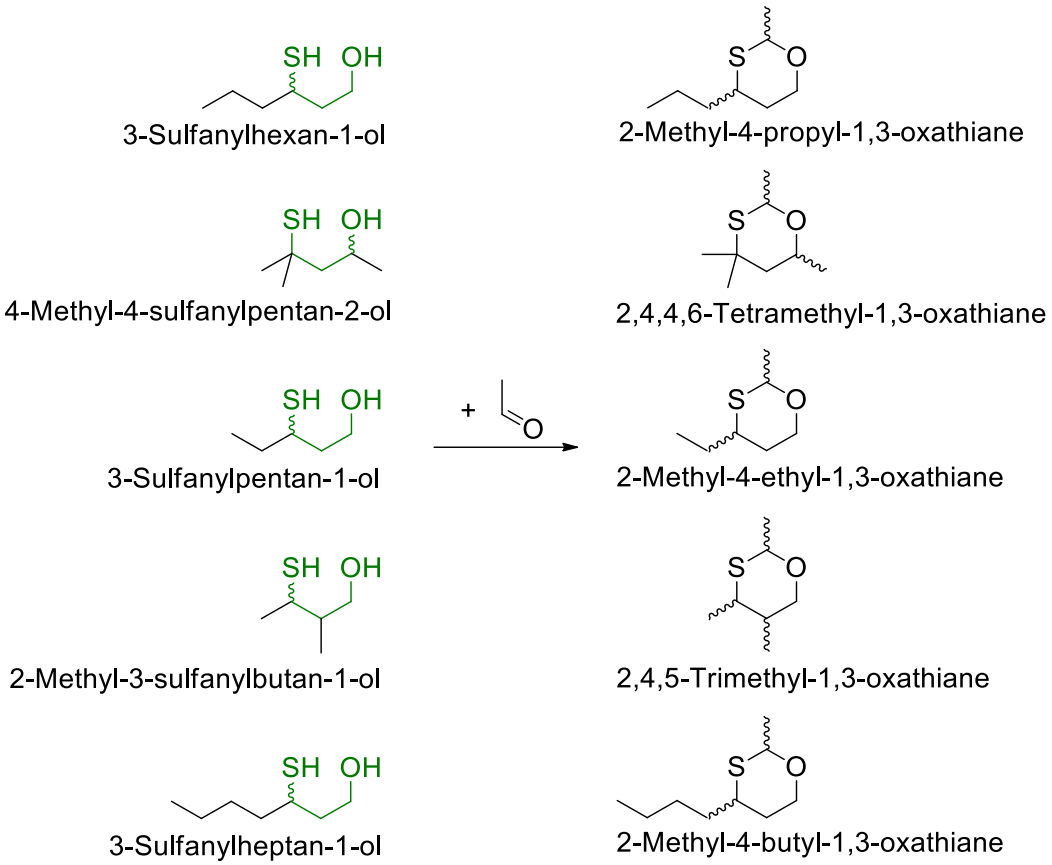

Figure 2. *Structures of oxathianes produced from reactions between 1,3-sulfanylalkanols and acetaldehyde.*

1.4 Alternative proposed biogenesis pathways to varietal thiols

The main source of H_2S in grape juice or must is from yeast metabolism during AF (step a in Scheme 4),[97] and H_2S was suggested react with (*E*)-2-hexenal catalysed by yeast strains during AF to produce 3-sulfanylhexanal (step b) which is then reduced into 3-SH by alcohol dehydrogenase from yeasts (step c).[61,98-99] The pathway is supported by the results that adding $NaSH{\cdot}xH_2O$, which releases free H_2S in acidic wine medium, to Sauvignon blanc grape must has significantly improved the concentration of 3-SH and 3-SHA in the final wines[98] and adding elemental sulfur, which could be reduced into H_2S, to fresh Sauvignon blanc juice improved the level of 3-SH in the resultant wine.[99] However, steps b and c need further evidence since the direct addition of H_2S and (*E*)-2-hexenal has never been proved. There is also possibility that mesityl oxide reacts with H_2S to form 4-MSP according to the discussion in Scheme 2, where mesityl oxide existing in paint or ink[78] reacts with H_2S in food to form 4-MSP as a known food taint.

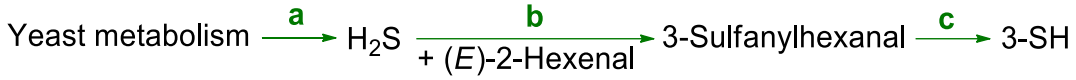

Scheme 4. *Proposed alternative formation pathway of 3-SH.*[98-99] *Steps: a, production of H_2S from yeast metabolism; b, combination of H_2S and (E)-2-hexenal to form 3-sulfanylhexanal by yeast; c, enzymatic reduction by yeast of the aldehyde group in 3-sulfanylhexanal.*

1.5 Factors impacting concentrations of varietal thiols and their precursors

1.5.1 Vineyard environment

Water and nitrogen status: Grapevine water status, normally measured as leaf water potential, is influenced by factors including not only precipitation and irrigation, but also soil texture and different water-holding capacity. For instance, the leaf water potential of Sauvignon blanc grown on sandy and gravelly soil (low water-holding capacity) is generally more negative than that of clay soil (high water-holding capacity).[100] Mild water deficit could improve the concentration of varietal thiols precursors (GSH-3-SH and Cys-3-SH) in grape leaves and berries,[48] whereas Peyrot des Gachons, et al.[100] showed that severe water deficit caused lower concentration of the precursors although the precursors were quantified by measuring the volatile thiols in juice treated by apotrypophanase.

Grapevine nitrogen status has an impact on the concentrations of varietal thiols and their precursors. Ammonium nitrate supplementation of soil significantly improved the concentrations of Cys-4-MSP, 4-*S*-cysteinyl-4-methylpentan-2-ol (Cys-4-MSPOH), and Cys-3-SH by 76 %, 171 %, and 341 % in Sauvignon blanc juice, respectively.[101] In contrast, another study pointed that vine nitrogen status did not affect Cys-3-SH concentration whereas GSH-3-SH was increased (195 % in Bordeaux, 165 % in Sancerre) significantly in Sauvignon blanc must from one of the two vintages studied.[102] Aside from the amount of nitrogen, the method of nitrogen supplementation also showed impact on thiol precursors. Compared with soil nitrogen fertilisation, which causes vigorous growth of vegetative parts of vines,[101,103] foliar spray of urea before véraison showed to improve the concentration of 4-MSP (402 ng/L) in the resultant wine compared with the control (308 ng/L).[104] Also, the combination spray of urea and micronised sulfur increased the concentrations of 4-MSP, 3-SH, and 3-SHA by 124 %, 164 %, and 234 %, respectively, compared with the control that was not fertilised.[104]

Crop level: A good deal of effort has been devoted to investigating the effect of crop level

on the quality of grape berries[105-108] and wine aroma compounds.[109-112] However, the influence of crop level on the concentrations of varietal thiol precursors in grape berries and varietal thiols in the final wines does not appear to have been explored.

Canopy management: Various canopy management practices exploring the influence on thiol precursors have been explored. For instance, different training systems in two adjacent vineyards, namely Royat cordon and Guyot, caused significant differences in the concentrations of cysteinylated and glutathionylated precursors of 3-SH, 4-MSP, and 4-MSPOH in Grechetto grapes.[32] Controlling canopy temperature under 30 °C by spraying nebulised water was revealed to elevate the concentrations of 3-SH (134 %), 3-SHA (122 %), and 4-MSP (improving from 2 to 9 ng/L) in the wines compared with the control, where the canopy temperature was not modulated.[113] However, the increase of varietal thiols may also relate to the difference in grapevine water potential induced by canopy water spray, but the water potential was not monitored in the study. Defoliation before blossom was reported to improve concentrations of GSH-3-SH, GSH-4-MSP, and Cys-4-MSP in Sauvignon blanc grapes.[28] The concentrations of 3-SH and 3-SHA were higher when defoliation was conducted when grape berries were at peppercorn size (2014 vintage) or two weeks before véraison (2016 vintage) compared with the control treatment that foliage was kept.[114-115]

Ripeness: Evolution study revealed that the concentrations of precursors of 3-SH and 4-MSP increased during the grape ripening stage and a dramatic increase occurred in the later period of ripeness.[6,35,39] However, different results were also observed where the concentrations of Cys-3-SH and GSH-3-SH in Koshu grape variety continued to increase for 8-10 weeks from 8 weeks post-flowering before a decrease to trace level until harvest,[59] and similar dynamic trend for Cys-3-SH was also reported in Sauvignon blanc grapes during growing season.[100] Interestingly, the total concentration of GSH-3-SH, Cys-3-SH, and CysGly-3-SH increased in the early morning then decreased during the day, and grapes harvested in early morning had higher levels of GSH-3-SH, Cys-3-SH, and CysGly-3-SH than those harvested at other times, and the corresponding wines produced by the grapes obtained in the early morning had higher concentrations of 3-SH and 3-SHA.[38]

Fungus: Fungal infection can increase the concentrations of precursors in grape berries and varietal thiols in the resultant wine. Spraying spore suspension of *Botryotinia fuckeliana* on Sauvignon blanc, Chardonnay, Koshu, and Merlot berries improved the concentrations of GSH-3-SH and Cys-3-SH to 23-57 fold and 16-51 fold, respectively,[48] and the level of Cys-3-SH was 100-fold higher when the berries were affected by *Botrytis cinerea*.[116] Besides, the

percentage of rot in harvested bunches appeared to correlate well with the level of Cys-3-SH in healthy berries having a correlation coefficient of 0.745.[117] These results might be explained by the detoxification mechanism as discussed in Section 1.1.2 of plants against the stimulation of fungus. In addition, botrytisation of Sauvignon blanc or Semillon berries can elevate the concentration of 3-SH in the corresponding wines, with more severe infection leading to more abundant 3-SH, 3-sulfanylpentan-1-ol, 3-sulfanylheptan-1-ol, and 2-methyl-3-sulfanylbutan-1-ol in the final wines.[10]

UV light: UV light exposure was shown to increase concentrations of 3-SH, GSH-3-SH, and Cys-3-SH, and this could be the protective reaction of cells towards damage from UV radiation.[118] Contrast results with the use of Sauvignon blanc showed that UV light treatment in conjunction with low-temperature storage (–80 °C) could not significantly impact the concentrations of varietal thiols and their precursors.[119] More specifically, UV light is divided into UV-A (315-400 nm), UV-B (280-315 nm), and UV-C (100-280 nm) according to the electromagnetic spectrum. A study showed that artificial exposure of UV-C could increase concentrations of 3-SH, Cys-3-SH, and GSH-3-SH.[48,120] However, this is unlikely to happen in vineyards given UV-C from sunlight could not reach ground.

1.5.2 Pre-fermentation procedures

Harvesting methods: The concentrations of GSH-3-SH and Cys-3-SH can be affected by grape harvesting operations. Capone and Jeffery[22] showed that the concentrations of GSH-3-SH and Cys-3-SH were 70 % and 65 % lower in hand-picked grapes than in the machine-harvested grapes without the addition of antioxidants, and the two precursors declined when SO_2 was added during harvest. With respect to the concentrations of 3-SH and 3-SHA, wines produced by grapes harvested mechanically presented higher levels of 3-SH and 3-SHA than the hand-harvested grapes.[121-124] However, it seemed that 4-MSP was not affected by harvesting methods.[121]

Transporting and storage: Capone and Jeffery[22] found in a commercial-scale trial that after transportation for 800 km, Sauvignon blanc grape must presented a significantly higher amount of both diastereomers of GSH-3-SH and Cys-3-SH than those that were not transported. Inspired by this phenomenon, a prolonged storage experiment of Sauvignon blanc grapes was conducted, which showed that the concentration of Cys-3-SH was 3 times higher after 30 h storage and the concentrations of GSH-3-SH and CysGly-3-SH were approximately 1.5 times that of the original levels after 30 h storage.[125]

Freezing: Storing grape berries in a freezer for two months was found to significantly

improve the level of GSH-3-SH compared to the level measured in the juice from fresh grape berries, whereas the concentration of Cys-3-SH was not significantly different among the fresh juice, frozen juice, and frozen grape berries.[6] Only recently our laboratory showed the substantial elevation (up to 10-fold) of varietal thiols in wines produced from frozen grapes.[126]

Cold maceration: Cold maceration is beneficial to improving the concentration of Cys-3-SH[127-128] in grape juice and also 3-SH in the final wines.[129] Moreover, improving oxygen availability to Müller-Thurgau and Sauvignon blanc must during cold maceration skin contact increased the concentrations of GSH-3-SH and Cys-3-SH.[130] Though the technique is not commonly used in wine industry, cryogenic maceration, in which dry ice was applied to Sauvignon blanc grape must to decrease the temperature to –20 °C and the must was permitted to thaw at ambient temperature before pressing, was reported to increase the concentration of 3-SHA and to a lesser extent 3-SH in the final wines.[123] A recent study on a new grape crushing technique named "accentuated cut edges" revealed that it could accelerate the extraction of phenolics from Pinot noir grape skins during maceration by reducing the sizes of the broken grape skin compared with the conventional crushing.[131] This new technique could potentially be used in Sauvignon blanc wine production with the aim of increasing the concentration of thiol precursors in grape juice pending fermentation.

Pressing: The concentrations of GSH-3-SH and Cys-3-SH in grape juices were improved by applying harder pressing procedures,[127,129] which might be due to the higher pressure promoting the extraction into juice of precursors located in the skin.[129] Using a benchtop press to evaluate juice preparation method on thiol precursor concentrations, Capone and Jeffery[22] mentioned that 70 % of GSH-3-SH and Cys-3-SH in Sauvignon blanc grape juice was obtained from lighter pressure (440 kPa) juice and the following heavier pressure (670 kPa) contributed the rest in the combined pressed juice. Although having higher amount of thiol precursors induced by applying heavier pressing pressure, a concern was raised by the co-occurring higher amount of phenolics that could potentially increase the risk of browning and loss of varietal thiols due to wine oxidation.[127] For instance, wines produced from free run juice contained over 2-fold higher amounts of 3-SH and 3-SHA than those made from the pressed juice.[132]

1.5.3 Winemaking practices

Must composition: Nitrogen content in grape must/juice plays an important role in fermentation. Ammonium and amino acids constitute the major proportion of yeast assimilable nitrogen (YAN) content in grape must or juice,[133] but due to insufficient nitrogen, supplementing inorganic nitrogen, such as diammonium phosphate (DAP), during the early

stage of AF has been a conventional practice in wine industry. Different forms of nitrogen can be utilised by *S. cerevisiae* yeasts, including ammonium and amino acids (proline is not consumed by yeasts under anaerobic conditions).[134] However, good nitrogen sources are metabolised first by yeasts (ammonium, glutamine, asparagine) before other poor nitrogen sources (alanine, arginine), which is regulated by Nitrogen Catabolite Repression (NCR).[135]

NCR is regulated by gene *URE2* which produces Ure2p (step a, Scheme 5) that inhibits transcription of *GLN3* and *GAT1* genes with optimal nitrogen sources (steps b1 and c1) and binds Gln3p and Gat1p from the cytoplasm (steps b2 and c2).[136-137] The two genes (*GLN3* and *GAT1*) are transcriptional activators when only poor nitrogen sources are in the environment, which enables yeast to uptake such nitrogen sources. The NCR of yeast strains showed to impact the concentrations of varietal thiols. Such examples include the yeast with a deletion of *GLN3* gene produced significantly lower concentrations of 4-MSP, and to a lesser extent, of 3-SH and 3-SHA.[137] The deletion of the gene *URE2* stopped the production of Ure2p, which subsequently silenced NCR (step d) and therefore resulted in a normal functionality of *GAT1* and *GLN3*. As a result of this deletion, the expression of gene *IRC7* that encodes β-lyase was enhanced (step e, Scheme 5),[79,137] improving the production of 4-MSP and 3-SH from their cysteinylated precursors, and also the (*R*)/(*S*) ratio of 3-SH from 50/50 to 78/22 (Step f, Scheme 5).[137]

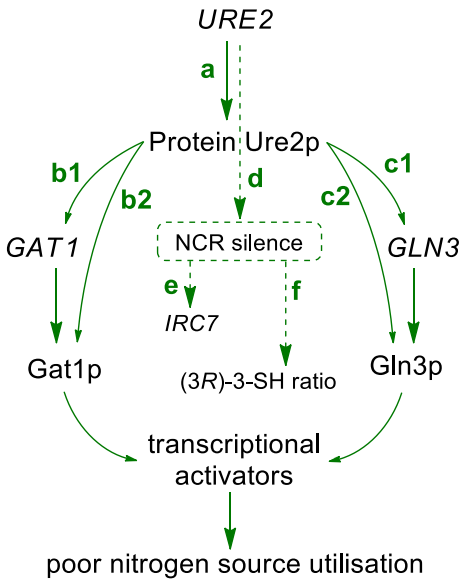

Scheme 5. *Gene regulation of nitrogen catabolite repression stream in yeasts.*[136-137] *Steps, a, transcription of gene URE2 to produce protein ure2p; b1 & c1, inhibition on the transcription of genes GAT1 & GLN3, respectively, by protein ure2p; b2 & c2, binding of protein Gat1p & Gln3p, respectively, by Ure2p; d, deletion of URE2 gene triggered NCR silence; e, IRC7 gene expression was enhanced by deletion of URE2 gene; f, increase of (3R)/(3S)-3-SH ratio as a function of URE2*

gene deletion.

As a result of nitrogen supplementation to grape juice, the concentrations of varietal thiols in final wines were affected differently. For example, the addition of DAP at 200 mg/L to Sauvignon blanc juice significantly increased the concentrations of both 3-SH and 3-SHA,[138] whereas contrasting results showed that DAP addition led to double the amount of 3-SHA but had no significant impact on both 3-SH and 4-MSP.[139] Compared with using DAP alone, using urea as the sole nitrogen resource in a synthetic medium showed higher conversion yield of Cys-3-SH into free 3-SH, although addition of urea during winemaking is forbidden.

Lipids: Studies showed that adding linoleic acid and lipase to Sauvignon blanc juice or increasing the content of β-sitosterol in a synthetic medium could improve the concentrations of 3-SH, or 3-SH and 4-MSP, respectively, while decreasing the level of 3-SHA.[140-141] Since all acetates were reduced by supplying lipase[141] but the total level of 3-SH and 3-SHA did not change,[140] it could be hypothesised that adding lipase could decrease the acetylation of 3-SH into 3-SHA. Furthermore, a positive correlation between linoleic acid in Sauvignon blanc juice and 3-SH in the resultant wine (R = 0.37) was revealed,[139] although the correlation was poor.

Microorganisms: Other than the effect of *Botrytis cinerea* discussed earlier (Section 1.1.1), yeasts and bacteria play key roles in the concentration of varietal thiols in wines as a result of fermentations. Table 4 illustrates some commercial *S. cerevisiae* yeasts that are advantageous in releasing varietal thiols possibly due to the full length *IRC7* gene[79] and gene-modified *S. cerevisiae* strains used to testify the effect of some targeted genes in releasing varietal thiols. Both Enoferm M2 (behaves well under low AF temperatures) and Zymaflore X5 (commonly used strain in Marlborough Sauvignon blanc fermentation) yeast strains produced high concentrations of 3-SH (940–4080 ng/L for M2, 1350-5280 ng/L for X5) and 3-SHA (60–250 ng/L for M2, 150–270 ng/L for X5).[142] VIN7 yeast strain produced higher concentrations of 4-MSP and 3-SHA than VL3 and VIN13.[143]

Table 4. *Yeast and lactic acid bacteria used in releasing varietal thiols during winemaking.*

Microorganism	Medium	Features	Ref
***S. cerevisiae* yeasts**			
Enoferm M2, Zymaflore X5	Sauvignon blanc	Release 3-SH and 3-SHA	[142]
VIN7, VIN13, VL3	Sauvignon blanc	Release 4-MSP, 3-SHA, and 3-SH	[143]

Table 4. Contd.

Microorganism	Medium	Features	Ref
S. cerevisiae Diana and *S. cerevisiae* Revelación	Verdejo must	Release 3-SH, 3-SHA, or/and 4-MSP	[14]
Zymaflore F15 (*IRC7*)	Sauvignon blanc juice	Improve 4-MSP, 3-SH, and 3-SHA	[79]
VIN13 (*STR3*)	Sauvignon blanc juice	Release 3-SH and 4-MSP, improve 3-SH in wine	[144]
VIN13 and VIN13 (*CSL1*)	Model juice	VIN13 (*CLS1*) release 3-SH from Cys-3-SH and GSH-3-SH	[40]
Non-*Saccharomyces* yeasts			
T. delbrueckii Viniferm NS-TD	Verdejo must	Improve 3-SH, 4-MSP	[14]
T. delbrueckii	Sauvignon blanc must	Improve 3-SH and 3-SHA	[145]
K. thermotolerans Lm5LT1; *M. pulcherrima* Q6LT26 and Q4LT1; Mixed use of *S. cerevisiae* X5, *Hanseniaspora uvarum, Candida zemplinina, M. pulcherrima, T. delbrueckii, Issatchenkia orientalis*	Sauvignon blanc must	Improve 3-SH	[82]
Pichia kluyveri/VL3=9/1	Sauvignon blanc	Improve 3-SH and 3-SHA	[146]
M. pulcherrima	Verdejo must	Improved 4-MSP	[147]
Lactic acid bacteria			
Lactobacillus plantarum	Concentrated Chardonnay juice	Release 3-SH from Cys-3-SH and CysGly-3-SH	[148]

Genes regulating the release of varietal thiols have been studied, with the overexpression of some genes such as *IRC7* (Zymaflore F15), *STR3* (VIN13), and *CSL1* (a gene from *Escherichia coli* encodes tryptophanase with β-lyase), could significantly increase the concentration of varietal thiols.[40,79,144] Exploring *IRC7* gene further, the yeast strain Viniferm Reverlación with full length *IRC7* gene and yeast strain Diana with an inactivated *IRC7* gene produced identical amount of 3-SH, but 4-MSP was only produced by Viniferm Reverlación yeast,[14] suggesting the important role of *IRC7* gene in the production of 4-MSP.[79]

The mixed use of *S. cerevisiae* and non-*Saccharomyces* yeasts in AF could modify both chemical and sensory aroma profiles,[149] and some studies addressed the impact of non-*Saccharomyces* strains on the release of varietal thiols (Table 4). Specifically, *Torulaspora delbrueckii* yeast, characterised with a full length of *IRC7* gene,[14] showed to affect the concentrations of varietal thiols in wine. For instance, over 4-fold higher concentration of 4-

MSP was reported by the sequential inoculation treatment of *T. delbrueckii*/*S. cerevisiae* than the control in Verdejo wine,[14] and over 4-fold and 2-fold higher concentrations of 3-SH and 3-SHA, respectively, were revealed by sequential inoculation of *T. delbrueckii*/*S. cerevisiae* than the single inoculation of *S. cerevisiae* in Sauvignon blanc wine.[145] Other non-*Saccharomyces* yeasts such as *Pichia kluyveri*, *Candida zemplinina*, *Kluyveromyces thermotolerans* Lm5LT1/X5, *Metschnikowia pulcherrima* Q6LT26/X5, and *Metschnikowia pulcherrima* Q4LT1/X5 could increase 3-SH significantly when co-fermenting with *S. cerevisiae* yeasts.[82,146]

The effect of co-inoculation of *S. cerevisiae* yeasts on varietal thiols has been evaluated but mixed results were obtained. For instance, co-inoculation of VIN7/QA23 resulted in the highest concentration of 3-SHA (~60 ng/L) but relatively high 3-SH (< 1000 ng/L) and 4-MSP (approximately 2.0 ng/L); VIN7/VIN13 treatment produced a high level of 3-SH (approximately 1200 ng/L) and low level of 3-SHA (approximately 20 ng/L), but 4-MSP was not detected.[150] A mixture use of three strains of *S. cerevisiae* yeast produced the highest concentrations of 3-SH (approximately 800 ng/L) and 3-SHA (> 250 ng/L) in Sauvignon blanc wine compared with the individual inoculation treatments.[151]

Much less work has been done with respect to lactic acid bacteria (LAB) that conduct malolactic fermentation (MLF) (and few white wine styles make use of MLF) but recently Takase, et al.[148] found that a strain of *L. plantarum* could release 3-SH from Cys-3-SH and CysGly-3-SH with conversion rates of 9.1 % and 38.5 % in citrate buffer, respectively (Table 4). This highlighted the potential of LAB in releasing varietal thiols from thiol precursors during MLF. However, further study is required to characterise enzymes capable of catalysing thiol precursors in LAB. MLF trials with wines should be conducted to explore the ability of LAB in the production of varietal thiols.

Fermentation temperature: Results for the influence of fermentation temperature on the concentration of varietal thiols are conflicting. Specifically, some research showed that higher temperatures (i.e., 20 or 25 °C) resulted in higher levels of varietal thiols in Sauvignon blanc than the lower temperature fermentation treatment (13 or 12.5 °C),[142,152] whereas other research conducted on model grape juice fermentation reported that more typical white wine fermentation temperatures (16 or 18 °C) could produce higher levels of 3-SHA or 4-MSP than the higher temperature treatments (24 or 28 °C).[45,140]

1.6 Analytical methods of volatile thiols and their precursors

1.6.1 Analytical methods for volatile thiols

Varietal thiols are present at very low levels in wines as shown in Table 1 and they are chemically reactive compounds that can be readily consumed by aldehydes and quinones in wine.[87] Therefore, extra care must be taken to minimise the artificial impact on the loss of thiols and choice of sample extraction protocols (i.e., liquid-liquid extraction, solid-phase microextraction, or solid-phase extraction) and analytical instruments (i.e., GC-MS or LC-MS). As extensively reviewed by Roland, et al,[153] a number of methods have been investigated and applied in the past three decades to the analysis of varietal thiols (and polyfunctional thiols in wine more generally). Table 5 presents some details of sample preparation, analytical instrumentation, method validation, and quantification.

The combination between *p*-hydroxymercuribenzoic acid (*p*-HMB) and thiols is reversible,[154] making it an easy way to measure thiols in wines, but the disadvantages are consuming large volume of wine, pH of wines should be adjusted to alkaline (pH 8-10), sample preparation is tedious, methods are not sensitive, and using 4-methoxy-2-methyl-2-mercaptobutane as internal standard.[3,154-157] Though these drawbacks were optimised years later,[13] it is still time-consuming and the most serious issue is that *p*-HMB is highly toxic.

The derivatives between pentafluorobenzyl bromide (PFBBr) and thiols could be determined by negative chemical ionisation MS.[158] An on-fibre derivatisation SPME method was developed, which was limited by the linear range[158] and an in-cartridge derivatisation SPE method encountered low repeatability, especially for 3-SH (15.6–19.2 % relative standard deviation, RSD).[159] Based on the method of Capone, et al.[6], which only targeted 3-SH, a new method combining PFBBr derivatisation, LLE, SPME, and SIDA gives a satisfactory result for determining 3-SH, 3-SHA, and 4-MSP,[160] but the pH of wine should be adjusted to 12 before derivatisation and the LOD for 3-SHA (17.3 ng/L) is much higher than the perception threshold (4.2 ng/L[155]).

Table 5. *Analytical methods used for determination of varietal thiols (3-SH, 3-SHA, and 4-MSP) in wine or model system.*

Thiols	Medium [sample volume /mL][a]	Preparation [pH] [b]	Qualification [year] [c]	LOD (ng/L)	Repeatability (RSD %)	Quantification [d]	Ref
4-MSP	Sb wine [750]	Diethyl ether/pentane + *p*-HMB extraction + re-extract with diethyl ether/pentane [pH 8]	GC-MS [1995]	-	-	GC-O	154
3-SHA	Sb wine [1500]	Dichloromethane+ *p*-HMB extraction + release thiols by cysteine [pH 8.5]	GC-MS [1996]	-	-	-	155
4-MSP, 3-SH	Sb wine [1000]	Dichloromethane+ *p*-HMB extraction + release thiols by cysteine [pH 8.5]	GC-MS [1998]	-	-	-	156
3-SH, 3-SHA, 4-MSP	Sb wine [500]	Dichloromethane+ *p*-HMB extraction + AEC + release thiols by cysteine [pH 7.0]	GC-MS (SIM) [1998]	-	SD %: 3-SH: 36.5 3-SHA: 2.59 4-MSP: 2.62	IS: 4-methoxy-2-methyl-2-mercaptobutane	157
(*S*)-/(*R*)-3-SH, (*S*)-/(*R*)-3-SHA	Sb and Semillon wine and must [500]	Ethyl acetate + *p*-HMB extraction + AEC + cysteine solution + dichloromethane [wine pH]	GC-MS (SCAN & SIM) [2006]	-	-	IS: 4-methoxy-2-methyl-2-mercaptobutane	3
3-SHA	Wine [10]	Derivatisation on SPME fibre preconditioned with PFBBr and tributylamine [wine pH]	GC-NCI-MS (SIM) [2006]	~3	10.1-15.2	IS: 1-hexanethiol, benzylthiol	158
3-SH, 3-SHA, 4-MSP	Wine [200]	SPE + LLE (dichloromethane + *p*-HMB + dithioerythritol in HEPES + dichloromethane) [wine pH]	GC-ion trap-MS (SCAN & SIS) [2007]	3-SH: 15 & 3 3-SHA: 25 & 5 4-MSP: 0.8 & 0.5	3-SH: 5-14 3-SHA: 3.5-11 4-MSP: 8-15	IS: 2-octanol	161
3-SH, 3-SHA, 4-MSP	Wine [10]	SPE + PFBBr derivatisation in cartridge + elute with hexane 25 % in diethyl ether [wine pH]	GC-NCI-MS [2008]	3-SH: 2 3-SHA: 0.3 4-MSP: 0.1	3-SH: 15.6-19.2 3-SHA: 3.6-5.1 4-MSP: 6.1-11	SIDA (IS: d_2-3-SH-d_2, d_5-3-SHA, d_{10}-4-MSP)	159
(*S*)-/(*R*)-3-SH	Model fermentation [10]	SPME [wine pH]	Chiral GC-MS (SIM) [2010, 2008]	-	-	SIDA (IS: d_{10}-3-SH)	40, 41
3-SH	Wine and grape juice [~200]	Pentane + derivatisation with PFBBr + HS-SPME [pH 4-5 after derivatisation]	GC-EI-MS [2011]	30	SD %: 1.4-2.5	SIDA (IS: d_{10}-3-SH)	6
3-SH, 3-SHA	Sb wine [50]	Dichloromethane+ *p*-HMB extraction + AEC + release thiols by cysteine [pH 7.0]	GC-MS [2012]	-	3-SH: 5.1 3-SHA: 7.1 4-MSP: 9.4	SIDA (IS: d_2-3-SH, d_2-3-SHA)	13
3-SH, 3-SHA, 4-MSP	Wine and model wine [50]	ETP derivatisation + SPE purification + dichloromethane extraction [pH 10]	GC-MS (SIM) [2013]	3-SH: 194.6 & 9.0 (wine & model wine) 3-SHA: 120.9 & 1.5 4-MSP: 24.5 & 1.7	3-SH: 1.9-4.2 3-SHA: 1.9-7.8 4-MSP: 2.7-16.7	SIDA (IS: d_2-3-SH, d_2-3-SHA, 4-MSP was quantified with d_2-3-SHA)	162

Table 5. Contd.

Thiols	Medium [sample volume /mL][a]	Preparation [pH] [b]	Qualification [year] [c]	LOD (ng/L)	Repeatability (RSD %)	Quantification [d]	Ref
4-MSP	Sb wine [3]	Derivatised by adding EDTA, L-cysteine hydrochloride monohydrate, and *o*-methylhydroxylamine hydrochloride in SPME vial containing wine sample [wine pH]	GC-MS/MS (SCAN) [2014]	0.19	7	SIDA (IS: d_{10}-4-MSP)	[163]
3-SH, 3-SHA, 4-MSP	Wine [20]	DTDP derivatisation + SPE [wine pH]	HPLC-MS/MS [2015]	3-SH: 5.4-10.6 3-SHA: 1.2-4.3 4-MSP: 0.8-1.6	3-SH: 1.2-5.6 3-SHA: 1.3-5.6 4-MSP: 1.6-4.8	SIDA (IS: d_{10}-4-MSP, d_{10}-3-SH, d_5-3-SHA)	[164]
3-SH, 3-SHA, 4-MSP	Wine [40]	Derivatisation by PFBBr + LLE (pentane:diethyl ether=1:3 (v/v)) + SPME [pH 12]	GC-EI-MS (SIM) [2015]	3-SH: 1 3-SHA: 17 4-MSP: 0.9	3-SH: 5.4-6.9 3-SHA: 5.6-11.1 4-MSP: 6.6-9.8	SIDA (IS: d_8-3-SH, d_5-3-SHA, d_{10}-4-MSP)	[160]
3-SH, 3-SHA, and the corresponding disulfides	Wine [2]	Derivatised by *N*-phenylmaleimide, followed by SPE purification; disulfide was reduced by TCEP before derivatisation and purification [wine pH]	HPLC-Chip-MS/MS [2016]	3-SH: 0.7 3-SHA: 0.5	3-SH: 14 3-SHA: 15	SIDA (d_2-3-SH, d_5-3-SHA)	[92]
(*S*)-/(*R*)-3-SH, (*S*)-/(*R*)-3-SHA	Wine [20]	DTDP derivatisation + SPE [wine pH]	HPLC-MS/MS [2018]	(*S*)-3-SH: 0.3-0.6 (*R*)-3-SH: 0.3-0.7 (*S*)-3-SHA: 0.1 (*R*)-3-SHA: 0.1	(*S*)-3-SH: 3.2-7.9 (*R*)-3-SH: 1.4-6.0 (*S*)-3-SHA: 1.1-4.2 (*R*)-3-SHA: 1.8-5.0	SIDA (IS: d_{10}-3-SH, d_5-3-SHA)	[4]
3-SH, 3-SHA, 4-MSP	Sb and Chenin blanc wine [50]	ETP derivatisation + SPE purification + dichloromethane extraction [pH 10]	GC-MS/MS (SIM) [2018]	3-SH: 1-2.1 3-SHA: 3.8-25 4-MSP: 0.5-10	3-SH: 10.5-11.3 3-SHA: 4.8-12.1 4-MSP: 10.8-12.5	IS: 4-methoxy-2-methyl-2-mercaptobutane	[165]
3-SH, 3-SHA	Chardonnay wine [-]	LLE + IEC purification [-]	GC-MS (SIM) [2018]	-	-	IS: 4-methoxy-2-methyl-2-mercaptobutane	[148]
3-SH, 3-SHA, 4-MSP	Wine [20]	DTDP derivatisation + SPE [wine pH]	UPC²-MS/MS [2018]	3-SH: 3.5-4.0 3-SHA: 2.1-3.4 4-MSP: 0.15-0.42	3-SH: 9-18 3-SHA: 11-13 4-MSP: 8-12	IS: 6-SH	[166]

[a]: Sb indicates Sauvignon blanc; [b]: pH: the pH of wine when derivatisation reaction was conducted. *p*-HMB: *p*-hydroxymercuribenzoic acid. AEC: anion exchanger column. TCEP: tris(carboxyethyl)-phosphine. PFBBr: pentafluorobenzyl bromide. DTDP: 4,4'-dithiodipyridine. HEPES: 4-(2-hydroxyethyl)piperazine-1-ethanesulfonic acid. ETP: ethyl propiolate. IEC: ion exchange column.
[c] year: publication year of the method. NCI: negative chemical ionisation. SIS: selected ion storage mode. UPC²: ultra-performance convergence chromatography.
[d] SIDA: stable isotope dilution assay. IS: internal standard.

A novel method by using 4,4'-dithiodipyridine (DTDP) as the derivatisation regent was developed,[164] which overcomes the shortcomings that earlier derivatisation approaches had. For instance, DTDP reacts quickly with thiols at wine pH, the method uses only 20 mL of wine for analysis, and has very low LOD and RSD values using either SIDA or 6-sulfanylhexan-1-ol as internal standard.[4,166] Based on this method, Chen, et al.[4] quantified the enantiomers of 3-SH and 3-SHA in 23 commercial wines using an HPLC column with a chiral stationary phase, yielding even lower LOD and LOQ values than the original achiral method.

Roland, et al.[92] developed a SIDA methodology using *N*-phenylmaleimide as the derivatisation reagent, which provides a robust method for determining 3-SH and 3-SHA in red, white and rosé wines. Other SIDA methods using derivatisation regents, such as *o*-methylhydroxylamine hydrochloride (for determining 4-MSP only)[163] and ethyl propriolate,[162] also yielded satisfactory results. The LODs of 3-SH, 3-SHA, and 4-MSP derivatised with ethyl propriolate were higher than those measured by other methods,[162] but the approach was improved by Coetzee, et al.[165] with the use of more sensitive MS/MS detector. Chen, et al.[96] presented a robust SIDA method using headspace SPME coupled with GC-MS to analyse *cis*-2-methyl-4-propyl-1,3-oxathiane in wine.

1.6.2 Analytical methods for the precursors of varietal thiols

Table 6 presents the methods applied in determining precursors in the past three decades. GC-MS was initially utilised to analyse precursors thiol research when precursors were either derivatised into volatile forms or enzymatically hydrolysed to release free thiols that were quantified by SIDA.[36,128,167] Although years later, GC-MS/MS or GC-MS was still in use to quantify precursors after derivatisation with heptafluorobutyric anhydride (HFBA) and heptafluorobutanol (HFOH).[42,137] More directly, various methods of SIDA utilising HPLC coupled with mass spectrometer or tandem mass spectrometer were developed for thiol precursors in juice samples after concentration by SPE, with diastereomers of GSH-3-SH, Cys-3-SH, and CysGly-3-SH resolved.[29,31,34,54]

Table 6. *Analytical methods used for determination of precursors of varietal thiols in grapes and wine.*

Precursors	Medium [sample volume/mL][a]	Sample preparation [b]	Qualification [year]	LOD (ng/L)[c]	Repeatability (RSD %)	Quantification	Ref
Cys-4-MSP, Cys-3-SH	SB must [45000]	C_{18} column to concentrate + AEC to purify + BSTFA/TMCS/pyridine (3/1/3) to derivative	GC-MS (SIM) [1998]	-	-	IS: *S*-ethylcysteine	36
Cys-4-MSP, Cys-3-SH	SB must [~3 kg]	DEAE column to eliminate affections + tryptophanase column to release thiols	GC-MS (SCAN) [2000]	-	Cys-4-MSP: 2.2 Cys-3-SH: 173	SIDA (IS: d_1-Cys-3-SH, d_1-Cys-4-MSP)	167
Cys-3-SH	Grape berries [0.5]	Purification by Chelating Sepharose 4B column + derivatisation as 36	GC-MS (SIM) [2001]	-	-	SIDA (IS: $^{15}N_2$-Cys-3-SH)	128
(*R*)-Cys-3-SH, (*S*)-Cys-3-SH	Grape juice, synthetic must, fermenting must, wine [0.5]	Purification by Chelating Sepharose column + HFBA and HFOH derivatisation	GC-MS/MS (Scan & MS/MS) [2008]	Cys-3-SH: 333	Cys-3-SH: 2.6-7.1	IS: *S*-benzyl-L-cysteine	42
GSH-3-SH, Cys-3-SH	Grape must of SB, Riesling, and Gewurztraminer [1.2]	Extraction by CER, purification by SPE	Nano-LC-MS/MS (ESI+), SRM mode [2010]	GSH-3-SH: 59, Cys-3-SH: 195	GSH-3-SH: 6, Cys-3-SH: 5	SIDA (IS: d_2/d_3-GSH-3-SH, d_2-Cys-3-SH)	51
GSH-3-SH, Cys-3-SH, GSH-4-MSP, Cys-4-MSP	Melon B, SB must or juice [1.2]	Extraction by CER, purification by SPE	Nano-LC-MS/MS (ESI+), SRM or MRM mode [2010]	GSH-3-SH: 61 Cys-3-SH: 319 GSH-4-MSP: 8 Cys-4-MSP: 127	GSH-3-SH: 3-7 Cys-3-SH: 3-7 GSH-4-MSP: 7-27 Cys-4-MSP: 4-12	SIDA (IS: d_2-GSH-3-SH, d_2-Cys-3-SH, d_6-Cys-4-MSP, d_{10}-GSH-4-MSP), external calibration	34
(*R*/*S*)-Cys-3-SH, (*R*/*S*)-GSH-3-SH	Juice and wine [9.9]	Purification by SPE	HPLC-MS/MS [2010]	(*R*)-Cys-3-SH: 60-120 (*R*)-GSH-3-SH: 80 (*S*)-Cys-3-SH: 10-40 (*S*)-GSH-3-SH: 90-130	Standard error ng/L (*R*)-Cys-3-SH: 50-710 (*R*)-GSH-3-SH: 230-600 (*S*)-Cys-3-SH: 200-950 (*S*)-GSH-3-SH: 400-790	SIDA (IS: d_8-(*R*/*S*)-Cys-3-SH, d_9-(*R*/*S*)-GSH-3-SH)	29
GSH-3-SH, Cys-3-SH	Koshu berry [5]	Grinded in liquid N_2 + LLE	LC-MS/MS [2010]	GSH-3-SH: 41 Cys-3-SH: 44	GSH-3-SH: 1.7 Cys-3-SH: 2.7	External calibration	59
CysGly-3-SH	SB grapes [9.9]	SPE + N_2 dryness + reconstitution	HPLC-MS/MS [2011]	200	5.8	IS: d_8-Cys-3-SH	30
GSH-3-SH, Cys-3-SH, CysGly-3-SH, GluCys-3-SH, Cys-4-MSP	SB must [1.2]	Extraction by CER	UPLC-MS/MS [2017]	10-18	CV % < 5 %	SIDA (IS: corresponding deuterated compounds)	31
GSH-3-SH, GSH-4-MSP, Cys-3-SH, Cys-4-MSP, CysGly-3-SH, CysGly-4-MSP, GluCys-3-SH, GluCys-4-MSP	Model juice [1.2]	Extraction by CER	UPLC-MS/MS [2018]	-	-	SIDA (IS: corresponding deuterated compounds)	54
GSH-3-SHal, GSH-3-SH, Cys-3-SH	CBC and Grillo grapes, must, and wine [2]	Purification by SPE	UPLC-ESI-HRMS [2018]	-	-	IS: d_1-GSH-3-SH	25

[a]: SB, Sauvignon blanc; CBC, Catarratto BC; [b]: AEC: anion exchanger column. BSTFA: *N*,*O*-bis(trimethylsilyl)trifluoroacetamide. TMCS: trimethylchlorosilane. HFBA: heptafluorobutyric anhydride. HFOH: heptafluorobutanol. CER: cation exchange resin. SPE: solid phase extraction. LSIMS: liquid secondary ion mass spectrometry. [c]: the unit is ng/L unless specified. IS, internal standard.

1.7 Potential for undiscovered volatile thiols and precursors

As discussed in Section 1.2, only a small portion of precursors in grape berries is hydrolysed to release free thiols, which may only account for a minor proportion of thiols in wines. Although Bonnaffoux, et al.[54] explained a major part of 3-SH by simply combining conversion rates from each individual precursor. However, the difficulty arises from the complexity of the degradation pathways shown in Scheme 1 & 2. Furthermore, except for the loss of free thiols during AF, precursors may undergo other pathways in grape berries similar to that in *Arabidopsis thaliana*,[168] peanut,[169] and wheat[170] and exist in different forms that are currently not measured, such as *N*-acetylcysteine, *N*-malonylcysteine conjugates, or the sulfoxide form of these precursors (Figure 3).

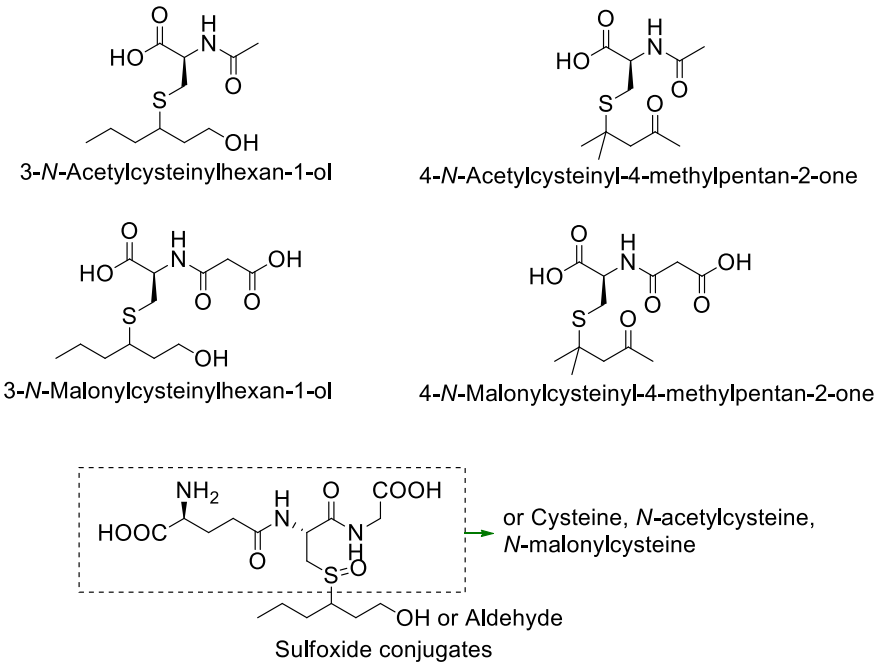

Figure 3. *Structures of potential precursors of varietal thiols.*

The presence of *N*-malonylcysteinylated and *N*-acetylcysteinylated conjugates have been proposed in *Arabidopsis thaliana* as is shown in Scheme 6.[168] In that case, 4,6-dichloro-2-phenylpyrimidine (a herbicide safener) was bound to GSH to form GSH-fenclorim (step a), which was subsequently metabolised into the relevant cysteine conjugate (*S*-cysteine-fenclorim, step b) as a result of the usual GSH detoxification mechanism. Besides being catalysed by β-lyase and *S*-methyltransferase to release 4-chloro-6-(methylthio)-phenylpyrimidine (step c), Cys-fenclorim also underwent the pathway to form an *N*-malonylcysteinylated conjugate catalysed by *N*-malonyl-CoA-dependent *N*-

malonyltransferase (step d) and a subsequent *N*-acetylcysteinylated conjugate (step e). Furthermore, similar conjugates have also been detected in other plants, such as *S*-(pentachlorophenyl)-*N*-malonylcysteine in peanut[169] and *N*-acetylcysteine conjugates of mycotoxin 4-deoxynivalenol in wheat.[170] However, neither the *N*-acetylcysteine conjugates nor *N*-malonylcysteine conjugates of thiols have so far been reported in grapes although a similar enzyme, malonyl-CoA:4-coumaroyl-CoA malonyltransferase (EC 2.3.1.95) which is involved in resveratrol biosynthesis in young Cabernet Sauvignon grape plants, has been determined.[171]

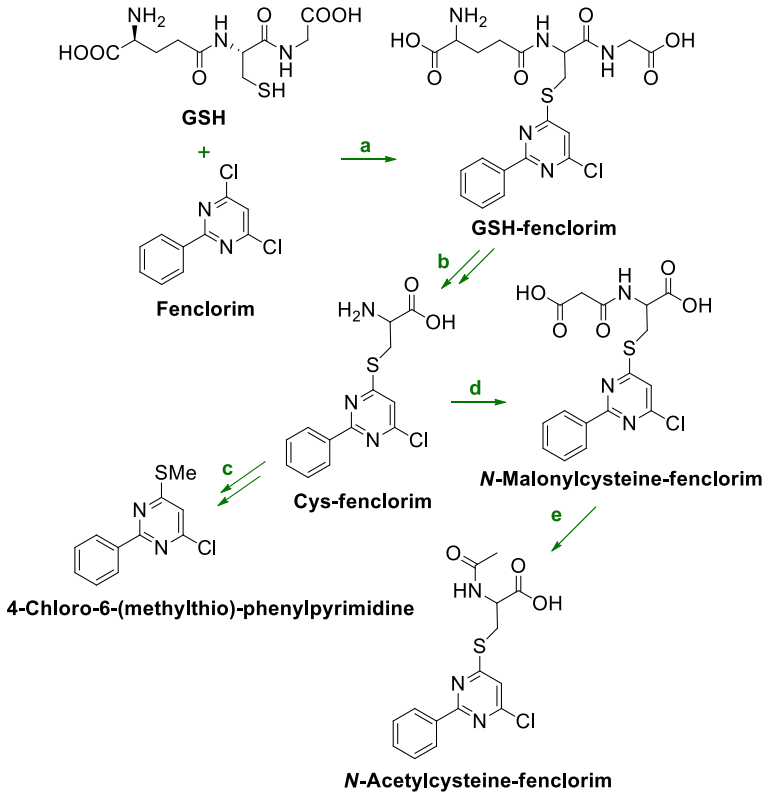

Scheme 6. *Potential pathway to the formation and degradation of GSH conjugated fenclorim.*[168] *Steps: a, glutathionylation of fenclorim to form GSH-fenclorim; b, stepwise removal of glycine and glutamate moiety to produce Cys-fenclorim; c, cleavage of cysteine moiety by β-lyase then S-methylation by S-methyltransferase to produce 4-chloro-6-(methylthio)-phenylpyrimidine; d, N-malonylation of Cys-fenclorim to produce N-malonylcysteine-fenclorim; e, decarboxylation of N-malonylcysteine-fenclorim to produce N-acetylcysteine-fenclorim.*

Since GSH-3-SH-SO_3 has been discovered in grape juice,[23] there might also be other

undiscovered precursors in which sulfur is in higher oxidised states, such as sulfoxide conjugates shown in Figure 3. Tominaga, et al.[36] showed that 4-MSP could be released from Cys-4-MSP sulfoxide by either Alliin lyase or β-lyase but did not provide the direct evidence of whether Cys-conjugate sulfoxides occur in Sauvignon blanc juice. However, the Cys-conjugate sulfoxides do exist in many other plants, such as cabbage[172] and garlic.[173]

As discussed in Section 1.3, thiols with similar structure to 3-SH might form the corresponding 1,3-oxathianes. Such thiols include 4-MSPOH, 3-sulfanylpentan-1-ol, 3-sulfanylheptan-1-ol, and 2-methyl-3-sulfanylbutan-1-ol (Figure 4). Furthermore, two other thiols are potential to be identified in wine (Figure 4), namely grapefruit mercaptan ((*R*)-(+)-1-*p*-menthene-8-thiol) and blackcurrant mercaptan (4-methoxy-2-methylbutane-2-thiol). A formal identification of grapefruit mercaptan in wine is to be conducted despite its tentative identification in some wines.[174] Grapefruit mercaptan is in fact a chiral molecule, with a low odour detection threshold (ODT) of 0.02 ng/L and 0.08 ng/L for the respective *R*-(+)- and *S*-(–)-enantiomers determined in water.[175] It has been synthesised from D-limonene with hydrogen sulfide.[176] Blackcurrant mercaptan, which also has a low ODT of 1 ng/L in water[177], is a natural aroma compound in blackcurrants. Despite the available ODTs being determined in water or other matrices but not hydroalcoholic solution or wine, grapefruit mercaptan and blackcurrant mercaptan are considered to be odour impact compounds. Thus, the presence of either of these two mercaptans in wine could potentially modify wine aroma profile.

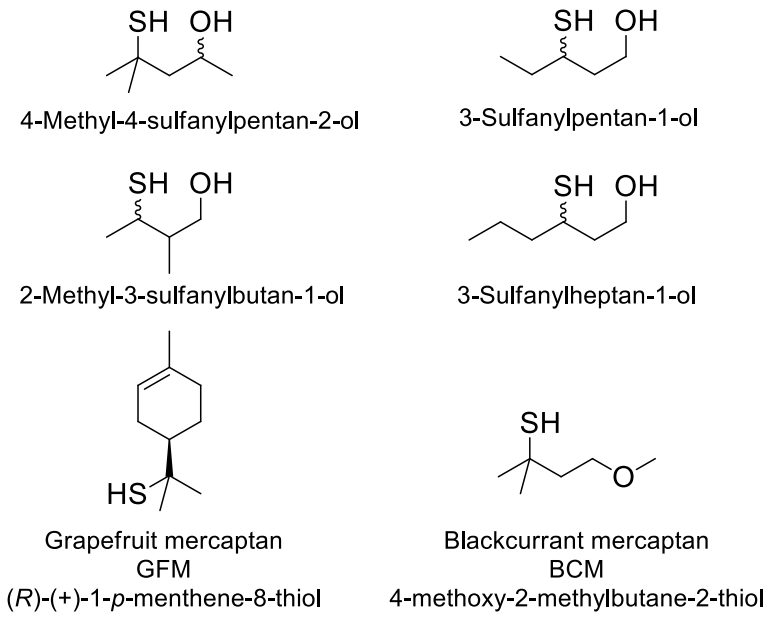

Figure 4. *Structures of four varietal thiols, grapefruit mercaptan, and blackcurrant mercaptan.*

1.8 Research questions

1.8.1 The formation of 4-MSP precursors

As discussed in section 1.2, one of the proposed precursors of GSH-4-MSP, namely mesityl oxide, has not been detected in grapes and the origin of mesityl oxide is a mystery that requires further effort to explore. The formation of 4-MSP precursors from mesityl oxide in grape requires investigation.

1.8.2 New precursors to 3-SH

Based on the previous conclusions in section 1.7, it is reasonable to hypothesise that one of the proposed precursors, namely *N*-malonylcysteinylated 3-SH (MalCys-3-SH), could potentially present in grapes and is undiscovered. In addition, the conversion rate from this new precursor to free thiols and factors influencing the concentration of the new precursor would be worthy of exploring upon the identification of MalCys-3-SH.

1.8.3 New sulfur-containing volatiles and chiral analysis of 4-MSPOH in wines

Although *cis*-2-MPO was identified in wine,[96] its production during fermentation, influence of oenological practices on its production, the correlation with varietal thiols and acetaldehyde during fermentation, and the stability in wine during storage require further investigation. Besides, the possibility that other thiols (4-methyl-4-sulfanylpentan-2-ol, 3-sulfanylpentan-1-ol, 3-sulfanylheptan-1-ol, and 2-methyl-3-sulfanylbutan-1-ol, etc.) bearing a 3-sulfanylalkan-1-ol substitution in their structures could react with acetaldehyde to produce their corresponding 1,3-oxathianes is to be verified.

Moreover, the potential presence of BCM and GFM (Figure 4) proposed in Section 1.7 requires study. The enantiomeric distribution of 4-MSPOH enantiomers in wine should also be explored.

1.8.4 Influence of winemaking practices on thiols and precursors concentrations

Given the finding that the new grape crushing technique, namely "accentuated cut edges", accelerated the extraction rate of phenolics from grape skin, it is hypothesised that this technique could accelerate the extraction rate of thiol precursors from grape skin and therefore the concentrations of varietal thiols in the resultant wine. Besides, the impact of wine microflora on the release of enantiomers of 3-SH and 3-SHA could potentially be different given the stereoselectivity of enzymes involved in the release of varietal thiols from their precursors.

1.9 Aims/objectives of the project

Varietal thiols have been an important focus of wine flavour research in recent decades, but more effort is required considering the importance to wine quality of thiols. The focus of this project is to contribute knowledge in understanding the relationship between varietal thiols in wines and their precursors in grapes and to explore winemaking practices with a view to improving the concentration of thiols in wines. The aims are proposed to be achieved by means of following objectives:

(1) Examine the hypothesis of a potential pathway for uptake of exogenous mesityl oxide by grapevines and transformation into the precursors of 4-MSP by feeding grapevines with deuterated mesityl oxide. Qualification of corresponding deuterated GSH-4-MSP or Cys-4-MSP in grape berries or leaves could help confirm the pathway.

(2) Identify *N*-malonylcysteinylated 3-SH in grapes after optimising a HPLC-MS/MS method with a chemically synthesised MalCys-3-SH standard and explore its evolution profile during growing season upon its identification in grapes.

(3) Evaluate the kinetics of *cis*-2-methyl-4-propyl-1,3-oxathiane formation during AF conducted with different yeasts, examine its stability under different storage conditions, and explore its chirality and chiral relationship with 3-SH enantiomers. Exploring the potential existence of *cis*-2,4,4,6-tetramethyl-1,3-oxathiane in wine, a potential sulfur-containing volatile compound derived from acetaldehyde and 4-MSPOH.

Identify grapefruit mercaptan and blackcurrant mercaptan in wine with a previously developed DTDP derivatisation approach coupled with HPLC-MS/MS using the reference standards.

Optimise a published chiral HPLC-MS/MS method to resolve 4-MSPOH enantiomers using the DTDP derivatisation approach and explore the enantiomeric distribution of 4-MSPOH enantiomers in wine.

(4) Assess influences of some novel winemaking practices, such as grape crushing method, yeast strain, and lactic acid bacteria, on the concentration of thiol precursors in grape must and varietal thiols in the final wine, with particular interest in the enantiomer profiles of 3-SH and 3-SHA.

1.10 References

1. Tominaga, T.; Baltenweck-Guyot, R.; Peyrot des Gachons, C.; Dubourdieu, D., Contribution of volatile thiols to the aromas of white wines made from several *Vitis vinifera*

grape varieties. *Am. J. Enol. Vitic.* **2000,** *51* (2), 178-181.

2. Rigou, P.; Triay, A.; Razungles, A., Influence of volatile thiols in the development of blackcurrant aroma in red wine. *Food Chem.* **2014,** *142*, 242-248.

3. Tominaga, T.; Niclass, Y.; Frerot, E.; Dubourdieu, D., Stereoisomeric distribution of 3-mercaptohexan-1-ol and 3-mercaptohexyl acetate in dry and sweet white wines made from *Vitis vinifera* (Var. Sauvignon blanc and Semillon). *J. Agric. Food Chem.* **2006,** *54* (19), 7251-7255.

4. Chen, L.; Capone, D. L.; Jeffery, D. W., Chiral analysis of 3-sulfanylhexan-1-ol and 3-sulfanylhexyl acetate in wine by high-performance liquid chromatography–tandem mass spectrometry. *Anal. Chim. Acta* **2018,** *998*, 83-92.

5. King, E. S.; Osidacz, P.; Curtin, C.; Bastian, S. E. P.; Francis, I. L., Assessing desirable levels of sensory properties in Sauvignon blanc wines – consumer preferences and contribution of key aroma compounds. *Aust. J. Grape Wine Res.* **2011,** *17* (2), 169-180.

6. Capone, D. L.; Sefton, M. A.; Jeffery, D. W., Application of a modified method for 3-mercaptohexan-1-ol determination to investigate the relationship between free thiol and related conjugates in grape juice and wine. *J. Agric. Food Chem.* **2011,** *59* (9), 4649-4658.

7. Capone, D. L.; Barker, A.; Williamson, P. O.; Francis, I. L., The role of potent thiols in Chardonnay wine aroma. *Aust. J. Grape Wine Res.* **2018,** *24* (1), 38-50.

8. Bouchilloux, P.; Darriet, P.; Henry, R.; Lavigne-Cruege, V.; Dubourdieu, D., Identification of volatile and powerful odorous thiols in Bordeaux red wine varieties. *J. Agric. Food Chem.* **1998,** *46* (8), 3095-3099.

9. Dominguez, A. M.; Agosin, E., Gas chromatography coupled with mass spectrometry detection for the volatile profiling of *Vitis vinifera* cv. Carmenere wines. *J. Chil. Chem. Soc.* **2010,** *55* (3), 385-391.

10. Sarrazin, E.; Shinkaruk, S.; Tominaga, T.; Bennetau, B.; Frerot, E.; Dubourdieu, D., Odorous impact of volatile thiols on the aroma of young botrytized sweet wines: Identification and quantification of new sulfanyl alcohols. *J. Agric. Food Chem.* **2007,** *55* (4), 1437-1444.

11. Jouanneau, S. Survey of aroma compounds in Marlborough Sauvignon blanc wines-regionality and small scale winemaking. The University of Auckland, 2011.

12. Lund, C. M.; Thompson, M. K.; Benkwitz, F.; Wohler, M. W.; Triggs, C. M.; Gardner, R.; Heymann, H.; Nicolau, L., New Zealand Sauvignon blanc distinct flavor characteristics: Sensory, chemical, and consumer aspects. *Am. J. Enol. Vitic.* **2009,** *60* (1), 1-12.

13. Benkwitz, F.; Tominaga, T.; Kilmartin, P. A.; Lund, C.; Wohlers, M.; Nicolau, L., Identifying the chemical composition related to the distinct aroma characteristics of New

Zealand Sauvignon blanc wines. *Am. J. Enol. Vitic.* **2012,** *63* (1), 62-72.

14. Belda, I.; Ruiz, J.; Beisert, B.; Navascués, E.; Marquina, D.; Calderón, F.; Rauhut, D.; Benito, S.; Santos, A., Influence of *Torulaspora delbrueckii* in varietal thiol (3-SH and 4-MSP) release in wine sequential fermentations. *Int. J. Food Microbiol.* **2017,** *257*, 183-191.

15. Cheynier, V.; Souquet, J. M.; Moutounet, M., Glutathione content and glutathione to hydroxycinnamic acid ratio in *Vitis vinifera* grapes and musts. *Am. J. Enol. Vitic.* **1989,** *40* (4), 320-324.

16. Alscher, R. G., Biosynthesis and antioxidant function of glutathione in plants. *Physiol. Plant.* **1989,** *77* (3), 457-464.

17. Noctor, G.; Mhamdi, A.; Chaouch, S.; Han, Y. I.; Neukermans, J.; Marquez-Garcia, B.; Queval, G.; Foyer, C. H., Glutathione in plants: An integrated overview. *Plant, Cell & Environment* **2012,** *35* (2), 454-484.

18. Kritzinger, E. C.; Bauer, F. F.; du Toit, W. J., Role of glutathione in winemaking: A review. *J. Agric. Food Chem.* **2013,** *61* (2), 269-277.

19. Lamoureux, G. L.; Rusness, D. G., EPTC metabolism in corn, cotton, and soybean: Identification of a novel metabolite derived from the metabolism of a glutathione conjugate. *J. Agric. Food Chem.* **1987,** *35* (1), 1-7.

20. Kishimoto, K.; Matsui, K.; Ozawa, R.; Takabayashi, J., Direct fungicidal activities of C6-aldehydes are important constituents for defense responses in Arabidopsis against *Botrytis cinerea*. *Phytochemistry* **2008,** *69* (11), 2127-2132.

21. Zebelo, S. A.; Matsui, K.; Ozawa, R.; Maffei, M. E., Plasma membrane potential depolarization and cytosolic calcium flux are early events involved in tomato (*Solanum lycopersicon*) plant-to-plant communication. *Plant Sci.* **2012,** *196*, 93-100.

22. Capone, D. L.; Jeffery, D. W., Effects of transporting and processing Sauvignon blanc grapes on 3-mercaptohexan-1-ol precursor concentrations. *J. Agric. Food Chem.* **2011,** *59* (9), 4659-4667.

23. Thibon, C.; Böcker, C.; Shinkaruk, S.; Moine, V.; Darriet, P.; Dubourdieu, D., Identification of *S*-3-(hexanal)-glutathione and its bisulfite adduct in grape juice from *Vitis vinifera* L. cv. Sauvignon blanc as new potential precursors of 3SH. *Food Chem.* **2016,** *199*, 711-719.

24. Clark, A. C.; Deed, R. C., The chemical reaction of glutathione and *trans*-2-hexenal in grape juice media to form wine aroma precursors: The impact of pH, temperature, and sulfur dioxide. *J. Agric. Food Chem.* **2018,** *66* (5), 1214-1221.

25. Fracassetti, D.; Stuknytė, M.; La Rosa, C.; Gabrielli, M.; De Noni, I.; Tirelli, A., Thiol precursors in Catarratto Bianco Comune and Grillo grapes and effect of clarification conditions on the release of varietal thiols in wine. *Aust. J. Grape Wine Res.* **2018,** *24*, 125-133.

26. Chen, L.; Capone, D. L.; Tondini, F. A.; Jeffery, D. W., Chiral polyfunctional thiols and their conjugated precursors upon winemaking with five *Vitis vinifera* Sauvignon blanc clones. *J. Agric. Food Chem.* **2018,** *66* (18), 4674-4682.

27. Vanzo, A.; Janeš, L.; Požgan, F.; Velikonja Bolta, Š.; Sivilotti, P.; Lisjak, K., UHPLC-MS/MS determination of varietal thiol precursors in Sauvignon blanc grapes. *Sci. Rep.* **2017,** *7* (1), 13122.

28. Sivilotti, P.; Falchi, R.; Herrera, J. C.; Škvarč, B.; Butinar, L.; Sternad Lemut, M.; Bubola, M.; Sabbatini, P.; Lisjak, K.; Vanzo, A., Combined effects of early season leaf removal and climatic conditions on aroma precursors in Sauvignon blanc grapes. *J. Agric. Food Chem.* **2017,** *65* (38), 8426-8434.

29. Capone, D. L.; Sefton, M. A.; Hayasaka, Y.; Jeffery, D. W., Analysis of precursors to wine odorant 3-mercaptohexan-1-ol using HPLC-MS/MS: Resolution and quantitation of diastereomers of 3-*S*-cysteinylhexan-1-ol and 3-*S*-glutathionylhexan-1-ol. *J. Agric. Food Chem.* **2010,** *58* (3), 1390-1395.

30. Capone, D. L.; Pardon, K. H.; Cordente, A. G.; Jeffery, D. W., Identification and quantitation of 3-*S*-cysteinylglycinehexan-1-ol (Cysgly-3-MH) in Sauvignon blanc grape juice by HPLC-MS/MS. *J. Agric. Food Chem.* **2011,** *59* (20), 11204-11210.

31. Bonnaffoux, H.; Roland, A.; Rémond, E.; Delpech, S.; Schneider, R.; Cavelier, F., First identification and quantification of *S*-3-(hexan-1-ol)-γ-glutamyl-cysteine in grape must as a potential thiol precursor, using UPLC-MS/MS analysis and stable isotope dilution assay. *Food Chem.* **2017,** *237*, 877-886.

32. Cerreti, M.; Ferranti, P.; Benucci, I.; Liburdi, K.; De Simone, C.; Esti, M., Thiol precursors in Grechetto grape juice and aromatic expression in wine. *Eur. Food Res. Technol.* **2017,** *243*, 753-760.

33. Fedrizzi, B.; Pardon, K. H.; Sefton, M. A.; Elsey, G. M.; Jeffery, D. W., First identification of 4-*S*-glutathionyl-4-methylpentan-2-one, a potential precursor of 4-mercapto-4-methylpentan-2-one, in Sauvignon blanc juice. *J. Agric. Food Chem.* **2009,** *57* (3), 991-995.

34. Roland, A.; Vialaret, J.; Moniatte, M.; Rigou, P.; Razungles, A.; Schneider, R., Validation of a nanoliquid chromatography-tandem mass spectrometry method for the identification and the accurate quantification by isotopic dilution of glutathionylated and cysteinylated

precursors of 3-mercaptohexan-1-ol and 4-mercapto-4-methylpentan-2-one in white grape juices. *J. Chromatogr. A* **2010,** *1217* (10), 1626-1635.

35. Cerreti, M.; Esti, M.; Benucci, I.; Liburdi, K.; de Simone, C.; Ferranti, P., Evolution of *S*-cysteinylated and *S*-glutathionylated thiol precursors during grape ripening of *Vitis vinifera* L. cvs Grechetto, Malvasia del Lazio and Sauvignon blanc. *Aust. J. Grape Wine Res.* **2015,** *21* (3), 411-416.

36. Tominaga, T.; Peyrot des Gachons, C.; Dubourdieu, D., A new type of flavor precursors in *Vitis vinifera* L. cv. Sauvignon blanc: *S*-Cysteine conjugates. *J. Agric. Food Chem.* **1998,** *46* (12), 5215-5219.

37. Peyrot des Gachons, C.; Tominaga, T.; Dubourdieu, D., Sulfur aroma precursor present in *S*-glutathione conjugate form: Identification of *S*-3-(hexan-1-ol)-glutathione in must from *Vitis vinifera* L. cv. Sauvignon blanc. *J. Agric. Food Chem.* **2002,** *50* (14), 4076-4079.

38. Kobayashi, H.; Matsuyama, S.; Takase, H.; Sasaki, K.; Suzuki, S.; Takata, R.; Saito, H., Impact of harvest timing on the concentration of 3-mercaptohexan-1-ol precursors in *Vitis vinifera* berries. *Am. J. Enol. Vitic.* **2012,** *63* (4), 544-548.

39. Roland, A.; Vialaret, J.; Razungles, A.; Rigou, P.; Schneider, R., Evolution of *S*-cysteinylated and *S*-glutathionylated thiol precursors during oxidation of Melon B. and Sauvignon blanc musts. *J. Agric. Food Chem.* **2010,** *58* (7), 4406-4413.

40. Grant-Preece, P. A.; Pardon, K. H.; Capone, D. L.; Cordente, A. G.; Sefton, M. A.; Jeffery, D. W.; Elsey, G. M., Synthesis of wine thiol conjugates and labeled analogues: Fermentation of the glutathione conjugate of 3-mercaptohexan-1-ol yields the corresponding cysteine conjugate and free thiol. *J. Agric. Food Chem.* **2010,** *58* (3), 1383-1389.

41. Pardon, K. H.; Graney, S. D.; Capone, D. L.; Swiegers, J. H.; Sefton, M. A.; Elsey, G. M., Synthesis of the individual diastereomers of the cysteine conjugate of 3-mercaptohexanol (3-MH). *J. Agric. Food Chem.* **2008,** *56* (10), 3758-3763.

42. Thibon, C.; Shinkaruk, S.; Tominaga, T.; Bennetau, B.; Dubourdieu, D., Analysis of the diastereoisomers of the cysteinylated aroma precursor of 3-sulfanylhexanol in *Vitis vinifera* grape must by gas chromatography coupled with ion trap tandem mass spectrometry. *J. Chromatogr. A* **2008,** *1183* (1-2), 150-157.

43. Duhamel, N.; Piano, F.; Davidson, S. J.; Larcher, R.; Fedrizzi, B.; Barker, D., Synthesis of alkyl sulfonic acid aldehydes and alcohols, putative precursors to important wine aroma thiols. *Tetrahedron Lett.* **2015,** *56* (13), 1728-1731.

44. Jeffery, D. W., Spotlight on varietal thiols and precursors in grapes and wines. *Aust. J.*

Chem. **2016,** *69*, 1323-1330.

45. Howell, K. S.; Swiegers, J. H.; Elsey, G. M.; Siebert, T. E.; Bartowsky, E. J.; Fleet, G. H.; Pretorius, I. S.; de Barros Lopes, M. A., Variation in 4-mercapto-4-methyl-pentan-2-one release by *Saccharomyces cerevisiae* commercial wine strains. *FEMS Microbiol. Lett.* **2004,** *240* (2), 125-129.

46. Dubourdieu, D.; Tominaga, T.; Masneuf, I.; Peyrot des Gachons, C.; Murat, M. L., The role of yeasts in grape flavor development during fermentation: The example of Sauvignon blanc. *Am. J. Enol. Vitic.* **2006,** *57* (1), 81-88.

47. Kalua, C. M.; Boss, P. K., Comparison of major volatile compounds from Riesling and Cabernet Sauvignon grapes (*Vitis vinifera* L.) from fruitset to harvest. *Aust. J. Grape Wine Res.* **2010,** *16* (2), 337-348.

48. Kobayashi, H.; Takase, H.; Suzuki, Y.; Tanzawa, F.; Takata, R.; Fujita, K.; Kohno, M.; Mochizuki, M.; Suzuki, S.; Konno, T., Environmental stress enhances biosynthesis of flavor precursors, *S*-3-(hexan-1-ol)-glutathione and *S*-3-(hexan-1-ol)-l-cysteine, in grapevine through glutathione *S*-transferase activation. *J. Exp. Bot.* **2011,** *62* (3), 1325-1336.

49. Molina, I.; Nicolas, M.; Crouzet, J., Grape alcohol dehydrogenase. I. Isolation and characterization. *Am. J. Enol. Vitic.* **1986,** *37* (3), 169-173.

50. Kuhn, A.; van Zyl, C.; van Tonder, A.; Prior, B. A., Purification and partial characterization of an aldo-keto reductase from *Saccharomyces cerevisiae*. *Appl. Environ. Microbiol.* **1995,** *61* (4), 1580-1585.

51. Roland, A.; Schneider, R.; Guernevé, C. L.; Razungles, A.; Cavelier, F., Identification and quantification by LC-MS/MS of a new precursor of 3-mercaptohexan-1-ol (3MH) using stable isotope dilution assay: Elements for understanding the 3MH production in wine. *Food Chem.* **2010,** *121*, 847-855.

52. Winter, G.; Van Der Westhuizen, T.; Higgins, V. J.; Curtin, C.; Ugliano, M., Contribution of cysteine and glutathione conjugates to the formation of the volatile thiols 3-mercaptohexan-1-ol (3MH) and 3-mercaptohexyl acetate (3MHA) during fermentation by *Saccharomyces cerevisiae*. *Aust. J. Grape Wine Res.* **2011,** *17* (2), 285-290.

53. Cordente, A. G.; Capone, D. L.; Curtin, C. D., Unravelling glutathione conjugate catabolism in *Saccharomyces cerevisiae*: The role of glutathione/dipeptide transporters and vacuolar function in the release of volatile sulfur compounds 3-mercaptohexan-1-ol and 4-mercapto-4-methylpentan-2-one. *Appl. Microbiol. Biotechnol.* **2015,** *99* (22), 9709-9722.

54. Bonnaffoux, H.; Delpech, S.; Rémond, E.; Schneider, R.; Roland, A.; Cavelier, F.,

Revisiting the evaluation strategy of varietal thiol biogenesis. *Food Chem.* **2018,** *268*, 126-133.

55. Dubourdieu, D.; Tominaga, T., Polyfunctional thiol compounds. In *Wine chemistry and biochemistry*, Moreno-Arribas, M. V.; Polo, M. C., Eds. Springer New York, 2009; pp 275-293.

56. Belda, I.; Ruiz, J.; Navascués, E.; Marquina, D.; Santos, A., Improvement of aromatic thiol release through the selection of yeasts with increased β-lyase activity. *Int. J. Food Microbiol.* **2016,** *225*, 1-8.

57. Subileau, M.; Schneider, R.; Salmon, J.-M.; Degryse, E., New insights on 3-mercaptohexanol (3MH) biogenesis in Sauvignon blanc wines: Cys-3MH and (*E*)-hexen-2-al are not the major precursors. *J. Agric. Food Chem.* **2008,** *56* (19), 9230-9235.

58. Swiegers, J. H.; Capone, D. L.; Pardon, K. H.; Elsey, G. M.; Sefton, M. A.; Francis, I. L.; Pretorius, I. S., Engineering volatile thiol release in *Saccharomyces cerevisiae* for improved wine aroma. *Yeast* **2007,** *24* (7), 561-574.

59. Kobayashi, H.; Takase, H.; Kaneko, K.; Tanzawa, F.; Takata, R.; Suzuki, S.; Konno, T., Analysis of *S*-3-(hexan-1-ol)-glutathione and *S*-3-(hexan-1-ol)-L-cysteine in *Vitis vinifera* L. cv. Koshu for aromatic wines. *Am. J. Enol. Vitic.* **2010,** *61* (2), 176-185.

60. Swiegers, J. H.; Willmott, R.; Hill-Ling, A.; Capone, D. L.; Pardon, K. H.; Elsey, G. M.; Howell, K. S.; de Barros Lopes, M. A.; Sefton, M. A.; Lilly, M.; Pretorius, I. S., Modulation of volatile thiol and ester aromas by modified wine yeast. In *Developments in Food Science*, Bredie, W. L. P.; Petersen, M. A., Eds. Elsevier: Amsterdam, The Netherlands, 2006; Vol. 43, pp 113-116.

61. Schneider, R.; Charrier, F.; Razungles, A.; Baumes, R., Evidence for an alternative biogenetic pathway leading to 3-mercaptohexanol and 4-mercapto-4-methylpentan-2-one in wines. *Anal. Chim. Acta* **2006,** *563* (1-2), 58-64.

62. Stoj, A.; Czernecki, T.; Domagala, D.; Targonski, Z., Application of volatile compound analysis for distinguishing between red wines from Poland and from other European countries. *S. Afr. J. Enol. Vitic.* **2017,** *38* (2), 245-263.

63. Batovska, D. I.; Todorova, I. T.; Popov, S. S., Seasonal variations in the leaf surface composition of field grown grapevine plants. *J. Serb. Chem. Soc.* **2009,** *74* (11), 1229-1240.

64. Kaack, K.; Christensen, L. P., Effect of packing materials and storage time on volatile compounds in tea processed from flowers of black elder (*Sambucus nigra* L.). *Eur. Food Res. Technol.* **2008,** *227* (4), 1259-1273.

65. Stevens, M. A., Relationship between polyene-carotene content and volatile compound composition of tomatoes. *Journal of the American Society for Horticultural Science* **1970,** *95* (4), 461-&.

66. Jüttner, F.; Leonhardt, J.; Möhren, S., Environmental factors affecting the formation of mesityloxide, dimethylallylic alcohol and other volatile compounds excreted by *Anabaena cylindrica*. *J. Gen. Microbiol.* **1983,** *129* (2), 407-412.

67. Cole, E. R.; Kapur, N. S., The stability of lycopene. I.-Degradation by oxygen. *J. Sci. Food Agric.* **1957,** *8* (6), 360-365.

68. Suwanaruang, T., Analyzing lycopene content in fruits. *Agric. Agric. Sci. Procedia* **2016,** *11*, 46-48.

69. Famiani, F.; Moscatello, S.; Ferradini, N.; Gardi, T.; Battistelli, A.; Walker, R. P., Occurrence of a number of enzymes involved in either gluconeogenesis or other processes in the pericarp of three cultivars of grape (*Vitis vinifera* L.) during development. *Plant Physiol. Biochem.* **2014,** *84*, 261-270.

70. Malkar, R. S.; Yadav, G. D., Selectivity engineering in one pot synthesis of raspberry ketone: Crossed aldol condensation of *p*-hydroxybenzaldehyde and acetone and hydrogenation over novel Ni/Zn-La mixed oxide. *ChemistrySelect* **2019,** *4* (7), 2140-2152.

71. Rice, S.; Maurer, D. L.; Fennell, A.; Dharmadhikari, M.; Koziel, J. A., Evaluation of volatile metabolites emitted in-vivo from cold-hardy grapes during ripening using SPME and GC-MS: A proof-of-concept. *Molecules* **2019,** *24* (3), 536.

72. Garbeva, P.; Hordijk, C.; Gerards, S.; de Boer, W., Volatile-mediated interactions between phylogenetically different soil bacteria. *Front. Microbiol.* **2014,** *5*, 289.

73. Kanchiswamy, C. N.; Malnoy, M.; Maffei, M. E., Chemical diversity of microbial volatiles and their potential for plant growth and productivity. *Front. Plant Sci.* **2015,** *6* (151), 1-23.

74. Jørgensen, U.; Hansen, M.; Christensen, L. P.; Jensen, K.; Kaack, K., Olfactory and quantitative analysis of aroma compounds in elder flower (*Sambucus nigra* L.) drink processed from five cultivars. *J. Agric. Food Chem.* **2000,** *48* (6), 2376-2383.

75. Dresow, J. F.; Bohm, H., The influence of volatile compounds of the flavour of raw, boiled and baked potatoes: Impact of agricultural measures on the volatile components. *Landbauforsch. Volkenrode* **2009,** *59* (4), 309-338.

76. Macdonald, R. C.; Fall, R., Acetone emission from conifer buds. *Phytochemistry* **1993,** *34* (4), 991-994.

77. Ridgway, K.; Lalljie, S. P. D.; Smith, R. M., Analysis of food taints and off-flavours: A review. *Food Additives & Contaminants: Part A: Chemistry, Analysis, Control, Exposure & Risk Assessment* **2010,** *27* (2), 146-168.

78. Saxby, M. J., A survey of chemicals causing taints and off-flavours in food. In *Food Taints*

and Off-Flavours, Saxby, M. J., Ed. Springer US: Boston, MA, 1996; pp 41-71.

79. Roncoroni, M.; Santiago, M.; Hooks, D. O.; Moroney, S.; Harsch, M. J.; Lee, S. A.; Richards, K. D.; Nicolau, L.; Gardner, R. C., The yeast *IRC7* gene encodes a β-lyase responsible for production of the varietal thiol 4-mercapto-4-methylpentan-2-one in wine. *Food Microbiol.* **2011,** *28* (5), 926-935.

80. Santiago, M.; Gardner, R. C., Yeast genes required for conversion of grape precursors to varietal thiols in wine. *FEMS Yeast Res.* **2015,** *15* (5), 1-10.

81. Murat, M.-L.; Masneuf, I.; Darriet, P.; Lavigne, V.; Tominaga, T.; Dubourdieu, D., Effect of *Saccharomyces cerevisiae* yeast strains on the liberation of volatile thiols in Sauvignon blanc wine. *Am. J. Enol. Vitic.* **2001,** *52* (2), 136-139.

82. Zott, K.; Thibon, C.; Bely, M.; Lonvaud-Funel, A.; Dubourdieu, D.; Masneuf-Pomarede, I., The grape must non-*Saccharomyces* microbial community: Impact on volatile thiol release. *Int. J. Food Microbiol.* **2011,** *151* (2), 210-215.

83. Coetzee, C.; Van Wyngaard, E.; Suklje, K.; Ferreira, A. C. S.; du Toitt, W. J., Chemical and sensory study on the evolution of aromatic and nonaromatic compounds during the progressive oxidative storage of a Sauvignon blanc wine. *J. Agric. Food Chem.* **2016,** *64* (42), 7979-7993.

84. Herbst-Johnstone, M.; Nicolau, L.; Kilmartin, P. A., Stability of varietal thiols in commercial Sauvignon blanc wines. *Am. J. Enol. Vitic.* **2011,** *62* (4), 495-502.

85. Murat, M.-L.; Tominaga, T.; Saucier, C.; Glories, Y.; Dubourdieu, D., Effect of anthocyanins on stability of a key odorous compound, 3-mercaptohexan-1-ol, in Bordeaux rosé wines. *Am. J. Enol. Vitic.* **2003,** *54* (2), 135-138.

86. Blanchard, L.; Darriet, P.; Dubourdieu, D., Reactivity of 3-mercaptohexanol in red wine: Impact of oxygen, phenolic fractions, and sulfur dioxide. *Am. J. Enol. Vitic.* **2004,** *55* (2), 115-120.

87. Nikolantonaki, M.; Waterhouse, A. L., A method to quantify quinone reaction rates with wine relevant nucleophiles: A key to the understanding of oxidative loss of varietal thiols. *J. Agric. Food Chem.* **2012,** *60* (34), 8484-8491.

88. Kreitman, G. Y.; Danilewicz, J. C.; Jeffery, D. W.; Elias, R. J., Reaction mechanisms of metals with hydrogen sulfide and thiols in model wine. Part 1: Copper-catalyzed oxidation. *J. Agric. Food Chem.* **2016,** *64*, 4095-4104.

89. Kreitman, G. Y.; Danilewicz, J. C.; Jeffery, D. W.; Elias, R. J., Reaction mechanisms of metals with hydrogen sulfide and thiols in model wine. Part 2: Iron- and copper-catalyzed oxidation. *J. Agric. Food Chem.* **2016,** *64*, 4105-4113.

90. Nikolantonaki, M.; Magiatis, P.; Waterhouse, A. L., Measuring protection of aromatic wine thiols from oxidation by competitive reactions vs wine preservatives with *ortho*-quinones. *Food Chem.* **2014,** *163*, 61-67.

91. Kreitman, G. Y.; Laurie, V. F.; Elias, R. J., Investigation of ethyl radical quenching by phenolics and thiols in model wine. *J. Agric. Food Chem.* **2013,** *61* (3), 685-692.

92. Roland, A.; Delpech, S.; Dagan, L.; Ducasse, M.-A.; Cavelier, F.; Schneider, R., Innovative analysis of 3-mercaptohexan-1-ol, 3-mercaptohexylacetate and their corresponding disulfides in wine by stable isotope dilution assay and nano-liquid chromatography tandem mass spectrometry. *J. Chromatogr. A* **2016,** *1468*, 154-163.

93. Dekker, S.; Nardin, T.; Mattana, M.; Fochi, I.; Larcher, R., Identification and characterisation of thiolated polysulfides in must and wine using online SPE UHPLC-HRMS. *Anal. Bioanal. Chem.* **2020,** *412*, 5229-5245.

94. Kreitman, G. Y.; Elias, R. J.; Jeffery, D. W.; Sacks, G. L., Loss and formation of malodorous volatile sulfhydryl compounds during wine storage. *Crit. Rev. Food Sci. Nutr.* **2018**, 1-25.

95. Winter, M.; Furrer, A.; Willhalm, B.; Thommen, W., Identification and synthesis of two new organic sulfur compounds from the yellow passion fruit (*Passiflora edulis* f. *flavicarpa*). *Helv. Chim. Acta* **1976,** *59* (5), 1613-1620.

96. Chen, L.; Capone, D. L.; Jeffery, D. W., Identification and quantitative analysis of 2-methyl-4-propyl-1,3-oxathiane in wine. *J. Agric. Food Chem.* **2018,** *66* (41), 10808-10815.

97. Waterhouse, A. L.; Sacks, G. L.; Jeffery, D. W., *Understanding Wine Chemistry*. John Wiley & Sons, Ltd: Chichester, U.K., 2016.

98. Harsch, M. J.; Benkwitz, F.; Frost, A.; Colonna-Ceccaldi, B.; Gardner, R. C.; Salmon, J.-M., A new precursor of 3-mercaptohexan-1-ol in grape juice: Thiol-forming potential and kinetics during early stages of must fermentation. *J. Agric. Food Chem.* **2013,** *61*, 3703-3713.

99. Araujo, L. D.; Vannevel, S.; Buica, A.; Callerot, S.; Fedrizzi, B.; Kilmartin, P. A.; du Toit, W. J., Indications of the prominent role of elemental sulfur in the formation of the varietal thiol 3-mercaptohexanol in Sauvignon blanc wine. *Food Res. Int.* **2017,** *98*, 79-86.

100. Peyrot des Gachons, C.; Leeuwen, C. V.; Tominaga, T.; Soyer, J.-P.; Gaudillère, J.-P.; Dubourdieu, D., Influence of water and nitrogen deficit on fruit ripening and aroma potential of *Vitis vinifera* L cv Sauvignon blanc in field conditions. *J. Sci. Food Agric.* **2005,** *85* (1), 73-85.

101. Chone, X.; Lavigne-Cruege, V.; Tominaga, T.; Van Leeuwen, C.; Castagnede, C.; Saucier, C.; Dubourdieu, D., Effect of vine nitrogen status on grape aromatic potential: Flavor precursors (*S*-cysteine conjugates), glutathione and phenolic content in *Vitis vinifera* L. cv. Sauvignon

blanc grape juice. *J. Int. Sci. Vigne Vin* **2006,** *40* (1), 1-6.

102. Helwi, P.; Guillaumie, S.; Thibon, C.; Keime, C.; Habran, A.; Hilbert, G.; Gomes, E.; Darriet, P.; Delrot, S.; van Leeuwen, C., Vine nitrogen status and volatile thiols and their precursors from plot to transcriptome level. *BMC Plant Biol.* **2016,** *16* (1), 173.

103. Helwi, P.; Thibon, C.; Habran, A.; Hilbert, G.; Guillaumie, S.; Delrot, S.; Darriet, P.; van Leeuwen, C., Effect of vine nitrogen status, grapevine variety and rootstock on the levels of berry *S*-glutathionylated and *S*-cysteinylated precursors of 3-sulfanylhexan-1-ol. *J. Int. Sci. Vigne Vin* **2015,** *49* (4), 253-265.

104. Lacroux, F.; Trégoat, O.; van Leeuwen, C.; Pons, A.; Tominaga, T.; Lavigne-Cruège, V.; Dubourdieu, D., Effect of foliar nitrogen and sulphur application on aromatic expression of *Vitis vinifera* L. cv. Sauvignon blanc. *J. Int. Sci. Vigne Vin* **2008,** *42* (3), 125-132.

105. Kliewer, W.; Weaver, R., Effect of crop level and leaf area on growth, composition, and coloration of 'Tokay' grapes. *Am. J. Enol. Vitic.* **1971,** *22* (3), 172-177.

106. Reynolds, A. G.; Yerle, S.; Watson, B.; Price, S. F.; Wardle, D. A., Fruit environment and crop level effects on Pinot noir. III. Composition and descriptive analysis of Oregon and British Columbia wines. *Am. J. Enol. Vitic.* **1996,** *47* (3), 329-339.

107. Reynolds, A. G.; Price, S. F.; Wardle, D. A.; Watson, B. T., Fruit environment and crop level effects on Pinot noir. I. Vine performance and fruit composition in British Columbia. *Am. J. Enol. Vitic.* **1994,** *45* (4), 452-459.

108. Gamero, E.; Moreno, D.; Vilanova, M.; Uriarte, D.; Prieto, M. H.; Valdés, M. E., Effect of bunch thinning and water stress on chemical and sensory characteristics of Tempranillo wines. *Aust. J. Grape Wine Res.* **2014,** *20* (3), 394-400.

109. Sinton, T.; Ough, C.; Kissler, J.; Kasimatis, A., Grape juice indicators for prediction of potential wine quality. I. Relationship between crop level, juice and wine composition, and wine sensory ratings and scores. *Am. J. Enol. Vitic.* **1978,** *29* (4), 267-271.

110. Bowen, A. J.; Reynolds, A. G., Aroma compounds in Ontario Vidal and Riesling icewines. II. Effects of crop level. *Food Res. Int.* **2015,** *76*, 550-560.

111. Bowen, A. J.; Reynolds, A. G.; Lesschaeve, I., Harvest date and crop level influence sensory and chemical profiles of Ontario Vidal blanc and Riesling icewines. *Food Res. Int.* **2016,** *89*, 591-603.

112. Talaverano, I.; Valdés, E.; Moreno, D.; Gamero, E.; Mancha, L.; Vilanova, M., The combined effect of water status and crop level on Tempranillo wine volatiles. *J. Sci. Food Agric.* **2017,** *97* (5), 1533-1542.

113. Paciello, P.; Mencarelli, F.; Palliotti, A.; Ceccantoni, B.; Thibon, C.; Darriet, P.; Pasquini, M.; Bellincontro, A., Nebulized water cooling of the canopy affects leaf temperature, berry composition and wine quality of Sauvignon blanc. *J Sci Food Agric* **2017,** *97* (4), 1267-1275.

114. Šuklje, K.; Antalick, G.; Coetzee, Z.; Schmidtke, L. M.; Baša Česnik, H.; Brandt, J.; du Toit, W. J.; Lisjak, K.; Deloire, A., Effect of leaf removal and ultraviolet radiation on the composition and sensory perception of *Vitis vinifera* L. cv. Sauvignon blanc wine. *Aust. J. Grape Wine Res.* **2014,** *20* (2), 223-233.

115. Šuklje, K.; Antalick, G.; Buica, A.; Langlois, J.; Coetzee, Z. A.; Gouot, J.; Schmidtke, L. M.; Deloire, A., Clonal differences and impact of defoliation on Sauvignon blanc (*Vitis vinifera* L.) wines: A chemical and sensory investigation. *J. Sci. Food Agric.* **2016,** *96* (3), 915-926.

116. Thibon, C.; Dubourdieu, D.; Darriet, P.; Tominaga, T., Impact of noble rot on the aroma precursor of 3-sulfanylhexanol content in *Vitis vinifera* L. cv Sauvignon blanc and Semillon grape juice. *Food Chem.* **2009,** *114* (4), 1359-1364.

117. Luisier, J.-L.; Buettner, H.; Volker, S.; Rausis, T.; Frey, U., Quantification of cysteine *S*-conjugate of 3-sulfanylhexan-1-ol in must and wine of petite arvine vine by stable isotope dilution analysis. *J. Agric. Food Chem.* **2008,** *56* (9), 2883-2887.

118. Gil, M.; Bottini, R.; Berli, F.; Pontin, M.; Silva, M. F.; Piccoli, P., Volatile organic compounds characterized from grapevine (*Vitis vinifera* L. cv. Malbec) berries increase at pre-harvest and in response to UV-B radiation. *Phytochemistry* **2013,** *96* (0), 148-157.

119. Parish-Virtue, K.; Herbst-Johnstone, M.; Bouda, F.; Fedrizzi, B., The impact of postharvest ultra-violet light irradiation on the thiol content of Sauvignon blanc grapes. *Food Chem.* **2019,** *271*, 747-752.

120. Maurer, L. H.; Bersch, A. M.; Santos, R. O.; Trindade, S. C.; Costa, E. L.; Peres, M. M.; Malmann, C. A.; Schneider, M.; Bochi, V. C.; Sautter, C. K.; Emanuelli, T., Postharvest UV-C irradiation stimulates the non-enzymatic and enzymatic antioxidant system of 'Isabel' hybrid grapes (*Vitis labrusca* × *Vitis vinifera* L.). *Food Res. Int.* **2017,** *102*, 738-747.

121. Allen, T.; Herbst-Johnstone, M.; Girault, M.; Butler, P.; Logan, G.; Jouanneau, S.; Nicolau, L.; Kilmartin, P. A., Influence of grape-harvesting steps on varietal thiol aromas in Sauvignon blanc wines. *J. Agric. Food Chem.* **2011,** *59* (19), 10641-10650.

122. Herbst-Johnstone, M.; Araujo, L. D.; Allen, T. A.; Logan, G.; Nicolau, L.; Kilmartin, P. A., Effects of mechanical harvesting on 'Sauvignon blanc' aroma. In *International Workshop on Vineyard Mechanization and Grape and Wine Quality*, Poni, S., Ed. 2013; Vol. 978.

123. Olejar, K. J.; Fedrizzi, B.; Kilmartin, P. A., Influence of harvesting technique and

maceration process on aroma and phenolic attributes of Sauvignon blanc wine. *Food Chem.* **2015,** *183*, 181-189.

124. Parr, W. V.; Schlich, P.; Theobald, J. C.; Harsch, M. J., Association of selected viniviticultural factors with sensory and chemical characteristics of New Zealand Sauvignon blanc wines. *Food Res. Int.* **2013,** *53* (1), 464-475.

125. Capone, D. L.; Black, C. A.; Jeffery, D. W., Effects on 3-mercaptohexan-1-ol precursor concentrations from prolonged storage of Sauvignon blanc grapes prior to crushing and pressing. *J. Agric. Food Chem.* **2012,** *60* (13), 3515-3523.

126. Chen, L.; Capone, D. L.; Nicholson, E. L.; Jeffery, D. W., Investigation of intraregional variation, grape amino acids, and pre-fermentation freezing on varietal thiols and their precursors for *Vitis vinifera* Sauvignon blanc. *Food Chem.* **2019,** *295*, 637-645.

127. Maggu, M.; Winz, R.; Kilmartin, P. A.; Trought, M. C. T.; Nicolau, L., Effect of skin contact and pressure on the composition of Sauvignon blanc must. *J. Agric. Food Chem.* **2007,** *55* (25), 10281-10288.

128. Murat, M.-L.; Tominaga, T.; Dubourdieu, D., Assessing the aromatic potential of Cabernet Sauvignon and Merlot musts used to produce rose wine by assaying the cysteinylated precursor of 3-mercaptohexan-1-ol. *J. Agric. Food Chem.* **2001,** *49* (11), 5412-5417.

129. Roland, A.; Schneider, R.; Charrier, F.; Cavelier, F.; Rossignol, M.; Razungles, A., Distribution of varietal thiol precursors in the skin and the pulp of Melon B. and Sauvignon blanc grapes. *Food Chem.* **2011,** *125* (1), 139-144.

130. Larcher, R.; Nicolini, G.; Tonidandel, L.; Román Villegas, T.; Malacarne, M.; Fedrizzi, B., Influence of oxygen availability during skin-contact maceration on the formation of precursors of 3-mercaptohexan-1-ol in Müller-Thurgau and Sauvignon Blanc grapes. *Aust. J. Grape Wine Res.* **2013,** *19* (3), 342-348.

131. Sparrow, A. M.; Smart, R. E.; Dambergs, R. G.; Close, D. C., Skin particle size affects the phenolic attributes of Pinot noir wine: Proof of concept. *Am. J. Enol. Vitic.* **2016,** *67* (1), 29-37.

132. Patel, P.; Herbst-Johnstone, M.; Lee, S. A.; Gardner, R. C.; Weaver, R.; Nicolau, L.; Kilmartin, P. A., Influence of juice pressing conditions on polyphenols, antioxidants, and varietal aroma of Sauvignon blanc microferments. *J. Agric. Food Chem.* **2010,** *58* (12), 7280-7288.

133. Henschke, P. A.; Jiranek, V., Yeasts - metabolism of nitrogen compounds. In *Wine microbiology and biotechnology*, Fleet, G. H., Ed. Harwood Academic Publishers: Chur, Switzerland, 1993; pp 77-164.

134. Deed, N.; van Vuuren, H.; Gardner, R., Effects of nitrogen catabolite repression and di-

ammonium phosphate addition during wine fermentation by a commercial strain of *S. cerevisiae*. *Appl. Microbiol. Biotechnol.* **2011,** *89* (5), 1537-1549.

135. Beltran, G.; Novo, M.; Rozès, N.; Mas, A.; Guillamón, J. M., Nitrogen catabolite repression in *Saccharomyces cerevisiae* during wine fermentations. *FEMS Yeast Res.* **2004,** *4* (6), 625-632.

136. Howell, K. S.; Klein, M.; Swiegers, J. H.; Hayasaka, Y.; Elsey, G. M.; Fleet, G. H.; Hoj, P. B.; Pretorius, I. S.; Lopes, M. A. D., Genetic determinants of volatile-thiol release by *Saccharomyces cerevisiae* during wine fermentation. *Appl. Environ. Microbiol.* **2005,** *71* (9), 5420-5426.

137. Thibon, C.; Marullo, P.; Claisse, O.; Cullin, C.; Dubourdieu, D.; Tominaga, T., Nitrogen catabolic repression controls the release of volatile thiols by *Saccharomyces cerevisiae* during wine fermentation. *FEMS Yeast Res.* **2008,** *8* (7), 1076-1086.

138. Harsch, M. J.; Gardner, R. C., Yeast genes involved in sulfur and nitrogen metabolism affect the production of volatile thiols from Sauvignon blanc musts. *Appl. Microbiol. Biotechnol.* **2013,** *97* (1), 223-235.

139. Pinu, F. R.; Edwards, P. J. B.; Jouanneau, S.; Kilmartin, P. A.; Gardner, R. C.; Villas-Boas, S. G., Sauvignon blanc metabolomics: Grape juice metabolites affecting the development of varietal thiols and other aroma compounds in wines. *Metabolomics* **2014,** *10*, 556-573.

140. Deroite, A.; Legras, J. L.; Rigou, P.; Ortiz-Julien, A.; Dequin, S., Lipids modulate acetic acid and thiol final concentrations in wine during fermentation by *Saccharomyces cerevisiae* × *Saccharomyces kudriavzevii* hybrids. *AMB Express* **2018,** *8*, 130.

141. Tumanov, S.; Pinu, F. R.; Greenwood, D. R.; Villas-Boas, S. G., Effect of free fatty acids and lipolysis on Sauvignon blanc fermentation. *Aust. J. Grape Wine Res.* **2018,** *24* (4), 398-405.

142. Deed, R. C.; Fedrizzi, B.; Gardner, R. C., Influence of fermentation temperature, yeast strain, and grape juice on the aroma chemistry and sensory profile of Sauvignon blanc wines. *J. Agric. Food Chem.* **2017,** *65* (40), 8902-8912.

143. Swiegers, J.; Francis, I.; Herderich, M.; Pretorius, I., Meeting consumer expectations through management in vineyard and winery. *Aust. NZ Wine Ind. J* **2006,** *21*, 34-42.

144. Holt, S.; Cordente, A. G.; Williams, S. J.; Capone, D. L.; Jitjaroen, W.; Menz, I. R.; Curtin, C.; Anderson, P. A., Engineering *Saccharomyces cerevisiae* to release 3-mercaptohexan-1-ol during fermentation through overexpression of an *S. cerevisiae* gene, *STR3*, for improvement of wine aroma. *Appl. Environ. Microbiol.* **2011,** *77* (11), 3626-3632.

145. Renault, P.; Coulon, J.; Moine, V.; Thibon, C.; Bely, M., Enhanced 3-sulfanylhexan-1-ol

production in sequential mixed fermentation with *Torulaspora delbrueckii*/*Saccharomyces cerevisiae* reveals a situation of synergistic interaction between two industrial strains. *Front Microbiol.* **2016,** *7*.

146. Anfang, N.; Brajkovich, M.; Goddard, M. R., Co-fermentation with *Pichia kluyveri* increases varietal thiol concentrations in Sauvignon blanc. *Aust. J. Grape Wine Res.* **2009,** *15* (1), 1-8.

147. Ruiz, J.; Belda, I.; Beisert, B.; Navascués, E.; Marquina, D.; Calderón, F.; Rauhut, D.; Santos, A.; Benito, S., Analytical impact of *Metschnikowia pulcherrima* in the volatile profile of Verdejo white wines. *Appl. Microbiol. Biotechnol.* **2018,** *102* (19), 8501-8509.

148. Takase, H.; Sasaki, K.; Kiyomichi, D.; Kobayashi, H.; Matsuo, H.; Takata, R., Impact of *Lactobacillus plantarum* on thiol precursor biotransformation leading to production of 3-sulfanylhexan-1-ol. *Food Chem.* **2018,** *259*, 99-104.

149. Jolly, N. P.; Varela, C.; Pretorius, I. S., Not your ordinary yeast: Non-*Saccharomyces* yeasts in wine production uncovered. *FEMS Yeast Res.* **2014,** *14* (2), 215-237.

150. King, E. S.; Swiegers, J. H.; Travis, B.; Francis, I. L.; Bastian, S. E. P.; Pretorius, I. S., Coinoculated fermentations using *Saccharomyces* yeasts affect the volatile composition and sensory properties of *Vitis vinifera* L. cv. Sauvignon blanc wines. *J. Agric. Food Chem.* **2008,** *56* (22), 10829-10837.

151. King, E. S.; Kievit, R. L.; Curtin, C.; Swiegers, J. H.; Pretorius, I. S.; Bastian, S. E. P.; Francis, I. L., The effect of multiple yeasts co-inoculations on Sauvignon blanc wine aroma composition, sensory properties and consumer preference. *Food Chem.* **2010,** *122* (3), 618-626.

152. Masneuf-Pomarede, I.; Mansour, C.; Murat, M. L.; Tominaga, T.; Dubourdieu, D., Influence of fermentation temperature on volatile thiols concentrations in Sauvignon blanc wines. *Int. J. Food Microbiol.* **2006,** *108* (3), 385-390.

153. Roland, A.; Schneider, R.; Razungles, A.; Cavelier, F., Varietal thiols in wine: Discovery, analysis and applications. *Chem. Rev.* **2011,** *111* (11), 7355-7376.

154. Darriet, P.; Tominaga, T.; Lavigne, V.; Boidron, J.-N.; Dubourdieu, D., Identification of a powerful aromatic component of *Vitis vinifera* L. var. Sauvignon wines: 4-Mercapto-4-methylpentan-2-one. *Flavour Fragr. J.* **1995,** *10* (6), 385-392.

155. Tominaga, T.; Darriet, P.; Dubourdieu, D., Identification of 3-mercaptohexyl acetate in Sauvignon wine, a powerful aromatic compound exhibiting box-tree odor. *Vitis* **1996,** *35* (4), 207-210.

156. Tominaga, T.; Furrer, A.; Henry, R.; Dubourdieu, D., Identification of new volatile thiols

in the aroma of *Vitis vinifera* L. var. Sauvignon blanc wines. *Flavour Fragr. J.* **1998,** *13* (3), 159-162.

157. Tominaga, T.; Murat, M.-L.; Dubourdieu, D., Development of a method for analyzing the volatile thiols involved in the characteristic aroma of wines made from *Vitis vinifera* L. Cv. Sauvignon blanc. *J. Agric. Food Chem.* **1998,** *46* (3), 1044-1048.

158. Mateo-Vivaracho, L.; Ferreira, V.; Cacho, J., Automated analysis of 2-methyl-3-furanthiol and 3-mercaptohexyl acetate at ng L^{-1} level by headspace solid-phase microextraction with on-fibre derivatisation and gas chromatography-negative chemical ionization mass spectrometric determination. *J. Chromatogr. A* **2006,** *1121* (1), 1-9.

159. Mateo-Vivaracho, L.; Cacho, J.; Ferreira, V., Improved solid-phase extraction procedure for the isolation and in-sorbent pentafluorobenzyl alkylation of polyfunctional mercaptans: Optimized procedure and analytical applications. *J. Chromatogr. A* **2008,** *1185* (1), 9-18.

160. Musumeci, L.; Ryona, I.; Pan, B.; Loscos, N.; Feng, H.; Cleary, M.; Sacks, G., Quantification of polyfunctional thiols in wine by HS-SPME-GC-MS following extractive alkylation. *Molecules* **2015,** *20* (7), 12280-12299.

161. Ferreira, V.; Ortin, N.; Cacho, J. F., Optimization of a procedure for the selective isolation of some powerful aroma thiols: Development and validation of a quantitative method for their determination in wine. *J. Chromatogr. A* **2007,** *1143* (1-2), 190-198.

162. Herbst-Johnstone, M.; Piano, F.; Duhamel, N.; Barker, D.; Fedrizzi, B., Ethyl propiolate derivatisation for the analysis of varietal thiols in wine. *J. Chromatogr. A* **2013,** *1312* (0), 104-110.

163. Dagan, L.; Reillon, F.; Roland, A.; Schneider, R., Development of a routine analysis of 4-mercapto-4-methylpentan-2-one in wine by stable isotope dilution assay and mass tandem spectrometry. *Anal. Chim. Acta* **2014,** *821*, 48-53.

164. Capone, D. L.; Ristic, R.; Pardon, K. H.; Jeffery, D. W., Simple quantitative determination of potent thiols at ultratrace levels in wine by derivatization and high-performance liquid chromatography–tandem mass spectrometry (HPLC-MS/MS) analysis. *Anal. Chem.* **2015,** *87* (2), 1226-1231.

165. Coetzee, C.; Schulze, A.; Mokwena, L.; du Toit, W. J.; Buica, A., Investigation of thiol levels in young commercial South African Sauvignon blanc and Chenin blanc wines using propiolate derivatization and GC-MS/MS. *S. Afr. J. Enol. Vitic.* **2018,** *39* (2), 180-184.

166. Mafata, M.; Stander, M. A.; Thomachot, B.; Buica, A., Measuring thiols in single cultivar South African red wines using 4,4-dithiodipyridine (DTDP) derivatization and ultraperformance convergence chromatography-tandem mass spectrometry. *Foods* **2018,** *7* (9),

138.

167. Peyrot des Gachons, C.; Tominaga, T.; Dubourdieu, D., Measuring the aromatic potential of *Vitis vinifera* L. cv. Sauvignon blanc grapes by assaying *S*-cysteine conjugates, precursors of the volatile thiols responsible for their varietal aroma. *J. Agric. Food Chem.* **2000,** *48* (8), 3387-3391.

168. Brazier-Hicks, M.; Evans, K. M.; Cunningham, O. D.; Hodgson, D. R. W.; Steel, P. G.; Edwards, R., Catabolism of glutathione conjugates in *Arabidopsis thaliana*: Role in metabolic reactivation of the herbicide safener fenclorim. *J. Biol. Chem.* **2008,** *283* (30), 21102-21112.

169. Lamoureux, G. L.; Rusness, D. G., Pentachloronitrobenzene metabolism in peanut. 1. Mass spectral characterization of seven glutathione-related conjugates produced in vivo or in vitro. *J. Agric. Food Chem.* **1980,** *28* (6), 1057-1070.

170. Uhlig, S.; Stanic, A.; Hofgaard, I. S.; Kluger, B.; Schuhmacher, R.; Miles, C. O., Glutathione-conjugates of deoxynivalenol in naturally contaminated grain are primarily linked via the epoxide group. *Toxins* **2016,** *8* (11).

171. Wang, W.; Tang, K.; Yang, H.-R.; Wen, P.-F.; Zhang, P.; Wang, H.-L.; Huang, W.-D., Distribution of resveratrol and stilbene synthase in young grape plants (*Vitis vinifera* L. cv. Cabernet Sauvignon) and the effect of UV-C on its accumulation. *Plant Physiol. Biochem.* **2010,** *48* (2), 142-152.

172. Chin, H.-W.; Lindsay, R. C., Mechanisms of formation of volatile sulfur compounds following the action of cysteine sulfoxide lyases. *J. Agric. Food Chem.* **1994,** *42* (7), 1529-1536.

173. Kubec, R.; Svobodova, M.; Velisek, J., Gas chromatographic determination of S-alk(en)ylcysteine sulfoxides. *J. Chromatogr. A* **1999,** *862* (1), 85-94.

174. Gürbüz, O.; Rouseff, J.; Talcott, S. T.; Rouseff, R., Identification of Muscadine wine sulfur volatiles: Pectinase versus skin-contact maceration. *J. Agric. Food Chem.* **2013,** *61* (3), 532-539.

175. Demole, E.; Enggist, P.; Ohloff, G., 1-*p*-Menthene-8-thiol: A powerful flavor impact constituent of grapefruit juice (*Citrus parodisi* Macfayden). *Helv. Chim. Acta* **1982,** *65* (6), 1785-1794.

176. Thomas, A.; Bessiere, Y., Limonene. *Nat. Prod. Rep.* **1989,** *6* (3), 291-309.

177. Jung, K.; Fastowski, O.; Engel, K.-H., Occurrence of 4-methoxy-2-methyl-2-butanethiol in blackcurrant (*Ribes nigrum* L.) berries. *Flavour Fragr. J.* **2016,** *31* (6), 438-441.

CHAPTER 2

Preliminary Study of the Potential New Precursors to 3-Sulfanylhexan-1-ol and 4-Methyl-4-sulfanylpentan-2-one

Xingchen Wang,[†] Dimitra L. Capone,[†,‡]Aurélie Roland,[§] Sue Maffei,[⸸] David W. Jeffery[†,‡,*]

[†] Department of Wine Science and Waite Research Institute, The University of Adelaide (UA), PMB 1, Glen Osmond, SA 5064, Australia

[‡] Australian Research Council Training Centre for Innovative Wine Production, UA, PMB 1, Glen Osmond, SA 5064, Australia

[§] SPO, Univ Montpellier, INRAE, Institut Agro, Montpellier, France

[⸸] CSIRO Agriculture and Food, Waite Campus, Locked Bag No. 2, Glen Osmond, South Australia 5064, Australia

Statement of Authorship

Title of Paper	Preliminary studies of a potential new precursor to 3-sulfanylhexan-1-ol and the formation pathway of 4-methyl-4-sulfanylpentan-2-one conjugates in grape
Publication Status	☐ Published ☐ Accepted for Publication ☐ Submitted for Publication ☑ Unpublished and Unsubmitted work written in manuscript style
Publication Details	Prepared in manuscript format based primarily on the author guidelines for Journal of Agricultural and Food Chemistry.

Principal Author

Name of Principal Author (Candidate)	Xingchen Wang		
Contribution to the Paper	Designed experiments, conducted experiments, collected, processed, analysed, and visualised data. Produced original manuscript and revised and edited manuscript.		
Overall percentage (%)	75		
Certification:	This paper reports on original research I conducted during the period of my Higher Degree by Research candidature and is not subject to any obligations or contractual agreements with a third party that would constrain its inclusion in this thesis. I am the primary author of this paper.		
Signature		Date	21/06/2022

Co-Author Contributions

By signing the Statement of Authorship, each author certifies that:

i. the candidate's stated contribution to the publication is accurate (as detailed above);

ii. permission is granted for the candidate in include the publication in the thesis; and

iii. the sum of all co-author contributions is equal to 100% less the candidate's stated contribution.

Name of Co-Author	Dimitra L. Capone		
Contribution to the Paper	Designed experiments, supervised the work, interpreted data. Reviewed and edited manuscript.		
Signature		Date	09/08/2022

Name of Co-Author	Aurélie Roland
Contribution to the Paper	Contributed to the design of experiments, interpreted data, and supervised the work. Reviewed and edited the manuscript.

Signature		Date	22/06/2022

Name of Co-Author	Sue Maffei		
Contribution to the Paper	Method development and sample analysis by HPLC-MS/MS; sample analysis by HPLC-Q-TOF MS.		
Signature		Date	20/7/22

Name of Co-Author	David W. Jeffery		
Contribution to the Paper	Conceived of and designed experiments, interpreted data, supervised the project, and provided resources. Reviewed and edited the manuscript and acted as the principal supervisor.		
Signature		Date	21/06/2022

Please cut and paste additional co-author panels here as required.

Abstract: A major pathway to varietal thiols such as 3-sulfanylhexan-1-ol (3-SH) and 4-methyl-4-sulfanylpentan-2-one (4-MSP) present in wine involves their release during fermentation from L-glutathione and L-cysteine conjugated precursors that originate in the grape. However, discrepancies exist in the formation and degradation of the precursors, such that the concentration of thiols such as 3-SH cannot be completely accounted for based on consumption of known precursors. This implied the potential existence of undiscovered precursors, with *N*-malonyl-3-*S*-cysteinylhexan-1-ol (MalCys-3-SH) being one of the potential candidates based on other plant metabolites. Thus, the presence of MalCys-3-SH in grape juice was investigated. The tandem mass spectrometer (MS/MS) and source parameters were optimised using a synthesised MalCys-3-SH standard but analysis of a few concentrated Sauvignon blanc juice extracts by HPLC-MS/MS did not enable positive identification of MalCys-3-SH. Further study would be required, however, to identify and then quantify MalCys-3-SH in a larger range of juice and wine samples to evaluation of the potential of MalCys-3-SH to produce 3-SH during fermentation. Regarding the precursors of 4-MSP, mesityl oxide has not been detected in grapes despite reasonable speculation of its involvement in the formation of precursors of 4-MSP. It was hypothesised that mesityl oxide might be secreted by soil bacteria and absorbed by grapevine roots for subsequent translocation and transformation to 4-MSP precursors in vine organs, including berries. Preliminary experiments were conducted by feeding grape leaves and berries of potted grapevines of three varieties with d_{10}-mesityl oxide. Analysis by HPLC-MS/MS of samples prepared from the treated tissues provided tentative identification of the corresponding deuterium labelled precursors of 4-MSP. However, future investigations are warranted to apply d_{10}-mesityl oxide to the potted grapevine in the soil and detect 4-MSP precursors in grapevine tissues, as well as screening soil bacteria for their ability to secrete mesityl oxide in vineyards.

Keywords: mesityl oxide, varietal thiols, MalCys-3-SH, Sauvignon blanc, Cabernet Sauvignon, Shiraz, Pinot Meunier

INTRODUCTION

Varietal thiol precursors are a group of odourless non-volatile compounds present in grape, with the initial identification of 3-*S*-cysteinylhexan-1-ol (Cys-3-SH) being made in Sauvignon blanc grape juice.[1] In subsequent decades, a relatively integral formation and degradation metabolic pathway for thiol precursors has been achieved via the identification of a series of thiol precursors and fermentation trials, particularly in its ability to produce 3-sulfanylhexan-1-ol (3-SH). The formation of known 3-SH precursors originates from the incorporation of L-glutathione (GSH) with (*E*)-2-hexenal (degradation of unsaturated fatty acids) to form 3-*S*-glutathionylhexanal (GSH-3-SHal) as a function of detoxification mechanisms linked to GSH.[2-4] This is followed by the enzymatic reduction of the aldehyde in GSH-3-SHal to yield the alcohol, 3-*S*-glutathionylhexan-1-ol (GSH-3-SH). Subsequently, GSH-3-SH metabolism occurs through either 3-*S*-cysteinylglycinehexan-1-ol (CysGly-3-SH)[5] or 3-*S*-glutamylcysteinehexan-1-ol (GluCys-3-SH)[6] to yield Cys-3-SH,[7] which is a substrate for β-lyase to release 3-SH.[8]

Despite the metabolic pathway of 3-SH precursors outlined above (of which aspects could occur in grape berry, juice, or during fermentation), discrepancies exist in fully accounting for the relationship between free 3-SH in wines and the identified precursors. For example, up to 72 % of 3-SH in wine could be accounted for by the previously identified precursors (i.e., GSH-3-SHal, GSH-3-SH and its bisulfite adduct, Cys-3-SH, CysGly-3-SH, and GluCys-3-SH) that are consumed during fermentation.[9] An additional 11.8 % of 3-SH could be accounted for due to acetylation to form 3-sulfanylhexyl acetate,[3] thus a total of 83.8 % 3-SH in wine could so far be explained. On the other hand, this means that up to ~ 16 % of 3-SH in wine may be unaccounted for, implying the possibility of novel precursors awaiting identification (and/or alternative fates for thiols such as 3-SH).

By comparing the metabolic pathway of GSH conjugates in other plants, such as soybean, corn, cotton, radish, peanut, and thale cress (*Arabidopsis thaliana*),[10-14] with that in grape, one of the metabolic intermediates of GSH conjugation of xenobiotics (e.g., fungicide, herbicide, or pesticide), namely an *N*-malonylcysteine (MalCys) type conjugate, has drawn recent attention. Specifically, the GSH conjugated fenclorim (a herbicide safener) was found to be enzymatically metabolised to L-cysteine conjugated fenclorim (Cys-fenclorim) in a similar way to that of GSH-3-SH, but an alternative pathway exists for Cys-fenclorim which involved the generation of MalCys conjugated fenclorim catalysed by malonyl-CoA-dependent *N*-

malonyltransferase.[13] Although such an enzyme has not been identified in grape, there remained the possibility that *N*-malonyl-3-*S*-cysteinylhexan-1-ol (MalCys-3-SH) could potentially be present and thus required exploration.

Regarding the formation and production of 4-methyl-4-sulfanylpentan-2-one (4-MSP) and its precursors, the metabolic pathways are understood to be similar to that of 3-SH. Briefly, L-glutathionylated 4-MSP (GSH-4-MSP) was proposed to originate from L-glutathione and mesityl oxide,[15] which was supported by the identification of GSH-4-MSP in grape juice.[16] Further implicating a role for mesityl oxide, a spiking experiment using d_{10}-mesityl oxide in Sauvignon blanc fermentation led to the formation of deuterium labelled 4-MSP in the resultant wine.[17] The identification of other intermediate precursors of 4-MSP, including L-cysteinylated 4-MSP (Cys-4-MSP),[1] 4-*S*-cysteinylglycine-4-methylpentan-2-one (CysGly-4-MSP), and 4-*S*-glutamylcysteine-4-methylpentan-2-one (GluCys-4-MSP),[6] have helped elucidate the fate of precursors in releasing 4-MSP via a series of fermentation trials.[9] However, one of the remaining discrepancies is that the origin of mesityl oxide is not clear yet, although it was tentatively qualified in wines and "cold-hardy" grape surface.[18-20] Interestingly, mesityl oxide was identified recently in glycoside extract of kiwifruit juice after β-glycosidase treatment.[21] Apart from that, several possible other origins of mesityl oxide have been proposed in the Section of 1.2 in Chapter 1, with one hypothesis being that mesityl oxide is secreted by soil bacteria (i.e., *Collimonas pratensis*[22]) as a function of interaction with either other soil microorganisms or plant roots.[22] Subsequent uptake by the plant and translocation/transformation of mesityl oxide into 4-MSP precursors would also need to occur and this has not been verified.

Considering the gaps in the literature, one of the aims of this chapter was to explore the potential presence of MalCys-3-SH in grape juice extracts concentrated and isolated using chromatography on C18 sorbent, after optimisation of HPLC-MS/MS parameters using a synthesised standard of MalCys-3-SH. The other focus of this chapter was to verify the hypothesis that grapevine can uptake mesityl oxide and use it to synthesise 4-MSP precursors.

MATERIALS AND METHODS

Chemicals and materials. Chemical grade methanol was obtained from ChemSupply (Gillman, SA, Australia). HPLC gradient grade ethanol, methanol, acetonitrile, d_{10}-mesityl oxide (98 % atom), and C18 sorbent were purchased from Sigma-Aldrich (Castle Hill, NSW, Australia). Authentic MalCys-3-SH was synthesised for another project, and deuterium

labelled GSH-4-MSP was available from a previous study.[23] Phenomenex SDB-L cartridges (500 mg, 6 mL) was bought from Phenomenex (Lane Cove, NSW, Australia). Milli-Q water was obtained from a Milli-Q purification system (Millipore, North Ryde, NSW, Australia).

Study of MalCys-3-SH. *Grape samples and process.* Sauvignon blanc grapes (clone H5V10) were randomly picked from both sides of the canopy across multiple rows from a commercial vineyard in Adelaide Hills wine region in the early morning and transported to a 4 °C cold room at the university research laboratory. Grapes samples were collected 4 times until commercial harvest: 15 February, 22 February, 1 March, and 8 March 2021.

The grapes were destemmed manually and 50 mg/kg of SO_2 was added as potassium metabisulfite (PMS). This was followed by the manual crush of grape berries, and the juice was collected in plastic bottles and stored at –20 °C before further processing. Grape juice parameters, including total soluble solids (TSS, °Brix), titratable acidity (g/L as tartaric acid, titration endpoint of pH 8.2), and pH, were measured using a digital refractometer (Atago, PAL-1, VIC, Australia) and T50 autotitrator (Mettler Toledo, Melbourne, Australia), respectively.

Preparation of extracts from grape juice. Isolation of components from grape juice was conducted according to a previous method.[16] The frozen juice (harvest date 15th February) was defrosted overnight in a 4 °C cold room before being centrifuged (3128*g*, at 22 °C for 20 min). The supernatant was collected (1.06 L) and a proportion (approximately 200 mL) was loaded onto a C18 sorbent bed prepared on a sintered glass funnel (100 mm diameter, 30–35 mm bed height) using 100 g of C18 sorbent. The sorbent was activated with two bed volumes of acetonitrile followed by equilibration with Milli-Q water before the loading of grape juice. Two bed volumes of Milli-Q water were used to wash off polar constituents before two bed volumes of methanol were used to elute the sorbent bed with aid of vacuum. This was repeated with the remaining portions of juice after the re-equilibration of the sorbent bed with three bed volumes of Milli-Q water. All methanol eluates were pooled and then concentrated under vacuum at 30 °C.

The residue (~ 11 mL) obtained after the removal of methanol was diluted with 4 mL of Milli-Q water and 5 mL was then loaded onto a C18 low-pressure column (15 mm diameter, 200 mm bed height) that was preconditioned with acetonitrile and Milli-Q water. Then, 100 mL of Milli-Q water was applied as a wash, followed by elution with 150 mL methanol. The column was equilibrated with two bed volumes of Milli-Q water before loading the next aliquot of crude extract (aqueous residue). This was repeated two more times and the pooled methanol eluates underwent concentration under vacuum and residue was reconstituted using 5 mL of

Milli-Q water. Samples were filtered using 0.45 µm membrane filter before instrumental analysis. This juice extraction procedure was repeated with the Sauvignon blanc juice samples prepared on the other three harvest dates, using refreshed C18 sorbent flushing with two bed volumes of methanol and equilibrated with one bed volume of Milli-Q water.

Analysis of Sauvignon blanc juice extracts. The synthetic standard of MalCys-3-SH (50 µg/mL prepared in water) was used for a preliminary automated MRM method development using an Agilent 1200 HPLC coupled with a 6410 triple quadrupole mass spectrometer (QQQ MS). The flow injection MS experiment was conducted by injecting 4 µL of MalCys-3-SH standard with a mobile phase (50 % of 0.5 % aqueous formic acid and 50 % of 0.5 % formic acid in acetonitrile) flow rate of 0.3 mL/min. The mass spectrometer was operated in positive electrospray ionisation (ESI+) mode with capillary voltage, nebuliser pressure, drying gas temperature, and drying gas flow rate of 4000 V, 241 kPa, 300 °C, and 8 L/min, respectively. The optimised fragmentor voltage and collision energy are illustrated in Table 1 and a dwell time of 100 ms was used. The Agilent MassHunter Optimizer software (version B.03.01) in conjunction with MassHunter Workstation data acquisition for triple quadrupole (version B.03.01) were used for the mass spectrometric parameter optimisation.

Table 1. *Optimised MS/MS parameters for MalCys-3-SH with Agilent 6410 and G6470A triple quadrupole mass spectrometer.*

Instrument	Precursor ion (m/z)	Product ion (m/z)	Fragmentor (V)	Collision energy (V)
Agilent 6410 QQQ MS	308.1	174.1	66	8
		162.1	66	16
		159.1	66	8
		55.1	66	40
Agilent G6470A QQQ MS	308.1	174	94	12
		159	94	12
		83	94	24
		55.1	94	40

Further method optimisation was performed using an Agilent 1260 HPLC coupled with an Agilent G6470A MS/MS, with an Alltima C18 column (250 × 2.1 mm i.d., 5 µm, 100 A particle size, HiChrom, Phenomenex, Lane Cove, NSW, Australia) protected by a guard cartridge (7.5 × 2.1 mm i.d.) of the same material used for separation. Source conditions including drying gas

flow (7–12 L/min with a 1 L/min gradient), drying gas temperature (150–350 °C with a 50 °C gradient), nebuliser pressure (138–414 Kpa with a 35 Kpa gradient), sheath gas temperature (200–400 °C with a 50 °C gradient), sheath gas flow (10, 11, 12 L/min), capillary voltage (1000–6000 V with a 500 V gradient), and nozzle voltage (0–2000 V with a 500 V gradient) were optimised with the MalCys-3-SH standard (50 µg/mL, injection volume of 1 µL). The electron multiplier voltage (EMV) was increased from 0 to 200 V, and fragmentor voltage and collision energy were again optimised for this instrument, with parameters illustrated in Table 1. Mobile phase at a flow rate of 0.3 mL/min consisted of 0.5 % aqueous formic acid (A) and 0.5 % formic acid in acetonitrile (B). The gradient of mobile phase for B was 0 min, 5 %; 10 min, 15 %; 20 min, 30 %; 21 min, 80 %; 25 min, 80 %; 25.1 min, 5 %; and 35 min, 5 %. The Sauvignon blanc juice extracts were screened with an injection volume of 4 µL with optimised source conditions: drying gas temperature and flow rate were 300 °C and 8 L/min, respectively; nebuliser pressure was 241 Kpa; sheath gas temperature and flow rate were 350 °C and 12 L/min, respectively; capillary and nozzle voltages were 4000 V and 2000 V, respectively.

Study of d_{10}-mesityl oxide to 4-MSP precursors. *Grapevines.* Three varieties of own-rooted grapevines were grown in a commercial potting mix in a glasshouse at 21 °C: dwarf Pinot Meunier,[24] Shiraz (BV186), and Cabernet Sauvignon (ENTAV 338).

Application of d_{10}-mesityl oxide to grape leaves and berries. Two aqueous solutions of d_{10}-mesityl oxide (5 mg/L and 30 mg/L) were prepared by diluting an ethanolic solution of d_{10}-mesityl oxide (0.946 g/L) with Milli-Q water. The application of d_{10}-mesityl oxide solutions to grape leaves and berries followed a previous method.[25] Generally, 10 mL of d_{10}-mesityl oxide solution (concentration as specified later) was added to a plastic resealable bag and a grape leaf was placed in the bag, with both bag and grape leaf gently folded to maximise the contact with d_{10}-mesityl oxide solution. A similar protocol was applied to grape bunches and careful mixing (twice per day) of the bunches with d_{10}-mesityl oxide solution was conducted to maintain some contact of berries with the solution. Harvested grape and leaf samples from the trials were instantly frozen with liquid N_2 and stored at –80 °C before further use.

The first trial was conducted with potted Shiraz leaves, with one old grape leaf (formed near the roots of the vines) and one young leaf (formed near the end of the vines) from one grapevine dipped in 10 mL of either 5 mg/L or 30 mg/L d_{10}-mesityl oxide solution in resealable plastic bags for 2 days before harvest (4^{th}–6^{th} November 2020) (Figure 1(1)). Three pots of Shiraz vine were treated in the same manner.

The second trial on Cabernet Sauvignon leaves was conducted in the same manner as

for Shiraz grape leaves but for a 7-day treatment duration (from 18th–25th November). Grape bunches of the Cabernet Sauvignon were also treated with 5 mg/L or 30 mg/L d_{10}-mesityl oxide solution for 3 days (8th–11th January 2021, duplicate) or 6 days (8th–14th January 2021, triplicate) before harvest (Figure 1(2)). In total, 5 pots of Cabernet Sauvignon vine were utilised.

The third trial was conducted on nine potted Pinot Meunier vines using only 30 mg/L d_{10}-mesityl oxide solution for 3-day, 6-day, and 9-day of treatment on tissues of grape leaf, younger grape berry (bunches formed near the end of the vines), and older grape berry (bunches formed near the roots of the vines) in triplicate (Figure 1(3)). In total, 9 pots of Pinot Meunier were used for the trial. Treatments started from 8th December and harvest was conducted on 11th, 14th, and 17th of December 2020.

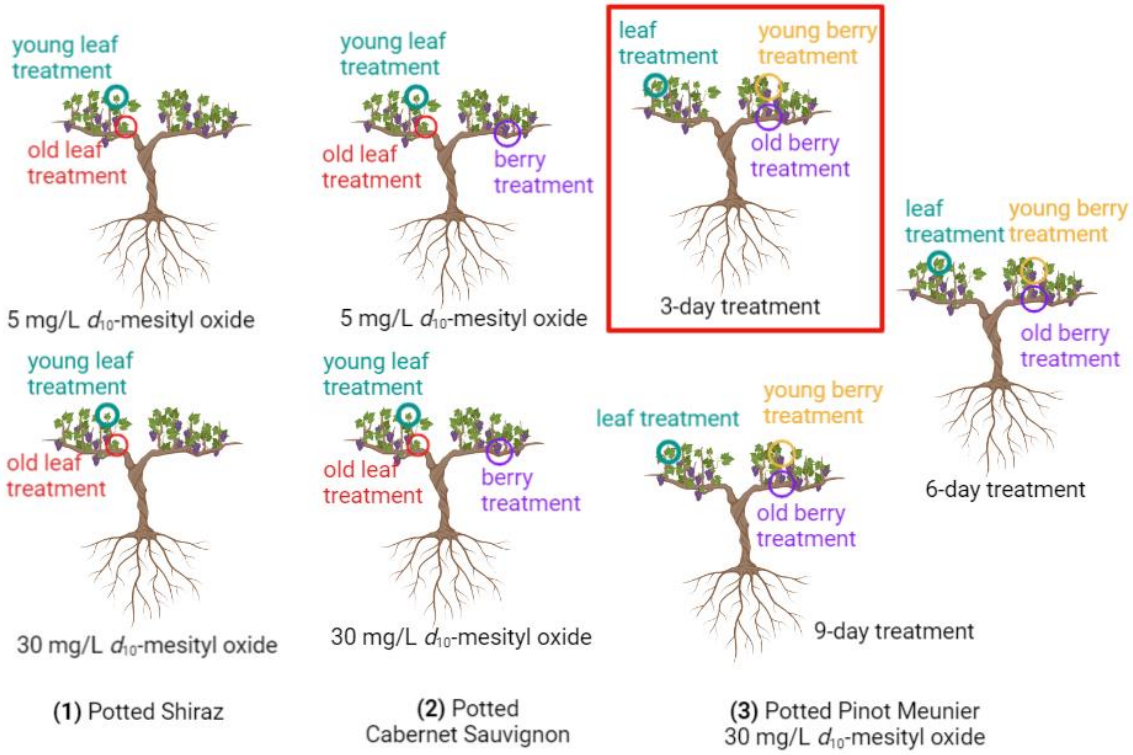

Figure 1. *Experimental setup for applying d_{10}-mesityl oxide to grape leaves and berries of potted (1) Shiraz (2-day treatment with 5 mg/L or 30 mg/L solution), (2) Cabernet Sauvignon (3-day or 6-day treatment with 5 mg/L or 30 mg/L solution), and (3) Pinot Meunier (3-day, 6-day, or 9-day treatment with 30 mg/L solution). Old berry sample from Pinot Meunier highlighted with red border was to be used as an illustration in Figure 4.*

Sample preparation. The frozen grape leaves were ground using a mortar and pestle with the aid of liquid N_2 and 1 g of leaf ground was weighed and transferred to a 12 mL glass vial. Five millilitres of aqueous ethanol solution (50/50) was added and the vial was vortexed for 1 min

followed by ultrasonic treatment for 15 min in a sonicator water bath (50 Hz frequency, Unisonics, Sydney, Australia). The clear supernatant was collected after centrifugation at 3857*g* at 10 °C for 10 min. This extraction procedure using aqueous ethanol solution was repeated another time and the two portions of 5 mL aqueous ethanol extract were pooled before being concentrated under reduced pressure. Milli-Q water was added to top up the volume of the extract to 10 mL and extracts were stored at 4 °C before SPE processing.

Frozen berries were collected from frozen grape bunches treated with liquid N_2 before being ground using a coffee grinder. Liquid N_2 was occasionally added to the grinder to prevent the contents from defrosting. The ground berry material was quickly transferred to plastic tubes and stored at –80 °C before use. Before the SPE process, frozen grape berry homogenate was defrosted overnight at 4 °C, then the supernatant was collected after centrifugation at 3857*g*, 5 °C for 15 min.

SPE of grape leaf and berry isolates. Previous thiol precursor procedures of extraction were followed.[26] Briefly, Strata SDB-L cartridges were activated with 6 mL of methanol followed by 6 mL of Milli-Q water under vacuum. Then 10 mL of either grape leaf extracts or grape juice from berry ground was loaded onto the cartridges before being dried by air under SPE manifold vacuum for 5 min. This was followed by elution using 2 mL of methanol. The methanol fraction was dried under N_2 (138–170 kPa) at 30 °C using a 24-channel manifold fitted with a nitrogen regulator and reconstituted with 500 µL of methanol and 200 µL of Milli-Q water. The extracts were filtered through 0.45 µm membrane filters prior to instrumental analysis.

Analysis of grape leaf and berry extracts. HPLC conditions were identical for different instruments, with separation achieved using an Alltima C18 column (250 × 2.1 mm i.d., 5 µm, HiChrom, Phenomenex, Lane Cove, NSW, Australia) operated at 25 °C. Solvents A and B were 0.5 % aqueous formic acid and 0.5 % formic acid in acetonitrile, respectively, with the gradient for solvent B as follows: 0 min, 5 %; 10 min, 15 %; 20 min, 30 %; 21 min, 80 %; and 25 min, 80 %. Mobile phase flow rate was set at 0.3 mL/min and an injection volume of 10 µL was used, except for 2 µL injection volume when undertaking accurate mass analysis. The ion source for each MS was operated in ESI+ mode.

A ThermoFinnigan Surveyor HPLC coupled to a ThermoFinnigan LCQ Deca XP Plus mass spectrometer (MS) was used for preliminary sample screening. The ions of the deuterium labelled GSH-4-MSP recorded in selected reaction monitoring (SRM) mode were deduced from the results for unlabelled GSH-4-MSP.[16] The capillary temperature, sheath gas flow rate (N_2), and sweep gas flow rate were 250 °C, 30 arbitrary unit, and 19 arbitrary unit, respectively.

The ion spray voltage, capillary voltage, and tube lens offset voltage were 4500 V, 18 V, and 10 V, respectively. Helium was used as collision gas, and normalised collision energy, activation Q, activation time, and isolation width were 35 %, 0.25, 30 ms, and *m*/*z* 1.6, respectively. Instrument control, data acquisition, and data processing were performed with a Xcalibur software (version 1.3).

An Agilent 1200 HPLC coupled with a 6410 triple quadrupole MS was used for the analysis of $d_{6\text{-}10}$-GSH-4-MSP (i.e., the range of isotopologues present in the deuterated standard) in both grape berry and grape leaf extracts with MRM ion pairs shown in Table 2. The dwell time, fragmentor voltage, and collision energy were 100 ms, 122 V, and 20 V, respectively. The drying gas temperature, drying gas flow rate, nebuliser pressure, and capillary voltage were 300 °C, 8 L/min, 241 kPa, and 4000 V, respectively.

High resolution mass spectrometry (HRMS) analysis of the suspected peaks that were observed with the 6410 triple quadrupole MS were obtained with an Agilent 1200 HPLC coupled with an Agilent G6530B quadrupole time-of-flight (Q-TOF) MS. The MS scan range was *m*/*z* 100–1000 with a scan rate of 2 spectra per second; and N_2 was used as drying gas, 300 °C, 8 L/min; nebuliser gas, 276 kPa; sheath gas, 350 °C, 11 L/min. The capillary voltage, nozzle voltage, fragmentor, skimmer1, and octopoleRFPeak were 4000 V, 1000 V, 100 V, 65 V, and 750 V, respectively.

Table 2. *MRM ion pairs for the analysis of deuterium labelled GSH-4-MSP.*

Compounds	Ion pairs (*m*/*z*)
d_{10}-GSH-4-MSP	416.3→341.1
	416.3→269.3
	416.3→178.9
d_9-GSH-4-MSP	415.3→340.1
	415.3→268.3
d_8-GSH-4-MSP	414.3→339.1
	414.3→267.1
d_7-GSH-4-MSP	413.3→338.1
	413.3→266.1
d_6-GSH-4-MSP	412.3→337.1
	412.3→265.1

Statistical analysis. Mean values and standard deviations were calculated with Microsoft Excel (Microsoft Office Pro Plus 2019, USA).

RESULTS AND DISCUSSION

MS/MS analysis of MalCys-3-SH. The basic parameters of Sauvignon blanc juice from the four harvest dates were measured, with total soluble solids increasing to 21.8 °Brix, TA decreasing to 8.1 g/L, and pH being stable at approximately 3.0, as shown in Figure 2.

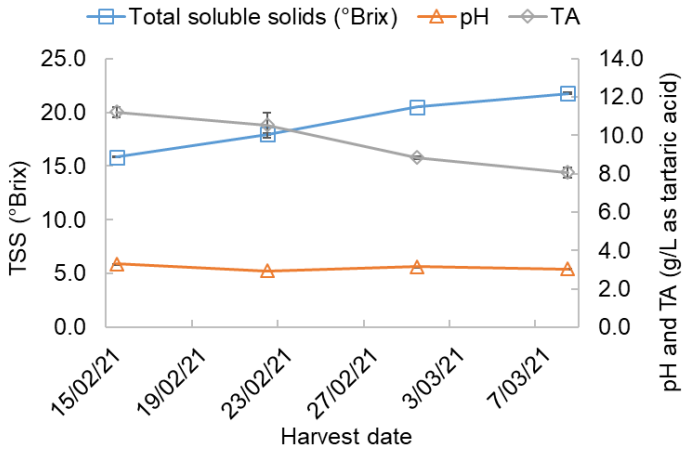

Figure 2. *Evolution of mean values (n = 3) for total soluble solids (°Brix), pH, and titratable acidity (g/L as tartaric acid) in Sauvignon blanc H5V10 grape juice from four harvest dates. Error bars represent the standard derivation replicated measurement (n = 3).*

The grape juice samples were isolated and concentrated using C18 sorbent before being analysed by HPLC-MS/MS. The MS/MS and source conditions were initially optimised with a 6410 QQQ MS, followed by further optimisation with a G6470A QQQ MS using a synthesised MalCys-3-SH standard, with total ion chromatograms from the two instruments shown in Figure 3. Comparing the peak areas and with the consideration of injection volume difference (4 µL for 6410 MS/MS vs. 1 µL for G6470A MS/MS), an increase in sensitivity of over 20-times was achieved with the G6470A QQQ MS. Thus, the optimised method on G6470A QQQ MS operated in MRM mode with monitored ion pairs is shown in Table 1 and this was utilised to screen MalCys-3-SH in Sauvignon blanc juice extracts, but MalCys-3-SH was not found in the current set of samples. Time did not permit further experimentation, but a larger selection of samples should be screened in the future to reach a more objective conclusion. Furthermore, model fermentation with MalCys-3-SH standard could be performed to evaluate its ability to release 3-SH and act as a new precursor form.

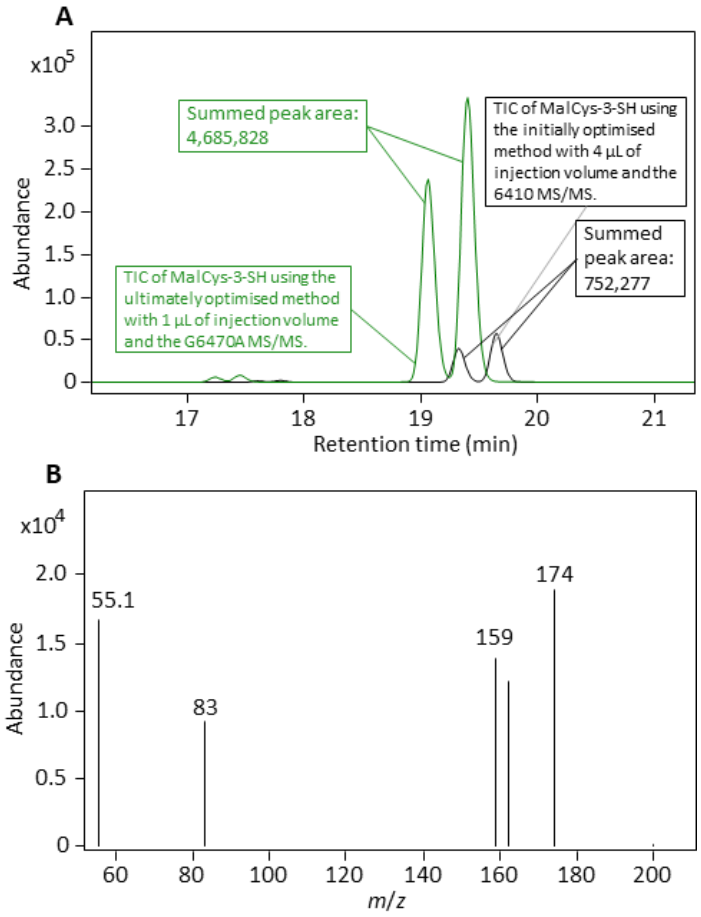

Figure 3. *HPLC-MS/MS analysis of MalCys-3-SH standard using optimised methods showing (A) total ion chromatograms analysed with G6470A QQQ MS (green trace) and 6410 QQQ MS (black trace) (B) MRM mass spectrum of MalCys-3-SH by G6470A under optimised conditions.*

Qualification of $d_{6\text{-}10}$-GSH-4-MSP in grape leaf and berry samples. The identification of natural GSH-4-MSP in Sauvignon blanc grape juice employing HPLC-MS/MS in MRM mode utilised the mass transitions of *m/z* 406→331 and *m/z* 406→259, derived from the respective loss of glycine and glutamic acid residues from GSH-4-MSP.[16] It was speculated that $d_{6\text{-}10}$-GSH-4-MSP would undergo the same fragmentation under the similar mass spectrometry conditions. Thus, due to the deuterium labelling positions on the mesityl oxide residue of GSH-4-MSP, the mass transitions for $d_{6\text{-}10}$-GSH-4-MSP were deduced, as shown in Table 2. Synthesised $d_{6\text{-}10}$-GSH-4-MSP standard was used for characterisation, showing the deuterium labelling (d_6 to d_{10}-labelling) of GSH-4-MSP (Figure 4A and 4B) with the d_6-labelled compound being the most abundant. This was not likely to be caused by the acidic environment in the mobile phase during analysis as a stability study of d_{10}-GSH-4-MSP showed that it was stable over 4 days of storage at pH 3.2.[23] On the contrary, it may originate from the labile structure of GSH-4-MSP where deuteration at enolisable positions (i.e., adjacent to the

carbonyl) could be lost due to the change of pH values during synthesis from d_{10}-mesityl oxide.[27] These aspects are of importance when considering which isotoplogues to analyse for when conducting feeding experiments with d_{10}-mesityl oxide. The expected mass transitions were associated with the loss of glycine residue (Figure 4A) and glutamic acid residue (Figure 4B) from $d_{6\text{-}10}$-GSH-4-MSP reference standard, respectively.

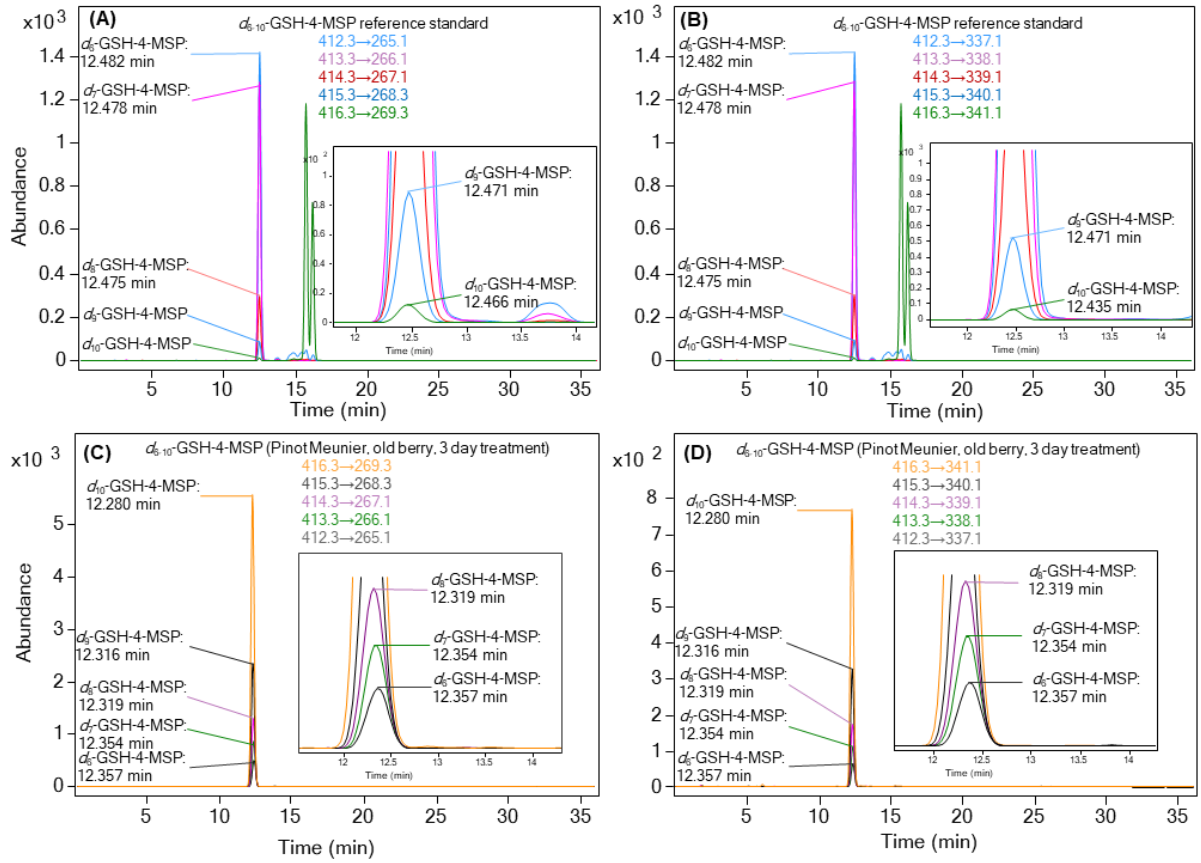

Figure 4. *Overlaid MRM chromatograms obtained from HPLC-MS/MS showing mass transitions for loss of (A) glycine residue and (B) glutamic acid residue from $d_{6\text{-}10}$-GSH-4-MSP reference standard and the respective transitions (C) and (D) from Pinot Meunier extracts of older grape berry from the 3-day treatment (refer to the treatment highlighted with a red border in Figure 1).*

The analysis of grape leaf and berry sample extracts revealed $d_{6\text{-}10}$-labelled GSH-4-MSP in all treatments of Cabernet Sauvignon and Pinot Meunier that were identical to that of the standard. Representative chromatograms from one of the samples (older Pinot Meunier berries from a 3-day treatment) are shown Figure 4C and 4D. This agreed with the observations for the $d_{6\text{-}10}$-GSH-4-MSP standard (Figure 4A and 4B), showing a successively earlier retention time as the extent of deuterium labelling of GSH-4-MSP increased. The d_{10}-GSH-4-MSP was the most

abundant deuterium labelled analogue in d_{10}-mesityl oxide treated grape tissues, being different to that observed for $d_{6\text{-}10}$-GSH-4-MSP standard (but not an anomalous situation). Samples from Shiraz grape leaves did not yield any detectable amount of any labelled GSH-4-MSP, potentially due to the shorter duration of contact with labelled mesityl oxide (2 days) compared to those for Cabernet Sauvignon and Pinot Meunier (3 to 9 days).

Accurate masses of the tentatively assigned peaks obtained from triple quadrupole MS were acquired with HPLC Q-TOF-MS using Pinot Meunier extract samples from grape leaf, younger berry, and older berry, as well as one Cabernet Sauvignon grape extract. As shown in the Table 3, the mass errors between the theoretical values and the obtained values for $d_{6\text{-}10}$-GSH-4-MSP were within 5 ppm, showing high confidence in the assignment of the peaks found in the material fed with d_{10}-mesityl oxide.

Table 3. *HRMS analysis of deuterium labelled GSH-4-MSP and Cys-4-MSP.*

Compounds	Theoretical m/z $[M + H]^+$	Observed m/z $[M + H]^+$	Mass error (ppm)
d_{10}-GSH-4-MSP	416.2276	416.2262	−3.36
d_9-GSH-4-MSP	415.2213	415.2199	−3.37
d_8-GSH-4-MSP	414.2150	414.2136	−3.38
d_7-GSH-4-MSP	413.2087	413.2076	−2.66
d_6-GSH-4-MSP	412.2025	412.2016	−2.18
d_{10}-Cys-4-MSP	230.1635	230.1635	0
d_6-Cys-4-MSP	226.1384	226.1377	−3.10

Although ions were not included in the triple quadrupole MS screening method, the accurate mass of d_6-Cys-4-MSP and d_{10}-Cys-4-MSP was also determined by HRMS (Table 3) with mass errors between the theoretical and observed values within 5 ppm. This provided further strong evidence of 4-MSP precursor formation due to the presence of d_{10}-mesityl oxide applied to berry or leaf, even though the abundances of both peaks were substantially different and had a ratio of d_6:d_{10} of approximately 150:1. The difference in abundance between d_6-Cys-4-MSP and d_{10}-Cys-4-MSP could reasonably be due to the loss of labels at enolisable positions during biochemical processes such as the conjugation of L-cysteine with d_{10}-mesityl oxide or the enzymatic degradation from d_{10}-GSH-4-MSP to its Cys counterpart. In accord with the earlier explanation for the different isotopologues of 4-GSH-MSP, such a loss of deuteration has been reported previously, where d_6-Cys-4-MSP was obtained from chemical synthesis using

d_{10}-mesityl oxide and cysteine as the starting materials.[28]

CONCLUSION

In summary, based on the proposed existence of a *N*-malonylcysteine conjugate of 3-SH, MS/MS and source conditions for two tandem mass spectrometers were optimised for MalCys-3-SH using a synthetic reference standard, and a few Sauvignon blanc juice extract samples were screened. However, MalCys-3-SH was not identified in the limited number of samples that were screened and this may infer that C18 sorbent was not optimal for MalCys-3-SH isolation in grape juice. Thus, optimisation of MalCys-3-SH isolation procedures, including the selection of different sorbent materials, is to be performed. Apart from assessing a larger selection of juice and wine samples in the future, a method for the quantification of MalCys-3-SH would need to be developed and validated, if the presence of this new precursor form is verified. Besides, evolution profiles of MalCys-3-SH in grapes during growing season and in grape must/juice during fermentation and model fermentation experiments spiked with MalCys-3-SH standard could be performed to investigate the quantitative relationship between MalCys-3-SH and 3-SH (i.e., conversion yield), to ascertain the potential contribution of such a precursor to the pool of 3-SH found in wine.

In other experiments utilising mass spectrometry, preliminary feeding trials involving deuterium labelled mesityl oxide and potted grapevines showed that grape leaves or berries could convert deuterated mesityl oxide to GSH-4-MSP and Cys-4-MSP containing the deuterium labels. However, further studies using a balanced number of grapevines are required to verify the hypothesis involving soil-borne bacteria, first by applying d_{10}-mesityl oxide to the soil of potted grapevines during the growing season followed by analysing for $d_{6\text{-}10}$-GSH-4-MSP and $d_{6\text{-}10}$-Cys-4-MSP in grapevine tissues, such as grape berries, leaves, and roots. At the same time, grape berry compositional parameters, such as total soluble solids, pH, and titratable acidity could be determined. This could be followed by the screening of soil bacteria in vineyards for their ability to secrete mesityl oxide and then relating this to the concentrations of GSH-4-MSP and Cys-4-MSP in grapevine tissues.

ACKNOWLEDGEMENTS

We thank University of Adelaide colleagues including Lishi Cai and Ross Sanders for donating their potted grapevines for the experiment and valuable discussions in setting up the trials. Christine Bottcher (Commonwealth Scientific and Industrial Research Organisation) is acknowledged for helping with HRMS data analysis. Alan Dean (The Deanery Vineyard) is

thanked for the donation of Sauvignon blanc grape materials used for potential new precursor identification. Cory Black (formerly from the Australian Wine Research Institute) is acknowledged for undertaking the synthesis of MalCys-3-SH. Xingchen Wang is a recipient of the joint scholarship of the University of Adelaide and China Scholarship Council (201806300044) and is supported by a Wine Australia Supplementary Scholarship (WA Ph1803). The Australian Research Council Training Centre for Innovative Wine Production (www.ARCwinecentre.org.au; project number IC170100008) is funded by the Australian Government with additional support from Wine Australia, Waite Research Institute and industry partners. The University of Adelaide is a member of the Wine Innovation Cluster.

REFERENCES

1. Tominaga, T.; Peyrot des Gachons, C.; Dubourdieu, D., A new type of flavor precursors in *Vitis vinifera* L. cv. Sauvignon blanc: *S*-Cysteine conjugates. *J. Agric. Food Chem.* **1998,** *46* (12), 5215-5219.

2. Capone, D. L.; Jeffery, D. W., Effects of transporting and processing Sauvignon blanc grapes on 3-mercaptohexan-1-ol precursor concentrations. *J. Agric. Food Chem.* **2011,** *59* (9), 4659-4667.

3. Thibon, C.; Böcker, C.; Shinkaruk, S.; Moine, V.; Darriet, P.; Dubourdieu, D., Identification of *S*-3-(hexanal)-glutathione and its bisulfite adduct in grape juice from *Vitis vinifera* L. cv. Sauvignon blanc as new potential precursors of 3SH. *Food Chem.* **2016,** *199*, 711-719.

4. Clark, A. C.; Deed, R. C., The chemical reaction of glutathione and *trans*-2-hexenal in grape juice media to form wine aroma precursors: The impact of pH, temperature, and sulfur dioxide. *J. Agric. Food Chem.* **2018,** *66* (5), 1214-1221.

5. Capone, D. L.; Pardon, K. H.; Cordente, A. G.; Jeffery, D. W., Identification and quantitation of 3-*S*-cysteinylglycinehexan-1-ol (Cysgly-3-MH) in Sauvignon blanc grape juice by HPLC-MS/MS. *J. Agric. Food Chem.* **2011,** *59* (20), 11204-11210.

6. Bonnaffoux, H.; Roland, A.; Rémond, E.; Delpech, S.; Schneider, R.; Cavelier, F., First identification and quantification of *S*-3-(hexan-1-ol)-γ-glutamyl-cysteine in grape must as a potential thiol precursor, using UPLC-MS/MS analysis and stable isotope dilution assay. *Food Chem.* **2017,** *237*, 877-886.

7. Peyrot des Gachons, C.; Tominaga, T.; Dubourdieu, D., Measuring the aromatic potential of *Vitis vinifera* L. cv. Sauvignon blanc grapes by assaying *S*-cysteine conjugates,

precursors of the volatile thiols responsible for their varietal aroma. *J. Agric. Food Chem.* **2000,** *48* (8), 3387-3391.

8. Howell, K. S.; Klein, M.; Swiegers, J. H.; Hayasaka, Y.; Elsey, G. M.; Fleet, G. H.; Hoj, P. B.; Pretorius, I. S.; Lopes, M. A. D., Genetic determinants of volatile-thiol release by *Saccharomyces cerevisiae* during wine fermentation. *Appl. Environ. Microbiol.* **2005,** *71* (9), 5420-5426.

9. Bonnaffoux, H.; Delpech, S.; Rémond, E.; Schneider, R.; Roland, A.; Cavelier, F., Revisiting the evaluation strategy of varietal thiol biogenesis. *Food Chem.* **2018,** *268*, 126-133.

10. Lamoureux, G. L.; Rusness, D. G., Malonylcysteine conjugates as end-products of glutathione conjugate metabolism in plants. In *Mode of Action, Metabolism and Toxicology*, Matsunaka, S.; Hutson, D. H.; Murphy, S. D., Eds. Pergamon: 1983; pp 295-300.

11. Lamoureux, G. L.; Rusness, D. G., EPTC metabolism in corn, cotton, and soybean: Identification of a novel metabolite derived from the metabolism of a glutathione conjugate. *J. Agric. Food Chem.* **1987,** *35* (1), 1-7.

12. Onisko, B. C.; Barnes, J. P.; Staub, R. E.; Walker, F. H.; Kerlinger, N., Metabolism of cycloate in radish leaf: Metabolite identification by packed capillary flow fast atom bombardment tandem mass spectrometry. *Biol. Mass Spectrom.* **1994,** *23* (10), 626-636.

13. Brazier-Hicks, M.; Evans, K. M.; Cunningham, O. D.; Hodgson, D. R. W.; Steel, P. G.; Edwards, R., Catabolism of glutathione conjugates in *Arabidopsis thaliana*: Role in metabolic reactivation of the herbicide safener fenclorim. *J. Biol. Chem.* **2008,** *283* (30), 21102-21112.

14. Lamoureux, G. L.; Rusness, D. G., Pentachloronitrobenzene metabolism in peanut. 1. Mass spectral characterization of seven glutathione-related conjugates produced in vivo or in vitro. *J. Agric. Food Chem.* **1980,** *28* (6), 1057-1070.

15. Roland, A.; Vialaret, J.; Razungles, A.; Rigou, P.; Schneider, R., Evolution of *S*-cysteinylated and *S*-glutathionylated thiol precursors during oxidation of Melon B. and Sauvignon blanc musts. *J. Agric. Food Chem.* **2010,** *58* (7), 4406-4413.

16. Fedrizzi, B.; Pardon, K. H.; Sefton, M. A.; Elsey, G. M.; Jeffery, D. W., First identification of 4-*S*-glutathionyl-4-methylpentan-2-one, a potential precursor of 4-mercapto-4-methylpentan-2-one, in Sauvignon blanc juice. *J. Agric. Food Chem.* **2009,** *57* (3), 991-995.

17. Schneider, R.; Charrier, F.; Razungles, A.; Baumes, R., Evidence for an alternative biogenetic pathway leading to 3-mercaptohexanol and 4-mercapto-4-methylpentan-2-one in wines. *Anal. Chim. Acta* **2006,** *563* (1-2), 58-64.

18. Stoj, A.; Czernecki, T.; Domagala, D.; Targonski, Z., Application of volatile compound

analysis for distinguishing between red wines from Poland and from other European countries. *S. Afr. J. Enol. Vitic.* **2017,** *38* (2), 245-263.

19. Stój, A.; Czernecki, T.; Sosnowska, B.; Niemczynowicz, A.; Matwijczuk, A., Impact of grape variety, yeast and malolactic fermentation on volatile compounds and fourier transform infrared spectra in red wines. *Pol. J. food Nutr. Sci.* **2022,** *72* (1), 39-55.

20. Rice, S.; Maurer, D. L.; Fennell, A.; Dharmadhikari, M.; Koziel, J. A., Evaluation of volatile metabolites emitted in-vivo from cold-hardy grapes during ripening using SPME and GC-MS: A proof-of-concept. *Molecules* **2019,** *24* (3), 536.

21. Zhao, N.; Zhang, Y.; Liu, D.; Zhang, J.; Qi, Y.; Xu, J.; Wei, X.; Fan, M., Free and bound volatile compounds in 'Hayward' and 'Hort16A' kiwifruit and their wines. *Eur. Food Res. Technol.* **2020,** *246* (5), 875-890.

22. Garbeva, P.; Hordijk, C.; Gerards, S.; de Boer, W., Volatile-mediated interactions between phylogenetically different soil bacteria. *Front. Microbiol.* **2014,** *5*, 289.

23. Grant-Preece, P. A.; Pardon, K. H.; Capone, D. L.; Cordente, A. G.; Sefton, M. A.; Jeffery, D. W.; Elsey, G. M., Synthesis of wine thiol conjugates and labeled analogues: Fermentation of the glutathione conjugate of 3-mercaptohexan-1-ol yields the corresponding cysteine conjugate and free thiol. *J. Agric. Food Chem.* **2010,** *58* (3), 1383-1389.

24. Boss, P. K.; Thomas, M. R., Association of dwarfism and floral induction with a grape 'green revolution' mutation. *Nature* **2002,** *416* (6883), 847-850.

25. Hayasaka, Y.; Baldock, G. A.; Pardon, K. H.; Jeffery, D. W.; Herderich, M. J., Investigation into the formation of guaiacol conjugates in berries and leaves of grapevine *Vitis vinifera* L. Cv. Cabernet Sauvignon using stable isotope tracers combined with HPLC-MS and MS/MS analysis. *J. Agric. Food Chem.* **2010,** *58* (4), 2076-2081.

26. Capone, D. L.; Sefton, M. A.; Jeffery, D. W., Application of a modified method for 3-mercaptohexan-1-ol determination to investigate the relationship between free thiol and related conjugates in grape juice and wine. *J. Agric. Food Chem.* **2011,** *59* (9), 4649-4658.

27. Shinkaruk, S.; Thibon, C.; Schmitter, J.-M.; Babin, P.; Tominaga, T.; Degueil, M.; Desbat, B.; Jussier, C.; Bennetau, B.; Dubourdieu, D.; Bennetau-Pelissero, C., Surprising structural lability of a cysteine-*S*-conjugate precursor of 4-methyl-4-sulfanylpentan-2-one, a varietal aroma in wine of *Vitis vinifera* L. cv. Sauvignon blanc. *Chem. Biodivers.* **2008,** *5* (5), 793-810.

28. Hebditch, K. R.; Nicolau, L.; Brimble, M. A., Synthesis of isotopically labelled thiol volatiles and cysteine conjugates for quantification of Sauvignon blanc wine. *J. Labelled Compd. Radiopharm.* **2007,** *50* (4), 237-243.

CHAPTER 3

Evolution and Correlation of *cis*-2-Methyl-4-propyl-1,3-oxathiane, Varietal Thiols, and Acetaldehyde during Fermentation of Sauvignon blanc Juice

Xingchen Wang,[†] Liang Chen,[†] Dimitra L. Capone,[†,‡] Aurélie Roland,[§] David W. Jeffery[*,†,‡]

[†] Department of Wine and Food Science, and Waite Research Institute, The University of Adelaide (UA), PMB 1, Glen Osmond, SA 5064, Australia

[‡] Australian Research Council Training Centre for Innovative Wine Production, UA, PMB 1, Glen Osmond, SA 5064, Australia

[§] SPO, Univ Montpellier, INRAE, Institut Agro - Montpellier SupAgro, 2 place Pierre Viala, 34060 Montpellier, France

Journal of Agricultural and Food Chemistry, **2020**, 68(32), 8676-8687

DOI: 10.1021/acs.jafc.0c03183

Statement of Authorship

Title of Paper	Evolution and Correlation of *cis*-2-Methyl-4-propyl-1,3-oxathiane, Varietal Thiols and Acetaldehyde during Fermentation of Sauvignon blanc Juice
Publication Status	☑ Published ☐ Accepted for Publication ☐ Submitted for Publication ☐ Unpublished and Unsubmitted work written in manuscript style
Publication Details	Wang, X.; Chen, L.; Capone, D.L.; Roland, A.; Jeffery, D.W. (**2020**) Evolution and Correlation of *cis*-2-Methyl-4-propyl-1,3-oxathiane, Varietal Thiols and Acetaldehyde during Fermentation of Sauvignon blanc Juice. *Journal of Agricultural and Food Chemistry*, 68 (32), 8676-8687.

Principal Author

Name of Principal Author (Candidate)	Xingchen Wang		
Contribution to the Paper	Contributed to the design of experiments. Conducted experiments and prepared and analysed samples using a range of techniques, including GC-MS. Collected, processed, analysed, interpreted and visualised the data. Produced a complete first draft of the manuscript. Reviewed and edited the manuscript.		
Overall percentage (%)	65%		
Certification:	This paper reports on original research I conducted during the period of my Higher Degree by Research candidature and is not subject to any obligations or contractual agreements with a third party that would constrain its inclusion in this thesis. I am the primary author of this paper.		
Signature		Date	13/08/2020

Co-Author Contributions

By signing the Statement of Authorship, each author certifies that:

i. the candidate's stated contribution to the publication is accurate (as detailed above);

ii. permission is granted for the candidate in include the publication in the thesis; and

iii. the sum of all co-author contributions is equal to 100% less the candidate's stated contribution.

Name of Co-Author	Liang Chen		
Contribution to the Paper	Conceived of and designed the experiments. Prepared samples for storage trials. Interpreted data. Reviewed and edited the manuscript.		
Signature		Date	17/08/2020

Name of Co-Author	Dimitra L. Capone		
Contribution to the Paper	Conceived of and designed the experiments. Conducted HPLC-MS/MS analysis and collected, processed and interpreted data. Supervised the work. Reviewed and edited the manuscript.		
Signature		Date	27/08/2020

Name of Co-Author	Aurélie Roland		
Contribution to the Paper	Contributed to the design of experiments. Interpreted data and supervised the work. Reviewed and edited the manuscript.		
Signature		Date	26/08/2020

Name of Co-Author	David W. Jeffery		
Contribution to the Paper	Conceived of and designed the experiments. Interpreted data, supervised the project and provided resources. Reviewed and edited the manuscript and acted as corresponding author.		
Signature		Date	13/08/2020

Please cut and paste additional co-author panels here as required.

JOURNAL OF AGRICULTURAL AND FOOD CHEMISTRY

pubs.acs.org/JAFC Article

Evolution and Correlation of *cis*-2-Methyl-4-propyl-1,3-oxathiane, Varietal Thiols, and Acetaldehyde during Fermentation of Sauvignon blanc Juice

Xingchen Wang, Liang Chen, Dimitra L. Capone, Aurélie Roland, and David W. Jeffery*

Cite This: *J. Agric. Food Chem.* 2020, 68, 8676−8687 Read Online

ACCESS | Metrics & More | Article Recommendations | Supporting Information

ABSTRACT: *cis*-2-Methyl-4-propyl-1,3-oxathiane (*cis*-2-MPO) was recently identified in wine and proposed to arise from the reaction of 3-sulfanylhexan-1-ol (3-SH) and acetaldehyde. However, the evolution profile of *cis*-2-MPO during alcoholic fermentation (AF) and storage and its relationship with varietal thiols and acetaldehyde production were unknown. These aspects were investigated by fermenting Sauvignon blanc juice with J7 and/or VIN13 yeast strains and assessing the stability of *cis*-2-MPO during wine storage. Moderate to strong Pearson correlations verified similar evolution trends between acetaldehyde, 3-sulfanylhexyl acetate, and *cis*-2-MPO, with initial increases and a peak during the early to middle stages of AF before consecutive decreases until the end. Contrarily, 3-SH correlated moderately only at the end of AF. A consistent decrease observed for *cis*-2-MPO when spiked into Sauvignon blanc wine and assessed during 1-year storage revealed its general instability, but acetaldehyde addition (100 mg/L), pH 3.0, and storage at 4 °C all appeared to retain *cis*-2-MPO. These results have implications for wine aroma and the potential for *cis*-2-MPO to act as a sink (or source) for 3-SH in wine over time.

KEYWORDS: *3-sulfanylhexan-1-ol, 3-sulfanylhexyl acetate, analysis, thiol precursors, stable isotope dilution assay, wine aroma, Vitis vinifera*

INTRODUCTION

As one of the most important groups of aroma impact compounds in wine, varietal thiols have attracted intensive attention from researchers due to not only their contribution to wine aroma characteristics but also their intriguing biogenesis pathways.[1] Varietal thiols have exceptionally low odor detection thresholds (ODTs) that are often exceeded by their typical concentrations in wine. 4-Methyl-4-sulfanylpentan-2-one (4-MSP, **1** in Figure 1) was the first varietal thiol identified in a Sauvignon blanc wine and contributes aromas of "boxwood" and "broom" with an ODT measured in model wine of 0.8 ng/L.[2] However, 4-MSP is orders of magnitude less abundant than 3-sulfanylhexan-1-ol (3-SH, **2** in Figure 1) and 3-sulfanylhexyl acetate (3-SHA, **3** in Figure 1), which were subsequently identified in wines.[3,4] Thus, with its aromas of "grapefruit" and "passionfruit", 3-SH is generally a more important contributor than 4-MSP to the aroma of Sauvignon blanc wines from different origins due to having a higher odor activity value (i.e., concentration in wine ÷ ODT), despite having a higher ODT (60 ng/L in model wine[3]). 3-SHA (the *O*-acetate of 3-SH) also makes an important contribution to wine aroma by imparting "passionfruit" and "boxwood-like" nuances. With an ODT of 4.2 ng/L determined in a model wine,[4] 3-SHA exists in wines at concentrations that are around tenfold lower than 3-SH, based on the molar conversion yield of 3-SH to 3-SHA.[5]

Inspired by their significance to Sauvignon blanc wine aroma in particular, additional varietal thiols have been identified, including 3-sulfanylpentan-1-ol, 3-sulfanylheptan-1-ol, 2-methyl-3-sulfanylbutan-1-ol, and 3-sulfanyl-3-methylbutan-1-ol in botrytized white wines.[6,7] Besides, varietal thiols have been reported in wines from a range of other grape cultivars, including Chardonnay,[8] Melon B.,[9] Cabernet Sauvignon,[10,11] and Merlot,[10,11] although their sensory contributions are less understood compared to Sauvignon blanc wines. The wide prevalence and sensory significance of varietal thiols have attracted much interest in understanding their formation/degradation mechanisms so that there can be better control over their concentrations in wines.

3-SH and 4-MSP in wine predominantly arise from bound forms, existing in grape berries as L-glutathione (GSH) or L-cysteine conjugates and intermediates, such as 3-*S*-glutathionylhexan-1-ol (GSH-3-SH, **4**), 3-*S*-cysteinylhexan-1-ol (Cys-3-SH, **5**), 4-*S*-glutathionyl-4-methylpentan-2-one (GSH-4-MSP, **6**), and 4-*S*-cysteinyl-4-methylpentan-2-one (Cys-4-MSP, **7**, Figure 1).[12,13] Related to the breakdown of GSH, 3-*S*-cysteinylglycinehexan-1-ol (Cysgly-3-SH, **8**, Figure 1) was identified in Sauvignon blanc juice (0−28.5 μg/L) some years ago,[14] whereas the other related dipeptide (Glucys-3-SH, **9**, Figure 1) was reported more recently.[15] In parallel, two dipeptide precursors of 4-MSP, namely, L-cysteinylglycine-4-MSP (Cysgly-4-MSP, **10**) and γ-L-glutamyl-L-cysteine-4-MSP

Received: May 20, 2020
Revised: July 13, 2020
Accepted: July 13, 2020
Published: July 29, 2020

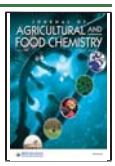

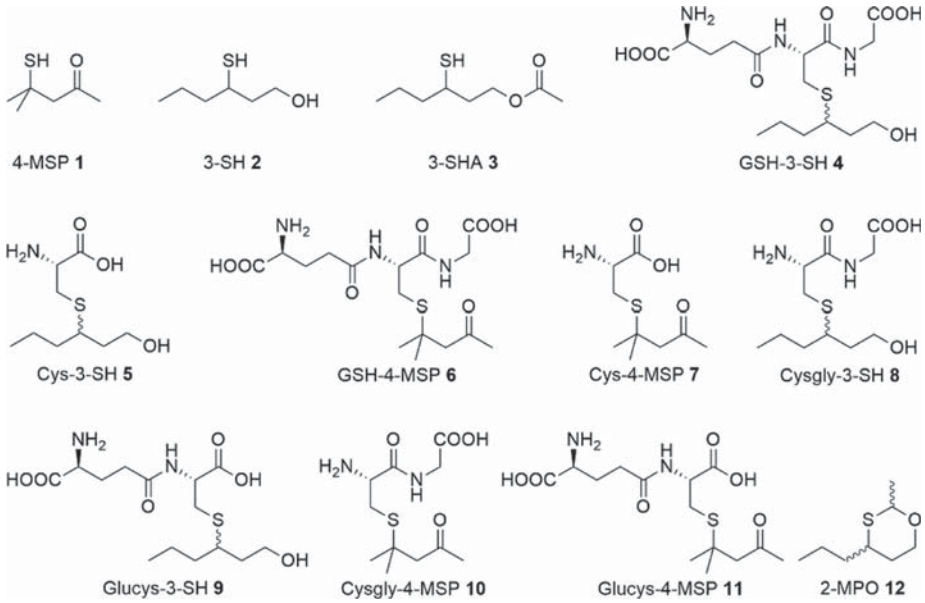

Figure 1. Structures of 4-MSP (**1**), 3-SH (**2**), 3-SHA (**3**), and their precursors (**4**−**11**),[15,16] as well as 2-MPO (**12**) that can be derived from 3-SH (**2**).[17] 4-MSP, 4-methyl-4-sulfanylpentan-2-one; 3-SH, 3-sulfanylhexan-1-ol; 3-SHA, 3-sulfanylhexyl acetate; GSH-3-SH, 3-*S*-glutathionylhexan-1-ol; Cys-3-SH, 3-*S*-cysteinylhexan-1-ol; GSH-4-MSP, 4-*S*-glutathionyl-4-methylpentan-2-one; Cys-4-MSP, 4-*S*-cysteinyl-4-methylpentan-2-one; Cysgly-3-SH, L-cysteinylglycine-3-SH; Glucys-3-SH, γ-L-glutamyl-L-cysteine-3-SH; Cysgly-4-MSP, L-cysteinylglycine-4-MSP; Glucys-4-MSP, γ-L-glutamyl-L-cysteine-4-MSP; 2-MPO, 2-methyl-4-propyl-1,3-oxathiane.

(Glucys-4-MSP, **11**, Figure 1) have also been identified in Sauvignon blanc grape juice but never quantified due to their very low abundances.[15] These nonvolatile precursors are enzymatically cleaved by yeast during alcoholic fermentation (AF) to release the free thiols, with only limited amounts of free 3-SH (around 100 ng/L) having been quantified in grape berries.[18] Much research has been devoted to accounting for thiol formation, and most recently, Bonnaffoux et al.[19] revisited some key steps of thiol biogenesis from precursors, providing a relatively integral view of current research.

Apart from understanding the biochemical release from precursors, the fate of thiols has also been considered, including the potential for oxidation. Indirect quantitation of disulfides of both 3-SH and 3-SHA under reducing conditions showed that a large proportion of "lost" 3-SH (7−53%) and 3-SHA (44−96%) could be explained.[20] Combining the quantitation of free thiols and disulfides in wines, and precursors consumed during fermentation, Bonnaffoux et al.[19] estimated that 27% of 3-SH in final wines could be explained and a minimum of 45% considering the yields of other potential precursors, including Cys-3-SH, (*E*)-2-hexenal, and 3-*S*-glutathionylhexanal along with its bisulfite adduct.[5,21,22] Highlighting some inconsistencies, however, the percentage of 3-SH produced from the alternative pathway of 1,4-addition of H_2S to (*E*)-2-hexenal has been reported by Schneider et al.[22] to be approximately 10% and by Subileau et al.[21] to be less than 0.1%. There is also an issue of timing in terms of the co-occurrence of H_2S and (*E*)-2-hexenal during winemaking under reductive conditions, making this pathway less plausible for contributing meaningful amounts of 3-SH. Furthermore, the *S*-glutathionylated conjugate of 4-MSP is barely consumed by yeast,[19] which is in stark contrast to GSH-3-SH, and more research is required to understand the pathways involved in thiol biogenesis and fate.

One of the discrepancies to date in trying to perform a mass balance to account for thiols is that greater amounts of free thiols appear to be produced than theoretically possible based on the experimentally determined conversion yields of each precursor type during AF. This is despite the relatively ample abundance of precursors in grape juice, but accounting for thiol yields from AF is further complicated by the various fates of free thiols once released. This leads to studies aimed at identifying new precursors and potential pathways of precursor utilization, along with those that investigate secondary products formed from varietal thiols, such as via their reaction with quinones and oxidation to disulfides,[20,23] or even formation of (diorgano)polysulfanes as seen with other sulfur compounds.[24,25] Pursuing the fate of 3-SH in particular, and encouraged by the existence in passionfruit[26] and formation from 3-SH and acetaldehyde,[27,28] *cis*-2-methyl-4-propyl-1,3-oxathiane (*cis*-2-MPO, **12**, Figure 1) was recently identified in wine for the first time.[17] This oxathiane was quantified in 35 of 42 commercial white wines and could account for up to 390 ng/L (or an additional 8% on a molar basis) of 3-SH in those wines.[17] The aromas of *cis*-2-MPO have been described as "fruity", "green", and "slightly burnt",[26] and the ODT of *cis*-2-MPO in a neutral white wine was determined to be 7.1 μg/L, which was much higher than its typical concentrations in the set of wines that had been analyzed so far.[17]

Investigating the relationships of *cis*-2-MPO with 3-SH, 3-SHA, and acetaldehyde has the potential to shed light on both the production of *cis*-2-MPO during winemaking and the formation and fate of varietal thiols. Given that the formation of *cis*-2-MPO is a chemical equilibrium reaction between acetaldehyde and 3-SH, thus potentially acting as a sink or source for 3-SH in wines, this study aimed to monitor the evolution of *cis*-2-MPO during AF of Sauvignon blanc juice using two yeast strains and to assess its stability in wine during storage. Addressing these aspects, diastereomers of GSH-3-SH,

https://dx.doi.org/10.1021/acs.jafc.0c03183
J. Agric. Food Chem. 2020, 68, 8676−8687

Cys-3-SH, and Cysgly-3-SH were quantified in both juice and wines along with 3-SH, 3-SHA, 4-MSP, acetaldehyde, and *cis*-2-MPO during AF. The stability of *cis*-2-MPO was assessed in a commercial Sauvignon blanc wine under different conditions involving pH; storage temperature; and the presence of acetaldehyde, SO_2, or CO_2, over a period of 1 year.

MATERIALS AND METHODS

Chemicals and Solutions. Deuterium-labeled and unlabeled standards including 3-SH, [$^2H_8$]-3-sulfanylhexan-1-ol (3-SH-d_8), 3-SHA, [$^2H_8$]-3-sulfanylhexyl acetate (3-SHA-d_8), 4-MSP, [$^2H_{10}$]-4-methyl-4-sulfanylpentan-2-one (4-MSP-d_{10}), [$^2H_4$]-2-methyl-4-propyl-1,3-oxathiane (*cis*-2-MPO-d_4), GSH-3-SH, [$^2H_9$]-3-*S*-glutathionylhexan-1-ol (GSH-3-SH-d_9), Cysgly-3-SH, Cys-3-SH, and [$^2H_8$]-3-*S*-cysteinylhexan-1-ol (Cys-3-SH-d_8) were previously prepared as described elsewhere.[17,29] *cis*-2-MPO (≥98% pure, determined to be an 85:15 ratio of *cis*/*trans*[17]), ethylenediaminetetraacetic acid disodium salt (EDTA 2Na), formic acid, 4,4′-dithiodipyridine (DTDP), and acetaldehyde (anhydrous, ≥99.5%) were purchased from Sigma-Aldrich (Castle Hill, NSW, Australia). Bond Elut C18 cartridges (500 mg, 6 mL) and Strata SDB-L cartridges (500 mg, 6 mL) were acquired from Agilent (Mulgrave, VIC, Australia) and Phenomenex (Lane Cove, NSW, Australia), respectively. High-performance liquid chromatography (HPLC) gradient-grade methanol, ethanol, and acetonitrile were sourced from Merck (Noble Park, VIC, Australia), and water was obtained from a Milli-Q purification system (Millipore, North Ryde, NSW, Australia). Model wine was prepared freshly and consisted of 10% (v/v) ethanol, saturated with potassium hydrogen tartrate and pH adjusted to 3.4 with tartaric acid solution (1 M). DTDP reagent was prepared according to a previous procedure,[30] and aliquots were stored at −20 °C prior to use.

Grape Juice and Basic Chemical Parameters. Grape juice was stored at −20 °C after harvest and consisted of a mixture of five Sauvignon blanc clones harvested in March 2018 as reported in a previous study.[31] In duplicate, the measurement of total soluble solids (TSS) was performed with a digital refractometer (Atago, PAL-1, VIC, Australia), and the titratable acidity (TA) and pH were determined with a T50 autotitrator (Mettler Toledo, Melbourne, Australia). Yeast assimilable nitrogen (YAN) was measured commercially by the Australian Wine Research Institute (AWRI) using a Randox Daytona enzymatic analyzer. Ethanol was measured with a DMA 4500M/Alcolyzer Wine ME (Anton Parr, Graz, Austria), and free and total SO_2 were measured with a GlassChem Kombo-4-OH VA/SO_2/OH still (Adelab Scientific, Adelaide, Australia) for the replicates of each treatment.

Formation and Evolution of *cis*-2-MPO during Alcoholic Fermentation and Storage. *Yeast Preparation.* VIN13 (Anchor, Cape Town, South Africa) and J7 (*Saccharomyces cerevisiae* AWRI 81, AWRI Wine Microorganism Culture Collection) were initially plated on yeast extract peptone dextrose (YPD) solid media to grow for 2 days (28 °C) followed by picking a single colony of each strain and inoculating separately into YPD liquid media and cultivating overnight on a platform incubator (180 rpm, 28 °C). Each inoculum was expanded in filter-sterilized (0.2 μm cellulose nitrate) Sauvignon blanc juice diluted to 50% with Milli-Q water and cultivated for 24 h (180 rpm, 28 °C) prior to inoculation.

Fermentation. The frozen juice was thawed at 4 °C for approximately 5 days and distributed into 2 L fermenters fitted with air-locks. Single yeast inoculation with VIN13 or J7 (2×10^6 cfu/mL per strain) in triplicate and co-inoculation of both VIN13 and J7 (1×10^6 cfu/mL of each strain) in duplicate (due to a lack of juice volume) were undertaken when the temperature of the juice had reached 15 °C. Fermentations were conducted in a temperature-controlled room at 16 °C until residual sugars were around 10 g/L (on day 17) and at 22 °C to complete the fermentation. Daily samples were taken 24 h after inoculation for the quantitation of varietal thiols, acetaldehyde, and *cis*-2-MPO from day 1 to 9 of fermentation; then on days 11, 13, 15, and 17; and finally on day 18. Once ferments were dry (<2.8 g/L residual sugar), tested by a ChemWell 2910 autoanalyzer (Awareness Technology, Palm City, FL) with a D-glucose and D-fructose test kit for discrete analyzers (Vintessential, Rowe Scientific, Adelaide, SA, Australia), wine samples were taken for the quantitation of varietal thiols, acetaldehyde, *cis*-2-MPO, and precursors of varietal thiols before 60 mg/L SO_2 (as potassium metabisulfite, PMS) was added and wines were cold-settled at 4 °C. After 2 weeks, the clear wines were racked under the protection of dry ice, bottled in amber beer bottles, sealed with crown caps, and stored at 4 °C prior to further analysis. Wines were sampled for the analysis of wine basic chemical parameters, varietal thiols, acetaldehyde, and *cis*-2-MPO after 4 months of storage in a bottle. After this 4-month period, a duplicate series of each wine was subsampled (5 mL) into clear ampoules (10 mL), sparged with N_2, and then sealed and stored at 16 °C, for analysis at each time point (day 7, 31, 59, 92, and 183) over a storage period of 6 months to investigate the influence of wine aging on the concentration of *cis*-2-MPO.

Stability of *cis*-2-MPO under Different Conditions. The stability of *cis*-2-MPO was evaluated by periodically monitoring a commercial Sauvignon blanc wine (2016, 12.4% v/v alcohol) spiked with *cis*-2-MPO (final concentration of 471 ng/L according to gas chromatography−mass spectrometry (GC−MS) analysis). The effects of pH, acetaldehyde, SO_2, CO_2, and temperature were separately investigated, with treatments prepared in large volumes and split prior to storage. Samples for pH 3.0, 3.7, and 4.0 treatments were prepared by adjusting the wine from pH 3.4 to 3.0 with saturated tartaric acid solution and to pH 3.7 and 4.0 with sodium hydroxide solution (1 M). The addition of acetaldehyde (100 mg/L), SO_2 (100 mg/L, added as PMS using a 52.6 g/L solution), or CO_2 (added as dry ice to displace air prior to adding wine) was used to prepare acetaldehyde, SO_2, or CO_2 treatments, respectively. In duplicate, a series of *cis*-2-MPO spiked wine (5 mL) for each treatment was sealed in 10 mL clear ampoules and stored in the dark at 22 °C, except for temperature treatments that were also stored at 4, 40, or 60 °C. Samples were taken for analysis on days 13, 20, 27, 33, 42, 70, 105, 129, 223, 315, and finally on day 364 of the storage period.

Organic Acids in Wines. Analysis of organic acids was undertaken with an Agilent 1100 HPLC (Agilent, Melbourne, VIC, Australia) coupled with a diode-array detector (DAD) at 210 nm, as previously reported,[32] using ChemStation software (version B.04.03, Agilent). Wine samples were centrifuged (3857*g* at 15 °C for 10 min) prior to the analysis of the supernatant.

Stable Isotope Dilute Assay (SIDA)−HPLC−Tandem Mass Spectrometry (MS/MS) for Thiol Precursor Quantitation. The method of Capone et al.[18] was used for the extraction and analysis of precursors in juice and wine.

SIDA−HPLC−MS/MS for Thiol Quantitation. 3-SH, 3-SHA, and 4-MSP were analyzed after derivatization with DTDP, according to the method of Capone et al.,[17] using an Agilent 1200 HPLC coupled with a 6410 triple quadrupole mass spectrometer. HPLC and MS parameters were the same as reported previously for the optimized method, except that the dwell time was 40 ms, and the fragmentor voltage and collision energy were as detailed in Table S1 of the Supporting Information.

SIDA−Headspace-Solid-Phase Microextraction (HS-SPME)−GC−MS for *cis*-2-MPO Quantitation. *cis*-2-MPO was quantitated by the previously reported method using an Agilent 7890A GC coupled with a Agilent 5975C inert XL MSD with a triple-axis detector[17] but with separation using a DB-WAXetr column (60 m × 0.25 mm, 0.25 μm, J&W Agilent). Sample preparation and GC−MS parameters were the same as the optimized method.[17]

Acetaldehyde Quantitation. Samples (800 μL) obtained for analysis were immediately placed on dry ice and then stored at −20 °C prior to analysis using a ChemWell 2910 autoanalyzer and a Megazyme K-ACHYD enzyme kit (Deltagen Australia, Kilsyth, VIC, Australia) following the manufacturer's instructions.

Statistical Analysis. Mean and standard deviation (SD) values were determined with Excel (Microsoft 2019). Figures were constructed using GraphPad Prism 7 (version 7.02, GraphPad Software Inc., San Diego, CA). Repeated-measures analysis of variance (ANOVA) with the estimation method and constraints set

https://dx.doi.org/10.1021/acs.jafc.0c03183
J. Agric. Food Chem. 2020, 68, 8676−8687

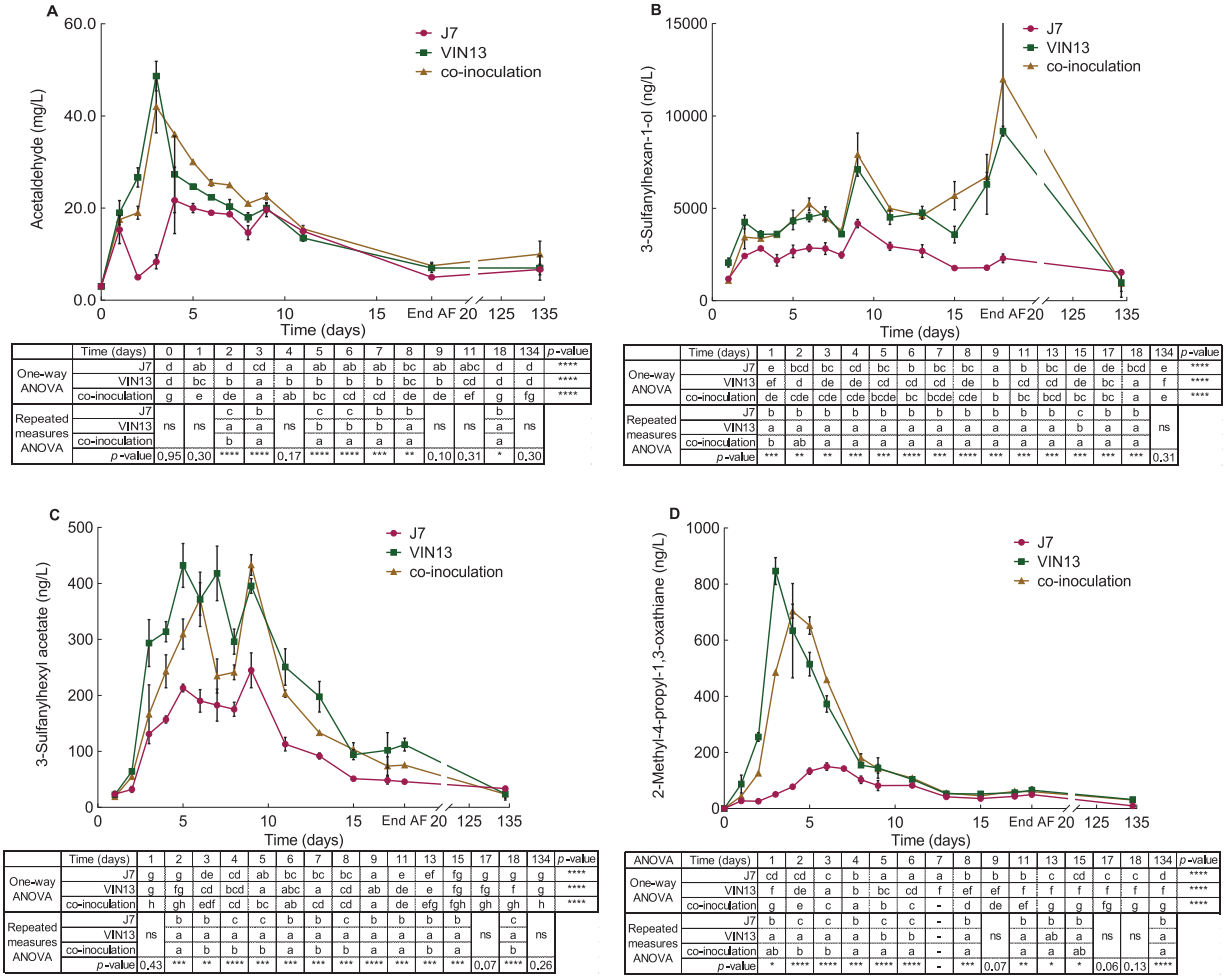

	Time (days)	0	1	2	3	4	5	6	7	8	9	11	18	134	p-value
One-way ANOVA	J7	d	ab	d	cd	a	ab	ab	ab	bc	ab	abc	d	d	****
	VIN13	d	bc	b	a	b	b	b	b	bc	b	cd	d	d	****
	co-inoculation	g	e	de	a	ab	bc	cd	cd	de	de	ef	g	fg	****
Repeated measures ANOVA	J7			c	b		c	c	b	b			b		
	VIN13	ns	ns	a	a	ns	b	b	b	a	ns	ns	a	ns	
	co-inoculation			b	a		a	a	a	a			a		
	p-value	0.95	0.30	****	****	0.17	****	****	***	**	0.10	0.31	*	0.30	

	Time (days)	1	2	3	4	5	6	7	8	9	11	13	15	17	18	134	p-value
One-way ANOVA	J7	e	bcd	bc	cd	bc	b	bc	bc	a	b	bc	de	de	bcd	e	****
	VIN13	ef	d	de	de	cd	cd	cd	de	b	cd	cd	de	bc	a	f	****
	co-inoculation	de	cde	cde	cde	bcde	bc	bcde	cde	b	bc	bcd	bc	bc	a	e	****
Repeated measures ANOVA	J7	b	b	b	b	b	b	b	b	b	b	b	c	b	b		
	VIN13	a	a	a	a	a	a	a	a	a	a	a	b	a	a	ns	
	co-inoculation	b	ab	a	a	a	a	a	a	a	a	a	a	a	a		
	p-value	***	**	**	***	***	****	***	****	***	***	***	***	***	***	0.31	

	Time (days)	1	2	3	4	5	6	7	8	9	11	13	15	17	18	134	p-value
One-way ANOVA	J7	g	g	de	cd	ab	bc	bc	bc	a	e	ef	fg	g	g	g	****
	VIN13	g	fg	cd	bcd	a	abc	a	cd	ab	de	e	fg	fg	f	g	****
	co-inoculation	h	gh	edf	cd	bc	ab	cd	cd	a	de	efg	fgh	gh	gh	h	****
Repeated measures ANOVA	J7		b	b	c	c	b	b	c	b	b	b	b		c		
	VIN13	ns	a	a	a	a	a	a	a	a	a	a	a	ns	a	ns	
	co-inoculation		a	b	b	b	a	b	b	a	a	b	a		b		
	p-value	0.43	***	**	****	***	***	***	***	****	***	***	***	0.07	****	0.26	

ANOVA	Time (days)	1	2	3	4	5	6	7	8	9	11	13	15	17	18	134	p-value
One-way ANOVA	J7	cd	cd	c	b	a	a	a	b	b	b	c	cd	c	c	d	****
	VIN13	f	de	a	b	bc	cd	f	ef	ef	f	f	f	f	f	f	****
	co-inoculation	g	e	c	a	b	c	-	d	de	ef	g	g	fg	g	g	****
Repeated measures ANOVA	J7	b	c	c	b	c	c	-	b		b	b	b			b	
	VIN13	a	a	a	a	b	b	-	a	ns	a	ab	a	ns	ns	a	
	co-inoculation	ab	b	b	a	a	a	-	a		a	a	ab			a	
	p-value	*	****	****	***	****	****	-	***	0.07	**	*	*	0.06	0.13	****	

Figure 2. Evolution profiles during alcoholic fermentation and after 4 months of storage in a bottle at 4 °C for (A) acetaldehyde, (B) 3-SH, (C) 3-SHA, and (D) *cis*-2-MPO. Error bars represent the standard deviation of replicate fermentations. Tables below the figures show the results of one-way ANOVA, revealing differences between sampling days within treatments, and repeated-measures ANOVA, revealing differences between treatments within sampling days. Different letters in each row of one-way ANOVA or each column of repeated-measures ANOVA indicate significant differences at $\alpha = 0.05$. *: $p < 0.05$, **: $p < 0.01$, ***: $p < 0.005$, ****: $p < 0.001$. Data points on days 13, 15, and 17 for acetaldehyde and on day 7 for *cis*-2-MPO in VIN13 and co-inoculation treatments were not obtained due to instrumentation issues. Data points on day 9 for 3-SH and 3-SHA appear to be aberrant values. Values of 3-SH were extrapolated when outside the calibration level of 5000 ng/L.

as least squares (LS) and $a_1 = 0$, respectively, followed by Tukey's multiple comparisons ($\alpha = 0.05$) using XLSTAT (version 2020.1, Addinsoft, Qi Statistics, Reading, U.K.), was conducted to test for differences according to the treatment for acetaldehyde, 3-SH, 3-SHA, 4-MSP, and *cis*-2-MPO during AF and the evolution of *cis*-2-MPO during storage on the basis of time and treatment, with treatment as the fixed effect. One-way ANOVA followed by Tukey's multiple comparisons ($\alpha = 0.05$) was undertaken on the basis of treatment using XLSTAT for basic chemical parameters, precursors of varietal thiols in both juice and wines, and organic acids in wines. Two-tailed Pearson correlation analysis with $\alpha = 0.05$ was applied to verify the correlation between *cis*-2-MPO and other analytes using SPSS Statistics (version 25.0, IBM, Armonk, NY).

RESULTS AND DISCUSSION

Basic Chemical Parameters of Grape Juice and Final Wines. As summarized in Table S2 of the Supporting Information, the TSS, pH, and TA of the grape juice were 19.3 °Bx, 3.43, and 8.9 g/L (as tartaric acid at pH 8.2), respectively, which were in the range of those reported for the individual juices of each Sauvignon blanc clone.[31] YAN was determined to be 97 mg/L (Table S2 of the Supporting Information), which was lower than the typical minimum concentration (140 mg/L[33]) in grape juice required to ferment to dryness but was in the range of Adelaide Hills Sauvignon blanc grape juices that were fermented to completion in a previous study.[29] The juice was fermented separately with VIN13 and J7 yeast strains and with co-inoculation using both strains, yielding experimental wines with basic chemical parameters (ethanol, free and total SO_2, TA, pH, and residual sugar) as presented in Table S3 of the Supporting Information. The ethanol content in the VIN13 treatment (11.9% v/v) was significantly higher than those in the other two treatments but of little practical consequence given the small numerical difference (0.2 and 0.3% v/v). Both free and total SO_2 varied but were not significantly different among the wines, although the concentrations in VIN13 replicate 3 and co-inoculation replicate 1 were much lower than those in their other replicates. Neither TA nor pH was significantly different across the wines (Table S3 of the Supporting Information).

https://dx.doi.org/10.1021/acs.jafc.0c03183
J. Agric. Food Chem. 2020, 68, 8676−8687

Organic acids (tartaric, malic, citric, acetic, lactic) in the wines were quantified by HPLC-DAD (Figure S1 of the Supporting Information). Tartaric acid (2.48−2.71 g/L) and malic acid (2.65−2.98 g/L) were the major organic acids in the wine samples, as expected. Citric and acetic acids (each ∼0.20 g/L) were the other two organic acids measured, with concentrations in line with the typical range.[34] Lactic acid (0.10−0.21 g/L) was a minor analyte, given that malolactic fermentation was not specifically conducted, and was present within the usual concentration range (0−3 g/L) for wines.[34] One-way ANOVA showed that only lactic acid was significantly different among the treatments for the various acids, being approximately double in the J7 treatment (215 mg/L).

Evolution Profile of Acetaldehyde. *cis*-2-MPO is presumably produced by the reaction of acetaldehyde with 3-SH in wines,[17] thus monitoring the evolution of these three compounds during winemaking could potentially explain (at least partially) the origin of *cis*-2-MPO. J7 is a strain of flor yeast that has been characterized by its ability to generate acetaldehyde during production of sherry-style wines.[35] It has also been shown to produce more acetaldehyde upon fermentation of grape juice in comparison with Port yeast 350 and Champagne yeast 352[35] and was therefore investigated in conjunction with VIN13 (often used with Sauvignon blanc and known as a good thiol releaser[36]) to assess the influence of acetaldehyde accumulation on the production of *cis*-2-MPO during AF. Both VIN13 and co-inoculation treatments showed a similar trend for evolution of acetaldehyde (Figure 2A), with concentrations having increased significantly and peaking at 49 and 42 mg/L, respectively, on the third day of fermentation, and then decreasing gradually thereafter to 7 and 5 mg/L, respectively. Notably, acetaldehyde in the J7 treatment was generally lower than in the other two treatments (Figure 2A) and appeared to be produced at a slower rate. J7 fermentations showed a gradual increase of acetaldehyde, which peaked at 22 mg/L on the fourth day (except for a significant decrease from day 1 to 2 as shown in Figure 2A) and then decreased in parallel with the other two treatments to a final level of 5 mg/L on day 18. Overall, the concentration profile for acetaldehyde during AF was in accordance with previous studies using different grape varieties or yeast strains.[37−39] After a 4-month period of storage at 4 °C in the dark, acetaldehyde was determined to be up to 4 mg/L higher (up to 33% increase on average) in all ferments, except for the decrease from 6 to 4 mg/L in one of the VIN13 ferments (−33%), although the difference was not statistically significant compared to the levels at the end of AF.

Evolution Profiles of Varietal Thiols. Despite the passage of more than two decades since varietal thiols were identified in wines, only limited data was available in terms of the evolution of varietal thiols during alcoholic fermentation. Tominaga et al.[12] monitored 3-SH, 4-MSP, and 4-methyl-4-sulfanylpentan-2-ol during Sauvignon blanc fermentation over 5 days, showing that the concentration of 3-SH increased in the first 4 days of fermentation and decreased on the last day. In a Sauvignon blanc and Semillon fermentation study, 3-SH increased continuously during AF, while 3-SHA initially increased before decreasing at the end of AF.[40] In a Merlot fermentation study, a general trend was observed for 3-SH, 3-SHA, and 4-MSP, whereby their concentrations increased as residual sugar decreased.[41] Differently, 3-SH and 4-MSP were found to increase at an early stage of AF for Sauvignon blanc juice followed by a general plateau with fluctuations until the end of fermentation.[19] In the present study, 3-SH, 3-SHA, and 4-MSP were quantified during AF of Sauvignon blanc juice inoculated with two different yeast strains (Figures 2 and 3).

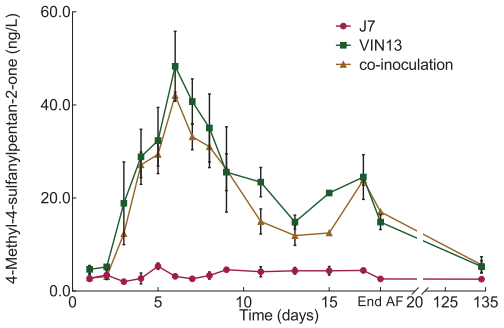

	Time (days)	1	2	3	4	5	6	7	8	9	11	13	15	17	18	134	*p*-value
One-way ANOVA	J7	bc	abc	c	bc	a	bc	bc	abc	ab	ab	ab	ab	ab	bc	bc	****
	VIN13	f	f	def	bcde	bcd	a	ab	abc	cde	cde	ef	cde	cde	ef	f	****
	co-inoculation	g	g	efg	bcd	bc	a	ab	ab	bcd	defg	efg	efg	bcde	cdef	fg	****
Repeated measures ANOVA	J7	b	ab	b	b	b	b	b	b	b	c	b	c	b	c		
	VIN13	a	a	a	a	a	a	a	a	a	a	a	a	a	b	ns	
	co-inoculation	b	b	ab	a	a	a	a	a	a	b	a	b	a	a		
	p-value	*	*	*	***	***	****	****	***	**	***	***	****	***	****	0.05	

Figure 3. Evolution profile during alcoholic fermentation and after 4 months of storage in a bottle at 4 °C for 4-methyl-4-sulfanylpentan-2-one. Error bars represent the standard deviation of replicate fermentations. The table below the figure shows the results of one-way ANOVA, revealing differences between sampling days within treatments, and repeated-measures ANOVA, revealing differences between treatments within sampling days. Different letters in each row of one-way ANOVA or each column of repeated-measures ANOVA indicate significant differences at $\alpha = 0.05$. *: $p < 0.05$, **: $p < 0.01$, ***: $p < 0.005$, ****: $p < 0.001$.

After the first day of fermentation (24 h after inoculation), the concentration of 3-SH in VIN13 treatments was 2068 ng/L and significantly higher than those of J7 (1181 ng/L) and co-inoculation (1095 ng/L) treatments (Figure 2B). In contrast, the concentration of 3-SH on the first sampling date was much lower in previous reports, ranging from below the limit of quantitation (LOQ, 8.0 ng/L) to 64 ng/L in the Merlot fermentation study[41] and less than 100 ng/L in another Sauvignon blanc study.[12] A number of factors could explain the differences, including grape variety (Sauvignon blanc vs Merlot), grape region (Australia vs Spain vs France), yeast strain, and the knowledge from recent findings that frozen juice can lead to significantly higher concentrations of varietal thiols in the corresponding wine.[31]

Except for the aberrant value on day 9, the concentration of 3-SH increased on the second day of fermentation and remained relatively stable with fluctuations at around 4000−5000 ng/L for both VIN13 (days 2−15) and co-inoculation (day 2−17) and 2000−3000 ng/L for J7 between days 2 and 13, with these results being in agreement with those of Tominaga et al.[12] and Bonnaffoux et al.[19] This was followed by a significant and consecutive increase from 3580 to 9177 ng/L (extrapolated values used when outside the calibration range of 5000 ng/L) in the last 3 days of fermentation (day 15−18) for VIN13 and from 5688 to 11 988 ng/L (significant increase only from day 17 to 18) for co-inoculation, whereas a general decrease was evident between days 13 and 17 followed by a minor and insignificant increase from day 17 to 18 for the J7 treatment (Figure 2B). Similar results were also observed by Concejero et al.[41] in the Merlot fermentation trial, where 3-SH increased during an early stage of AF and peaked at a density

https://dx.doi.org/10.1021/acs.jafc.0c03183
J. Agric. Food Chem. 2020, 68, 8676−8687

of around 1030−1060 g/L (early to middle stage of AF), before a decrease until the density had reached 1015−1020 g/L (late stage of AF), followed by another increase at the end of AF. The increase of 3-SH at the end of AF could potentially be related to yeast autolysis that normally occurs at the end of fermentation with the release of a series of enzymes,[42] which could potentially include enzymes involved in 3-SH release. This could be supported by the identification of aminopeptidases in yeast autolysate,[43] enzymes known to be involved with yeast autolysis[44] and thiol precursor degradation.[45] The different profiles for 3-SH at the end of AF in the J7 treatment compared to VIN13 and co-inoculation could have been related to VIN13 potentially yielding enzymes upon autolysis that were related to thiol release. Given that degradation of precursors of varietal thiols occurs within yeast cells,[45] the outcome could also partially be from the release of intracellular 3-SH upon yeast autolysis.

In terms of the influence of different yeast strains on 3-SH production, VIN13 yielded significantly higher concentrations than J7 from day 1 of AF (Figure 2B), whereas the co-inoculation treatment had a similar concentration of 3-SH to J7, before increasing to levels that were consistent with VIN13 after the third day of AF. The lower initial concentration and a swift increase of 3-SH on the second and third days in the co-inoculation treatment might be explained by VIN13 taking over AF after producing toxins that killed J7.[46] After a 4-month storage period at 4 °C, the concentration of 3-SH in both VIN13 and co-inoculation treatments significantly decreased to 983 and 928 ng/L, respectively, affording concentrations that were approximately 90% less than those at the end of AF (day 18). The J7 treatment also witnessed a significant decrease after storage of 33%, ending up at 1527 ng/L. The relatively large standard deviation (RSD of 25.4%) obtained in the co-inoculation treatment on day 18 resulted from the substantial difference in concentrations between the duplicates (9838 and 14 134 ng/L). The concentrations of 3-SH in VIN13 treatment replicate 3 and co-inoculation replicate 1 on day 134 were 437 and 404 ng/L, respectively, which caused high standard deviation values for both of these treatments and possibly resulted from the low level of free SO_2 in these two samples (Table S3 of the Supporting Information). The significant decrease of 3-SH concentration after storage could be related to fermentations being conducted with relatively small volumes so that a limited amount of O_2 could be sufficient to oxidize 3-SH and due to free SO_2 in VIN13 and co-inoculation treatments being lower than that in the J7 treatment (Table S3 of the Supporting Information). SO_2 plays a vital role in protecting 3-SH in wines,[47] but losses of 3-SH have been reported previously for Bordeaux rosé wines with free SO_2 maintained at 25 mg/L, where an average 34% of 3-SH was lost after 3 months of storage on lees for ten wines, and an average of 53% was lost after 1 year of bottle storage for another set of nine wines.[48]

The evolution of 3-SHA during fermentation (Figure 2C) was different from that of 3-SH. One day after yeast inoculation, 3-SHA was determined to be at a similar level in all of the wines with 24, 22, and 19 ng/L in J7, VIN13, and co-inoculation treatments, respectively. From there, the concentrations peaked at 432 ng/L for VIN13, 372 ng/L for co-inoculation, and 262 ng/L for J7 on day 5 or 6 of fermentation, before decreasing until the end of fermentation to 160, 109, and 72 ng/L, respectively. The decrease in 3-SHA was on the order of 74−80% on average compared with the highest concentrations in each treatment, which accorded with the observations of Tominaga et al.[40] and Concejero et al.,[41] who found more than 30 and 50% decreases in 3-SHA in Sauvignon blanc and Merlot winemaking trials, respectively. The reason for the decrease of 3-SHA during the latter stage of AF was unknown but was possibly caused by hydrolysis or oxidation phenomena as outlined below or was potentially due to a change in yeast metabolism as a function of lipid concentration[49] when yeast began to autolyse.[50] Such aspects would need to be the subject of future studies. Moreover, the peak and final concentrations of 3-SHA in the present study were in the same ranges as those in the Sauvignon blanc and Merlot studies.[40,41] Similar to the results for 3-SH, VIN13 produced the most 3-SHA during AF and J7 yielded the least (Figure 2C). However, after the 4-month storage period, concentrations of 3-SHA in each treatment had decreased to approximately 24−33 ng/L, which represented a loss of 27−79% of 3-SHA compared to the values determined at the end of AF (day 18). Analogous results have been reported for commercial Sauvignon blanc wines, where up to 46% of 3-SHA was lost during 3 months of storage at 15 °C in the dark and, on average, 69% was lost after 7 months.[51] Hydrolysis is one important reason for the loss of 3-SHA in wines,[51] with lower pH accelerating the process.[52] Moreover, the formation of disulfides from 3-SHA caused by thiol oxidation[20,53] or the loss of 3-SH during storage, caused by a reaction with quinones originating from oxidation of wine phenolics,[23] potentially prompted an equilibrium shift toward 3-SH that enhanced the hydrolysis of 3-SHA. The lower levels of free SO_2 in VIN13 and co-inoculation wines (Table S3 of the Supporting Information) might account for the greater decrease of 3-SHA in these two treatments compared to that in J7.

The evolution of 4-MSP was also monitored during AF (Figure 3), although it was not the focus of the present study. Values for 4-MSP between 0.9 and 3.1 ng/L, which were at the limit of detection (LOD) and LOQ of the method,[30] were extrapolated and shown in the figure to provide a complete evolution profile for the J7 treatment in particular. Twenty-four hours after inoculation, the concentration of 4-MSP was determined to be significantly higher in VIN13 (5 ng/L) compared with 3 ng/L in both J7 and co-inoculation treatments. The concentrations remained relatively stable for another 24 h before a significant increase to 48 ng/L and 40 ng/L in VIN13 and co-inoculation treatments on day 5, respectively (aside from an insignificant increase from day 2 to 3). This was followed by a consistent decrease for 7 days, reaching a low of 15 and 12 ng/L in these two treatments on day 13. The concentrations increased again for 4 days to approximately 24 ng/L on day 17 in both VIN13 and co-inoculation treatments and dropped slightly at the end of AF to 15 and 17 ng/L in VIN13 and co-inoculation, respectively. These values were in agreement with previous results where 4-MSP in Sauvignon blanc wine made from each of the individual clones present in the juice of the current study were determined to be between undetectable to 97 ng/L.[31] In contrast to VIN13 and co-inoculation, 4-MSP in the J7 treatment remained at low levels (between 2 and 5 ng/L) throughout the fermentation period. Compared with the highest concentrations reached during AF in VIN13 and co-inoculation treatments (day 6), 4-MSP decreased by 69 and 59% at the end of AF. Evolution of 4-MSP in VIN13 and co-inoculation treatments during the first 6 days of AF was similar to the results reported by Tominaga et al.,[12] who found that 4-

https://dx.doi.org/10.1021/acs.jafc.0c03183
J. Agric. Food Chem. 2020, 68, 8676−8687

MSP continued to increase during AF of Sauvignon blanc must. However, this was in contrast to the results determined for Merlot fermentation where 4-MSP was mainly observed at the end of AF; such a difference may be caused by a lower concentration of precursors of 4-MSP in the Merlot grape must.[41] After 4 months of storage in a bottle, 4-MSP in VIN13 and co-inoculation treatments declined to 5 and 6 ng/L, leading to respective decreases of 64 and 67% on average compared with those at the end of AF, whereas 4-MSP remained at low abundance in the J7 treatment.

Evolution Profile of *cis*-2-MPO. The concentration of *cis*-2-MPO was determined in the treatments during AF, as shown in Figure 2D. *cis*-2-MPO was not detected in grape juice (below the LOD of 2.6 ng/L) prior to initiation of AF but was found 24 h postinoculation: 27 ng/L for J7, 87 ng/L for VIN13, and 44 ng/L for co-inoculation. The concentration continued to significantly increase and reached 847 ng/L on day 3 of AF before a constant decrease until the end of fermentation in VIN13. Production of *cis*-2-MPO in the co-inoculation treatment was slightly slower than that of VIN13, having significantly increased to 704 ng/L by day 4 and then decreasing continually to concentrations similar to VIN13 at the end of fermentation (65 ng/L in VIN13 vs 60 ng/L in co-inoculation). J7 produced the least *cis*-2-MPO during the early to middle stages of AF, revealing a gradual increase (only significant from day 3 to 5) to 150 ng/L on day 6 and then a decrease to 50 ng/L (day 18). The concentrations of *cis*-2-MPO at the end of fermentation in all of the ferments were in line with the range previously reported for commercial Sauvignon blanc wines from Australia and France (14−80 ng/L).[17] Notably, the evolution of *cis*-2-MPO during AF (Figure 2D) was comparable to that of acetaldehyde (Figure 2A), indicating for the first time a potential correlation between these two parameters.

During the storage period of 4 months post-AF at 4 °C, *cis*-2-MPO decreased to 32 ng/L in the VIN13 wine, 30 ng/L in the co-inoculation wine, and 10 ng/L in the J7 wine (Figure 2D), or by around 50−81%. The declines in concentration of *cis*-2-MPO during both AF and the storage period were likely to be related to changes in equilibrium between the *cis*-2-MPO, 3-SH, and acetaldehyde. Although acetaldehyde increased during storage (albeit not in a statistically significant manner), the substantial decrease of 3-SH during storage could be the reason why *cis*-2-MPO also decreased, as a result of a shift in equilibrium (which implies the potential for some buffering against 3-SH loss).

Stability of *cis*-2-MPO in Wines. After the initial 4-month bottle storage period, samples were sealed in a series of glass ampoules and stored at 16 °C for 6 months to explore the evolution of *cis*-2-MPO during cellaring under relatively anoxic conditions (Figure 4A). Over the time course of analyses, the concentration of *cis*-2-MPO in both J7 and co-inoculation treatments respectively decreased significantly by 9 and 27% on average, whereas its concentration in VIN13 decreased by 13%, although this change was not statistically different (one-way ANOVA in Figure 4A). With respect to the concentration of *cis*-2-MPO in different treatments, J7 was always significantly lower than the other two during the storage period (repeated-measures ANOVA in Figure 4A).

Examining the stability further, the concentration of *cis*-2-MPO was periodically monitored for 1 year using a commercial Sauvignon blanc wine that was spiked with 471 ng/L of *cis*-2-MPO and maintained under different conditions

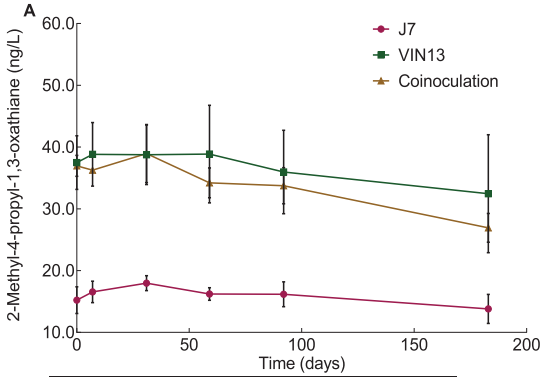

	Time (days)	0	7	31	59	92	183	*p*-value
One-way ANOVA	J7	ab	ab	a	ab	ab	b	*
	VIN13	ns						0.52
	co-inoculation	a	a	a	a	a	b	****
Repeated measures ANOVA	J7	b	b	b	b	b	b	
	VIN13	a	a	a	a	a	a	
	co-inoculation	a	a	a	a	a	a	
	p-value	****	****	****	****	****	***	

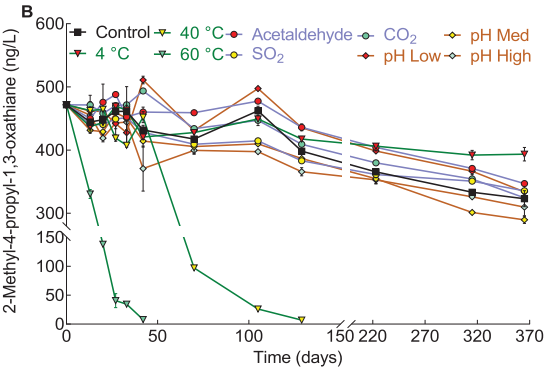

	Time (days)	0	13	20	27	33	42	70	105	129	223	315	364	*p*-value
One-way ANOVA	Control	a	bc	bc	ab	ab	cd	de	ab	e	f	g	g	****
	4 °C	a	cd	bc	a	ab	de	cde	abc	de	ef	f	f	****
	40 °C	a	ab	ab	c	c	b	d	e	f				****
	60 °C	a	b	c	d	d	e							****
	Acetaldehyde	a	ab	a	a	ab	ab	ab	a	abc	bcd	cd	d	****
	SO_2	a	bc	bc	b	b	cd	d	d	e	f	fg	g	****
	CO_2	ab	ab	bc	ab	ab	a	cd	bc	d	e	e	f	****
	pH low	bc	cd	cd	cde	ef	a	def	ab	de	fg	gh	h	****
	pH medium	a	bc	bcd	a	ab	cd	de	cde	e	f	g	g	****
	pH high	a	ab	abcd	abc	abc	def	bcde	cde	defg	efg	fg	g	****
Repeated measures ANOVA	Control	ns	ab	abc	ab	a	c	bc	bc	bc	bc	d	bc	
	4 °C		ab	abc	ab	a	cd	b	c	ab	a	a	a	
	40 °C		ab	ab	c	a	bc	e	f	e	d	f	e	
	60 °C		c	d	d	b	e	f	g	e	d	f	e	
	Acetaldehyde		ab	a	a	a	abc	a	b	a	a	b	b	
	SO_2		ab	abc	abc	a	c	cd	d	cd	c	c	bc	
	CO_2		a	abc	ab	a	ab	b	c	b	b	c	bc	
	pH low		ab	ab	bc	a	a	b	a	a	a	bc	bc	
	pH medium		b	bc	abc	a	cd	cd	de	c	c	e	d	
	pH high		ab	c	bc	a	d	d	e	d	c	d	cd	
	p-values	1.0	****	****	****	****	****	****	****	****	****	****	****	

Figure 4. Stability of *cis*-2-MPO in (A) Sauvignon blanc research wine during storage for 6 months at 16 °C; (B) commercial Sauvignon blanc wine under various conditions including different temperatures (4, 22, 40, and 60 °C), pH values (3.0, 3.4, 3.7, and 4.0), inclusion of acetaldehyde or SO_2, and sparging the samples with CO_2. The tables below the figures show the results of one-way ANOVA, revealing differences between sampling days within treatments, and repeated-measures ANOVA, revealing differences between treatments within sampling days. Values in 60 and 40 °C treatments from day 70 and 223, respectively, were set as 0 for the repeated-measures ANOVA. Different letters in each row of one-way ANOVA or each column of repeated-measures ANOVA indicate significant difference at $\alpha = 0.05$. *: $p < 0.05$, **: $p < 0.01$, ***: $p < 0.005$, ****: $p < 0.001$.

of temperature, pH, acetaldehyde, etc., as specified in the Materials and Methods section (Figure 4B). The decrease of *cis*-2-MPO was gradual and consistent in most treatments, with 17−39% being lost by the end of the trial, except for wine

https://dx.doi.org/10.1021/acs.jafc.0c03183
J. Agric. Food Chem. 2020, 68, 8676−8687

samples stored at 40 and 60 °C (Figure 4B). Samples stored at 60 °C witnessed the fastest disappearance of *cis*-2-MPO, with the concentration no longer quantifiable after 42 days. This was followed by the treatment at 40 °C, where the concentration of *cis*-2-MPO was indeterminable after 129 days of storage. However, *cis*-2-MPO in the treatment at 4 °C showed the slowest decrease, leading to a significantly higher concentration than the other treatments after 223 days of storage, except for acetaldehyde and low-pH treatments, but these were significantly lower than 4 °C from 315 days of storage. The different evolution profiles of *cis*-2-MPO for the temperature treatments showed that lower storage temperature could slow down the loss of *cis*-2-MPO in wine over time.

As for the other conditions, the concentration of *cis*-2-MPO in pH 3.0 treatment was significantly higher than those for pH 3.7 and 4.0 treatments from 42 days of storage to the end of the experiment, which implied that lower pH could potentially retain *cis*-2-MPO. In the acetaldehyde treatment, the *cis*-2-MPO concentration was significantly higher than those for CO_2 and SO_2 addition (each aimed at preventing oxidation, particularly of ethanol to acetaldehyde) from 70 days of storage until the last data point, when there was no significant difference between these three treatments. The slower decreasing trend with acetaldehyde addition implied a role for acetaldehyde in preserving *cis*-2-MPO levels.[17] The relative stability of *cis*-2-MPO in the wine samples during storage revealed the potential for different effects of the conditions, with some promoting the faster disappearance of *cis*-2-MPO via hydrolysis back into 3-SH and acetaldehyde or some other degradation pathway, thus acting either as an aroma source or a sink with respect to 3-SH during wine storage.

Correlation Analysis. In a previous study that determined the concentrations of *cis*-2-MPO, 3-SH, and 3-SHA in commercial wines, a strong correlation was only found between *cis*-2-MPO and 3-SH.[17] Herein, the correlations between the evolution of *cis*-2-MPO and each of 3-SH, 3-SHA, and acetaldehyde during AF were explored by Pearson correlation analysis, and the influence of different yeast strains was compared (Figure 5). In the J7 ferment, *cis*-2-MPO was significantly correlated with acetaldehyde and 3-SHA, showing correlation coefficients of 0.671 ($p < 0.001$) and 0.791 ($p < 0.001$), respectively. VIN13 and co-inoculation ferments showed significant correlations for *cis*-2-MPO with acetaldehyde and 3-SHA, albeit somewhat opposite to that of J7: correlation coefficients with acetaldehyde were 0.872 ($p < 0.001$) and 0.824 ($p < 0.001$) for VIN13 and co-inoculation, respectively, and with 3-SHA were 0.515 ($p = 0.001$) and 0.503 ($p = 0.009$), respectively. However, correlations between *cis*-2-MPO and 3-SH in both VIN13 and co-inoculation ferments were not significant, with moderately weak and negative correlation coefficients of −0.304 and −0.267, respectively, in contrast to that of J7 with a moderate and significant correlation coefficient of 0.430 ($p = 0.005$). Generally, J7 showed higher correlation coefficients between *cis*-2-MPO and 3-SH or 3-SHA, but lower between *cis*-2-MPO and acetaldehyde than VIN13 and co-inoculation. In the end, specific experiments could be conducted with wine spiked with 3-SH and acetaldehyde (or labeled analogues) to further assess this correlation as well as verify causation (i.e., confirming that *cis*-2-MPO arises from the chemical reaction of 3-SH with acetaldehyde).

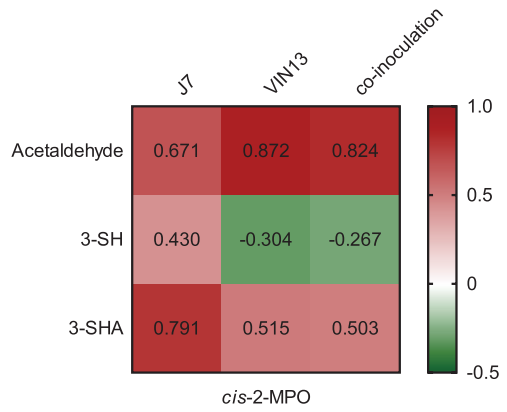

Figure 5. Pearson correlation coefficients between the evolution of *cis*-2-MPO compared to acetaldehyde, 3-SH, and 3-SHA during AF of Sauvignon blanc juice with J7, VIN13, and their co-inoculation treatment. Two-tailed Pearson correlation analysis was conducted with $\alpha = 0.05$.

In combination with the observations in Figure 2, the evolution of *cis*-2-MPO during AF was generally found to parallel that of acetaldehyde, whereas its evolution did not appreciably follow that of 3-SH, especially considering *cis*-2-MPO kept decreasing when 3-SH increased at the end of AF. This implied that acetaldehyde could be a limiting factor in the formation/stability of *cis*-2-MPO instead of 3-SH, although more work is required to verify this proposition. On the other hand, the significant correlation of 3-SHA with *cis*-2-MPO in all three treatments was most likely because 3-SHA and *cis*-2-MPO arise from 3-SH, with their production from 3-SH being related to yeast activity (i.e., enzymatic acetylation and acetaldehyde formation). However, when only considering the concentrations of all four compounds in the wines at the end of AF, moderate to strong correlations were revealed by Pearson correlation analysis between *cis*-2-MPO/acetaldehyde, *cis*-2-MPO/3-SH, and *cis*-2-MPO/3-SHA ($r = 0.414$, 0.489, and 0.612, respectively), which were in line with the results determined in a previous study.[17] Considering that 3-SHA is the *O*-acetate of 3-SH, their overall correlation was also explored, revealing a significant and strong correlation coefficient ($r = 0.752$, $p = 0.031$) at the end of fermentation: notably, the correlation during AF for J7 was strong ($r = 0.727$), but it was weak in the VIN13 and co-inoculation treatments ($r = 0.005$ and 0.107, respectively).

Precursors of Varietal Thiols in Juice and Wines. As a final piece of the biogenesis story, concentrations of precursors of 3-SH in both grape juice and wines were quantified (Figure 6) based on a previous method.[18] The concentrations of GSH-3-SH and Cys-3-SH in juice were 100.1 and 12.8 μg/L, respectively, which were similar to a range of fresh juices from the Adelaide Hills reported previously (33.7−170.7 μg/L for GSH-3-SH and 10.7−44.6 μg/L for Cys-3-SH) but much lower (unsurprisingly) than in the juice obtained from prefermentation freezing treatment of berries (724.3 and 73.1 μg/L).[31] The domination of GSH-3-SH over Cys-3-SH in the juice was in agreement with previous studies.[9,16] Additionally, the concentrations of (*R*)-Cys-3-SH and (*S*)-3-Cys-3-SH in grape juice were 3.8 and 9.0 μg/L, respectively, which was in line with the results of Capone et al.[54] where the concentration of (*S*)-3-Cys-3-SH was higher than that of the *R* counterpart. The (*R*)- and (*S*)-diastereomers of GSH-3-SH in grape juice were 27.2 and 73.0 μg/L, respectively, again

https://dx.doi.org/10.1021/acs.jafc.0c03183
J. Agric. Food Chem. 2020, 68, 8676−8687

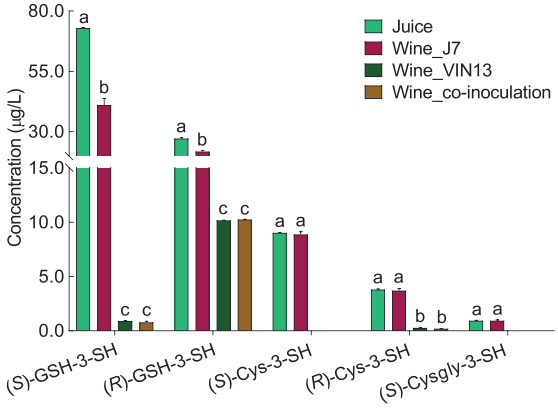

Figure 6. Precursors of varietal thiols in Sauvignon blanc juice and wines produced with two different yeast strains (VIN13 and J7) and with their co-inoculation. Error bars represent the standard deviation of replicate measurements (juice) or replicate ferments. Different letters above the bars for each precursor type indicate significant differences between means evaluated by one-way ANOVA followed by Tukey's multiple comparisons with $\alpha = 0.05$.

aligning with previous studies where (*S*)-GSH-3-SH was more abundant.[18,29,54] Only the (*S*)-isomer of Cysgly-3-SH was able to be quantified in grape juice, at 0.93 μg/L (LOQ and LOD were 0.5 and 0.2 μg/L, respectively[14]), which was in accordance with previous studies using Adelaide Hills Sauvignon blanc[14,31] but lower than that found in another report for Sauvignon blanc juice.[15]

Precursors were also quantified in wines after fermentation, showing that the J7 treatment had statistically greater amounts of precursors than VIN13 and co-inoculation treatments and was more similar to the initial juice concentrations (Figure 6). In contrast, mean values for VIN13 and co-inoculation treatments were not statistically different. Specifically, (*S*)-GSH-3-SH was mostly consumed in VIN13 and co-inoculation treatments, with only 0.9 and 0.8 μg/L remaining, respectively, whereas 41.0 μg/L was left in the J7 treatment. There were 10.2 and 10.3 μg/L of (*R*)-GSH-3-SH left in VIN13 and co-inoculation treatments but 21.8 μg/L left in the J7 treatment. The disproportionate consumption of (*S*)-GSH-3-SH (the more abundant diastereomer) might imply a certain stereoselectivity of the enzymatic thiol release reaction,[55] although a previous work did not find a strong link between the precursor and free thiol stereochemistries.[29] The J7 treatment barely affected (*S*)-Cysgly-3-SH and both (*R*/*S*)-Cys-3-SH, whereas (*S*)-Cysgly-3-SH and (*S*)-Cys-3-SH were undetectable in VIN13 and co-inoculation treatments and only 0.19 and 0.27 μg/L of (*R*)-Cys-3-SH remained in VIN13 and co-inoculation treatments, respectively.

Given that thiol precursors lead to the release of 3-SH, which is a necessary component for forming *cis*-2-MPO, a potential correlation could exist given the general tendency of greater precursor consumption in treatments where higher amounts of *cis*-2-MPO were quantified. However, there were not enough data points for conducting the correlation analysis between precursors and *cis*-2-MPO. Considering the concentrations of precursors before and after fermentation and the total concentration of 3-SH and 3-SHA in the wines, the yield of 3-SH from precursors was calculated on a molar basis, giving mean values of 19% for J7, 27% for VIN13, and 32% for co-inoculation. These values were generally in line with a previous report that specified that at least 33% of the origin of 3-SH could be explained by considering GSH-3-SH, Cysgly-3-SH, and Cys-3-SH.[19] Finally, it remains to develop a chiral analytical method for determination of *cis*-2-MPO enantiomers for comparison with precursor diastereomers and enantiomers of 3-SH and 3-SHA to enable a complete exploration of the stereochemical relationships from precursors to thiols to oxathiane.

In summary, the evolution profiles of *cis*-2-MPO, varietal thiols, and acetaldehyde were monitored during AF of Sauvignon blanc juice elaborated with monocultures and co-inoculation of J7 and VIN13 yeast strains. The concentrations of acetaldehyde, 3-SHA, and *cis*-2-MPO increased during the early stage of AF before a continuous decrease to the end, with the evolution of *cis*-2-MPO generally paralleling that of acetaldehyde and 3-SHA. The correlations of *cis*-2-MPO/acetaldehyde and *cis*-2-MPO/3-SHA were significant and moderate to strong, according to Pearson correlation analysis. In contrast, the production of 3-SH increased at the initial stage of AF and remained stable during the middle part of AF, followed by a slight decrease before an increase toward the end. The correlation of 3-SH with *cis*-2-MPO was insignificant but weakly negative in VIN13 and co-inoculation treatments, in contrast to the moderate and significant correlation in the J7 treatment. These observations suggested that the limiting factor in the formation/stability of *cis*-2-MPO in wine could be acetaldehyde.

With respect to the influence of yeast strain on the production of acetaldehyde, 3-SH, 3-SHA, and *cis*-2-MPO, the VIN13 treatment had higher concentrations of these compounds than the J7 treatment, whereas the co-inoculation treatment was similar to J7 at the initial stage of AF but quickly reached the higher levels seen for the VIN13 treatment. The results for 3-SH profiles were in line with the observation that higher concentrations of precursors were consumed in VIN13 and co-inoculation treatments than in the J7 treatment. Isomerically, the (*S*)-configured isomers of GSH-3-SH, Cysgly-3-SH, and Cys-3-SH were more abundant than their (*R*)-configured diastereomers in juice and were preferably consumed during AF of all treatments.

After a 4-month period of bottle storage at 4 °C, the concentrations of 3-SH, 3-SHA, 4-MSP, and *cis*-2-MPO all decreased, whereas that of acetaldehyde increased slightly, highlighting that *cis*-2-MPO was unstable in the longer term. The general instability of *cis*-2-MPO was further confirmed by a 1-year storage trial, which showed the potential of a source/sink relationship with 3-SH, and if acting as a source, *cis*-2-MPO may have the potential to compensate for 3-SH losses during wine aging. Lower storage temperature (4 °C), the addition of acetaldehyde (100 mg/L), and lower pH (3.0) of wine all appeared to retain *cis*-2-MPO, which may have implications should wines be found to possess suprathreshold levels of *cis*-2-MPO. Although some of the complex factors underlying formation and fate of thiols remain to be answered, this study identified the link between acetaldehyde production and *cis*-2-MPO formation, which can help guide future research into related phenomena.

■ ASSOCIATED CONTENT

Supporting Information

The Supporting Information is available free of charge at https://pubs.acs.org/doi/10.1021/acs.jafc.0c03183.

https://dx.doi.org/10.1021/acs.jafc.0c03183
J. Agric. Food Chem. 2020, 68, 8676−8687

Organic acids in final wines (Figure S1), mass spectrometer parameters for quantitation of varietal thiols by HPLC−MS/MS (Table S1), and basic parameters of grape juice and wine (Tables S2 and S3) (PDF)

AUTHOR INFORMATION

Corresponding Author

David W. Jeffery − *Department of Wine and Food Science, and Waite Research Institute and Australian Research Council Training Centre for Innovative Wine Production, The University of Adelaide (UA), Glen Osmond, SA 5064, Australia;* orcid.org/0000-0002-7054-0374; Phone: +61 8313 6649; Email: david.jeffery@adelaide.edu.au

Authors

Xingchen Wang − *Department of Wine and Food Science, and Waite Research Institute, The University of Adelaide (UA), Glen Osmond, SA 5064, Australia*

Liang Chen − *Department of Wine and Food Science, and Waite Research Institute, The University of Adelaide (UA), Glen Osmond, SA 5064, Australia*

Dimitra L. Capone − *Department of Wine and Food Science, and Waite Research Institute and Australian Research Council Training Centre for Innovative Wine Production, The University of Adelaide (UA), Glen Osmond, SA 5064, Australia;* orcid.org/0000-0003-4424-0746

Aurélie Roland − *SPO, Institut Agro—Montpellier SupAgro, INRAE, Univ Montpellier, 34060 Montpellier, France*

Complete contact information is available at: https://pubs.acs.org/10.1021/acs.jafc.0c03183

Funding

X.W. is the recipient of the joint scholarship of the University of Adelaide and China Scholarship Council (201806300044) and is supported by a Wine Australia supplementary scholarship (WA Ph1803). L.C. was also the recipient of the joint scholarship of the University of Adelaide and China Scholarship Council and supported by a Wine Australia supplementary scholarship (AGW Ph1512). The Australian Research Council Training Centre for Innovative Wine Production (www.ARCwinecentre.org.au; project number IC170100008) is funded by the Australian Government with additional support from Wine Australia, Waite Research Institute, and industry partners. The University of Adelaide is a member of the Wine Innovation Cluster.

Notes

The authors declare no competing financial interest.

ACKNOWLEDGMENTS

We thank Paul Boss and Sue Maffei (CSIRO) for providing access and advice regarding HPLC−MS/MS instrumentation. We acknowledge UA colleagues Ross Sanders, for helping with varietal thiol precursor analysis, Ana Hranilovic, for assistance with yeast cultivation and wine bottling, and Nick van Holst, for assistance with ChemWell operation and analysis of organic acids. Simon Dillon from the AWRI Wine Microorganism Culture Collection is thanked for providing a sample of J7 yeast strain.

ABBREVIATIONS

3-SH, 3-sulfanylhexan-1-ol; 3-SHA, 3-sulfanylhexyl acetate; 4-MSP, 4-methyl-4-sulfanylpentan-2-one; AF, alcoholic fermentation; *cis*-2-MPO, *cis*-2-methyl-4-propyl-1,3-oxathiane; Cys-3-SH, 3-*S*-cysteinylhexan-1-ol; Cys-4-MSP, 4-*S*-cysteinyl-4-methylpentan-2-one; Cysgly-3-SH, 3-*S*-cysteinylglycinehexan-1-ol; Cysgly-4-MSP, L-cysteinylglycine-4-MSP; DTDP, 4,4′-dithiodipyridine; Glucys-3-SH, γ-L-glutamyl-L-cysteine-3-SH; Glucys-4-MSP, γ-L-glutamyl-L-cysteine-4-MSP; GSH, L-glutathione; GSH-3-SH, 3-*S*-glutathionylhexan-1-ol; GSH-4-MSP, 4-*S*-glutathionyl-4-methylpentan-2-one; HPLC−MS/MS, high-performance liquid chromatography-tandem mass spectrometry; HS-SPME−GC−MS, headspace-solid phase microextraction−gas chromatography−mass spectrometry; LOD, limit of detection; LOQ, limit of quantitation; ODT, odor detection threshold; SD, standard deviation; SIDA, stable isotope dilute assay; TA, titratable acidity; TSS, total soluble solids; YPD, yeast extract peptone dextrose

REFERENCES

(1) Roland, A.; Schneider, R.; Razungles, A.; Cavelier, F. Varietal thiols in wine: Discovery, analysis and applications. *Chem. Rev.* **2011**, *111*, 7355−7376.

(2) Darriet, P.; Tominaga, T.; Lavigne, V.; Boidron, J.-N.; Dubourdieu, D. Identification of a powerful aromatic component of *Vitis vinifera* L. var. Sauvignon wines: 4-Mercapto-4-methylpentan-2-one. *Flavour Fragr. J.* **1995**, *10*, 385−392.

(3) Tominaga, T.; Furrer, A.; Henry, R.; Dubourdieu, D. Identification of new volatile thiols in the aroma of *Vitis vinifera* L. var. Sauvignon blanc wines. *Flavour Fragr. J.* **1998**, *13*, 159−162.

(4) Tominaga, T.; Darriet, P.; Dubourdieu, D. Identification of 3-mercaptohexyl acetate in Sauvignon wine, a powerful aromatic compound exhibiting box-tree odor. *Vitis* **1996**, *35*, 207−210.

(5) Thibon, C.; Böcker, C.; Shinkaruk, S.; Moine, V.; Darriet, P.; Dubourdieu, D. Identification of *S*-3-(hexanal)-glutathione and its bisulfite adduct in grape juice from *Vitis vinifera* L. cv. Sauvignon blanc as new potential precursors of 3SH. *Food Chem.* **2016**, *199*, 711−719.

(6) Sarrazin, E.; Shinkaruk, S.; Tominaga, T.; Bennetau, B.; Frerot, E.; Dubourdieu, D. Odorous impact of volatile thiols on the aroma of young botrytized sweet wines: Identification and quantification of new sulfanyl alcohols. *J. Agric. Food Chem.* **2007**, *55*, 1437−1444.

(7) Tominaga, T.; Baltenweck-Guyot, R.; Peyrot des Gachons, C.; Dubourdieu, D. Contribution of volatile thiols to the aromas of white wines made from several *Vitis vinifera* grape varieties. *Am. J. Enol. Vitic.* **2000**, *51*, 178−181.

(8) Capone, D. L.; Barker, A.; Williamson, P. O.; Francis, I. L. The role of potent thiols in Chardonnay wine aroma. *Aust. J. Grape Wine Res.* **2018**, *24*, 38−50.

(9) Roland, A.; Schneider, R.; Charrier, F.; Cavelier, F.; Rossignol, M.; Razungles, A. Distribution of varietal thiol precursors in the skin and the pulp of Melon B. and Sauvignon blanc grapes. *Food Chem.* **2011**, *125*, 139−144.

(10) Bouchilloux, P.; Darriet, P.; Henry, R.; Lavigne-Cruege, V.; Dubourdieu, D. Identification of volatile and powerful odorous thiols in Bordeaux red wine varieties. *J. Agric. Food Chem.* **1998**, *46*, 3095−3099.

(11) Darriet, P.; Bouchilloux, P.; Poupot, C.; Bugaret, Y.; Clerjeau, M.; Sauris, P.; Medina, B.; Dubourdieu, D. Effects of copper fungicide spraying on volatile thiols of the varietal aroma of Sauvignon blanc, Cabernet Sauvignon and Merlot wines. *Vitis* **2001**, *40*, 93−99.

(12) Tominaga, T.; Peyrot des Gachons, C.; Dubourdieu, D. A new type of flavor precursors in *Vitis vinifera* L. cv. Sauvignon blanc: *S*-Cysteine conjugates. *J. Agric. Food Chem.* **1998**, *46*, 5215−5219.

(13) Peyrot des Gachons, C.; Tominaga, T.; Dubourdieu, D. Sulfur aroma precursor present in *S*-glutathione conjugate form: Identi-

https://dx.doi.org/10.1021/acs.jafc.0c03183
J. Agric. Food Chem. 2020, 68, 8676−8687

fication of *S*-3-(hexan-1-ol)-glutathione in must from *Vitis vinifera* L. cv. Sauvignon blanc. *J. Agric. Food Chem.* **2002**, *50*, 4076−4079.
(14) Capone, D. L.; Pardon, K. H.; Cordente, A. G.; Jeffery, D. W. Identification and quantitation of 3-*S*-cysteinylglycinehexan-1-ol (Cysgly-3-MH) in Sauvignon blanc grape juice by HPLC-MS/MS. *J. Agric. Food Chem.* **2011**, *59*, 11204−11210.
(15) Bonnaffoux, H.; Roland, A.; Rémond, E.; Delpech, S.; Schneider, R.; Cavelier, F. First identification and quantification of *S*-3-(hexan-1-ol)-γ-glutamyl-cysteine in grape must as a potential thiol precursor, using UPLC-MS/MS analysis and stable isotope dilution assay. *Food Chem.* **2017**, *237*, 877−886.
(16) Jeffery, D. W. Spotlight on varietal thiols and precursors in grapes and wines. *Aust. J. Chem.* **2016**, *69*, 1323−1330.
(17) Chen, L.; Capone, D. L.; Jeffery, D. W. Identification and quantitative analysis of 2-methyl-4-propyl-1,3-oxathiane in wine. *J. Agric. Food Chem.* **2018**, *66*, 10808−10815.
(18) Capone, D. L.; Sefton, M. A.; Jeffery, D. W. Application of a modified method for 3-mercaptohexan-1-ol determination to investigate the relationship between free thiol and related conjugates in grape juice and wine. *J. Agric. Food Chem.* **2011**, *59*, 4649−4658.
(19) Bonnaffoux, H.; Delpech, S.; Rémond, E.; Schneider, R.; Roland, A.; Cavelier, F. Revisiting the evaluation strategy of varietal thiol biogenesis. *Food Chem.* **2018**, *268*, 126−133.
(20) Roland, A.; Delpech, S.; Dagan, L.; Ducasse, M.-A.; Cavelier, F.; Schneider, R. Innovative analysis of 3-mercaptohexan-1-ol, 3-mercaptohexylacetate and their corresponding disulfides in wine by stable isotope dilution assay and nano-liquid chromatography tandem mass spectrometry. *J. Chromatogr. A* **2016**, *1468*, 154−163.
(21) Subileau, M.; Schneider, R.; Salmon, J.-M.; Degryse, E. New insights on 3-mercaptohexanol (3MH) biogenesis in Sauvignon blanc wines: Cys-3MH and (*E*)-hexen-2-al are not the major precursors. *J. Agric. Food Chem.* **2008**, *56*, 9230−9235.
(22) Schneider, R.; Charrier, F.; Razungles, A.; Baumes, R. Evidence for an alternative biogenetic pathway leading to 3-mercaptohexanol and 4-mercapto-4-methylpentan-2-one in wines. *Anal. Chim. Acta* **2006**, *563*, 58−64.
(23) Nikolantonaki, M.; Magiatis, P.; Waterhouse, A. L. Measuring protection of aromatic wine thiols from oxidation by competitive reactions vs wine preservatives with *ortho*-quinones. *Food Chem.* **2014**, *163*, 61−67.
(24) Starkenmann, C.; Chappuis, C. J.-F.; Niclass, Y.; Deneulin, P. Identification of hydrogen disulfanes and hydrogen trisulfanes in H_2S bottle, in flint, and in dry mineral white wine. *J. Agric. Food Chem.* **2016**, *64*, 9033−9040.
(25) Kreitman, G. Y.; Danilewicz, J. C.; Jeffery, D. W.; Elias, R. J. Copper(II)-mediated hydrogen sulfide and thiol oxidation to disulfides and organic polysulfanes and their reductive cleavage in wine: Mechanistic elucidation and potential applications. *J. Agric. Food Chem.* **2017**, *65*, 2564−2571.
(26) Winter, M.; Furrer, A.; Willhalm, B.; Thommen, W. Identification and synthesis of two new organic sulfur compounds from the yellow passion fruit (*Passiflora edulis* f. *flavicarpa*). *Helv. Chim. Acta* **1976**, *59*, 1613−1620.
(27) Pickenhagen, W.; Brönner-Schindler, H. Enantioselective synthesis of (+)- and (-)-*cis*-2-methyl-4-propyl-1,3-oxathiane and their olfactive properties. *Helv. Chim. Acta* **1984**, *67*, 947−952.
(28) Scafato, P.; Colangelo, A.; Rosini, C. A new efficient enantioselective synthesis of (+)-*cis*-2-methyl-4-propyl-1,3-oxathiane, a valuable ingredient for the aroma of passion fruit. *Chirality* **2009**, *21*, 176−182.
(29) Chen, L.; Capone, D. L.; Tondini, F. A.; Jeffery, D. W. Chiral polyfunctional thiols and their conjugated precursors upon wine-making with five *Vitis vinifera* Sauvignon blanc clones. *J. Agric. Food Chem.* **2018**, *66*, 4674−4682.
(30) Capone, D. L.; Ristic, R.; Pardon, K. H.; Jeffery, D. W. Simple quantitative determination of potent thiols at ultratrace levels in wine by derivatization and high-performance liquid chromatography−tandem mass spectrometry (HPLC-MS/MS) analysis. *Anal. Chem.* **2015**, *87*, 1226−1231.
(31) Chen, L.; Capone, D. L.; Nicholson, E. L.; Jeffery, D. W. Investigation of intraregional variation, grape amino acids, and pre-fermentation freezing on varietal thiols and precursors for *Vitis vinifera* Sauvignon blanc. *Food Chem.* **2019**, *295*, 637−645.
(32) Li, S. J.; Bindon, K.; Bastian, S. E. P.; Jiranek, V.; Wilkinson, K. L. Use of winemaking supplements to modify the composition and sensory properties of Shiraz wine. *J. Agric. Food Chem.* **2017**, *65*, 1353−1364.
(33) Bely, M.; Sablayrolles, J.-M.; Barre, P. Automatic detection of assimilable nitrogen deficiencies during alcoholic fermentation in oenological conditions. *J. Ferment. Bioeng.* **1990**, *70*, 246−252.
(34) Waterhouse, A. L.; Sacks, G. L.; Jeffery, D. W. Acids. *Understanding Wine Chemistry*; John Wiley & Sons, Ltd.: Chichester, U.K., 2016; pp 19−20.
(35) Fornachon, J. C. M. Fermentation of Grape Juice by the Flor Yeasts. *Studies on the Sherry Flor*; Australian Wine Board: Adelaide, Australia, 1972; p 25.
(36) Swiegers, J. H.; Kievit, R. L.; Siebert, T.; Lattey, K. A.; Bramley, B. R.; Francis, I. L.; King, E. S.; Pretorius, I. S. The influence of yeast on the aroma of Sauvignon blanc wine. *Food Microbiol.* **2009**, *26*, 204−211.
(37) Jackowetz, J. N.; Dierschke, S.; Mira de Orduña, R. Multifactorial analysis of acetaldehyde kinetics during alcoholic fermentation by *Saccharomyces cerevisiae*. *Food Res. Int.* **2011**, *44*, 310−316.
(38) Li, E. H.; de Orduna, R. M. Acetaldehyde kinetics of enological yeast during alcoholic fermentation in grape must. *J. Ind. Microbiol. Biotechnol.* **2017**, *44*, 229−236.
(39) Benito, S.; Hofmann, T.; Laier, M.; Lochbuhler, B.; Schuttler, A.; Ebert, K.; Fritsch, S.; Rocker, J.; Rauhut, D. Effect on quality and composition of Riesling wines fermented by sequential inoculation with non-*Saccharomyces* and *Saccharomyces cerevisiae*. *Eur. Food Res. Technol.* **2015**, *241*, 707−717.
(40) Tominaga, T.; Niclass, Y.; Frerot, E.; Dubourdieu, D. Stereoisomeric distribution of 3-mercaptohexan-1-ol and 3-mercaptohexyl acetate in dry and sweet white wines made from *Vitis vinifera* (Var. Sauvignon blanc and Semillon). *J. Agric. Food Chem.* **2006**, *54*, 7251−7255.
(41) Concejero, B.; Hernandez-Orte, P.; Astrain, J.; Lacau, B.; Baron, C.; Ferreira, V. Evolution of polyfunctional mercaptans and their precursors during Merlot alcoholic fermentation. *LWT—Food Sci. Technol.* **2016**, *65*, 770−776.
(42) Fleet, G. H. Growth of yeasts during wine fermentations. *J. Wine Res.* **1990**, *1*, 211−223.
(43) Masuda, T.; Hayashi, R.; Hata, T. Aminopeptidases in the acidic fraction of the yeast autolysate. *Agric. Biol. Chem.* **1975**, *39*, 499−505.
(44) Babayan, T. L.; Bezrukov, M. G. Autolysis in yeasts. *Acta Biotechnol.* **1985**, *5*, 129−136.
(45) Cordente, A.; Capone, D.; Curtin, C. Unravelling glutathione conjugate catabolism in *Saccharomyces cerevisiae*: The role of glutathione/dipeptide transporters and vacuolar function in the release of volatile sulfur compounds 3-mercaptohexan-1-ol and 4-mercapto-4-methylpentan-2-one. *Appl. Microbiol. Biotechnol.* **2015**, *99*, 9709−9722.
(46) Mocke, B. A. *The Breeding of Yeast Strains for Novel Oenological Outcomes*; University of Stellenbosch: Stellenbosch, 2005; pp 44−45.
(47) Blanchard, L.; Darriet, P.; Dubourdieu, D. Reactivity of 3-mercaptohexanol in red wine: Impact of oxygen, phenolic fractions, and sulfur dioxide. *Am. J. Enol. Vitic.* **2004**, *55*, 115−120.
(48) Murat, M.-L.; Tominaga, T.; Saucier, C.; Glories, Y.; Dubourdieu, D. Effect of anthocyanins on stability of a key odorous compound, 3-mercaptohexan-1-ol, in Bordeaux rosé wines. *Am. J. Enol. Vitic.* **2003**, *54*, 135−138.
(49) Deroite, A.; Legras, J. L.; Rigou, P.; Ortiz-Julien, A.; Dequin, S. Lipids modulate acetic acid and thiol final concentrations in wine during fermentation by *Saccharomyces cerevisiae* × *Saccharomyces kudriavzevii* hybrids. *AMB Express* **2018**, *8*, 130.

https://dx.doi.org/10.1021/acs.jafc.0c03183
J. Agric. Food Chem. 2020, 68, 8676−8687

(50) Hernawan, T.; Fleet, G. Chemical and cytological changes during the autolysis of yeasts. *J. Ind. Microbiol. Biotechnol.* **1995**, *14*, 440−450.
(51) Herbst-Johnstone, M.; Nicolau, L.; Kilmartin, P. A. Stability of varietal thiols in commercial Sauvignon blanc wines. *Am. J. Enol. Vitic.* **2011**, *62*, 495−502.
(52) Ramey, D. D.; Ough, C. S. Volatile ester hydrolysis or formation during storage of model solutions and wines. *J. Agric. Food Chem.* **1980**, *28*, 928−934.
(53) Bencomo-Rodriguez, J.; Gambetta, J.; Rigou, P.; Canelo, N.; Roland, A.; Salmon, J.-M.; Bouvier, N. In *Quantitative Determination of Varietal Disulfides in Wine and Their Behavior during Alcoholic Fermentation*, 9e Symposium international d'oenologie de Bordeaux-Oeno 2011, Bordeaux, France, Bordeaux, France, 2011.
(54) Capone, D. L.; Sefton, M. A.; Hayasaka, Y.; Jeffery, D. W. Analysis of precursors to wine odorant 3-mercaptohexan-1-ol using HPLC-MS/MS: Resolution and quantitation of diastereomers of 3-*S*-cysteinylhexan-1-ol and 3-*S*-glutathionylhexan-1-ol. *J. Agric. Food Chem.* **2010**, *58*, 1390−1395.
(55) Chen, L.; Capone, D. L.; Jeffery, D. W. Chiral analysis of 3-sulfanylhexan-1-ol and 3-sulfanylhexyl acetate in wine by high-performance liquid chromatography−tandem mass spectrometry. *Anal. Chim. Acta* **2018**, *998*, 83−92.

https://dx.doi.org/10.1021/acs.jafc.0c03183
J. Agric. Food Chem. 2020, 68, 8676−8687

SUPPORTING INFORMATION FOR

Evolution and Correlation of *cis*-2-Methyl-4-propyl-1,3-oxathiane, Varietal Thiols and Acetaldehyde During Fermentation of Sauvignon blanc Juice

Xingchen Wang,[†] Liang Chen,[†,#] Dimitra L. Capone,[†,‡] Aurélie Roland,[§] David W. Jeffery[*,†,‡]

[†]Department of Wine and Food Science, and Waite Research Institute, The University of Adelaide (UA), PMB 1, Glen Osmond, SA 5064, Australia

[‡]Australian Research Council Training Centre for Innovative Wine Production, UA, PMB 1, Glen Osmond, SA 5064, Australia

[§]SPO, Institut Agro—Montpellier SupAgro, INRAE, Univ Montpellier, 2 Place Pierre Viala, 34060 Montpellier, France

[#]Current address: Institut des Sciences de la Vigne et du Vin, Université de Bordeaux, 210 Chemin de Leysotte CS 50008, 33882 Villenave d'Ornon Cedex, France

Corresponding Author

*Tel: +61 8313 6649. E-mail: david.jeffery@adelaide.edu.au.

Table of Contents

Table S1. Mass Spectrometer Parameters for Quantitation of Varietal Thiols by HPLC-MS/MS.

Compounds	MRM pairs	Fragmentor voltage (V)	Collision energy (eV)
d_8-3-SH	252.3 → 144.1	122	17
	252.0 → 143.9	105	20
	252.0 → 111.0	105	40
3-SH	244.5 → 144.1	102	17
	244.1 → 144.0	120	16
	244.1 → 111.0	120	40
	244.1 → 67.0	120	40
d_8-3-SHA	294.3 → 144.1	122	21
	294.0 → 144.1	120	20
	294.3 → 85.2	122	13
	294.0 → 86.0	120	13
3-SHA	286.4 → 144.2	122	21
	286.1 → 143.9	120	20
	286.4 → 111.0	122	30
	286.1 → 83.1	120	16
d_{10}-4-MSP	252.0 → 144.9	105	16
	252.0 → 111.0	105	40
4-MSP	242.1 → 144.0	105	16
	242.1 → 111.0	105	40
	242.2 → 144.2	100	13

Table S2. Basic Parameters of the Sauvignon blanc Juice Used for Fermentation.

Parameter	Result
TSS (°Brix)	19.3 ± 0.4
pH	3.43 ± 0.01
TA (g/L as tartaric acid, pH 8.2)	8.9 ± 0.2
Ammonia (mg/L)	47
Alpha amino nitrogen (mg/L)	58
YAN (mg/L)	97

Table S3. Ethanol, Free and Total SO_2, Titratable Acidity, pH, and Residual Sugar in Sauvignon blanc Wines Produced with J7 and VIN13 Yeast Strains after 4 Months of Bottle Storage.[a]

Wine samples	Parameters					
	Ethanol (%v/v)	Free SO_2 (mg/L)	Total SO_2 (mg/L)	Titratable acidity (g/L)	pH	Residual sugar (g/L)
J7_R1	11.7	9.6	42.4	7.7	2.89	2.8
J7_R2	11.7	13.6	45.6	7.6	2.90	1.8
J7_R3	11.7	12.8	46.4	7.7	2.90	1.8
Mean ± SD (J7)	11.7 ± 0.0 b	12.0 ± 2.1 a	44.8 ± 2.1 a	7.7 ± 0.0 a	2.90 ± 0.01 a	2.1 ± 0.6 a
VIN13_R1	11.9	10.4	38.4	7.6	2.90	0.9
VIN13_R2	11.9	2.4	22.4	7.6	2.89	0.8
VIN13_R3	11.8	0.8	2.4	7.7	2.89	0.5
Mean ± SD (VIN13)	11.9 ± 0.0 a	4.5 ± 5.1 a	21.1 ±18.0 a	7.6 ± 0.0 a	2.89 ± 0.01 a	0.7 ± 0.2 b
Co-inoculation_R1	11.6	0.8	5.6	7.6	2.89	1.6
Co-inoculation_R2	11.6	8.0	39.2	7.6	2.88	1.6
Mean ± SD (co-inoculation)	11.6 ± 0.0 b	4.4 ± 5.1 a	22.4 ±23.8 a	7.6 ± 0.0 a	2.89 ± 0.01 a	1.6 ± 0.0 ab

[a]Different letters within a column indicate significant differences between the means evaluated by one-way ANOVA followed by Tukey's multiple comparison with $\alpha = 0.05$.

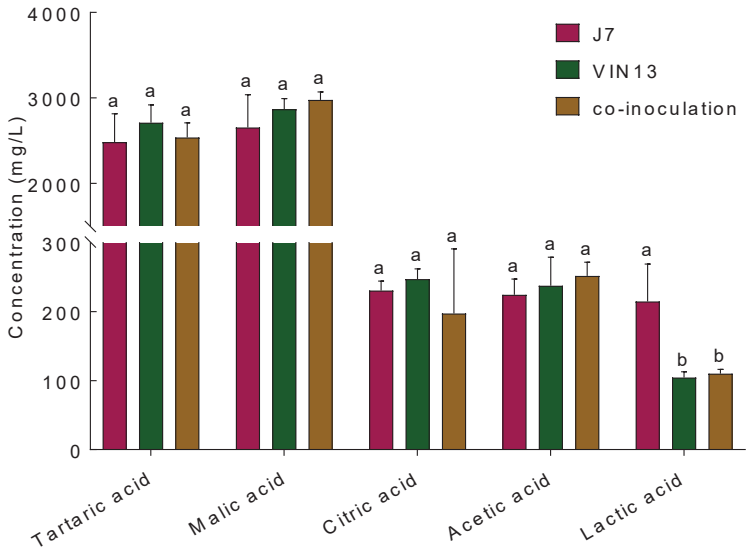

Figure S1. Mean concentrations (mg/L) of organic acids in Sauvignon blanc wines produced with J7 and VIN13 yeast strains either as monoculture or in co-inoculation. Different letters above the bars in each group indicate significant differences between the means evaluated by one-way ANOVA followed by Tukey's multiple comparisons with $\alpha = 0.05$.

CHAPTER 4

Chiral Analysis of *cis*-2-Methyl-4-propyl-1,3-oxathiane and Identification of *cis*-2,4,4,6-Tetramethyl-1,3-oxathiane in Wine

Xingchen Wang,[a] Dimitra L. Capone,[a,b] Aurélie Roland,[c] David W. Jeffery[a,b,*]

[a] Department of Wine Science and Waite Research Institute, The University of Adelaide (UA), PMB 1, Glen Osmond, SA 5064, Australia

[b] Australian Research Council Training Centre for Innovative Wine Production, UA, PMB 1, Glen Osmond, SA 5064, Australia

[c] SPO, INRAE, Univ Montpellier, Institut, Montpellier, France

Food Chemistry, **2021**, 357, 129406

DOI: 10.1016/j.foodchem.2021.129406

Statement of Authorship

Title of Paper	Chiral analysis of *cis*-2-methyl-4-propyl-1,3-oxathiane and identification of *cis*-2,4,4,6-tetramethyl-1,3-oxathiane in wine
Publication Status	☑ Published ☐ Accepted for Publication ☐ Submitted for Publication ☐ Unpublished and Unsubmitted work written in manuscript style
Publication Details	Wang, X., Capone, D.L., Roland, A., Jeffery, D.W. (**2021**) Chiral analysis of *cis*-2-methyl-4-propyl-1,3-oxathiane and identification of *cis*-2,4,4,6-tetramethyl-1,3-oxathiane in wine, *Food Chemistry*, 357, 129406.

Principal Author

Name of Principal Author (Candidate)	Xingchen Wang		
Contribution to the Paper	Contributed to the design of experiments. Conducted experiments and prepared and analysed samples using GC-MS and HPLC-MS/MS. Collected, processed, analysed, interpreted and visualised the data. Produced a complete first draft of the manuscript. Reviewed and edited the manuscript.		
Overall percentage (%)	70%		
Certification:	This paper reports on original research I conducted during the period of my Higher Degree by Research candidature and is not subject to any obligations or contractual agreements with a third party that would constrain its inclusion in this thesis. I am the primary author of this paper.		
Signature		Date	03/07/2021

Co-Author Contributions

By signing the Statement of Authorship, each author certifies that:

i. the candidate's stated contribution to the publication is accurate (as detailed above);

ii. permission is granted for the candidate in include the publication in the thesis; and

iii. the sum of all co-author contributions is equal to 100% less the candidate's stated contribution.

Name of Co-Author	Dimitra L. Capone		
Contribution to the Paper	Conceived of and designed the experiments. Developed the method, supervised the work and interpreted data. Reviewed and edited the manuscript.		
Signature		Date	03/07/2021

Name of Co-Author	Aurélie Roland
Contribution to the Paper	Contributed to the design of experiments. Interpreted data and supervised the work. Reviewed and edited the manuscript.

Signature		Date	03/07/2021

Name of Co-Author	David W. Jeffery		
Contribution to the Paper	Conceived of and designed the experiments. Interpreted data, supervised the project and provided resources. Reviewed and edited the manuscript and acted as the corresponding author.		
Signature		Date	04/07/2021

Please cut and paste additional co-author panels here as required.

Food Chemistry 357 (2021) 129406

Contents lists available at ScienceDirect

Food Chemistry

journal homepage: www.elsevier.com/locate/foodchem

Analytical Methods

Chiral analysis of *cis*-2-methyl-4-propyl-1,3-oxathiane and identification of *cis*-2,4,4,6-tetramethyl-1,3-oxathiane in wine

Xingchen Wang [a], Dimitra L. Capone [a,b], Aurélie Roland [c], David W. Jeffery [a,b,*]

[a] Department of Wine Science and Waite Research Institute, The University of Adelaide (UA), PMB 1, Glen Osmond, SA 5064, Australia
[b] Australian Research Council Training Centre for Innovative Wine Production, UA, PMB 1, Glen Osmond, SA 5064, Australia
[c] SPO, INRAE, Univ Montpellier, Institut Agro, Montpellier, France

ARTICLE INFO

Keywords:
3-Sulfanylhexan-1-ol
4-Methyl-4-sulfanylpentan-2-ol
Enantiomers
Stable isotope dilution assay
Chiral analysis

ABSTRACT

cis-2-Methyl-4-propyl-1,3-oxathiane (*cis*-2-MPO), arising from 3-sulfanylhexan-1-ol (3-SH) and acetaldehyde, was recently identified in wine, but the enantiomeric distribution was unknown. Such information could reveal influences on wine aroma, given the impact of chirality on odorant molecules. Herein, a stable isotope dilution assay employing headspace solid-phase microextraction with chiral gas chromatography–mass spectrometry was developed, validated, and applied to a selection of wines. Studies with (3*R*)-3-SH revealed the elution order of the *cis*-2-MPO enantiomers and the concentrations of (2*R*,4*S*)-2-MPO and (2*S*,4*R*)-2-MPO in the studied wines ranged from undetected to 250 ng/L and 303 ng/L, respectively. Strong positive correlations were found between (3*R*)-3-SH and (2*S*,4*R*)-2-MPO (r = 0.654), and (3*S*)-3-SH and (2*R*,4*S*)-2-MPO (r = 0.860). Additionally, *cis*-2,4,4,6-tetramethyl-1,3-oxathiane, constituted from acetaldehyde and 4-methyl-4-sulfanylpentan-2-ol (4-MSPOH), was identified in wine for the first time. This new 1,3-oxathiane, which presents a novel fate for 4-MSPOH, was detected in wines as a single enantiomer at up to 28 ng/L.

1. Introduction

Sauvignon blanc has long been a focus for wine researchers, given the interest in understanding the conversion of non-odorous grape berries into wines with powerful 'tropical' aroma characteristics imparted by varietal thiols (Coetzee & du Toit, 2012). The discovery of these character impact odorants, which includes 3-sulfanylhexan-1-ol (3-SH, 'grapefruit'), 3-sulfanylhexyl acetate (3-SHA, 'box tree', 'grapefruit', 'passion fruit'), 4-methyl-4-sulfanylpentan-2-one (4-MSP, 'guava', 'boxwood', 'broom'), and 4-methyl-4-sulfanylpentan-2-ol (4-MSPOH, 'citrus zest'), has since underpinned knowledge of the characteristic aromas of Sauvignon blanc wine (Darriet, Tominaga, Lavigne, Boidron, & Dubourdieu, 1995; Tominaga, Darriet, & Dubourdieu, 1996; Tominaga, Furrer, Henry, & Dubourdieu, 1998). In furthering the understanding of varietal thiols in wine, studies have revealed the influences on wine aroma characteristics of enantiomeric pairs of 3-SH and 3-SHA (Fig. 1A) (King, Osidacz, Curtin, Bastian, & Francis, 2011), which resulted from the differences in their aroma notes and detection thresholds (Tominaga, Niclass, Frerot, & Dubourdieu, 2006). The enantiomeric distributions of 3-SH and 3-SHA in different wines have also been studied analytically, revealing that 3-SH enantiomers are present more or less in equal proportions in dry wines, although (3*S*)-3-SH can be slightly more abundant than (3*R*)-3-SH. In contrast, 3-SHA enantiomers distribute much more unevenly, with (3*S*)-3-SHA accounting for approximately 70% of the total concentration of 3-SHA in dry wines (Chen, Capone, & Jeffery, 2018a; Tominaga et al., 2006). Noble rot wines tend to differ to dry white wine, however, with ratios of 3*S*-:3*R*-configured 3-SH and 3-SHA being close to 70:30 (Chen et al., 2018a; Tominaga et al., 2006). Also bearing a chiral centre, 4-MSPOH would be present as a pair of enantiomers in wine (Fig. 1A), but the aroma notes, odour detection thresholds, and distribution of enantiomers of 4-MSPOH have not yet been studied.

Abbreviations: 3-SH, 3-sulfanylhexan-1-ol; 3-SHA, 3-sulfanylhexyl acetate; 4-MSP, 4-methyl-4-sulfanylpentan-2-one; 4-MSPOH, 4-methyl-4-sulfanylpentan-2-ol; ANOVA, analysis of variance; *cis*-2-MPO, *cis*-2-methyl-4-propyl-1,3-oxathiane; EI, electron ionisation; FB, frozen berry; FJ, frozen juice; GC–MS, gas chromatography–mass spectrometry; HS-SPME, headspace–solid-phase microextraction; LOD, limit of detection; LOQ, limit of quantification; LRI, linear retention index; NMR, nuclear magnetic resonance; ODT, odour detection threshold; *p*-TsOH, *p*-toluenesulfonic acid; Rs, peak resolution; SD, standard deviation; SIDA, stable isotope dilution assay; SIM, selected ion monitoring; TLC, thin layer chromatography; TTMO, 2,4,4,6-tetramethyl-1,3-oxathiane.

* Corresponding author at: Department of Wine Science and Waite Research Institute, The University of Adelaide (UA), PMB 1, Glen Osmond, SA 5064, Australia.
E-mail address: david.jeffery@adelaide.edu.au (D.W. Jeffery).

https://doi.org/10.1016/j.foodchem.2021.129406
Received 3 December 2020; Received in revised form 16 February 2021; Accepted 16 February 2021
Available online 2 March 2021

Being enzymatically released from their grape-derived precursors during alcoholic fermentation (AF) or malolactic fermentation (Roland, Schneider, Razungles, & Cavelier, 2011; Takase, Sasaki, Kiyomichi, Kobayashi, Matsuo, & Takata, 2018), varietal thiols play a key role in Sauvignon blanc wine aroma. However, they are not stable over time and their concentrations can rapidly decrease, particularly after bottling (Murat, Tominaga, Saucier, Glories, & Dubourdieu, 2003). For example, 3-SH in rosé wines was found to decline substantially (by around 30–50%) during ageing on lees for 3 months or in bottle for one year (Murat et al., 2003), which could severely weaken the 'tropical' or 'fruity' aromas of such wines (Lopes et al., 2009). This phenomenon has highlighted the importance of exploring the fate of varietal thiols in wine so that measures could be taken to slow down the rate of their decrease. Additionally, detailed studies are still required to explain the disconnect between the amounts of varietal thiols present in wine and the concentrations of precursors in juice and after fermentation.

As chemically reactive nucleophiles, varietal thiols are able to react with electrophiles such as quinones and aldehydes in wine, and can also form disulfides (Bencomo-Rodriguez et al., 2011; Nikolantonaki & Waterhouse, 2012); each of these pathways relates to wine oxidation phenomena. Some of these reactions are potentially reversible, leading to a latent pool of thiols such as 3-SH that might be unmasked at a later stage as the wine matrix evolves. Highlighting this point, a study addressing the fate of 3-SH identified *cis*-2-methyl-4-propyl-1,3-oxathiane (*cis*-2-MPO) in wines – likely resulting from an acid-catalysed reaction between 3-SH and acetaldehyde – that could account for the disappearance of up to approximately 3 nmol/L of 3-SH (i.e., close to 400 ng/L and explaining 9% of initial 3-SH concentration) (Chen, Capone, & Jeffery, 2018b). This is of interest not only from the perspective of alternative thiol reaction pathways, but also with regard to chirality of aroma compounds. Stereochemically, 2-MPO has two pairs of enantiomers that relate to the two enantiomers of 3-SH: these are (2*S*,4*R*)-2-MPO and (2*R*,4*R*)-2-MPO derived from (3*R*)-3-SH, and (2*R*,4*S*)-2-MPO and (2*S*,4*S*)-2-MPO from (3*S*)-3-SH (Fig. 1). As with the enantiomers of 3-SH (and for chiral molecules more generally), the 2-MPO stereoisomers can impart different odour qualities, as detailed previously (Singer, Heusinger, Froehlich, Schreier, & Mosandl, 1986), and the possible existence of two pairs of enantiomers is due to geometric isomerism (i.e., enantiomers of both *cis*- and *trans*-isomers). However, only *cis*-2-MPO has been identified in wine and yellow passion fruit (Chen et al., 2018b; Singer et al., 1986), due to the equatorial positioning of both methyl and propyl groups on the 1,3-oxathiane ring being favoured. Moreover, because the *cis*-enantiomers of 2-MPO (i.e., (2*S*,4*R*)- and (2*R*,4*S*)-2-MPO, Fig. 1B) are directly related to (3*R*)- and (3*S*)-3-SH configurations, it is of interest to explore the distribution of *cis*-2-MPO enantiomers in wines, as mentioned in a recent review by Engel (2020) on chirality of flavour compounds.

In addition to 3-SH reacting with acetaldehyde in wine to produce 2-MPO, it is also possible that other thiols with similar structures to 3-SH could undergo the same reaction to produce the corresponding 1,3-oxathianes. Such candidates are 3-sulfanylpentan-1-ol, 2-methyl-3-sulfanylbutan-1-ol, 3-sulfanylheptan-1-ol, and 4-MSPOH, which all bear a 1,3-sulfanylalkanol substitution pattern and with the first three thiols having only been identified in noble rot wines. On the other hand, although 4-MSPOH is not as widely present (or abundant) in wines as 3-SH and 3-SHA, it has been reported in botrytised Semillon, Gewurztraminer, Muscat, Pinot Gris, and Riesling, and has an odour detection threshold of 55 ng/L in model wine (Tominaga, Baltenweck-Guyot, Peyrot des Gachons, & Dubourdieu, 2000). As with the other potent thiols, even trace concentrations of 4-MSPOH could have an impact on the perceived aromas of wine, and alternative fates for this compound were worthy of investigation. One example is the potential formation of 2,4,4,6-tetramethyl-1,3-oxathiane (TTMO, Fig. 1C), the product hypothetically arising from condensation of 4-MSPOH and acetaldehyde.

Taking chiral analysis and 1,3-oxathiane discovery together, this study aimed to determine the enantiomeric profiles of *cis*-2-MPO in wines for correlation with the enantiomers of 3-SH, and as a supplementary aim, to identify the existence of TTMO, given that the possible enantiomers of *cis*- and *trans*-TTMO related to the enantiomers of 4-MSPOH can be hypothesised (Fig. 1C). This necessitated the development and validation of a stable isotope dilution assay (SIDA) using headspace–solid-phase microextraction (HS-SPME) and gas chromatography–mass spectrometry (GC–MS), after selecting a suitable chiral GC column. The method was then applied to the quantitative analysis of enantiomers of both *cis*-2-MPO and TTMO (after verification of its presence) in a selection of wines.

2. Material and methods

2.1. Chemicals and materials

The following chemicals were sourced from commercial suppliers: HPLC gradient grade ethanol and acetonitrile, GC grade dichloromethane (SupraSolv), ammonium bicarbonate, acetaldehyde, d_4-acetaldehyde, NaCl, anhydrous $MgSO_4$, 4 Å sieves, $C_7 - C_{40}$ *n*-alkanes, thin layer chromatography (TLC) plates, $NaHCO_3$, *p*-toluenesulfonic acid (*p*-TsOH), and 2-MPO (≥98% pure, *cis/trans* ratio of 85/15 according to Chen et al. (2018b)) were from Sigma-Aldrich, Castle Hill, NSW,

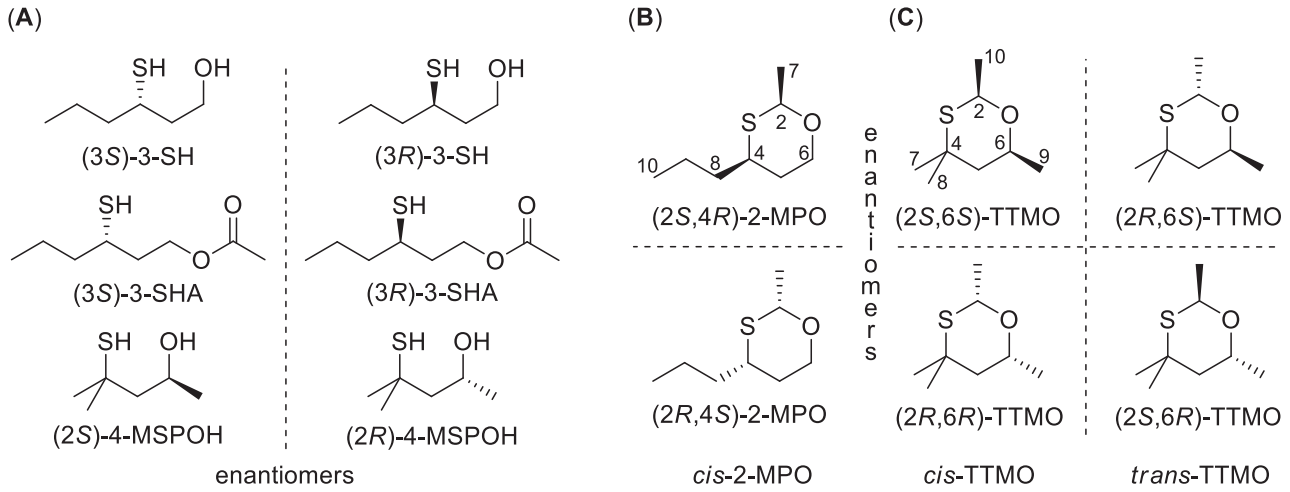

Fig 1. Structures for (A) enantiomers of 3-SH, 3-SHA, and 4-MSPOH, (B) enantiomers of *cis*-2-methyl-4-propyl-1,3-oxathiane (2-MPO), and (C) enantiomers of *cis*- and *trans*-2,4,4,6-tetramethyl-1,3-oxathiane (TTMO) that could arise from condensation of 4-MSPOH with acetaldehyde.

Australia; 4-MSPOH (98% pure) was from Thermo Fisher Scientific, Scoresby, VIC, Australia; analytical reagent–grade dichloromethane was from Chem-Supply Pty Ltd (Gillman, SA Australia). d_4-*cis*-2-MPO and (3*R*)-3-SH ethanolic solution were previously synthesised (Chen et al., 2018a, 2018b). Solutions of standards were prepared in ethanol, and Milli-Q water (Millipore, North Ryde, NSW, Australia) was used to prepare aqueous solutions. Details for the synthesis of TTMO and d_4-2,4,4,6-tetramethyl-1,3-oxathiane (d_4-TTMO) have been provided in Section A.1 of Appendix A. Commercial and experimental wines from previous studies were used for screening of the target 1,3-oxathianes and enantiomers of 3-SH (Table B.1 of Appendix B). Commercial wines consisted of Sauvignon blanc (SB, n = 14), Chardonnay (C, n = 21), rosé (R, n = 3), Pinot Grigio (PG, n = 1), Muscat (M, n = 1), white blend (WB, n = 1), and Riesling (RIE, n = 1), the details of which have been provided previously (Chen et al., 2018b). Experimental wines included Sauvignon blanc juice fermented with different yeast strains (J7 and VIN13 in triplicate, and their co-inoculation in duplicate, n = 8) (Wang, Chen, Capone, Roland, & Jeffery, 2020) and pre-fermentation freezing treatment of Sauvignon blanc juice and berries (frozen juice (FJ) and frozen berries (FB), respectively, with each treatment fermented in triplicate, n = 30) (Chen, Capone, Nicholson, & Jeffery, 2019).

2.2. Method development and validation

The process followed a general workflow of GC column screening using chiral stationary phases, GC–MS parameter optimisation, SPME fibre selection, method validation, elution order assignment for *cis*-2-MPO enantiomers, and verification of TTMO in wine (Fig. B.1 in Appendix B).

2.2.1. Sample preparation

Liquid injection was used for screening of chiral GC columns and initial method optimisation. An injection volume of 1 μL was used with standards (approximately 5.0 mg/L *cis*-TTMO, 5.0 mg/L *cis*-2-MPO, and 4.8 mg/L d_4-*cis*-2-MPO) dissolved in GC grade dichloromethane. At the stage of conversion from liquid injection to HS-SPME, Milli-Q water or model wine (10% v/v ethanol, saturated with potassium hydrogen L-tartrate and adjusted to pH 3.4 with 1 M tartaric acid solution) spiked with standards was used during the initial stages of HS-SPME method optimisation to determine the retention time for each analyte. Then a commercial Sauvignon blanc wine was used for GC–MS parameter optimisation and wine samples used for screening of the two analytes were prepared according to the published method (Chen et al., 2018b). Briefly, 5 mL of wine sample and an aliquot of ethanolic solution of d_4-*cis*-2-MPO (final concentration of 200 ng/L) were spiked into a 20 mL SPME vial containing NaCl (2 g). Vials were instantly capped and the contents were mixed well prior to GC–MS analysis. Upon completion of the synthesis, d_4-*cis*-TTMO, prepared as an ethanolic solution, was added into the developed method as an internal standard at a concentration of 200 ng/L.

2.2.2. GC–MS instrumentation and parameters

Analyses were conducted on an Agilent 6890N GC coupled with an Agilent 5973N mass selective detector (MSD) using ultra-pure helium (BOC, North Ryde, NSW, Australia) as carrier gas. The GC was equipped with a Gerstel MPS autosampler (Lasersan Australasia, Robina, QLD, Australia) with sample incubation parameters as detailed previously (Chen et al., 2018b). MS source and quadrupole temperatures were set at 230 °C and 150 °C, respectively throughout the study, with transfer line temperatures for each GC column trialled during method development as detailed in Section A.2 of Appendix A. Electron ionisation (EI) mass spectra were recorded at 70 eV in full scan (35–350 amu) or selected ion monitoring (SIM) modes. Instrument control and data acquisition were performed using MSD ChemStation (EA02.02, Agilent). Data analysis was performed using MassHunter software (version B.08.00, Agilent). Three GC columns with chiral stationary phases were investigated: CycloSil-B (30 m × 0.32 mm, 0.25 μm, Agilent J&W), Cyclodex-B (30 m × 0.32 mm, 0.25 μm, Agilent J&W), and Rt-βDEXcst (30 m × 0.25 mm, 0.25 μm, Restek).

Preliminary method development has been detailed in Section A.2 of Appendix A. The column that gave the best separation was the Rt-βDEXcst column utilising a carrier gas flow rate of 1.1 mL/min. Samples were extracted with a 2 cm DVB/CAR/PDMS fibre (50/30 μm, Sigma-Aldrich) at 35 °C for 30 min with an agitator speed of 500 rpm (agitator on 10 s and off 1 s) prior to desorption for 15 min at 220 °C into the GC-inlet (ultra inert SPME liner, 0.75 mm i.d., Agilent) in pulsed splitless mode at a pressure of 54.7 kPa. The oven program was 37 °C for 5 min, ramping to 90 °C at 1.5 °C/min, then to 130 °C at 3.0 °C/min, and to 220 °C at 30.0 °C/min, with a hold time of 10 min. The temperature of the transfer line was set at 220 °C and the ions monitored (20 ms dwell time) were *m/z* 164, 146, 116, 101, and 83 for d_4-*cis*-TTMO; *m/z* 160, 145, 116, 101, and 83 for *cis*-TTMO; *m/z* 164, 146, and 101 for d_4-*cis*-2-MPO; *m/z* 160, 145, and 101 for *cis*-2-MPO. Underlined ions were used for quantification and the others were used as qualifier ions.

2.2.3. SIDA GC–MS method validation and quantitative chiral analysis

Method validation was performed with a commercial Sauvignon blanc wine (containing 23 ng/L in total of *cis*-2-MPO, alcohol 12.0% v/v, 2018, Red Cliffs, VIC, Australia), a Chardonnay wine (alcohol 13.5% v/v, 2018, Red Cliffs, VIC, Australia), a Grenache rosé wine (alcohol 13.5% v/v, 2016, McLaren Vale, SA, Australia), and a Cabernet Sauvignon wine (alcohol 13.5% v/v, 2018, Red Cliffs, VIC, Australia). The authentic standards of racemic *cis*-2-MPO and *cis*-TTMO were spiked in the Sauvignon blanc wine at seven calibration levels (0, 50, 100, 250, 500, 750, and 1000 ng/L for *cis*-2-MPO and 0, 48, 93, 246, 472, 718, 944 ng/L for *cis*-TTMO) in duplicate. Seven replicates were spiked in the Sauvignon blanc wine with both *cis*-TTMO and *cis*-2-MPO at low (93 and 99 ng/L) and high (472 and 500 ng/L) levels for precision and accuracy evaluation. Recovery from different wine matrices was assessed by spiking low (93 and 99 ng/L) and high (472 and 500 ng/L) levels of both authentic compounds in duplicate into the commercial Chardonnay, Grenache rosé, and Cabernet Sauvignon wines. Deuterium labelled internal standards (d_4-*cis*-2-MPO and d_4-*cis*-TTMO) were added to all samples at 200 ng/L. Limit of detection (LOD) and limit of quantification (LOQ) were expressed as 3 and 10 times the standard error of the *y* intercept divided by the slope of the calibration equation. The method was applied to the quantitative analysis of a selection of wines as detailed in Table B.1 of Appendix B.

2.3. Verification of cis-TTMO in wine

2.3.1. Linear retention index (LRI)

Retention indices were calculated on a HP-INNOWAX column (60 m × 0.25 mm, 0.25 μm, J&W Agilent) and a DB-5ms UI column (60 m × 0.25 mm, 0.25 μm, J&W Agilent) by injecting 1 μL of $C_7 - C_{40}$ *n*-alkanes standard into the GC inlet. The GC–MS parameters were adapted from the published method for *cis*-2-MPO (Chen et al., 2018b) by converting the MS acquisition mode from SIM to scan with a gain factor of 10.

2.3.2. Co-injection experiments with authentic standard

Co-injections were conducted on HP-INNOWAX, DB-5ms UI, and Rt-βDEXcst columns. Increasing concentrations of *cis*-TTMO at 30, 60, and 90 ng/L for HP-INNOWAX and DB-5ms UI columns using the published method (Chen et al., 2018b), and 60, 120, and 180 ng/L for Rt-βDEXcst column using the validated SIDA chiral GC–MS method detailed in Section 2.2.2, were spiked into a commercial Sauvignon blanc wine (SB_7, Table B.1 of Appendix B) that was found to contain 28 ng/L of *cis*-TTMO.

2.4. Elution order for enantiomers of cis-2-MPO

An ethanolic solution of (3*R*)-3-SH, which had been previously

prepared (Chen et al., 2018a) was spiked in 1 mL of commercial Sauvignon blanc wine at increasing levels (0, 56, and 112 mg/L) together with acetaldehyde (20 μL). After 3 days of storage at room temperature, the samples were spiked with 200 ng/L of d_4-*cis*-2-MPO before analysis with the validated SIDA GC–MS method.

2.5. Quantification of 3-SH enantiomers by SIDA HPLC-MS/MS

Wine extracts used for the determination of 3-SH after derivatisation had been previously prepared (Chen et al., 2018b; Chen et al., 2019; Wang et al., 2020) and underwent HPLC-MS/MS analysis to determine (3*R*)- and (3*S*)-3-SH concentrations as detailed previously (Chen et al., 2018a) with modifications to the instrumentation. A ThermoFinnigan Surveyor HPLC coupled to a ThermoFinnigan LCQ Deca XP Plus MS with positive electrospray ionisation (ESI) was used for sample analysis. Xcalibur software (version 1.3) was utilised for instrument control, data acquisition, and processing. The MS data were recorded in selected reaction monitoring (SRM) mode with SRM transition pairs based on those reported previously for multiple reaction monitoring (Chen et al., 2018a). Nitrogen was used for the sheath gas (35 arbitrary units) and auxiliary gas (20 arbitrary units). The ion spray voltage, capillary voltage, tube lens offset voltage, and capillary temperature were 4500 V, 18 V, 10 V, and 250 °C, respectively. Ultra-pure helium was used as the collision gas and isolation width, normalised collision energy, activation Q, and activation time were *m/z* 1.4, 36.0%, 0.250, and 30.0 msec, respectively.

2.6. Evolution of 3-SH and 3-SHA enantiomers during AF of Sauvignon blanc juice

The concentrations of 3-SH and 3-SHA enantiomers were determined using an Agilent 1200 HPLC coupled with a 6410 triple quadrupole mass spectrometer based on the published method (Chen et al., 2018a) with MS instrumentation parameters as reported previously (Wang et al., 2020).

2.7. Sensory evaluation of TTMO

The odour detection threshold (ODT) of TTMO was determined according to ASTM standard practice E 679–04 (reapproved 2011) (ASTM, 2011) and odour quality testing was undertaken, using a neutral white wine stripped with charcoal. Full details of the procedures are provided in Section A.3 of Appendix A.

2.8. Statistical analysis

Mean values, standard deviations (SD), peak resolution (Rs), linear regressions of calibrations, and lack-of-fit *F*-test for regressions were calculated with Microsoft Excel (Microsoft Office Professional Plus 2019 for Windows). One-way analysis of variance (ANOVA) followed by Tukey's multiple comparisons ($\alpha = 0.05$) was conducted with XLSTAT (version 2020.1, Addinsoft, Qi Statistics, Reading, U.K.). Figures showing concentrations and ratios of enantiomers of analytes were constructed with GraphPad Prism (version 7.02, GraphPad Software Inc., San Diego, CA). Data were standardised before Pearson correlation analysis using SPSS (version 25.0, IBM, Armonk, NY, USA).

3. Results and discussion

3.1. Method development

A GC–MS method with a chiral stationary phase was required for the quantitative analysis of *cis*-2-MPO enantiomers to investigate the chiral relationships with 3-SH enantiomers. This also presented an opportunity to further test the hypothesis regarding 1,3-oxathiane formation from acetaldehyde and varietal thiols such as 4-MSPOH. To this end, TTMO (Fig. 1C) was firstly synthesised based on the procedure reported previously for d_4-*cis*-2-MPO (Chen et al., 2018b). As shown in Fig. B.2 of Appendix B, the two adjacent peaks in the chromatogram of both TTMO (rt = 10.49 min and 10.63 min, Fig. B.2A) and d_4-TTMO (rt = 10.88 min and 11.03 min, Fig. B.2D) have the same background subtracted mass spectra (Fig. B.2B and C, and B.2E and F), showing peak ratios of 94.4:5.6 for TTMO and 93.0:7.0 for d_4-TTMO, indicating the presence of *cis*- and *trans*-isomers for both compounds. Proton and carbon NMR spectra were recorded (Fig. B.3 to B.6 of Appendix B) and the *cis*-/*trans*-isomers of TTMO were assigned based on the chemical shifts of protons on C-2 and C-6. The two axial protons (i.e., H_{2ax} and H_{6ax}) in *cis*-TTMO were deemed to be upfield (4.84 ppm and 3.67–3.62 ppm, respectively) compared with their equatorial counterparts in *trans*-TTMO (5.12 ppm for H_{2eq} and 4.14–4.08 ppm for H_{6eq}) due to the steric shielding effect of the axial methyl group attached to C-4 (Perlin & Koch, 1970). Moreover, C-2 and C-6 in *cis*-TTMO showed the opposite effect, being downfield at 75.6 and 71.4 ppm, respectively, compared to 71.2 and 67.2 ppm in the minor *trans*-isomer (Fig. B.4 of Appendix B; signals for C-2 and C-6 for the minor isomer were elucidated by comparing unlabelled and labelled ^{13}C spectra), as a result of the equatorial orientation of the attached methyl groups (i.e., C-10 and C-9, respectively) in the *cis*-isomer (Perlin & Koch, 1970). This information also accords with the greater thermodynamic stability of *cis*-oxathianes (Winter, Furrer, Willhalm, & Thommen, 1976), whereby the two methyl substituents attached to C-2 and C-6 are proposed to be in the more favourable equatorial position. Therefore, *cis*-TTMO and d_4-*cis*-TTMO were determined to be the major constituents from the synthesis of these oxathianes.

Peak resolution (Rs) values were calculated to evaluate the separation between enantiomers at the method development stage, with a value of 1.5 showing baseline separation between two adjacent peaks and a value of 1.0 indicating incomplete baseline resolution but good enough for peak area calculation (Ettre, 1993). For the initial stage of screening chiral GC stationary phases, the authentic 1,3-oxathianes were analysed by liquid injection as detailed in Section 2.2.1 to obtain retention time and mass spectral data, and to estimate the separation of enantiomers of each compound before the transition to a HS-SPME method. Three GC columns with chiral stationary phases were screened during this process.

CycloSil-B column (30% heptakis(2,3-di-*O*-methyl-6-*O*-*t*-butyldimethylsilyl)-β-cyclodextrin in DB-1701) was initially trialled and the enantiomers of both *cis*-2-MPO and *cis*-TTMO were not separated, with severe tailing of peaks being evident (data not shown). A Cyclodex-B column (10.5% β-cyclodextrin in DB-1701) was then tested with the same method, which permitted the full separation of the enantiomers of *cis*-2-MPO and d_4-*cis*-2-MPO (Rs values of 1.4), but those of *cis*-TTMO were partially overlapped (Rs = 0.9). Thus, parameters including oven temperature program and carrier gas flow rate were optimised using full scan MS mode as detailed in Section A.2 of Appendix A. Under the optimised conditions, the Rs values for enantiomers of *cis*-TTMO, *cis*-2-MPO, and d_4-*cis*-2-MPO were 1.4, 2.0, and 3.0, respectively, and deemed adequate for quantitative analysis (Ettre, 1993). Based on the optimised parameters for the Cyclodex-B column, the liquid injection method with MS in scan mode was converted to HS-SPME (PDMS/DVB fibre) with SIM. The method was tested/optimised in both a model wine and a commercial Sauvignon blanc wine spiked with authentic standards. There was suitable resolution of *cis*-TTMO, but the qualifier ion at *m/z* 101 for *cis*-2-MPO and d_4-*cis*-2-MPO suffered from interference by a co-eluting compound in the Sauvignon blanc wine, thus necessitating either a longer column or one with a narrower diameter to be trialled.

Consequently, an Rt-βDEXcst column (proprietary cyclodextrin material in 14% cyanopropylphenyl/86% dimethylpolysiloxane) having a narrower diameter (0.25 mm id) compared to the other two columns (0.32 mm id) was evaluated with some minor GC parameter modifications (as specified in Section A.2 of Appendix A). In parallel, d_4-TTMO was synthesised and included during method optimisation. Under the

optimised conditions, the four pairs of enantiomers (i.e., two analytes and their internal standards) were well separated, with Rs values for the enantiomers of d_4-*cis*-TTMO (rt = 33.24 and 33.93 min), *cis*-TTMO (rt = 33.50 and 34.09 min), d_4-*cis*-2-MPO (rt = 46.51 and 46.99 min), and *cis*-2-MPO (rt = 46.65 and 47.09 min) being 1.6, 1.7, 3.1, and 1.7, respectively. Selected ion chromatograms of *m/z* 164 for d_4-*cis*-TTMO and d_4-*cis*-2-MPO, and *m/z* 160 for *cis*-TTMO and *cis*-2-MPO, illustrate the resolution of the enantiomers (Fig. B.7A and B in Appendix B).

3.2. Method validation

Linearity, repeatability, recovery from different wine matrices, LOD, and LOQ were evaluated (Table B.2 in Appendix B). The calibrations conducted in a commercial Sauvignon blanc wine were linear throughout the concentration range for each analyte, with R^2 values > 0.9997 and non-significant *p*-values from a lack-of-fit *F*-test (i.e., relationship is linear). Repeatability spikes for the four analytes showed that the relative standard deviation ranged from 1 to 3% for both low and high spiked concentrations in a commercial Sauvignon blanc wine. Recovery from different wine matrices was assessed in commercial Chardonnay, rosé, and Cabernet Sauvignon wines at low and high spiked concentrations, and ranged from 95% to 108%. LOD and LOQ values for all four analytes were within the range of 4–5 ng/L and 14–18 ng/L, respectively (Table B.2 in Appendix B).

3.3. Elution order of enantiomers of cis-2-MPO

The elution order of the two enantiomers of *cis*-2-MPO was determined in a commercial Sauvignon blanc wine spiked with increasing amounts of (3*R*)-3-SH along with 20 μL of acetaldehyde. After 3 days of storage at room temperature, samples were spiked with d_4-*cis*-2-MPO as internal standard and analysed with the validated method. In the control wine sample, neither enantiomer of *cis*-2-MPO was detected (Fig. 2). In contrast, sample spiked with 56 mg/L of (3*R*)-3-SH (Spike_low) showed a substantially higher peak at rt = 47.09 min than the peak at rt = 46.68 min, with ratios of analyte to internal standard of 1608 and 67, respectively. These ratios approximately doubled with a spike of 112 mg/L of (3*R*)-3-SH (Spike_high, 3226 and 129, respectively, Fig. 2). Thus, the elution order of the two enantiomers of *cis*-2-MPO was determined to be (2*R*,4*S*)-2-MPO at 46.69 min followed by (2*S*,4*R*)-2-MPO at 47.09 min, as labelled in Fig. B.7A of Appendix B. This elution order was identical to a previous study using a column with octakis(2,3-di-*O*-butyryl-6-*O*-*tert*-butyldimethylsilyl)-γ-cyclodextrin as the stationary phase (Weber, Maas, & Mosandl, 1995), but the reverse of that of another study conducted with a chiral nickel (II) bis[3-(heptafluorobutyryl)-l-(*R*)-camphorate] capillary column (Singer et al., 1986). Based on the unlabelled analytes, the elution order of the d_4-*cis*-2-MPO enantiomers was accordingly assigned as d_4-(2*R*,4*S*)-2-MPO (rt = 46.51 min) and d_4-(2*S*,4*R*)-2-MPO (rt = 46.99 min) (Fig. B.7A of Appendix B). The reported ratios of (2*R*,4*S*)-2-MPO to (2*S*,4*R*)-2-MPO (Fig. 2) depending on spiking level of (3*R*)-3-SH can be readily explained by the presence of a minor proportion of (3*S*)-3-SH in the ethanolic solution of (3*R*)-3-SH arising from the synthesis (Tominaga et al., 2006). Importantly, these experiments used to assign the *cis*-2-MPO enantiomer elution order also helped to verify that *cis*-2-MPO could be formed chemically in wine when 3-SH and acetaldehyde were both present (albeit both added in relatively high concentrations in this case).

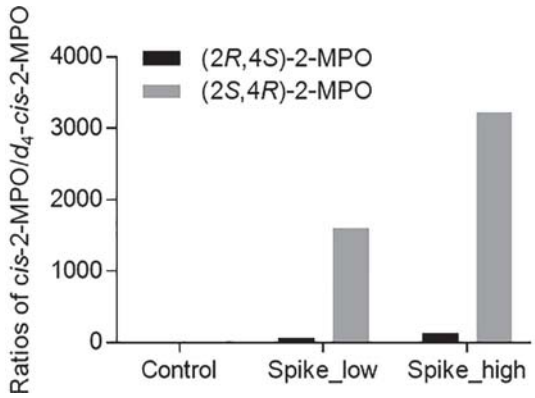

Fig 2. Ratios of respective enantiomers for unlabelled *cis*-2-MPO and d_4-*cis*-2-MPO in Sauvignon blanc wine spiked with (3*R*)-3-SH and acetaldehyde, and analysed after a 3-day storage period. Control wine was spiked only with 200 ng/L of d_4-*cis*-2-MPO before analysis; Spike_low wine sample was spiked with 56 mg/L of (3*R*)-3-SH and 20 μL of acetaldehyde, then d_4-*cis*-2-MPO before analysis; Spike_high wine sample was spiked with 112 mg/L of (3*R*)-3-SH and 20 μL of acetaldehyde, then d_4-*cis*-2-MPO before analysis.

3.4. Quantification of cis-2-MPO enantiomers in wine

The validated method was applied to a series of commercial and experimental wines to investigate the concentrations and ratios of enantiomers of *cis*-2-MPO, covering both white and rosé wines (Fig. 3A and B, with grey coloured bars showing (2*S*,4*R*)-2-MPO arising from (3*R*)-3-SH and black coloured bars showing (2*R*,4*S*)-2-MPO from (3*S*)-3-SH). Of the commercial wines (detailed in Table B.1 of Appendix B), both enantiomers of *cis*-2-MPO were determined in 8 Sauvignon blanc (SB), 11 Chardonnay (C), 3 rosé (R), a Muscat (M), a white blend (WB), and a Riesling (RIE, Fig. 3), with the concentration of (2*S*,4*R*)-2-MPO in rosé 2 (R_2) being between the LOD and LOQ of the method. The concentrations of (2*R*,4*S*)-2-MPO and (2*S*,4*R*)-2-MPO ranged from below the LOQ (<14 ng/L) to 250 ng/L and from below the LOQ (<18 ng/L) to 303 ng/L, respectively, with roughly equal distribution of the enantiomers (Fig. 3B), although (2*S*,4*R*)-2-MPO (arising from (3*R*)-3-SH) was higher on average, at 55% of the total concentration (ranging from 50 to 70%). Generally, the summed concentrations of (2*R*,4*S*)-2-MPO and (2*S*,4*R*)-2-MPO ranged from not detected (ND, lower than the LOD of 4–5 ng/L, Table B.2 of Appendix B) to 541 ng/L (Fig. 3A), which accorded with the results from *cis*-2-MPO analysis using an achiral stationary phase (ND to 460 ng/L) (Chen et al., 2018b). Notably, Sauvignon blanc (SB) wines tended to have the highest concentrations, although the Riesling (RIE) also had a relatively high concentration, followed by Chardonnay wines C_14 and C_21 (Fig. 3A).

For the eight experimental Sauvignon blanc wines from fermentation experiments using different yeast strains (Table B.1 of Appendix B) (Wang et al., 2020), neither of the enantiomers was detected in SB_J7 wines, thus SB_J7 was not included in Fig. 3. One of the replicate ferments of SB_VIN13 and both ferments of SB_co-inoculation had concentrations of both enantiomers of *cis*-2-MPO below the LOQ of the method (14–18 ng/L, Table B.2 of Appendix B) and were excluded when calculating the mean concentrations for the treatments. In general, concentrations of (2*R*,4*S*)-2-MPO and (2*S*,4*R*)-2-MPO ranged from below the LOQ to 15 ng/L and 20 ng/L, respectively, with the latter enantiomer (arising from (3*R*)-3-SH) accounting for 57% of the total concentration (Fig. 3B). The sum of the concentrations of (2*R*,4*S*)-2-MPO and (2*S*,4*R*)-2-MPO in SB_VIN13 was 35 ng/L, and well in line with result obtained previously by GC–MS analysis with an achiral stationary phase (32 ng/L at the end of fermentation) (Wang et al., 2020). In experimental Sauvignon blanc wines from a pre-fermentation freezing study involving juice or berry (Chen et al., 2019), both enantiomers of *cis*-2-MPO were determined in all wine samples except for FJ_Q9720 and FJ_5385, where neither enantiomer was detectable. Concentrations of (2*R*,4*S*)-2-MPO and (2*S*,4*R*)-2-MPO in these frozen juice (FJ) and frozen berry (FB) wines ranged from below the LOQ (FB_Q9720 wine, Table B.2 of Appendix B) to 63 ng/L, and from 24 to 253 ng/L, respectively, with the proportion of (2*S*,4*R*)-2-MPO ranging from 55 to 90% of the total concentration with an average of 66% (Fig. 3B). The summed concentrations of (2*R*,4*S*)-2-MPO and (2*S*,4*R*)-2-MPO ranged from 38 to 282 ng/L. Inexplicably, the large SD for

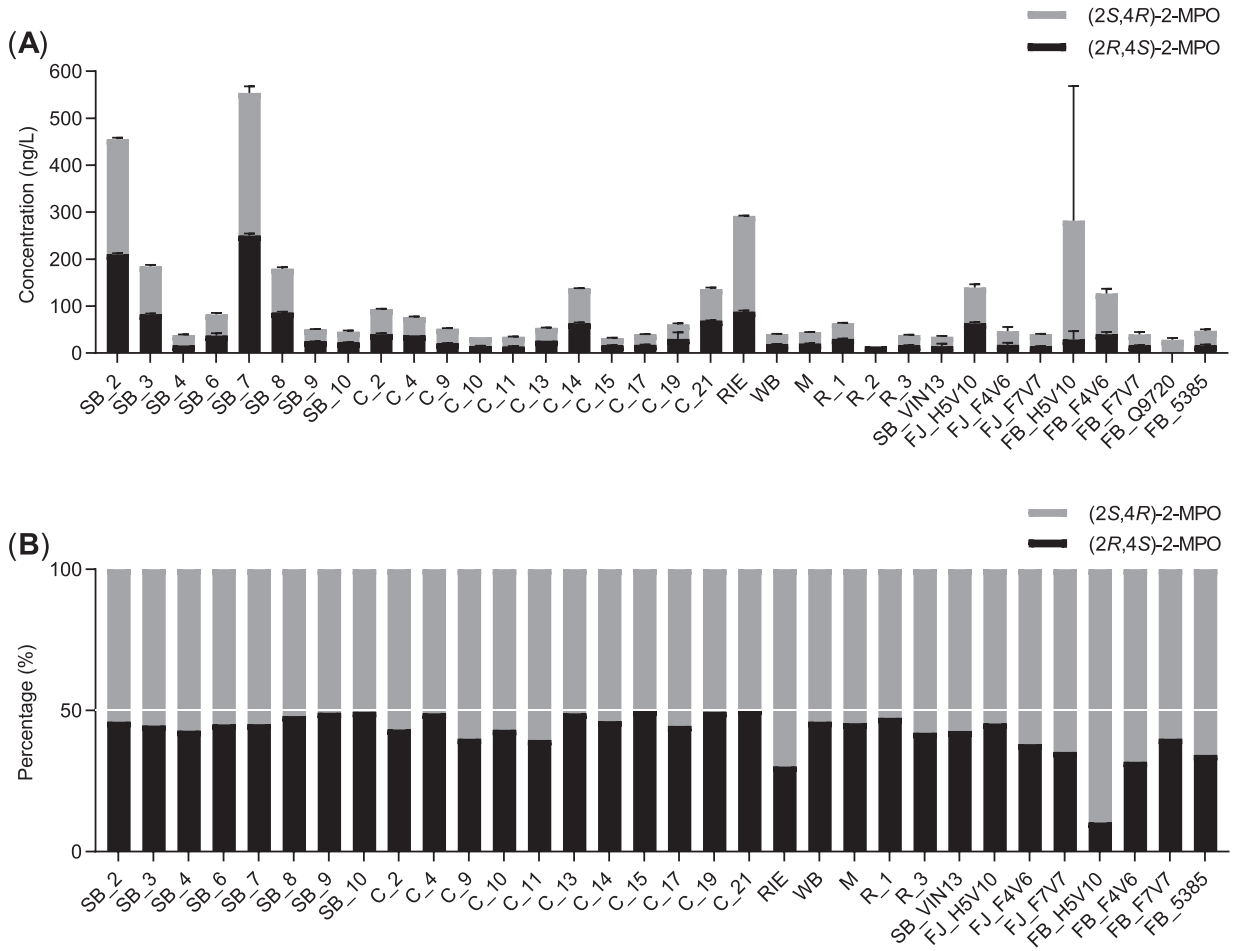

Fig 3. Results from GC–MS analysis of (2*S*,4*R*)-2-MPO and (2*R*,4*S*)-2-MPO in wines showing (A) the concentration of each enantiomer (ng/L) and (B) relative enantiomer ratios. Grey bars show (2*S*,4*R*)-2-MPO arising from (3*R*)-3-SH and black bars show (2*R*,4*S*)-2-MPO from (3*S*)-3-SH. Error bars represent standard deviation for commercial wines (n = 2) and experimental wines (n = 3, except for SB_VIN13 with n = 2). Abbreviations and details of each wine are presented in Table B.1 of Appendix B along with the concentrations of each *cis*-2-MPO enantiomer.

the concentration of (2*S*,4*R*)-2-MPO in FB_H5V10 wine resulted from a substantially higher concentration in one replicate of FB_H5V10 wines, which was extrapolated at 582 ng/L (outside the upper calibration value of 500 ng/L), whereas the other biological replicates were determined to be 117 and 58 ng/L. When taking all wines into consideration, including both experimental and commercial wines, the average proportion of the two enantiomers was slightly in favour of (2*S*,4*R*)-2-MPO, at 57%. This differed to the results obtained for yellow passion fruit, where only 4*S*-configured (2*R*,4*S*)-2-MPO and (2*S*,4*S*)-2-MPO were determined. This was hypothesised to result from enantioselective transformation of (3*S*)-3-SH (Weber et al., 1995) although this has not been verified. In contrast, the chemical production of *cis*-2-MPO from 3-SH and acetaldehyde outlined in Section 3.3 leads to equal production of enantiomers of *cis*-2-MPO in wine. Therefore, further studies are required to examine why (2*S*,4*R*)-2-MPO was slightly favoured when (3*R*)-3-SH, the corresponding thiol enantiomer, is generally less abundant in wine.

3.5. Verification and quantification of cis-TTMO in wine

Pure enantiomers of 4-MSPOH were not available to determine the elution order of *cis*-TTMO enantiomers in the same manner as achieved for *cis*-2-MPO (Section 3.3). The resolved enantiomers of *cis*-TTMO were thus tentatively assigned as (2*R*,6*R*)-TTMO and (2*S*,6*S*)-TTMO according to the analogy with the elution order of *cis*-2-MPO (Fig. B.7A and B of Appendix B), and so were the enantiomers of d_4-*cis*-TTMO. Interestingly, results from the quantitative analysis showed that only the tentatively assigned (2*R*,6*R*)-TTMO was detected in 10 of the wines that were analysed: SB_2 and SB_7 contained 17 and 28 ng/L of (2*R*,6*R*)-TTMO (equivalent to 14 and 23 ng/L of 4-MSPOH, respectively) and SB_3, SB_8, RIE, FJ_H5V10, FJ_F7V7, FB_H5V10, FB_F4V6, and FB_Q9720 (only detected in one of the triplicate wines) had (2*R*,6*R*)-TTMO between the LOD (5 ng/L) and LOQ (16 ng/L) for this compound (Table B.2 of Appendix B). Given the limited prevalence and low abundance of 4-MSPOH in wines (0–111 ng/L according to Tominaga et al. (1998)), it was reasonable that *cis*-TTMO was found at much lower concentration in wines compared to *cis*-2-MPO. Nonetheless, its presence gave weight to the general nature of 1,3-oxathiane formation from acetaldehyde and thiols bearing the 1,3-sulfanylalkanol substitution pattern.

It is noteworthy that only (2*R*,6*R*)-TTMO (tentatively assigned) appeared to be present in these wine samples, which could imply the predominant existence of (2*R*)-4-MSPOH (structure shown in Fig. 1A) in wine that can react with acetaldehyde. In support of this proposition, ketones can be asymmetrically reduced to their corresponding alcohols by fermenting yeast (MacLeod, Prosser, Fikentscher, Lanyi, & Mosher, 1964) and 4-MSP, a ketone form of varietal thiol, could possibly be reduced stereoselectively during fermentation to yield a single enantiomer of 4-MSPOH. However, more work is required to verify this proposal and a method to investigate the presence of 4-MSPOH

enantiomers in wine is required.

To help confirm the existence of this new oxathiane compound in wine, a commercial wine (SB_7, determined to contain 28 ng/L of tentatively assigned (2*R*,6*R*)-TTMO) was used for linear retention index determination on two achiral GC phases, namely HP-INNOWAX and DB-5ms UI. The peaks on the two phases were at rt = 17.3 min and 17.9 min, respectively, and five ions (*m/z* 160, *m/z* 145, *m/z* 116, *m/z* 101, and *m/z* 83) had the same ratios as authentic *cis*-TTMO (data not shown). LRIs on the two phases were calculated as 1353 and 1067, respectively. Further confirmation of the natural existence of *cis*-TTMO in wine was obtained from the co-injection experiments, which were conducted on two different achiral GC columns and the chiral Rt-βDEXcst GC column, using the same wine sample (SB_7) that was used for determination of LRIs. As observed in Fig. 4A and B, with higher spiking level of *cis*-TTMO, the intensities of selected ions were enhanced correspondingly on both achiral columns, though *m/z* 83 on both achiral phases and *m/z* 101 on HP-INNOWAX suffered from interference of background ions. A slight shift in retention time (<0.037 min) was also observed on HP-INNOWAX phase, but the increasing intensities of the target ions were still evident and the selected ions for d_4-*cis*-TTMO drifted in retention time simultaneously (data not shown). Moreover, the selected ion mass spectra of natural *cis*-TTMO in SB_7 (Fig. 4C) matched with that of a commercial Sauvignon blanc wine (used for calibration and not containing any TTMO) spiked with 246 ng/L of *cis*-TTMO (Fig. 4D) on a DB-5ms UI column. The intensity of the selected ion (*m/z* 160) of (2*R*,6*R*)-TTMO was also found to increase with higher spiking level of authentic TTMO on the chiral column (Fig. B.7C of Appendix B). In combination, this information confirmed that (2*R*,6*R*)-TTMO (as the tentatively assigned enantiomer) was present in wine. Indeed, this was the first time that this compound appeared to have been identified in any beverage, having only been reported previously as a potential perfuming agent (Winter, 1980).

In order to evaluate the potential influence on wine aroma characteristics, the ODT of TTMO in a charcoal stripped neutral white wine was investigated using a 3-alternative forced choice (3-AFC) sensory study (detailed in Section A.3 of Appendix A). The ODT from the panel was calculated to be 14.9 μg/L and informal assessment of the aroma quality revealed descriptors for TTMO that included 'citrus', 'green', 'sweet/caramel', and 'mango' when spiked at concentrations of 5 and 10 μg/L, and 'mango/tropical', 'sweet/caramel', and 'onion/sulfur/sweaty' at

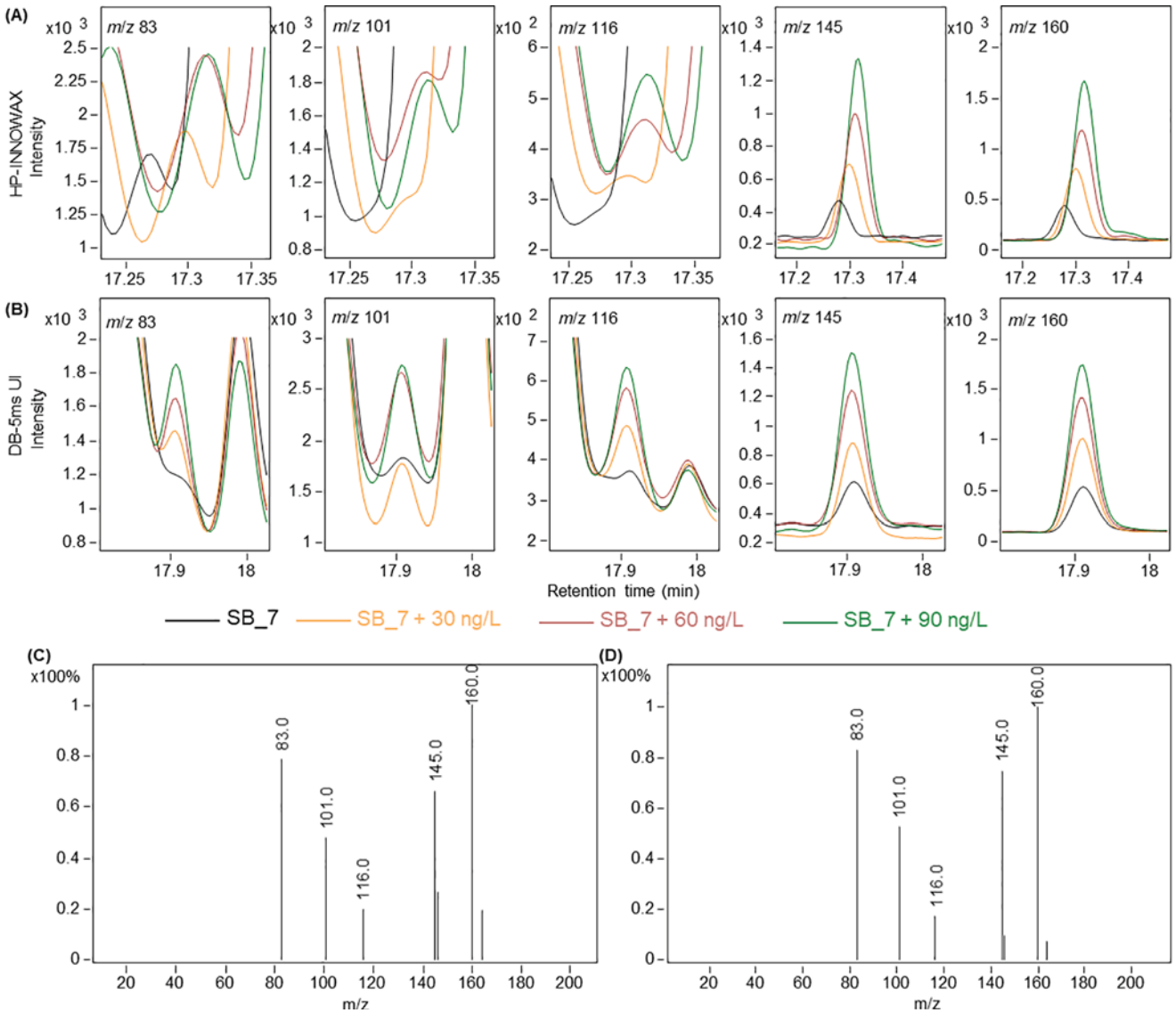

Fig 4. Co-injection experiments for *cis*-TTMO on (A) HP-INNOWAX column and (B) DB-5ms UI column using authentic *cis*-TTMO spiked at concentrations of 30 ng/L, 60 ng/L, and 90 ng/L into SB_7 wine containing 28 ng/L of (2*R*,6*R*)-TTMO. Background subtracted SIM mass spectra at 17.9 min on DB-5ms UI column for (C) natural *cis*-TTMO in SB_7 wine sample and (D) a commercial Sauvignon blanc wine sample (with no detectable TTMO) spiked with 246 ng/L of authentic *cis*-TTMO.

higher concentrations (19 to 100 μg/L).

3.6. Distribution of chiral thiols in the wines

In parallel to undertaking chiral analysis of *cis*-2-MPO, the distribution of chiral 3-SH was also studied (Table B.1 of Appendix B) in the wines sourced from previous studies (Chen et al., 2018b; Chen et al., 2019; Wang et al., 2020) to assess the correlation between the enantiomers of *cis*-2-MPO and those of 3-SH. In general, the concentrations of (3*S*)-3-SH and (3*R*)-3-SH ranged from 359 to 4412 ng/L and 297 to 4170 ng/L (extrapolated values used when outside the calibration range of 2500 ng/L for each enantiomer), respectively, in the commercial Sauvignon blanc (SB) wines (Fig. 5A). These values were generally higher than those determined for the commercial Chardonnay (C) wines, which had 277–1920 ng/L for (3*S*)-3-SH and 264–1619 ng/L for (3*R*)-3-SH (Fig. 5A). The remaining seven commercial wines of different varieties showed concentrations of 3-SH enantiomers approximately in the same range (although not to the same maximum) as those for Chardonnay, with concentrations between 373 and 637 ng/L for (3*S*)-3-SH, and 247 and 582 ng/L for (3*R*)-3-SH (Fig. 5A). Enantiomers of 3-SH distributed approximately equally in these wines, albeit with a slight preference for (3*S*)-3-SH, which accounted for 53% of total 3-SH on average (Fig. 5B). This enantiomeric distribution of 3-SH was in line with previous reports (Chen et al., 2018a; Tominaga et al., 2006).

In terms of the experimental Sauvignon blanc wines sourced from previous studies (Chen et al., 2019; Wang et al., 2020), as shown in Fig. 5A, the concentrations of (3*S*)-3-SH and (3*R*)-3-SH were 1472–6294 ng/L and 1237–7474 ng/L (extrapolated values used when outside the calibration range of 2500 ng/L for each enantiomer), respectively, in the wines made with different yeast strains (SB_J7, SB_VIN13, and SB_co-inoculation); 186–422 ng/L and 207–608 ng/L, respectively, in pre-fermentation frozen juice treatment wines (FJ wine samples); and 357–912 ng/L and 512–1073 ng/L, respectively, in pre-fermentation frozen berry treatment wines (FB wine samples). (3*R*)- and (3*S*)-3-SH were approximately equally distributed in these wines (Fig. 5B), with (3*R*)-3-SH accounting for 55% of the total concentration of 3-SH on average. This slight predominance of (3*R*)-3-SH was opposite to what has been observed in the commercial wines (Chen, Capone, Tondini, & Jeffery, 2018), with differences potentially arising due to grape variety/clone and yeast strain used for winemaking. Taking all wines into consideration (i.e., commercial and experimental wines), (3*S*)-3-SH accounted for 51% of the total concentrations of 3-SH on average. The

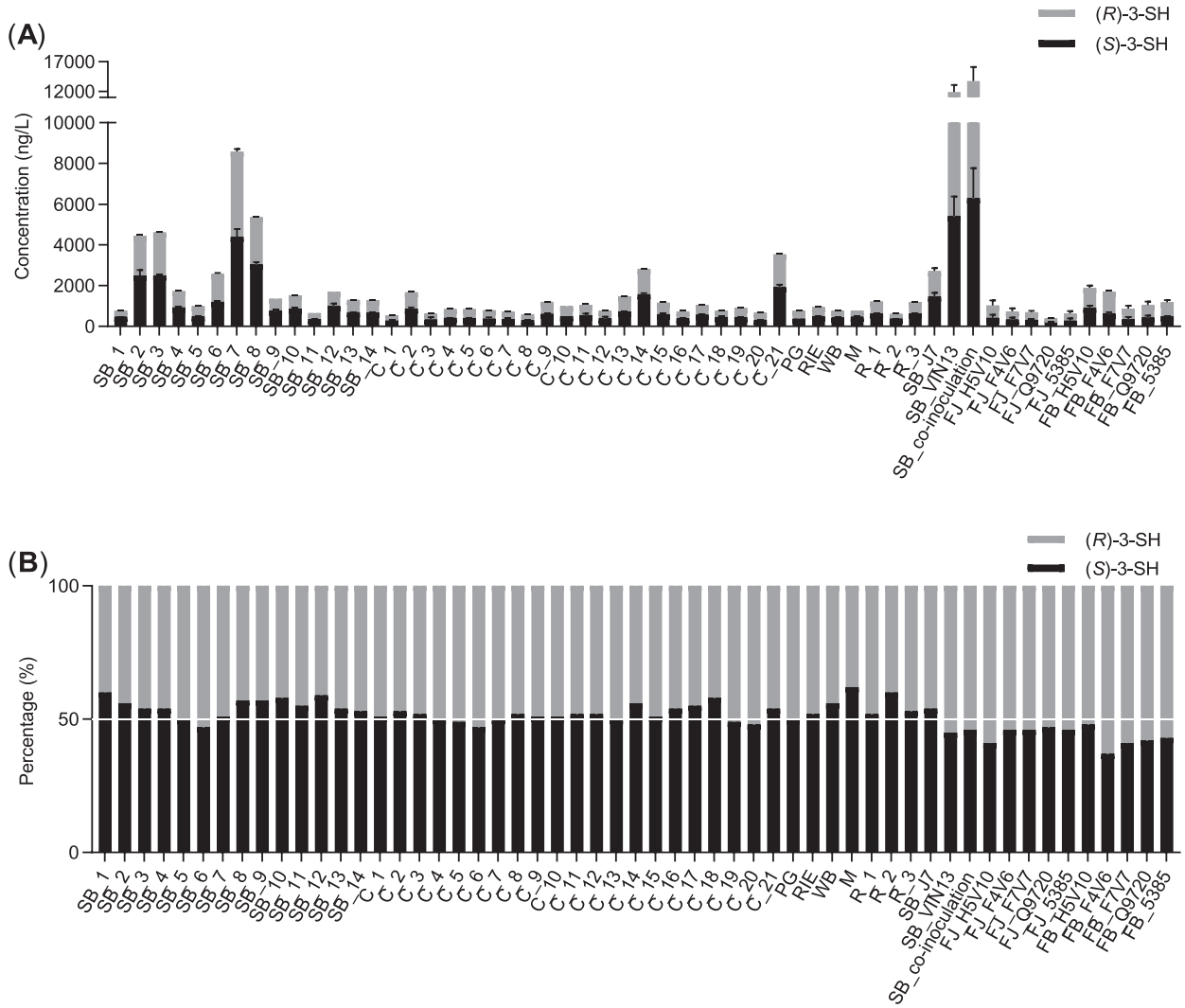

Fig 5. Results from chiral HPLC-MS/MS analysis of derivatives of (3*R*)-3-SH and (3*S*)-3-SH in wines showing (A) enantiomer concentrations (ng/L) and (B) relative enantiomer ratios. Error bars represent standard deviation of commercial wines (n = 2) and experimental wines (n = 3, except for SB_co-inoculation with n = 2). Abbreviations and details of each wine are presented in Table B.1 of Appendix B along with the concentrations of each 3-SH enantiomer.

slight predominance of (3*S*)-3-SH is at odds with the higher proportion of (2*S*,4*R*)-2-MPO noted earlier, if assuming purely chemical formation of oxathianes. The possible influence of enantioselective enzymatic reactions (during fermentation) on the production of *cis*-2-MPO enantiomers could potentially be explored in future studies.

In order to explore the evolution of (3*S*)-/(3*R*)-3-SH and (3*S*)-/(3*R*)-3-SHA during AF, the wine extracts used for monitoring the evolution of achiral thiols during AF from a previous study were reanalysed on the same instrument (Wang et al., 2020) with the published method using a chiral stationary phase (Chen et al., 2018a). As shown in Fig. B.8 of Appendix B, (3*S*)-3-SH accounted for about 70% of total 3-SH from an early stage of AF then gradually decreased to 47% by the end of AF (Fig. B.8A). On the other hand, (3*S*)-3-SHA maintained a relatively stable proportion of total 3-SHA, at nearly 70% throughout fermentation (Fig. B.8B). Both of these outcomes were in line with the only other reported study of thiol enantiomer profiles during fermentation (Tominaga et al., 2006). The results of one-way ANOVA (Fig. B.8A of Appendix B) revealed that the ratio of (3*S*)-3-SH declined significantly ($p < 0.05$) within the first three days of fermentation whereas the ratio of (3*S*)-3-SHA showed no significant change ($p > 0.05$) throughout the whole fermentation stage.

3.7. Correlation analysis of chiral cis-2-MPO and chiral thiols

cis-2-MPO had been proposed to originate from the combination of 3-SH and acetaldehyde when both are present in wine, and the previously determined strong correlation (r = 0.720) between *cis*-2-MPO and 3-SH using achiral analyses further supported this assumption (Chen et al., 2018b). However, the relationship between the enantiomers of 3-SH and those of *cis*-2-MPO had not been studied and was worthy of exploration. Having developed a method for the determination of enantiomers of *cis*-2-MPO and with 3-SH enantiomers quantified, Pearson correlation analysis was conducted for (3*S*)-3-SH with (2*R*,4*S*)-2-MPO, and (3*R*)-3-SH with (2*S*,4*R*)-2-MPO, to assess the relationship between enantiomers of 3-SH (Fig. 5A) and those of *cis*-2-MPO (Fig. 3A). With all wine samples containing both *cis*-2-MPO and 3-SH enantiomers included in the analysis, only (3*S*)-3-SH correlated moderately with (2*R*,4*S*)-2-MPO (r = 0.584, $p < 0.001$) whereas (3*R*)-3-SH correlated poorly with (2*S*,4*R*)-2-MPO (r = 0.314, $p = 0.080$). However, the correlations between respective enantiomers became strong and significant (r = 0.860 and 0.654, respectively, $p < 0.001$) when data points for SB_VIN13 wines from yeast fermentation experiments were eliminated from the analysis. This result was in line with the previous strong correlation obtained from achiral analyses (Chen et al., 2018b). The substantial 3-SH concentrations extrapolated in those Sauvignon blanc wines from yeast fermentation experiments (SB_VIN13 and SB_co-inoculation in Fig. 5A) may explain their large impact on the correlations.

Given the range of enantiomeric distributions of 3-SH and *cis*-2-MPO in the studied wines, Pearson correlation analysis was also performed with the ratios of (3*S*)-3-SH/(3*R*)-3-SH against (2*R*,4*S*)-2-MPO/(2*S*,4*R*)-2-MPO, revealing a significant and moderate correlation with r = 0.586 ($p < 0.001$). Taking these correlation results with the data presented earlier (Section 3.3), where spiking wine with (3*R*)-3-SH was shown to lead to a corresponding increase in a single enantiomer assigned as (2*S*,4*R*)-2-MPO, this study has provided direct evidence to verify the causation regarding likely pathways to 1,3-oxathiane formation. In other words, this work has shown that 1,3-oxathianes can arise from the chemical reaction of thiols such as 3-SH and 4-MSPOH with acetaldehyde in the acidic matrix of wines. Furthermore, it has provided a method for studying the link between chirality of thiols and their related 1,3-oxathianes, which may be important for future studies intending to assess the impact on wine sensory properties as a result of differences in enantiomer distribution.

4. Conclusion

In summary, given the importance of varietal thiols to wine aroma and of stereochemistry to aroma qualities more generally, a SIDA HS-SPME-GC–MS method using a chiral stationary phase was developed for quantification of the two enantiomers of *cis*-2-MPO, namely (2*R*,4*S*)-2-MPO and (2*S*,4*R*)-2-MPO, and applied to a selection of commercial and experimental wines. The elution order of enantiomers of *cis*-2-MPO was assigned based on the corresponding increase in peak area ratio against labelled internal standard of one *cis*-2-MPO enantiomer when spiking with increasing levels of (3*R*)-3-SH. This experiment also revealed the ability to form 1,3-oxathiane in wine when the thiol was present with acetaldehyde. Generally, the concentration of (2*S*,4*R*)-2-MPO ranged from undetectable to 303 ng/L, and (2*R*,4*S*)-2-MPO was determined between undetectable and 250 ng/L. The (2*S*,4*R*)-enantiomer had an average proportion of 57% across the studied commercial and experimental wines. In parallel, (3*R*)-3-SH and (3*S*)-3-SH were quantified in the studied wines, showing that the enantiomers were distributed roughly equally but with a disposition towards (3*S*)-3-SH, with a mean percentage of 51% across commercial and experimental wines. Pearson correlation analysis revealed strong correlations between (3*S*)-3-SH with (2*R*,4*S*)-2-MPO and (3*R*)-3-SH with (2*S*,4*R*)-2-MPO.

Inspired by the identification of *cis*-2-MPO in wines, *cis*-TTMO (assigned as *cis* on the basis of NMR data and thermodynamic considerations) was positively identified and found in 10 of the wines that were analysed, with concentrations ranging from between the LOD (5 ng/L) and LOQ (16 ng/L) to 28 ng/L. The ODT of TTMO in a charcoal stripped neutral white wine was determined to be 14.9 μg/L, with aromas imparted at lower concnetrations described as ‘citrus’, ‘green’, ‘sweet/caramel’, and ‘mango’, then tending toward ‘mango/tropical’, ‘sweet/caramel’, and ‘onion/sulfur/sweaty’ ‘sulfurous’ at higher concentrations. With a similar structure to 2-MPO, there is the potential for formation of two pairs of enantiomers of TTMO due to chirality and *cis*/*trans* isomerism, but only one of the two possible *cis*-enantiomers was detected. Further work is needed to assign this enantiomer of *cis*-TTMO and to develop a method to analyse the prospective enantiomers of 4-MSPOH, so the relationship between *cis*-TTMO and 4-MSPOH can be investigated. Nonetheless, with the identification of this new 1,3-oxathiane and evidence for the chemical formation of *cis*-2-MPO, it seems plausible that the corresponding 1,3-oxathianes of other thiols could exist, such as 3-sulfanylpentan-1-ol, 2-methyl-3-sulfanylbutan-1-ol, and 3-sulfanylheptan-1-ol found in noble rot wines.

CRediT authorship contribution statement

Xingchen Wang: Conceptualization, Formal analysis, Funding acquisition, Investigation, Methodology, Visualization, Writing - original draft, Writing - review & editing. **Dimitra L. Capone:** Conceptualization, Methodology, Supervision, Writing - review & editing. **Aurélie Roland:** Conceptualization, Supervision, Writing - review & editing. **David W. Jeffery:** Conceptualization, Funding acquisition, Methodology, Project administration, Supervision, Writing - review & editing.

Declaration of Competing Interest

The authors declare that they have no known competing financial interests or personal relationships that could have appeared to influence the work reported in this paper.

Acknowledgments

We thank Tracey Siebert (The Australian Wine Research Institute) for kindly lending us the Rt-βDEXcst column and Sijing Li (National Wine and Grape Industry Centre) for accurate mass results of synthesised standards. We acknowledge Paul Boss (Commonwealth Scientific and

Industrial Research Organisation, CSIRO) for the access to instrumentation and Sue Maffei (CSIRO) for assistance with the chiral analysis of thiols. Christine Bottcher (CSIRO) is thanked for initial assistance with accurate mass analysis. X. W. is a recipient of the joint scholarship of the University of Adelaide and China Scholarship Council (201806300044) and is supported by a Wine Australia supplementary scholarship (WA Ph1803). The Australian Research Council Training Centre for Innovative Wine Production (www.ARCwinecentre.org.au; project number IC170100008) is funded by the Australian Government with additional support from Wine Australia, Waite Research Institute and industry partners. The University of Adelaide is a member of the Wine Innovation Cluster.

Appendix A. Supplementary experimental section

A.1 Synthesis of TTMO and d_4-2,4,4,6-tetramethyl-1,3-oxathiane (d_4-TTMO)

The procedures were adapted from the previously reported synthesis of d_4-*cis*-2-MPO (Chen et al., 2018b). Briefly, 4-MSPOH (83 μL, 80 mg, 0.60 mmol) and acetaldehyde (168 μL, 131 mg, 3.0 mmol) were reacted under N_2 in 1.5 mL of dichloromethane containing 7.0 mg of *p*-TsOH and 270 mg of 4 Å sieves. The reaction was stirred for 30 min at room temperature (~25 °C) and monitored by TLC every 10 min using ceric ammonium molybdate dip ($R_f = 0.55$, dichloromethane). After consumption of the alcohol (as indicated by TLC), the reaction mixture was diluted with 1.5 mL of dichloromethane and washed sequentially with 3 mL of 10% aqueous $NaHCO_3$ and 3 mL of brine, then dried over $MgSO_4$. The solvent was removed *in vacuo* to afford 86 mg (0.54 mmol, 90.5% crude yield based on 4-MSPOH) of a colourless oil with purity of >99% according to GC–MS analysis. d_4-TTMO was prepared in the same manner except for using d_4-acetaldehyde (143 mg, 167 μL, 3.0 mmol), yielding 59 mg (60% crude yield based on 4-MSPOH) to afford a colourless oil with purity of >99%. As expected from the achiral synthesis, standards were subsequently found to be racemic mixtures (i.e., comprising enantiomer ratios of 50:50) according to chiral GC–MS analysis.

Proton and carbon nuclear magnetic resonance (NMR) spectra for TTMO and d_4-TTMO (Fig. B.3 to B.6 of Appendix B) were recorded with an Agilent 600 MHz NMR spectrometer with a cryoprobe using VnmrJ 4.2 software (Agilent, Santa Clara, CA). Spectra were acquired in chloroform-*d* at 25 °C with chemical shifts recorded as δ values in parts per million (ppm) and referenced to the residual $CHCl_3$ solvent signals. High resolution mass spectra for TTMO and d_4-TTMO were recorded using an Agilent 7200A quadrupole time-of-flight GC–MS equipped with a DB-WAXetr column (30 m × 250 μm × 0.25 μm, Agilent J&W). Samples were diluted in GC grade dichloromethane to a concentration of approximately 5 mg/L and a 2 μL injection volume was used. The inlet was set at 250 °C with a split ratio of 5:1. Carrier gas (helium) flow rate was 1.5 mL/min with an oven programme of 50 °C for 5 min, then ramping to 250 °C at 10 °C/min, and holding for 10 min.

^{1}H NMR (600 MHz, $CDCl_3$). TTMO: δ (ppm) 4.84 (1H, q, $J = 6.2$, H_{2ax}), 3.67–3.62 (1H, m, H_{6ax}), 1.38–1.35 (8H, m, H_5, H_8, H_{10}), 1.17 (3H, s, H_7), 1.12 (3H, d, $J = 6.2$ Hz, CH_9). d_4-TTMO: δ (ppm) 3.67–3.62 (1H, m, H_{6ax}), 1.37–1.35 (5H, m, H_5, H_8), 1.17 (3H, s, CH_7), 1.12 (3H, d, $J = 6.2$ Hz, CH_9).

^{13}C NMR (600 MHz, $CDCl_3$). TTMO: δ (ppm) 75.6 (C-2), 71.4 (C-6), 46.6 (C-5), 41.1 (C-4), 32.5 (C-7), 27.8 (C-8), 22.4 (C-9), 21.8 (C-10); d_4-TTMO: δ (ppm) 71.4 (C-6), 46.7 (C-5), 41.0 (C-4), 32.5 (C-7), 27.9 (C-8), 22.4 (C-9).

EI-HRMS (*m/z*). Calculated for $C_8H_{16}OS$, 160.0922 Da, found, 160.0873 Da. Calculated for $C_8H_{12}D_4OS$, 164.1173 Da, found, 164.1119 Da.

EI-MS, *m/z* (%). TTMO: 160 (M^+, 100), 145 (77), 116 (21), 101 (77), 83 (60), 74 (92), 60 (98); d_4-TTMO: 164 (M^+, 100), 146 (72), 116 (22), 101 (73), 83 (55), 74 (84), 60 (63).

A.2 Preliminary method development of SIDA-HS-SPME-GC–MS

With CycloSil-B column initially equipped, only liquid injection was used with an inlet temperature of 200 °C and carrier gas flow rate of 1.5 mL/min. The inlet was set to pulsed splitless mode with pulse pressure of 241.3 kPa at 0.5 min. Two oven temperature programmes were assessed: 40 °C for 1 min, then ramping to 240 °C at 5 °C/min and holding for 10 min; 40 °C for 1 min, then ramping to 120 °C at 3 °C/min, then to 240 °C at 20 °C/min and holding for 10 min. MS source, quadrupole, and transfer line temperatures were set at 230 °C, 150 °C, and 240 °C, respectively, and EI (70 eV) mass spectra were recorded in full-scan mode with a gain factor of 1.

With Cyclodex-B column installed, parameters including initial oven temperature (65, 40, and 36 °C), initial isocratic time (1, 5, and 10 min), oven temperature ramp programmes, and carrier gas flow rates (2.0, 1.9, and 1.7 mL/min) were investigated using liquid injection with inlet temperature of 200 °C. The optimised oven programme was 36 °C for 5 min, ramping to 90 °C at 1.5 °C/min, then to 120 °C at 3.0 °C/min, and to 240 °C at 20 °C/min with a hold time of 10 min, using a flow rate of 1.7 mL/min. MS source, quadrupole, and transfer line temperatures were set at 230 °C, 150 °C, and 240 °C, respectively. The MS was set to full-scan mode with a gain factor of 1. Consequently, the optimised conditions with liquid injection in full-scan mode were converted to a HS-SPME method with the MS in SIM mode and sample incubation parameters reported previously (Chen et al., 2018b), using a 1 cm PDMS/DVB SPME fibre (65 μm, Sigma-Aldrich) after being conditioned following manufacturer's instructions. A model wine spiked at a single level of *cis*-TTMO (1007 ng/L), *cis*-2-MPO (2000 ng/L), and d_4-*cis*-2-MPO (2000 ng/L) was prepared for obtaining retention times and a commercial Sauvignon blanc wine spiked with five levels of *cis*-TTMO (0–235 ng/L), *cis*-2-MPO (0–1000 ng/L), and d_4-*cis*-2-MPO (200 ng/L) were prepared for further method optimisation. Mass spectra were recorded with a gain factor of 10, and two SIM windows with dwell times of 25 ms were set: the first window (12 to 35 min) monitored ions of *m/z* 160, 145, 116, 101, 83, and 60 for *cis*-TTMO and the second window (35 to 65 min) monitored ions of *m/z* 164, 160, 146, 145, 114, 101, and 87 to detect d_4-*cis*-2-MPO and *cis*-2-MPO.

Lastly, with the Rt-βDEXcst column installed and synthesis of d_4-TTMO completed, the optimised method from the Cyclodex-B column was modified to account for the difference in column size and maximum temperature. Liquid injection of authentic standards dissolved in GC grade dichloromethane (section 2.2.1) with MS in scan mode was firstly conducted for the determination of retention times before further HS-SPME method optimisation. The sample extraction parameters for the HS-SPME method development stage were the same as those used for Cyclodex-B column and inlet temperature was 220 °C with helium flow rate of 1.3 mL/min. The initial oven temperature was 37 °C for 5 min, and increased to 90 °C at 1.5 °C/min, then to 120 °C at 3.0 °C/min, and to 220 °C at 30.0 °C/min with a hold time of 10 min, giving a total run time of 63.7 min. The oven temperature programme and SIM windows were then optimised by increasing the second ramp target temperature from 120 to 130 °C and setting first SIM window at 12 to 40 min and second SIM window 40 to 66.7 min. MS source, quadrupole, and transfer line temperatures were set at 230 °C, 150 °C, and 220 °C, respectively. A 2 cm DVB/CAR/PDMS fibre (50/30 μm, Sigma-Aldrich) was conditioned and used for the optimisation of extraction of *cis*-TTMO from a wine matrix with carrier gas flow rate of 1.1 mL/min to increase separation and sensitivity of enantiomers of d_4-*cis*-TTMO and *cis*-TTMO. The previous two SIM time windows were combined with d_4-*cis*-TTMO included in the method, with *m/z* 164, 146, 116, 101, and 83 being used to monitor d_4-*cis*-2-MPO (excluding *m/z* 83) and d_4-*cis*-TTMO, and *m/z* 160, 145, 116, 101, and 83 for the enantiomers of *cis*-2-MPO (excluding *m/z* 83) and *cis*-TTMO, with dwell times set at 20 ms. The underlined ions were used for quantification and the remainder were used as qualifiers.

A.3 Odour detection threshold (ODT) and aroma description of TTMO

The ODT of TTMO was determined by a 3-alternative forced choice study according to ASTM standard practice E 679-04 (reapproved 2011) (ASTM, 2011). The study was approved by Human Research Ethics Committee of the University of Adelaide (Ethics approval number: H-2019–135). Informed consent was obtained from panellists prior to beginning the study. The panel (n = 39) consisted of 12 males and 26 females, with age ranging from 18 to over 65. Half of the panellists had received wine related education, 17 worked in wine industry, and 27 people consumed wine at least once per week. A commercial neutral white wine (Chardonnay, 2019, 13.5% v/v, unoaked) was used as the base wine, with 25 × 750 mL bottles being pooled to maintain homogeneity of the base wine. The pooled wine was stripped by stirring for 30 min with 4.5 g/L of food grade charcoal (Winequip, Magill, SA, Australia) to minimise the influence of other volatiles. The charcoal was removed by careful batch-wise filtration (0.45 μm filter membrane, Millipore, US), the filtered wine was pooled, and then divided into seven lots, with six for spiking and the other one to act as the control.

Sample preparation was based on that reported by Cooke et al. (2009). An ethanolic solution of TTMO (<0.1 mL) was spiked into the charcoal stripped Chardonnay wine to prepare ascending concentrations of TTMO with a constant factor of three (0.46 μg/L, 1.37 μg/L, 4.12 μg/L, 12.36 μg/L, 37.07 μg/L, and 111.20 μg/L). An equal amount of ethanol was spiked into control wines at each spiking level to eliminate the influence from ethanol. Wines were stored at 4 °C prior to use and samples (25 mL) were presented in four-digit coded clear glasses covered with plastic lids. The sensory study was conducted in sensory booths and serving order of samples was designed with RedJade software (Redwood City, CA). Panellists were required to indicate the odd wine according to aroma only and a forced choice had to be made if the odd wine sample could not be determined. The best estimate threshold (BET) for each panellist was calculated and the group ODT was expressed as the geometric mean of the BETs of each panellist.

Another group of charcoal stripped Chardonnay wines spiked with six levels of TTMO (5, 10, 19, 30, 40, and 100 μg/L) was prepared for the aroma description analysis by an informal panel consisting of eight wine researchers. Each panellist was served with the group of six samples at once and was instructed to describe aromas of wine samples from lower to higher spiking levels in their own words in writing. A discussion was then conducted to identify common terms and aroma descriptors used by at least four panellists have been reported.

Appendix B. Supplementary data

Supplementary data to this article can be found online at https://doi.org/10.1016/j.foodchem.2021.129406.

References

ASTM. (2011). Standard E679-04. In Standard practice for determination of odor and taste thresholds by a forced-choice ascending concentration series method of limits, vol. E679-04 (pp. 1-7). ASTM International: West Conshohocken, PA, United States.

Bencomo-Rodriguez, J. J., Gambetta, J., Rigou, P., Canelo, N., Bouvier, N., Roland, A., & Salmon, J.-M. (2011). Quantitative determination of varietal disulfides in wine and their behavior during alcoholic fermentation. In P. Darriet (Ed.), *9e Symposium international d'œnologie de Bordeaux-Oeno 2011*. Dunod.

Chen, L., Capone, D. L., & Jeffery, D. W. (2018a). Chiral analysis of 3-sulfanylhexan-1-ol and 3-sulfanylhexyl acetate in wine by high-performance liquid chromatography–tandem mass spectrometry. *Analytica Chimica Acta, 998*, 83–92. https://doi.org/10.1016/j.aca.2017.10.031.

Chen, L., Capone, D. L., & Jeffery, D. W. (2018b). Identification and quantitative analysis of 2-methyl-4-propyl-1,3-oxathiane in wine. *Journal of Agricultural and Food Chemistry, 66*(41), 10808–10815. https://doi.org/10.1021/acs.jafc.8b04027.

Chen, L., Capone, D. L., Nicholson, E. L., & Jeffery, D. W. (2019). Investigation of intraregional variation, grape amino acids, and pre-fermentation freezing on varietal thiols and their precursors for *Vitis vinifera* Sauvignon blanc. *Food Chemistry, 295*, 637–645. https://doi.org/10.1016/j.foodchem.2019.05.126.

Chen, L., Capone, D. L., Tondini, F. A., & Jeffery, D. W. (2018). Chiral polyfunctional thiols and their conjugated precursors upon winemaking with five Vitis vinifera Sauvignon blanc clones. *Journal of Agricultural and Food Chemistry, 66*(18), 4674–4682. https://doi.org/10.1021/acs.jafc.8b01806.

Coetzee, C., & du Toit, W. J. (2012). A comprehensive review on Sauvignon blanc aroma with a focus on certain positive volatile thiols. *Food Research International, 45*(1), 287–298. https://doi.org/10.1016/j.foodres.2011.09.017.

Cooke, R. C., van Leeuwen, K. A., Capone, D. L., Gawel, R., Elsey, G. M., & Sefton, M. A. (2009). Odor detection thresholds and enantiomeric distributions of several 4-alkyl substituted γ-lactones in Australian red wine. Journal of Agricultural and Food Chemistry, 57(6), 2462-2467. doi: 10.1021/jf802866f.

Darriet, P., Tominaga, T., Lavigne, V., Boidron, J.-N., & Dubourdieu, D. (1995). Identification of a powerful aromatic component of *Vitis vinifera* L. var. Sauvignon wines: 4-Mercapto-4-methylpentan-2-one. *Flavour and Fragrance Journal, 10*(6), 385–392. https://doi.org/10.1002/ffj.2730100610.

Engel, K.-H. (2020). Chirality: An important phenomenon regarding biosynthesis, perception, and authenticity of flavor compounds. *Journal of Agricultural and Food Chemistry, 68*(38), 10265–10274. https://doi.org/10.1021/acs.jafc.0c01512.

Ettre, L. S. (1993). Nomenclature for chromatography (IUPAC Recommendations 1993). *Pure and Applied Chemistry, 65*(4), 819–872.

King, E. S., Osidacz, P., Curtin, C., Bastian, S. E. P., & Francis, I. L. (2011). Assessing desirable levels of sensory properties in Sauvignon blanc wines – consumer preferences and contribution of key aroma compounds. *Australian Journal of Grape and Wine Research, 17*(2), 169–180. https://doi.org/10.1111/j.1755-0238.2011.00133.x.

Lopes, P., Silva, M. A., Pons, A., Tominaga, T., Lavigne, V., Saucier, C., … Dubourdieu, D. (2009). Impact of oxygen dissolved at bottling and transmitted through closures on the composition and sensory properties of a Sauvignon blanc wine during bottle storage. *Journal of Agricultural and Food Chemistry, 57*(21), 10261–10270. https://doi.org/10.1021/jf9023257.

MacLeod, R., Prosser, H., Fikentscher, L., Lanyi, J., & Mosher, H. S. (1964). Asymmetric reductions. XII. Stereoselective ketone reductions by fermenting yeast. *Biochemistry, 3*(6), 838–846. https://doi.org/10.1021/bi00894a020.

Murat, M.-L., Tominaga, T., Saucier, C., Glories, Y., & Dubourdieu, D. (2003). Effect of anthocyanins on stability of a key odorous compound, 3-mercaptohexan-1-ol, in Bordeaux rosé wines. *American Journal of Enology and Viticulture, 54*(2), 135–138.

Nikolantonaki, M., & Waterhouse, A. L. (2012). A method to quantify quinone reaction rates with wine relevant nucleophiles: A key to the understanding of oxidative loss of varietal thiols. *Journal of Agricultural and Food Chemistry, 60*(34), 8484–8491. https://doi.org/10.1021/jf302017j.

Perlin, A. S., & Koch, H. J. (1970). Carbon-13 and proton chemical shifts of cyclohexanes in relation to interaction energy. *Canadian Journal of Chemistry, 48*(16), 2639–2643. https://doi.org/10.1139/v70-445.

Roland, A., Schneider, R., Razungles, A., & Cavelier, F. (2011). Varietal thiols in wine: Discovery, analysis and applications. *Chemical Reviews, 111*(11), 7355–7376. https://doi.org/10.1021/cr100205b.

Singer, G., Heusinger, G., Froehlich, O., Schreier, P., & Mosandl, A. (1986). Chirality evaluation of 2-methyl-4-propyl-1,3-oxathiane from the yellow passion fruit. *Journal of Agricultural and Food Chemistry, 34*(6), 1029–1033. https://doi.org/10.1021/jf00072a025.

Takase, H., Sasaki, K., Kiyomichi, D., Kobayashi, H., Matsuo, H., & Takata, R. (2018). Impact of *Lactobacillus plantarum* on thiol precursor biotransformation leading to production of 3-sulfanylhexan-1-ol. *Food Chemistry, 259*, 99–104. https://doi.org/10.1016/j.foodchem.2018.03.116.

Tominaga, T., Baltenweck-Guyot, R., Peyrot des Gachons, C., & Dubourdieu, D. (2000). Contribution of volatile thiols to the aromas of white wines made from several *Vitis vinifera* grape varieties. *American Journal of Enology and Viticulture, 51*(2), 178–181.

Tominaga, T., Darriet, P., & Dubourdieu, D. (1996). Identification of 3-mercaptohexyl acetate in Sauvignon wine, a powerful aromatic compound exhibiting box-tree odor. *Vitis, 35*(4), 207–210. https://doi.org/10.5073/vitis.1996.35.207-210.

Tominaga, T., Furrer, A., Henry, R., & Dubourdieu, D. (1998). Identification of new volatile thiols in the aroma of *Vitis vinifera* L. var. Sauvignon blanc wines. *Flavour and Fragrance Journal, 13*(3), 159–162. https://doi.org/10.1002/(SICI)1099-1026(199805/06)13:3<159::AID-FFJ709>3.0.CO;2-7.

Tominaga, T., Niclass, Y., Frerot, E., & Dubourdieu, D. (2006). Stereoisomeric distribution of 3-mercaptohexan-1-ol and 3-mercaptohexyl acetate in dry and sweet white wines made from *Vitis vinifera* (Var. Sauvignon blanc and Semillon). *Journal of Agricultural and Food Chemistry, 54*(19), 7251–7255. https://doi.org/10.1021/jf061566v.

Wang, X., Chen, L., Capone, D. L., Roland, A., & Jeffery, D. W. (2020). Evolution and correlation of *cis*-2-methyl-4-propyl-1,3-oxathiane, varietal thiols, and acetaldehyde during fermentation of Sauvignon blanc juice. *Journal of Agricultural and Food Chemistry, 68*(32), 8676–8687. https://doi.org/10.1021/acs.jafc.0c03183.

Weber, B., Maas, B., & Mosandl, A. (1995). Stereoisomeric flavor compounds. 72. Stereoisomeric distribution of some chiral sulfur-containing trace components of yellow passion fruits. *Journal of Agricultural and Food Chemistry, 43*(9), 2438–2441. https://doi.org/10.1021/jf00057a023.

Winter, M. (1980). Oxathiane and oxathiolane derivatives as perfuming agents. *U.S. Patent No. 4220561A*. Washington D.C.: U.S. Patent and Trademark Office.

Winter, M., Furrer, A., Willhalm, B., & Thommen, W. (1976). Identification and synthesis of two new organic sulfur compounds from the yellow passion fruit (*Passiflora edulis* f. *flavicarpa*). *Helvetica Chimica Acta, 59*(5), 1613–1620. https://doi.org/10.1002/hlca.19760590520.

APPENDIX B

Supplementary data for

Chiral analysis of *cis*-2-methyl-4-propyl-1,3-oxathiane and identification of *cis*-2,4,4,6-tetramethyl-1,3-oxathiane in wine

Xingchen Wang[a], Dimitra L. Capone[a,b], Aurélie Roland[c], David W. Jeffery[a,b,*]

[a] Department of Wine Science and Waite Research Institute, The University of Adelaide (UA), PMB 1, Glen Osmond, SA 5064, Australia
[b] Australian Research Council Training Centre for Innovative Wine Production, UA, PMB 1, Glen Osmond, SA 5064, Australia
[c] SPO, INRAE, Univ Montpellier, Institut Agro, Montpellier, France

*Corresponding author
E-mail address: david.jeffery@adelaide.edu.au (David W. Jeffery)

Table of Contents

Table B.1 Details of commercial and experimental wines used for quantification of 1,3-oxathianes and varietal thiols, and concentrations (ng/L) of enantiomers of *cis*-2-MPO and 3-SH.

wine	code	(2*R*,4*S*)-2-MPO	(2*S*,4*R*)-2-MPO	(3*S*)-3-SH	(3*R*)-3-SH
Commercial [a]					
Sauvignon blanc	SB_1 [b]	– [f]	–	470±6	316±9
Sauvignon blanc	SB_2	210±3	246±3	2510±252	1945±31
Sauvignon blanc	SB_3	82±2	102±3	2510±39	2097±30
Sauvignon blanc	SB_4	16±0	22±2	925±31	800±42
Sauvignon blanc	SB_5 [b]	–	–	495±23	500±3
Sauvignon blanc	SB_6	37±5	45±3	1208±37	1359±60
Sauvignon blanc	SB_7	250±4	303±14	4412±367 [g]	4170±126 [g]
Sauvignon blanc	SB_8	86±2	93±3	3045±104 [g]	2310±49
Sauvignon blanc	SB_9	25±0	26±1	782±34	579±4
Sauvignon blanc	SB_10	23±1	23±2	880±36	644±8
Sauvignon blanc	SB_11 [b]	–	–	359±11	297±1
Sauvignon blanc	SB_12 [b]	–	–	1003±128	703±4
Sauvignon blanc	SB_13 [b]	–	–	700±9	602±11
Sauvignon blanc	SB_14 [b]	–	–	688±6	604±6
Chardonnay	C_1	–	–	277±27	264±14
Chardonnay	C_2	41±1	53±1	882±54	792±35
Chardonnay	C_3	-	-	338±114	309±13
Chardonnay	C_4	37±0	39±1	425±13	425±6
Chardonnay	C_5	–	–	412±24	431±13
Chardonnay	C_6	–	–	374±76	413±18
Chardonnay	C_7	–	–	365±33	364±14
Chardonnay	C_8	–	–	317±4	288±3
Chardonnay	C_9	21±0	31±1	611±46	597±15
Chardonnay	C_10	15±1	19±0	508±1	492±2
Chardonnay	C_11	15±0	21±1	544±81	510±38
Chardonnay	C_12	–	–	398±71	365±12
Chardonnay	C_13	26±0	27±0	734±3	735±8
Chardonnay	C_14	63±1	74±1	1576±60	1239±18
Chardonnay	C_15	16±0	16±0	598±41	571±28
Chardonnay	C_16	–	–	399±3	344±23
Chardonnay	C_17	18±0	22±1	570±33	474±13
Chardonnay	C_18	–	–	457±47	329±24
Chardonnay	C_19	30±14	31±3	442±37	468±2
Chardonnay	C_20 [b]	69±1	68±3	326±16	356±20
Chardonnay	C_21	–	–	1920±134	1619±15
Pinot Grigio	PG	–	–	383±2	381±12
Riesling	RIE	88±2	204±1	490±21	452±21
White blend (variety not specified)	WB	19±1	22±0	429±18	335±18
Muscat	M	20±1	24±1	480±33	297±2
Rosé (Pinot noir)	R_1	30±1	34±1	637±20	582±42
Rosé (Sangiovese)	R_2	14±0	< LOQ	373±8	247±8
Rosé (variety not specified)	R_3	16±1	22±1	632±12	566±10

Table B.1 contd.

wine	code	(2*R*,4*S*)-2-MPO	(2*S*,4*R*)-2-MPO	(3*S*)-3-SH	(3*R*)-3-SH
Experimental [c]					
J7 yeast inoculation [d]	SB_J7	–	–	1472±182	1237±152
VIN13 yeast inoculation [d]	SB_VIN13	15±4	20±2	5415±965 [g]	6519±1176 [g]
J7 & VIN13 yeasts co-inoculation [d]	SB_co-inoculation	< LOQ (14 ng/L)	< LOQ (18 ng/L)	6294±1479 [g]	7474±2336 [g]
Pre-fermentation freezing juice (clone H5V10) [e]	FJ_H5V10	63±2	76±7	422±150	608±246
Pre-fermentation freezing juice (clone F4V6) [e]	FJ_F4V6	18±4	29±9	337±94	401±158
Pre-fermentation freezing juice (clone F7V7) [e]	FJ_F7V7	14±0	26±1	318±40	377±67
Pre-fermentation freezing juice (clone Q9720) [e]	FJ_Q9720	–	–	186±25	207±8
Pre-fermentation freezing juice (clone 5385) [e]	FJ_5385	–	–	287±103	337±123
Pre-fermentation freezing berry (clone H5V10) [e]	FB_H5V10	29±17	253±287	912±106	981±118
Pre-fermentation freezing berry (clone F4V6) [e]	FB_F4V6	40±4	87±10	633±62	1073±38
Pre-fermentation freezing berry (clone F7V7) [e]	FB_F7V7	16±1	24±5	357±103	512±143
Pre-fermentation freezing berry (clone Q9720) [e]	FB_Q9720	< LOQ	29±3	440±95	605±179
Pre-fermentation freezing berry (clone 5385) [e]	FB_5385	16±2	31±3	508±14	677±103

[a] Commercial wines sourced from a previous study (Chen, Capone, & Jeffery, 2018). [b] Wines not studied for 1,3-oxathianes quantification due to a lack of volume. [c] Variety of experimental wines are Sauvignon blanc. [d] Wines from a previous study (Wang, Chen, Capone, Roland, & Jeffery, 2020). [e] Wines from a previous study (Chen, Capone, Nicholson, & Jeffery, 2019). [f]– not detected (LOD = 4 ng/L for (2*R*,4*S*)-2-MPO and 5 ng/L for (2*S*,4*R*)-2-MPO). [g] Extrapolated, outside the calibration range (0–2500 ng/L).

Table B.2 Method validation for the stable isotope dilution assay using headspace–solid-phase microextraction with gas chromatography-mass spectrometry.

Parameter			(2*R*,6*R*)-TTMO [d]	(2*S*,6*S*)-TTMO [d]	(2*R*,4*S*)-2-MPO	(2*S*,4*R*)-2-MPO
Calibration range (ng/L)			LOQ – 472		LOQ – 500	
Linearity (R^2)			0.9998	0.9998	0.9999	0.9998
Repeatability [a]	Low		3%	2%	2%	2%
	High		1%	2%	2%	3%
Recovery [b]	Chardonnay	Low	94% ± 0.00	99% ± 0.03	100% ± 0.07	106% ± 0.00
		High	108% ± 0.01	106% ± 0.02	108% ± 0.01	104% ± 0.04
	Grenache rosé	Low	96% ± 0.01	98% ± 0.02	102% ± 0.06	97% ± 0.07
		High	107% ± 0.02	102% ± 0.00	95% ± 0.02	105% ± 0.04
	Cabernet Sauvignon	Low	96% ± 0.02	98% ± 0.02	96% ± 0.02	107% ± 0.01
		High	103% ± 0.00	105% ± 0.04	101% ± 0.04	104% ± 0.03
	LOD (ng/L) [c]		5	4	4	5
	LOQ (ng/L) [c]		16	15	14	18

[a] Repeatability in a commercial Sauvignon blanc expressed as relative standard deviation (n = 7); low spiking level was 46.5 ng/L for both (2*R*,6*R*)-TTMO and (2*S*,6*S*)-TTMO, and 50 ng/L for both (2*R*,4*S*)-2-MPO and (2*S*,4*R*)-2-MPO; high spiking level was 236 ng/L for both (2*R*,6*R*)-TTMO and (2*S*,6*S*)-TTMO, and 500 ng/L for both (2*R*,4*S*)-2-MPO and (2*S*,4*R*)-2-MPO. [b] Recovery in different matrices as a percentage of spiked amount ± standard deviation (n = 2). [c] Limits of detection (LOD) and quantification (LOQ) determined in a commercial Sauvignon blanc. [d] The configuration was tentatively assigned.

Table B.3 Analyte concentrations (ng/L) existing in wines used for calibration and method validation.

Analyte	Sauvignon blanc	Chardonnay	Rosé	Cabernet Sauvignon
(2*R*,6*R*)-TTMO	ND [a]	ND	ND	ND
(2*S*,6*S*)-TTMO	ND	ND	ND	ND
(2*R*,4*S*)-2-MPO	10	NQ [b]	18	NQ
(2*S*,4*R*)-2-MPO	13	NQ	25	NQ

[a] ND, not detected (analyte concentration below limit of detection). [b] NQ, not quantified (analyte concentration below limit of quantification).

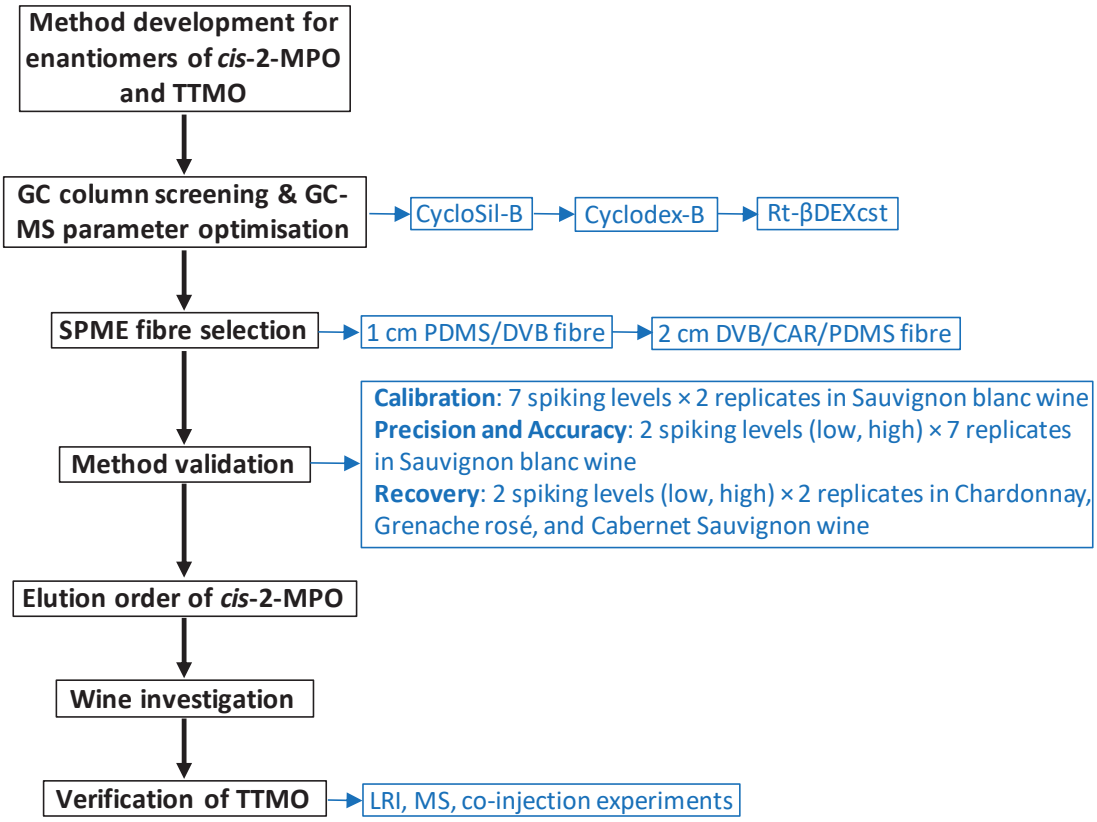

Fig. B.1 Workflow illustrating the method development process for enantiomers of *cis*-2-methyl-4-propyl-1,3-oxathiane and 2,4,4,6-tetramethyl-1,3-oxathiane.

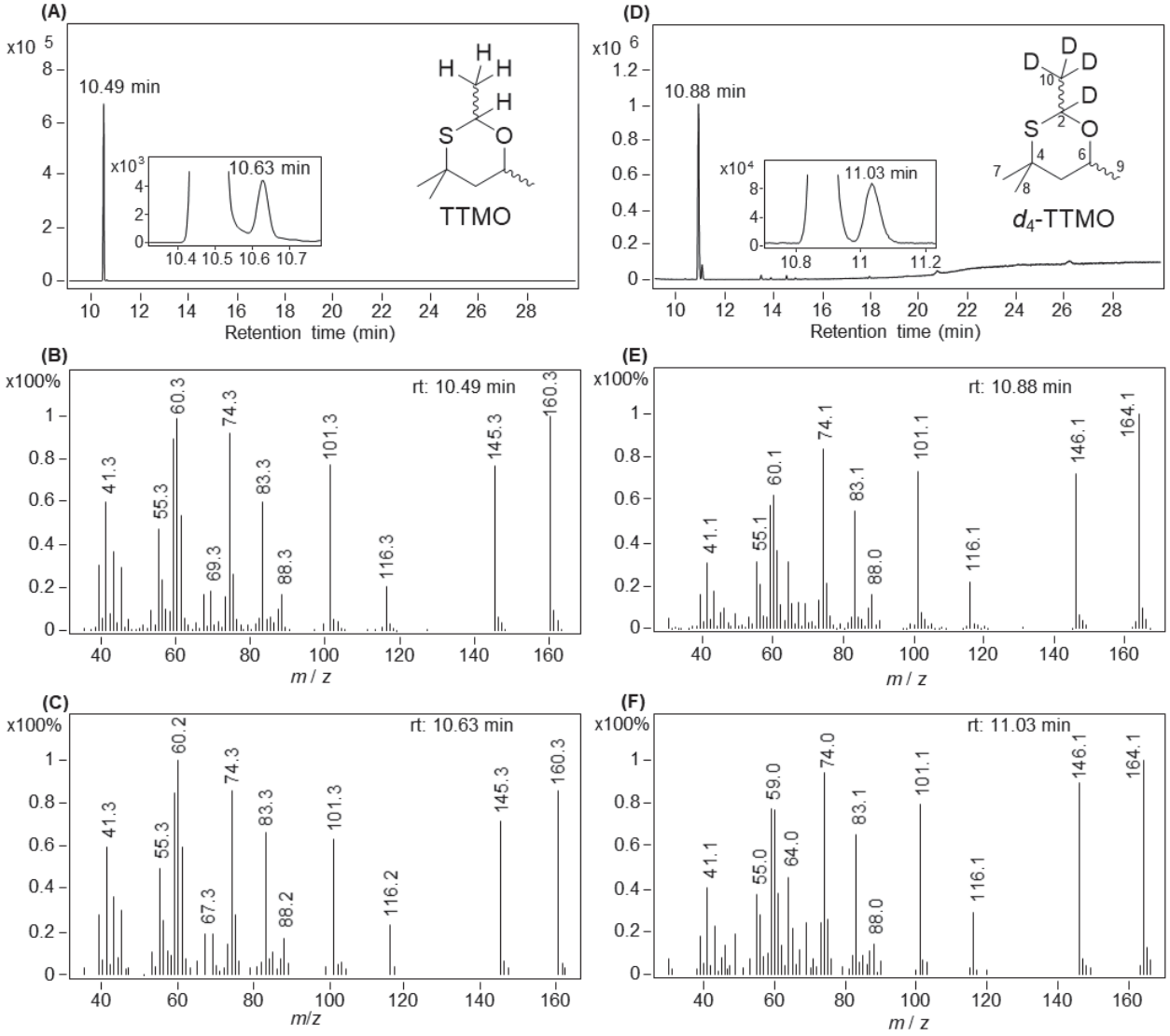

Fig. B.2 Total ion chromatogram (TIC) of (A) synthesised TTMO and background subtracted mass spectra of (B) *cis*-TTMO and (C) *trans*-TTMO; TIC of (D) synthesised d_4-TTMO and background subtracted mass spectra of (E) d_4-*cis*-TTMO and (F) d_4-*trans*-TTMO. Data recorded using liquid injection of compound in dichloromethane: DB-WAXetr column; 40 °C for 1 min, then 10 °C/min to 250 °C and holding at 250 °C for 8 min; 1.5 mL/min He as carrier gas; inlet was set at 200 °C, MS source and quadrupole were 230 °C and 150 °C, respectively; transfer line was 240 °C or 250 °C; scan range of *m*/*z* 30-350.

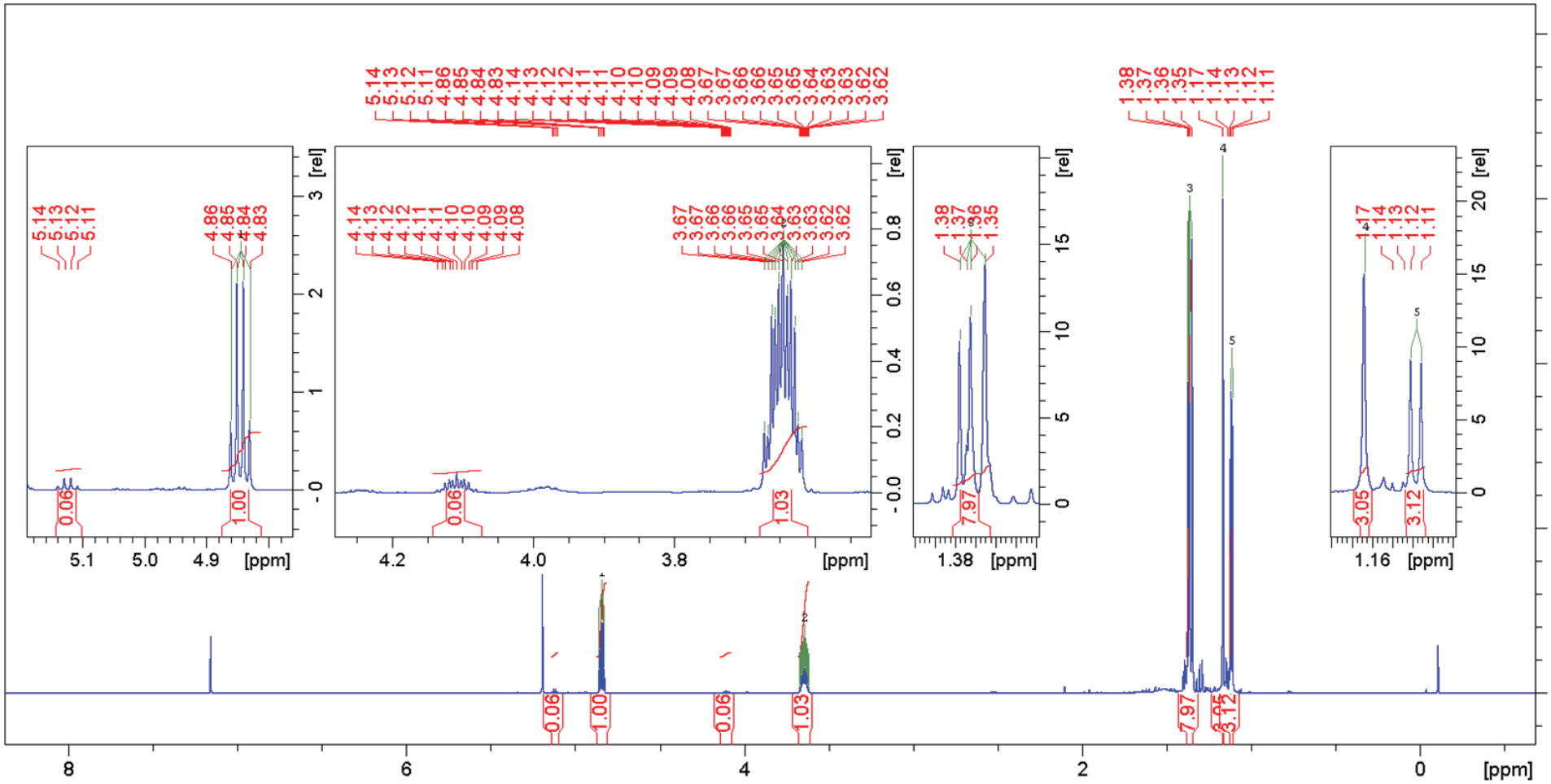

Fig. B.3 ^{1}H NMR spectrum of 2,4,4,6-tetramethyl-1,3-oxathiane ($CDCl_3$, 600 MHz).

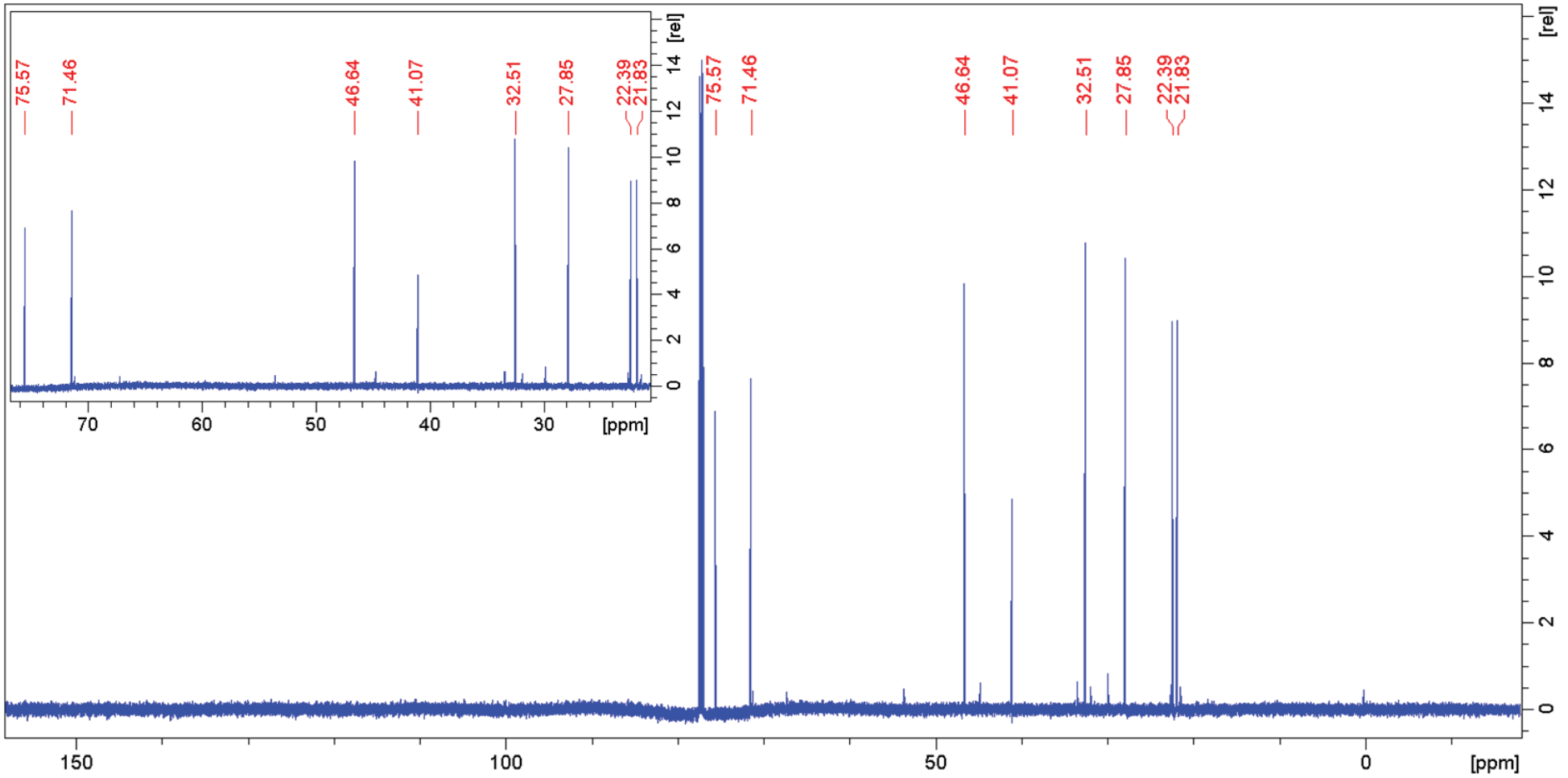

Fig. B.4 ^{13}C NMR spectrum of 2,4,4,6-tetramethyl-1,3-oxathiane ($CDCl_3$, 150 MHz).

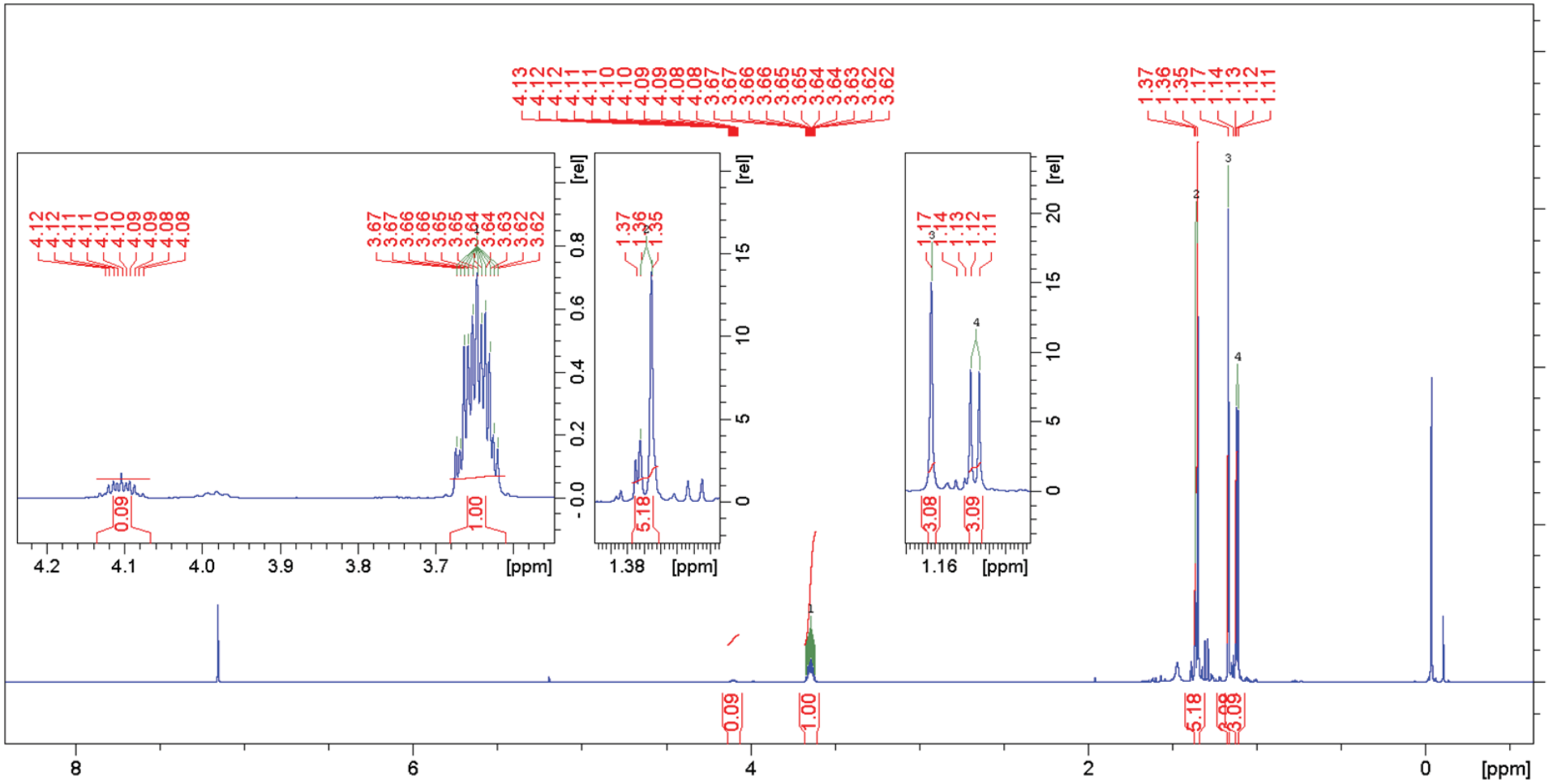

Fig. B.5 ^{1}H NMR spectrum of d_4-2,4,4,6-tetramethyl-1,3-oxathiane ($CDCl_3$, 600 MHz).

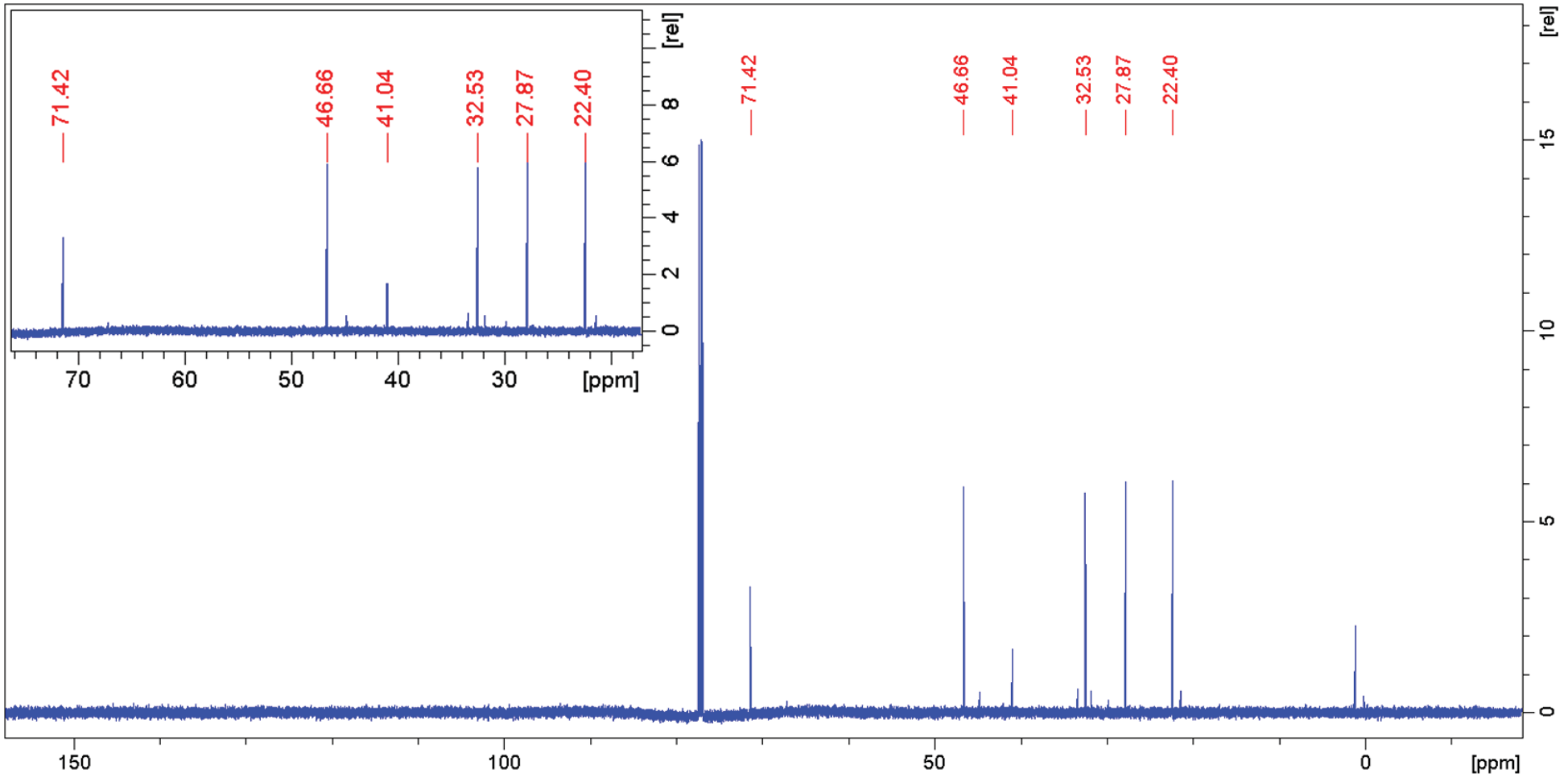

Fig. B.6 ^{13}C NMR spectrum of d_4-2,4,4,6-tetramethyl-1,3-oxathiane ($CDCl_3$, 150 MHz).

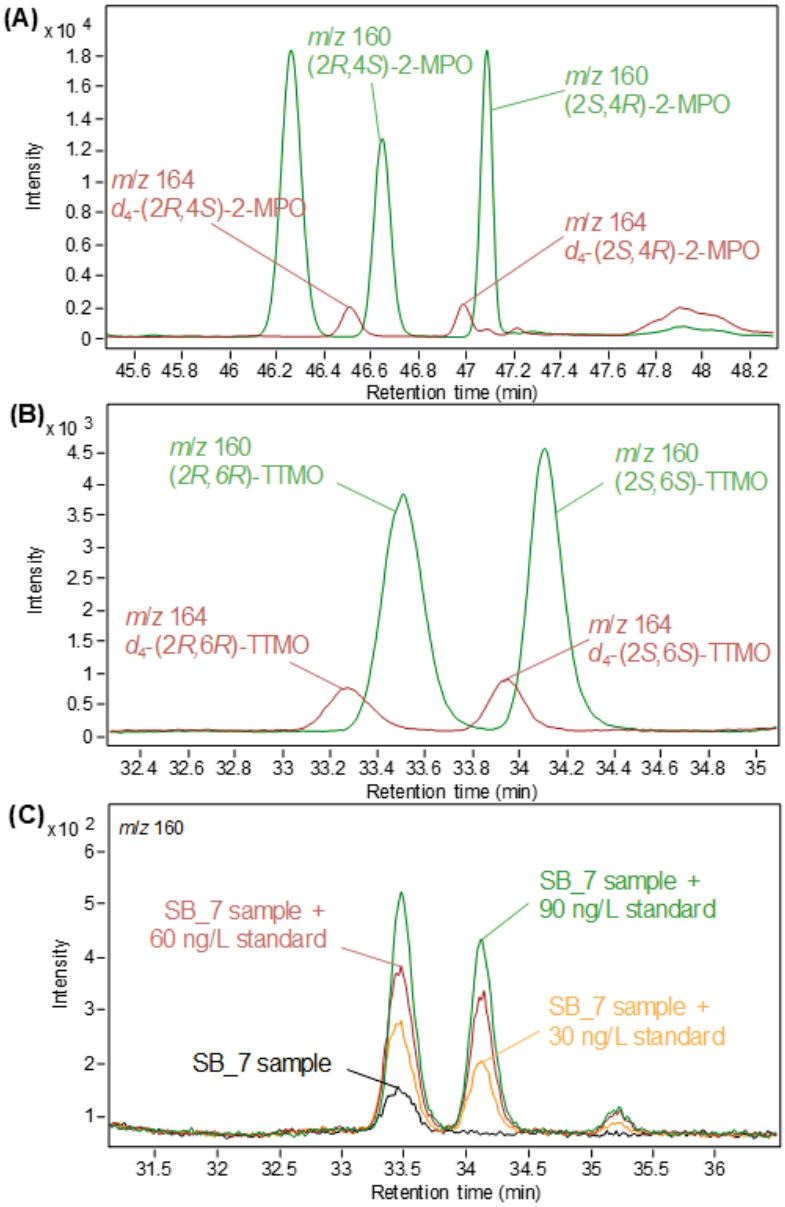

Fig. B.7 Selected ion chromatograms of (A) *cis*-2-MPO (spiked at 500 ng/L for each enantiomer) and d_4-*cis*-2-MPO (spiked at 100 ng/L for each enantiomer) in a commercial Sauvignon blanc wine and (B) *cis*-TTMO (spiked at 500 ng/L for each enantiomer) and d_4-*cis*-TTMO (spiked at 100 ng/L for each enantiomer), and (C) co-injection experiments of *cis*-TTMO added at concentrations of 60 ng/L, 120 ng/L, and 180 ng/L to SB_7 wine sample (already containing 28 ng/L of *cis*-TTMO), showing the increasing intensities of *m/z* 160 of *cis*-TTMO when analysed by the validated SIDA HS-SPME GC-MS method. The concentrations of the analytes in the commercial Sauvignon blanc wine used for calibration are detailed in Table B.3.

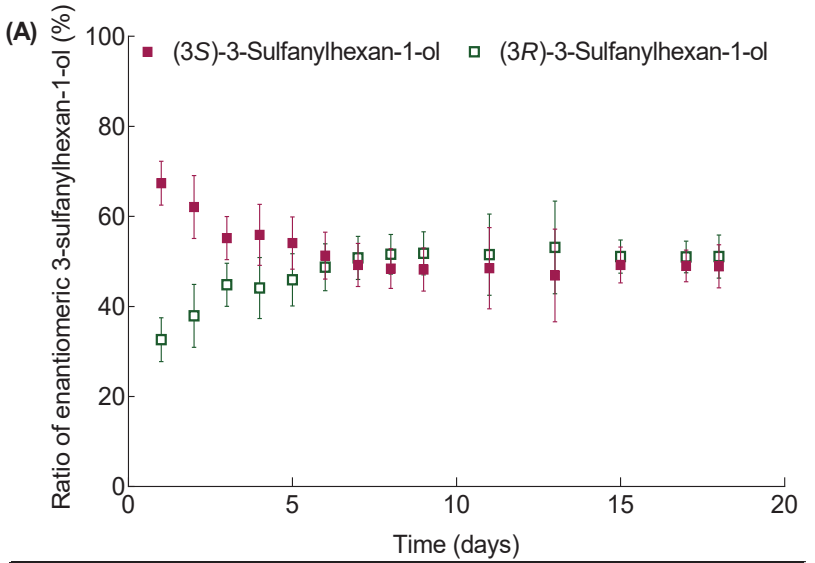

Time (days)	1	2	3	4	5	6	7	8	9	11	13	15	17	18	*p*-value
(3*S*)-3-Sulfanylhexan-1-ol	a	ab	bc	bc	bc	c	c	c	c	c	c	c	c	c	<0.0001
(3*R*)-3-Sulfanylhexan-1-ol	c	bc	ab	ab	ab	a	a	a	a	a	a	a	a	a	<0.0001

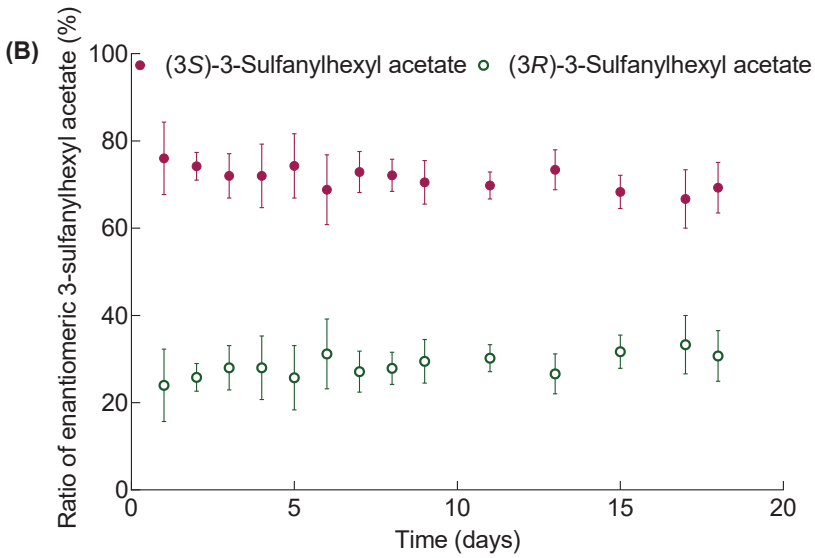

Fig. B.8 Evolution of enantiomeric ratios of (A) (3*R*)/(3*S*)-3-sulfanylhexan-1-ol and (B) (3*R*)/(3*S*)-3-sulfanylhexyl acetate during alcoholic fermentation of Sauvignon blanc juice based on HPLC-MS/MS analysis of derivatives. Error bars represent standard deviations across the treatments (n = 8). The table below Fig. B.8A illustrates results of one-way analysis of variance (ANOVA) followed by Tukey's multiple comparisions, showing the differences between sampling days for a given enantiomer (no significant differences were found for 3-SHA enantiomers). Different letters within a row reveal significant difference at $\alpha = 0.05$.

References

Chen, L., Capone, D. L., & Jeffery, D. W. (2018). Identification and quantitative analysis of 2-methyl-4-propyl-1,3-oxathiane in wine. *Journal of Agricultural and Food Chemistry, 66*(41), 10808-10815.

Chen, L., Capone, D. L., Nicholson, E. L., & Jeffery, D. W. (2019). Investigation of intraregional variation, grape amino acids, and pre-fermentation freezing on varietal thiols and their precursors for *Vitis vinifera* Sauvignon blanc. *Food Chemistry, 295*, 637-645.

Wang, X., Chen, L., Capone, D. L., Roland, A., & Jeffery, D. W. (2020). Evolution and correlation of *cis*-2-methyl-4-propyl-1,3-oxathiane, varietal thiols, and acetaldehyde during fermentation of Sauvignon blanc juice. *Journal of Agricultural and Food Chemistry, 68*(32), 8676-8687.

CHAPTER 5

Preliminary Study of the Presence of 4-Methyl-4-sulfanylpentan-2-ol Enantiomers and Other Sulfur-containing Volatile Compounds in Wine

Xingchen Wang,[†] Dimitra L. Capone,[†,‡] Aurélie Roland,[§] David W. Jeffery[†,‡,*]

[†] Department of Wine Science and Waite Research Institute, The University of Adelaide (UA), PMB 1, Glen Osmond, SA 5064, Australia

[‡] Australian Research Council Training Centre for Innovative Wine Production, UA, PMB 1, Glen Osmond, SA 5064, Australia

[§] SPO, Univ Montpellier, INRAE, Institut Agro, Montpellier, France

Statement of Authorship

Title of Paper	Preliminary study of 4-methyl-4-sulfanylpentan-2-ol enantiomers and other sulfur-containing volatile compounds in wine
Publication Status	☐ Published ☐ Accepted for Publication ☐ Submitted for Publication ☑ Unpublished and Unsubmitted work written in manuscript style
Publication Details	Prepared in manuscript format based on the author instructions for Journal of Agricultural and Food Chemistry.

Principal Author

Name of Principal Author (Candidate)	Xingchen Wang		
Contribution to the Paper	Designed experiments, conducted experiments, collected, processed, analysed, and visualised data. Produced original manuscript and revised and edited manuscript.		
Overall percentage (%)	80 %		
Certification:	This paper reports on original research I conducted during the period of my Higher Degree by Research candidature and is not subject to any obligations or contractual agreements with a third party that would constrain its inclusion in this thesis. I am the primary author of this paper.		
Signature		Date	01/06/2022

Co-Author Contributions

By signing the Statement of Authorship, each author certifies that:

i. the candidate's stated contribution to the publication is accurate (as detailed above);
ii. permission is granted for the candidate in include the publication in the thesis; and
iii. the sum of all co-author contributions is equal to 100% less the candidate's stated contribution.

Name of Co-Author	Dimitra L. Capone		
Contribution to the Paper	Designed experiments, supervised the work, interpreted data. Reviewed and edited manuscript.		
Signature		Date	08/06/2022

Name of Co-Author	Aurélie Roland		
Contribution to the Paper	Contributed to the design of experiments, interpreted data, and supervised the work. Reviewed and edited the manuscript.		
Signature		Date	10/06/2022

Name of Co-Author	David W. Jeffery		
Contribution to the Paper	Conceived of and designed experiments, interpreted data, supervised the project, and provided resources. Reviewed and edited the manuscript and acted as the principal supervisor.		
Signature		Date	01/06/2022

Please cut and paste additional co-author panels here as required.

Abstract: The identification of a single *cis*-2,4,4,6-tetramethyl-1,3-oxathiane (*cis*-TMO) enantiomer in wines indicated that only one of the possible 4-methyl-4-sulfanylpentan-2-ol (4-MSPOH) enantiomers was present in wine. In order to verify this, part of the study aimed to resolve 4-MSPOH enantiomers based on modification of a published stable isotope dilution assay (SIDA) utilising high performance liquid chromatography (HPLC) coupled with tandem mass spectrometry. Different HPLC parameters were trialled and the enantiomers could be partially separated with an Amylose-1 column, but baseline resolution was not achieved. Upon applying the method to a selection of wine samples that were previously quantified with *cis*-TMO, neither enantiomer of 4-MSPOH was detected. Further work would therefore be required to optimise a method for the accurate quantification of 4-MSPOH enantiomers and study a larger selection of wine samples. Additionally, the preliminary identification of blackcurrant mercaptan and grapefruit mercaptan in wine was investigated. An initial method for blackcurrant mercaptan was developed and applied to a small selection of wine samples, but this thiol was not detected in any of these samples. Furthermore, a brief study on grapefruit mercaptan showed it was unstable and could spontaneously degrade, although the derived product (may relate to thiocineole) is still to be confirmed. Overall, further method optimisation is required for the resolution of 4-MSPOH enantiomers and additional effort for the identification of volatile thiols in wine, including BCM, is required. Time constraints prevented further pursuit of these aspects.

Keywords: varietal thiols, chiral analysis, grapefruit mercaptan, blackcurrant mercaptan, synthesis, wine aroma

INTRODUCTION

The geometric property of volatile compounds that cannot be superimposable on their mirror images, namely chirality, plays an important part in characterisation of different food and beverage aroma profiles. This is especially so for varietal thiols in wine, given their sensory impact.[1] Bearing chiral centres, 3-sulfanylhexan-1-ol (3-SH) and 3-sulfanylhexyl acetate (3-SHA) are present in different proportions as (3*S*)- and (3*R*)-enantiomers in dry and sweet white wines.[2] As stereochemically-related progenitors to the enantiomers of 3-SH and 3-SHA, the L-glutathionylated and L-cysteinylated conjugate precursors of 3-SH (i.e., GSH-3-SH and Cys-3-SH, respectively) are present as pairs of diastereomers in grape.[3] Fermentation experiments conducted in model grape juice medium demonstrated that a diastereomerically pure precursor, (*R*)-GSH-3-SH (and (*R*)-Cys-3-SH as an intermediate), can be metabolised to produce the corresponding enantiomeric varietal thiols, namely (3*R*)-3-SH and (3*R*)-3-SHA.[4-5] Comparing the differences in (*S*):(*R*) diastereomeric ratio of GSH-3-SH (2 to 7[3] and 3 to 3.6[6]) and Cys-3-SH (1 to 3[3,7] and 2.1 to 2.5[6]) in healthy grapes to the (*S*):(*R*) enantiomeric ratio of 3-SH (0.79 to 1.38[2,6]) and 3-SHA (1.34 to 2.71[2,6]) in wine (such as Sauvignon blanc), (*S*)-configured GSH-3-SH, Cys-3-SH, and 3-SHA dominated over their (*R*)-configured counterparts, but 3-SH enantiomers were approximately equally distributed in dry wines. This change in the (*S*):(*R*) ratios from precursors to varietal thiols pointed the potential of diastereomeric or enantiomeric selectivity of enzymes from yeast strains.

Compared with studies investigating the chirality of 3-SH and 3-SHA and the conjugated precursors, similar knowledge for 4-methyl-4-sulfanylpentan-2-ol (4-MSPOH), another potent thiol in wine, is lacking. 4-MSPOH is generally lower in concentration than other varietal thiols, i.e., less than 90 ng/L,[8] but it also bears a chiral centre, meaning that its enantiomers, (2*S*)-4-MSPOH and (2*R*)-4-MSPOH, should also be present in wine. The analysis of 4-MSPOH enantiomers had not yet been reported; however, a previous study pointed to the possibility that a single enantiomer of 4-MSPOH may be present in wine, given that only a single enantiomer of *cis*-2,4,4,6-tetramethyl-1,3-oxathiane (*cis*-TMO), produced from acetaldehyde and 4-MSPOH, had been identified.[9]

As with the biogenesis of other varietal thiols, the occurrence of 4-MSPOH is likely related to the presence of non-volatile precursors in grapes. L-Cysteinylated 4-MSPOH (Cys-4-MSPOH) was identified in grape materials indirectly by enzymatically releasing and analysing 4-MSPOH using gas chromatography coupled with mass spectrometry (GC-MS).[10] This work

simultaneously verified that 4-MSPOH could be released from Cys-4-MSPOH due to the action of tryptophanase. The potential metabolic pathway from GSH-4-MSPOH to Cys-4-MSPOH and the subsequent release of 4-MSPOH is an open question. On the other hand, 4-MSPOH enantiomers may also arise from enzymatic reduction of 4-MSP during fermentation, with such enzymes, for instance the aldo-keto reductase family,[11] potentially showing enantiomeric selectivity (thus perhaps favouring one 4-MSPOH enantiomer).

Aside from the research gap in understanding the production and chirality of 4-MSPOH in wine, exploring the presence of other sulfur-containing volatile compounds could be important for further understanding the complexity of wine aroma, especially as it relates to potent thiols. As such, two compounds, namely 1-*p*-menthen-8-thiol (grapefruit mercaptan, GFM, Figure 1) and 4-methoxy-2-methyl-2-butanethiol (blackcurrant mercaptan, BCM, Figure 1), were proposed in Section 1.7 of Chapter 1 to be present in wine.

1-*p*-menthen-8-thiol
grapefruit mercaptan (GFM)

4-methoxy-2-methyl-2-butanethiol
blackcurrant mercaptan (BCM)

Figure 1. *Structures of grapefruit mercaptan and blackcurrant mercaptan.*

GFM is a chiral molecule with low odour detection thresholds (ODTs) of 0.02 ng/L and 0.08 ng/L for the respective *R*-(+)- and *S*-(–)- enantiomers in water,[12] and has long been known for characterising grapefruit aroma.[13] Its wide prevalence in other fruits, including honey and red pomelo, blood orange, mandarin, and lime, makes it a potential aroma marker for citrus fruits.[14] The formation of GFM in concentrated grapefruit juice was presumed to arise from the addition of hydrogen sulfide (H_2S) to limonene,[15] with the chemical synthesis of GFM by additive reaction of H_2S and limonene having been summarised in a review.[16] This is akin to the formation of the alcohol analogue, α-terpineol, from the hydration of limonene under acidic conditions.[17] A previous study established that GFM is not stable and can spontaneously cyclise into isothiocineole in the presence of light, explaining the co-occurrence of GFM and isothiocineole in grapefruit.[13] GFM can also cyclise into thiocineole at acidic pH, which is more likely to happen in a wine environment if GFM was present initially.

BCM has an ODT of 1 ng/L in water[18] and 0.08–0.3 pg/L in air,[19] and was first identified

in virgin olive oil and found to contribute 'blackcurrant' like aroma.[19] It characterises the aroma profile of blackcurrant[12] and was quantified between 0.16–4.5 µg/kg in blackcurrant berries.[18] Although L-cysteine conjugated BCM (Cys-BCM) was qualified in blackcurrant bud before bud burst,[20] the biogenesis from Cys-BCM to BCM and the reactivity of BCM were unclear.[18] Nonetheless, if present in wine, BCM or GFM could potentially impact sensory profiles, although the typical trace abundance of thiols presents an analytical challenge.

The analysis of 4-MSPOH enantiomers and exploration for new thiols such as BCM and GFM could be based around a sensitive approach that combines thiol derivatisation with 4,4'-dithiodipyridine (DTDP) and high-performance liquid chromatography coupled with tandem mass spectrometry (HPLC-MS/MS).[21] Therefore, one of the aims of this chapter was to optimise a previously published method[22] to resolve the enantiomers of 4-MSPOH and quantify them in a selection of wine samples. An additional aim was to explore the presence of GFM and BCM in wine by adapting a published HPLC-MS/MS approach used for the analysis of the usual varietal thiols.

MATERIAL AND METHODS

Chemicals. (±)-4-MSPOH (98 %) was purchased from Thermo Fisher Scientific (Scoresby, VIC, Australia). Acetaldehyde (≥ 99.5 %), acetic acid (≥ 80 %), ammonium bicarbonate (99 %), BCM (≥ 98 %), α-terpineol (≥ 95 %), DTDP (98 %), EDTA 2Na (≥ 99 %), ethyl acetate (≥ 99.5 %), formic acid (≥ 98 %), isothiocineole (95 %), Lawesson's reagent (97 %), *N*,*N*'-diisopropylcarbodiimide (DIC, 99 %), *N*-(*tert*-butoxycarbonyl)-L-phenylalanine (*N*-Boc-L-Phe-OH, ≥ 99 %), palladium(II) chloride (99 %), silica gel 60 (15–40 µm mesh), and thin layer chromatography (TLC) plates (20 × 20 cm) were purchased from Sigma-Aldrich (Castle Hill, NSW, Australia). AR grade hydrochloric acid (36.5 %–38 %), 4-dimethylaminopyridine (DMAP, ≥ 99 %), dichloromethane (99.8 %), diethyl ether (99.7 %), methanol (99.9 %), sodium chloride (≥ 99.7 %), and *n*-hexane (95 %) were obtained from ChemSupply (Port Adelaide, SA, Australia). Gas chromatography grade dichloromethane, HPLC gradient grade acetonitrile, ethanol, and methanol were purchased from Merck (Noble Park, VIC, Australia). Bond Elut C18 (500 mg, 6 mL) and Strata SDB-L (500 mg, 6 mL) solid phase extraction (SPE) cartridges were acquired from Agilent Technologies (Mulgrave, VIC, Australia) and Phenomenex (Lane Cove, NSW, Australia), respectively. Milli-Q water obtained from a purification system (Millipore, North Ryde, NSW, Australia) was used for preparation of aqueous solutions. DTDP reagent was prepared and stored at –20 °C,[21] with aliquots thawed before use. A palladium(II)

chloride reagent was used for TLC visualisation and prepared by dissolving 0.5 g palladium chloride in 100 mL water containing several drops of 25 % hydrochloric acid. After being dipped in the reagent, TLC plates were developed by heating for a brief period with a heat gun.

Preliminary method development for 4-MSPOH enantiomers. *Preparation of reference standard*. A reference solution of 4-MSPOH derivatised with DTDP was prepared in model wine (10 % aqueous ethanol solution saturated with potassium hydrogen tartrate and pH-adjusted to 3.2 with 1 M tartaric acid solution) according to the published method (excluding acetaldehyde).[21] Briefly, 20 µL of ethanolic 4-MSPOH solution (0.732 g/L) was spiked into 5 mL of model wine, followed by the addition of 20 mg EDTA 2Na and 100 µL DTDP derivatisation reagent. The mixture was left for 1 h prior to use for the method development.[9]

Preliminary preparation of 4-MSPOH enantiomers. The synthesis of *bis*-(*N*-Boc-L-Phe)-4-MSPOH (**1**) diastereomers followed the previous method with modifications.[23] To a stirred solution of (±)-4-MSPOH (100 mg, 0.75 mmol) in dry dichloromethane (5 mL) at 0 °C under N_2, *N*-Boc-L-Phe-OH (1592 mg, 6 mmol), DMAP (7.3 mg, 0.06 mmol), and DIC (464 µL, 379 mg, 3 mmol) were added. After stirring for 16 h at room temperature, the solvent was removed under reduced pressure. The residue was redissolved in diethyl ether (5 mL) and the mixture was filtered, with the solids being washed with diethyl ether (3 × 5 mL). The combined organic solvent was washed with 1 M HCl solution (3 × 5 mL), then brine (5 mL), and dried over $MgSO_4$. The solvent was removed under reduced pressure to yield a colourless oil (1.78 g), which was redissolved in a minimum amount of solvent mixture **A** (81.3% hexane/17.1% ethyl acetate/1.6% acetic acid) purified by flash silica gel chromatography, eluting with solvent mixture **A**. Eluted fractions were pooled according to TLC monitoring using palladium(II) chloride reagent and further analysed by HPLC-MS as detailed below after dissolving in the crude product in methanol/water mixture (50/50). Solvent from the pooled fractions containing product was removed under reduced pressure and the residue was redissolved in a small amount of solvent mixture **A**. Preparative TLC of this mixture was undertaken to separate the two diastereomers of *bis*-(*N*-Boc-L-Phe)-4-MSPOH, affording R_f values of 0.26 (**1a**) and 0.23 (**1b**) using solvent mixture **A**. The silica gel band with a single diastereomer was scraped from the TLC plate and stirred with dichloromethane. After filtration, the dichloromethane was removed under reduced pressure, affording the mixture with R_f value of 0.26 (185.2 mg) containing of **1** with 53.2 % purity and presenting a diastereomeric ratio of **1a**/**1b** of 93.7 %/6.3 %; and mixture with R_f value of 0.23 (32.6 mg) containing **1** with 90.3 % purity and a diastereomeric ratio of **1a**/**1b** of 28.9 %/70.2 % (HPLC-MS). The conversion yields from starting material to **1a** and **1b** were 18 %

and 5.7 %, respectively.

HPLC-MS instrumentation. Method development for analysis of 4-MSPOH enantiomers was conducted on a ThermoFinnigan Surveyor HPLC coupled to a ThermoFinnigan LCQ Deca XP Plus ion trap mass spectrometer operated in positive electrospray ionisation mode.

Purity of fractions from chemical synthesis was determined in full scan MS mode (*m*/*z* 100–1000) with voltages of source, capillary, tube lens offset being 4500 kV, 26 V, and 40 V, respectively, and capillary temperature, sheath gas flow, and sweep gas flow of 250 °C, 30 arbitrary units, and 20 arbitrary units, respectively. Helium was used as collision gas.

The fragmentation pattern was obtained by full scan MS/MS experiments and two ion pairs were selected for the qualification of 4-MSPOH by selected reaction monitoring (SRM): *m*/*z* 244.2→144.1 and *m*/*z* 244.2→111.0. The LCQ source conditions were: N_2 was used as sheath gas and auxiliary gas at 60 and 20 arbitrary units; the ion spray voltage, capillary voltage, tube lens offset voltage, and capillary temperature were 4500 V, 13 V, 25 V, and 250 °C, respectively. For MS/MS, helium was used as the collision gas, with normalised collision energy, activation Q, activation time, and isolation width being 36 %, 0.250, 30.0, and 1.4, respectively. Xcalibur software (version 1.3) was used for instrument control, data acquisition, and data processing.

HPLC conditions and optimisation. Separation of samples from chemical synthesis was achieved with a Kinetex Evo C18 column (150 × 2.1 mm, 100 Å, Phenomenex Australia, Lane Cove NSW, Australia) with an injection volume of 10 µL. Eluents consisted of aqueous 0.5 % formic acid (A) and acetonitrile with 0.5 % formic acid (B), with a flow rate of 0.2 mL/min. The program for solvent B was 0 min, 70 %; 2 min, 70 %; 10 min, 50 %; 15 min, 20 %; 20 min, 20 %; 21 min, 70 %; 25 min 70 %.

The initial HPLC conditions for chiral 4-MSPOH enantiomers separation were the same as the previously reported method for analysis of thiol enantiomers.[22] Separation was performed with either Lux Amylose-1 or Amylose-2 column (250 × 2.1 mm i.d., 5 µm, HiChrom, Phenomenex, Lane Cove, NSW, Australia) protected by a guard cartridge (4.0 × 2.0 mm i.d.) of the same material as the column. The initial column temperature was 25 °C and eluents were 5 mM aqueous ammonium bicarbonate (A) and acetonitrile (B), with a flow rate of 0.3 mL/min and injection volume of 10 µL. An assessment of HPLC parameters included column temperature (5, 10, 15, 20, 25, and 30 °C), isocratic eluent conditions (30 % B, 35 % B, and 60 % B), eluent flow rates (0.20, 0.25, 0.26, 0.28, and 0.30 mL/min), and concentration of ammonium bicarbonate (5, 10, and 20 mM). Wine samples found to contain *cis*-TMO were screened,

including Riesling (n= 1) and Sauvignon blanc (n = 5).[9]

Preliminary method development for GFM and BCM. *Synthesis of GFM.* The synthesis followed the previous method[24] with modifications. α-Terpineol (1.00 g, 6.48 mmol) and Lawesson's reagent (1.31 g, 3.24 mmol) were dissolved in dry toluene (220 mL) protected by N_2 and the mixture was stirred under reflux for 0.5 h with exclusion of light. The reaction was monitored with TLC, with the product having a R_f value of 0.27 in *n*-hexane. The reaction solvent was removed under reduced pressure and the residue was redissolved in a minimal amount of *n*-hexane before being purified by a flash chromatography on silica gel, with exclusion of light. The purities of fractions were determined using the GC-MS, namely three GFM fractions of 4.7 mg (95.6 % pure), 21.4 mg (94.4 % pure), and 19.8 mg (81.9 % pure), and relevant fractions were combined to afford a final yield of 3.7 %.

Purity checks of fractions arising from synthesis were conducted using an Agilent 6890N GC coupled with an Agilent 5973N mass spectrometer using ultra-pure helium as the carrier gas at a flow rate of 1.5 mL/min. Separation was performed with an Agilent DB-WAXetr column (60 m × 0.25 mm i.d., 0.25 µm df). The Gerstel MPS autosampler (Lasersan Australasia, Tanunda, SA, Australia) was fitted with a 10 µL glass syringe used for liquid injection. The GC inlet was fitted with an inlet liner (ultra inert tapered with glass wool, Agilent) and operated in pulsed splitless mode, was maintained at 200 °C and the sample previously dissolved in GC grade dichloromethane was injected (1 µL) for analysis. The initial GC oven temperature was held at 40 °C for 1 min, then ramped to 250 °C at 10 °C/min, and holding at this temperature for 8 min. The temperatures of the transfer line, mass spectrometer source, and quadrupole were 240, 230, and 150 °C, respectively. Positive ion electron ionisation mass spectra (70 eV) were collected in scan mode (*m*/*z* 35–350) with a solvent delay time of 9 min.

Wine sample preparation for analysis. Samples for HPLC-MS/MS analysis were prepared according to a previous method.[21] Calibration samples were prepared by spiking separate ethanolic solutions of GFM (0.01419 and 0.1419 mg/mL) and BCM (0.0124 and 0.124 mg/mL), and 50 µL of deuterium labelled internal standard (d_8-3-SH, at a final concentration of 500 ng/L) into 20 mL of commercial Chardonnay wine at levels of 0, 11.4, 26.6, 40.4, 53.2, 78.0, and 99.3 ng/L for GFM, and 0, 11.8, 25.1, 38.2, 50.2, 77.5, and 102.3 ng/L for BCM. Sequentially, EDTA 2Na (20 mg), aqueous acetaldehyde (50/50, 80 µL), and DTDP (200 µL) derivatisation reagent were added to the respective solutions. Mixtures were left for 30 min before being loaded onto pre-activated Bond Elut SPE cartridges and treated according to the previous method.[21] Eluates from the SPE cartridges were dried under N_2 before being reconstituted with 10 % aqueous

ethanol solution. Samples were stored at –20 °C prior to analysis.

Wines used for the screening of GFM and BCM were previously prepared according to the published method[21] and included experimental wines (Shiraz from vintage 2019 (n = 6)[25] and Sauvignon blanc from vintages 2019 (n = 42)[26]) and commercial wines (n = 42), consisting mainly of either Chardonnay or Sauvignon blanc.[27]

HPLC-MS instrumentation. The LCQ HPLC-MS instrument specified in Section 2.2.2 was used for the precursor ion scan analysis and an Agilent 1200 HPLC coupled with a 6410 triple quadrupole mass spectrometer was used for further method development. The HPLC parameters on both instruments were the same as the previous method.[21] Multiple reaction monitoring (MRM) ion pairs acquired for both DTDP derivatives of GFM and BCM are shown in Table 1. The Agilent MassHunter Workstation software (B.03.01) was used for instrument control and data acquisition.

Table 1. *Mass spectrometry parameters for the qualification and quantification of grapefruit mercaptan (GFM) and blackcurrant mercaptan (BCM) after DTDP derivatisation.*

Compound	MRM ion pairs	Dwell time (mS)	Fragmentor (V)	Collision energy (eV)
GFM-DTDP	280.0→144.0	40	100	12
	280.0→137.0	40	100	30
	280.0→111.0	40	100	20
	280.0→79.0	40	100	40
BCM-DTDP	244.0→143.9*	40	105	12
	244.0→111.0	40	105	36
	244.0→67.0	40	105	40

* Ion pair used for BCM quantification.

Statistical analysis. Microsoft Excel (Microsoft Office Professional Plus 2019 for Windows) was used for all basic statistical calculations. Limit of detection (LOD) and limit of quantification (LOQ) were calculated where applicable and expressed as 3 and 10 times the standard error of *y* intercept divided by the slope of calibration equation.

RESULTS AND DISCUSSION

Analysis of 4-MSPOH enantiomers. *HPLC-MS/MS method development for the resolution of 4-MSPOH enantiomers.* The previously developed method to quantify the

enantiomers of 3-SH and 3-SHA by a stable isotope dilution assay (SIDA) with HPLC-MS/MS,[22] did not include 4-MSPOH most likely due to its lower prevalence in wines. Nonetheless, 4-MSPOH could present as a pair of enantiomers, namely (2*S*)- and (2*R*)-4-MSPOH, which could have implications for wine aroma in the same way as the enantiomers of 3-SH and 3-SHA. However, using the HPLC conditions developed for the enantiomers of 3-SH and 3-SHA,[22] the DTDP derivatives of 4-MSPOH enantiomers (prepared using a racemic standard) were not resolved on either an Amylose-1 or Amylose-2 column. Decreasing the proportion of acetonitrile from 65 % to 35 % on the Amylose-1 column showed signs of enantiomeric separation, which was further increased by the optimisation of other parameters, including decreasing the acetonitrile proportion to 30 %, adjusting the flow rate from 0.3 mL/min to 0.2 mL/min, and modifying the column temperature from 25 °C to 10 °C. The increase of ammonium bicarbonate from 5 mM to 20 mM improved the separation only marginally by increasing the selectivity value of 0.01, thus 5 mM was chosen as per the original method. Ultimately, better separation on Amylose-1 column was achieved compared with the Amylose-2 column, using isocratic 30 % acetonitrile with an eluent flow rate of 0.2 mL/min and a column temperature of 10 °C. This was in line with the observation from a previous study[22] whereby the enantiomers of derivatised 3-SH were better separated on Amylose-1 column rather than Amylose-2. As proposed earlier for 3-SH, this could be due to the stronger interaction between the hydroxy group in 4-MSPOH with amylose 3,5-dimethylphenylcarbamates (Amylose-1). Figure 2 illustrates the resolution of 4-MSPOH enantiomers under the best HPLC conditions, with retention factors for the two peaks of 15.2 and 16.6, respectively, a selectivity value of 1.10, and a resolution value of 0.79.

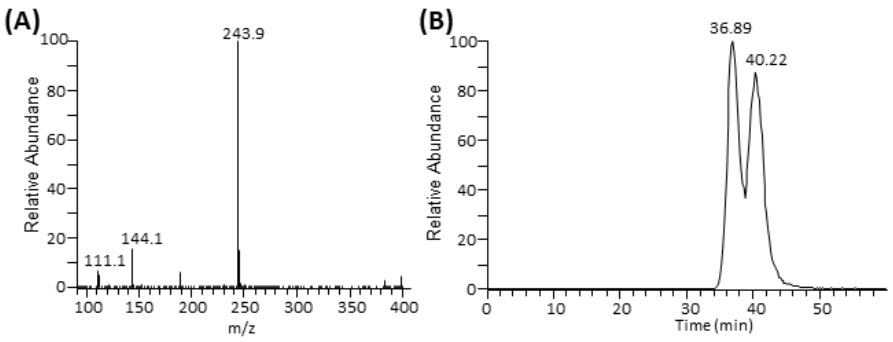

Figure 2. *HPLC-MS/MS analysis of derivatised (±)-4-MSPOH standard at a concentration of 5.23 µg/L showing (A) full scan MS/MS spectrum and (B) selected reaction monitoring chromatogram of m/z 244.1→144.1 showing partial separation of 4-MSPOH enantiomers. The HPLC conditions were isocratic 30 % acetonitrile and 70 % 5 mM ammonium bicarbonate with*

a flow rate of 0.2 mL/min and column temperature of 10 °C.

Despite base line resolution of the enantiomers not being achieved (Figure 2), it was still practical to apply the method with improved chromatographic parameters to wine samples for the verification of the hypothesis that only one of the 4-MSPOH enantiomers may be present in wine. Thus, wine samples that were quantified for *cis*-TMO in a previous study,[9] including Riesling (n= 1) and Sauvignon blanc (n = 5), were screened for 4-MSPOH with an Amylose-1 column. However, neither enantiomer of 4-MSPOH was detected in this small set of wines, which may be due to a lack of sensitivity of the ion trap instrument that was used. If the present HPLC method is to be used for further investigation of the enantiomers of 4-MSPOH in wine, MRM experiments with a triple quadrupole mass spectrometer followed by screening a larger set of wine samples would be advisable.

In spite of these initial efforts, the current Amylose-1 column may not be the most suitable phase for the resolution of 4-MSPOH enantiomers, although a smaller particle size (i.e., 3 µm) may potentially increase the separation. A cellulose-based chiral stationary phase showed greater selectivity values for separation of alcohol enantiomers compared with an amylose-based counterpart,[28] meaning that a cellulose based 3,5-dimethylphenylcarbamate chiral stationary phase could potentially be beneficial to 4-MSPOH enantiomeric separation. Successfully achieving the first aim of the study to integrate the enantiomers of 4-MSPOH into the previously method would require screening of other chiral stationary phases. Given the cost of HPLC columns for chiral separation, this would likely need to be facilitated with column screening by Phenologix or similar application development services, as undertaken in the previous work of this kind.[22]

Synthetic protocols for the preparation of 4-MSPOH enantiomers. In parallel to the method development for resolution of 4-MSPOH enantiomers on a chiral stationary phase, synthesis was initiated to obtain single enantiomers of 4-MSPOH for use as standards to assign the elution order of the enantiomers according to the HPLC-MS/MS method.[22] Asymmetric reduction of ketones to the corresponding alcohols by yeast has been achieved, but only up to 90 % enantiopure alcohol could be obtained and yeasts were not efficient in reducing branched-chain ketones.[29] In comparison, the approach using porcine pancreas lipase preparation in the asymmetric reduction of 4-acetylthio-2-heptanone, obtained by Michael addition of thioacetic acid to 3-hepten-2-one, afforded (4*S*)-4-acetylthio-2-heptanone with enantiomeric purity of 98 % as the remaining substrate after kinetic resolution. Chemical

reduction with lithium aluminium hydride was used to obtain the thiol and alcohol functionalities so that the elution order of enantiomers of 4-sulfanyl-2-heptanol could be assigned.[30] This approach has been applied to other 4-sulfanyl-2-alkanols and 2-sulfanyl-4-alkanols,[31-32] but it is not suitable for 4-MSPOH resolution given the only chiral centre in 4-MSPOH is at C-2 compared with the C-2 and C-4 chiral centres in those other polyfunctional thiols. A previous study revealed that the double acylation of the alcohol and thiol groups in 3-SH by *N*-Boc-L-Phe-OH could help resolve the subsequently formed diastereomers of *bis*-(*N*-Boc-L-Phe)-3-SH, using chiral preparative HPLC.[23] This synthetic approach was considered for the protection of alcohol and thiol functional groups in 4-MSPOH in the present study (Scheme 1, part a). However, compared with using chiral preparative HPLC method to separate *bis*-(*N*-Boc-L-Phe)-3-SH diastereomers,[23] preparative TLC was used to achieve the separation, after a preliminary purification with flash silica chromatography and optimisation of the solvent system for TLC to at least partly resolve the diastereomers (Scheme 1, part b).

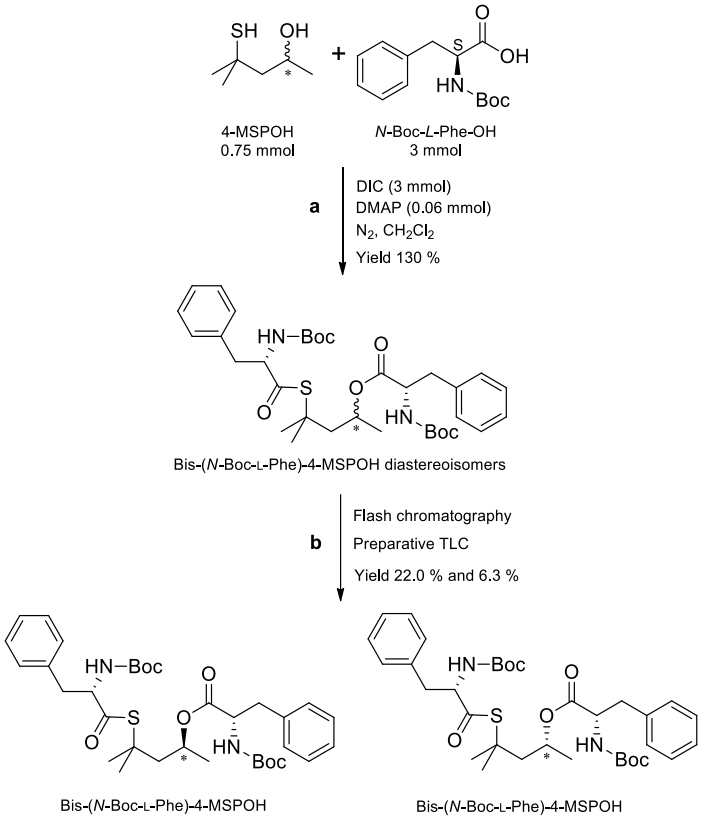

Scheme 1. *Synthetic protocols for the preparation of two diastereomers of bis-(N-Boc-L-Phe)-4-MSPOH with a view to obtaining individual enantiomers of 4-MSPOH.*

The separated fractions from preparative TLC were analysed with HPLC-MS/MS in full scan MS mode (Figure 3). The total ion chromatogram (TIC) of the TLC band with a R_f value

of 0.26 had a lower overall purity (53.2 %) due to the impurities at 3.8 min and 6.2 min (Figure 3A), but had a higher diastereomeric excess of product **1a** (14.1 min) than **1b** (12.5 min). In comparison, the TIC of the TLC band with R_f value of 0.23 (Figure 3B) had higher purity of 90.3 %, but a lower diastereomeric excess of **1b** (12.14 min, Figure 3B) than **1a** (13.7 min, Figure 3B). Identical mass spectra associated with the peaks for **1a** and **1b** are shown in Figure 3C and 3D, respectively. The ion at *m/z* 629 was the protonated molecule ($[M + H]^+$), and 651 was $[M + Na]^+$. The ions at *m/z* 573, 529, 473, and 429 were supposedly from the sequential loss of 2-methylprop-1-ene (*m/z* 56) and subsequent elimination of CO_2 (*m/z* 44) from the two Boc moieties (Figure 3C), with a similar fragmentation pattern of the Boc moiety for positive ESI-MS/MS having been previously discussed.[33] However, both TLC isolates were not pure enough for diastereomeric characterisation by HRMS and NMR at this point. Considering 4-MSPOH enantiomers were not separated by the chiral HPLC-MS method (Section 3.1.1) by this stage, further experiments in characterisation of **1a** and **1b** were ceased. If taken further, however, having at least one relatively pure diastereomer would have been enough to confirm the elution order of 4-MSPOH enantiomers by HPLC – after diastereomer deprotection,[23] the relative stereochemistry of the obtained enantiomer could be determined according to chemical shifts with NMR experiments.[34]

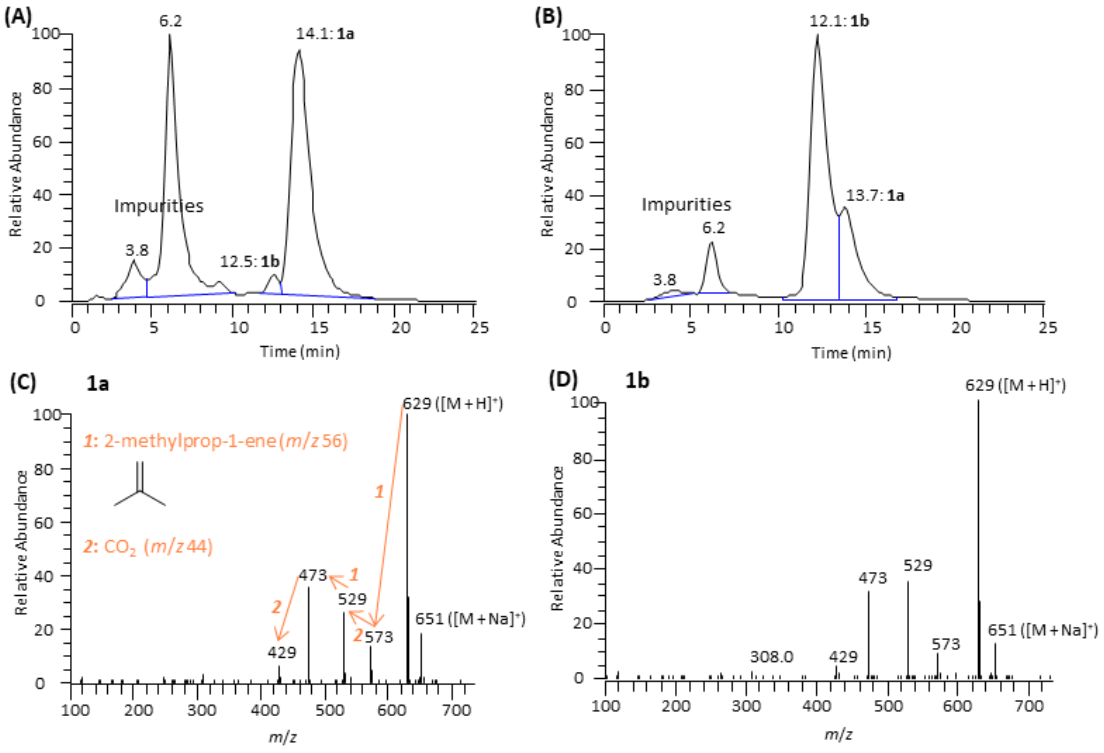

Figure 3. *Total ion chromatograms of TLC isolates with R_f values of (A) 0.26 and (B) 0.23, and full scan mass spectra of diastereomers eluting as (C) **1a** with proposed fragmentation pattern*

and (D) ***1b****.*

Method development for GFM and BCM. A direct route to the formation of GFM is from α-terpineol, the corresponding tertiary alcohol, was achieved with Lawesson's reagent as previously reported (Scheme 2).[24] Given the light-sensitive property of GFM, whereby radical cyclisation could yield 2,8-epithio-*cis*-*p*-menthane,[13] reaction and purification procedures were protected from ambient light. The conversion yield was calculated to be 3.7 % (Scheme 2), which was substantially lower than that in the previous report (20 %)[24] but provided ample product (> 40 mg) for the present study's needs.

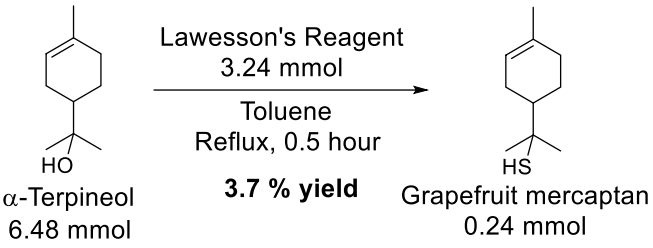

Scheme 2. *Synthesis of grapefruit mercaptan from α-terpineol.*

The purity of the crude material from synthesis of GFM that was used for method development was 94.4 % according to GC-MS analysis (Figure 4A). The mass spectrum of the synthesised GFM (Figure 4B) showed ions identical to the previous result (Figure 4C).[35]

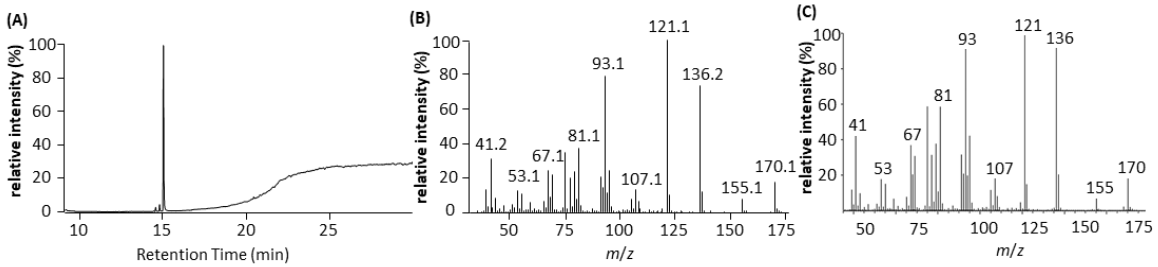

Figure 4. *GC-MS analysis of a freshly prepared solution of synthesised grapefruit mercaptan provided (A) a total ion chromatogram showing the purity and (B) the corresponding background subtracted mass spectrum that can be compared to (C) a reference mass spectrum of GFM.*[35]

BCM and GFM were derivatised with DTDP and used for compound characterisation according to a previous HPLC-MS/MS method.[21] Full scan MS and product ion scan MS/MS

experiments were performed to select ion pairs for MRM analysis, with the overlaid MRM chromatograms for derivatised BCM and GFM illustrated in Figure 5A and 5B, respectively. Ion transitions from precursor ions of derivatised BCM (*m/z* 244) and GFM (*m/z* 280) to product ions of *m/z* 144 and *m/z* 111 were derived from the protonated molecules fragmenting to the derivatised potion of each molecule, in complete accord with the fragmentation pattern of thiol derivatives such as 3-SH and 4-MSP using the DTDP approach.[21] The additional ion pair of *m/z* 244.1→67 for BCM was potentially due to the fragment $CH_2CHCHCHCH_2^+$ that presumably originated from pyridyl cation after the loss of N and rearrangement, in a similar way to that observed for 1-methylpyridine.[36] The transitions of *m/z* 280.0→79 and →137 could be attributed to the protonated pyridyl cation and the α-terpinyl cation, akin to the fragmentation seen for furfural thiol and benzyl mercaptan derivatives.[21]

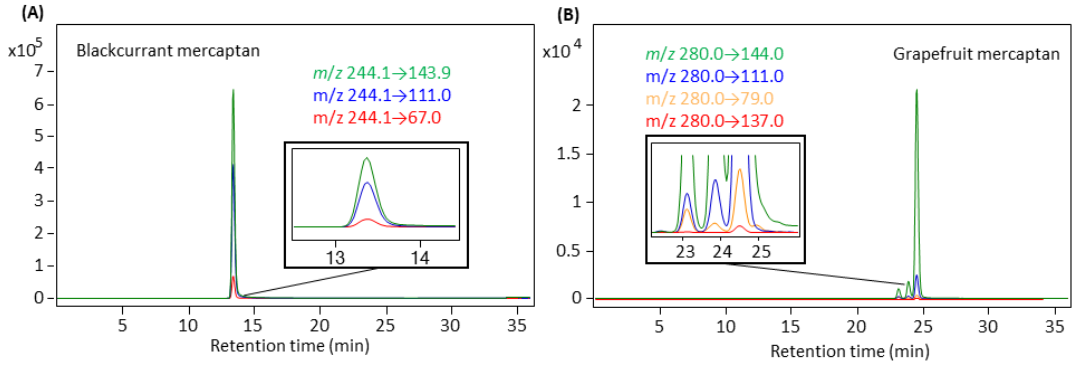

Figure 5. *Overlaid MRM chromatograms (inset) for thiopyridine derivatives of (A) blackcurrant mercaptan and (B) grapefruit mercaptan.*

Based on the newly acquired parameters, preliminary seven-point calibrations for both mercaptans were prepared from 0 to 100 ng/L using d_8-3-SH as the internal standard. The calibration for BCM was linear, with a coefficient of determination (R^2) > 0.99. The *p*-value was < 0.0001 from the goodness of fit test for the linear regression model, showing there was not lack of fit for the calibration. LOD and LOQ values calculated for BCM were 4.8 and 15 ng/L, respectively. The previous method[21] containing the new MRM transitions was applied to screening for BCM in 84 white wines (Sauvignon blanc and Chardonnay) and 6 Shiraz wines (detailed in Section 2.3.2). BCM was not identified in any of the wines, however, this may be attributable to the small sample size, and additional wine samples would need to be screened in future attempts to verify its existence. Apart from this rather targeted approach, other possibilities for discovering volatile thiols in wine such as BCM include mass spectrometry in

precursor ion scan mode, as used for the identification of thiols in vegetables after derivatisation using DTDP,[37] or volatile thiol screening using selective silver ion SPE coupled with multidimensional GC-MS.[38]

In contrast to BCM, the analysis of GFM as its derivative was not so straightforward. Although the full scan MS/MS spectrum of GFM could be obtained using a freshly prepared standard solution, the calibration for GFM prepared with a diluted ethanolic stock solution of GFM (stored for 3 months at 4 °C) failed and peaks were not detected at any concentration. Degradation of the synthesised GFM standard prior to derivatisation was suspected and partly verified by the mass spectrum (Figure 6A) obtained from the main new chromatographic peak, which eluted approximately 1 min later that GFM, upon the analysis of a stored ethanolic solution of synthesised GFM. This was in contrast to the correct mass spectrum obtained for GFM analysed soon after synthesis (see Figure 4B). Mass spectral library searches (Wiley275.L and NIST14.L) of the degradation product suggested the compound to be 2,8-epithio-*cis*-*p*-menthane (isothiocineole) with a similarity of 92 %, or 1,8-epithio-*p*-menthane (thiocineole) with 72 % similarity. Although the mass spectrum of authentic 2,8-epithio-*cis*-*p*-menthane shown in Figure 6B does not match well with the product from GFM degradation in Figure 6A (identical ions but different ion intensities), conversion of GFM to either of these bicyclic compounds is plausible, given the lability of GFM reported previously.[13] Thus, GFM can readily cyclise into 1,8-epithio-*p*-menthane under protic conditions (Scheme 3, path a) or 2,8-epithio-*cis*-*p*-menthane under radical-forming conditions (Scheme 3, path b) in the presence of light.[13] Indeed, the co-occurrence of GFM and 2,8-epithio-*cis*-*p*-menthane in grapefruit juice with an approximate ratio of 4 to 1 has been reported.[13]

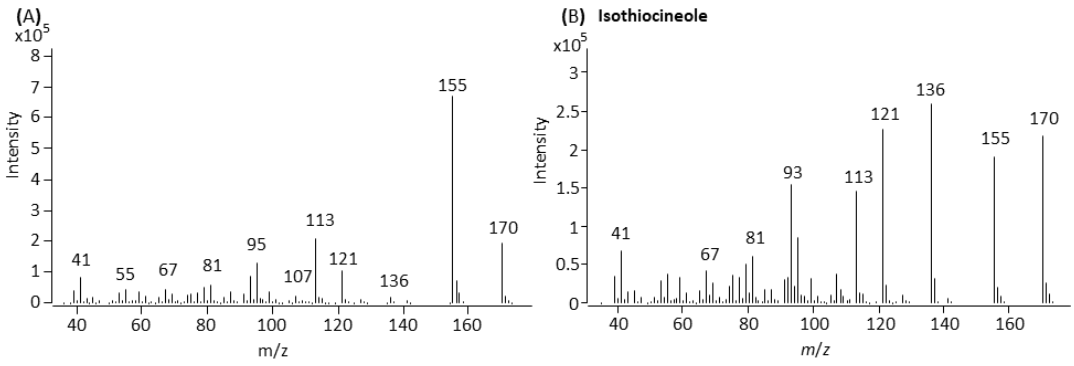

Figure 6. *Background subtracted mass spectra of (A) unknown compound degraded from grapefruit mercaptan solution and (B) a commercial standard of 2,8-epithio-cis-p-menthane (isothiocineole).*

Interestingly, the proposed cyclisation of GFM into 1,8-epithio-*p*-menthane under protic conditions (which would include those found in wine) could be viewed analogously to the cyclisation of α-terpineol into 1,8-cineole (Scheme 3, path c) that was illustrated in model wine.[39] A commercial standard of thiocineole was not available to help verify the identity of the degradation product, but the occurrence of pathway (Scheme 3, path a) in the present case was not well supported when considering differences in the mass spectrum of thiocineole obtained from online database (https://spectrabase.com/spectrum/4QgMOrrbmVs, SpectraBase, Wiley).

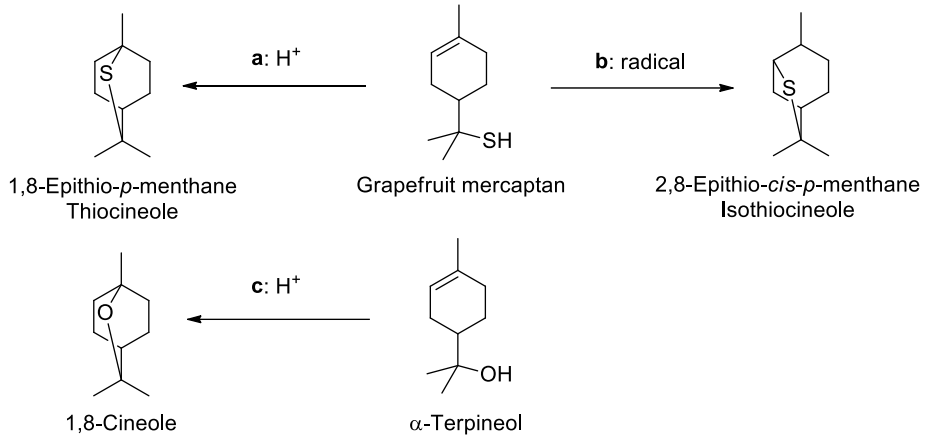

Scheme 3. *Cyclisation of grapefruit mercaptan to thiocineole under protic conditions (path a) and isothiocineole due to light-induced radical formation (path b),*[13] *and cyclisation of α-terpineol to 1,8-cineole in model wine (path c).*[39]

CONCLUSION

This study was devoted to the analysis of thiol enantiomers and investigation of potential new thiols in wine. Attempts were made to resolve 4-MSPOH enantiomers after thiol derivatisation in an attempt to confirm their relative distribution. Secondary to this, identification of BCM and GFM in wine utilising preliminarily optimised or developed methods was initiated. Despite substantial progress, time constraints prevented the work from being taken any further. As for GFM and BCM, which were not identified in wine at the present time, the results indicated that GFM is unstable and identifying the breakdown product of GFM could facilitate further studies in wine. The presence of the breakdown product could point to GFM as the labile precursor, even if GFM itself may not exist long in wine. In comparison, BCM was more stable, and additional work such as using DTDP derivatisation followed by precursor ion scan mass spectrometry experiments or novel extraction techniques

coupled with GC-MS analysis have been proposed for the identification of BCM or indeed other volatile thiols in wine. Aside from exploring the potential presence of both mercaptans in wine, their ODTs in wine matrix would need to be determined to enable evaluation of their contribution to wine sensory characteristics.

ACKNOWLEDGEMENTS

We would like to thank University of Adelaide colleagues, Liang Chen for his preliminary work on the synthesis and analysis of grapefruit mercaptan, and Ross Sanders and Carolyn Puglisi for their valuable advice on the synthesis of grapefruit mercaptan. Sue Maffei (The Commonwealth Scientific and Industrial Research Organisation) is acknowledged for the help and advice with HPLC-MS/MS instrumentation. X.W. is the recipient of the joint scholarship of the University of Adelaide and China Scholarship Council (201806300044) and is supported by a Wine Australia supplementary scholarship (WA Ph1803). The Australian Research Council Training Centre for Innovative Wine Production (www.ARCwinecentre.org.au;project number IC170100008) is funded by the Australian Government with additional support from Wine Australia, Waite Research Institute, and industry partners. The University of Adelaide is a member of the Wine Innovation Cluster.

Notes

The authors declare no competing financial interest.

REFERENCES

1. Engel, K.-H., Chirality: An important phenomenon regarding biosynthesis, perception, and authenticity of flavor compounds. *J. Agric. Food Chem.* **2020,** *68* (38), 10265-10274.

2. Tominaga, T.; Niclass, Y.; Frerot, E.; Dubourdieu, D., Stereoisomeric distribution of 3-mercaptohexan-1-ol and 3-mercaptohexyl acetate in dry and sweet white wines made from *Vitis vinifera* (Var. Sauvignon blanc and Semillon). *J. Agric. Food Chem.* **2006,** *54* (19), 7251-7255.

3. Capone, D. L.; Sefton, M. A.; Hayasaka, Y.; Jeffery, D. W., Analysis of precursors to wine odorant 3-mercaptohexan-1-ol using HPLC-MS/MS: Resolution and quantitation of diastereomers of 3-*S*-cysteinylhexan-1-ol and 3-*S*-glutathionylhexan-1-ol. *J. Agric. Food Chem.* **2010,** *58* (3), 1390-1395.

4. Grant-Preece, P. A.; Pardon, K. H.; Capone, D. L.; Cordente, A. G.; Sefton, M. A.; Jeffery, D. W.; Elsey, G. M., Synthesis of wine thiol conjugates and labeled analogues: Fermentation of the glutathione conjugate of 3-mercaptohexan-1-ol yields the corresponding cysteine conjugate and free thiol. *J. Agric. Food Chem.* **2010,** *58* (3), 1383-1389.

5. Pardon, K. H.; Graney, S. D.; Capone, D. L.; Swiegers, J. H.; Sefton, M. A.; Elsey, G. M., Synthesis of the individual diastereomers of the cysteine conjugate of 3-mercaptohexanol (3-MH). *J. Agric. Food Chem.* **2008,** *56* (10), 3758-3763.

6. Chen, L.; Capone, D. L.; Tondini, F. A.; Jeffery, D. W., Chiral polyfunctional thiols and their conjugated precursors upon winemaking with five *Vitis vinifera* Sauvignon blanc clones. *J. Agric. Food Chem.* **2018,** *66* (18), 4674-4682.

7. Thibon, C.; Shinkaruk, S.; Tominaga, T.; Bennetau, B.; Dubourdieu, D., Analysis of the diastereoisomers of the cysteinylated aroma precursor of 3-sulfanylhexanol in *Vitis vinifera* grape must by gas chromatography coupled with ion trap tandem mass spectrometry. *J. Chromatogr. A* **2008,** *1183* (1-2), 150-157.

8. Roland, A.; Schneider, R.; Razungles, A.; Cavelier, F., Varietal thiols in wine: Discovery, analysis and applications. *Chem. Rev.* **2011,** *111* (11), 7355-7376.

9. Wang, X.; Capone, D. L.; Roland, A.; Jeffery, D. W., Chiral analysis of *cis*-2-methyl-4-propyl-1,3-oxathiane and identification of *cis*-2,4,4,6-tetramethyl-1,3-oxathiane in wine. *Food Chem.* **2021,** *357*, 129406.

10. Peyrot des Gachons, C.; Tominaga, T.; Dubourdieu, D., Measuring the aromatic potential of *Vitis vinifera* L. cv. Sauvignon blanc grapes by assaying *S*-cysteine conjugates, precursors of the volatile thiols responsible for their varietal aroma. *J. Agric. Food Chem.* **2000,** *48* (8), 3387-3391.

11. Kawai, Y.; Saitou, K.; Hida, K.; Ohno, A., Asymmetric reduction of α,β-unsaturated ketones with Bakers' yeast. *Tetrahedron: Asymmetry* **1995,** *6* (9), 2143-2144.

12. Demole, E.; Enggist, P.; Ohloff, G., 1-*p*-Menthene-8-thiol: A powerful flavor impact constituent of grapefruit juice (*Citrus parodisi* Macfayden). *Helv. Chim. Acta* **1982,** *65* (6), 1785-1794.

13. Cheetham, P. S. J., Natural sources of flavours. In Taylor, A. J.; Linforth, R. S., *Food flavour technology*. Wiley Online Library: 2002; pp 127-177.

14. Schoenauer, S.; Schieberle, P., Screening for novel mercaptans in 26 fruits and 20 wines using a thiol-selective isolation procedure in combination with three detection methods. *J. Agric. Food Chem.* **2019,** *67* (16), 4553-4559.

15. Cannon, R. J.; Ho, C.-T., Volatile sulfur compounds in tropical fruits. *J. Food Drug Anal.* **2018,** *26* (2), 445-468.

16. Thomas, A.; Bessiere, Y., Limonene. *Nat. Prod. Rep.* **1989,** *6* (3), 291-309.

17. Haleva-Toledo, E.; Naim, M.; Zehavi, U.; Rouseff, R. L., Formation of α-terpineol in

citrus juices, model and buffer solutions. *J. Food Sci.* **1999,** *64* (5), 838-841.

18. Jung, K.; Fastowski, O.; Engel, K.-H., Occurrence of 4-methoxy-2-methyl-2-butanethiol in blackcurrant (*Ribes nigrum* L.) berries. *Flavour Fragr. J.* **2016,** *31* (6), 438-441.

19. Guth, H.; Grosch, W., A comparative study of the potent odorants of different virgin olive oils. *Lipid / Fett* **1991,** *93* (9), 335-339.

20. Garland, S. M. Improving the yield and quality of blackcurrant (*Ribes nigrum* L.) extracts. University of Tasmania, 2007.

21. Capone, D. L.; Ristic, R.; Pardon, K. H.; Jeffery, D. W., Simple quantitative determination of potent thiols at ultratrace levels in wine by derivatization and high-performance liquid chromatography–tandem mass spectrometry (HPLC-MS/MS) analysis. *Anal. Chem.* **2015,** *87* (2), 1226-1231.

22. Chen, L.; Capone, D. L.; Jeffery, D. W., Chiral analysis of 3-sulfanylhexan-1-ol and 3-sulfanylhexyl acetate in wine by high-performance liquid chromatography–tandem mass spectrometry. *Anal. Chim. Acta* **2018,** *998*, 83-92.

23. Petit, E.; Jacquet, R.; Pouységu, L.; Deffieux, D.; Quideau, S., About the impact of oak ellagitannins on wine odoriferous thiols under acidic and oxidation conditions. *Tetrahedron* **2015,** *71* (20), 2991-2998.

24. Nishio, T., Direct conversion of alcohols into thiols. *J. Chem. Soc. Perkin Trans. I 1* **1993,** (10), 1113-1117.

25. Wang, X.; Capone, D. L.; Kang, W.; Roland, A.; Jeffery, D. W., Impact of accentuated cut edges (ACE) technique on volatile and sensory profiles of Shiraz wines. *Food Chem.* **2022,** *372*, 131222.

26. Wang, X.; Chen, L.; Capone, D. L.; Roland, A.; Jeffery, D. W., Evolution and correlation of *cis*-2-methyl-4-propyl-1,3-oxathiane, varietal thiols, and acetaldehyde during fermentation of Sauvignon blanc juice. *J. Agric. Food Chem.* **2020,** *68* (32), 8676-8687.

27. Chen, L.; Capone, D. L.; Jeffery, D. W., Identification and quantitative analysis of 2-methyl-4-propyl-1,3-oxathiane in wine. *J. Agric. Food Chem.* **2018,** *66* (41), 10808-10815.

28. Kim, I.-W.; Ryu, J.-K.; Ahn, S.-D.; Park, J.-H.; Lee, K.-P.; Ryoo, J.-J.; Hyun, M.-H.; Okamoto, Y.; Yamamoto, C.; Carr, P. W., Comparison of chiral separation on amylose and cellulose tris(3,5-dimethylphenylcarbamate)-coated zirconia in HPLC. *Bull. Korean Chem. Soc.* **2003,** *24* (2), 239-242.

29. MacLeod, R.; Prosser, H.; Fikentscher, L.; Lanyi, J.; Mosher, H. S., Asymmetric reductions. XII. Stereoselective ketone reductions by fermenting yeast. *Biochemistry* **1964,** *3*

(6), 838-846.

30. Nörenberg, S.; Reichardt, B.; Andelfinger, V.; Eisenreich, W.; Engel, K.-H., Influence of the stereochemistry on the sensory properties of 4-mercapto-2-heptanol and its acetyl-derivatives. *J. Agric. Food Chem.* **2013,** *61* (9), 2062-2069.

31. Nörenberg, S.; Kiske, C.; Reichardt, B.; Andelfinger, V.; Pfeiffer, A.; Schmidts, F.; Eisenreich, W.; Engel, K.-H., Analysis and sensory evaluation of the stereoisomers of a homologous series (C5–C10) of 4-mercapto-2-alkanols. *J. Agric. Food Chem.* **2017,** *65* (40), 8913-8922.

32. Riegel, A. D.; Kiske, C.; Dudko, V.; Poplacean, I.; Eisenreich, W.; Engel, K. H., Absolute configurations and sensory properties of the stereoisomers of a homologous series (C6-C10) of 2-mercapto-4-alkanols. *J. Agric. Food Chem.* **2020,** *68* (9), 2738-2746.

33. Garner, G. V.; Gordon, D. B.; Tetler, L. W.; Sedgwick, R. D., Fast atom bombardment mass spectrometry of butyloxycarbonyl protected (BOC) amino acids. *Org. Mass Spectrom.* **1983,** *18* (11), 486-488.

34. Dale, J. A.; Mosher, H. S., Nuclear magnetic resonance enantiomer reagents. Configurational correlations via nuclear magnetic resonance chemical shifts of diastereomeric mandelate, *O*-methylmandelate, and α-methoxy-α-trifluoromethylphenylacetate (MTPA) esters. *J. Am. Chem. Soc.* **1973,** *95* (2), 512-519.

35. Schoenauer, S.; Schieberle, P., Structure–odor activity studies on monoterpenoid mercaptans synthesized by changing the structural motifs of the key food odorant 1-*p*-menthene-8-thiol. *J. Agric. Food Chem.* **2016,** *64* (19), 3849-3861.

36. Hau, J.; Stadler, R.; Jenny, T. A.; Fay, L. B., Tandem mass spectrometric accurate mass performance of time-of-flight and Fourier transform ion cyclotron resonance mass spectrometry: A case study with pyridine derivatives. *Rapid Commun. Mass Spectrom.* **2001,** *15* (19), 1840-1848.

37. Millan, S.; Jeffery, D. W.; Dall'Acqua, S.; Masi, A., A novel HPLC-MS/MS approach for the identification of biological thiols in vegetables. *Food Chem.* **2021,** *339*, 127809.

38. Chen, L.; Darriet, P., Qualitative screening of volatile thiols in wine by selective silver ion solid-phase extraction with heart-cutting multidimensional gas chromatography mass spectrometry/olfactometry. *J. Agric. Food Chem.* **2022,** *70* (15), 4701-4711.

39. Capone, D. L.; Van Leeuwen, K.; Taylor, D. K.; Jeffery, D. W.; Pardon, K. H.; Elsey, G. M.; Sefton, M. A., Evolution and occurrence of 1,8-cineole (eucalyptol) in Australian wine. *J. Agric. Food Chem.* **2011,** *59* (3), 953-959.

CHAPTER 6

Impact of Accentuated Cut Edges (ACE) Technique on Volatile and Sensory Profiles of Shiraz Wines

Xingchen Wang,[a] Dimitra L. Capone,[a,b] Wenyu, Kang,[a] Aurélie Roland,[c] David W. Jeffery[a,b,*]

[a] Department of Wine Science and Waite Research Institute, The University of Adelaide (UA), PMB 1, Glen Osmond, SA 5064, Australia

[b] Australian Research Council Training Centre for Innovative Wine Production, UA, PMB 1, Glen Osmond, SA 5064, Australia

[c] SPO, Univ Montpellier, INRAE, Institut Agro, Montpellier, France

Food Chemistry, **2022**, 372, 131222

DOI: 10.1016/j.foodchem.2021.131222

Statement of Authorship

Title of Paper	Impact of accentuated cut edges (ACE) technique on volatile and sensory profiles of Shiraz wines
Publication Status	☑ Published ☐ Accepted for Publication ☐ Submitted for Publication ☐ Unpublished and Unsubmitted w ork w ritten in manuscript style
Publication Details	Wang, X., Capone, D.L., Kang, W., Roland, A., Jeffery, D.W. (**2022**) Impact of accentuated cut edges (ACE) technique on volatile and sensory profiles of Shiraz wines, *Food Chemistry*, 372, 131222.

Principal Author

Name of Principal Author (Candidate)	Xingchen Wang		
Contribution to the Paper	Contributed to the design of experiments. Conducted experiments and prepared and analysed samples using GC-MS and HPLC-MS/MS. Collected, processed, analysed, interpreted and visualised the data. Produced a complete first draft of the manuscript. Reviewed and edited the manuscript.		
Overall percentage (%)	70%		
Certification:	This paper reports on original research I conducted during the period of my Higher Degree by Research candidature and is not subject to any obligations or contractual agreements with a third party that would constrain its inclusion in this thesis. I am the primary author of this paper.		
Signature		Date	10/02/2022

Co-Author Contributions

By signing the Statement of Authorship, each author certifies that:

i. the candidate's stated contribution to the publication is accurate (as detailed above);

ii. permission is granted for the candidate in include the publication in the thesis; and

iii. the sum of all co-author contributions is equal to 100% less the candidate's stated contribution.

Name of Co-Author	Dimitra L. Capone		
Contribution to the Paper	Conceived and designed the experiments, supervised the work, and interpreted data. Reviewed and edited the manuscript.		
Signature		Date	14/02/2022

Name of Co-Author	Wenyu Kang
Contribution to the Paper	Conceived, designed, and performed experiments. Reviewed and edited the manuscript.

Signature		Date	14/02/2022

Name of Co-Author	Aurélie Roland		
Contribution to the Paper	Contributed to the design of experiments, interpreted data, and supervised the work. Reviewed and edited the manuscript.		
Signature		Date	14/02/2022

Name of Co-Author	David W. Jeffery		
Contribution to the Paper	Conceived of and designed the experiments, interpreted data, supervised the project, and provided resources. Reviewed and edited the manuscript and acted as the corresponding author.		
Signature		Date	14/02/2022

Please cut and paste additional co-author panels here as required.

Food Chemistry 372 (2022) 131222

Contents lists available at ScienceDirect

Food Chemistry

journal homepage: www.elsevier.com/locate/foodchem

Impact of accentuated cut edges (ACE) technique on volatile and sensory profiles of Shiraz wines

Xingchen Wang [a], Dimitra L. Capone [a,b], Wenyu Kang [a,1], Aurélie Roland [c], David W. Jeffery [a,b,*]

[a] Department of Wine Science and Waite Research Institute, The University of Adelaide (UA), PMB 1, Glen Osmond, SA 5064, Australia
[b] Australian Research Council Training Centre for Innovative Wine Production, UA, PMB 1, Glen Osmond, SA 5064, Australia
[c] SPO, Univ Montpellier, INRAE, Institut Agro, Montpellier, France

ARTICLE INFO

Keyword:
Varietal thiols
Thiol precursors
Rate-all-that-apply
Dilution
GC-MS
Maceration

ABSTRACT

Varietal thiols are important wine aroma compounds that are generally less abundant in red wines. Accentuated cut edges (ACE), known for accelerating phenolic extraction, was applied to Shiraz winemaking and compared with conventional crushing (NOACE) to examine the effects on varietal thiol precursor extraction and thiol formation. Water addition to grape must and skin contact time (SCT) during fermentation were also assessed. Although there was no difference for precursors in the must, ACE significantly decreased 3-*S*-glutathionylhexan-1-ol concentration during fermentation. 3-Sulfanylhexan-1-ol and ethyl esters were significantly influenced by crushing method and/or SCT, with NOACE or shorter SCT yielding higher concentrations. Acetates, higher alcohols, fatty acids, and isoprenoids differed according to the interaction of crushing method and SCT, with ACE and shorter SCT significantly enhancing all groups except acetates. Volatiles in Sauvignon blanc and Pinot noir wines produced at commercial scale with ACE were briefly evaluated, suggesting an impact of grape variety.

1. Introduction

Wine is an extremely complex matrix that consists of numerous non-volatile and volatile compounds characterising its aroma, flavour, and texture. Illustrating the chemical complexity, over one thousand volatile compounds have been detected in wines, but not all play a role in the sensory perception of wine. Any impact on aroma needs consideration due to the wide range of volatile compound concentrations (orders of magnitude), their various odour detection thresholds (ODTs), and the interactions among volatiles and with non-volatile compounds in the wine matrix (Ferreira et al., 2002).

Notably, there are very few aroma impact compounds, with varietal thiols forming one of the most influential and studied groups. Present in the nanogram-*per*-litre to low microgram-*per*-litre range, varietal thiols are polyfunctional compounds (i.e., thiols also containing other functional groups such as hydroxyl, carbonyl or ester) recognised for their ability to strongly influence wine aroma due to their extremely low ODTs (Roland et al., 2011). In terms of grape variety, varietal thiols are often relatively more abundant in Sauvignon blanc wines and mainly include 3-sulfanylhexan-1-ol (3-SH) and 3-sulfanylhexyl acetate (3-SHA), and to a lesser extent 4-methyl-4-sulfanylpentan-2-one (4-MSP). They give rise to the characteristic aromas of Sauvignon blanc wine that are described as 'tropical', 'grapefruit', 'passionfruit', and 'boxwood'; hence the inclusion of "varietal" in the description of these thiols (in contrast to fermentative thiols).

Nevertheless, varietal thiols are not unique to Sauvignon blanc wines, having also been reported in other white and red varieties (Roland et al., 2011). Cabernet Sauvignon and Merlot wines were the first red wines found to contain varietal thiols, with 3-SH, 3-SHA, and newly identified 3-sulfanyl-2-methylpropanol being qualified (Bouchilloux et al., 1998). Over the subsequent two decades, other red wines have been found to contain varietal thiols, such as Grenache, Pinot noir,

Abbreviations: 3-SH, 3-sulfanylhexan-1-ol; 3-SHA, 3-sulfanylhexyl acetate; 4-MSP, 4-methyl-4-sulfanylpentan-2-one; ACE, accentuated cut edges; ANOVA, analysis of variance; Cys-3-SH, 3-*S*-cysteinylhexan-1-ol; DAD, diode array detector; DTDP, 4,4'-dithiodipyridine; EDTA 2Na, ethylenediaminetetraacetic acid disodium salt; GC-MS, gas chromatography–mass spectrometry; GSH-3-SH, 3-*S*-glutathionylhexan-1-ol; HPLC, high performance liquid chromatography; HS-SPME, headspace-solid phase microextraction; MLF, malolactic fermentation; MS/MS, tandem mass spectrometry; OAV, odour active value; ODT, odour detection threshold; PCA, principal component analysis; SD, standard deviation; SIDA, stable isotope dilution assay; TA, titratable acidity.

* Corresponding author at: Department of Wine Science and Waite Research Institute, The University of Adelaide (UA), PMB 1, Glen Osmond, SA 5064, Australia.
E-mail address: david.jeffery@adelaide.edu.au (D.W. Jeffery).
[1] Present address: College of Chemistry and Chemical Engineering, Xiamen University, Xiamen 361005, China.

https://doi.org/10.1016/j.foodchem.2021.131222
Received 11 May 2021; Received in revised form 20 September 2021; Accepted 23 September 2021
Available online 25 September 2021

Pinotage, Shiraz, Sangiovese, and Cabernet Franc (Capone et al., 2021; Mafata et al., 2018; Rigou et al., 2014; Wang et al., 2016), revealing the broad presence of varietal thiols and their impacts on aroma characteristics of red and rosé wines. For instance, 3-SH was found to substantially affect the 'fruity' and 'citric' notes in Grenache rosé wine (Ferreira et al., 2002) and 4-MSP has been demonstrated to play a key role in impacting 'blackcurrant' aroma in blended red wines comprising 30% to 80% Shiraz (Rigou et al., 2014), the perception of which varied according to interactions between 4-MSP and 3-SH or 3-SHA. Shiraz was of particular interest due to being Australia's most important red grape varietal, but data on varietal thiol concentrations in Shiraz wines was limited and the presence of precursors of varietal thiols in Shiraz grapes appeared not to have been reported.

Compared to Sauvignon blanc wines, lower concentrations of varietal thiols in red wines could be a function of the winemaking process or may relate to precursor concentrations arising from the grapes. Varietal thiols are enzymatically released by yeast during fermentation from their L-glutathione, L-cysteine conjugated precursors or dipeptide derivatives that are present in both grape pulp and skin (Bonnaffoux et al., 2018; Capone et al., 2011; Roland et al., 2011), and increasing the concentrations of precursors in grape must prior to fermentation may provide an opportunity for increasing varietal thiols in the corresponding wines (in the absence of another major pathway to thiol formation, and despite a general lack of correlation between precursor and thiol concentrations (Chen et al., 2019)). Although attention has been paid mostly to Sauvignon blanc, the knowledge gained from viticultural and oenological aspects could also potentially be suitable for red wine production. Of particular relevance to red winemaking are techniques that seek to enhance disruption and extraction of grape solids. Skin contact time is an obvious one, whereby a gradual increase in the concentration of thiol precursor 3-*S*-cysteinylhexan-1-ol (Cys-3-SH) in Merlot grape must has been found with longer skin contact time (Murat et al., 2001). Similarly, pre-fermentation cold storage of Sauvignon blanc grape must or freezing of berries led to increased concentrations of precursors in juice (3-*S*-glutathionylhexan-1-ol (GSH-3-SH), Cys-3-SH, and 3-*S*-cysteinylglycinehexan-1-ol according to Capone et al. (2012) and of both GSH-3-SH and Cys-3-SH as reported by Chen et al. (2019)), as well as varietal thiols in experimental Sauvignon blanc wines (Chen et al., 2019; Roland et al., 2011).

In view of the importance of the maceration and extraction phase to red wine production, a novel approach known as accentuated cut edges (ACE) has been designed to mechanically break down grape skins into smaller fragments (i.e., ~ 10% of original size) while maintaining the integrity of grape seeds, so as to increase the amount of broken edges of grape skin and thus accelerate and improve the extraction of compounds from grape skins into grape must (Sparrow et al., 2016). ACE is used after conventional crushing of the grapes (e.g., with equipment such as a maceration accelerator from Della Toffola) and has been shown to increase colour density and hue, and content of total tannin, total phenolics, and stable pigments in McLaren Vale Shiraz and Tasmania Pinot noir wines (Kang et al., 2020; Sparrow et al., 2016). Ultimately, ACE could shorten the duration of skin contact while increasing the level of phenolics, thus minimising the time required for pump-over or other cap management techniques and helping to improve the efficiency of fermentor usage during increasingly compressed vintages. The technique has been reported to impact wine aroma characteristics, with an enhanced 'dark fruit' aroma in ACE treated Pinot noir wine (Sparrow, Holt, et al., 2016) in contrast to an intensified 'earthy/dusty' flavour in ACE treated Shiraz wine (Kang et al., 2020). The Pinot noir study also showed that ACE treatment wines had higher levels of some acetates and higher alcohols, but lower concentrations of ethyl esters (Sparrow et al., 2016), although the influence of ACE on the biogenesis of these fermentative volatiles has not been elucidated. Moreover, it remains unclear how ACE treatment could influence the concentration of grape derived aroma compounds, such as varietal thiols, which can play an important role in characterising young wine aromas.

Considering the potential impact on wine aroma quality from ACE and the economic importance of Shiraz grape variety to the Australian wine industry, this study aimed to investigate the concentrations of varietal thiol precursors in ACE treated Shiraz grape must before fermentation and concentrations of varietal thiols in wines compared to those produced from a conventional approach. The work addressed the hypothesis that ACE treatment could improve the concentration of thiol precursors in must and free thiols in the resulting wines. Additionally, other volatile compounds were determined, including C_6 compounds, higher alcohols, fatty acids, ethyl esters, acetates, and isoprenoids, to provide a broader evaluation of the effect of ACE on wine volatile compounds. The impact of pre-fermentative water addition (to dilute grape must total soluble solids to the regulated limit of 13.5 Baumé as permitted in Australia by FSANZ (2016)) and skin contact time (3 or 6 days) during fermentation in conjunction with ACE treatment were also evaluated, along with a brief assessment of commercial-scale Sauvignon blanc and Pinot noir wines that had undergone ACE treatment.

2. Material and methods

2.1. Chemicals and materials

Standards, reagents, and solid-phase extraction cartridges used for quantitative analysis of varietal thiols and their precursors were the same as outlined previously (Capone et al., 2015; Capone et al., 2011). 4,4′-Dithiodipyridine (DTDP), ethylenediaminetetraacetic acid disodium salt, formic acid, and acetaldehyde (anhydrous, ≥ 99.5%) were obtained from Sigma-Aldrich (Castle Hill, NSW, Australia). Bond Elut C18 cartridges (500 mg, 6 mL) and Strata SDB-L cartridges (500 mg, 6 mL) were from Agilent (Mulgrave, VIC, Australia) and Phenomenex (Lane Cove, NSW, Australia). Standards used for determination of C_6 compounds, higher alcohols, ethyl esters, acetates, fatty acids, isoprenoids, and other volatile compounds were from commercial suppliers (> 97% purity), as detailed previously (Capone et al., 2012; Wang et al., 2016), except for ethyl decanoate (> 99%, Eastman Organic Chemicals, New York, USA), d_8-(*E*)-2-hexen-1-ol (> 92% by GC–MS), synthesised as reported in Previtali et al. (2021)), and d_{15}-ethyl octanoate (> 98%), d_{11}-hexanoic acid (> 98%), d_7-butanoic acid (> 98%), and d_{15}-octanoic acid (> 98%) (CDN Isotopes, Pointe-Claire, Canada). Commercial Sauvignon blanc and Pinot noir wines were obtained from producers who used grapes harvested in 2020 from the Riverland region of South Australia.

2.2. Grape samples and fermentation

Details of Shiraz grapes (sourced from McLaren Vale in South Australia during vintage 2019) and procedures for winemaking have been outlined previously (Kang et al., 2020). Briefly, six treatments were performed in triplicate (25 kg scale): wines fermented after ACE treatment of crushed grapes (Della Toffola Maceration Accelerator, Della Toffola, Treviso, Italy) or using conventionally crushed grapes (control) were racked off grape skins on the third day (ACE_Short and NOACE_Short) or the sixth day (ACE_Long and NOACE_Long); grape must from ACE or conventional crushing was diluted with 0.5 L of spring water (2% v/w proportion) to yield a must with 13.5 Baumé after yeast inoculation and the wines were racked off skins on the sixth day of fermentation (ACE_Long_Dil and NOACE_Long_Dil).

Commercial-scale winemaking (unreplicated) involved Sauvignon blanc and Pinot noir from separate ACE experiments using a Della Toffola Maceration Accelerator. Sauvignon blanc trials included a control wine (SB_CTRL, titratable acidity: 5.2 g/L; pH 3.3; alcohol: 12.9% v/v), in which the juice for fermentation was obtained from conventionally crushed grapes, and three treatments prior to pressing and winemaking: treatment 1, ACE treated must (SB_ACE, titratable acidity: 5.9 g/L; pH 3.4; alcohol: 12.5% v/v); treatment 2, ACE treated must with 24 h of cold maceration (SB_ACE+M, titratable acidity: 5.7 g/L; pH 3.2; alcohol:

12.0% v/v); treatment 3, conventionally crushed grapes with 24 h of cold maceration (SB_M, titratable acidity: 6.4 g/L; pH 3.4; alcohol: 13.3% v/v). Pinot noir trials included a control wine (PN_CTRL, titratable acidity: 5.9 g/L; pH 3.7; alcohol: 13.9% v/v), produced from conventionally crushed grapes, and a treatment wine (PN_ACE, titratable acidity: 5.5 g/L; pH 3.8; alcohol: 13.6% v/v), produced using ACE treatment of crushed grapes.

2.3. Basic chemical analyses of wine

Methods and instruments used to determine pH, titratable acidity (TA), volatile acidity, sulfur dioxide, residual sugars, malic acid (particularly during malolactic fermentation (MLF)), and alcohol content have been reported (Kang et al., 2020). Organic acids were analysed in duplicate with an Agilent 1100 HPLC (Agilent, Melbourne, VIC, Australia) coupled with a diode-array detector as outlined previously (Li et al., 2017).

2.4. Stable isotope dilution assay (SIDA) with HPLC-MS/MS for analysis of varietal thiols and precursors

2.4.1. Analysis of varietal thiols in wine

The extracts of varietal thiol derivatives were prepared in duplicate following the published SIDA method (Capone et al., 2015), in which 20 mL of wine spiked with internal standard was derivatised with DTDP and extracted by solid phase extraction (SPE). Extracts were dried, reconstituted, and analysed with an Agilent 1200 HPLC coupled with a 6410 triple quadrupole mass spectrometer using the parameters detailed previously (Wang et al., 2020). Additional details are provided in a supplementary methods section in Appendix A.

2.4.2. Analysis of precursors of varietal thiols in must and wine

The extraction of precursors from must and wine was conducted in duplicate according to the published method (Capone et al., 2011), using 9.9 mL wine sample that was spiked with internal standard and extracted by SPE. Extracts were dried and reconstituted before analysis with an Agilent 1200 HPLC coupled with a 4000 QTRAP triple quadrupole mass spectrometer (Applied Biosystems/MDS Sciex, Concord, ON, Canada) according to (Capone et al., 2011). Additional details are provided in a supplementary methods section in Appendix A.

2.5. GC–MS analysis of C_6 compounds and other volatiles in wines

Both groups of volatiles were analysed in duplicate with an Agilent 7890A GC coupled with an Agilent 5975C inert XL MSD with triple-axis detector. C_6 compounds were analysed according to a previous method (Capone et al., 2012), where 1 mL of wine and 9 mL of Milli-Q water were added to a pre-salted (2 g NaCl) 20 mL amber solid-phase microextraction (SPME) vial followed by deuterium labelled internal standard mixture. The method was slightly modified with the inclusion of d_8-(*E*)-2-hexen-1-ol as an additional internal standard (ethanolic solution added to samples to yield 166 μg/L, quantifier ion at *m/z* 90 and qualifier ions at *m/z* 89 and 78) for the quantification of (*E*)-2-hexen-1-ol and (*Z*)-2-hexen-1-ol (Previtali et al., 2021). Other volatiles were determined following the method of Wang et al. (2016), where 0.5 mL of wine and 4.5 mL of Milli-Q water were added to a pre-salted (2 g NaCl) 20 mL amber SPME vial followed by deuterium labelled internal standard mixture. The method was slightly modified with the inclusion of additional authentic standards and deuterated internal standards as detailed in Table A.1 in Appendix A. Additional details for these analyses are provided in a supplementary methods section in Appendix A.

2.6. Sensory analysis

The experimental Shiraz wines were previously evaluated by 61 untrained regular wine consumers (Kang et al., 2020) using the validated rate-all-that-apply (RATA) sensory methodology (Danner et al., 2018). Aroma and flavour attributes from that assessment were discussed with the current dataset.

2.7. Statistical analysis

Mean values and standard deviation (SD) were calculated using Microsoft Excel (Microsoft Office Pro Plus 2019, USA). Independent sample *t*-test, two-way analysis of variance (ANOVA, with crushing method and skin contact time/water addition as fixed factors) followed by Tukey's HSD multiple comparison test ($\alpha = 0.05$), and principal component analysis (PCA) were conducted with XLSTAT (version 2020.1, Addisoft, Q-statistics, Reading, U.K.). Bar graphs were constructed with GraphPad Prism (version 7.02, GraphPad Software Inc., San Diego, CA).

3. Results and discussion

3.1. Basic chemical parameters of Shiraz wines

The basic parameters of experimental Shiraz wines (i.e., alcohol % v/v, residual sugar, pH, TA, volatile acidity, malic acid, and free and total SO_2) have been discussed previously, showing that water addition significantly decreased alcohol and TA whereas it increased the pH (Kang et al., 2020), although the differences were negligible. The concentrations of tartaric, lactic, citric, and malic acids determined in the present work (Fig. 1) were not significantly different according to two-way ANOVA ($p \geq 0.183$). Generally, tartaric acid ranged from 2.24 to 2.46 g/L, close to the lower limit of the typical range (2–6 g/L) in wine (Waterhouse et al., 2016). Lactic acid produced from malic acid during MLF (hence the negligible concentrations of malic acid, Fig. 1) ranged between 1.65 and 1.78 g/L and citric acid was between 0.65 and 0.73 g/L, in line with expected concentrations in wine (Waterhouse et al. (2016).

3.2. Precursors of varietal thiols in Shiraz grape must and wine

As reported for Melon B., Sauvignon blanc, Merlot, and Cabernet

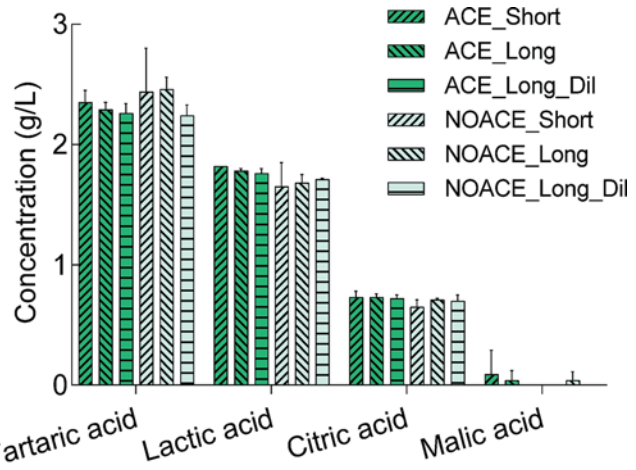

Fig. 1. Concentrations of organic acids in Shiraz wine samples arising from different treatments. Results represent mean values and standard deviation as error bars for replicate fermentations (n = 3). There were no significant differences due to treatment according to two-way ANOVA ($\alpha = 0.05$). ACE_Short and ACE_Long, wines made with ACE treated grape must and fermented with skin contact for 3 or 6 days; NOACE_Short and NOACE_Long, wines made from conventionally crushed grape must and fermented with skin contact for 3 or 6 days; ACE_Long_Dil and NOACE_Long_Dil, wines made with ACE or conventionally crushed grape must with water addition and fermented with skin contact for 6 days.

Sauvignon, precursors of varietal thiols are more abundant in grape skins (Murat et al., 2001; Roland et al., 2011). Thus, ACE was evaluated with the aim of improving the extraction of varietal thiol precursors from grape skin in a similar way to its capacity to accelerate the extraction of phenolics from the skin of Pinot noir (Sparrow et al., 2016).

To the best of our knowledge, this is the first time that the varietal thiol precursors have been quantified in Shiraz grape must (as the sum of diastereomers, Fig. 2), revealing that the concentration of GSH-3-SH in ACE and NOACE treatments was 208 and 177 μg/L, respectively, and the concentration of Cys-3-SH was 4.8 and 4.4 μg/L, respectively. Neither GSH-3-SH nor Cys-3-SH was significantly different between ACE and NOACE treated musts. The mean concentration of GSH-3-SH (sum of diastereomers) in Shiraz grape must (193 μg/L, average of both treatments) was higher than that reported in Cabernet Sauvignon at 52 μg/L (Helwi et al., 2015)) and Merlot at approximately 150 nM or equivalent to 61 μg/L (Kobayashi et al., 2011), but lower than determined for Garnacha (1422 μg/L) and Tempranillo (1284 μg/L) by Concejero et al. (2014). Compared with the concentrations in white grape varieties, the Shiraz in the present work was much lower than Sauvignon blanc (416 and 643 μg/L) and Pinot gris (466 μg/L) juice, being more similar to Chardonnay (176 μg/L) and Riesling (89 to 275 μg/L) (Capone et al., 2011). At 4.6 μg/L (sum of diastereomers, average of both treatments), Cys-3-SH was less abundant than GSH-3-SH and similar in concentration to Cabernet Sauvignon at ripeness (6.4 μg/L, Helwi et al. (2015)), but lower than Garnacha and Tempranillo (172 and 205 μg/L, respectively, Concejero et al. (2014)), and Merlot (80 nM, equivalent to 17.7 μg/L, Kobayashi et al. (2011)). Cys-3-SH was also reported as equivalent to approximately 16 ng/g of potential 3-SH (i.e., ~26 μg/kg of Cys-3-SH) in Cabernet Sauvignon grape skin and juice and between 17 and 22 ng/g (i.e., ~28–36 μg/kg of Cys-3-SH) in Merlot grape (Murat et al., 2001), although these higher concentrations compared to the ACE/NOACE processed Shiraz grape must in the present case could possibly be explained by the frozen storage of grape must in that previous work (Murat et al., 2001).

Thiol precursors in grape must are not necessarily consumed in their entirety during fermentation (Bonnaffoux et al., 2018), so the concentrations of GSH-3-SH and Cys-3-SH were also determined for the experimental Shiraz wines (Fig. 2). Precursor concentrations were not significantly different according to two-way ANOVA ($p \geq 0.11$) and only small differences were found for skin contact time and water addition treatments (Fig. 2). Approximately 100 μg/L of GSH-3-SH was found in the wine samples, pointing to the consumption of an average of about 100 μg/L in ACE treated wines and significantly less ($p < 0.01$, *t*-test) in NOACE treated wines (average of 70 μg/L). This decrease in GSH-3-SH (< 50%) was 23% lower than reported in a Sauvignon blanc study (from 1429 nmol/L to < 500 nmol/L, equalling 582 μg/L to < 204 μg/L in the work of Bonnaffoux et al. (2018)) and 47% lower than a study involving synthetic medium that imitated the amino acid profile of different grape varieties (1000 μg/L to < 50 μg/L according to Alegre et al. (2017)). This may point to the influences of grape juice/must composition and yeast strain on the utilisation of varietal thiol precursors during fermentation. In contrast to GSH-3-SH, the presence of Cys-3-SH in the experimental Shiraz wines was not detectable, which accorded with results from a Sauvignon blanc study (Wang et al., 2020) and grape juice composition appears to play an important role in the consumption of Cys-3-SH during fermentation (Alegre et al., 2017). The precursors remaining in the Shiraz wines were not significantly different with respect to treatment according to two-way ANOVA, which was of interest when comparing ACE and NOACE wines with their diluted counterparts. The addition of water was not significantly influential on the consumption of GSH-3-SH and Cys-3-SH, likely due to the limited amount used (Kang et al., 2020).

3.3. Volatile compounds in Shiraz wine

3.3.1. Varietal thiols in Shiraz wine

Although varietal thiols have been extensively studied in a wide range of varietal wines, they have rarely been reported for Australian red or rosé wines containing Shiraz (Bekker et al., 2021; Capone et al., 2021). The impact of ACE and skin contact time on the concentrations of varietal thiols (3-SH and 3-SHA only; 4-MSP was not detected) in Shiraz

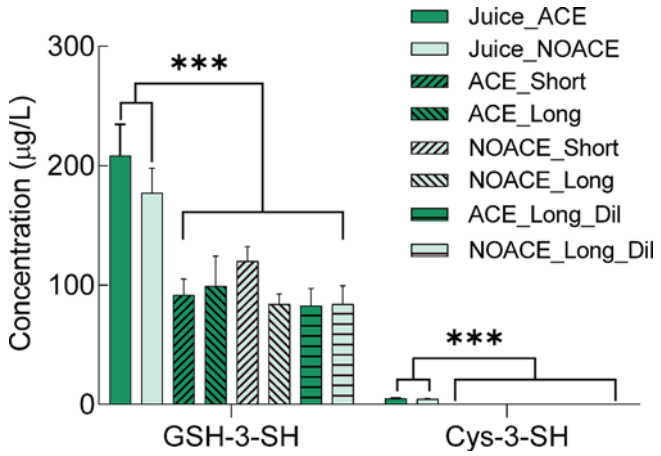

Fig. 2. Concentrations of varietal thiol precursors in Shiraz must arising from different treatments and remaining in the wine. Results represent mean values and standard deviation as error bars for must and replicate fermentations (n = 3). *** indicates significant difference between means of must or wine at $p < 0.0001$ (independent samples *t*-test). There were no significant differences between must treatments (independent samples *t*-test, α = 0.05) and wine treatments according to two-way ANOVA (α = 0.05). ACE_Short and ACE_Long, wines made with ACE treated grape must and fermented with skin contact for 3 or 6 days; NOACE_Short and NOACE_Long, wines made from conventionally crushed grape must and fermented with skin contact for 3 or 6 days; ACE_Long_Dil and NOACE_Long_Dil, wines made with ACE or conventionally crushed grape must with water addition and fermented with skin contact for 6 days.

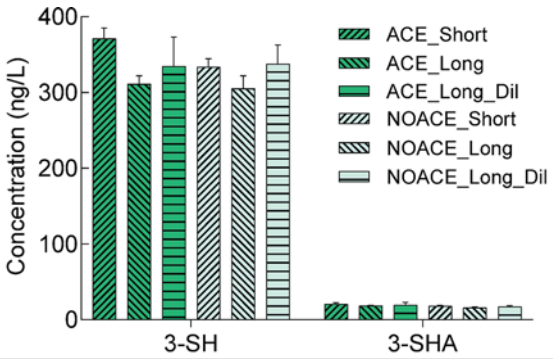

Compounds	3-SH	3-SHA
Crushing method	n.s.	n.s.
Skin contact time	0.001 (a, b, ab)*	n.s.
Interaction	n.s.	n.s.

Fig. 3. Concentrations of varietal thiols in Shiraz wines arising from different treatments. Results represent mean values and standard deviation as error bars for replicate fermentations (n = 3). ACE_Short and ACE_Long, wines made with ACE treated grape must and fermented with skin contact for 3 or 6 days; NOACE_Short and NOACE_Long, wines made from conventionally crushed grape must and fermented with skin contact for 3 or 6 days; ACE_Long_Dil and NOACE_Long_Dil, wines made with ACE or conventionally crushed grape must with water addition and fermented with skin contact for 6 days. The table below the figure shows results of two-way ANOVA followed by Tukey's HSD multiple comparisons (α = 0.05). n.s., not significant. *Different lower-case letters in brackets in the skin contact time row indicate significantly different means for 3-SH concentration in Short, Long, and Long_Dil treatments, respectively.

wines was evaluated for the first time in the present work (Fig. 3). 3-SH ranged from 305 ng/L to 371 ng/L (approximately 5–6 times above the ODT) across the treatments, which agreed with previous results for experimental McLaren Vale Shiraz wines (320–379 ng/L, Bekker et al. (2021)) and commercial South African Shiraz wines (69–363 ng/L, Mafata et al. (2018)), but lower than Adelaide Hills Shiraz wines (414–792 ng/L, Capone et al., 2021) and commercial Australian rosé wines (490–734 ng/L for monovarietal Shiraz and 347–2132 ng/L for Shiraz blend, Wang et al. (2016)). Except for yeast strain, vintage, wine region, and other factors that potentially influence 3-SH concentrations in wine, the lower concentrations of 3-SH in Shiraz red wines from the present study compared to the Adelaide Hills Shiraz wines (and the commercial rosé wines for that matter) could potentially be ascribed to higher levels of polyphenols – generally 55–63 a.u. for total phenolics in this set of Shiraz wines (Kang et al., 2020) compared with 7–33 a.u. for total phenolics in the Adelaide Hills Shiraz wines (Capone et al., 2021) – whose oxidised forms (i.e. *o*-quinones) can readily react with varietal thiols (Nikolantonaki & Waterhouse, 2012). Somewhat related to this, 3-SH was significantly affected by the main effect of skin contact time ($p = 0.001$, Fig. 3), whereby treatments with shorter skin contact time (352 μg/L, average of ACE/NOACE_Short) had significantly higher concentrations of 3-SH than those with longer contact time (308 μg/L, average of ACE/NOACE_Long), most likely due to additional oxidation and binding with *o*-quinones with the longer duration (Nikolantonaki & Waterhouse, 2012). Longer skin contact time coupled with water dilution was essentially in between and not significantly different to either of the other two treatments (336 μg/L, average of ACE/NOACE_Long_Dil).

Concentrations of 3-SHA ranged between 16 and 21 ng/L (Fig. 3) and were not significantly different as a function of the treatments. The values were similar to those determined for Adelaide Hills Shiraz wines (3–25 ng/L, Capone et al., 2021), but higher than reported for commercial South African Shiraz wines (≤ 8.4 ng/L, Mafata et al. (2018)) and Australian rosé wines (≤ 1.4 ng/L, Wang et al. (2016)). Notwithstanding the likely effect of different yeast strains among the studies, small differences in 3-SHA concentration could also be attributable to variation of acetate hydrolysis during the latter stage of fermentation or upon completion (Hernandez-Orte et al., 2006; Wang et al., 2020), and lipid and amino acid profiles of grape must can have an influence (Alegre et al., 2017; Deroite et al., 2018). Nonetheless, the data showed that 3-SHA may be important to Shiraz aroma profile, considering that calculated odour activity values (OAV) were ≥ 4. The molar esterification rate of 3-SH to 3-SHA ranged from 3.6% to 4.4%, which was similar to that reported previously in commercial Shiraz wines (Mafata et al., 2018).

Conversion yields from precursors to free thiols have often been a focus of varietal thiol studies when trying to rationalise thiol biogenesis through winemaking. Molar conversion yields calculated on summed values of 3-SH and 3-SHA divided by that of precursors consumed during alcoholic fermentation (i.e., precursor content in grape juice minus that in final wine) could provide an improved view of consumption of precursors during fermentation (Bonnaffoux et al., 2018). Based on this, the conversion yield of precursors for ACE treated wines was approximately 0.9%, whereas for NOACE treated wines it was slightly higher at roughly 1.2% but not significant (*t*-test, $p = 0.167$). Any apparent discrepancy in conversion yield, caused by similar levels of varietal thiols between ACE and NOACE wines but significantly higher amount of precursors consumed in ACE than NOACE treatment (detailed above in Section 3.2), could hypothetically relate to a higher proportion of varietal thiols in ACE treatment being subjected to the formation of other thiol-related products such as thiol-tannin adducts (Nikolantonaki & Waterhouse, 2012) as a result of the higher concentrations of total tannin in the ACE treatment compared to NOACE (Kang et al., 2020). Meanwhile, the potential formation of disulfides (Bonnaffoux et al., 2018) or oxathianes (Wang et al., 2020), for example, may also play an important role in influencing the results of the conversion yield calculation.

3.3.2. C_6 compounds in Shiraz wine

C_6 compounds are derived from polyunsaturated fatty acids (i.e., linoleic acid and linolenic acid) when grape berries are crushed in the presence of air (Cordonnier & Bayonove, 1981). Their contribution to the bouquet of wine is interesting given the correlation revealed between 1-hexanol and (*Z*)-3-hexen-1-ol with aroma notes of 'confectionery' and 'red fruits' in Shiraz wine (Capone et al., 2021) despite their individual 'green' and 'grassy' attributes (Table A.1). With total concentrations ranging from 2 to 3 mg/L, five C_6 compounds were quantified in the wines made from ACE/NOACE processed Shiraz grapes: 1-hexanol, (*Z*)-3-hexen-1-ol, (*E*)-3-hexen-1-ol, (*Z*)-2-hexen-1-ol, and (*E*)-2-hexen-1-ol (Fig. 4). Comparatively, 6-day skin contact time treatments (Long and Long_Dil with or without ACE) had significantly higher total concentrations of C_6 compounds than 3-day skin contact time treatments ($p = 0.003$, Fig. 4). This tended to agree with a previous report showing that Chardonnay juice pressed after 16 h of skin contact had a higher concentration of 1-hexanol compared to the directly pressed juice (Ferreira et al., 1995). Mean concentrations for water addition treatments (ACE_Long_Dil and NOACE_Long_Dil) were not different to their ACE_Long and NOACE_Long counterparts, due to the minimal amount of water added before fermentation (decrease in grape must sugar from 14.0 to 13.5 Baumé).

More specifically, 1-hexanol exceeded the concentrations of other C_6 compounds and (*Z*)-3-hexen-1-ol was the only C_6 compound found with an OAV > 1 (Fig. 4). Their concentrations (around 2000 μg/L and 414–607 μg/L, respectively) were similar but generally less abundant than reported previously in Shiraz wines (2339–5351 μg/L and 579–1357 μg/L, respectively, Table A.1 in Appendix A). The concentration of 1-hexanol was only impacted by skin contact time (Fig. 4), with 6-day skin contact time having a significantly higher level than 3-day skin contact time ($p = 0.004$, Fig. 4). (*Z*)-3-Hexen-1-ol was significantly increased by both ACE and 6-day skin contact time treatments ($p = 0.044$ and $p < 0.001$, respectively, Fig. 4), which agreed with previous observations for Shiraz wines produced with skin contact compared to those without (Capone et al., 2021). Notably, water addition treatment significantly decreased the concentration of (*Z*)-3-hexen-1-ol ($p < 0.001$, Fig. 4).

(*E*)-3-Hexen-1-ol and (*Z*)-2-hexen-1-ol were less abundant C_6 alcohols, with concentrations ranging from 45 to 59 μg/L and 19 to 43 μg/L, respectively, revealing a similar range to previous results for (*E*)-3-hexen-1-ol (49–58 μg/L, Table A.1 in Appendix A). These two compounds were significantly influenced by the interaction between crushing method and skin contact time; (*E*)-3-hexen-1-ol was significantly lower in NOACE_Short wine than the others ($p = 0.026$) and (*Z*)-2-hexen-1-ol was significantly higher in ACE_Short than ACE_Long, ACE_Long_Dil, and NOACE_Short treatments ($p = 0.008$). The concentration of (*E*)-2-hexen-1-ol, the least abundant of the measured C_6 compounds, ranged from 4.3 to 9.1 μg/L, in agreement with a previous report (not detected to 41 μg/L, Table A.1), and was significantly increased by ACE and longer skin contact time ($p \leq 0.034$, Fig. 4). Overall, skin contact time contributed significantly to the increment of C_6 compounds in the present study, in line with a previous Shiraz research (Capone et al., 2021) and potentially attributable to higher concentrations of unsaturated fatty acids extracted from grape solids during skin contact (Ferreira et al., 1995). ACE treatment had only limited impact on C_6 compounds and this tended to agree with a report on ACE treated Pinot noir wine where 1-hexanol was not significantly different to the control (Sparrow et al., 2016).

3.3.3. Other major volatile compounds in Shiraz wine

In total, fifty-three other volatiles in the wines, including ethyl esters, acetates, higher alcohols, fatty acids, isoprenoids, and others (Table A.1 in Appendix A) were analysed based on a validated method (Wang et al., 2016). Results showed that 20 of 35 quantified compounds (Table A.2) and 6 of 18 semi-quantified compounds (Table A.3) were significantly affected by the interaction of crushing method and skin contact time (*p*

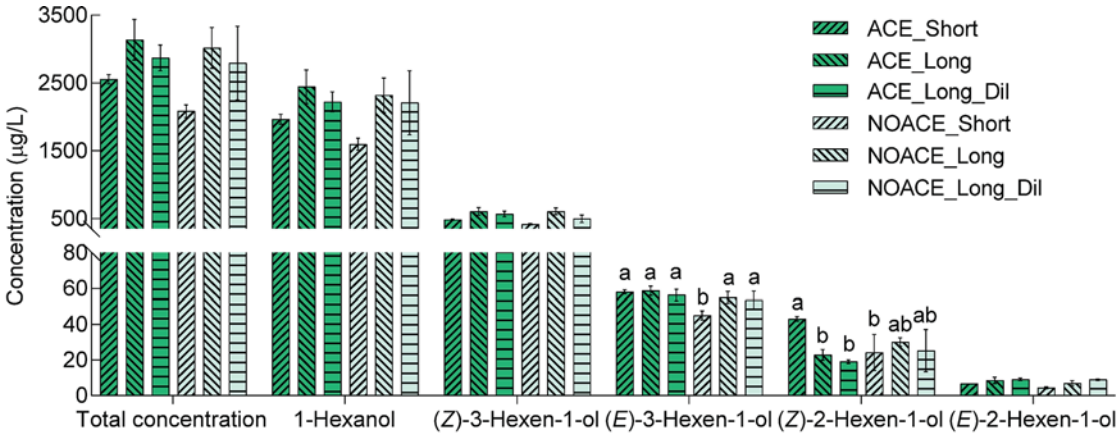

Compounds	Total concentration	1-Hexanol	(*Z*)-3-Hexen-1-ol	(*E*)-3-Hexen-1-ol	(*Z*)-2-Hexen-1-ol	(*E*)-2-Hexen-1-ol
Crushing method	n.s.	n.s.	0.044 (a, b)	0.001	n.s.	0.013 (a, b)
Skin contact time	0.003 (b, a, a)*	0.004 (b, a, a)	< 0.001 (c, a, b)	0.035	0.032	< 0.001 (b, a, a)
Interaction	n.s.	n.s.	n.s.	0.026	0.008	n.s.

Fig. 4. Concentrations of C_6 compounds in Shiraz wines arising from different treatments. Results represent mean values and standard deviation as error bars for replicate fermentations (n = 3). ACE_Short and ACE_Long, wines made with ACE treated grape must and fermented with skin contact for 3 or 6 days; NOACE_Short and NOACE_Long, wines made from conventionally crushed grape must and fermented with skin contact for 3 or 6 days; ACE_Long_Dil and NOACE_Long_Dil, wines made with ACE or conventionally crushed grape must with water addition and fermented with skin contact for 6 days. The table below the figure shows results of two-way ANOVA followed by Tukey's HSD multiple comparison ($\alpha = 0.05$). n.s. not significance. *Different lower-case letters in brackets in the crushing method row indicate significantly different means for analyte concentrations in ACE and NOACE, respectively, and in the skin contact time row indicate significantly different means for analyte concentrations in Short, Long, and Long_Dil treatments, respectively. Different lower-case letters above the bars indicate significantly different means for analyte concentrations in all treatments caused by interaction of crushing method and skin contact time.

≤ 0.032). Among the quantified compounds (Table A.2), the concentrations of 22 were above their respective ODT. Particularly, compounds with high OAV may be more important to the aroma profiles of these wines: these included 3-methylbutyl acetate (OAV $\geq$ 75), β-damascenone (OAV $\geq$ 43), ethyl hexanoate (OAV $\geq$ 39), 1-octanol (OAV $\geq$ 24), 3-methylbutanoic acid (OAV $\geq$ 22), nonanal (OAV $\geq$ 11), 3-methyl-1-butanol (OAV $\geq$ 10), ethyl octanoate (OAV $\geq$ 10), ethyl 2-methylbutanoate (OAV $\geq$ 8), octanoic acid (OAV $\geq$ 8), hexanoic acid (OAV $\geq$ 7), and ethyl nonanoate (OAV $\geq$ 6). The results were in agreement with previous reports showing that ethyl esters, acetates, and β-damascenone had high OAVs in Shiraz wines from the Adelaide Hills (Capone et al., 2021) as well as from Margaret River and Barossa Valley (Mayr et al., 2014).

Ethyl esters were more affected by the main effects of crushing method and skin contact time (Table A.2 in Appendix A) and only ethyl octanoate, presenting 'melon' and 'wood' aromas (Table A.1), had OAV > 1 and was significantly affected by the interaction of crushing method and skin contact time. Previously reported in Shiraz wines to be between 128 and 795 μg/L (Table A.1), ethyl octanoate was significantly more abundant in the NOACE treatments (299–337 μg/L) compared with the ACE_Long (210 μg/L) and ACE_Long_Dil wines (192 μg/L) in the present study. A similar effect was observed for ethyl propanoate (199–264 μg/L, OAV = 0.1) and ethyl butanoate (163–245 μg/L, OAV = 0.3–0.4), which can present 'banana' and 'apple' aromas (Table A.1) and could possibly contribute more to 'fruity' aroma in the NOACE treatments by acting as enhancers (de-la-Fuente-Blanco et al., 2020).

The main effect of crushing method revealed that the NOACE treatments had significantly higher concentrations ($p \leq 0.048$, Table A.2 in Appendix A) of ethyl 2-methylpropanoate (OAV $\leq$ 0.1), ethyl 2-methylbutanoate (OAV = 8–12), ethyl 3-methylbutanoate (OAV = 4–6), ethyl hexanoate (OAV = 39–55), and ethyl decanoate (OAV = 0.6–0.7), as well as ethyl 3-hexenoate and ethyl heptanoate in terms of the semi-quantified compounds ($p \leq 0.023$, Table A.3). The compounds all contribute 'fruity' aromas (Table A.1), with ethyl 2-methylbutanoate and ethyl hexanoate having been demonstrated as important to the aroma of young wine (de-la-Fuente-Blanco et al., 2020). The present results agreed with a previous study with NOACE processed Pinot noir wine presenting higher levels of some ethyl esters than the control (Sparrow et al., 2016). In contrast, ethyl lactate (OAV = 0.8–1.1, 'solvent' aroma, Table A.1) was significantly higher in ACE treatments (Table A.2), indicating the potential impact of ACE on the behaviours of yeast and bacteria used in the study. Additionally, skin contact time showed a significant enhancement of ethyl 2-methylpropanoate, ethyl 2-methylbutanoate, ethyl lactate, and ethyl decanoate in the 6-day skin contact time treatments ($p \leq 0.030$), with the first two volatiles being significantly higher only in Long_Dil treatments and the latter two being significantly higher in Long and Long_Dil treatments, when compared to 3-day skin contact time.

Of the four acetates determined, two (3-methylbutyl acetate and hexyl acetate) were significantly impacted by interaction of crushing method and skin contact time (Table A.2 in Appendix A). Similar in concentration range to a previous report on Shiraz wines (465–3880 μg/L, Table A.1), 3-methylbutyl acetate yielded the highest OAV among all esters and was significantly higher ($p = 0.011$) in NOACE_Long_Dil wine (3330 μg/L) than the ACE treatment (2238–2639 μg/L, Table A.2), indicating the potential for a more intense 'fruity' aroma in the NOACE_Long_Dil wine. Ethyl acetate, found in the range of 43–164 mg/L in other Shiraz wines (Table A.1), was significantly higher ($p = 0.004$) in NOACE treatments (65.3–67.6 mg/L) than in ACE treatments (53.3–54.2 mg/L, Table A.2). As mentioned in Section 3.3.1, lipid and amino acid profiles in grape must are important modulators of the volatile profiles of wine (Deroite et al., 2018; Hernandez-Orte et al., 2006), which could partly explain the difference in concentration of the acetates in the Shiraz wines. Hydrolysis of acetates at the latter stage of fermentation is also a possibility, however, potentially complicating the interpretation (Hernandez-Orte et al., 2006).

Higher alcohols were more significantly affected by the interaction of crushing method and skin contact time, including 6 of the 10 quantified compounds ($p \leq 0.031$, Table A.2 in Appendix A) and 3 of the 8 that were semi-quantified ($p \leq 0.002$, Table A.3). The concentration of 3-methyl-1-butanol, which ranged between 301 and 346 mg/L (OAV = 10–12, Table A.2) and agreed with the previously reported

concentrations (trace–310 mg/L, Table A.1), was significantly higher in ACE_Short treatment compared with the NOACE_Short treatment (p = 0.012, Table A.2). 1-Butanol and 2-phenylethanol, with respective concentrations of 0.9–1.1 mg/L and 53.0–67.3 mg/L and OAVs of 6–7 and 4–5 (Table A.2), were in the similar ranges reported previously (1.3–2.6 mg/L and trace–404 mg/L, respectively, Table A.1) and were found to be significantly more abundant in ACE_Short treatment than ACE_Long_Dil treatment. The concentration of 1-propanol (Table A.2), which ranged from 59.8 to 63.9 mg/L (OAV = 1.2–1.3) and was somewhat higher than previously reported (29.3–35.8 mg/L, Table A.1), was significantly higher in ACE_Short and NOACE_Long treatments compared with the ACE_Long_Dil treatment. Although most compounds in the higher alcohol grouping can be individually perceived as unpleasant (Table A.1), with descriptors such as 'alcohol', 'fusel', and 'solvent' aromas with the exception of 2-phenylethanol ('floral', 'rose'), their contribution to wine aroma profiles is reported to be dependent on the aroma context. For example, 2-methylpropanol and 3-methyl-1-butanol at a total concentration of 430 mg/L (i.e., similar concentration range to the Shiraz wines in the present work) significantly suppressed 'fruity' and 'coconut'/'wood'/'vanilla' notes when these alcohols were clearly perceived (de-la-Fuente-Blanco et al., 2016).

All seven quantified fatty acids were significantly affected by the interaction of crushing method and skin contact time ($p \leq 0.028$, Table A.2 in Appendix A). ACE_Short treatment had significantly higher concentrations of acetic, butanoic, 3-methylbutanoic, and decanoic acids than the other treatments ($p \leq 0.019$, Table A.2), although acetic acid in ACE_Long treatment was not significantly different to the other treatments. 2-Methylpropanoic, hexanoic, and octanoic acids were somewhat differently affected by the interaction effect, but in each case ACE_Short treatment had the highest concentrations. Of the compounds with OAV $\geq$ 1 in these Shiraz wines (Table A.2), the concentrations of acetic acid (434–648 mg/L), 3-methylbutanoic acid (740–1089 μg/L), and hexanoic acid (2743–3437 μg/L) were in line with previously reported values (Table A.1), but octanoic acid (3925–7029 μg/L, Table A.2) was considerably higher (253–3110 μg/L, Table A.1). Fatty acids have unpleasant aromas (Table A.1), such as 'sour', 'rancid', and 'cheesy', but they may only have a small impact on wine aroma (Ferreira et al., 2002) and serve as reactants in the production of desirable ethyl esters.

Isoprenoids were more impacted by the interaction of crushing method and skin contact time than the main effects (Table A.2 and A.3 in Appendix A) – these included α-terpineol (p = 0.001), terpinene-4-ol (p = 0.008), β-citronellol (p = 0.017), and nerol (p = 0.003) – being marginally differentially influenced, but ACE_Short treatment had the highest concentrations in each case. This outcome with ACE_Short was seemingly sensible, given the release of isoprenoids from their glycosidic precursors requires glycosidases (particularly β-glucosidase activity) that are most active when yeasts are in the exponential growth phase during fermentation (Fia et al., 2005). The 3-day skin contact time treatments (ACE/NOACE_Short) were racked off skins on the third day of fermentation, which potentially stimulated the growth of yeast by introducing oxygen at the end of exponential growth phase (Day et al., 2015). This contrasted with the 6-day skin contact time treatments, which were racked off skins long after this growth phase. Although the individual impact on wine aroma profile was likely to be limited apart from β-damascenone, these isoprenoids may still be important within the context of a synergistic effect (Ferreira et al., 2002).

The other three isoprenoids were influenced by the main effects, with NOACE treatments having significantly higher concentrations of vitispirane 1 and β-ionone than ACE treatments ($p \leq 0.030$, Table A.3 in Appendix A), and 3-day skin contact time treatments having significantly higher concentrations of vitispirane 1 and 2 ($p \leq 0.008$, Table A.3). The concentration of β-damascenone (2.2–3.0 μg/L, OAV > 43, Table A.2), imparting 'rose', 'apple', and 'honey' aromas to wine (Table A.1), matched with the previously reported concentrations in Shiraz wines (around 1 to 8.5 μg/L according to Capone et al., 2021; Ferreira et al., 2002), but was not significantly different among the present treatments. Nonetheless, β-damascenone may still play a part in affecting wine aroma by enhancing fruity notes of esters (Ferreira et al., 2002).

PCA was performed with the quantified volatiles that differed significantly in the wines, to further illustrate the impact of the applied treatments during winemaking (Fig. 5). Wines were separated by PC1 (49.2% total variance explained) according to skin contact time or dilution and by PC2 (29.2% total variance explained) according to the ACE process (Fig. 5). Specifically, ACE_Short was situated on its own to the right of the plot along PC1 and was characterised by higher concentrations of fatty acids, higher alcohols, 3-SH, and ethyl lactate, and lower amounts of some C_6 alcohols and ethyl esters (Fig. 5). Although the reason for this was unknown, higher levels in sugars or amino acids and lipids, the respective precursors of higher alcohols and fatty acids from fermentation, may have resulted from ACE and could be the drivers for determining the close location of ACE treatments relative to these two groups of volatiles. The location of 3-SH near ACE_Short agreed with the results presented in Fig. 3.

ACE_Long and ACE_Long_Dil were found to the left along PC1 (Fig. 5), where 1-hexanol, (*Z*)-3-hexen-1-ol, and (*E*)-2-hexen-1-ol were clustered, which affirmed the effect of longer skin contact time in increasing C_6 compounds. The three NOACE treatments were close to the PC2 axis in the positive direction (Fig. 5) and were relatively high in ethyl esters of various acids (2-methylpropanoate, 3-methylbutanoate, 2-methylbutanoate, hexanoate, octanoate, butanoate, and propanoate), ethyl acetate, and 3-methylbutyl acetate, but lower in some C_6 alcohols and higher alcohols. This could be attributable to the lower amount of lipids or unsaturated fatty acids in the conventional crushed grape must, with a similar result being shown for fermentation conducted with chemically-defined juice (Saerens et al., 2008). Together with this, winemaking parameters such as fermentation temperature, oxygen, and skin contact can further influence the production of ethyl esters (Antalick et al., 2014).

3.4. Sensory analysis of Shiraz wine

Sensory attributes of the wine samples were assessed by a RATA panel. Of the 22 aroma and corresponding flavour attributes evaluated, only 'floral/perfume/musk' and 'vanilla' aromas (Table A.4 in Appendix A) and 5 flavour attributes, including 'red fruits', 'earthy/dusty', 'floral/perfume/musk', 'herbaceous', and 'vanilla', were significantly different ($p < 0.1$, (Kang et al., 2020)). The more intense 'floral/perfume/musk' aroma in ACE_Short wine was likely due to the higher concentrations of isoprenoids in this treatment as a result of a synergistic effect, as mentioned earlier (Section 3.3.3). The 'red fruit' flavour being more intense in NOACE_Short and NOACE_Long mirrored the observations in Fig. 5 that NOACE treatments had higher concentrations of ethyl esters. Both 'vanilla' aroma and flavour were more intense in ACE_Short wine. The existence of a 'vanilla' trait was somewhat unexpected as oak products were not involved in the winemaking process, although it has been described for an unoaked Cabernet Sauvignon and could be associated with 2-methylbutanol in this case (Bindon et al., 2014).

3.5. Volatile compounds in commercial Sauvignon blanc and Pinot noir wines

Varietal thiols and other volatile compounds were analysed in a small number of Sauvignon blanc and Pinot noir wines from commercial trials addressing the effect of both ACE and cold maceration prior to fermentation (Table A.5 in Appendix A). This additional work involved unreplicated fermentations on a commercial scale and was aimed at providing general indications into the effect of ACE on the two varietal wines. In the Sauvignon blanc wines, varietal thiols, most higher alcohols, and linalool were much higher in SB_ACE+M than the other wine samples. An improvement of varietal thiols induced by cold maceration

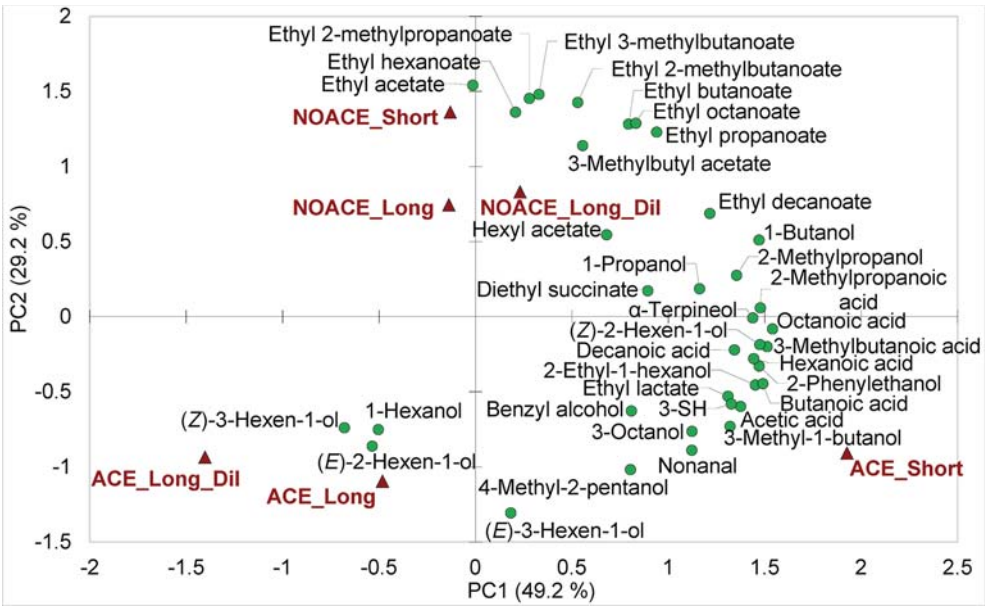

Fig. 5. PCA biplot showing scores and loadings of significantly different ($p < 0.05$ from two-way ANOVA) volatile compounds (green circles) in Shiraz wines from different treatments (brown triangles). ACE_Short and ACE_Long, wines made with ACE treated grape must and fermented with skin contact for 3 or 6 days; NOACE_Short and NOACE_Long, wines made from conventionally crushed grape must and fermented with skin contact for 3 or 6 days; ACE_Long_Dil and NOACE_Long_Dil, wines made with ACE or conventionally crushed grape must with water addition and fermented with skin contact for 6 days. (For interpretation of the references to colour in this figure legend, the reader is referred to the web version of this article.)

prior to fermentation, as reported previously in the case of pre-fermentation cold maceration (Roland et al., 2011), was not obvious in wine SB_M of the present work. Furthermore, the concentrations of 3-SH in these Sauvignon blanc wines were generally lower than those reported previously (i.e., can reach up to 19000 ng/L (Roland et al., 2011), which aside from differences resulting from fruit origin could potentially be related to processes used during commercial winemaking such as the use of fining agents (Vela et al., 2017). Higher alcohols being more abundant in SB_ACE+M wine could be attributed to the higher concentrations of amino acids in the grape must induced by the application of both the ACE process and cold maceration. Ethyl esters and fatty acids in Sauvignon blanc wines were not uniformly affected by any of the treatments. In contrast, acetates were mostly higher in the SB_CTRL wine sample, which accorded with the results for the Shiraz wines (Section 3.3.3).

With respect to the volatile compounds in Pinot noir, 3-SH was higher in PN_CTRL than PN_ACE (Table A.5 in Appendix A), which was different to the results of both Shiraz and Sauvignon blanc wines in the present work. This may result from the higher levels of phenolics associated with Pinot noir that has undergone ACE (Sparrow et al., 2016). ACE treatment affected both ethyl esters and acetates marginally, as only 5 esters (ethyl propanoate, ethyl butanoate, ethyl hexanoate, ethyl lactate, and ethyl acetate) of the 14 appeared to be higher in PN_ACE treatment than PN_CTRL, with the difference in concentrations of the remaining esters between the two wines being < 10 μg/L. Higher alcohols and fatty acids were generally more abundant in PN_ACE wine than in PN_CTRL (Table A.5), in accordance with previous observations for Shiraz wines as discussed in Section 3.3.3.

4. Conclusion

The influence of ACE in conjunction with skin contact time (3 or 6-day) and water addition on both the chemical and the sensory aroma profiles of Shiraz wines has been assessed, with a particular interest in varietal thiols and their precursors. To the best of our knowledge, the precursors of varietal thiols were determined in a Shiraz grape must and wine for the first time. Concentrations of precursors in grape must sampled immediately after crushing only showed marginal improvement (17%) in ACE processed grape must, but the consumption of GSH-3-SH was significantly higher (43%) in ACE treatments than the NOACE treatment. Production of 3-SH and 3-SHA was not significantly impacted by the ACE process, whereas 3-day skin contact time could significantly improve the amounts of 3-SH (by 14%) compared with the 6-day skin contact time treatment.

With respect to the other volatiles, six of eleven quantified ethyl esters and two of the three that were semi-quantified were affected by main effects of crushing method or skin contact time, with NOACE (increase of 4–33%, except for an 11% decline in ethyl lactate) and 3-day skin contact time (increment of 4–24%) enhancing their production. In contrast, acetates, higher alcohols, fatty acids, and isoprenoids were more impacted by the interaction of crushing method and skin contact time, with ACE_Short treatment showing the most potential to improve all groups of volatiles (increase of 3–47% for higher alcohols, 17–216% for fatty acids, and 20% for α-terpineol) except for acetates (decline of 14–21%). The significantly more intense 'floral/perfume/musk' aroma reported previously for ACE_Short wine was presumed to be driven by isoprenoids whereas 'red fruit' flavour, which was more intense in the NOACE_Short and NOACE_Long wines, was attributed to the higher concentrations of ethyl esters. Results from the analysis of volatile compounds in the experimental Shiraz and commercial Sauvignon blanc and Pinot noir wines indicated that the impact of ACE on varietal thiols in particular was dependent on grape variety, thus additional fermentation trials with Sauvignon blanc or other grape varieties are warranted.

CRediT authorship contribution statement

Xingchen Wang: Conceptualization, Formal analysis, Funding acquisition, Investigation, Visualization, Writing - original draft, Writing - review & editing. **Dimitra L. Capone:** Conceptualization, Supervision, Writing - review & editing. **Wenyu Kang:** Funding acquisition, Investigation, Writing - review & editing. **Aurélie Roland:** Conceptualization, Supervision, Writing - review & editing. **David W. Jeffery:** Conceptualization, Funding acquisition, Project administration, Resources, Supervision, Writing - review & editing.

Declaration of Competing Interest

The authors declare that they have no known competing financial interests or personal relationships that could have appeared to influence the work reported in this paper.

Acknowledgement

We acknowledge Mark Lloyd and Duncan Lloyd (Coriole Vineyards) for donation of grape material and kind help with winemaking. Richard Smart is especially acknowledged for his advice and valuable discussions on winemaking. Trentham Estate is acknowledged for the donation of Sauvignon blanc and Pinot noir wine samples. Paul Boss and Sue Maffei (CSIRO) are thanked for providing access to and advice on HPLC-MS/MS instrumentation. We acknowledge University of Adelaide (UA) colleagues, Ross Sanders for assistance with thiol precursor analysis in grape must, and Claire Armstrong and Pietro Previtali for their assistance with the experimental winemaking. X. W. is a receipt of the joint scholarship of the University of Adelaide and China Scholarship Council (201806300044) and is supported by a Wine Australia supplementary scholarship (WA Ph1803). W. K. acknowledges the support provided by the Adelaide Graduate Research Scholarship and Wine Australia (AGW Ph1605). The Australian Research Council Training Centre for Innovative Wine Production (www.ARCwinecentre.org.au; project number IC170100008) is funded by the Australian Government with additional support from Wine Australia, Waite Research Institute, and industry partners. The University of Adelaide is a member of the Wine Innovation Cluster.

Appendix A. Supplementary data

Supplementary data to this article can be found online at https://doi.org/10.1016/j.foodchem.2021.131222.

References

Alegre, Y., Culleré, L., Ferreira, V., & Hernández-Orte, P. (2017). Study of the influence of varietal amino acid profiles on the polyfunctional mercaptans released from their precursors. *Food Research International, 100*, 740–747. https://doi.org/10.1016/j.foodres.2017.07.081

Antalick, G., Perello, M.-C., & de Revel, G. (2014). Esters in wines: New insight through the establishment of a database of French wines. *American Journal of Enology and Viticulture, 65*(3), 293–304. https://doi.org/10.5344/ajev.2014.13133

Bekker, M. Z., Espinase Nandorfy, D., Kulcsar, A. C., Faucon, A., Bindon, K., & Smith, P. A. (2021). Comparison of remediation strategies for decreasing 'reductive' characters in Shiraz wines. *Australian Journal of Grape and Wine Research, 27*(1), 52–65. https://doi.org/10.1111/ajgw.12459

Bindon, K., Holt, H., Williamson, P. O., Varela, C., Herderich, M., & Francis, I. L. (2014). Relationships between harvest time and wine composition in *Vitis vinifera* L. cv. Cabernet Sauvignon 2. Wine sensory properties and consumer preference. *Food Chemistry, 154*, 90–101. https://doi.org/10.1016/j.foodchem.2013.12.099

Bonnaffoux, H., Delpech, S., Rémond, E., Schneider, R., Roland, A., & Cavelier, F. (2018). Revisiting the evaluation strategy of varietal thiol biogenesis. *Food Chemistry, 268*, 126–133. https://doi.org/10.1016/j.foodchem.2018.06.061

Bouchilloux, P., Darriet, P., Henry, R., Lavigne-Cruege, V., & Dubourdieu, D. (1998). Identification of volatile and powerful odorous thiols in Bordeaux red wine varieties. *Journal of Agricultural and Food Chemistry, 46*(8), 3095–3099. https://doi.org/10.1021/jf971027d

Capone, D. L., Barker, A., Pearson, W., & Francis, I. L. (2021). Influence of inclusion of grapevine leaves, rachis and peduncles during fermentation on the flavour and volatile composition of *Vitis vinifera* cv. Shiraz wine. *Australian Journal of Grape and Wine Research, 27*(3), 348–359. https://doi.org/10.1111/ajgw.12489

Capone, D. L., Black, C. A., & Jeffery, D. W. (2012). Effects on 3-mercaptohexan-1-ol precursor concentrations from prolonged storage of Sauvignon blanc grapes prior to crushing and pressing. *Journal of Agricultural and Food Chemistry, 60*(13), 3515–3523. https://doi.org/10.1021/jf300054h

Capone, D. L., Pardon, K. H., Cordente, A. G., & Jeffery, D. W. (2011). Identification and quantitation of 3-*S*-cysteinylglycinehexan-1-ol (Cysgly-3-MH) in Sauvignon blanc grape juice by HPLC-MS/MS. *Journal of Agricultural and Food Chemistry, 59*(20), 11204–11210. https://doi.org/10.1021/jf202543z

Capone, D. L., Ristic, R., Pardon, K. H., & Jeffery, D. W. (2015). Simple quantitative determination of potent thiols at ultratrace levels in wine by derivatization and high-performance liquid chromatography–tandem mass spectrometry (HPLC-MS/MS) analysis. *Analytical Chemistry, 87*(2), 1226–1231. https://doi.org/10.1021/ac503883s

Capone, D. L., Sefton, M. A., & Jeffery, D. W. (2011). Application of a modified method for 3-mercaptohexan-1-ol determination to investigate the relationship between free thiol and related conjugates in grape juice and wine. *Journal of Agricultural and Food Chemistry, 59*(9), 4649–4658. https://doi.org/10.1021/jf200116q

Chen, L., Capone, D. L., Nicholson, E. L., & Jeffery, D. W. (2019). Investigation of intraregional variation, grape amino acids, and pre-fermentation freezing on varietal thiols and their precursors for *Vitis vinifera* Sauvignon blanc. *Food Chemistry, 295*, 637–645. https://doi.org/10.1016/j.foodchem.2019.05.126

Concejero, B., Peña-Gallego, A., Fernandez-Zurbano, P., Hernández-Orte, P., & Ferreira, V. (2014). Direct accurate analysis of cysteinylated and glutathionylated precursors of 4-mercapto-4-methyl-2-pentanone and 3-mercaptohexan-1-ol in must by ultrahigh performance liquid chromatography coupled to mass spectrometry. *Analytica Chimica Acta, 812*, 250–257. https://doi.org/10.1016/j.aca.2014.01.004

Cordonnier, R., & Bayonove, C. (1981). Etude de la phase préfermentaire de la vinification: Extraction et formation de certains composés de l'arôme; cas des terpènols, des aldéhydes et des alcools en C_6. *Oeno One, 15*(4), 269–286. https://doi.org/10.20870/oeno-one.1981.15.4.1365

Danner, L., Crump, A. M., Croker, A., Gambetta, J. M., Johnson, T. E., & Bastian, S. E. P. (2018). Comparison of rate-all-that-apply and descriptive analysis for the sensory profiling of wine. *American Journal of Enology and Viticulture, 69*(1), 12–21. https://doi.org/10.5344/ajev.2017.17052

Day, M. P., Schmidt, S. A., Smith, P. A., & Wilkes, E. N. (2015). Use and impact of oxygen during winemaking. *Australian Journal of Grape and Wine Research, 21*(S1), 693–704. https://doi.org/10.1111/ajgw.12199

de-la-Fuente-Blanco, A., Sáenz-Navajas, M.-P., & Ferreira, V. (2016). On the effects of higher alcohols on red wine aroma. *Food Chemistry, 210*, 107–114. https://doi.org/10.1016/j.foodchem.2016.04.021

de-la-Fuente-Blanco, A., Sáenz-Navajas, M.-P., Valentin, D., & Ferreira, V. (2020). Fourteen ethyl esters of wine can be replaced by simpler ester vectors without compromising quality but at the expense of increasing aroma concentration. *Food Chemistry, 307*, 125553. https://doi.org/10.1016/j.foodchem.2019.125553

Deroite, A., Legras, J. L., Rigou, P., Ortiz-Julien, A., & Dequin, S. (2018). Lipids modulate acetic acid and thiol final concentrations in wine during fermentation by *Saccharomyces cerevisiae* × *Saccharomyces kudriavzevi*i hybrids. *AMB Express, 8*, 130. https://doi.org/10.1186/s13568-018-0657-5

Ferreira, B., Hory, C., Bard, M. H., Taisant, C., Olsson, A., & Le Fur, Y. (1995). Effects of skin contact and settling on the level of the C18:2, C18:3 fatty acids and C6 compounds in Burgundy Chardonnay musts and wines. *Food Quality and Preference, 6*(1), 35–41. https://doi.org/10.1016/0950-3293(94)P4210-W

Ferreira, V., Ortin, N., Escudero, A., Lopez, R., & Cacho, J. (2002). Chemical characterization of the aroma of Grenache rosé wines: Aroma extract dilution analysis, quantitative determination, and sensory reconstitution studies. *Journal of Agricultural and Food Chemistry, 50*(14), 4048–4054. https://doi.org/10.1021/jf0115645

Fia, G., Giovani, G., & Rosi, I. (2005). Study of β-glucosidase production by wine-related yeasts during alcoholic fermentation. A new rapid fluorimetric method to determine enzymatic activity. *Journal of Applied Microbiology, 99*(3), 509–517. https://doi.org/10.1111/j.1365-2672.2005.02657.x

FSANZ. (2016). Food Standards Australia New Zealand, Application A1119 – Addition of water to facilitate wine fermentation.

Helwi, P., Thibon, C., Habran, A., Hilbert, G., Guillaumie, S., Delrot, S., … Van Leeuwen, C. (2015). Effect of vine nitrogen status, grapevine variety and rootstock on the levels of berry *S*-glutathionylated and *S*-cysteinylated precursors of 3-sulfanylhexan-1-ol. *Oeno One, 49*(4), 253–265. https://doi.org/10.20870/oeno-one.2015.49.4.40

Hernandez-Orte, P., Ibarz, M. J., Cacho, J., & Ferreira, V. (2006). Addition of amino acids to grape juice of the Merlot variety: Effect on amino acid uptake and aroma generation during alcoholic fermentation. *Food Chemistry, 98*(2), 300–310. https://doi.org/10.1016/j.foodchem.2005.05.073

Kang, W., Bindon, K. A., Wang, X., Muhlack, R. A., Smith, P. A., Niimi, J., & Bastian, S. E. P. (2020). Chemical and sensory impacts of accentuated cut edges (ACE) grape must polyphenol extraction technique on Shiraz wines. *Foods, 9*(8), 1027. https://doi.org/10.3390/foods9081027

Kobayashi, H., Takase, H., Suzuki, Y., Tanzawa, F., Takata, R., Fujita, K., Kohno, M., Mochizuki, M., Suzuki, S., & Konno, T. (2011). Environmental stress enhances biosynthesis of flavor precursors, *S*-3-(hexan-1-ol)-glutathione and *S*-3-(hexan-1-ol)-l-cysteine, in grapevine through glutathione *S*-transferase activation. Journal of Experimental Botany, 62(3), 1325-1336. 10.1093/jxb/erq376.

Li, S., Bindon, K., Bastian, S. E. P., Jiranek, V., & Wilkinson, K. L. (2017). Use of winemaking supplements to modify the composition and sensory properties of Shiraz wine. *Journal of Agricultural and Food Chemistry, 65*(7), 1353–1364. https://doi.org/10.1021/acs.jafc.6b04505

Mafata, M., Stander, M. A., Thomachot, B., & Buica, A. (2018). Measuring thiols in single cultivar South African red wines using 4,4-dithiodipyridine (DTDP) derivatization and ultraperformance convergence chromatography-tandem mass spectrometry. *Foods, 7*(9), 138. https://doi.org/10.3390/foods7090138

Mayr, C. M., Geue, J. P., Holt, H. E., Pearson, W. P., Jeffery, D. W., & Francis, I. L. (2014). Characterization of the key aroma compounds in Shiraz wine by quantitation, aroma reconstitution, and omission studies. *Journal of Agricultural and Food Chemistry, 62*(20), 4528–4536. https://doi.org/10.1021/jf405731v

Murat, M.-L., Tominaga, T., & Dubourdieu, D. (2001). Assessing the aromatic potential of Cabernet Sauvignon and Merlot musts used to produce rose wine by assaying the cysteinylated precursor of 3-mercaptohexan-1-ol. *Journal of Agricultural and Food Chemistry, 49*(11), 5412–5417. https://doi.org/10.1021/jf0103119

Nikolantonaki, M., & Waterhouse, A. L. (2012). A method to quantify quinone reaction rates with wine relevant nucleophiles: A key to the understanding of oxidative loss of varietal thiols. *Journal of Agricultural and Food Chemistry, 60*(34), 8484–8491. https://doi.org/10.1021/jf302017j

Previtali, P., Dokoozlian, N., Capone, D. L., Wilkinson, K. L., & Ford, C. M. (2021). Exploratory study of sugar and C_6 compounds in single berries of grapevine (*Vitis vinifera* L.) cv. Cabernet Sauvignon throughout ripening. *Australian Journal of Grape and Wine Research, 27*(2), 194–205. https://doi.org/10.1111/ajgw.12472

Rigou, P., Triay, A., & Razungles, A. (2014). Influence of volatile thiols in the development of blackcurrant aroma in red wine. *Food Chemistry, 142*, 242–248. https://doi.org/10.1016/j.foodchem.2013.07.024

Roland, A., Schneider, R., Charrier, F., Cavelier, F., Rossignol, M., & Razungles, A. (2011). Distribution of varietal thiol precursors in the skin and the pulp of Melon B. and Sauvignon blanc grapes. *Food Chemistry, 125*(1), 139–144. https://doi.org/10.1016/j.foodchem.2010.08.050

Roland, A., Schneider, R., Razungles, A., & Cavelier, F. (2011). Varietal thiols in wine: Discovery, analysis and applications. *Chemical Reviews, 111*(11), 7355–7376. https://doi.org/10.1021/cr100205b

Saerens, S. M. G., Delvaux, F., Verstrepen, K. J., Van Dijck, P., Thevelein, J. M., & Delvaux, F. R. (2008). Parameters affecting ethyl ester production by *Saccharomyces cerevisiae* during fermentation. *Applied and Environmental Microbiology, 74*(2), 454–461. https://doi.org/10.1128/aem.01616-07

Sparrow, A. M., Holt, H. E., Pearson, W., Dambergs, R. G., & Close, D. C. (2016). Accentuated cut edges (ACE): Effects of skin fragmentation on the composition and sensory attributes of Pinot noir wines. *American Journal of Enology and Viticulture, 67*(2), 169–178. https://doi.org/10.5344/ajev.2015.15094

Sparrow, A. M., Smart, R. E., Dambergs, R. G., & Close, D. C. (2016). Skin particle size affects the phenolic attributes of Pinot noir wine: Proof of concept. *American Journal of Enology and Viticulture, 67*(1), 29–37. https://doi.org/10.5344/ajev.2015.15055

Vela, E., Hernández-Orte, P., Castro, E., Ferreira, V., & Lopez, R. (2017). Effect of bentonite fining on polyfunctional mercaptans and other volatile compounds in Sauvignon blanc wines. *American Journal of Enology and Viticulture, 68*(1), 30–38. https://doi.org/10.5344/ajev.2016.16052

Wang, J., Capone, D. L., Wilkinson, K. L., & Jeffery, D. W. (2016). Chemical and sensory profiles of rosé wines from Australia. *Food Chemistry, 196*, 682–693. https://doi.org/10.1016/j.foodchem.2015.09.111

Wang, X., Chen, L., Capone, D. L., Roland, A., & Jeffery, D. W. (2020). Evolution and correlation of *cis*-2-methyl-4-propyl-1,3-oxathiane, varietal thiols, and acetaldehyde during fermentation of Sauvignon blanc juice. *Journal of Agricultural and Food Chemistry, 68*(32), 8676–8687. https://doi.org/10.1021/acs.jafc.0c03183

Waterhouse, A. L., Sacks, G. L., & Jeffery, D. W. (2016). Acids. In *Understanding Wine Chemistry* (pp. 19–33). John Wiley & Sons. https://doi.org/10.1002/9781118730720.

APPENDIX A

SUPPLEMENTARY DATA FOR

Impact of accentuated cut edges (ACE) technique on volatile and sensory profiles of Shiraz wines

Xingchen Wang[a], Dimitra L. Capone[a,b], Wenyu Kang[a], Aurélie Roland[c], David W. Jeffery[a,b,*]

[a] Department of Wine Science and Waite Research Institute, The University of Adelaide (UA), PMB 1, Glen Osmond, SA 5064, Australia

[b] Australian Research Council Training Centre for Innovative Wine Production, UA, PMB 1, Glen Osmond, SA 5064, Australia

[c] SPO, Univ Montpellier, INRAE, Institut Agro, Montpellier, France

*Corresponding author

Email address: david.jeffery@adelaide.edu.au (D.W. Jeffery)

Table of Contents

Supplementary method information for Sections 2.4 and 2.5

2.4.1 Analysis of varietal thiols in wine

An aliquot (50 µL) of an ethanolic solution containing d_8-3-SH, d_8-3-SHA, and d_{10}-4-MSP (final concentrations of 500 ng/L of each internal standard) was added to 20 mL of wine followed by EDTA 2Na (20 mg), 50 % acetaldehyde (80 µL), and freshly thawed DTDP reagent (10 mM, 200 µL). After 30 minutes the derivatisation mixture was passed through a 6 mL, 500 mg Bond Elut C18 cartridge, previously conditioned with 6 mL of methanol followed by 6 mL of water. The cartridge was washed with 12 mL of 50% methanol and dried under air for 5 minutes, then eluted with 3 mL of methanol. The eluate was collected, concentrated to dryness with a gentle stream of nitrogen at 25 ºC using a TurboVap LV evaporator, and reconstituted for analysis with 200 µL of 10% aqueous ethanol.

HPLC separation was conducted using a 250 × 2.1 mm i.d., 5 µm, 100 Å Alltima C18 column operated at 25 ºC and protected by a 7.5 × 2.1 mm i.d. guard cartridge. The solvents were 0.5% aqueous formic acid (solvent A) and 0.5% formic acid in acetonitrile (solvent B), with a flow rate of 0.200 mL/min. The linear gradient for solvent B was: 0 min, 20%; 10 min, 50%; 15 min, 80%; 20 min, 80%; 21 min, 20%; and 15 min equilibration with 20% B. An injection volume of 10 µL was used. Electrospray ionisation was conducted in positive ion mode, mass spectrometer dwell times for multiple reaction monitoring (MRM) were 40 ms, and values for fragmentor voltage and collision energy were as shown below.

Compound	MRM pairs	Fragmentor voltage (V)	Collision energy (eV)
d_8-3-SH	252.3 → 144.1	122	17
	252.0 → 143.9	105	20
	252.0 → 111.0		40
3-SH	244.5 → 144.1	102	17
	244.1 → 144.0		16
	244.1 → 111.0	120	40
	244.1 → 67.0		40
d_8-3-SHA	294.3 → 144.1	122	21
	294.0 → 144.1	120	20
	294.3 → 86.0	122	13
	294.0 → 85.2	120	13
3-SHA	286.4 → 144.2	122	21
	286.1 → 143.9	120	20
	286.4 → 111.0	122	30
	286.1 → 83.1	120	16
d_{10}-4-MSP	252.0 → 144.9	105	16
	252.0 → 111.0		40
4-MSP	242.2 → 144.2	100	13
	242.1 → 144.0	105	16
	242.1 → 111.0		40

2.4.2 Analysis of precursors of varietal thiols in must and wine

An aliquot (100 µL) of an aqueous solution containing d_8-(*R*/*S*)-Cys-3-SH and d_9-(*R*/*S*)-GSH-3-SH (50 µg/L of each diastereomer) was added to 9.9 mL of grape must or wine. The sample was passed through a 6 mL, 500 mg Strata SDB-L cartridge (Phenomenex, Lane Cove, NSW, Australia), previously conditioned with 6 mL of methanol followed by 6 mL of water. The cartridge was dried under air for 5 min and eluted with 2 mL of methanol. The eluate was collected and concentrated to dryness using nitrogen at 25 °C on a TurboVap LV evaporator. The sample was then reconstituted with 500 µL of methanol, followed by the addition of 200 µL of Milli-Q water and vortexing for 10 s. The sample was filtered through a 0.45 µm syringe filter prior to HPLC-MS/MS analysis.

HPLC separation was conducted using a 250 × 2.1 mm i.d., 5 µm, 100 Å Alltima C18 column operated at 25 °C and protected by a 4 × 2 mm i.d. guard cartridge. The solvents were 0.5% aqueous formic acid (solvent A) and 0.5% formic acid in acetonitrile (solvent B), with a flow rate of 0.300 mL/min. The gradient for solvent B was as follows: 0 min, 5%; 10 min, 15%; 20 min, 30%; 21 min, 80%, and 25 min, 80%; and 10 min equilibration with 5% B. An injection volume of 10 µL was used. Electrospray ionisation was conducted in positive ion mode with a mass spectrometer collision energy of 20 eV and dwell times of 100 ms for multiple reaction monitoring (MRM) using the ion pairs shown below.

Compound	MRM pairs
d_8-(*R/S*)-Cys-3-SH	230.2 → 213.1
	230.2 → 109.2
	230.2 → 90.2
(*R/S*)-Cys-3-SH	222.2 → 205.1
	222.2 → 101.2
	222.2 → 83.2
d_9-(*R/S*)-GSH-3-SH	417.3 → 342.5
	417.3 → 288.5
	417.3 → 271.2
	417.3 → 162.1
(*R/S*)-GSH-3-SH	408.2 → 333.4
	408.2 → 279.3
	408.2 → 262.4
	408.2 → 162.3

2.5 GC-MS analysis of C_6 compounds and other volatiles in wines

For C_6 compounds, an aliquot (1 mL) of wine and 9 mL of Milli-Q water were added to a 20 mL glass screw cap amber SPME vial containing 2 g of NaCl and. An aliquot (100 µL) of an ethanol solution containing deuterium labelled C_6 standards (final concentrations of d_{13}-hexan-1-ol, 60.8 µg/L; d_9-(*E*)-2-hexenal, 300 µg/L; d_8-(*E*)-2-hexen-1-ol, 166 µg/L) was added, the contents were shaken, and the vials sealed for GC−MS analysis.

The autosampler was fitted with a 65 µm PDMS/DVB SPME fibre and samples were extracted at 40 °C for 30 min with agitation (500 rpm, 10 s on, 1 s off) before desorption into the inlet for 15 min at 240 °C. Injection was undertaken in pulsed/splitless mode with an inlet pressure of 45.0 psi maintained until splitting, with the splitter (90:1) being opened after 36 s. GC separation was conducted with a 60 m DB-WaxUI column (0.25 mm i.d., 0.25 µm film thickness). The carrier gas was helium with a flow rate of 1.5 mL/min. The oven temperature started at 45 °C, was held at this temperature for 5 min, then increased at 2 °C/min to 100 °C, then at 15 °C/min to 240 °C, and maintained at this temperature for 8 min. The transfer line was maintained at 240 °C. Positive ion electron ionisation mass spectra at 70 eV were recorded using the dwell times and selected ion monitoring (SIM) ions (**quantifier** and qualifier) as shown below.

Compound	SIM ions	Dwell time (ms)
d_9-(*E*)-2-Hexenal	**89**	
	107	25
	73	
(*E*)-2-Hexenal	**97**	
	98	25
	83	
d_{13}-Hexan-1-ol	**78**	
	96	20
	64	
Hexan-1-ol	**69**	
	84	20
	56	
(*E*)-3-Hexen-1-ol	**82**	
	69	20
	67	
(*Z*)-3-Hexen-1-ol	82	
	69	20
	67	
d_8-(*E*)-2-Hexen-1-ol	**90**	
	89	20
	78	
(*E*)-2-Hexen-1-ol	**82**	
	67	20
	57	
(*Z*)-2-Hexen-1-ol	**82**	
	67	20
	57	

For other volatile compounds, an aliquot (0.5 mL) of wine and 4.5 mL of Milli-Q water were added to a 20 mL glass screw cap amber SPME vial containing 2 g of NaCl and. An aliquot (10 µL) of an ethanol solution containing deuterium labelled standards (final concentrations of d_4-methylbutan1-ol, 48 µg/L; d_3-hexyl acetate, 0.5 µg/L; d_{13}-hexan-1-ol, 1 µg/L; d_5-2-phenylethanol, 10 µg/L; d_5-ethyl nonanoate, 0.024 µg/L; d_{15}-ethyl octanoate, 1 µg/L; d_{11}-hexanoic acid, 10 µg/L; d_{15}-octanoic acid, 20 µg/L; d_{19}-decanoic acid, 1 µg/L) was added, the contents were shaken, and the vials sealed for GC−MS analysis.

The autosampler was fitted with a DVB/CAR/PDMS SPME fibre (50/30 µm, 1 cm, 23 gauge) and samples were incubated for 10 min then extracted for 45 min, both at 50 °C with agitation speed of 500 rpm. Injection was undertaken in splitless mode for 10 min with a desorption temperature of 240 °C, using a deactivated SPME inlet liner (0.75 mm i.d., Supelco). GC separation was conducted with a 30 m DB-Waxetr column (0.25 mm i.d., 0.25 µm film thickness). The carrier gas was helium at a constant flow of 1 mL/min. The oven temperature started at 40 °C for 1 min, increased to 135 °C at 2 °C/min, then to 212 °C at 5 °C/min, and to 250 °C at 15 °C/min, remaining at 250 °C for 10 min. The transfer line was maintained at 200 °C. Positive ion electron ionisation mass spectra at 70 eV were recorded in the range m/z 35–350 for scan runs.

Table A.1. Qualification and quantification details of C_6 compounds and other major volatiles grouped according to compound type.

Compound[a]	Ions[b]	Calibration range (µg/L)[c]	R^2	Internal standard[d]	ODT (µg/L)[e]	Odour descriptors[f]	Typical range (refs)[g]
C_6 Compounds							
1-Hexanol	**69**, 56, 84	8.0–495	0.9999	d_{13}-Hexanol	8000 (Guth, 1997)	Resin, flower, green, cut grass (Benkwitz et al., 2012)	2339–5351 (1, 2)
(*E*)-3-Hexen-1-ol	**82**, 67, 69	0.6–495	0.9998	d_{13}-Hexanol	1550 (Waterhouse et al., 2016)	Green, cut grass (Benkwitz et al., 2012)	49–58 (2)
(*Z*)-3-Hexen-1-ol	**82**, 67, 69	1.7–495	0.9997	d_{13}-Hexanol	400 (Guth, 1997)	Green, cut grass (Benkwitz et al., 2012)	579–1357 (1, 2)
(*E*)-2-Hexen-1-ol	**82**, 57, 67	1.3–495	0.9999	**d_8-(*E*)-2-Hexen-1-ol**	400 (Waterhouse et al., 2016)	Green, cut grass (Benkwitz et al., 2012)	n.d.–41 (1)
(*Z*)-2-Hexen-1-ol	**82**, 67, 57	3.8–495	0.9998	**d_8-(*E*)-2-Hexen-1-ol**	Unknown	Green, cut grass (Benkwitz et al., 2012)	n.r.
Ethyl esters							
Ethyl propanoate	**57**, 75, 102	52.4–902	0.9987	**d_4-3-Methyl-1-butanol**	2100 (Moyano et al., 2002)	Banana, apple (Moyano et al., 2002)	143–723 (3, 4, 5, 6)
Ethyl 2-methylpropanoate	**71**, 88, 116	77.2–902	0.9972	**d_3-Hexyl acetate**	5600 (Moyano et al., 2002)	Fruity (Moyano et al., 2002)	30–353 (3, 4, 5, 6, 7)
Ethyl butanoate	**71**, 29, 88	26.8–902	0.9985	d_4-3-Methyl-1-butanol	600 (Moyano et al., 2002)	Banana, pineapple, strawberry (Moyano et al., 2002)	81–350 (3, 4, 5, 6, 7, 8, 9)
Ethyl 2-methylbutanoate	**57**, 85, 115	0.8–15.0	0.9954	d_3-Hexyl acetate	1 (Guth, 1997)	Fruity, anise strawberry (Ferreira et al., 2009)	4–76 (3, 4, 5, 6, 7, 8)
Ethyl 3-methylbutanoate	**88**, 57, 130	1.4–15.0	0.9940	d_3-Hexyl acetate	3 (Guth, 1997)	Fruit	27–100 (3, 7, 8)
Ethyl 2-butenoate	**69**, 99	equivalent to ethyl 2-methylbutanoate		d_3-Hexyl acetate	Unknown	Compost (Mayr et al., 2014)	n.r.
Ethyl hexanoate	**88**, 99, 60	187–1202	0.9909	d_4-3-Methyl-1-butanol	14 (Ferreira et al., 2000)	Apple peel, fruit	147–679 (3, 4, 5, 6, 7, 8, 9)
Ethyl 3-hexenoate	**69**, 41, 29	**equivalent to ethyl hexanoate**		**d_4-3-Methyl-1-butanol**	Unknown	Green, fruity (Burdock, 2010)	n.r.
Ethyl heptanoate	**88**, 32, 101	**equivalent to ethyl hexanoate**		**d_4-3-Methyl-1-butanol**	220 (Etiévant, 1991)	Fruity, perfumed, fatty (Meilgaard, 1975)	n.r.
Ethyl lactate	**45**, 29, 75	2.9–23.5 mg/L	0.9947	**d_4-3-Methyl-1-butanol**	146000 (Moyano et al., 2002)	Solvent (Mayr et al., 2014)	5.4–367 mg/L (3, 7, 9)
Ethyl octanoate	**88**, 101, 127	77.3–1200	0.9984	**d_{15}-Ethyl octanoate**	20 (Swiegers et al., 2005)	Melon, wood (Mayr et al., 2014)	128–795 (3, 4, 5, 6, 7, 8, 9)
Ethyl nonanoate	**88**, 101, 141	118–1200	0.9963	**d_{15}-Ethyl octanoate**	850 (Etiévant, 1991)	Fruity, rose, waxy, rum, tropical	n.r.
Ethyl decanoate	**88**, 101, 155	60.3–497	0.9918	d_4-3-Methyl-1-butanol	200 (Ferreira et al., 2000)	Fruity (Swiegers et al., 2005)	37–156 (3, 5, 6, 9)
Diethyl succinate	**129**, 101, 147	476–4500	0.9945	d_4-3-Methyl-1-butanol	500000 (Boscaino et al., 2019)	Light fruity (Boscaino et al., 2019)	1.9–8110 (4, 9)

[a] Quantification of compounds refers to the published method (Wang et al., 2016), with bolded compound names highlighting those that were newly added to the method. [b] Bolded ions were used as quantifiers and other ions were used as qualifiers. [c] Calibration range from limit of quantification to the highest level used (µg/L except where indicated). Bolding designates the use of a different standard for semi-quantification compared to the published method. [d] Bolding indicates the use of a different internal standard compared to the published method. d_{15}-Ethyl octanoate (*m*/*z* 91 as quantifier, *m*/*z* 105 and 142 as qualifiers), d_{11}-hexanoic acid (*m*/*z* 63 as quantifier, *m*/*z* 77 and 93 as qualifiers), and d_{15}-octanoic acid (*m*/*z* 63 as quantifier, *m*/*z* 125 and 109 as qualifiers) were also incorporated as new internal standards added to samples at 1.0, 10.0, and 20.0 µg/L, respectively. [e] ODT, odour detection threshold determined in hydroalcoholic solution. [f] Odour descriptors were from "Flavornet and human odor space" (http://www.flavornet.org/flavornet.html) by Terry Acree & Heinrich Arn, except for those specified. [g] Typical concentration ranges (µg/L except where indicated) of volatile compounds found in Shiraz wines according to: (1) (Capone et al., 2021); (2) (Hranilovic et al., 2018); (3) (Mayr et al., 2014); (4) (Ugliano et al., 2010); (5) (Antalick et al., 2015); (6) (Longo et al., 2018); (7) (Li et al., 2017); (8) (Kustos et al., 2020); (9) (Albanese et al., 2013); (10) (Wang et al., 2016), rose wines made of either Shiraz or blends including Shiraz; (11) (Chou et al., 2018). n.r., not reported, concentration range not found in literature.

Table A.1. contd.

Compound[a]	Ions[b]	Calibration range (µg/L)[c]	R^2	Internal standard[d]	ODT (µg/L)[e]	Odour descriptors[f]	Typical range (refs)[g]
Acetates							
Ethyl acetate	**61**, 88	8.6–120 mg/L	0.9981	d_4-3-Methyl-1-butanol	15000 (Moyano et al., 2002)	Pineapple, varnish, balsamic (Moyano et al., 2002)	43.0–164 mg/L (3, 4, 7, 8, 9)
3-Methylbutyl acetate	**70**, 55, 87	704–11585	0.9962	d_4-3-Methyl-1-butanol	30 (Guth, 1997)	Banana	465– 3880 (3, 4, 5, 6, 8, 9)
Hexyl acetate	**43**, 56, 69	16.6–276	0.9988	d_3-Hexyl acetate	670 (Peinado et al., 2004)	Fruity, floral (Peinado et al., 2004)	5–160 (3, 4, 5, 6, 8, 9)
2-Phenylethyl acetate	**104**, 65, 91	107–2100	0.9971	d_5-phenylethanol	250 (Guth, 1997)	Floral, rose, fruity (Swiegers et al., 2005)	5–360 (3, 6, 8, 9)
Higher alcohols							
1-Propanol	**31**, 42, 59	15.7–150 mg/L	0.9943	d_{13}-1-Hexanol	50000 (Song et al., 2016)	Alcohol (Meilgaard, 1975)	29.3–35.8 mg/L (9)
2-Methylpropanol	**31**, 55, 74	2.7–45.0 mg/L	0.9965	**d_4-3-Methyl-1-butanol**	40000 (Ferreira et al., 2000)	Wine, solvent, bitter banana	26.8–69.4 mg/L (3, 8, 9)
1-Butanol	**56**, 41, 31	0.1–1.2 mg/L	0.9955	**d_4-3-Methyl-1-butanol**	160 (Moyano et al., 2002)	Fruit, medicinal, wine	1.3–2.6 mg/L (3, 8)
4-Methyl-2-pentanol	**45**, 43, 41	12.1–120	0.9962	**d_4-3-Methyl-1-butanol**	Unknown	Unknown	n.r.
3-Methyl-1-butanol	**55**, 42, 70	11.9–150 mg/L	0.9969	d_4-3-Methyl-1-butanol	30000 (Guth, 1997)	Harsh, nail polish, fusel (Ferreira et al., 2009)	0.005–310 mg/L (3, 4, 6, 7, 8)
4-Methyl-1-pentanol	**41**, 56, 69	**equivalent to 4-methyl-2-pentanol**		**d_4-3-Methyl-1-butanol**	50000 (Zea et al., 2012)	Almond, toasted (Zea et al., 2012)	8–11 (3)
2-Heptanol	**55**, 41, 45	**equivalent to 3-octanol**		**d_4-3-Methyl-1-butanol**	70 (Du et al., 2010)	Coconut (Meilgaard, 1975)	n.r.
3-Methyl-1-pentanol	**69**, 56, 55	**equivalent to 4-methyl-2-pentanol**		**d_{13}-1-Hexanol**	50000 (Zea et al., 2012)	Vinous, herbaceous, cocoa (Zea et al., 2012)	n.r.
3-Octanol	**83**, 59, 101	12.8–120	0.9957	**d_{13}-1-Hexanol**	18–250 (Burdock, 2010)	Earthy, mushroom, rose, leather (Burdock, 2010; Mayr et al., 2014)	n.r.
1-Heptanol	**41**, 56, 71	**equivalent to 3-octanol**		**d_{13}-1-Hexanol**	2500 (Gómez García-Carpintero et al., 2014)	Oily (Gómez García-Carpintero et al., 2014)	n.r.
2-Methyl-6-hepten-1-ol	**69**, 110, 95	**equivalent to 3-octanol**		**d_{13}-1-Hexanol**	Unknown	Unknown	n.r.
2-Ethyl-1-hexanol	**57**, 70, 98	1.4–15.0	0.9966	d_{13}-1-Hexanol	270 (Pino & Queris, 2011)	Green, flowery, green cucumber (Komes et al., 2006)	25–59 (10)
1-Octanol	**56**, 70, 84	12.4–120	0.9960	d_{13}-1-Hexanol	0.8 (Etiévant, 1991)	Chemical, metal, burnt	9–34 (10)
1-Nonanol	**70**, 55, 41	**equivalent to 1-octanol**		d_{13}-1-Hexanol	80 (Meilgaard, 1975)	Coconut, walnut oily (Meilgaard, 1975)	n.r.
Methionol	**106**, 61, 73	**equivalent to α-terpineol**		**d_{13}-1-Hexanol**	1000 (Ferreira et al., 2000)	Cooked potato, cut hay (Zea et al., 2012)	2994–3130 (4)
1-Decanol	**55**, 83, 112	equivalent to 1-octanol		d_{13}-1-Hexanol	500 (Moyano et al., 2002)	Fat	n.r.
Benzyl alcohol	**108**, 107, 79	79.0–1200	0.9984	**d_5-Phenylethanol**	900000 (Zea et al., 2012)	Almonds, bitter (Meilgaard, 1975)	n.r.
2-Phenylethanol	**91**, 65, 122	0.9–17.5 mg/L	0.9991	d_5-Phenylethanol	14000 (Ferreira et al., 2000)	Floral, rose (Mayr et al., 2014)	0.006–404 mg/L (3, 4, 6, 8, 9)

[a] Quantification of compounds refers to the published method (Wang et al., 2016), with bolded compound names highlighting those that were newly added to the method. [b] Bolded ions were used as quantifiers and other ions were used as qualifiers. [c] Calibration range from limit of quantification to the highest level used (µg/L except where indicated). Bolding designates the use of a different standard for semi-quantification compared to the published method. [d] Bolding indicates the use of a different internal standard compared to the published method. d_{15}-Ethyl octanoate (*m/z* 91 as quantifier, *m/z* 105 and 142 as qualifiers), d_{11}-hexanoic acid (*m/z* 63 as quantifier, *m/z* 77 and 93 as qualifiers), and d_{15}-octanoic acid (*m/z* 63 as quantifier, *m/z* 125 and 109 as qualifiers) were also incorporated as new internal standards added to samples at 1.0, 10.0, and 20.0 µg/L, respectively. [e] ODT, odour detection threshold determined in hydroalcoholic solution. [f] Odour descriptors were from "Flavornet and human odor space" (http://www.flavornet.org/flavornet.html) by Terry Acree & Heinrich Arn, except for those specified. [g] Typical concentration ranges (µg/L except where indicated) of volatile compounds found in Shiraz wines according to: (1) (Capone et al., 2021); (2) (Hranilovic et al., 2018); (3) (Mayr et al., 2014); (4) (Ugliano et al., 2010); (5) (Antalick et al., 2015); (6) (Longo et al., 2018); (7) (Li et al., 2017); (8) (Kustos et al., 2020); (9) (Albanese et al., 2013); (10) (Wang et al., 2016), rose wines made of either Shiraz or blends including Shiraz; (11) (Chou et al., 2018). n.r., not reported, concentration range not found in literature.

Table A.1. contd.

Compound[a]	Ions[b]	Calibration range (µg/L)[c]	R^2	Internal standard[d]	ODT (µg/L)[e]	Odour descriptors[f]	Typical range (refs)[g]
Fatty acids							
Acetic acid	**43**, 45, 60	17.2–120 mg/L	0.9956	d_{19}-Decanoic acid	200000 (Guth, 1997)	Sour, vinegar (Mayr et al., 2014)	393–680 mg/L (3, 8)
2-Methylpropanoic acid	**73**, 88, 43	399–2413	0.9917	**d_{13}-1-Hexanol**	2300 (Gabrielli et al., 2017)	Rancid-butter-cheese (Gabrielli et al., 2017)	929–1634 (3)
Butanoic acid	**60**, 73, 42	550–5654	0.9968	**d_{13}-1-Hexanol**	10000 (Guth, 1997)	Buttery, cheesy, sweaty (Meilgaard, 1975)	174–433 (3)
3-Methylbutanoic acid	**60**, 43, 87	67.8–575	0.9952	**d_{13}-1-Hexanol**	33.4 (Ferreira et al., 2000)	Blue cheese	432–2797 (3, 4)
Hexanoic acid	**60**, 73, 87	884–10298	0.9973	**d_{11}-Hexanoic acid**	420 (Ferreira et al., 2000)	Cheese (Zea et al., 2012)	418–3280 (3, 4, 7, 8, 9)
Octanoic acid	**60**, 73, 101	1925–26713	0.9968	**d_{15}-Octanoic acid**	500 (Ferreira et al., 2000)	Butter, almond (Mayr et al., 2014)	253–3110 (4, 9)
Nonanoic acid	**60**, 73, 115	**equivalent to hexanoic acid**		**d_5-Phenylethanol**	3000 (Burdock, 2010)	Green, fat	119–893 (10)
Decanoic acid	**129**, 60, 172	311–4837	0.9969	d_{19}-Decanoic acid	1000 (Ferreira et al., 2000)	Rancid, fat	224–2690 (3, 7, 8, 9)
Isoprenoids							
Vitispirane 1	**93**, 121, 192	**equivalent to β-damascenone**		**d_{13}-1-Hexanol**	800 (Boscaino et al., 2019)	Woody, spicy (Boscaino et al., 2019)	0.32 (11)
Vitispirane 2	**93**, 121, 192	**equivalent to β-damascenone**		**d_{13}-1-Hexanol**	800 (Boscaino et al., 2019)	Woody, spicy (Boscaino et al., 2019)	0.28–0.32 (11)
Terpinen-4-ol	**71**, 43, 93	**equivalent to α-terpineol**		**d_{13}-1-Hexanol**	5000 (Franco et al., 2004)	Fir needle-like, peppermint (Schoenauer & Schieberle, 2016)	0.1 (6)
α-Terpineol	**59**, 93, 136	8.5–180	0.9989	d_{13}-1-Hexanol	250 (Ferreira et al., 2000)	Wine, fruity	< 0.7–9 (3, 6, 8)
β-Citronellol	**69**, 95, 123	equivalent to 3-octanol		d_{13}-1-Hexanol	100 (Guth, 1997)	Citrus	2–23 (6, 9)
β-Damascenone	**69**, 121, 190	2.5–128	0.9991	**d_5-Phenylethanol**	0.05 (Guth, 1997)	Rose, apple, honey	1.2–16 (3, 6, 8, 9)
Nerol	**69**, 93, 41	**equivalent to 3-octanol**		**d_{13}-1-Hexanol**	500 (Meilgaard, 1975)	Lime, flowery (Meilgaard, 1975)	n.r.
β-Ionone	**175**, 91, 43	**equivalent to β-damascenone**		**d_5-Phenylethanol**	0.09 (Ferreira et al., 2000)	Phenolic, pleasant (López et al., 1999)	0.1 (6)
Other							
Nonanal	**70**, 41, 82	9.9–150	0.9983	**d_{13}-1-Hexanol**	2.5 (Clarke & Bakker, 2004)	Astringent, bitter, aldehyde (Meilgaard, 1975)	13–44 (10)

[a] Quantification of compounds refers to the published method (Wang et al., 2016), with bolded compound names highlighting those that were newly added to the method. [b] Bolded ions were used as quantifiers and other ions were used as qualifiers. [c] Calibration range from limit of quantification to the highest level used (µg/L except where indicated). Bolding designates the use of a different standard for semi-quantification compared to the published method. [d] Bolding indicates the use of a different internal standard compared to the published method. d_{15}-Ethyl octanoate (*m/z* 91 as quantifier, *m/z* 105 and 142 as qualifiers), d_{11}-hexanoic acid (*m/z* 63 as quantifier, *m/z* 77 and 93 as qualifiers), and d_{15}-octanoic acid (*m/z* 63 as quantifier, *m/z* 125 and 109 as qualifiers) were also incorporated as new internal standards added to samples at 1.0, 10.0, and 20.0 µg/L, respectively. [e] ODT, odour detection threshold determined in hydroalcoholic solution. [f] Odour descriptors were from "Flavornet and human odor space" (http://www.flavornet.org/flavornet.html) by Terry Acree & Heinrich Arn, except for those specified. [g] Typical concentration ranges (µg/L except where indicated) of volatile compounds found in Shiraz wines according to: (1) (Capone et al., 2021); (2) (Hranilovic et al., 2018); (3) (Mayr et al., 2014); (4) (Ugliano et al., 2010); (5) (Antalick et al., 2015); (6) (Longo et al., 2018); (7) (Li et al., 2017); (8) (Kustos et al., 2020); (9) (Albanese et al., 2013); (10) (Wang et al., 2016), rose wines made of either Shiraz or blends including Shiraz; (11) (Chou et al., 2018). n.r., not reported, concentration range not found in literature.

Table A.2. Mean concentration with standard deviation of volatile compounds in Shiraz wines that underwent different treatments.

	Concentration (µg/L)[a]												Two-way ANOVA[b]		
Compound	ACE_Short	OAV[c]	ACE_Long	OAV	ACE_Long_Dil	OAV	NOACE_Short	OAV	NOACE_Long	OAV	NOACE_Long_Dil	OAV	Crushing method[d]	Skin contact time[e]	Interaction[f]
Ethyl esters															
Ethyl propanoate	253±14	0.1	200±1	0.1	199±8	0.1	264±14	0.1	258±5	0.1	258±31	0.1	<0.001	0.008	**0.03** (a, b, b, a, a, a)
Ethyl 2-methylpropanoate	266±3	0.0	263±2	0.0	259±6	0.0	286±3	0.1	276±5	0.0	273±8	0.0	**<0.001** (b, a)	**0.012** (a, ab, b)	n.s.
Ethyl butanoate	213±36	0.4	163±21	0.3	163±13	0.3	226±10	0.4	227±16	0.4	245±4	0.4	<0.001	n.s.	**0.027** (ab, b, b, a, a, a)
Ethyl 2-methylbutanoate	9.8±0.5	10	8.8±0.3	9	7.9±0.9	8	12.1±0.1	12	11.3±0.9	11	10.8±1.8	11	**<0.001** (b, a)	**0.030** (a, ab, b)	n.s.
Ethyl 3-methylbutanoate	14.4±0.2	5	13.7±0.4	5	12.3±1.6	4	18.3±0.5	6	18.3±1.4	6	17.4±3.3	6	**<0.001** (b, a)	n.s.	n.s.
Ethyl hexanoate	576±164	41	558±21	40	543±46	39	670±1	48	718±13	51	766±53	55	**0.001** (b, a)	n.s.	n.s.
Ethyl lactate (mg/L)	168±30	1.1	124±6	0.8	123±1	0.8	132±2	0.9	117±8	0.8	122±1	0.8	**0.033** (a, b)	**0.003** (a, b, b)	n.s.
Ethyl octanoate	284±41	14	210±16	11	192±58	10	314±14	16	299±25	15	337±16	17	<0.001	n.s.	**0.032** (ab, bc, c, a, a, a)
Ethyl nonanoate	6995±2578	8	5460±778	6	5466±796	6	5160±165	6	6710±154	8	5795±637	7	n.s.	n.s.	n.s.
Ethyl decanoate	142±10	0.7	125±1	0.6	122±5	0.6	142±2	0.7	130±1	0.6	132±0	0.7	**0.048** (b, a)	**<0.001** (a, b, b)	n.s.
Diethyl succinate	1462±199	0.0	986±68	0.0	1009±126	0.0	842±74	0.0	1477±340	0.0	1551±454	0.0	n.s.	n.s.	**0.003** (ab, ab, ab, b, ab, a)
Acetates															
Ethyl acetate (mg/L)	53.5±18.5	4	54.2±2.0	4	53.3±0.9	4	67.6±1.5	5	65.3±0.8	4	67.3±2.5	5	**0.004** (b, a)	n.s.	n.s.
3-Methylbutyl acetate	2639±237	88	2422±69	81	2238±516	75	2726±61	91	2992±37	100	3330±59	111	<0.001	n.s.	**0.011** (bc, bc, c, abc, ab, a)
Hexyl acetate	48.5±2.2	0.1	44.7±0.4	0.1	40.2±7.9	0.1	41.4±1.6	0.1	53.1±2.4	0.1	56.7±9.9	0.1	0.0	n.s.	**0.008** (ab, ab, b, b, ab, a)
2-Phenylethyl acetate	296±56	1.2	266±8	1.1	249±26	1.0	264±5	1.1	269±10	1.1	283±5	1.1	n.s.	n.s.	n.s.
Higher alcohols															
1-Propanol (mg/L)	63.7±0.6	1.3	62.0±0.2	1.2	59.8±1.4	1.2	61.3±0.2	1.2	63.9±1.7	1.3	62.1±1.6	1.2	n.s.	0.030	**0.007** (a, ab, b, ab, a, ab)
2-Methylpropanol (mg/L)	52.6±3.7	1.3	48.2±1.3	1.2	47.3±0.6	1.2	51.0±2.1	1.3	47.9±2.5	1.2	50.1±2.3	1.3	n.s.	**0.032** (a, b, ab)	n.s.
1-Butanol (mg/L)	1.1±0.1	7	1.0±0.1	6	0.9±0.1	6	1.0±0.1	6	1.0±0.1	6	1.1±0.0	7	n.s.	n.s.	**0.031** (a, ab, b, ab, ab, ab)
4-Methyl-2-pentanol	227±69	n.d.	178±11	n.d.	157±6	n.d.	157±12	n.d.	132±3	n.d.	106±20	n.d.	**0.002** (a, b)	**0.014** (a, ab, b)	n.s.
3-Methyl-1-butanol (mg/L)	346±32	12	315±6	11	309±6	10	301±1	10	310±10	10	320±4	11	n.s.	n.s.	**0.012** (a, ab, ab, b, ab, ab)
3-Octanol	14.4±0.3	n.d.	14.2±0.1	n.d.	14±0.1	n.d.	14±0.1	n.d.	14±0.1	n.d.	14.2±0.1	n.d.	n.s.	n.s.	**0.010** (a, ab, ab, ab, b, ab)
2-Ethyl-1-hexanol	9±0.9	0.0	6.6±0.6	0.0	6.1±0.2	0.0	6.4±0.3	0.0	6.3±0.5	0.0	7.3±0.4	0.0	0.037	0.005	**<0.001** (a, b, b, b, b, b)
1-Octanol	20.7±4.9	26	21.6±0.5	27	19.8±3.2	25	19±1	24	21±1.2	26	23.7±0.4	30	n.s.	n.s.	n.s.
Benzyl alcohol	238±13	0.0	224±10	0.0	220±28	0.0	204±1	0.0	212±9	0.0	241±4	0.0	n.s.	n.s.	n.s.
2-Phenylethanol (mg/L)	67.3±6.3	5	59.2±1.1	4	53.0±9.1	4	55.6±1.2	4	58.6±1.7	4	60.7±1.1	4	n.s.	n.s.	**0.011** (a, ab, b, ab, ab, ab)

[a] Data are present in mean ± SD (n = 3). Concentrations are expressed as µg/L except where indicated. [b] OAV: Odour activity value = compound concentration/odour detection threshold; n.d. represents OAV not determined due to the lack of odour detection threshold value. [c] *p*-values of two-way ANOVA followed by Tukey's HSD multiple comparison (α = 0.05) evaluating the effect of crushing method and skin contact time. Bolded *p*-values are the main or interaction effect to be considered. [d] Different letters in brackets following bolded *p*-values indicate significant differences caused by main effect of crushing method of ACE and NOACE treatments. [e] Different letters in brackets following bolded *p*-values indicate significant differences caused by main effect of skin contact time of Short, Long, and Long_Dil treatments. [f] Different letters in brackets following bolded *p*-values indicate significant differences caused by interaction effect between crushing method and skin contact time. The order of letters corresponds to that of the wines in the table (from left to right).

Table A.2. contd.

Compound	Concentration (µg/L)[a]												Two-way ANOVA[b]		
	ACE_Short	OAV[c]	ACE_Long	OAV	ACE_Long_Dil	OAV	NOACE_Short	OAV	NOACE_Long	OAV	NOACE_Long_Dil	OAV	Crushing method[d]	Skin contact time[e]	Interaction[f]
Fatty acids															
Acetic acid (mg/L)	648±78	3	537±59	3	434±61	2	488±10	2	493±49	3	475±27	2	n.s.	0.010	**0.019** (a, ab, b, b, b, b)
2-Methylpropanoic acid	2191±58	1.0	1882±62	0.8	1729±139	0.8	1988±36	0.9	1918±137	0.8	1880±117	0.8	n.s.	0.001	**0.028** (a, b, b, ab, ab, b)
Butanoic acid	2062±92	0.2	1842±44	0.2	1755±141	0.2	1819±26	0.2	1830±42	0.2	1835±15	0.2	n.s.	0.014	**0.007** (a, b, b, b, b, b)
3-Methylbutanoic acid	1089±94	33	836±19	25	740±92	22	865±11	26	863±85	26	835±81	25	n.s.	0.002	**0.006** (a, b, b, b, b, b)
Hexanoic acid	3437±275	8	3007±70	7	2743±367	7	2825±118	7	3071±59	7	3132±158	8	n.s.	n.s.	**0.004** (a, ab, b, b, ab, ab)
Octanoic acid	7029±1062	14	4730±351	10	3925±1260	8	5218±231	10	4828±412	10	5093±273	10	n.s.	0.005	**0.012** (a, b, b, ab, b, ab)
Decanoic acid	1149±204	1.1	480±6	0.5	364±77	0.4	737±55	0.7	433±49	0.4	421±19	0.4	0.011	<0.001	**0.003** (a, bc, c, b, c, c)
Isoprenoids															
α-Terpineol	15.1±0.4	0.1	13.4±0.3	0.1	12.6±1.2	0.1	13.1±0.2	0.1	13.6±0.5	0.1	14.5±0.5	0.1	n.s.	n.s.	**0.001** (a, abc, c, bc, abc, ab)
β-Damascenone	2.9±1.2	58	2.6±0	53	2.2±0.5	43	2.8±0.2	57	3±0.1	59	3±0.2	61	n.s.	n.s.	n.s.
Other															
Nonanal	31.1±1.2	12	29.2±3.7	12	28.2±1.6	11	27.8±1.2	11	27.5±1.3	11	26.8±1	11	**0.037** (a, b)	n.s.	n.s.

[a] Data are present in mean ± SD (n = 3). Concentrations are expressed as µg/L except where indicated. [b] OAV: Odour activity value = compound concentration/odour detection threshold; n.d. represents OAV not determined due to the lack of odour detection threshold value. [c] *p*-values of two-way ANOVA followed by Tukey's HSD multiple comparison (α = 0.05) evaluating the effect of crushing method and skin contact time. Bolded *p*-values are the main or interaction effect to be considered. [d] Different letters in brackets following bolded *p*-values indicate significant differences caused by main effect of crushing method of ACE and NOACE treatments. [e] Different letters in brackets following bolded *p*-values indicate significant differences caused by main effect of skin contact time of Short, Long, and Long_Dil treatments. [f] Different letters in brackets following bolded *p*-values indicate significant differences caused by interaction effect between crushing method and skin contact time. The order of letters corresponds to that of the wines in the table (from left to right).

Table A.3. Mean concentration with standard deviation of semi-quantified other volatile compounds in Shiraz wine samples that underwent different treatments.

	Concentration (µg/L)[a]						Two-way ANOVA[b]		
Compound	ACE_Short	ACE_Long	ACE_Long_Dil	NOACE_Short	NOACE_Long	NOACE_Long_Dil	Crushing method[c]	Skin contact time[d]	Interaction[e]
Ethyl esters									
Ethyl 2-butenoate	11.8±1.3	11.4±0.8	11±1.3	11.2±0.6	11.5±0.6	11.7±0.7	n.s.	n.s.	n.s.
Ethyl 3-hexenoate	112±1	112±0	112±0	112±0	113±1	113±1	**0.023** (b, a)	n.s.	n.s.
Ethyl heptanoate	112±1	111±0	111±0	112±0	113±1	113±1	**0.006** (b, a)	n.s.	n.s.
Higher alcohols									
4-Methyl-1-pentanol	50.9±2.8	50.5±2	48.3±4	47.3±0.9	49.1±0.7	50.9±0.4	n.s.	n.s.	n.s.
2-Heptanol	13.6±0.1	13.6±0	13.6±0	13.6±0	13.6±0	13.6±0	n.s.	n.s.	n.s.
3-Methyl-1-pentanol	237±22	213±8	199±20	207±4	219±2	223±4	n.s.	n.s.	**0.009** (a, ab, b, ab, ab, ab)
1-Heptanol	17.7±1	18.7±0.6	17.8±0.2	17.8±0.2	20.4±2	19.3±2.7	n.s.	n.s.	n.s.
2-Methyl-6-hepten-1-ol	15.7±0.2	15.5±0.2	15.2±0.4	15.3±0	15.7±0.1	15.9±0.2	n.s.	n.s.	**0.002** (ab, ab, b, b, ab, a)
1-Nonanol	13.4±1.5	14±0.6	13±1.7	13.8±0.3	14.6±0.1	15.1±0.7	**0.040** (b, a)	n.s.	n.s.
Methionol	14.1±0.4	11.8±0.5	11.1±1.2	12.1±0.5	11.6±0.2	12±0.2	n.s.	0.001	**0.004** (a, b, b, b, b, b)
1-Decanol	12.9±2.3	11.2±0.2	10.9±0.8	12.7±0.5	11.5±0.2	12.2±0.1	n.s.	n.s.	n.s.
Fatty acids									
Nonanoic acid	1778±79	1789±59	1778±41	1816±40	1848±20	1876±29	**0.016** (b, a)	n.s.	n.s.
Isoprenoids									
Vitispirane 1	21.8±2.2	16.8±2.8	13.2±4.2	21.5±1.1	19.4±1.6	19.4±1.1	**0.030** (b, a)	**0.008** (a, ab, b)	n.s.
Vitispirane 2	20.4±1.6	15.4±2.5	12.3±4	19.3±0.9	17.6±1.6	17.7±1	n.s.	**0.007** (a, ab, b)	n.s.
Terpinen-4-ol	8.8±0.1	8.2±0.1	8.2±0.3	8.3±0.1	8.2±0.1	8.2±0.1	n.s.	0.001	**0.008** (a, b, b, b, b, b)
β-Citronellol	18.9±1.4	17.3±0.1	16.9±0.9	16.9±0.3	17.3±0.4	17.7±0.4	n.s.	n.s.	**0.017** (a, ab, ab, b, ab, ab)
Nerol	15.9±0.4	15.5±0.3	15.1±0.5	14.6±0.2	15.0±0	15.5±0.2	0.008	n.s.	**0.003** (a, a, ab, b, ab, a)
β-Ionone	0.2±0	0.1±0	0.1±0.1	0.2±0	0.2±0	0.2±0	**0.001** (b, a)	n.s.	n.s.

[a] Data are present in mean ± SD (n = 3). [b] *p*-values of two-way ANOVA followed by Tukey's HSD multiple comparison (α = 0.05) evaluating the effect of crushing method and skin contact time. Bolded *p*-values are the main or interaction effect to be considered. [c] The two letters in bracket following bolded *p*-values indicate significant difference caused by main effect of crushing method of ACE and NOACE treatments. [d] The three letters in bracket following bolded *p*-values indicate significant difference caused by main effect of ski contact time of Short, Long, and Long_Dil treatments. [e] The six letters in bracket following bolded *p*-values indicate significant difference caused by interaction effect between crushing method and skin contact time. The order of letters corresponds to that of the wines in the table (from left to right).

Table A.4. Mean scores and *p*-values for each aroma attribute of Shiraz wines evaluated by RATA panellists.

Attribute	ACE_Short	ACE_Long	ACE_Long_Dil	NOACE_Short	NOACE_Long	NOACE_Long_Dil	*p*-Value
Dark fruit	3.61	3.67	3.71	3.67	3.69	3.75	0.971
Red fruit	3.22	2.94	2.94	3.04	3.13	3.02	0.490
Dried fruit	1.77	2.03	2.03	2.02	1.91	1.99	0.494
Jammy	2.31	2.24	2.19	2.23	2.13	2.07	0.703
Confectionery	2.04	1.85	2.07	2.02	1.87	1.80	0.313
Chocolate	1.27	1.34	1.34	1.32	1.17	1.45	0.409
Coconut	0.88	0.87	0.86	0.79	0.69	0.95	0.267
Cooked vegetables	0.80	0.85	0.97	0.85	0.85	0.96	0.738
Earthy/dusty	1.22	1.37	1.38	1.37	1.36	1.49	0.596
Eucalypt/mint	1.28	1.30	1.23	1.38	1.28	1.27	0.932
Floral/perfume/musk	2.27 a	1.99 bc	1.73 c	2.06 ab	1.96 bc	1.93 bc	**0.041**
Forest floor/mushrooms	0.83	0.91	1.10	1.02	0.93	1.14	0.164
Green pepper/capsicum	1.02	1.28	1.12	1.19	1.05	1.04	0.392
Herbaceous	1.40	1.46	1.59	1.47	1.44	1.32	0.497
Leather	1.02	1.12	1.06	1.10	1.15	1.14	0.918
Pepper	1.43	1.49	1.55	1.44	1.39	1.44	0.896
Savoury/meaty/gamey	1.19	1.41	1.46	1.39	1.57	1.34	0.159
Spice	2.43	2.49	2.28	2.36	2.14	2.35	0.327
Stemmy/stalky	0.89	0.95	1.08	0.95	0.99	0.96	0.618
Toasty/smoky	1.15	1.30	1.30	1.23	1.15	1.15	0.726
Vanilla	1.54 a	1.41 ab	1.16 c	1.44 ab	1.45 ab	1.23 bc	**0.057**
Woody	1.56	1.55	1.63	1.51	1.66	1.54	0.912

Table A.5. Mean concentrations and standard deviations of volatile compounds in commercial wine samples that underwent different treatments.

	Commercial Sauvignon blanc wines (µg/L)[a]				Commercial Pinot noir wines (µg/L)[b]	
Compound	**SB_CTRL**	**SB_ACE**	**SB_ACE+M**	**SB_M**	**PN_CTRL**	**PN_ACE**
Varietal thiols						
3-SH (ng/L)	17±1	25±2	612±19	37±1	139±2	83±3
3-SHA (ng/L)	7±0	6±1	71±0	10±1	n.d.[c]	n.d.
Ethyl esters						
Ethyl propanoate	84±7.7	182±13	137±5	92.2±6.1	278±90	415±25
Ethyl 2-methylpropanoate	61.1±1.9	41.3±2.3	81.5±5.9	59±0.3	85.2±7.3	79.3±5.2
Ethyl butanoate	541±44	252±20	513±16	378±28	109.8±25.9	173±9
Ethyl 2-methylbutanoate	4.5±0.2	2.1±0.1	6.5±0.3	3.5±0.1	15.5±2.6	15±0.7
Ethyl 3-methylbutanoate	11.2±0.1	6.1±0.3	16.7±1.1	7.1±0	21.2±2	20.3±1.1
Ethyl hexanoate	874±66	683±58	646±24	813±92	266±85	430±22
Ethyl lactate (mg/L)	5.7±0.3	14.1±0.5	12.6±1.0	6.1±0.9	152±6	173±5
Ethyl octanoate	359±3	355±3	353±3	363±3	340±0	342±0
Ethyl decanoate	182±20	163±3	137±2	188±16	111±7	117±0
Diethyl succinate	698±34	143±6	577±51	468±35	9286±421	7635±192
Acetates						
Ethyl acetate (mg/L)	89.9±7.8	78.8±4.5	57.2±2.8	87.0±4.1	67.4±12.9	83.3±3.4
3-Methylbutyl acetate	7890±471	2819±174	6316±47	5424±742	< LOQ[d]	< LOQ
Hexyl acetate	396±19	318±26	267±7	262±18	6.5±0.3	8.5±0.2
2-Phenylethyl acetate	448±7	276±17	353±3	346±13	104±9	113±1
Higher alcohols						
1-Propanol (mg/L)	30.2±1.4	31.8±0.7	31.3±0.8	33.1±0.9	42.9±1.0	54.4±0.4
2-Methylpropanol (mg/L)	16.0±0.0	11.9±0.3	19.0±1.3	14.8±2.5	28.5±1.1	35.6±0.2
1-Butanol	621±0	5366±70	472±10	938±57	864±5	1078±4
3-Methyl-1-butanol (mg/L)	113±4	79.7±1.1	146±6	109±4	295±9	372±2
1-Hexanol	1758±51	1373±39	1734±49	1235±28	1820±46	2503±26
2-Ethyl-1-hexanol	4.6±0.6	4.6±1	5.1±0.7	5±0.9	4.9±0.8	4.8±0.9
1-Octanol	9.5±0.2	6.5±0.2	11.8±0.1	9.1±0.3	21.4±1.8	29.9±0.8
Benzyl alcohol	1980±32	2484±7	2080±3	3478±107	10752±36	12025±107
2-Phenylethanol (mg/L)	11.7±0.2	6.5±0.0	13.0±0.7	10.5±0.6	57.5±0.5	71.6±0.4
Fatty acids						
Acetic acid (mg/L)	151±18	341±4	83±1	276±64	450±18	563±75
2-Methylpropanoic acid	1004±19	670±10	1121±55	1038±93	1890±29	2455±33
Butanoic acid	1687±41	1202±114	1567±13	1382±45	902±41	1233±4
3-Methylbutanoic acid	5759±133	4078±44	6659±5	4446±38	11621±393	14609±132
Hexanoic acid	5909±57	5308±107	5013±5	5560±210	2053±40	2882±51
Octanoic acid (mg/L)	24.2±0.2	21.8±0.2	21.0±0.8	23.5±1.0	9.6±0.2	12.3±0.0
Decanoic acid	2012±61	1743±91	1407±31	1832±92	984±57	1077±13
Isoprenoid						
Linalool	9.8±0.3	7.2±0.3	11.8±0.8	9.9±0.3	16.2±0.6	17.3±0.1

[a] Data are present in mean ± SD (n = 2). Concentrations are expressed as µg/L except where indicated. Commercial Sauvignon blanc wines abbreviated as SB_CTRL, Sauvignon blanc wine produced using juice pressed immediately from traditionally crushed must; SB_ACE, Sauvignon blanc wine produced using juice pressed from ACE treated must; SB_ACE+M, Sauvignon blanc wine produced using juice pressed from ACE treated must after 24 h of cold maceration; SB_M, Sauvignon blanc wine produced using juice pressed from traditionally crushed grape must after 24 h of cold maceration. [b] Commercial Pinot noir wines abbreviated as PN_CTRL, Pinot noir wine produced from traditionally crushed grape must; PN_ACE, Pinot noir wine produced from ACE treated grape must. [c] n.d., compound not detected. [d] < LOQ, concentration of compound below limit of quantification.

References

Albanese, D., Attanasio, G., Cinquanta, L., & Di Matteo, M. (2013). Volatile compounds in red wines processed on an industrial scale by short pre-fermentative cold maceration. *Food and Bioprocess Technology, 6*(11), 3266-3272. https://doi.org/10.1007/s11947-012-0798-5

Antalick, G., Šuklje, K., Blackman, J. W., Meeks, C., Deloire, A., & Schmidtke, L. M. (2015). Influence of grape composition on red wine ester profile: Comparison between Cabernet Sauvignon and Shiraz cultivars from Australian warm climate. *Journal of Agricultural and Food Chemistry, 63*(18), 4664-4672. https://doi.org/10.1021/acs.jafc.5b00966

Benkwitz, F., Tominaga, T., Kilmartin, P. A., Lund, C., Wohlers, M., & Nicolau, L. (2012). Identifying the chemical composition related to the distinct aroma characteristics of New Zealand Sauvignon blanc wines. *American Journal of Enology and Viticulture, 63*(1), 62-72. https://doi.org/10.5344/ajev.2011.10074

Boscaino, F., Ionata, E., La Cara, F., Guerriero, S., Marcolongo, L., & Sorrentino, A. (2019). Impact of *Saccharomyces cerevisiae* and *Metschnikowia fructicola* autochthonous mixed starter on Aglianico wine volatile compounds. *Journal of Food Science and Technology, 56*(11), 4982-4991. https://doi.org/10.1007/s13197-019-03970-9

Burdock, G. A. (2010). *Fenaroli's Handbook of Flavor Ingredients* (6th ed.). CRC Press.

Capone, D. L., Barker, A., Pearson, W., & Francis, I. L. (2021). Influence of inclusion of grapevine leaves, rachis and peduncles during fermentation on the flavour and volatile composition of *Vitis vinifera* cv. Shiraz wine. *Australian Journal of Grape and Wine Research, 27*(3), 348-359. https://doi.org/10.1111/ajgw.12489

Chou, H.-C., Šuklje, K., Antalick, G., Schmidtke, L. M., & Blackman, J. W. (2018). Late-season Shiraz berry dehydration that alters composition and sensory traits of wine. *Journal of Agricultural and Food Chemistry, 66*(29), 7750-7757. https://doi.org/10.1021/acs.jafc.8b01646

Clarke, R. J., & Bakker, J. (2004). Volatile components. In *Wine Flavour Chemistry* (pp. 120-188). Wiley-Blackwell. https://doi.org/10.1002/9781444346022.fmatter

Du, X., Finn, C. E., & Qian, M. C. (2010). Volatile composition and odour-activity value of thornless 'Black Diamond' and 'Marion' blackberries. *Food Chemistry, 119*(3), 1127-1134. https://doi.org/10.1016/j.foodchem.2009.08.024

Etiévant, P. X. (1991). Wine. In H. Maarse (Ed.), *Volatile compounds in foods and beverages* (pp. 483-546). Marcel Dekker.

Ferreira, V., López, R., & Cacho, J. F. (2000). Quantitative determination of the odorants of young red wines from different grape varieties. *Journal of the Science of Food and Agriculture, 80*(11), 1659-1667. https://doi.org/10.1002/1097-0010(20000901)80:11<1659::AID-JSFA693>3.0.CO;2-6

Ferreira, V., San Juan, F., Escudero, A., Cullere, L., Fernandez-Zurbano, P., Saenz-Navajas, M. P., & Cacho, J. (2009). Modeling quality of premium Spanish red wines from gas chromatography-olfactometry data. *Journal of Agricultural and Food Chemistry, 57*(16), 7490-7498. https://doi.org/10.1021/jf9006483

Franco, M., Peinado, R. A., Medina, M., & Moreno, J. (2004). Off-vine grape drying effect on volatile compounds and aromatic series in must from Pedro Ximénez grape variety. *Journal of Agricultural and Food Chemistry, 52*(12), 3905-3910. https://doi.org/10.1021/jf0354949

Gabrielli, M., Aleixandre-Tudo, J. L., Kilmartin, P. A., Sieczkowski, N., & du Toit, W. J. (2017). Additions of glutathione or specific glutathione-rich dry inactivated yeast preparation (DYP) to Sauvignon blanc must: Effect on wine chemical and sensory composition. *South African Journal of Enology and Viticulture, 38*(1), 18-28.

Gómez García-Carpintero, E., Sánchez-Palomo, E., & González Viñas, M. A. (2014). Volatile composition of Bobal red wines subjected to alcoholic/malolactic fermentation with oak chips. *LWT - Food Science and Technology, 55*(2), 586-594. https://doi.org/10.1016/j.lwt.2013.10.024

Guth, H. (1997). Quantitation and sensory studies of character impact odorants of different white wine varieties. *Journal of Agricultural and Food Chemistry, 45*(8), 3027-3032. https://doi.org/10.1021/jf970280a

Hranilovic, A., Li, S., Boss, P. K., Bindon, K., Ristic, R., Grbin, P. R., Van der Westhuizen, T., & Jiranek, V. (2018). Chemical and sensory profiling of Shiraz wines co-fermented with commercial non-*Saccharomyces* inocula. *Australian Journal of Grape and Wine Research, 24*(2), 166-180. https://doi.org/10.1111/ajgw.12320

Komes, D., Ulrich, D., & Lovric, T. (2006). Characterization of odor-active compounds in Croatian Rhine Riesling wine, subregion Zagorje. *European Food Research and Technology, 222*(1), 1-7. https://doi.org/10.1007/s00217-005-0094-y

Kustos, M., Gambetta, J. M., Jeffery, D. W., Heymann, H., Goodman, S., & Bastian, S. E. P. (2020). A matter of place: Sensory and chemical characterisation of fine Australian Chardonnay and Shiraz wines of provenance. *Food Research International, 130*, 108903. https://doi.org/10.1016/j.foodres.2019.108903

Li, S. J., Bindon, K., Bastian, S. E. P., Jiranek, V., & Wilkinson, K. L. (2017). Use of winemaking supplements to modify the composition and sensory properties of Shiraz wine. *Journal of Agricultural and Food Chemistry, 65*(7), 1353-1364. https://doi.org/10.1021/acs.jafc.6b04505

Longo, R., Blackman, J. W., Antalick, G., Torley, P. J., Rogiers, S. Y., & Schmidtke, L. M. (2018). Volatile and sensory profiling of Shiraz wine in response to alcohol management: Comparison of harvest timing versus technological approaches. *Food Research International, 109*, 561-571. https://doi.org/10.1016/j.foodres.2018.04.057

López, R., Ferreira, V., Hernández, P., & Cacho, J. F. (1999). Identification of impact odorants of young red wines made with Merlot, Cabernet Sauvignon and Grenache grape varieties: A comparative study. *Journal of the Science of Food and Agriculture, 79*(11), 1461-1467. https://doi.org/10.1002/(SICI)1097-0010(199908)79:11<1461::AID-JSFA388>3.0.CO;2-K

Mayr, C. M., Geue, J. P., Holt, H. E., Pearson, W. P., Jeffery, D. W., & Francis, I. L. (2014). Characterization of the key aroma compounds in Shiraz wine by quantitation, aroma reconstitution, and omission studies. *Journal of Agricultural and Food Chemistry, 62*(20), 4528-4536. https://doi.org/10.1021/jf405731v

Meilgaard, M. C. (1975). Flavor chemistry of beer: Part II: Flavor and threshold of 239 aroma volatiles. *Master Brewers Association of the Americas Technical Quarterly 12*(3), 151-168.

Moyano, L., Zea, L., Moreno, J., & Medina, M. (2002). Analytical study of aromatic series in sherry wines subjected to biological aging. *Journal of Agricultural and Food Chemistry, 50*(25), 7356-7361. https://doi.org/10.1021/Jf020645d

Peinado, R. A., Moreno, J., Bueno, J. E., Moreno, J. A., & Mauricio, J. C. (2004). Comparative study of aromatic compounds in two young white wines subjected to pre-fermentative cryomaceration. *Food Chemistry, 84*(4), 585-590. https://doi.org/10.1016/S0308-8146(03)00282-6

Pino, J. A., & Queris, O. (2011). Analysis of volatile compounds of mango wine. *Food Chemistry, 125*(4), 1141-1146. https://doi.org/10.1016/j.foodchem.2010.09.056

Schoenauer, S., & Schieberle, P. (2016). Structure–odor activity studies on monoterpenoid mercaptans synthesized by changing the structural motifs of the key food odorant 1-*p*-menthene-8-thiol. *Journal of Agricultural and Food Chemistry, 64*(19), 3849-3861. https://doi.org/10.1021/acs.jafc.6b01645

Song, C.-Z., Liu, M.-Y., Meng, J.-F., Shi, P.-B., Zhang, Z.-W., & Xi, Z.-M. (2016). Influence of foliage-sprayed zinc sulfate on grape quality and wine aroma characteristics of Merlot. *European Food Research and Technology, 242*(4), 609-623. https://doi.org/10.1007/s00217-015-2570-3

Swiegers, J. H., Bartowsky, E. J., Henschke, P. A., & Pretorius, I. S. (2005). Yeast and bacterial modulation of wine aroma and flavour. *Australian Journal of Grape and Wine Research, 11*(2), 139-173. https://doi.org/10.1111/j.1755-0238.2005.tb00285.x

Ugliano, M., Travis, B., Francis, I. L., & Henschke, P. A. (2010). Volatile composition and sensory properties of Shiraz wines as affected by nitrogen supplementation and yeast species: Rationalizing nitrogen modulation of wine aroma. *Journal of Agricultural and Food Chemistry, 58*(23), 12417-12425. https://doi.org/10.1021/jf1027137

Wang, J., Capone, D. L., Wilkinson, K. L., & Jeffery, D. W. (2016). Chemical and sensory profiles of rosé wines from Australia. *Food Chemistry, 196*, 682-693. https://doi.org/10.1016/j.foodchem.2015.09.111

Waterhouse, A. L., Sacks, G. L., & Jeffery, D. W. (2016). Higher alcohols. In *Understanding Wine Chemistry* (pp. 51-56). John Wiley & Sons. https://doi.org/10.1002/9781118730720

Zea, L., Ruiz, M. J., & Moyano, L. (2012). Using odorant series as an analytical tool for the study of the biological ageing of sherry wines. In B. Salih & Ö. Çelikbıçak (Eds.), *Gas chromatography in plant science, wine technology, toxicology and some specific applications* (pp. 91-108). IntechOpen.

CHAPTER 7

Impact of Accentuated Cut Edges, Yeast Strain, and Malolactic Fermentation on Chemical and Sensory Profiles of Sauvignon blanc Wine

Xingchen Wang,[a] Dimitra L. Capone,[a,b] Aurélie Roland,[c] David W. Jeffery[a,b,*]

[a] Department of Wine Science and Waite Research Institute, The University of Adelaide (UA), PMB 1, Glen Osmond, SA 5064, Australia

[b] Australian Research Council Training Centre for Innovative Wine Production, UA, PMB 1, Glen Osmond, SA 5064, Australia

[c] SPO, Univ Montpellier, INRAE, Institut Agro, Montpellier, France

Food Chemistry, **2023**, 400, 134051

DOI: 10.1016/j.foodchem.2022.134051

Statement of Authorship

Title of Paper	Impact of accentuated cut edges, yeast strain, and malolactic fermentation on chemical and sensory profiles of Sauvignon blanc wine
Publication Status	☑ Published ☐ Accepted for Publication ☐ Submitted for Publication ☐ Unpublished and Unsubmitted work written in manuscript style
Publication Details	Wang, X., Capone, D.L., Roland, A., Jeffery, D.W. (2023) Impact of accentuated cut edges, yeast strain, and malolactic fermentation on chemical and sensory profiles of Sauvignon blanc wine. Food Chemistry, 400, 134051.

Principal Author

Name of Principal Author (Candidate)	Xingchen Wang		
Contribution to the Paper	Contributed to the design of experiments. Conducted experiments and prepared and analysed samples using GC-MS, HPLC-MS/MS, and RATA sensory methodology. Collected, processed, analysed, interpreted and visualised the data. Produced a complete first draft of the manuscript. Reviewed and edited the manuscript.		
Overall percentage (%)	70 %		
Certification:	This paper reports on original research I conducted during the period of my Higher Degree by Research candidature and is not subject to any obligations or contractual agreements with a third party that would constrain its inclusion in this thesis. I am the primary author of this paper.		
Signature		Date	21/07/2022

Co-Author Contributions

By signing the Statement of Authorship, each author certifies that:

i. the candidate's stated contribution to the publication is accurate (as detailed above);
ii. permission is granted for the candidate in include the publication in the thesis; and
iii. the sum of all co-author contributions is equal to 100% less the candidate's stated contribution.

Name of Co-Author	Dimitra L. Capone		
Contribution to the Paper	Conceived and designed the experiments, supervised the work, and interpreted data. Reviewed and edited the manuscript.		
Signature		Date	10/08/2022

Name of Co-Author	Aurélie Roland		
Contribution to the Paper	Contributed to the design of experiments, interpreted data, and supervised the work. Reviewed and edited the manuscript.		
Signature		Date	10/08/2022

Name of Co-Author	David W. Jeffery		
Contribution to the Paper	Conceived of and designed the experiments, interpreted data, supervised the project, and provided resources. Reviewed and edited the manuscript and acted as the corresponding author.		
Signature		Date	8/08/2022

Please cut and paste additional co-author panels here as required.

Food Chemistry 400 (2023) 134051

Contents lists available at ScienceDirect

Food Chemistry

journal homepage: www.elsevier.com/locate/foodchem

Impact of accentuated cut edges, yeast strain, and malolactic fermentation on chemical and sensory profiles of Sauvignon blanc wine

Xingchen Wang [a], Dimitra L. Capone [a,b], Aurélie Roland [c], David W. Jeffery [a,b,*]

[a] Department of Wine Science and Waite Research Institute, The University of Adelaide (UA), PMB 1, Glen Osmond, SA 5064, Australia
[b] Australian Research Council Training Centre for Innovative Wine Production, UA, PMB 1, Glen Osmond, SA 5064, Australia
[c] SPO, Univ Montpellier, INRAE, Institut Agro, Montpellier, France

ARTICLE INFO

Keywords:
Varietal thiol
Thiol precursors
Chiral analysis
Enantiomers
Stable isotope dilution assay
Rate-all-that-apply

ABSTRACT

This pioneering investigation involved the application of accentuated cut edges (ACE) technique to Sauvignon blanc winemaking. The concentration of varietal thiol precursors in juice was significantly higher for ACE treatment compared to conventional crushing, with two-way or three-way interactions of the experimental factors, which included yeast strain and malolactic fermentation, being determined from the wine data. ACE yielded higher concentrations of 4-methyl-4-sulfanylpentan-2-one (4-MSP) and enantiomers of 3-sulfanylhexanol (3-SH) and 3-sulfanylhexyl acetate (3-SHA) in wines that were more abundant in phenolic compounds. Compared to Sauvy yeast strain, VIN13 produced greater amounts of 3-SH and 3-SHA but less 4-MSP with wines exhibiting lower intensity 'floral' and 'fruity' notes. MLF increased 3-SH and 4-MSP concentrations and led to wines that exhibited more non-fruity sensory attributes. The study revealed the potential of ACE for increasing varietal thiol concentrations in Sauvignon blanc wine and altering overall sensory profiles, with interactions involving yeast strain and MLF.

1. Introduction

Sauvignon blanc wine is characterised by distinctive aroma attributes such as 'tropical fruit', 'grapefruit', 'passionfruit', and 'blackcurrant' that are substantially contributed by potent varietal thiols, including 3-sulfanylhexan-1-ol (3-SH), 3-sufanylhexyl acetate (3-SHA), 4-methyl-4-sulfanylpentan-2-one (4-MSP) (Bonnaffoux et al., 2021). 3-SH and 3-SHA are chiral compounds, so are present as (3*S*)- and (3*R*)-enantiomers (Table 1), usually in enantiomeric ratios of approximately 50:50 for 3-SH and 70:30 for 3-SHA (Chen, Capone, & Jeffery, 2018). These ratios in Sauvignon blanc wine can be impacted by factors including grapevine clone, yeast strain, and nutrient or enzyme addition prior to fermentation (Chen, Capone, Tondini, et al., 2018). Given the differences in odour detection threshold (ODT) and aroma descriptors of varietal thiol enantiomers (Table 1) (Tominaga et al., 2006), changes in concentration or enantiomer ratio could substantially modify wine aroma characteristics (King et al., 2011).

The previous work has undoubtedly provided considerable knowledge regarding the enhancement of varietal thiol production, for example, pre-fermentation freezing treatment of grape berry/juice (Chen et al., 2019), and preservation in relation to oxidation and other reactions (Nikolantonaki & Waterhouse, 2012), but there is a need for further consideration in terms of the impact on the enantiomers of 3-SH and 3-SHA. This is especially so from the perspective of biogenesis, where precursors to 3-SH are present as non-volatile diastereomers that are mainly located in grape skins and released enzymatically during

Abbreviations: 3-SH, 3-sulfanylhexan-1-ol; 3-SHA, 3-sufanylhexyl acetate; 4-MSP, 4-methyl-4-sulfanylpentan-2-one; ACE, accentuated cut edges; ANOVA, analysis of variance; A-TEEM, absorbance-transmission and fluorescence excitation-emission matrix; CAE, caffeic acid equivalents; *cis*-2-MPO, *cis*-2-methyl-4-propyl-1,3-oxathianes; Cys-3-SH, 3-*S*-cysteinylhexan-1-ol; CysGly-3-SH, 3-*S*-cysteinylglycinehexan-1-ol; DTDP, 4,4′-dithiodipyridine; EDTA 2Na, ethylenediaminetetraacetic acid disodium salt; ESI, electrospray ionisation; GC–MS, gas chromatography-mass spectrometry; GLSW, generalised least squares weighting; GluCys-3-SH, L-cysteinylglycinehexan-1-ol; GSH-3-SH, 3-*S*-glutathionylhexan-1-ol; HPLC, high-performance liquid chromatography; MS/MS, tandem mass spectrometry; NaCl, sodium chloride; OAV, odour activity value; ODT, odour detection thresholds; PCA, principal component analysis; PLS, partial least-squares; PMS, potassium metabisulfite; RATA, rate-all-that-apply; SD, standard deviation; SIDA, stable isotope dilution assay; SPME, solid-phase microextraction; TA, titratable acidity; TSS, total soluble solids.

* Corresponding author at: Department of Wine Science and Waite Research Institute, The University of Adelaide (UA), PMB 1, Glen Osmond, SA 5064, Australia.
E-mail address: david.jeffery@adelaide.edu.au (D.W. Jeffery).

https://doi.org/10.1016/j.foodchem.2022.134051
Received 5 May 2022; Received in revised form 16 August 2022; Accepted 26 August 2022
Available online 30 August 2022

fermentation, with the formation and degradation pathway of 3-SH precursors and fate of 3-SH as proposed in Fig. A.1 (Appendix A). Such precursors include L-glutathione conjugates (i.e., 3-*S*-glutathionylhexan-1-ol, GSH-3-SH), L-cysteine conjugates (i.e., 3-*S*-cysteinylhexan-1-ol, Cys-3-SH), and dipeptide intermediates (i.e., 3-*S*-cysteinylglycinehexan-1-ol, CysGly-3-SH; 3-*S*-glutamylcysteinehexan-1-ol, GluCys-3-SH) (Bonnaffoux et al., 2021).

Although poor correlations generally exist between the concentrations of *known* precursors in juice and corresponding varietal thiols in resulting wines, practices that enhance the extraction of thiol precursors from grape skins into grape must or juice prior to fermentation still provide opportunities for increasing the production of varietal thiols during winemaking (Chen, Capone, Tondini, et al., 2018). As a recent example, Sauvignon blanc juice obtained from pre-fermentation freezing of grape berries showed significantly higher amounts of GSH-3-SH and Cys-3-SH than the juice from fresh berries, with wines from frozen berry treatment having significantly higher concentrations of 3-SH, 3-SHA, and 4-MSP than the wines produced from fresh grapes (Chen et al., 2019). Considering further research avenues, a novel maceration technique known as "accentuated cut edges" (ACE) drew attention. Designed to break down grape skin into smaller pieces while maintaining the integrity of grape seeds so as to accelerate the extraction of phenolics from grape skin through an increase in broken edges (Sparrow et al., 2016), ACE is employed sequentially after a conventional crusher. It has been shown to improve extraction of phenolic constituents from grape skin (Sparrow et al., 2016) and thus could proposedly also augment the extraction of aroma precursors from skin, leading to enhancement of varietal thiol concentrations in wine, for example. The only study reported to date involved Shiraz grape must, with the influence of ACE on concentrations of varietal thiol precursors found to be limited. The potential application of ACE in the production of other varietal wines was indicated, however, with preliminary results showing an increase in varietal thiols in Sauvignon blanc wine produced at commercial scale (Wang et al., 2022).

Other than practices aimed at enhancing the extraction of precursors in grape must or juice, microbes involved in alcoholic fermentation and malolactic fermentation (MLF), such as *Saccharomyces cerevisiae* yeasts and lactic acid bacteria (LAB), can play key roles in producing varietal thiols as a result of uptake and metabolism of their precursors (Cordente et al., 2015; Suklje & Čuš, 2021; Takase et al., 2018). Different yeast strains can yield diverse concentrations of varietal thiols due to various enzymes (Fig. A.1 of Appendix A) regulated by the expression of relevant genes, for instance *BNA3*, *CYS3*, *GLO1*, and *IRC7* (Howell et al., 2005). On the other hand, winemaking bacteria such as LAB used for MLF require further study to obtain more insight into their effect on varietal thiol release and the potential modification of wine aroma characteristics. Furthermore, while the foregoing studies have provided important contributions, they have almost exclusively focused on achiral analysis of 3-SH and 3-SHA (and 4-MSP), with the exception of a single study investigating chirality of precursors and thiols (Chen, Capone, Tondini, et al., 2018). Therefore, the impact of different strains of yeast or bacteria on the concentrations of 3-SH and 3-SHA enantiomers was essentially unknown.

From the viewpoint of wine aroma and flavour chemistry, this study explored the hypothesis that ACE treatment would improve both the release of varietal thiol precursors into Sauvignon blanc juice and the concentration of varietal thiols formed in the wine, in comparison to conventional crushing. The individual use of two yeast strains jointly with malolactic fermentation by LAB was also investigated in a quantitative assessment of their influence on the release of varietal thiols and the ensuing enantiomer profiles. Volatile compounds, including esters, acetates, higher alcohols, fatty acids, and isoprenoids, were also quantified to evaluate the effect of the studied winemaking practices from a broader viewpoint. The perceived effect of the experimental conditions on wine sensory profiles was evaluated by a rate-all-that-apply (RATA) panel and the sensory results were compared with the chemical composition of the wines with respect to varietal thiols, major volatiles, and phenolics.

2. Material and methods

2.1. Chemicals

Food-grade chemicals used for winemaking were from commercial suppliers, and other chemicals and consumables used for analysis were commercially available: ethylenediaminetetraacetic acid disodium salt (EDTA 2Na), formic acid (LC-MS grade), 4,4′-dithiodipyridine (DTDP), potassium hydrogen tartrate, and acetaldehyde (anhydrous, ≥ 99.5 %) were from Sigma-Aldrich (Castle Hill, NSW, Australia); sodium chloride (NaCl), high-performance liquid chromatography (HPLC) gradient-grade methanol, ethanol, and acetonitrile were from Merck (Noble Park, VIC, Australia); Bond Elut C18 cartridges (500 mg, 6 mL) and

Table 1
Structure, odour detection threshold (ODT), aroma descriptor(s), and concentration range of 3-SH and 3-SHA enantiomers, and 4-MSP.

Compound	Structure	ODT[a]	Aroma descriptor	Concentration range[b]
(3*S*)-3-SH	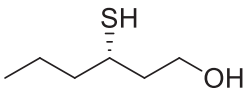	60 (ng/L)[1]	Passionfruit[1]	72–1663 ng/L[1,3]
(3*R*)-3-SH	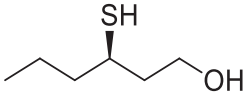	50 (ng/L)[1]	Grapefruit[1]	69–1320 ng/L[1,3]
(3*S*)-3-SHA	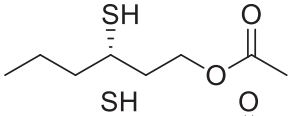	2.5 (ng/L)[1]	Boxwood[1]	1.1–196 ng/L[1,3]
(3*R*)-3-SHA	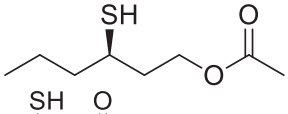	9.0 (ng/L)[1]	Passionfruit[1]	1.2–84 ng/L[1,3]
4-MSP	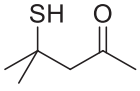	3.0 (ng/L)[2]	Box tree, cat urine[2]	n.d.–200 ng/L[4,5]

[a] Odour detection thresholds of 3-SH and 3-SHA enantiomers were determined in aqueous ethanol solution, and in wine for 4-MSP.
[b] Typical concentration range in dry wines. n.d. not detected. References: [1] (Tominaga et al., 2006); [2] (Darriet et al., 1995); [3] (Chen, Capone, & Jeffery, 2018); [4] (Dagan et al., 2014); [5] (Chen et al., 2019).

Strata SDB-L cartridges (500 mg, 6 mL) were from Agilent (Mulgrave, VIC, Australia) and Phenomenex (Lane Cove, NSW, Australia), respectively. Analytical standards were available from previous studies and included: 3-SH, d_8-3-SH, 3-SHA, d_8-3-SHA, 4-MSP, d_{10}-4-MSP, Cys-3-SH, d_8-Cys-3-SH, GSH-3-SH, and d_9-GSH-3-SH (Chen, Capone, Tondini, et al., 2018); isoprenoids, C_6 alcohols, ethyl esters, acetates, higher alcohols, and fatty acids from commercial suppliers (>97 % purity, except for d_8-(*E*)-2-hexen-1-ol with > 92 % purity) (Wang et al., 2016; Wang et al., 2022). Milli-Q water, obtained from a Milli-Q purification system (Millipore, North Ryde, NSW, Australia), was used for aqueous solutions where applicable and model wine was freshly prepared using 10 % v/v ethanol/water solution that was saturated with potassium hydrogen tartrate and adjusted to pH 3.4 with 1 M tartaric acid solution. DTDP reagent was prepared and stored at − 20 °C as previously detailed (Capone et al., 2015), with an aliquot thawed prior to use.

2.2. Grape samples and winemaking

Sauvignon blanc grapes were mechanically harvested on 30th March 2021 close to Kuitpo at the southern end of Adelaide Hills wine region. Details of winemaking have been provided in Supplementary Experimental Section A.1.1 (Appendix A) with the design of the trial illustrated in Fig. A.2 of Appendix A. Briefly, Sauvignon blanc grapes treated with accentuated cut edges (ACE) or conventional crushing (NoACE) techniques were subsequently inoculated with yeast strain (VIN13 or Sauvy) for alcoholic fermentation. Half of the ferments were inoculated with lactic acid bacteria (*Oenococcus oeni*, Lalvin VP41) after 48 h to induce malolactic fermentation (MLF) whereas the remaining ferments were not inoculated for MLF (NoMLF). In total, this yielded eight treatments (±ACE, 2 × yeast strains, ± MLF, in triplicate): ACE_VIN13_NoMLF, ACE_VIN13_MLF, ACE_Sauvy_NoMLF, ACE_Sauvy_MLF, NoACE_VIN13_NoMLF, NoACE_VIN13_MLF, NoACE_Sauvy_NoMLF, NoACE_Sauvy_MLF.

2.3. Basic chemical parameters

Parameters were measured in duplicate, with pH and TA analysed with a T50 AutoTitrator (Mettler Toledo, Melbourne, Australia), alcohol determined with a DMA 4500 M/Alcolyzer Wine ME (Anton Parr, Graz, Austria), and free and total SO_2 measured with a GlassChem Kombo-4-OH VA/SO_2/OH still (Adelab Scientific, Adelaide, Australia). Glucose, fructose, and organic acids in wines were measured as per a previous study (Wang et al., 2020).

2.4. Varietal thiol precursors in juice and wine by stable isotope dilution assay (SIDA) with HPLC-tandem mass spectrometry (MS/MS)

Juice samples taken periodically from grape must during the cold maceration stage and from wines at bottling were stored at −20 °C prior to the analysis of precursors (Cys-3-SH and GSH-3-SH). Freshly thawed juice or wine samples were centrifuged (3857*g*) at 15 °C for 15 min before extraction following the published method (Capone et al., 2011). Reconstituted extracts were analysed with a Thermo Finnigan Surveyor HPLC coupled to a Thermo Finnigan LCQ Deca XP Plus mass spectrometer operating in positive electrospray ionisation (ESI) mode. Chromatographic conditions and ion pairs for analytes were detailed by Capone et al. (2010) and MS parameters were the same as specified previously (Chen et al., 2019).

2.5. Varietal thiols in wine by SIDA with HPLC-MS/MS

Wine samples were taken at bottling and at the time of sensory analysis 4 months later, and derivatised and extracted according to the procedures of Capone et al. (2015). Reconstituted extracts were analysed for enantiomers of 3-SH and 3-SHA, and for 4-MSP using an Agilent 1200 HPLC coupled with a 6410 triple quadrupole mass spectrometer as reported previously (Chen, Capone, & Jeffery, 2018).

2.6. Other volatiles in wine by SIDA with gas chromatography-mass spectrometry (GC–MS)

cis-2-Methyl-4-propyl-1,3-oxathiane (*cis*-2-MPO) enantiomers were quantitated in wine samples taken at bottling and 4 months later (at the sensory analysis stage) using an Agilent 7890A for gas chromatography (GC) coupled with an Agilent 5975C for mass spectrometry (MS) following the published method (Wang et al., 2021). C_6 alcohols were analysed in samples taken at the time of sensory assessment using the method of Capone et al. (2012) with an Agilent 6890 N GC and an Agilent 5973 N MS. Isoprenoids, ethyl and acetate esters, higher alcohols, and fatty acids were analysed in samples taken at the time of sensory analysis with an Agilent 7890A GC and an Agilent 5975C MS according to a previous method (Wang et al., 2022).

2.7. Absorbance-transmission and fluorescence excitation-emission matrix (A-TEEM) analysis of wine

Samples were taken at bottling and analysed with a Horiba Scientific Aqualog spectrophotometer (version 4.2, Quark Photonics, Adelaide, SA, Australia) following the reported method (Ranaweera et al., 2021). The dilution factor for the wines was 1:50 and triplicate readings were obtained for each winemaking replicate. EEM data were processed and analysed following the procedures detailed previously (Ranaweera et al., 2021), and total phenolics (absorbance units, a.u.; calculated as 280 nm – 4) and hydroxycinnamates (mg/L of caffeic acid equivalents, CAE; calculated as (absorbance at 320 nm – 1.4) ÷ 0.9 × 10 mg/L) were obtained following the published method (Somers & Ziemelis, 1985).

2.8. Sensory profile of wines by RATA

Wines underwent an informal benchtop tasting by five experts prior to formal sensory analysis, in which all replicates from each treatment were deemed to be identical, except for one treatment replicate. Thus, the identical replicates of each respective treatment were blended proportionately for a RATA study conducted according to the established method (Danner et al., 2018). Details of the formal RATA study have been provided in the Supplementary Experimental Section A.1.2 of the Appendix A. Informed consent was obtained from panellists and the sensory study was conducted with the approval of the Human Research Ethics Committee of the University of Adelaide (Approval Number H-2019-135).

2.9. Statistical analysis

Mean and standard deviation (SD) were calculated using Excel (Microsoft 2019). Statistical methods involving analysis of variance (ANOVA), principal component analysis (PCA), and parallel factor analysis (PARAFAC) were variously applied to analyse the different datasets related to the treatments. Full details are provided in the Supplementary Experimental Section A.1.3 of the Appendix A.

3. Results and discussion

A previous study with commercial-scale Sauvignon blanc wine revealed that the joint use of ACE and cold maceration made substantial differences to wine volatile composition, particularly for 3-SH, compared with wines made by conventional crushing with or without cold maceration, or the sole use of ACE (Wang et al., 2022). Inspired by those results, the present study primarily intended to assess the possibility of applying the ACE technique to Sauvignon blanc wine production at experimental scale in association with two commercial yeast strains, with a particular focus on the impact of varietal thiols and their precursors. MLF was conducted on half of the treatments to explore the

potential ability of *O. oeni* for releasing varietal thiols. Other volatile compounds and the sensory profiles of the wines were also evaluated, to provide the first insight into the effects of ACE and the winemaking conditions on Sauvignon blanc wine.

3.1. Basic chemical parameters.

Briefly, Table A.1 of Appendix A shows that the wines at bottling had similar basic oenological parameters. Some significant differences were identified according to one-way ANOVA ($p < 0.05$), with the potential sensory implications discussed in Section 3.5.2. The lower concentration of free SO_2 in ACE treatment (8.3–18.1 mg/L) compared to NoACE treatment (19.6–26.9 mg/L) may be due to its reaction with *o*-quinones derived from oxidation because of the more abundant phenolics in the ACE treatments, as elaborated in the next section. Malic acid was undetectable in the MLF treatment samples, which signified the successful completion of malolactic fermentation in those wines.

3.2. A-TEEM analysis of wine

3.2.1. Absorbance profile

Total phenolics and hydroxycinnamates in wine were determined using the A-TEEM method (Ranaweera et al., 2021) to reveal the potential influence of the treatments, and particularly the crushing method, on phenolic extraction from grape skin. Values ranged between 2.7 and 5.8 a.u. and 43–65 mg/L CAE for total phenolics and hydroxycinnamates, respectively (Fig. A.3A and A.3B of Appendix A), in line with the previously reported typical ranges in a number of commercial white wines (5–15 a.u. and 17.8–129 mg/L CAE, respectively, (Somers & Ziemelis, 1985)). According to three-way ANOVA, total phenolics was significantly impacted by a three-way interaction ($p < 0.001$) and hydroxycinnamates was influenced by two-way interactions of crushing method × malolactic fermentation ($p = 0.009$) and yeast strain × malolactic fermentation ($p < 0.001$) (Table A.3 of Appendix A). Evaluation of the simple main effects highlighted that ACE had significantly higher values for total phenolics (Fig. A.4A and A.4B of Appendix A) and hydroxycinnamates (Fig. A.5A of Appendix A) compared to NoACE, reinforcing the potential of ACE for enhancing the release of compounds from grape skin. Objectively, the enhancement of hydroxycinnamates and total phenolics in white wine due to ACE may raise the potential concern of increased browning, yet values were well within the typical range of up to 129 mg/L reported for commercial white wines (Somers & Ziemelis, 1985). The impacts of yeast strain and malolactic fermentation varied under the different conditions (Fig. A.4 and A.5 of Appendix A), with MLF significantly increasing the content of total phenolics (Fig. A.4C of Appendix A) and hydroxycinnamates (Fig. A.5A of Appendix A) compared to the NoMLF treatment, but only in NoACE wines. Previous work on Chardonnay wine also showed that MLF yielded a greater amount of hydroxycinnamates than the absence of MLF (Pacheco et al., 2022), but the effect of ACE in the present case had no immediate explanation.

3.2.2. EEM profile

Aside from the absorbance values, the discrimination power of the A-TEEM analytical method has previously been illustrated with the successful classification of wines (Ranaweera et al., 2021). The technique was applied to the Sauvignon blanc wines for the first time in the present study, with robust PCA showing complete separation of treatments based on yeast strain along PC1 (85.6 % of total variance explained, Fig. A.6A of Appendix A), with VIN13 to the left and Sauvy to the right. Treatments were also well resolved as a function of crushing method along PC2 (12.1 % of total variance explained, Fig. A.6A of Appendix A), with ACE in the top half, and MLF and NoMLF treatments were separated along PC3 with 1.0 % of total variance explained (Fig. A.6B of Appendix A). PARAFAC modelling was used to ascertain the potential fluorescent compounds driving the differences, yielding three components (Fig. A.7 of Appendix A) as verified by split-half analysis affording 100 % similarity. Components 1 and 2 exhibited $\lambda_{ex}/\lambda_{em}$ wavelength couples of 275/300 and 285/340, respectively (Fig. A.7 of Appendix A), and were tentatively assigned as tyrosine and hydroxycinnamates (Coelho et al., 2015), with component 3 ($\lambda_{ex}/\lambda_{em} = 275/285$, Fig. A.7 of Appendix A) also likely to be related to aromatic amino acids (Christensen et al., 2006). The compositional differences could be induced by different levels of amino acid uptake and release by yeast strains as revealed in the PCA scores plots (Fig. A.6 of Appendix A) along PC1 and hydroxycinnamate extraction from grape skin by crushing method as seen along PC2, as well as from the effect of LAB on these aspects as indicated by PC3.

3.3. Varietal thiol precursors

The evolution profiles of GSH-3-SH and Cys-3-SH in grape juice were monitored during cold maceration for 21 h before pressing to reveal the impact of crushing method on thiol precursors extraction (Fig. 1A and 1B). Residual precursors in the resultant wines were determined to elucidate the biological influences of yeast strain and MLF (Fig. 1C and 1D).

3.3.1. Evolution of GSH-3-SH

Initially, the concentration of GSH-3-SH in ACE and NoACE grape juice was not significantly different (313 μg/L and 315 μg/L at 0 h, respectively, Fig. 1A), after which time the concentration in ACE treatment increased significantly ($p < 0.001$, one-way ANOVA) to 514 μg/L. The concentration remained stable until the end of maceration (at 21 h) and upon pressing and cold settling, with 513 μg/L of GSH-3-SH present at yeast inoculation (45 h). Conversely, GSH-3-SH in NoACE declined significantly ($p < 0.001$, one-way ANOVA, Fig. 1A) to 230–251 μg/L within the first 9 h before a significant increase ($p < 0.001$, Fig. 1A) to 382 μg/L at 21 h, but no change after pressing and cold settling (410 μg/L at 45 h, Fig. 1A). The general increase in concentration of GSH-3-SH in the ACE and NoACE treatments was similar to that reported previously for prolonged storage of Sauvignon blanc must (Capone et al., 2012) and an artificially oxygenated Sauvignon blanc juice (Roland et al., 2010). Comparing crushing method, the concentration of GSH-3-SH in ACE became significantly higher than NoACE after 3 h and then remained so for the rest of the maceration period ($p < 0.01$ to < 0.05, repeated-measures ANOVA, Fig. 1A), revealing the higher efficiency of ACE in extracting GSH-3-SH compared to the conventional crushing method (NoACE). The concentrations of GSH-3-SH in both treatments at yeast inoculation (410 and 513 μg/L for NoACE and ACE, respectively) were in the range reported for a previous study of Sauvignon blanc juice (245–642 μg/L, (Capone et al., 2010)), but were generally more abundant than in some other Sauvignon blanc studies (3 nmol/L or equivalent to 1.2 μg/L (Roland et al., 2010) and < 150 μg/L (Chen, Capone, Tondini, et al., 2018)).

3.3.2. Evolution of Cys-3-SH

Although being an order of magnitude lower in concentration compared to GSH-3-SH, the evolution profiles of Cys-3-SH during maceration in ACE and NoACE treatments were similar to those of the GSH-3-SH, increasing with maceration time and with ACE being higher than NoACE, with the exception that Cys-3-SH at yeast inoculation did not significantly differ (10 μg/L in NoACE and 15 μg/L in ACE, Fig. 1B). Overall, the evolution profile was in line with that noted in a prolonged storage of Sauvignon blanc must (Capone et al., 2012), although a generally stable evolution profile of Cys-3-SH in Sauvignon blanc juice (40–60 μg/L) has also been reported (Roland et al., 2010).

3.3.3. Varietal thiol precursors in wine

Quantifying remaining precursors in the wines helped evaluate the effect of the three factors on the release of varietal thiols from their precursors. The residual concentrations of GSH-3-SH and Cys-3-SH were

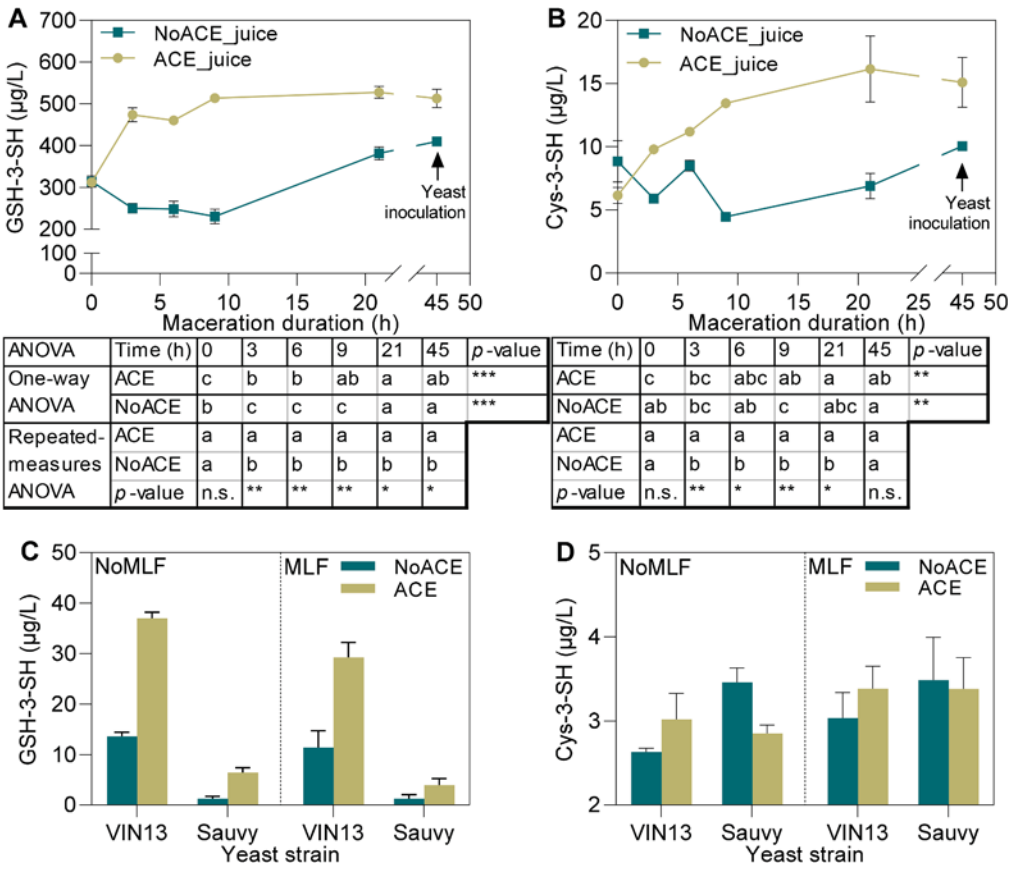

ANOVA	Time (h)	0	3	6	9	21	45	*p*-value
One-way ANOVA	ACE	c	b	b	ab	a	ab	***
	NoACE	b	c	c	c	a	a	***
Repeated-measures ANOVA	ACE	a	a	a	a	a	a	
	NoACE	a	b	b	b	b	b	
	p-value	n.s.	**	**	**	*	*	

Time (h)	0	3	6	9	21	45	*p*-value
ACE	c	bc	abc	ab	a	ab	**
NoACE	ab	bc	ab	c	abc	a	**
ACE	a	a	a	a	a	a	
NoACE	a	b	b	b	b	a	
p-value	n.s.	**	*	**	*	n.s.	

Fig. 1. Evolution of (A) GSH-3-SH and (B) Cys-3-SH in Sauvignon blanc juice of different treatments during cold maceration and at inoculation, and concentrations of (C) GSH-3-SH and (D) Cys-3-SH in the resulting wines at bottling. Cyan curves in A and B show analytes from NoACE treatment and olive curves show analytes from ACE treatment, with error bars representing standard deviation (n = 2 from duplicate measurement of grape juice from each crushing method). Tables below panels A and B illustrate the results of one-way ANOVA for differences between sampling times within treatments and repeated-measures ANOVA for differences between treatments within sampling times. Different letters in each row for one-way ANOVA or each column for repeated-measures ANOVA represent significant difference between the means (at $\alpha = 0.05$). n.s.: not significant; *: $p < 0.05$; **: $p < 0.01$; ***: $p < 0.001$. Cyan bars in C and D show analytes from NoACE treatment and olive bars show analytes from ACE treatment, with error bars representing standard deviation (n = 3 from single measurement of three biological replicates). (For interpretation of the references to colour in this figure legend, the reader is referred to the web version of this article.)

1.2–37 μg/L and 2.6–3.5 μg/L, respectively (Fig. 1C and 1D), in general agreement with previous results for Sauvignon blanc wine (11–63 μg/L (Wang et al., 2020) and 374–486 μg/L (Capone et al., 2010) for GSH-3-SH, and < 13 μg/L (Wang et al., 2020) and 39–50 μg/L (Capone et al., 2010) for Cys-3-SH). Based on the present values, 65.2 %–81.1 % of GSH-3-SH and 94.3 %–99.7 % of Cys-3-SH were apparently consumed during fermentation, although as revealed previously via the lack of a strong correlation, the disappearance of precursors is not necessarily accounted for by the concentration of free thiols determined in wine (Chen, Capone, Tondini, et al., 2018). Nonetheless, conversion yields based on precursors consumed and free thiols released could offer some insight into the thiol release process, as discussed in the next section.

Briefly interpreting the three-way ANOVA results (Table A.3 of Appendix A), ACE (Fig. A.8A and A.8C of Appendix A) and VIN13 (Fig. A.8B and A.8C of Appendix A) wines had significantly higher residual GSH-3-SH than NoACE and Sauvy, respectively. This may be due to the higher concentration of GSH-3-SH in ACE processed juice than NoACE prior to fermentation, and to VIN13 potentially consuming less GSH-3-SH than Sauvy. MLF had a lower amount of GSH-3-SH than NoMLF under certain conditions (Fig. A.8A and A.8B of Appendix A), reinforcing the notion that LAB (*O. oeni* in this case) is able to consume thiol precursors (Suklje & Čuš, 2021). Under certain conditions, ACE and Sauvy had greater amounts of residual Cys-3-SH than NoACE and VIN13, respectively, although there was minimal actual difference (<1 μg/L, Fig. A.8D of Appendix A).

3.4. Varietal thiols and cis-2-MPO at bottling

Enantiomers of 3-SH and 3-SHA along with 4-MSP were quantified in wines at bottling to assess the influence of the three factors on thiol-related phenomena. *cis*-2-MPO enantiomers, namely (2*R*,4*S*)-2-MPO and (2*S*,4*R*)-2-MPO, originating from (3*S*)-3-SH and (3*R*)-3-SH, respectively, were quantified at very low concentrations of 1.2–4.5 ng/L and 1.1–5.8 ng/L, so the influence of the winemaking factors has not been discussed further.

3.4.1. 3-SH enantiomers

The concentrations of (3*S*)-3-SH and (3*R*)-3-SH were 456–864 ng/L and 434–850 ng/L (Fig. 2A and 2B), leading to respective odour activity values (OAV) of 7.6–14.4 and 8.7–17.0 in wines at bottling. These concentration ranges were substantially higher than reported in a previous study for Sauvignon blanc wines from the same region (96–306 ng/L and 90–358 ng/L, respectively (Chen, Capone, Tondini, et al., 2018)), likely as a result of the difference in fruit composition due to location or yeast strains used (Chen et al., 2019; Chen, Capone, Tondini, et al., 2018). Nevertheless, the enantiomeric ratio of (3*S*)-/(3*R*)-3-SH averaged 51:49, in line with studies showing an approximately equal proportion of 3-SH enantiomers with a slight preference toward (3*S*)-3-SH (Chen, Capone, & Jeffery, 2018; Tominaga et al., 2006).

Enantiomers of 3-SH were significantly impacted by two-way interactions of crushing method × yeast strain ($p < 0.001$) and yeast strain × malolactic fermentation ($p = 0.023$ and $p < 0.001$, Table A.3 of Appendix A). The simple main effects showed that MLF and ACE had significantly higher concentrations of (3*S*)-3-SH (Fig. 2C) and (3*R*)-3-SH (Fig. 2D) than NoMLF and NoACE, respectively. The result for MLF indicated that *O. oeni* could produce additional 3-SH beyond that attributed to alcoholic fermentation by yeast, likely from its precursors given the lower concentration of GSH-3SH remaining in MLF wines, as discussed earlier and seen in Fig. 1. This result further implied that the enzymes releasing 3-SH enantiomers from their precursors could potentially be present in *O. oeni*, although this requires more research. This outcome agreed with previous work, in which spontaneous or inoculated MLF significantly increased concentrations of 3-SH in Welschriesling white wines (Suklje & Čuš, 2021), whereas *O. oeni* (Lalvin

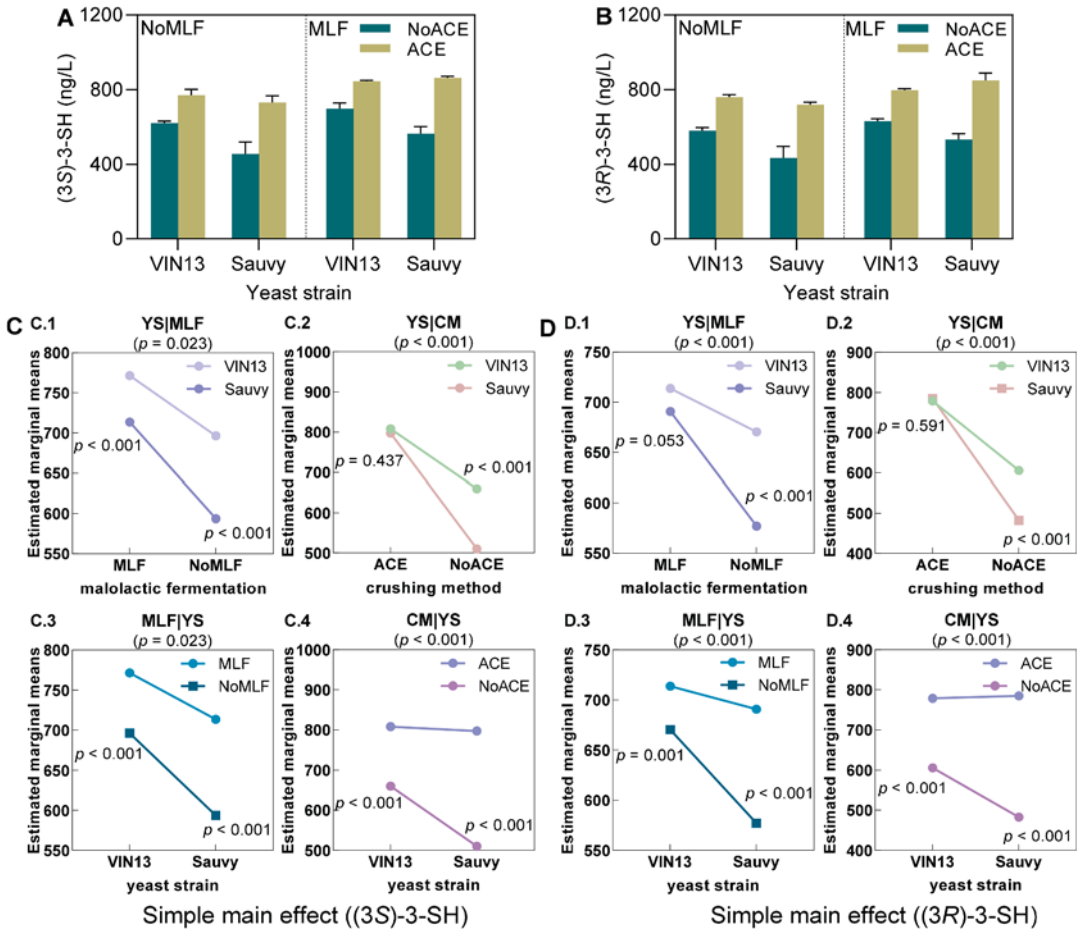

Fig. 2. Concentrations of (A) (3*S*)-3-sulfanylhexanol ((3*S*)-3-SH) and (B) (3*R*)-3-sulfanylhexanol ((3*R*)-3-SH), and simple main effect plots of significant two-way interactions from three-way ANOVA for Sauvignon blanc wines at bottling showing interactions of (C) yeast strain and malolactic fermentation, and yeast strain and crushing method for (3*S*)-3-SH, and (D) yeast strain and malolactic fermentation, and yeast strain and crushing method for (3*R*)-3-SH. Cyan bars in A and B show analytes from NoACE treatment and olive bars show analytes from ACE treatment, with error bars representing standard deviation (n = 6 from duplicate measurement of three biological replicates). Abbreviations above each plot in C and D represent significant interactions between factors followed by *p*-values in brackets. MLF, malolactic fermentation; YS, yeast strain; CM, crushing method. (For interpretation of the references to colour in this figure legend, the reader is referred to the web version of this article.)

VP41) as used in the present work was unable to release 3-SH from its precursors when undertaking whole-cell assays in citrate buffer, in contrast to *Lactobacillus plantarum* (Takase et al., 2018). The higher concentrations of 3-SH enantiomers in ACE wines seemingly resulted from the greater abundance of GSH-3-SH in the ACE treatment juice at yeast inoculation, as shown in Fig. 1A. The impact of yeast strain on 3-SH enantiomers varied: VIN13 increased the concentration of both enantiomers in NoMLF ($p < 0.001$, Fig. 2C and D) and in NoACE ($p < 0.001$, Fig. 2C and D) compared to Sauvy, whereas there were no significant differences in MLF ($p = 0.053$, Fig. 2D) and ACE ($p > 0.4$, Fig. 2C and D), except for (3*S*)-3-SH ($p < 0.001$, Fig. 2C). These results according to yeast strain may be related to different enzymes involved in uptake of thiol precursors (e.g., Opt1p (Cordente et al., 2015)) or release of 3-SH from its precursors (e.g., β-lyase (Howell et al., 2005)).

The enantiomeric ratio of (3*S*)-/(3*R*)-3-SH, which can potentially influence wine aroma (King et al., 2011; Tominaga et al., 2006), was only affected by the main effects, where NoACE, VIN13, and MLF (all 52:48) significantly increased the ratio ($p < 0.001$, < 0.006, and < 0.014, respectively, Table A.3 of Appendix A) compared to ACE, Sauvy, and NoMLF (all 51:49). The enantiomers of 3-SH are produced at least in part from their respective precursor diastereomers via enzymes (Bonnaffoux et al., 2021; Grant-Preece et al., 2010), thus potential differences in enzyme stereoselectivity between yeast strains or LAB may account for the change in the ratio, although asymmetric production of precursors or free thiols could also have an impact on enantiomer ratios, as previously proposed (Chen, Capone, Tondini, et al., 2018). With individual sensory attributes of 'passionfruit' and 'grapefruit' (Tominaga et al., 2006) and an OAV > 7.6 for each 3-SH enantiomer according to the concentrations shown in Fig. 2, the near-equal enantiomeric ratios of 3-SH may in combination contribute to 'solvent' and 'citrus' flavour in wine (King et al., 2011).

3.4.2. 3-SHA enantiomers

The concentrations of (3*S*)-3-SHA and (3*R*)-3-SHA at bottling were 13–29 ng/L and 6–15 ng/L, respectively (Fig. 3A and 3B), in reasonable accord with a previous study of Adelaide Hills Sauvignon blanc wines (2.1–13.1 ng/L and 1.6–5.9 ng/L for (3*S*)- and (3*R*)-3-SHA, respectively, (Chen, Capone, Tondini, et al., 2018)). The somewhat higher values in the present work could relate to different strains of yeast used for alcoholic fermentation, and a difference in the constitution of grape juice, for instance, variable amino acid and *p*-coumaric acid concentrations, could also play a key role (Pinu et al., 2014). Nonetheless, when expressed as total 3-SHA, the values for the summed enantiomers (i.e., 20–43 ng/L) aligned well with a previous study (Chen et al., 2019).

(3*S*)-3-SHA and (3*R*)-3-SHA were significantly affected by the three-way interaction of crushing method × yeast strain × malolactic fermentation ($p = 0.016$) and the two-way interaction of crushing method × malolactic fermentation ($p = 0.003$, Table A.3 of Appendix A),

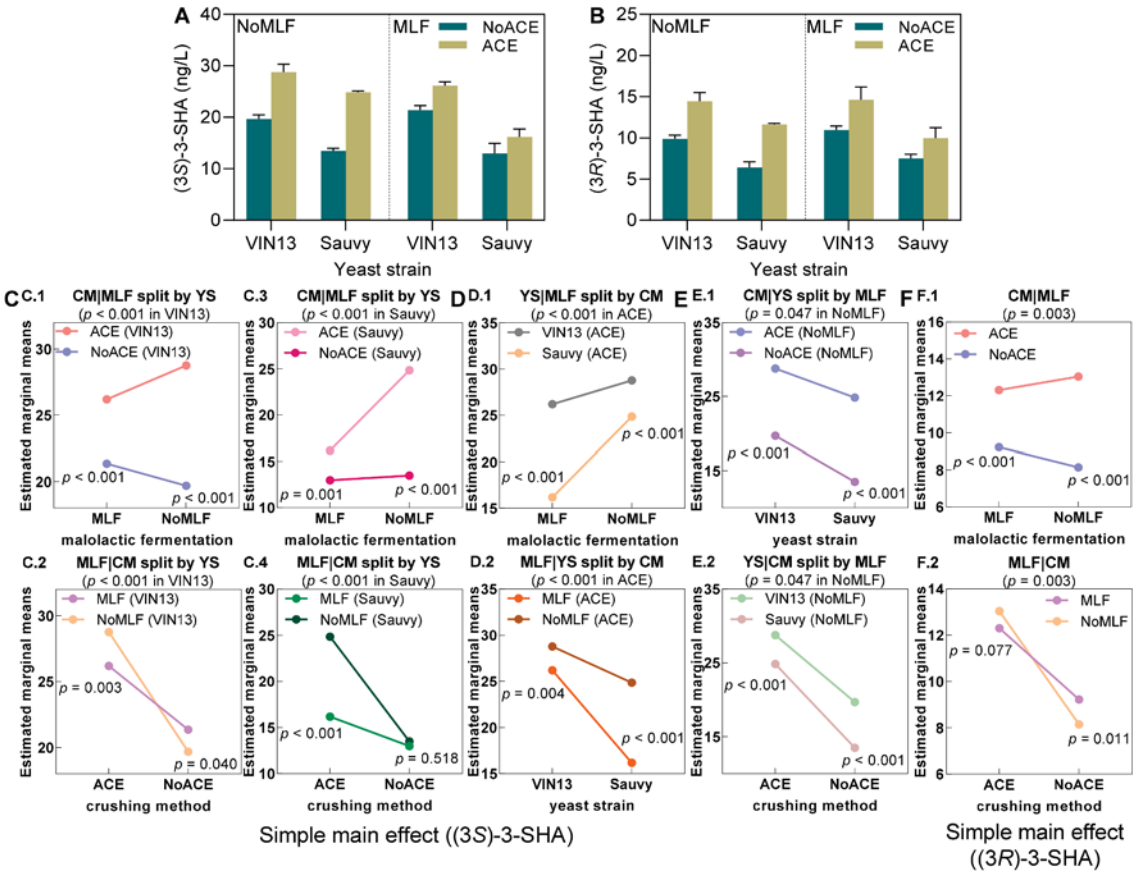

Fig. 3. Concentrations of (A) (3*S*)-3-SHA and (B) (3*R*)-3-SHA, and simple main effect plots of significant two-way interactions from three-way ANOVA for Sauvignon blanc wines at bottling showing interactions for (3*S*)-3-SHA of (C) crushing method and malolactic fermentation, (D) yeast strain and malolactic fermentation, and (E) crushing method and yeast strain, and for (3*R*)-3-SHA of (F) crushing method and malolactic fermentation. Cyan bars in A and B show analytes from NoACE treatment and olive bars show analytes from ACE treatment, with error bars representing standard deviation (n = 6 from duplicate measurement of three biological replicates). Abbreviations above each plot in C–F represent significant interactions between factors followed by *p*-values in brackets. MLF, malolactic fermentation; YS, yeast strain; CM, crushing method. (For interpretation of the references to colour in this figure legend, the reader is referred to the web version of this article.)

respectively. The simple main effects revealed that ACE and VIN13 significantly increased both 3-SHA enantiomers compared to NoACE (Fig. 3C, E, and F) and Sauvy (Fig. 3D and E), respectively, in line with the results for 3-SH enantiomers (Fig. 2). The impact of MLF varied, with lower levels of 3-SHA enantiomers compared to NoMLF for ACE (Fig. 3C and F), VIN13, and Sauvy treatments (Fig. 3D), whereas MLF had significantly higher (Fig. 3C and F) or similar amounts of 3-SHA enantiomers (Fig. 3C) than NoMLF in the NoACE treatments. The acetylation of 3-SH to produce 3-SHA is catalysed by alcohol acetyltransferase secreted by yeast, but not likely by LAB (Takase et al., 2018). However, the potential for yeast-bacteria interaction and hydrolysis of 3-SHA may cause the difference in 3-SHA enantiomer concentrations (Tristezza et al., 2016), with crushing method possibly complicating the effect. This differed from a report on Welschriesling wines, where the concentration of 3-SHA was not significantly impacted by MLF (Suklje & Čuš, 2021). These disparate outcomes may relate to factors such as the different grape varieties or yeast and bacterial strains used between the two studies, and the biological nature of malolactic fermentation may have contributed to greater variance, thus lack of significance, among replicates in the Welschriesling wine study (Suklje & Čuš, 2021).

The enantiomeric ratio of (3*S*)-/(3*R*)-3-SHA ranged between 62:38 and 68:32 (Fig. A.9A of Appendix A), with an average of 66:34, in reasonable accord with the previous reports of 70:30 (Chen, Capone, & Jeffery, 2018; Tominaga et al., 2006). This ratio was impacted by the two-way interaction of yeast strain × malolactic fermentation (p = 0.001, Table A.3 of Appendix A), with the simple main effects revealing that VIN13 produced a significantly higher ratio in MLF (p = 0.007, Fig. A.9B of Appendix A) but lower in NoMLF (p = 0.043, Fig. A.9B of Appendix A) than Sauvy. The varied ratio between VIN13 and Sauvy contrasted with the minimal difference between VIN13 and W28 (also a thiol-releasing yeast) in a previous study (Chen, Capone, Tondini, et al., 2018). MLF appeared to significantly decrease the ratio of (3*S*)-/(3*R*)-3-SHA compared to NoMLF in Sauvy treatment (p < 0.001, Fig. A.9B of Appendix A), implying, as mentioned earlier, that LAB may have affected the alcohol acetyltransferase activity of yeast in transforming 3-SH enantiomers into 3-SHA enantiomers through yeast-bacteria interaction (Tristezza et al., 2016), although LAB might not be directly involved in this acetylation (Takase et al., 2018). With respective OAVs of 5.2–11.6 and 0.67–1.7 for (3*S*)-3-SHA and (3*R*)-3-SHA calculated from their concentrations shown in Fig. 3, and sensory notes of 'boxwood' and 'passionfruit' (Tominaga et al., 2006), a higher ratio of (3*S*)-/(3*R*)-3-SHA as induced by VIN13 in the present case has been related to 'cooked green vegetal' and 'cat urine/sweaty' notes (King et al., 2011).

3.4.3. *Apparent molar conversion yields*

Based on the amounts of GSH-3-SH and Cys-3-SH consumed, the apparent molar conversion from precursors to the sum of 3-SH and 3-SHA ranged from 0.65 % to 1.01 % (Fig. A.10A of Appendix A), with significant two-way interactions of crushing method × yeast strain (p < 0.001, Table A.3 of Appendix A) and yeast strain × malolactic fermentation (p = 0.049, Table A.3 of Appendix A). The simple main effects showed that VIN13 (Fig. A.10B and A.10C of Appendix A), MLF (Fig. A.10B of Appendix A), and ACE (Fig. A.10C of Appendix A)

increased the conversion yield by around 0.15–0.2 % compared with their treatment counterparts. Although minor, the difference in conversion yield suggested an impact of ACE, VIN13, and MLF on the uptake and/or conversion of precursors, potentially attributable to the activity of the enzymes involved in these processes (Bonnaffoux et al., 2021).

The calculated molar conversion yield from 3-SH to 3-SHA ranged from 1.1 % to 2.2 % (Fig. A.11A of Appendix A) with an average of 1.7 %, agreeing with another study of Sauvignon blanc wines (1.1–4.7 %) (Chen, Capone, Tondini, et al., 2018). The simple main effects of the three significant two-way interactions ($p = 0.006$, < 0.001, and < 0.001, respectively, Table A.3 of Appendix A) showed that VIN13 (Fig. A.11C and A.11D of Appendix A) and NoMLF (Fig. A.11B and A.11C of Appendix A) appeared to significantly increase the yield of 3-SHA by an increment of 0.2–0.5 %, and ACE significantly increased the yield by up to 0.3 % in NoMLF ($p < 0.001$, Fig. A.11B of Appendix A) and VIN13 ($p = 0.002$, Fig. A.11D of Appendix A) but decreased it by 0.1 % in MLF ($p = 0.024$, Fig. A.11B of Appendix A). The slight differences implied an influence of the three studied factors on acetylation of 3-SH to form 3-SHA, with this transformation being associated with alcohol acetyltransferase activity (Swiegers et al., 2006).

3.4.4. *Effects on 4-MSP*

The concentration of 4-MSP ranged from 76 ng/L to 188 ng/L (Fig. 4A) and was relatively high but consistent with other reports on young Sauvignon blanc wines (Chen et al., 2019; Dagan et al., 2014). Having an ODT of 0.8 ng/L and thus an OAV range of 95–235 calculated from the concentrations shown in Fig. 4, 4-MSP was likely to contribute 'box-tree' and 'blackcurrant' sensory characters (Darriet et al., 1995). 4-MSP was significantly impacted by two-way interactions of crushing method × yeast strain ($p = 0.036$, Table A.3 of Appendix A), crushing method × malolactic fermentation ($p < 0.001$, Table A.3 of Appendix A), and yeast strain × malolactic fermentation ($p < 0.001$, Table A.3 of Appendix A). The simple main effects indicated that ACE (Fig. 4B and D), Sauvy (Fig. 4C and D), and MLF (Fig. 4B and C) significantly increased the concentration of 4-MSP, except for ACE with VIN13 ($p = 0.470$, Fig. 4D) and MLF with VIN13 ($p = 0.324$, Fig. 4C), with the impact of ACE and MLF being in line with the preceding discussion for 3-SH. The increase of 4-MSP induced by MLF agreed with the results in Welschriesling wines using three commercial strains of *O. oeni* (Suklje & Čuš, 2021), which included Lalvin VP41 as used in the present work.

Notably, the observation that VIN13 produced higher concentrations of 3-SH (Fig. 2) and lower amounts of 4-MSP than Sauvy (Fig. 4) may be attributed to the different expression levels of genes regulating the uptake and release of varietal thiols. Genes encoding β-lyase enzymes that cleave 4-MSP from its cysteinylated precursor (Cys-4-MSP) have been studied, such as *BNA*3, *GLO*1, *METC*, *CYS*3, and *IRC*7 (Howell et al., 2005; Roncoroni et al., 2011), of which *IRC*7 gene allele length and single-nucleotide polymorphism mutations play a synergistic role (Roncoroni et al., 2011). Besides, as with 3-SH precursors, genes regulating 4-MSP precursor uptake can affect the concentration of 4-MSP. Such genes include *OPT*1, which encodes a plasma membrane transporter that is important for conveying glutathionylated conjugates of 4-MSP and 3-SH into yeast cells (Cordente et al., 2015).

3.5. *Volatile and sensory profiles of wines*

3.5.1. *Volatile composition*

At the time of sensory analysis, 38 volatile compounds comprising 5

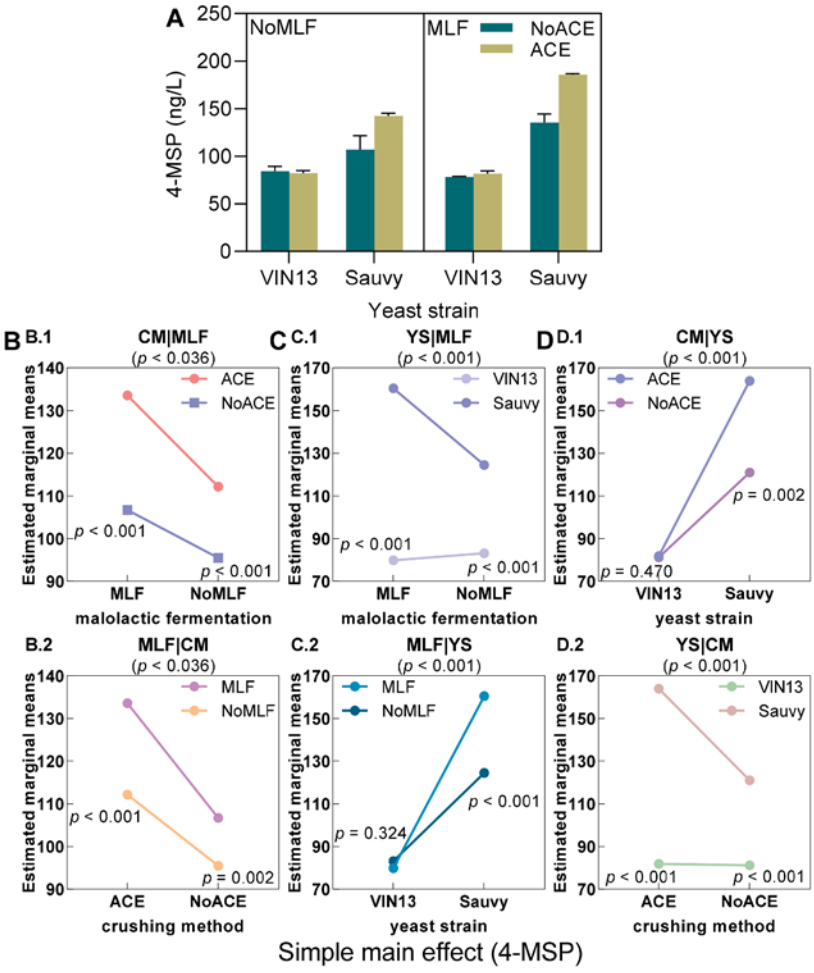

Fig. 4. Concentrations of (A) 4-methyl-4-sulfanylpentan-2-one (4-MSP) and simple main effect plots of significant two-way interactions from three-way ANOVA for Sauvignon blanc wines at bottling showing interactions for 4-MSP of (B) crushing method and malolactic fermentation, (C) yeast strain and malolactic fermentation, and (D) crushing method and yeast strain. Cyan bars in A show analytes from NoACE treatment and olive bars show analytes from ACE treatment, with error bars representing standard deviation (n = 6 from duplicate measurement of three biological replicates). Abbreviations above each plot in B–D represent significant two-way interactions between factors followed by *p*-values in brackets. MLF, malolactic fermentation; YS, yeast strain; CM, crushing method. (For interpretation of the references to colour in this figure legend, the reader is referred to the web version of this article.)

varietal thiols (i.e., 3-SH/3-SHA enantiomers and 4-MSP), 3 isoprenoids, 3 C_6 alcohols, 10 ethyl esters, 4 acetates, 8 higher alcohols, and 6 fatty acids were quantified (Table A.4 of Appendix A) and found to be significantly affected by either two-way or three-way interactions according to three-way ANOVA, except for (3*S*)-3-SHA. Enantiomers of *cis*-2-MPO were not detected in most treatments at this stage. It is well known that the manifestation of wine aroma is complicated due to the number of volatile constituents and the interactions among them and with the wine matrix, including an abundance of non-volatiles. Nonetheless, OAVs associated with aroma compounds as used in the current study can still provide an easy, initial, and general estimation of the relevance of given volatile compounds despite the limitations, such as ignoring the matrix effect (Benkwitz et al., 2012).

The concentrations of (3*S*)-3-SH, (3*S*)-3-SHA, (3*R*)-3-SHA, and 4-MSP decreased by an average of 6–20 % in contrast to those at bottling, conceivably due to the formation of quinone-thiol adducts via wine oxidation phenomena (Nikolantonaki & Waterhouse, 2012). An average 2 % increase of (3*R*)-3-SH was observed, and although hydrolysis of 3-SHA could ordinarily contribute to such an occurrence, the lower concentration of (3*R*)-3-SHA could not account for the increase of (3*R*)-3-SH in this case. This variable impact on 3-SH enantiomers was inexplicable, given that the potential chemical reactions would not be stereoselective and enzymatic reactions are implausible during storage.

Concentrations of linalool, α-terpineol, and β-damascenone were 12–16 μg/L, 1.5–5.0 μg/L, and 3.3–4.5 μg/L, respectively (Table A.4 of Appendix A), in general agreement with the previously reported concentrations in Sauvignon blanc wine (Coetzee et al., 2016; Swiegers et al., 2009). With respective OAVs ranging between 0.8 and 1.1 and 66–98 (Table A.4 of Appendix A), linalool and especially β-damascenone could be key contributors to the sensory traits of these wines, as noted previously (Benkwitz et al., 2012). The concentration of 1-hexanol (2.8–3.2 mg/L, Table A.4 of Appendix A) was higher and those of (*E*)-3-hexen-1-ol (60–69 μg/L) and (*Z*)-3-hexen-1-ol (151–180 μg/L) were lower than found in Marlborough Sauvignon blanc wine (Benkwitz et al., 2012), potentially due to the difference in amino acids in juice (Pinu et al., 2014). Their low OAVs (<1.0, Table A.4 of Appendix A) imply a lack of sensory impact, although these C_6 alcohols reportedly enhance 'passionfruit', 'flinty', and 'grassy' aromas according to omission studies (Benkwitz et al., 2012) and relate to 'confection' and 'red fruit' notes in Shiraz wines (Capone et al., 2021).

The concentrations of ethyl propanoate (276–361 μg/L), ethyl 2-methylpropanoate (189–201 μg/L, Table A.4 of Appendix A), ethyl 2-methylbutanoate (8.5–11 μg/L), ethyl 3-methylbutanoate (11–16 μg/L), and 3-methylbutyl acetate (192–614 μg/L) were generally higher than previous reports of Sauvignon blanc wine (Coetzee et al., 2016; Swiegers et al., 2009). Contrarily, ethyl esters of even numbered straight-chain fatty acids, including ethyl butanoate (7.4–137 μg/L), ethyl hexanoate (97–493 μg/L), ethyl octanoate (196–596 μg/L), and ethyl decanoate (210–290 μg/L), and acetates including ethyl acetate (7.2–32.9 mg/L), hexyl acetate (18–50 μg/L), and 2-phenylethyl acetate (101–196 μg/L) were lower than those reported in the previous studies (Coetzee et al., 2016; Swiegers et al., 2009). This could be related to differences in fruit ripeness and composition, vintage, or yeast strain and LAB (Chen et al., 2019; Suklje & Čuš, 2021; Swiegers et al., 2009). Regarding the sensory contribution of esters, as a group they can impact several fruity aroma notes of wine (Benkwitz et al., 2012), with most having an OAV around 1, such as ethyl decanoate (1.1–1.5) and ethyl lactate (1.1–1.6), and some with an OAV of up to 35, for instance, ethyl hexanoate (7–35), ethyl octanoate (9–30), and ethyl 2-methylbutanoate (8.5–11) (Table A.4 of Appendix A).

The concentrations of higher alcohols and fatty acids (Table A.4 of Appendix A) were generally in the same range as previous studies, although 1-propanol (10.4–17.0 mg/L), 1-butanol (576–837 μg/L), 2-phenylethanol (1.1–2.2 mg/L), hexanoic acid (1.5–2.5 mg/L), octanoic acid (32–59 μg/L), and decanoic acid (791–1462 μg/L) were lower and 2-methyl-1-propanol (28.4–40.3 mg/L), 3-methyl-1-butanol (223–243 mg/L), 2-methylpropanoic acid (0.9–1.6 mg/L), and butanoic acid (0.9–1.2 mg/L) were higher than reported for Sauvignon blanc wines (Coetzee et al., 2016; Swiegers et al., 2009). Some of these compounds had an OAV higher than 1 and others were below or close to 1 (Table A.4 of Appendix A) and have been shown to decrease the intensities of 'flinty' and 'bourbon' notes in Sauvignon blanc wine (Benkwitz et al., 2012). Although seemingly less relevant, these volatiles may still be important to 'fruity' aroma notes by acting as substrates for ester formation.

3.5.2. RATA sensory analysis

The sensory study showed that seven aroma (orthonasal), eight flavour (retronasal), and five taste/aftertaste attributes were significantly different according to two-way ANOVA ($\alpha = 0.1$, Table A.2 of Appendix A). PCA was conducted to visualise the sensory profiles among the treatments, with the inclusion of volatile composition and basic chemical parameters of the wines. As shown in Fig. 5A, PC1 (37.4 % variance explained) and PC2 (30.2 % variance explained) separated the treatments according to yeast strain and MLF combinations, with ACE and NoACE from each combination being clustered together.

AVM and NAVM were located to the left along PC1 (Fig. 5A), being close to 'sulfidic' and 'bacon' aroma notes, 'mineral', 'sulfidic', and 'citrus' flavours, and 'bitter' and 'length of non-fruity' aftertaste. These sensory attributes were close to several fatty acids (2-methylpropanoic, butanoic, hexanoic, and octanoic acids), varietal thiols (enantiomers of 3-SH and 3-SHA), ethyl esters (acetate, lactate, butanoate, hexanoate, octanoate), butanol, and 2-methyl-1-propanol.

ASNM and NASNM were plotted to the right along PC1 (Fig. 5A) and adjacent to pleasant aroma and flavour notes of 'floral', 'tropical fruit', 'melon', 'honey', and 'confectionery' and 'length of fruity', with volatiles including 2-ethyl-1-hexanol ('green', 'floral', 'green cucumber'), β-damascenone ('apple', 'rose', 'honey'), 2-phenylethyl acetate ('floral', 'rose', 'fruity'), 2-phenylethanol ('floral', 'rose'), and linalool ('flower', 'lavender') being close to the 'floral' note. This agreed with a lack of 3-SH, which has been related with more intense 'flowery' and 'peach', notes (Wilson et al., 2019). The fact that 3-SH and 3-SHA were located away from the usual 'tropical fruit' descriptor may be due to a suppression effect by other volatiles (Coetzee et al., 2015). Linalool may also contribute to 'stone fruit' flavour, with omission of linalool and α-terpineol found to decrease the intensities of 'apple lolly' and 'stone fruit' attributes (Benkwitz et al., 2012). Although 4-MSP could decrease the intensity of 'confectionery' note (Benkwitz et al., 2012), it was situated close to the 'confectionery' flavour in the present study, to the right along PC1 and lower half of PC2 (Fig. 5A).

AVNM and NAVNM were located in the upper section of PC2 (Fig. 5A), being close to 'grapefruit' aroma note and volatiles comprising (*Z*)-3-hexen-1-ol, hexyl acetate, decanoic acid, and ethyl decanoate. Opposite to these, ASM and NASM were in the lower section of PC2, where several ethyl esters, α-terpineol, 1-octanol, 3-methyl-1-butanol, and benzyl alcohol were also scattered. These latter two treatments were relatively moderate in their sensory profiles compared to the others, as indicated by them being furthest from the perceived attributes.

Treatments were separated according to PC3 (17.4 % variance explained, Fig. 5B) based on crushing method, with ACE located in the lower section of PC3 and close to acetates, C_6 alcohols, varietal thiols, isoprenoids, and higher alcohols that were relatively close to aromas of 'tropical fruit', 'honey', and 'bacon', and flavours of 'sulfidic', 'confectionery', 'floral', 'sweet', 'length of fruity', and 'length of non-fruity'. The higher perception of 'sweet' may be attributed to glycerol and alcohol in the ACE treatments. NoACE wines were found in the upper section of PC3, being relatively closer to ethyl esters and fatty acids along with aromas of 'sulfidic', 'grapefruit', 'melon', 'floral', and flavours of 'stone fruits', 'tropical fruit' and 'honey' as well as 'bitter' and 'acidity' taste. The higher 'acidity' in NoACE wines may be related with higher TA and tartaric acid values (Table A.2 of Appendix A). The separation of crushing methods along PC3 clearly showed that ACE could

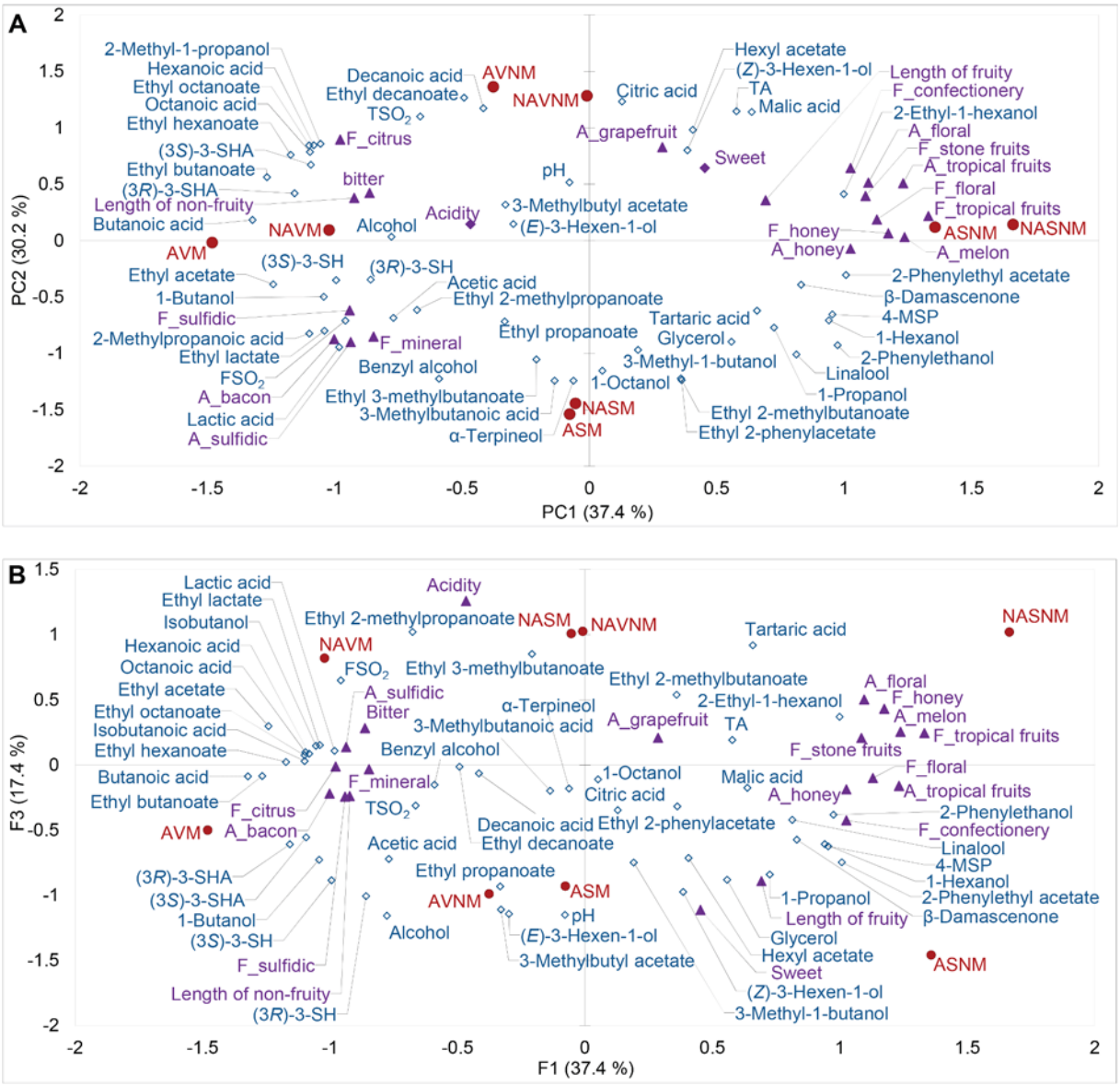

Fig. 5. PCA biplot of scores and loadings of significantly different wine sensory attributes (purple triangles, α = 0.10 from two-way ANOVA), volatile compounds and other basic chemical parameters (blue diamonds, α = 0.05 from one-way ANOVA) for Sauvignon blanc wines from different treatments (red circles) showing (A) PC1 vs PC2 and (B) the PC1 vs PC3. Wines were processed by accentuated cut edges (ACE) or conventional crusher (NoACE), fermented with one of two strains yeasts (VIN13 or Sauvy), and underwent malolactic fermentation (MLF) or not (NoMLF): AVNM, ACE_VIN13_NoMLF; ASNM, ACE_Sauvy_NoMLF; NAVNM, NoACE_-VIN13_NoMLF; NASNM, NoACE_Sauvy_NoMLF; AVM, ACE_VIN13_MLF; ASM, ACE_Sauvy_MLF; NAVM, NoACE_VIN13_MLF; NASM, NoACE_Sauvy_MLF. Prefix A indicates aroma attributes and F indicates flavour attributes. TSO_2, total SO_2; FSO_2, free SO_2; TA, titratable acidity.

alter both the volatile compounds composition and sensory profile of wine.

4. Conclusion

As a general summary, this novel study involving the ACE grape crushing approach revealed significant increases in the concentration of thiol precursors (GSH-3-SH and Cys-3-SH) during cold maceration of Sauvignon blanc grape must as well as in the concentrations of enantiomers of 3-SH and 3-SHA, along with 4-MSP in the resulting wines compared to conventional crushing (NoACE). The minor increases in total phenolics and hydroxycinnamates in the wines from ACE treatment may pose a heightened prospect of wine browning and thus decline in varietal aroma intensity, although the values were still below those reported for white wines in other work. The production of varietal thiols and oxathiane was different for the two strains of yeast used, with VIN13 tending to produce higher concentrations of enantiomers of 3-SH and 3-SHA and Sauvy producing significantly higher amounts of 4-MSP. MLF with *O. oeni* strain VP41 significantly increased the concentrations of 3-SH enantiomers and 4-MSP, decreased the concentration of (3*S*)-3-SHA, and had a variable impact on the concentrations of (3*R*)-3-SHA depending on the interaction with crushing method or yeast strain.

Sensory characterisation and analysis of volatile compounds after bottle ageing for 4 months revealed that NoMLF treatments tended to have more 'fruity' and 'floral' attributes than their MLF counterparts, with the latter being more abundant in savoury attributes, namely 'sulfidic', 'mineral', and 'bacon'. This can be ascribed to the overall chemical composition of the wines and changes attributed to MLF, despite it tending to yield greater amounts of varietal thiols, ethyl esters, higher alcohols, and fatty acids. Grape crushing method could modify the sensory profile, at least to a moderate extent, with ACE tending to have greater amounts of varietal aroma compounds and higher alcohols,

and higher intensity in 'confectionery', 'tropical fruits', 'bacon', 'sulfidic', and 'length of fruity/non-fruity' attributes, whereas NoACE had higher proportions of ethyl esters and fatty acids, and more intense attributes such as 'tropical fruits', 'floral', 'grapefruit', 'bitter', and 'sulfidic'. Sauvy yeast led to higher concentrations of isoprenoids, ethyl esters of branched-chain fatty acids, and higher alcohols than VIN13, whereas VIN13 yielded a greater abundance of ethyl esters of straight-chain fatty acids and fatty acids. Overall, the novel ACE grape-crushing technique appears to be a potentially useful tool for white winemaking, especially for tailoring Sauvignon blanc wine composition and sensory properties in combination with other winemaking techniques as assessed in this work.

CRediT authorship contribution statement

Xingchen Wang: Conceptualisation, Formal analysis, Funding acquisition, Investigation, Visualisation, Writing – original draft, Writing – review & editing. **Dimitra L. Capone:** Conceptualisation, Supervision, Writing – review & editing. **Aurélie Roland:** Conceptualisation, Supervision, Writing – review & editing. **David W. Jeffery:** Conceptualisation, Funding acquisition, Project administration, Resources, Supervision, Writing – review & editing.

Declaration of Competing Interest

The authors declare that they have no known competing financial interests or personal relationships that could have appeared to influence the work reported in this paper.

Data availability

Additional data is provided in the supporting information file

Acknowledgement

We thank Duncan Lloyd (Coriole Vineyards) for the donation and process of Sauvignon blanc grapes as well as the participation in the informal benchtop taste panel. Eveline Bartowsky (Lallemand, Edwardstown, SA, Australia) is acknowledged for the donation of Sauvy yeast. Sue Maffei (Commonwealth Scientific and Industrial Research Organisation) is thanked for the help with chiral analysis of thiols. We acknowledge University of Adelaide colleagues including Claire Armstrong for the help with the sensory study and use of the Aqualog instrument, Ruchira Ranaweera for assistance with Aqualog data analysis, Susan Bastian and Pietro Previtali for the participation in the informal benchtop taste panel, Nick van Holst for the assistance with organic acids analysis, and Renata Ristic for valuable winemaking advice. X.W. is a recipient of the joint scholarship of the University of Adelaide and China Scholarship Council (201806300044) and is supported by a Wine Australia Supplementary Scholarship (WA Ph1803). The Australian Research Council Training Centre for Innovative Wine Production (www.ARCwinecentre.org.au; project number IC170100008) is funded by the Australian Government with additional support from Wine Australia, Waite Research Institute and industry partners. The University of Adelaide is a member of the Wine Innovation Cluster.

Appendix A. Supplementary data

Supplementary data to this article can be found online at https://doi.org/10.1016/j.foodchem.2022.134051.

References

Benkwitz, F., Nicolau, L., Lund, C., Beresford, M., Wohlers, M., & Kilmartin, P. A. (2012). Evaluation of key odorants in Sauvignon blanc wines using three different methodologies. *Journal of Agricultural and Food Chemistry, 60*(25), 6293–6302. https://doi.org/10.1021/jf300914n

Bonnaffoux, H., Roland, A., Schneider, R., & Cavelier, F. (2021). Spotlight on release mechanisms of volatile thiols in beverages. *Food Chemistry, 339*, Article 127628. https://doi.org/10.1016/j.foodchem.2020.127628

Capone, D. L., Barker, A., Pearson, W., & Francis, I. L. (2021). Influence of inclusion of grapevine leaves, rachis and peduncles during fermentation on the flavour and volatile composition of *Vitis vinifera* cv. Shiraz wine. *Australian Journal of Grape and Wine Research, 27*(3), 348–359. https://doi.org/10.1111/ajgw.12489

Capone, D. L., Black, C. A., & Jeffery, D. W. (2012). Effects on 3-mercaptohexan-1-ol precursor concentrations from prolonged storage of Sauvignon blanc grapes prior to crushing and pressing. *Journal of Agricultural and Food Chemistry, 60*(13), 3515–3523. https://doi.org/10.1021/jf300054h

Capone, D. L., Ristic, R., Pardon, K. H., & Jeffery, D. W. (2015). Simple quantitative determination of potent thiols at ultratrace levels in wine by derivatization and high-performance liquid chromatography–tandem mass spectrometry (HPLC-MS/MS) analysis. *Analytical Chemistry, 87*(2), 1226–1231. https://doi.org/10.1021/ac503883s

Capone, D. L., Sefton, M. A., Hayasaka, Y., & Jeffery, D. W. (2010). Analysis of precursors to wine odorant 3-mercaptohexan-1-ol using HPLC-MS/MS: Resolution and quantitation of diastereomers of 3-*S*-cysteinylhexan-1-ol and 3-*S*-glutathionylhexan-1-ol. *Journal of Agricultural and Food Chemistry, 58*(3), 1390–1395. https://doi.org/10.1021/jf903720w

Capone, D. L., Sefton, M. A., & Jeffery, D. W. (2011). Application of a modified method for 3-mercaptohexan-1-ol determination to investigate the relationship between free thiol and related conjugates in grape juice and wine. *Journal of Agricultural and Food Chemistry, 59*(9), 4649–4658. https://doi.org/10.1021/jf200116q

Chen, L., Capone, D. L., & Jeffery, D. W. (2018). Chiral analysis of 3-sulfanylhexan-1-ol and 3-sulfanylhexyl acetate in wine by high-performance liquid chromatography–tandem mass spectrometry. *Analytica Chimica Acta, 998*, 83–92. https://doi.org/10.1016/j.aca.2017.10.031

Chen, L., Capone, D. L., Nicholson, E. L., & Jeffery, D. W. (2019). Investigation of intraregional variation, grape amino acids, and pre-fermentation freezing on varietal thiols and their precursors for *Vitis vinifera* Sauvignon blanc. *Food Chemistry, 295*, 637–645. https://doi.org/10.1016/j.foodchem.2019.05.126

Chen, L., Capone, D. L., Tondini, F. A., & Jeffery, D. W. (2018). Chiral polyfunctional thiols and their conjugated precursors upon winemaking with five *Vitis vinifera* Sauvignon blanc clones. *Journal of Agricultural and Food Chemistry, 66*(18), 4674–4682. https://doi.org/10.1021/acs.jafc.8b01806

Christensen, J., Nørgaard, L., Bro, R., & Engelsen, S. B. (2006). Multivariate autofluorescence of intact food systems. *Chemical Reviews, 106*(6), 1979–1994. https://doi.org/10.1021/cr050019q

Coelho, C., Aron, A., Roullier-Gall, C., Gonsior, M., Schmitt-Kopplin, P., & Gougeon, R. D. (2015). Fluorescence fingerprinting of bottled white wines can reveal memories related to sulfur dioxide treatments of the must. *Analytical Chemistry, 87*(16), 8132–8137. https://doi.org/10.1021/acs.analchem.5b00388

Coetzee, C., Brand, J., Emerton, G., Jacobson, D., Silva Ferreira, A. C., & du Toit, W. J. (2015). Sensory interaction between 3-mercaptohexan-1-ol, 3-isobutyl-2-methoxypyrazine and oxidation-related compounds. *Australian Journal of Grape and Wine Research, 21*(2), 179–188. https://doi.org/10.1111/ajgw.12133

Coetzee, C., Van Wyngaard, E., Suklje, K., Silva Ferreira, A. C., & du Toit, W. J. (2016). Chemical and sensory study on the evolution of aromatic and nonaromatic compounds during the progressive oxidative storage of a Sauvignon blanc wine. *Journal of Agricultural and Food Chemistry, 64*(42), 7979–7993. https://doi.org/10.1021/acs.jafc.6b02174

Cordente, A. G., Capone, D. L., & Curtin, C. D. (2015). Unravelling glutathione conjugate catabolism in *Saccharomyces cerevisiae*: The role of glutathione/dipeptide transporters and vacuolar function in the release of volatile sulfur compounds 3-mercaptohexan-1-ol and 4-mercapto-4-methylpentan-2-one. *Applied Microbiology and Biotechnology, 99*(22), 9709–9722. https://doi.org/10.1007/s00253-015-6833-5

Dagan, L., Reillon, F., Roland, A., & Schneider, R. (2014). Development of a routine analysis of 4-mercapto-4-methylpentan-2-one in wine by stable isotope dilution assay and mass tandem spectrometry. *Analytica Chimica Acta, 821*, 48–53. https://doi.org/10.1016/j.aca.2014.03.004

Danner, L., Crump, A. M., Croker, A., Gambetta, J. M., Johnson, T. E., & Bastian, S. E. P. (2018). Comparison of rate-all-that-apply and descriptive analysis for the sensory profiling of wine. *American Journal of Enology and Viticulture, 69*(1), 12–21. https://doi.org/10.5344/ajev.2017.17052

Darriet, P., Tominaga, T., Lavigne, V., Boidron, J.-N., & Dubourdieu, D. (1995). Identification of a powerful aromatic component of *Vitis vinifera* L. var. Sauvignon wines: 4-mercapto-4-methylpentan-2-one. *Flavour and Fragrance Journal, 10*(6), 385–392. https://doi.org/10.1002/ffj.2730100610

Grant-Preece, P. A., Pardon, K. H., Capone, D. L., Cordente, A. G., Sefton, M. A., Jeffery, D. W., & Elsey, G. M. (2010). Synthesis of wine thiol conjugates and labeled analogues: Fermentation of the glutathione conjugate of 3-mercaptohexan-1-ol yields the corresponding cysteine conjugate and free thiol. *Journal of Agricultural and Food Chemistry, 58*(3), 1383–1389. https://doi.org/10.1021/jf9037198

Howell, K. S., Klein, M., Swiegers, J. H., Hayasaka, Y., Elsey, G. M., Fleet, G. H., … de Barros Lopes, M. A. (2005). Genetic determinants of volatile-thiol release by *Saccharomyces cerevisiae* during wine fermentation. *Applied and Environmental Microbiology, 71*(9), 5420–5426. https://doi.org/10.1128/AEM.71.9.5420-5426.2005

King, E. S., Osidacz, P., Curtin, C., Bastian, S. E. P., & Francis, I. L. (2011). Assessing desirable levels of sensory properties in Sauvignon blanc wines – consumer preferences and contribution of key aroma compounds. *Australian Journal of Grape and Wine Research, 17*(2), 169–180. https://doi.org/10.1111/j.1755-0238.2011.00133.x

Nikolantonaki, M., & Waterhouse, A. L. (2012). A method to quantify quinone reaction rates with wine relevant nucleophiles: A key to the understanding of oxidative loss of varietal thiols. *Journal of Agricultural and Food Chemistry, 60*(34), 8484–8491. https://doi.org/10.1021/jf302017j

Pacheco, M., Winckler, P., Marin, A., Perrier-Cornet, J.-M., & Coelho, C. (2022). Multispectral fluorescence sensitivity to acidic and polyphenolic changes in Chardonnay wines – The case study of malolactic fermentation. *Food Chemistry, 370*, Article 131370. https://doi.org/10.1016/j.foodchem.2021.131370

Pinu, F. R., Edwards, P. J. B., Jouanneau, S., Kilmartin, P. A., Gardner, R. C., & Villas-Boas, S. G. (2014). Sauvignon blanc metabolomics: Grape juice metabolites affecting the development of varietal thiols and other aroma compounds in wines. *Metabolomics, 10*, 556–573. https://doi.org/10.1007/s11306-013-0615-9

Ranaweera, R. K. R., Gilmore, A. M., Capone, D. L., Bastian, S. E. P., & Jeffery, D. W. (2021). Authentication of the geographical origin of Australian Cabernet Sauvignon wines using spectrofluorometric and multi-element analyses with multivariate statistical modelling. *Food Chemistry, 335*, Article 127592. https://doi.org/10.1016/j.foodchem.2020.127592

Roland, A., Vialaret, J., Razungles, A., Rigou, P., & Schneider, R. (2010). Evolution of *S*-cysteinylated and *S*-glutathionylated thiol precursors during oxidation of Melon B. and Sauvignon blanc musts. *Journal of Agricultural and Food Chemistry, 58*(7), 4406–4413. https://doi.org/10.1021/jf904164t

Roncoroni, M., Santiago, M., Hooks, D. O., Moroney, S., Harsch, M. J., Lee, S. A., … Gardner, R. C. (2011). The yeast *IRC7* gene encodes a β-lyase responsible for production of the varietal thiol 4-mercapto-4-methylpentan-2-one in wine. *Food Microbiology, 28*(5), 926–935. https://doi.org/10.1016/j.fm.2011.01.002

Somers, T. C., & Ziemelis, G. (1985). Spectral evaluation of total phenolic components in *Vitis vinifera*: Grapes and wines. *Journal of the Science of Food and Agriculture, 36*(12), 1275–1284. https://doi.org/10.1002/jsfa.2740361212

Sparrow, A. M., Smart, R. E., Dambergs, R. G., & Close, D. C. (2016). Skin particle size affects the phenolic attributes of Pinot noir wine: Proof of concept. *American Journal of Enology and Viticulture, 67*(1), 29–37. https://doi.org/10.5344/ajev.2015.15055

Suklje, K., & Čuš, F. (2021). Modulation of Welschriesling wine volatiles through the selection of yeast and lactic acid bacteria. *OENO One, 55*(3), 245–260. https://doi.org/10.20870/oeno-one.2021.55.3.4563

Swiegers, J. H., Kievit, R. L., Siebert, T., Lattey, K. A., Bramley, B. R., Francis, I. L., … Pretorius, I. S. (2009). The influence of yeast on the aroma of Sauvignon blanc wine. *Food Microbiology, 26*(2), 204–211. https://doi.org/10.1016/j.fm.2008.08.004

Swiegers, J. H., Willmott, R., Hill-Ling, A., Capone, D. L., Pardon, K. H., Elsey, G. M., Howell, K. S., de Barros Lopes, M. A., Sefton, M. A., Lilly, M., & Pretorius, I. S. (2006). Modulation of volatile thiol and ester aromas by modified wine yeast. In W. L. P. Bredie & M. A. Petersen (Eds.), *Developments in Food Science* (pp. 113-116). Elsevier. 10.1016/S0167-4501(06)80027-0.

Takase, H., Sasaki, K., Kiyomichi, D., Kobayashi, H., Matsuo, H., & Takata, R. (2018). Impact of *Lactobacillus plantarum* on thiol precursor biotransformation leading to production of 3-sulfanylhexan-1-ol. *Food Chemistry, 259*, 99–104. https://doi.org/10.1016/j.foodchem.2018.03.116

Tominaga, T., Niclass, Y., Frerot, E., & Dubourdieu, D. (2006). Stereoisomeric distribution of 3-mercaptohexan-1-ol and 3-mercaptohexyl acetate in dry and sweet white wines made from *Vitis vinifera* (Var. Sauvignon blanc and Semillon). *Journal of Agricultural and Food Chemistry, 54*(19), 7251–7255. https://doi.org/10.1021/jf061566v

Tristezza, M., di Feo, L., Tufariello, M., Grieco, F., Capozzi, V., Spano, G., … Grieco, F. (2016). Simultaneous inoculation of yeasts and lactic acid bacteria: Effects on fermentation dynamics and chemical composition of Negroamaro wine. *LWT - Food Science and Technology, 66*, 406–412. https://doi.org/10.1016/j.lwt.2015.10.064

Wang, J., Capone, D. L., Wilkinson, K. L., & Jeffery, D. W. (2016). Chemical and sensory profiles of rosé wines from Australia. *Food Chemistry, 196*, 682–693. https://doi.org/10.1016/j.foodchem.2015.09.111

Wang, X., Capone, D. L., Kang, W., Roland, A., & Jeffery, D. W. (2022). Impact of accentuated cut edges (ACE) technique on volatile and sensory profiles of Shiraz wines. *Food Chemistry, 372*, Article 131222. https://doi.org/10.1016/j.foodchem.2021.131222

Wang, X., Capone, D. L., Roland, A., & Jeffery, D. W. (2021). Chiral analysis of *cis*-2-methyl-4-propyl-1,3-oxathiane and identification of *cis*-2,4,4,6-tetramethyl-1,3-oxathiane in wine. *Food Chemistry, 357*, Article 129406. https://doi.org/10.1016/j.foodchem.2021.129406

Wang, X., Chen, L., Capone, D. L., Roland, A., & Jeffery, D. W. (2020). Evolution and correlation of *cis*-2-methyl-4-propyl-1,3-oxathiane, varietal thiols, and acetaldehyde during fermentation of Sauvignon blanc juice. *Journal of Agricultural and Food Chemistry, 68*(32), 8676–8687. https://doi.org/10.1021/acs.jafc.0c03183

Wilson, C., Brand, J., du Toit, W., & Buica, A. (2019). Matrix effects influencing the perception of 3-mercaptohexan-1-ol (3MH) and 3-mercaptohexyl acetate (3MHA) in different Chenin Blanc wines by Projective Mapping (PM) with Ultra Flash profiling (UFP) intensity ratings. *Food Research International, 121*, 633–640. https://doi.org/10.1016/j.foodres.2018.12.032

Appendix A: Supplementary data

Impact of accentuated cut edges, yeast strain, and malolactic fermentation on chemical and sensory profiles of Sauvignon blanc wine

Xingchen Wang,[a] Dimitra L. Capone,[a,b] Aurélie Roland,[c] David W. Jeffery[a,b,*]

[a] Department of Wine Science and Waite Research Institute, The University of Adelaide (UA), PMB 1, Glen Osmond, SA 5064, Australia

[b] Australian Research Council Training Centre for Innovative Wine Production, UA, PMB 1, Glen Osmond, SA 5064, Australia

[c] SPO, Univ Montpellier, INRAE, Institut Agro, Montpellier, France

Corresponding author

E-mail address: david.jeffery@adelaide.edu.au (D.W. Jeffery)

Table of Contents

A.1 Supplementary Experimental Details

A.1.1 Winemaking protocols

Fruit was transferred to a commercial winery within an hour of being harvested and was crushed using a conventional crusher (Miller MC250) with the addition of 50 mg/L of SO_2 as a solution of potassium metabisulfite (PMS, Laffort, Woodville North, SA, Australia). A single lot of conventionally crushed grape must (100 kg, NoACE) with total soluble solids (TSS) of 21.0 °Brix, pH of 3.4, titratable acidity (TA) of 4.1 g/L, and yeast assimilable nitrogen (YAN) of 175 mg/L was retained and another single lot of 100 kg portion of crushed grape must underwent processing with a Della Toffola Maceration Accelerator (Della Toffola, Treviso, Italy), yielding ACE treatment must with TSS of 21.9 °Brix, pH of 3.4, titratable acidity (TA) of 4.6 g/L, and 182 mg/L YAN. Replication of this processing by the winery was not possible due to commercial imperatives. Both must parcels were transferred to the experimental facility within an hour and underwent cold maceration at 5 °C for 21 h. After maceration, grape must from each processing treatment was pressed with a water-bag press at 200 kPa for 10 min before being cold settled at 5 °C overnight. Clear juice was racked and each 3.2 L of juice was dispatched into a 5 L glass fermenter fitted with an airlock. Two strains of commercial yeast, namely VIN13 (Winequip, Dudley Park, SA, Australia) and Sauvy (Lallemand, Edwardstown, SA, Australia), selected for their ability to release varietal thiols, were activated according to the manufacturers' instructions and inoculated at 300 mg/L, yielding four treatments: ACE_VIN13_NoMLF (AVNM), ACE_Sauvy_NoMLF (ASNM), NoACE_VIN13_NoMLF (NAVNM), and NoACE_Sauvy_NoMLF (NASNM). Fermentations were conducted at 16–18 °C in a temperature-controlled room and 48 h after yeast inoculation, *Oenococcus oeni* (Lalvin VP41, Lallemand, Edwardstown, SA, Australia) was inoculated into half of the abovementioned treatments at a rate of 15 mg/L, resulting in an additional four treatments: ACE_VIN13_MLF (AVM), ACE_Sauvy_MLF (ASM), NoACE_VIN13_MLF (NAVM), and NoACE_Sauvy_MLF (NASM). All alcoholic and MLF fermentation treatments were conducted in triplicate.

Specific gravity was measured with a hydrometer (EasyDens, Anton Paar, Graz, Austria) during alcoholic fermentation until the value was below 0.994 and remained constant. MLF was monitored by measuring malic acid and acetic acid weekly with an L-malic acid enzyme assay kit (K-LMALQR, Megazyme, Deltagen, Kilsyth, Victoria, Australia) and an acetic acid enzyme assay kit (K-ACETAF, Megazyme), respectively, until malic acid was undetectable for MLF treatments. At the end of alcoholic or malolactic fermentation, fermenters were settled at 4 °C overnight before being racked into 2 L narrow-necked glass flagons with the addition of 50 mg/L of SO_2 (as PMS solution). TA was adjusted to 7.0 g/L as necessary with a 1 M solution of tartaric acid (Winequip, Dudley Park, SA, Australia). Wines were stored at 4 °C for 3 weeks before being bottled in 375 mL bottles under screwcap and then stored at a 16 °C in the dark for 4 months until sensory analysis.

A.1.2 Sensory study of Sauvignon blanc wines by rate-all-that-apply (RATA)

During the formal sensory study, a panel of 41 regular wine consumers was recruited, comprising 25 females and 16 males aged from 18 to over 65, with 31 panellists having consumed wine at least once a week. Twenty-seven panellists either held a wine-related qualification (e.g., Wine and Spirit Education Trust, sommelier or tertiary level such as oenology) or worked in wine industry, meaning they are wine experts according to Parr et al. (2002). Wine samples (25 mL) were served in

a single session in coded, clear ISO XL5 glasses covered by glass lids, with Red Jade software used to randomise the serving order. Breaks (1-min between samples and a 5-min after every four samples) were enforced and crackers and water were available for panellists to cleanse their palate. Panellists were provided with a list of forty-nine attributes, including aroma, mouthfeel, and aftertaste attributes (Table A.2) to choose from using a 7-point scale (from "extremely low" = 1 to "extremely high" = 7), with those that were not perceived being left blank.

A.1.3 Statistical analysis

Three-way analysis of variance **(**ANOVA) was applied using SPSS (version 27, IBM, Armonk, NY, USA) to explore the impact of the three factors and their interactions (crushing method × yeast strain × malolactic fermentation) on parameters related to varietal thiols in wines at bottling, and these and other volatile compounds at the time of sensory analysis. The simple main effects of significant interactions were further evaluated where necessary. The following analyses were undertaken with XLSTAT (version 2020.1, Addinsoft, Paris, France): repeated-measures ANOVA to assess the evolution of varietal thiol precursors in grape juice during cold maceration; one-way ANOVA followed by Tukey's multiple comparison post-hoc test ($\alpha = 0.05$) for varietal thiol precursor evolution profile and basic chemical parameters; two-way ANOVA for RATA sensory data with treatment as a fixed factor and panellist as a random factor, followed by Fisher's least significant difference post-hoc test ($\alpha = 0.1$); principal component analysis (PCA) using significant sensory and chemical datasets. A-TEEM data was processed using Solo (version 8.7.1, Eigenvector Research, Inc., Manson, WA, USA) following the procedure of (Ranaweera et al., 2021) with the unfolded EEMs being pre-processed by de-cluttering with generalised least squares weighting (GLSW) at 0.2 before robust PCA and parallel factor analysis (PARAFAC), with the latter models assessed with split-half analysis.

Table A.1
Basic composition of Sauvignon blanc wines from different treatments at bottling involving accentuated cut edges, VIN13 or Sauvy yeast strain, and malolactic fermentation.[a]

Parameter	Treatments[b]								*p*-value
	AVNM	ASNM	AVM	ASM	NAVNM	NASNM	NAVM	NASM	
pH	3.44±0.06 a	3.40±0.03 ab	3.36±0.01 b	3.34±0.03 b	3.32±0.03 ab	3.29±0.01 ab	3.31±0.04 b	3.32±0.02 b	0.005
Titratable acidity (g/L)	6.9±0.35 ab	6.8±0.22 abc	7.1±0.20 a	6.7±0.07 abc	6.2±0.05 d	6.3±0.05 cd	6.5±0.05 bcd	6.4±0.05 cd	< 0.0001
Alcohol % v/v	13.0±0.01 b	12.8±0.02 c	12.5±0.01 e	12.1±0.06 f	13.1±0.01 a	12.9±0.03 b	12.6±0.01 d	12.4±0.06 e	< 0.0001
Total SO_2 (mg/L)	89.3±10 ab	73.3±2 ab	84.8±2 a	71.7±1 ab	80.5±1 ab	75.2±15 ab	79.2±1 ab	67.7±1 b	0.024
Free SO_2 (mg/L)	8.27±3.3 c	8.27±3.0 c	18.1±1.8 b	9.87±0.5 c	23.5±1.2 ab	19.6±2.6 b	26.7±2.8 a	26.9±2.6 a	< 0.0001
Glucose (g/L)	0.04±0.03 c	0.07±0.01 b	0.02±0.00 cd	0.01±0.00 d	0.02±0.00 cd	0.17±0.03 a	0.01±0.01 d	0.03±0.01 cd	< 0.0001
Fructose (g/L)	0.54±0.54 ab	0.85±0.11 a	0.02±0.03 c	0.50±0.14 ab	0.32±0.05 bc	0.87±0.16 a	0.01±0.01 c	0.18±0.04 bc	< 0.0001
Glycerol (g/L)	7.5±0.06 e	8.8±0.01 a	7.0±0.02 g	7.9±0.04 c	7.6±0.02 e	8.5±0.04 b	7.1±0.02 f	7.7±0.05 d	< 0.0001
Malic acid (g/L)	2.2±0.1 a	1.5±0.03 b	0.0±0.0 d	0.0±0.03 d	2.1±0.14 a	1.3±0.02 c	0.0±0.03 d	0.0±0.0 d	< 0.0001
Tartaric acid (g/L)	2.2±0.03 g	3.0±0.02 d	2.6±0.08 f	2.8±0.03 e	2.8±0.01 e	3.6±0.01 a	3.2±0.01 c	3.4±0.01 b	< 0.0001
Citric acid (g/L)	0.27±0.01 a	0.26±0.02 ab	0.24±0.01 bc	0.09±0.01 e	0.24±0.01 c	0.23±0.01 c	0.20±0.0 d	0.06±0.01 f	< 0.0001
Lactic acid (g/L)	0.07±0.01 c	0.05±0.03 c	3.65±0.35 a	3.14±0.39 b	0.06±0.01 c	0.05±0.01 c	3.34±0.41 ab	3.01±0.34 b	< 0.0001
Acetic acid (g/L)	0.52±0.02 bc	0.45±0.04 bc	0.60±0.06 ab	0.71±0.08 a	0.44±0.02 bc	0.37±0.04 c	0.48±0.05 bc	0.49±0.23 bc	< 0.0001

[a] Data are presented as mean ± standard deviation (n = 6 from duplicate measurement of three biological replicates). Different letters in the same row indicate significant differences between means according to one-way ANOVA with Tukey's post hoc test ($\alpha = 0.05$).
[b] AVNM, ACE_VIN13_NoMLF; ASNM, ACE_Sauvy_NoMLF; NAVNM, NoACE_VIN13_NoMLF; NASNM, NoACE_Sauvy_NoMLF; AVM, ACE_VIN13_MLF; ASM, ACE_Sauvy_MLF; NAVM, NoACE_VIN13_MLF; NASM, NoACE_Sauvy_MLF. Titratable acidity is expressed as equivalent to tartaric acid.

Table A.2
Mean score and *p*-value for each attribute of Sauvignon blanc wines evaluated on a 7-point scale by RATA panellists.[a]

Attribute	Treatment[b]								*p*-value
	AVNM	ASNM	AVM	ASM	NAVNM	NASNM	NAVM	NASM	
Aroma									
Tropical fruit	3.95 ab	4.22 a	3.22 d	3.46 bcd	3.85 abc	3.39 cd	3.61 bcd	3.24 d	**0.03**
Passion fruit	3.22	3.41	3.10	3.49	3.56	3.39	3.00	3.24	0.76
Grapefruit	2.66 a	2.61 a	2.49 a	1.88 b	2.83 a	2.68 a	2.59 a	2.39 a	**0.05**
Citrus	2.71	2.88	2.80	2.37	3.24	2.63	2.66	2.41	0.14
Apple/pear	2.37	2.07	1.88	1.93	2.24	2.39	1.80	1.59	0.11
Melon	2.27 ab	2.56 a	1.78 bc	1.98 bc	1.76 bc	2.02 bc	2.24 ab	1.54 c	**0.04**
Floral	2.22 bc	2.80 a	1.76 c	2.07 bc	2.27 b	2.05 bc	2.39 ab	2.10 bc	**0.07**
Green/grassy/herbaceous	2.39	2.15	2.41	1.85	2.27	2.02	2.39	2.63	0.32
Chemical	0.88	0.56	0.80	0.88	0.71	1.00	0.80	0.93	0.75
Confectionery	1.00	1.39	0.88	1.02	0.80	1.34	0.80	0.93	0.26
Stone fruits	2.61	2.73	2.12	2.46	2.68	2.80	2.20	2.49	0.33
Honey	1.49 a	1.37 ab	0.73 c	1.39 ab	0.80 c	0.78 c	1.24 ab	1.05 bc	**0.01**
Toffee/caramel/buttery	0.39	1.05	0.85	0.61	0.80	1.00	0.95	0.61	0.12
Nutty	0.46	0.71	0.68	0.71	0.63	0.39	0.76	0.49	0.43
Spice	0.90	0.88	0.68	0.80	0.83	0.63	0.63	0.59	0.71
Sulfidic	0.95 d	0.85 d	2.02 ab	1.54 bc	1.02 cd	2.10 a	0.71 d	1.88 ab	**<0.0001**
Mineral	1.15	1.44	1.68	1.56	1.46	1.49	1.68	1.59	0.67
Bread/yeast/leesy	0.76	1.12	1.44	1.22	0.83	1.00	1.02	1.00	0.23
Cheesy/creamy	0.83	0.68	0.76	1.07	0.56	0.61	0.71	0.68	0.60
Bacon	0.27 bc	0.24 c	0.71 a	0.76 a	0.34 bc	0.51 abc	0.29 bc	0.59 ab	**0.05**
Blackcurrant bud/sweaty	1.29	1.37	1.51	1.49	1.10	1.27	1.39	1.51	0.79
Flavour									
Tropical fruit	3.61 ab	4.02 a	2.63 d	3.20 bc	3.27 bc	3.29 bc	3.51 b	2.83 cd	**<0.001**
Passion fruit	2.88	2.85	3.17	2.95	2.80	3.34	2.90	2.68	0.59
Grapefruit	2.78	2.39	2.56	2.66	3.00	2.54	2.73	2.71	0.74
Citrus	3.02 bcd	2.95 cd	3.63 a	2.78 d	3.49 ab	2.98 cd	3.32 abc	3.44 abc	**0.04**
Apple/pear	1.71	2.32	1.93	1.73	2.07	2.27	1.80	1.66	0.13
Melon	1.34	1.95	1.98	1.95	1.54	2.02	1.44	1.83	0.16
Floral	1.90 ab	2.12 a	1.61 bc	1.46 c	1.51 bc	1.46 c	1.51 bc	1.34 c	**0.06**
Green/grassy/herbaceous	2.29	2.17	2.02	2.17	1.85	1.83	1.90	2.02	0.81
Chemical	0.95	0.85	0.83	0.80	0.59	0.90	0.66	0.88	0.67
Confectionery	1.32 a	1.32 a	0.85 bc	0.90 bc	1.05 ab	0.61 c	0.98 abc	0.88 bc	**0.06**
Stone fruit	2.39 b	3.17 a	1.98 b	2.22 b	2.41 b	2.00 b	2.27 b	2.15 b	**<0.01**
Honey	1.12 bc	1.63 a	0.83 bcd	1.00 bcd	0.78 cd	0.95 bcd	1.20 b	0.71 d	**0.01**
Toffee/caramel/buttery	0.59	0.95	0.51	0.63	0.56	0.85	0.46	0.49	0.39
Nutty	0.44	0.66	0.59	0.71	0.54	0.59	0.61	0.49	0.89
Spice	0.90	0.68	0.80	0.90	0.68	0.73	0.88	0.78	0.76

Table A.2 contd.

Attribute	Treatment[b]								*p*-value
	AVNM	ASNM	AVM	ASM	NAVNM	NASNM	NAVM	NASM	
Sulfidic	1.12 bcd	0.80 cd	1.78 a	1.15 bc	1.07 bcd	1.46 ab	0.66 d	1.46 ab	**< 0.01**
Mineral	1.29 b	1.22 b	1.83 a	1.56 ab	1.37 b	1.83 a	1.29 b	1.39 b	**0.07**
Bread/yeast/leesy	0.66	1.05	1.10	0.88	0.78	0.88	1.05	1.07	0.52
Cheesy/creamy	0.68	0.71	0.59	0.68	0.39	0.80	0.71	0.54	0.65
Bacon	0.34	0.29	0.44	0.37	0.22	0.22	0.20	0.59	0.13
Blackcurrant bud/sweaty	1.20	1.15	1.20	0.95	0.85	0.88	1.10	1.39	0.44
Taste									
Balance	3.22	3.27	3.32	3.29	3.32	3.54	3.07	3.59	0.33
Acidity	3.80 cd	3.71 d	4.07 abc	3.76 cd	4.39 a	4.05 bc	4.32 ab	4.27 ab	**< 0.01**
Alcohol	3.61	3.24	3.61	3.39	3.29	3.29	3.24	3.32	0.25
Sweet	3.15 a	3.41 a	2.73 b	2.76 b	2.76 b	2.66 bc	2.63 bc	2.41 c	**< 0.0001**
Bitter	2.66 bc	2.00 d	2.83 ab	2.80 ab	3.15 a	2.34 cd	2.66 bc	2.29 cd	**< 0.0001**
Aftertaste									
Length of fruity	3.98 b	4.37 a	3.76 b	3.90 b	3.83 b	3.88 b	3.93 b	3.68 b	**0.10**
Length of non-fruity	3.90 a	3.34 c	3.90 a	3.88 a	3.78 ab	3.56 abc	3.71 abc	3.41 bc	**0.06**

[a] Different letters in the same row indicate significant differences in mean attribute scores (two-way ANOVA followed by Fisher's least significant difference, $\alpha = 0.1$). Bolded *p*-values indicate significant differences at $\alpha = 0.1$. "Aroma" and "Flavour" refer respectively to the orthonasal and retronasal perception of sensory attributes.
[b] AVNM, ACE_VIN13_NoMLF; ASNM, ACE_Sauvy_NoMLF; NAVNM, NoACE_VIN13_NoMLF; NASNM, NoACE_Sauvy_NoMLF; AVM, ACE_VIN13_MLF; ASM, ACE_Sauvy_MLF; NAVM, NoACE_VIN13_MLF; NASM, NoACE_Sauvy_MLF.

Table A.3
Results of three-way ANOVA conducted with different parameters at bottling for Sauvignon blanc wines from different treatments.[a]

Parameter	Crushing method (CM)	Yeast strain (YS)	Malolactic fermentation (MLF)	CM × YS[b]	CM × MLF[b]	YS ×MLF[b]	CM ×YS × MLF[c]
Total phenolics	< 0.001	< 0.001	< 0.001	< 0.001	< 0.001	< 0.001	**< 0.001** (Fig. A.3 & 4)
Hydroxycinnamates	< 0.001	< 0.001	< 0.001	0.866	**0.009** (Fig. A.3 & A.5)	**< 0.001** (Fig. A3 & A .5)	0.782
GSH-3-SH	< 0.001	< 0.001	< 0.001	**< 0.001** (Fig. 1 & A.8)	**0.013** (Fig. 1 & A8)	**0.021** (Fig. 1 & A.8)	0.292
Cys-3-SH	0.975	0.035	0.014	**0.008** (Fig. 1 & A.8)	0.347	0.666	0.274
(3*S*)-3-SH	< 0.001	< 0.001	< 0.001	**< 0.001** (Fig. 2)	0.581	**0.023** (Fig. 2)	0.466
(3*R*)-3-SH	< 0.001	< 0.001	< 0.001	**< 0.001** (Fig. 2)	0.566	**< 0.001** (Fig. 2)	0.172
(3*S*)-/(3*R*)-3-SH ratio	< 0.001	0.006	0.014	0.517	0.965	0.097	0.697
(3*S*)-3-SHA	< 0.001	< 0.001	< 0.001	0.701	< 0.001	< 0.001	**0.016** (Fig. 3)
(3*R*)-3-SHA	< 0.001	< 0.001	0.549	0.622	**0.003** (Fig. 3)	0.122	0.104
(3*S*)-/(3*R*)-3-SHA ratio	0.191	0.608	< 0.001	0.794	0.169	**0.001** (Fig. A.9)	0.846
Apparent molar conversion yield of precursors to thiols	< 0.001	< 0.001	< 0.001	**< 0.001** (Fig. A.10)	0.523	**0.049** (Fig. A.10)	0.621
Apparent molar conversion yield of 3-SH to 3-SHA	0.078	< 0.001	< 0.001	**0.006 (**Fig. A.11)	**< 0.001** (Fig. A.11)	**< 0.001** (Fig. A.11)	0.087
4-MSP	< 0.001	< 0.001	< 0.001	**0.036** (Fig. 4)	**< 0.001** (Fig. 4)	**< 0.001** (Fig. 4)	0.243

[a] *p*-Value of each three-way ANOVA model. Bolded *p*-values indicate significant two-way or three-way interactions, with the location of results showing the simple main effects given in brackets.
[b] Two-way interactions between different factors.
[c] Three-way interactions between the factors.

Table A.4
Mean concentration and standard deviation of volatile compounds at the time of sensory analysis in Sauvignon blanc wines that underwent different treatments.[a]

Compound	Concentration (µg/L)[b]								ODT[c]	OAV[d]
	AVM	ASM	NAVM	NASM	AVNM	ASNM	NAVNM	NASNM		
Varietal thiols (ng/L)										
(3*S*)-3-SH	819±36	830±39	684±1	591±27	704±5	640±16	565±51	396±36	60[1]	7–14
(3*R*)-3-SH	802±11	868±12	677±14	608±16	751±28	683±10	576±11	415±31	50[1]	8–17
(3*S*)-3-SHA	23±1	15±1	19±1	11±1	23±3	14±1	17±1	9±0	2.5[1]	4–9
(3*R*)-3-SHA	13±1	10±1	10±1	8±1	13±2	8±1	10±1	5±0	9[1]	0.6–1.4
4-MSP	60±2	116±6	61±4	105±1	74±7	143±37	72±9	90±2	0.8[1]	76–179
Isoprenoids										
Linalool	12.5±0.3	16.4±0.6	12.1±0.4	14.8±0.5	12.8±1	15.0±0.9	12.3±0.4	14.8±0.5	15[2]	0.8–1.1
α-Terpineol	2.2±0.2	5.0±0.3	2.0±0.3	4.4±0.3	2.2±0.6	2.1±0.2	1.5±0.2	2.1±0.2	250[3]	<0.1
β-Damascenone	4.2±0.4	4.4±0.1	3.5±0.1	3.9±0.1	4.1±0.3	4.5±0.2	3.3±0.2	4.9±0.4	0.05[2]	66–98
C_6 alcohols										
1-Hexanol (mg/L)	2.90±0.08	3.16±0.08	2.78±0.03	2.92±0.31	2.84±0.08	3.12±0.06	2.84±0.04	3.08±0.05	8.0[2]	0.3–0.4
(*E*)-3-Hexen-1-ol	68.7±2	67.7±1	62.6±2	59.6±4	66.3±3	67.0±1	63.9±1	63.0±1	1550[4]	<0.1
(*Z*)-3-Hexen-1-ol	163±8	156±13	157±4	151±13	171±2	180±5	163±4	158±6	400[2]	0.4–0.5
Ethyl esters										
Ethyl propanoate	307±8	361±9	315±10	300±3	310±12	321±7	286±7	276±10	2100[5]	0.1–0.2
Ethyl 2-methylpropanoate	199±2	196±2	201±2	201±1	191±4	189±2	196±2	197±1	5600[5]	<0.1
Ethyl butanoate	137±6	42±6	121±13	40±3	117±14	19±10	79±6	7.4±3	600[5]	≤0.2
Ethyl 2-methylbutanoate	9.9±0.3	11.2±0.2	10.3±0.3	11.7±0.6	8.5±0.5	9.5±0.3	9.5±0.3	10.9±0.4	1[2]	8.5–11
Ethyl 3-methylbutanoate	13.9±0.6	14.3±0.4	14.4±0.3	15.6±0.5	11.2±0.5	11.9±0.6	12.9±0.5	14.3±0.4	3[2]	3.7–5.3
Ethyl hexanoate	493±62	171±10	468±27	195±11	489±49	127±24	405±13	97±5	14[3]	7–35
Ethyl octanoate	596±47	188±8	530±20	217±9	518±18	199±11	491±22	186±5	20[6]	9–30
Ethyl decanoate	258±14	210±1	252±3	226±3	290±5	240±3	283±9	229±2	200[3]	1.1–1.5
Ethyl 2-phenylacetate	1.5±0.02	1.6±0.02	1.5±0.03	1.6±0.02	1.4±0.01	1.6±0.01	1.4±0.01	1.5±0.01	650[7]	<0.1
Ethyl lactate (mg/L)	230±39	158±10	229±10	160±4	n.d.	n.d.	n.d.	n.d.	146[5]	1.1–1.6

Table A.4 contd.

Compound	Concentration (µg/L)[b]								ODT[c]	OAV[d]
	AVM	ASM	NAVM	NASM	AVNM	ASNM	NAVNM	NASNM		
Acetates										
Ethyl acetate (mg/L)	29.7±2	26.1±1	31.3±1	32.9±1	24.9±1	7.24±1	22.4±1	8.11±0.3	15[5]	0.5–2.2
Hexyl acetate	34.0±3	18.4±2	26.5±1	21.9±1	46.5±3	49.8±3	33.1±1	32.4±3	670[8]	≤0.1
2-Phenylethyl acetate	131±17	139±5	101±2	134±4	125±3	196±5	106±2	155±7	250[2]	0.4–0.8
Higher alcohols										
1-Propanol (mg/L)	12.9±0.3	15.2±0.5	10.5±0.5	14.5±0.7	12.6±0.5	17.0±0.4	10.4±0.4	13.4±0.6	50[9]	0.2–0.3
2-Methyl-1-propanol (mg/L)	40.2±1	28.4±5	38.0±1	32.2±1	40.3±2	29.1±1	37.2±1	30.1±2	40[3]	0.7–1.0
1-Butanol	821±22	837±30	740±39	686±27	742±68	662±23	633±21	576±2	160[5]	3.6–5.2
3-Methyl-1-butanol (mg/L)	237±3	243±4	231±5	243±6	238±6	240±6	223±6	235±2	30[2]	7.4–8.1
2-Ethyl-1-hexanol	4.1±0.3	4.0±0.1	4.7±0.4	5.4±1.0	5.2±1.1	5.5±0.9	5.0±0.5	5.6±1.3	270[10]	<0.1
1-Octanol	4.4±0.3	6.1±0.3	3.4±0.3	8.4±0.6	4.1±0.2	4.9±0.2	2.8±0.2	3.8±0.3	0.8[11]	3.5–10.5
Benzyl alcohol	361±15	423±13	324±6	418±14	290±4	288±3	265±4	263±4	900000[12]	<0.1
2-Phenylethanol (mg/L)	1.20±0.02	2.13±0.05	1.09±0.03	1.97±0.05	1.20±0.03	2.22±0.04	1.09±0.02	1.94±0.07	14[3]	0.1–0.2
Fatty acids										
2-Methylpropanoic acid (mg/L)	1.59±0.07	1.42±0.06	1.49±0.07	1.45±0.04	1.07±0.05	0.97±0.02	0.97±0.03	0.93±0.04	2.3[13]	0.4–0.6
Butanoic acid (mg/L)	1.25±0.03	1.03±0.02	1.14±0.04	1.03±0.04	1.10±0.06	0.94±0.02	1.03±0.02	0.94±0.03	10[2]	0.1
3-Methylbutanoic acid	794±14	799±11	746±21	832±17	714±22	757±11	654±15	753±25	33.4[3]	20–25
Hexanoic acid (mg/L)	2.53±0.10	1.45±0.03	2.31±0.04	1.63±0.04	2.29±0.06	1.57±0.04	2.22±0.04	1.52±0.04	0.42[3]	3.5–6.0
Octanoic acid	59.0±5	31.9±0.4	52.2±2	37.7±1	51.6±1	35.1±1	49.1±0.4	35.4±1	500[3]	0.1
Decanoic acid (mg/L)	1.44±0.16	0.79±0.05	1.07±0.07	0.98±0.03	1.46±0.04	1.11±0.02	1.37±0.04	1.13±0.07	1.0[3]	0.8–1.5

[a] Data are presented as mean ± standard deviation (n = 6 from duplicate measurement of three biological replicates). According to three-way ANOVA, all compounds were significantly influenced by two-way or three-way interactions with the exception of (3*S*)-3-SHA (α = 0.05).

[b] Concentrations are given as µg/L unless specified otherwise in the Compound column. AVNM, ACE_VIN13_NoMLF; ASNM, ACE_Sauvy_NoMLF; NAVNM, NoACE_VIN13_NoMLF; NASNM, NoACE_Sauvy_NoMLF; AVM, ACE_VIN13_MLF; ASM, ACE_Sauvy_MLF; NAVM, NoACE_VIN13_MLF; NASM, NoACE_Sauvy_MLF. n.d., compound not detected.

[c] ODT, odour detection threshold (µg/L for all compounds unless a different concentration unit is specified in the **Compound** column). References used: [1] (Tominaga et al., 2006); [2] (Guth, 1997); [3] (Ferreira et al., 2000); [4] (Waterhouse et al., 2016); [5] (Moyano et al., 2002); [6] (Swiegers et al., 2005); [7] (Burdock, 2010); [8] (Peinado et al., 2004); [9] (Song et al., 2016); [10] (Pino & Queris, 2011); [11] (Etiévant, 1991); [12] (Zea et al., 2012); [13] (Gabrielli et al., 2017).

[d] OAV, odour activity value.

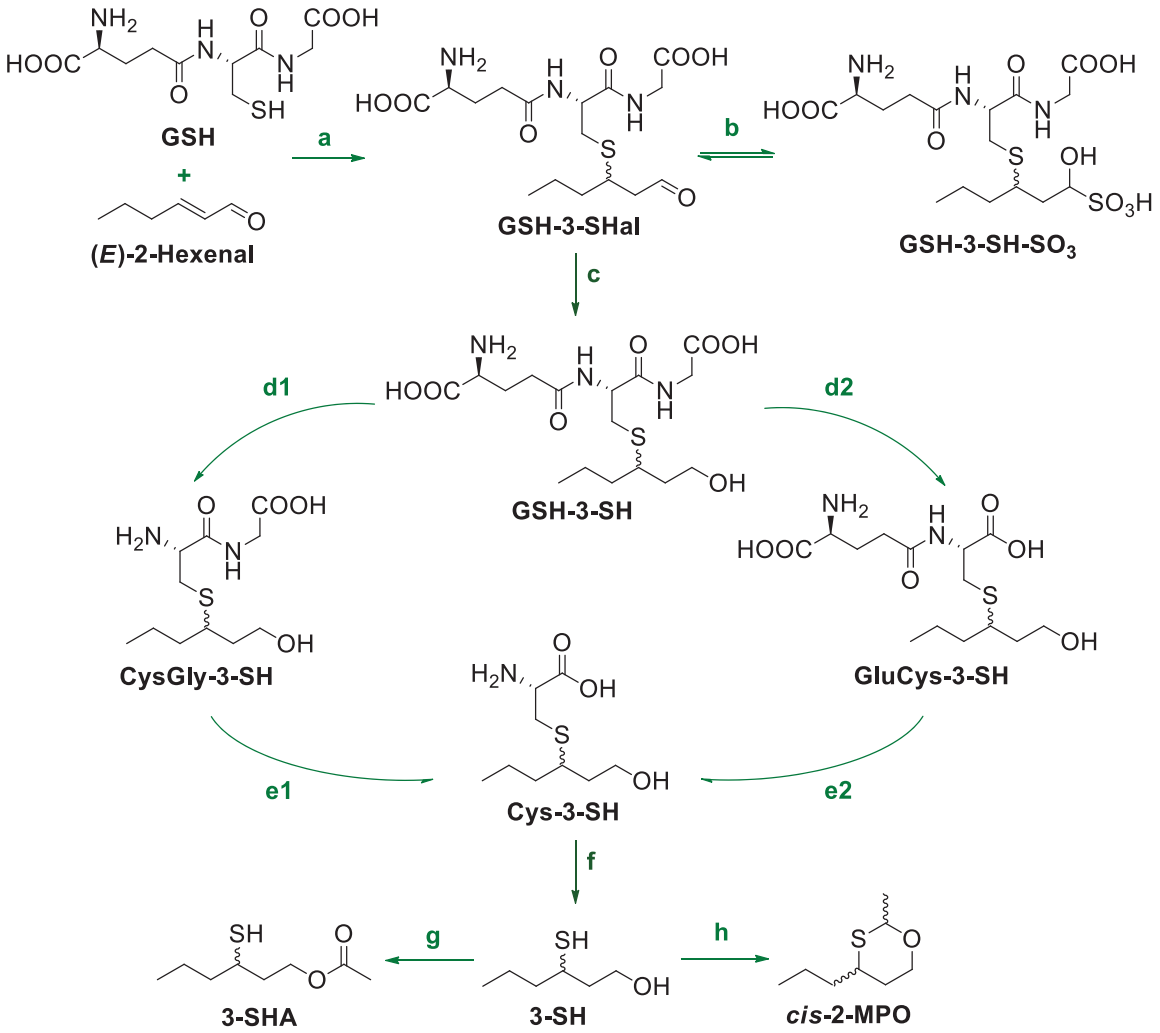

Fig. A.1. Proposed metabolic pathways for the formation of 3-SH precursor diastereomers and fate of subsequently-released 3-SH enantiomers (Bonnaffoux et al., 2017; Capone et al., 2011; Chen et al., 2018; Clark & Deed, 2018; Jeffery, 2016; Peyrot des Gachons et al., 2002; Thibon et al., 2016; Tominaga et al., 1998). Steps: a, conjugation of GSH and (*E*)-2-hexenal catalysed by GST or from chemical reaction; b, interconversion between GSH-3-SHal and GSH-3-SH-SO_3 in the presence of bisulfite; c, enzymatic aldehyde reduction by alcohol dehydrogenase or aldo-keto reductase; d1, degradation of GSH-3-SH to Cysgly-3-SH catalysed by γ-glutamyl-transpeptidase; d2, degradation of GSH-3-SH to GluCys-3-SH catalysed by phytochelatin synthase or carboxypeptidase; e1, degradation of CysGly-3-SH to Cys-3-SH catalysed by carboxypeptidase; e2, degradation of GluCys-3-SH to Cys-3-SH, enzymes unclear; f, release of 3-SH from Cys-3-SH catalysed by yeast carbon-sulfur lyase; g, acetylation of 3-SH catalysed by alcohol acetyltransferase or other potential enzymes; h, formation of *cis*-2-methyl-4-propyl-1,3-oxathiane (*cis*-2-MPO) via condensation of 3-SH and acetaldehyde.

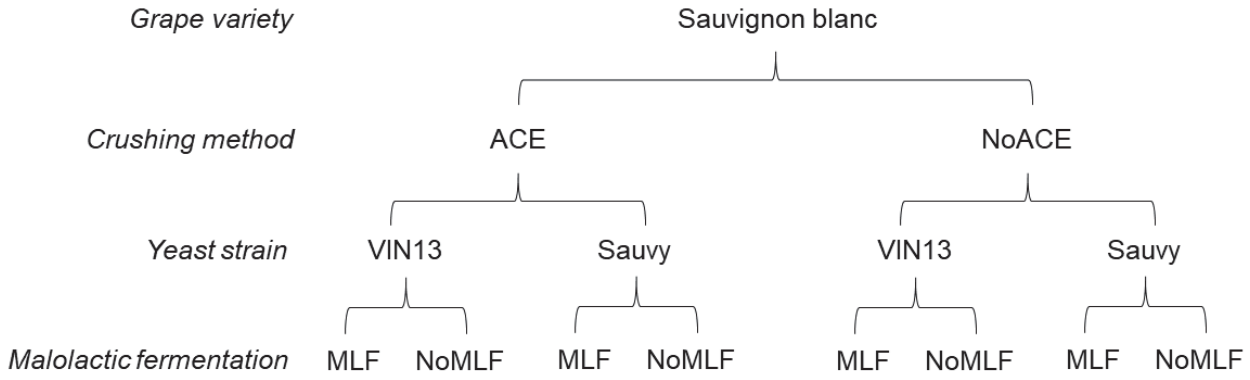

Fig. A.2 Outline of treatments for Sauvignon blanc winemaking trial showing the parameters of grape crushing method (accentuated cut edges (ACE) and conventional crushing method (NoACE)), yeast strain (VIN13 and Sauvy), and with/without malolactic fermentation (MLF and NoMLF). Fermentation of each treatment was conducted in triplicate.

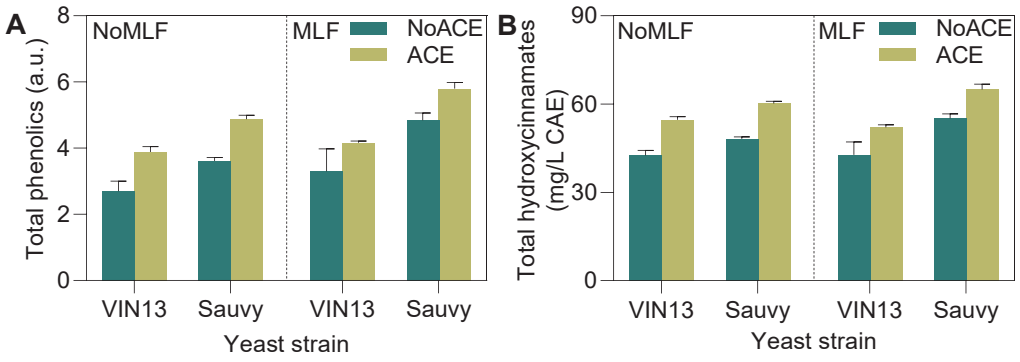

Fig. A.3. Results of (A) total phenolics (a.u.) and (B) hydroxycinnamates (mg/L caffeic acid equivalents, CAE) in Sauvignon blanc wines from different treatments at bottling. Cyan bars show analytes from NoACE treatment and olive bars show analytes from ACE treatment, with error bars representing standard deviation (n = 9 from triplicate measurements obtained for each winemaking replicate). MLF, malolactic fermentation; YS, yeast strain; CM, crushing method.

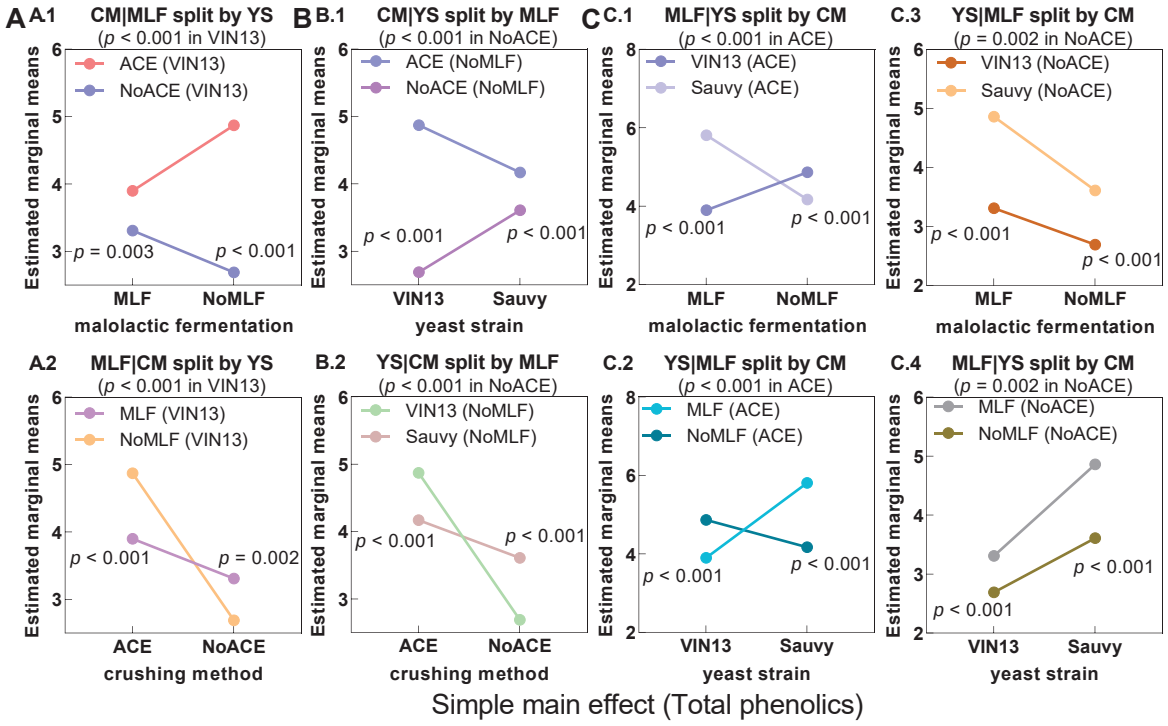

Fig. A.4. Simple main effect plots of significant two-way interactions from three-way ANOVA for total phenolics in Sauvignon blanc wines at bottling showing interaction of (A) crushing method and malolactic fermentation, (B) crushing method and yeast strain, and (C) malolactic fermentation and yeast strain. Abbreviations above each plot represent the significant interactions between factors followed by *p*-values in brackets. MLF, malolactic fermentation; YS, yeast strain; CM, crushing method.

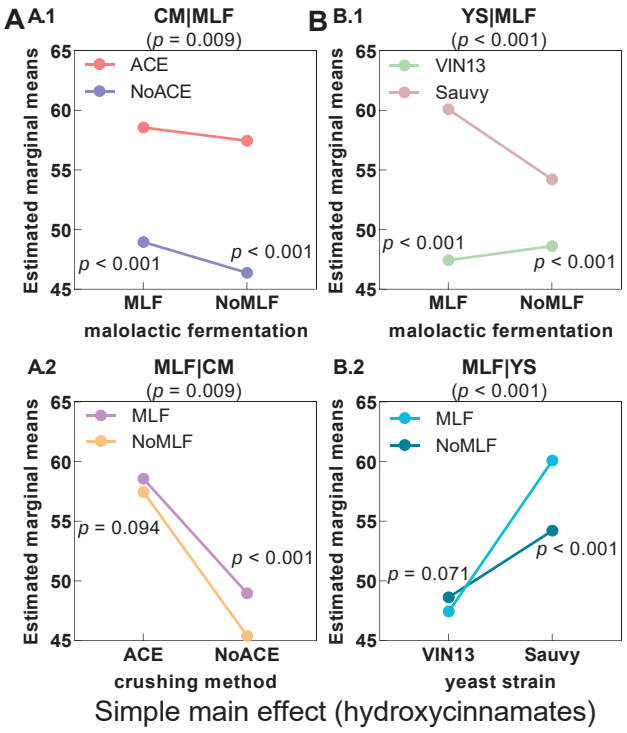

Fig. A.5. Simple main effect plots of significant two-way interactions from three-way ANOVA for hydroxycinnamates in Sauvignon blanc wines at bottling showing interaction of (A) crushing method and malolactic fermentation, and (B) yeast strain and malolactic fermentation. Abbreviations above each plot represent significant interactions between factors followed by *p*-values in brackets. MLF, malolactic fermentation; YS, yeast strain; CM, crushing method.

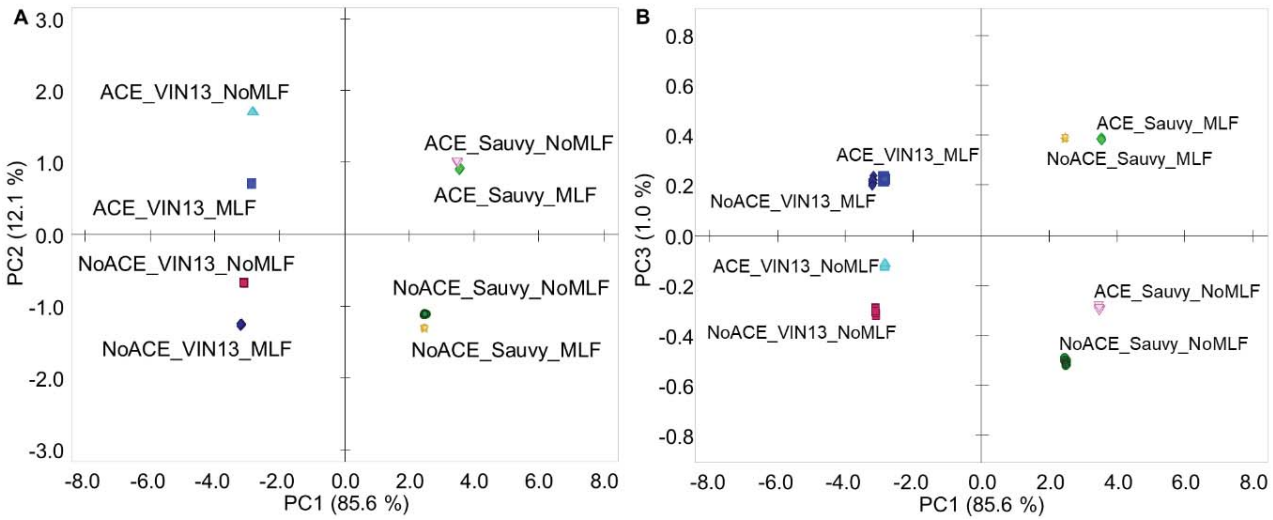

Fig. A.6. PCA scores plots of Sauvignon blanc wines from different treatments according to EEM data showing (A) PC1 and PC2, and (B) PC1 and PC3. Note that the nine data points associated with winemaking (n = 3) and analysis (n = 3) replicates for each treatment are essentially overlapped in the plots.

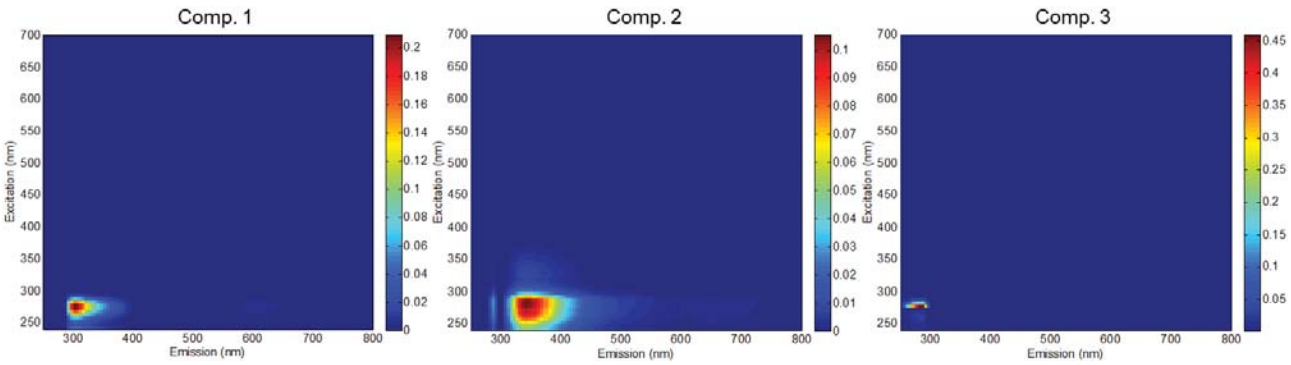

Fig. A.7. EEM contour plots of the PARAFAC model with three components for Sauvignon blanc treatment wines, illustrating the fluorescent properties of typical fluorophores in white wine. Tentative assignments: Comp. 1: Tyrosine; Comp. 2: hydroxycinnamates; Comp. 3: aromatic amino acids.

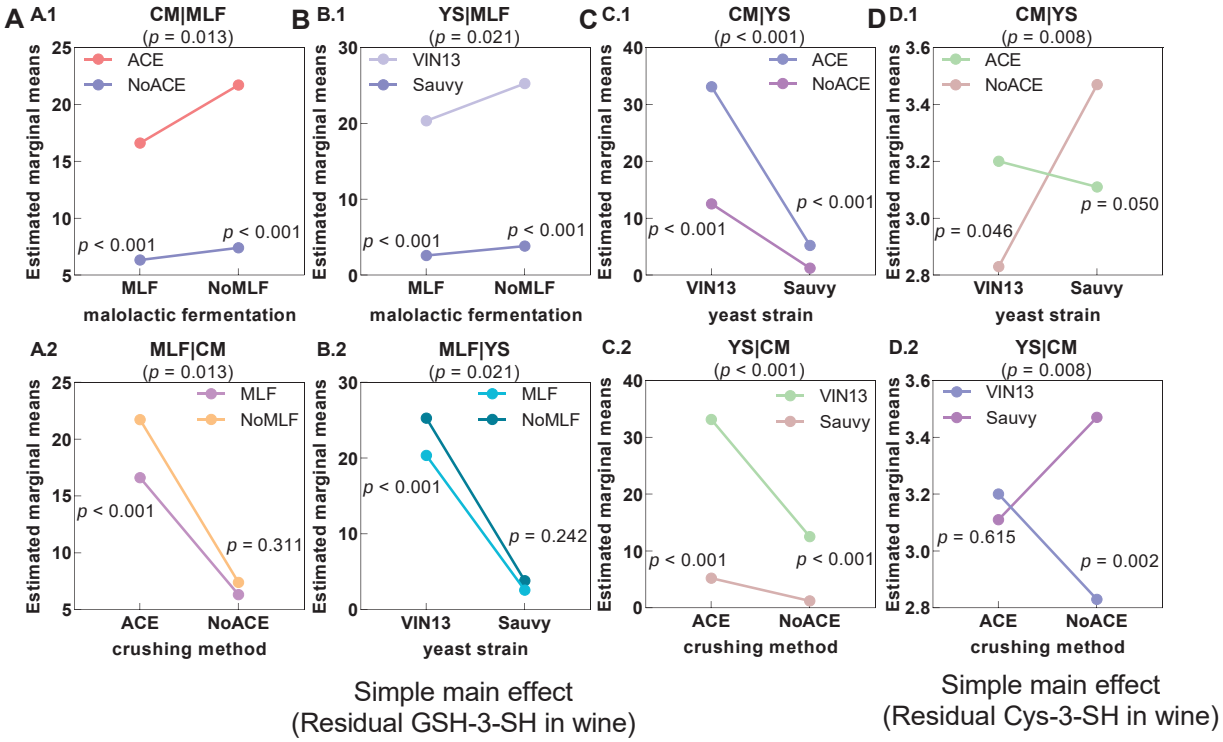

Fig. A.8. Simple main effect plots of significant two-way interactions from three-way ANOVA for residual GSH-3-SH in Sauvignon blanc wines at bottling showing interaction of (A) crushing method and malolactic fermentation, (B) yeast strain and malolactic fermentation, and (C) crushing method and yeast strain; and for residual Cys-3-SH in wines at bottling showing interaction (D) crushing method and yeast strain. Abbreviations above each plot represent significant interactions between factors followed by *p*-values in brackets. MLF, malolactic fermentation; YS, yeast strain; CM, crushing method.

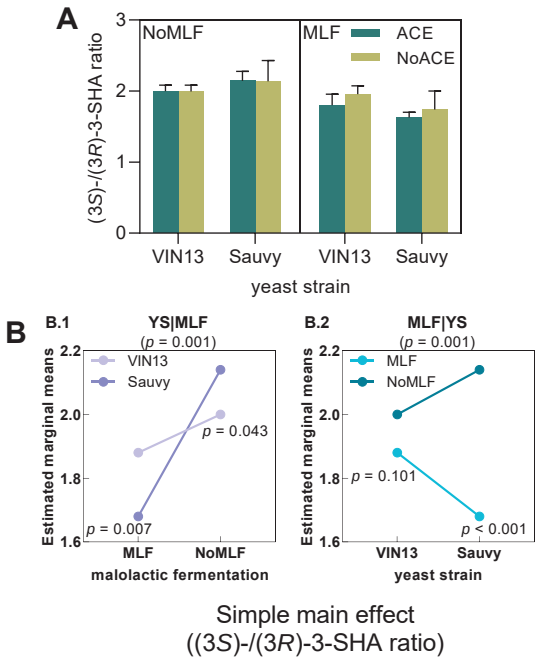

Fig. A.9. Plot showing (A) enantiomeric ratio of (3*S*)-/(3*R*)-3-SHA and simple main effect plots of significant two-way interactions from three-way ANOVA for (3*S*)-/(3*R*)-3-SHA ratios in Sauvignon blanc wines at bottling showing interaction of (B) yeast strain and malolactic fermentation. Cyan bars in A show analytes from NoACE treatment and olive bars show analytes from ACE treatment, with error bars representing standard deviation (n = 6 from duplicate measurement of three biological replicates). Abbreviations above each plot in B represent significant interactions between factors followed by *p*-values in brackets. MLF, malolactic fermentation; YS, yeast strain.

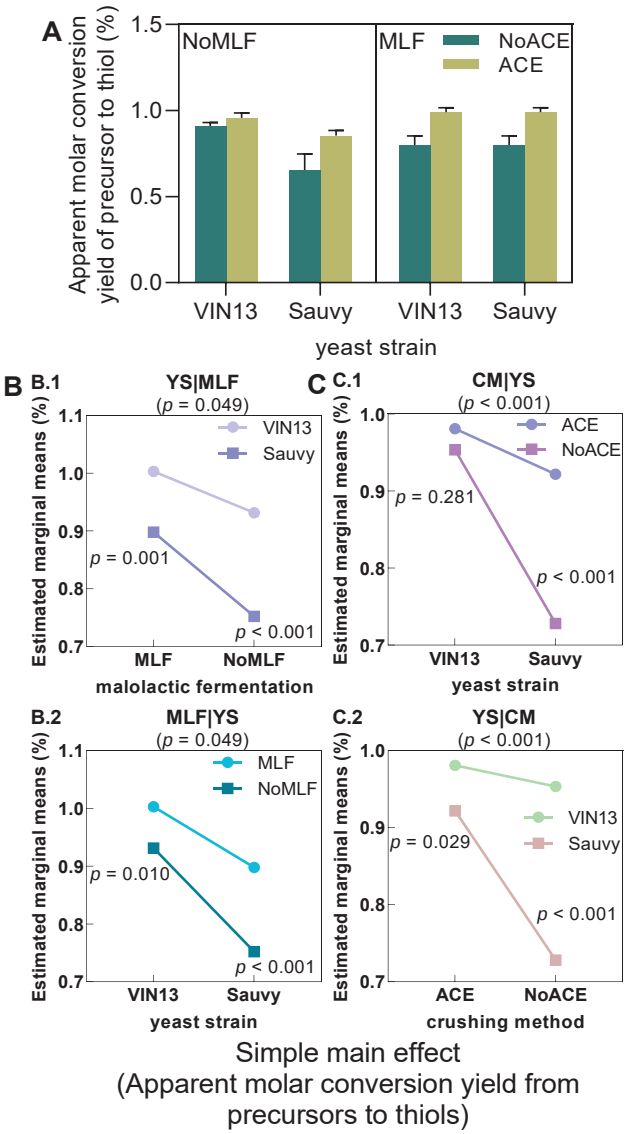

Fig. A.10. Apparent molar conversion yield from (A) thiol precursors to free thiols and simple main effect of significant two-way interactions from three-way ANOVA for conversion yield of precursors to the sum of 3-SH and 3-SHA in Sauvignon blanc wines at bottling showing interaction of (B) yeast strain and malolactic fermentation and (C) crushing method and yeast strain. Cyan bars in A show analyte from NoACE treatment and olive bars show analytes from ACE treatment, with error bars representing standard deviation (n = 6 from duplicate measurement of three biological replicates). Abbreviations above each plot in B and C represent significant two-way interactions between factors followed by *p*-values in brackets. MLF, malolactic fermentation; YS, yeast strain; CM, crushing method.

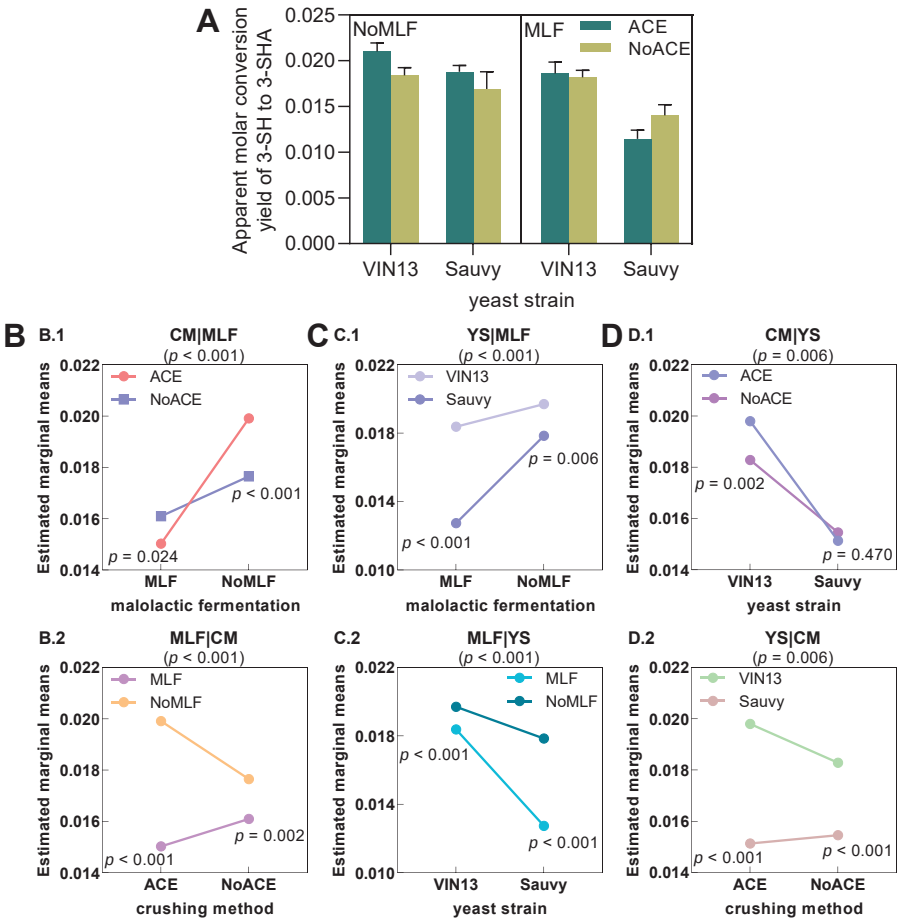

Fig. A.11. Apparent molar conversion yield from (A) 3-SH to 3-SHA and simple main effect of significant two-way interactions from three-way ANOVA for conversion yield of 3-SH to 3-SHA in Sauvignon blanc wines at bottling showing interaction of (B) crushing method and malolactic fermentation, (C) yeast strain and malolactic fermentation and (D) crushing method and yeast strain. Cyan bars in A show analyte from NoACE treatment and olive bars show analytes from ACE treatment, with error bars representing standard deviation (n = 6 from duplicate measurement of three biological replicates). Abbreviations above each plot in B, C, and D represent significant two-way interactions between factors followed by *p*-values in brackets. MLF, malolactic fermentation; YS, yeast strain; CM, crushing method.

References

Bonnaffoux, H., Roland, A., Rémond, E., Delpech, S., Schneider, R., & Cavelier, F. (2017). First identification and quantification of *S*-3-(hexan-1-ol)-γ-glutamyl-cysteine in grape must as a potential thiol precursor, using UPLC-MS/MS analysis and stable isotope dilution assay. *Food Chemistry, 237*, 877-886. https://doi.org/10.1016/j.foodchem.2017.05.116

Burdock, G. A. (2010). *Fenaroli's Handbook of Flavor Ingredients* (6th ed.). CRC Press.

Capone, D. L., Pardon, K. H., Cordente, A. G., & Jeffery, D. W. (2011). Identification and quantitation of 3-*S*-cysteinylglycinehexan-1-ol (Cysgly-3-MH) in Sauvignon blanc grape juice by HPLC-MS/MS. *Journal of Agricultural and Food Chemistry, 59*(20), 11204-11210. https://doi.org/10.1021/jf202543z

Chen, L., Capone, D. L., & Jeffery, D. W. (2018). Identification and quantitative analysis of 2-methyl-4-propyl-1,3-oxathiane in wine. *Journal of Agricultural and Food Chemistry, 66*(41), 10808-10815. https://doi.org/10.1021/acs.jafc.8b04027

Clark, A. C., & Deed, R. C. (2018). The chemical reaction of glutathione and *trans*-2-hexenal in grape juice media to form wine aroma precursors: The impact of pH, temperature, and sulfur dioxide. *Journal of Agricultural and Food Chemistry, 66*(5), 1214-1221. https://doi.org/10.1021/acs.jafc.7b04991

Etiévant, P. X. (1991). Wine. In H. Maarse (Ed.), *Volatile compounds in foods and beverages* (pp. 483-546). Marcel Dekker.

Ferreira, V., López, R., & Cacho, J. F. (2000). Quantitative determination of the odorants of young red wines from different grape varieties. *Journal of the Science of Food and Agriculture, 80*(11), 1659-1667. https://doi.org/10.1002/1097-0010(20000901)80:11

Gabrielli, M., Aleixandre-Tudo, J. L., Kilmartin, P. A., Sieczkowski, N., & du Toit, W. J. (2017). Additions of glutathione or specific glutathione-rich dry inactivated yeast preparation (DYP) to Sauvignon blanc must: Effect on wine chemical and sensory composition. *South African Journal of Enology and Viticulture, 38*(1), 18-28.

Guth, H. (1997). Quantitation and sensory studies of character impact odorants of different white wine varieties. *Journal of Agricultural and Food Chemistry, 45*(8), 3027-3032. https://doi.org/10.1021/jf970280a

Jeffery, D. W. (2016). Spotlight on varietal thiols and precursors in grapes and wines. *Australian Journal of Chemistry, 69*, 1323-1330. https://doi.org/10.1071/CH16296

Moyano, L., Zea, L., Moreno, J., & Medina, M. (2002). Analytical study of aromatic series in sherry wines subjected to biological aging. *Journal of Agricultural and Food Chemistry, 50*(25), 7356-7361. https://doi.org/10.1021/Jf020645d

Parr, W. V., Heatherbell, D., & White, K. G. (2002). Demystifying wine expertise: Olfactory threshold, perceptual skill and semantic memory in expert and novice wine judges. *Chemical Senses, 27*(8), 747-755. https://doi.org/10.1093/chemse/27.8.747

Peinado, R. A., Moreno, J., Bueno, J. E., Moreno, J. A., & Mauricio, J. C. (2004). Comparative study of aromatic compounds in two young white wines subjected to pre-fermentative cryomaceration. *Food Chemistry, 84*(4), 585-590. https://doi.org/10.1016/S0308-8146(03)00282-6

Peyrot des Gachons, C., Tominaga, T., & Dubourdieu, D. (2002). Sulfur aroma precursor present in *S*-glutathione conjugate form: Identification of *S*-3-(hexan-1-ol)-glutathione in must from *Vitis vinifera* L. cv. Sauvignon blanc. *Journal of Agricultural and Food Chemistry, 50*(14), 4076-4079. https://doi.org/10.1021/jf020002y

Pino, J. A., & Queris, O. (2011). Characterization of odor-active compounds in Guava wine. *Journal of Agricultural and Food Chemistry, 59*(9), 4885-4890. https://doi.org/10.1021/jf2011112

Ranaweera, R. K. R., Gilmore, A. M., Capone, D. L., Bastian, S. E. P., & Jeffery, D. W. (2021). Authentication of the geographical origin of Australian Cabernet Sauvignon wines using spectrofluorometric and multi-element analyses with multivariate statistical modelling. *Food Chemistry, 335*, 127592. https://doi.org/10.1016/j.foodchem.2020.127592

Song, C.-Z., Liu, M.-Y., Meng, J.-F., Shi, P.-B., Zhang, Z.-W., & Xi, Z.-M. (2016). Influence of foliage-sprayed zinc sulfate on grape quality and wine aroma characteristics of Merlot. *European Food Research and Technology, 242*(4), 609-623. https://doi.org/10.1007/s00217-015-2570-3

Swiegers, J. H., Bartowsky, E. J., Henschke, P. A., & Pretorius, I. S. (2005). Yeast and bacterial modulation of wine aroma and flavour. *Australian Journal of Grape and Wine Research, 11*(2), 139-173. https://doi.org/10.1111/j.1755-0238.2005.tb00285.x

Thibon, C., Böcker, C., Shinkaruk, S., Moine, V., Darriet, P., & Dubourdieu, D. (2016). Identification of *S*-3-(hexanal)-glutathione and its bisulfite adduct in grape juice from *Vitis vinifera* L. cv. Sauvignon blanc as new potential precursors of 3SH. *Food Chemistry, 199*, 711-719. https://doi.org/10.1016/j.foodchem.2015.12.069

Tominaga, T., Niclass, Y., Frerot, E., & Dubourdieu, D. (2006). Stereoisomeric distribution of 3-mercaptohexan-1-ol and 3-mercaptohexyl acetate in dry and sweet white wines made from *Vitis vinifera* (Var. Sauvignon blanc and Semillon). *Journal of Agricultural and Food Chemistry, 54*(19), 7251-7255. https://doi.org/10.1021/jf061566v

Tominaga, T., Peyrot des Gachons, C., & Dubourdieu, D. (1998). A new type of flavor precursors in *Vitis vinifera* L. cv. Sauvignon blanc: *S*-Cysteine conjugates. *Journal of Agricultural and Food Chemistry, 46*(12), 5215-5219. https://doi.org/10.1021/jf980481u

Waterhouse, A. L., Sacks, G. L., & Jeffery, D. W. (2016). Higher alcohols. In *Understanding Wine Chemistry* (pp. 51-56). John Wiley & Sons. https://doi.org/10.1002/9781118730720

Zea, L., Ruiz, M. J., & Moyano, L. (2012). Using odorant series as an analytical tool for the study of the biological ageing of sherry wines. In B. Salih & Ö. Çelikbıçak (Eds.), *Gas chromatography in plant science, wine technology, toxicology and some specific applications* (pp. 91-108). IntechOpen. https://doi.org/10.5772/31803

CHAPTER 8

Concluding Remarks and Future Perspectives

8.1 Conclusions

The scope of this thesis was to obtain a better comprehension of varietal thiols from the perspectives of investigating potential new thiol precursors and sulfur-containing volatile compounds. As well as examining the reactivity and chirality of varietal thiols and assessing the impact of different winemaking practices.

8.1.1 Preliminary exploration of potential new precursors of 4-MSP and 3-SH

Addressing Objective 1 of the project, preliminary experiments were conducted by applying deuterium labelled mesityl oxide to grape leaves and berries. Analysis of the grape leaf and berry extracts using HPLC-QQQ-MS revealed the presence of deuterium labelled GSH-4-MSP. The identity of deuterium labelled GSH-4-MSP and Cys-4-MSP was further confirmed utilising high-resolution time-of-flight mass spectrometry, demonstrating that mesityl oxide can act as a precursor of GSH-4-MSP and that grapevine tissues could utilise mesityl oxide (when applied in this case) to synthesise GSH-4-MSP (**Chapter 2**).

Complying with Objective 2 that hypothesised the potential for MalCys-3-SH to be a precursor of 3-SH, synthesised MalCys-3-SH standard was used to optimise MS and source conditions of an HPLC-MS/MS method. This was followed by the analysis of Sauvignon blanc juice extracts prepared by percolating approximately 1 L of Sauvignon blanc juice through C18 sorbent and concentrating the juice into an extract. Despite trialling extracts at different grape maturity time points, MalCys-3-SH was not identified in the current set of samples.

8.1.2 The production, stability, and chirality of cis-2-MPO and identification of sulfur-containing volatile compounds

In line with Objective 3 of the thesis, a winemaking study showed that *cis*-2-MPO was produced from the second day of the alcoholic fermentation of Sauvignon blanc wine, with the concentration peaking in the early to middle stage of fermentation before a continuous decrease occurred until the end of fermentation (**Chapter 3**). Significantly different evolution profiles of *cis*-2-MPO induced by different yeast strains were illustrated by comparing the use of single inoculation with VIN13 yeast (advantageous in producing considerable amounts of

varietal thiols) or J7 (*Saccharomyces cerevisiae* AWRI 81, a flor yeast with reported ability to produce high concentrations of acetaldehyde), or co-inoculation of VIN13 and J7. Strong to moderate Pearson correlations of the evolution profiles of *cis*-2-MPO occurred with that of acetaldehyde, but weak correlation with 3-SH, indicated that acetaldehyde may be the restricting factor in the production of *cis*-2-MPO. Additionally, *cis*-2-MPO was unstable in wine during storage, with its concentration continuously decreasing under various conditions, such as different storage temperature, pH of wine, and addition of SO_2 or acetaldehyde. However, *cis*-2-MPO was retained by low storage temperature (4 °C), pH 3.0, and acetaldehyde addition.

Despite the weak correlation between the evolution profiles of 3-SH and *cis*-2-MPO, their concentrations determined in wine were strongly correlated. To study the enantiomeric relationships of (3*R*)-3-SH with (2*S*,4*R*)-2-MPO and (3*S*)-3-SH with (2*R*,4*S*)-2-MPO, SIDA with HS-SPME-GC-MS was developed to resolve and quantify the enantiomers of *cis*-2-MPO using a chiral stationary phase (**Chapter 4**). The chemical formation of *cis*-2-MPO was verified by spiking (3*R*)-3-SH as a single enantiomer and acetaldehyde standards in a commercial white wine, with subsequent detection of the corresponding *cis*-2-MPO enantiomer after a short storage period, which was also used to determine the elution order of *cis*-2-MPO enantiomers. Concentrations of (2*S*,4*R*)-2-MPO and (2*R*,4*S*)-2-MPO in a selection of wines were determined, ranging from undetected to 303 ng/L and 250 ng/L, respectively. Accordingly, SIDA with HPLC-MS/MS was utilised to quantify (3*R*)-3-SH and (3*S*)-3-SH in the same wine samples, which the concentrations were 207–7474 ng/L and 186–6294 ng/L respectively. Strong Pearson correlation of (3*R*)-3-SH with (2*S*,4*R*)-2-MPO (r = 0.654) and (3*S*)-3-SH with (2*R*,4*S*)-2-MPO (r = 0.860) were revealed. Furthermore, one of the enantiomers of *cis*-TMO, originating from condensation of acetaldehyde and 4-MSPOH, was identified in wine with a concentration of up to 28 ng/L.

Based on a single *cis*-TMO enantiomer having been identified, it was hypothesised that a single enantiomer of 4-MSPOH may be present in wine. Thus, a HPLC-MS/MS method for chiral thiol analysis was adapted to resolve and quantify 4-MSPOH enantiomers in wine. HPLC parameters, including eluent composition, mobile phase flow rate, concentration of eluent additive, chiral column phase, and column temperature were evaluated (**Chapter 5**). The most optimised method, which partially resolved 4-MSPOH enantiomers, was applied to screen wine samples that were determined to contain *cis*-TMO. However, neither enantiomer of 4-MSPOH was detected at the current stage, most likely due to the small number of wine samples

analysed or the poor sensitivity of the instrument used.

Aside from investigating 4-MSPOH enantiomers, it was considered that additional thiols, namely blackcurrant mercaptan (BCM) and grapefruit mercaptan (GFM), could potentially be present in wine. Using commercially purchased BCM and synthesised GFM standards, a published method utilising thiol derivatisation by DTDP and SIDA HPLC-MS/MS was modified for the characterisation and identification of GFM and BCM in wine (**Chapter 5**). A preliminary calibration for BCM was achieved, followed by the screening of a selection of wine samples, but BCM was not detected. Study of GFM showed that it was unstable and could spontaneously degrade, with the identity of the derived compound of GFM being explored but not positively confirmed.

8.1.3 Impact of oenological factors on chemical and sensory profiles of Shiraz and Sauvignon blanc wines

Fulfilling Objective 4, the impact of accentuated cut edges (ACE), jointly with water dilution of grape must and skin contact time, on the volatile and sensory profiles of Shiraz wine was investigated (**Chapter 6**), with a focus on varietal thiols and their precursors. GSH-3-SH and Cys-3-SH were quantified in Shiraz grape must with average concentrations of 193 μg/L and 4.6 μg/L, respectively. ANOVA revealed that the use of ACE did not increase the concentrations of thiol precursors in the must or varietal thiols, including 3-SH and 3-SHA, in the resultant wine. However, 3-day skin contact significantly increased concentration of 3-SH compared with a 6-day treatment. Two-way ANOVA revealed that other volatile compounds were significantly affected by crushing method and skin contact time. Briefly, most ethyl esters were significantly increased by the conventional crushing technique and 3-day skin contact time. In contrast, acetates, higher alcohols, fatty acids, and isoprenoids were affected by the interactive effect of crushing method and skin contact time: ACE coupled with 3-day skin contact time significantly increased all volatiles apart from the acetates. Sensory analysis of the wines outlined that 'floral/perfume/musk' aroma was significantly more intense in the treatment with ACE coupled with 3-day skin contact time and this was potentially related to the more abundant isoprenoids in the treatment; 'red fruit' flavour was more potent in the conventional crushing treatment with either 3-day or 6-day skin contact time, which was likely relevant to the higher concentrations of ethyl esters. In addition, the chapter provided some insight into volatile profiles of commercially produced Sauvignon blanc and Pinot noir wine arising from ACE treatment. Although the winemaking was not replicated in this case, the results showed that the impact of ACE could potentially be grape variety dependent, thus

providing inspiration for study of the impact of this pre-fermentation technique on other varieties.

As such, the influence of ACE, yeast strain, and malolactic fermentation on the phenolic, volatile, and sensory profiles of Sauvignon blanc was subsequently studied (**Chapter 7**). During a cold maceration stage of grape must, the extraction rate and concentration of GSH-3-SH and Cys-3-SH were both significantly increased by ACE treatment. Analysis of total phenolics and hydroxycinnamates in the resultant wines showed minor increases by ACE compared with the conventional crushing, which should be considered in relation to an increased chance of wine browning. The impact of the three winemaking practices on varietal thiols varied: the concentration of 4-MSP and enantiomers of 3-SH and 3-SHA being significantly increased by ACE treatment; VIN13 yeast produced a greater amount of 3-SH and 3-SHA enantiomers and Sauvy generated a higher amount of 4-MSP; MLF increased the concentration of 3-SH enantiomers and 4-MSP, but decreased 3-SHA enantiomers. Analysis of other volatile compounds and sensory profiles of the wines showed that most volatiles were significantly affected by three-way interactions of crushing method, yeast strain, and malolactic fermentation. Yeast strain and MLF had greater impacts on the sensory profile than crushing method, with treatments that did not undergo malolactic fermentation having more 'fruity' and 'floral' notes compared with the more savoury attributes (i.e., 'sulfidic', 'mineral', and 'bacon') in the MLF treatments. MLF tended to increase concentrations of varietal thiols, ethyl esters, higher alcohols, and fatty acids. Sauvy yeast strain produced greater amounts of isoprenoids, ethyl esters of branched-chain fatty acids, and higher alcohols than VIN13, with the latter characterised by higher levels of fatty acids and ethyl esters of straight-chain fatty acids. ACE crushing method tended to increase varietal aroma compounds and higher alcohols, and was more intense in 'confectionery' and 'sulfidic' flavour, 'tropical fruits' and 'bacon' aroma, and 'length of fruity/non-fruity' attributes. This differed to the conventional crushing treatment, which had higher concentrations of ethyl esters and fatty acids, and greater intensity of 'tropical fruits' flavour, 'floral' and 'sulfidic' aroma, and 'bitter' sensory traits.

8.2 Future perspectives

8.2.1 Precursors of varietal thiols

The potential presence of MalCys-3-SH in a limited number of Sauvignon blanc juice extracts was explored (**Chapter 2**). Although it was not detected in this study, a larger selection of grape juice and wine samples are recommended to be screened in the future. If positive identification of MalCys-3-SH can be accomplished, development of a fully validated HPLC-

MS/MS method is warranted to enable the accurate quantification of MalCys-3-SH in grape and wine samples. Profiling the concentration of MalCys-3-SH in grapes during both grape growing season and in grape juice/must during fermentation could be conducted, as it has been done with other precursor types, to further understanding biochemical relationships. Correlation between the concentration of MalCys-3-SH and 3-SH could also be studied in model fermentations spiked with MalCys-3-SH standard, to examine the potential contribution of MalCys-3-SH to the pool of 3-SH found in wine.

It was verified that grape leaf and grape berry could use deuterium labelled mesityl oxide to synthesise the corresponding labelled GSH-4-MSP (**Chapter 2**). However, proceeding experiments using a balanced number of grapevines are recommended to explore the origin and metabolism of mesityl oxide: firstly, deuterium labelled mesityl oxide could be applied to the soil of potted grape vines and deuterium labelled GSH-4-MSP and Cys-4-MSP could be evaluated in grapevine tissues; secondly, soil bacteria that are characterised to release mesityl oxide in commercial vineyards could be explored.

8.2.2 Reactivity of known varietal thiols and identification of new sulfur-containing volatile compounds

cis-2-MPO was identified in wine because of the reaction between 3-SH and acetaldehyde. Although its typical concentrations in wine are below the odour detection threshold, the potential sensory contribution of *cis*-2-MPO to wine as a function of interaction with other constituents (e.g., 3-SH and 3-SHA) could be studied. Aside from this, quantification of 4-MSPOH enantiomers in wine with a fully optimised and validated HPLC-MS/MS could be revisited. Relevant to the reaction between varietal thiols and acetaldehyde (or indeed other aldehydes), potential 1,3-oxathianes corresponding to 3-sulfanylpentan-1-ol, 2-methyl-3-sulfanylbutan-1-ol, and 3-sulfanylheptan-1-ol could be identified and their sensory importance, formation and fate were studied.

Moreover, it could be worthwhile to develop a more sensitive method for the identification of BCM in wine, along with screening a larger number of wines. GFM has been proven to be unstable in wine and the presence of its potential derived product in wine, namely thiocineole, could also be verified and its relevance determined. To ascertain the potential sensory importance of BCM and GFM to wine aroma, odour detection thresholds of both mercaptans in wine matrix would need to be obtained. For a broader screening of potential new thiols in wine, using thiol selective extraction techniques, such as DTDP derivatisation[1] and silver ion solid phase extraction protocols[2], coupled with mass spectrometry or

olfactometry experiments could be alternative methods.

8.2.3 Impact of novel winemaking practices on chemical and sensory profiles of wine

To fully understand the influence of the ACE technique on wine chemical and sensory profiles, commercial scale fermentation trials would be advantageous. Given the impact of ACE seeming to depend on grape variety, the influence of ACE on grape varieties other than Shiraz, Sauvignon blanc, Pinot noir, and Marquette, which have already been studied, requires detailed investigation. Despite the uncommon usage of malolactic fermentation in Sauvignon blanc wine production, the study in **Chapter 7** revealed the potential of lactic acid bacteria for varietal thiol production, which may be exploitable in other wine varieties. However, enzymes in lactic acid bacteria that may be involved with varietal thiol release from their conjugated precursors, such as β-lyase, would need to be characterised.

References

1. Millan, S.; Jeffery, D. W.; Dall'Acqua, S.; Masi, A., A novel HPLC-MS/MS approach for the identification of biological thiols in vegetables. *Food Chem.* **2021,** *339*, 127809.

2. Chen, L.; Darriet, P., Qualitative screening of volatile thiols in wine by selective silver ion solid-phase extraction with heart-cutting multidimensional gas chromatography mass spectrometry/olfactometry. *J. Agric. Food Chem.* **2022,** *70* (15), 4701-4711.

APPENDIX

Chemical and Sensory Impacts of Accentuated Cut Edges (ACE) Grape Must Polyphenol Extraction Technique on Shiraz Wines

Wenyu Kang,[1] Keren A. Bindon,[2] **Xingchen Wang**,[1] Richard A. Muhlack,[1] Paul A. Smith,[3] Jun Niimi,[1,4] Susan E.P. Bastian[1,*]

[1] Department of Wine Science and Waite Research Institute, The University of Adelaide (UA), PMB 1, Glen Osmond, SA 5064, Australia

[2] The Australian Wine Research Institute, Hartley Grove, Urrbrae, Adelaide, SA 5064, Australia

[3] Wine Australia, Industry House, Corner Hackney and Botanic Roads, Adelaide, SA 5000, Australia

[4] Institute for Molecular Biosciences, Goethe University Frankfurt, 60438 Frankfurt am Main, Germany

Foods, ***2020***, *9(8), 1027.*

DOI: 10.3390/foods9081027

foods

MDPI

Article

Chemical and Sensory Impacts of Accentuated Cut Edges (ACE) Grape Must Polyphenol Extraction Technique on Shiraz Wines

Wenyu Kang [1], Keren A. Bindon [2], Xingchen Wang [1], Richard A. Muhlack [1], Paul A. Smith [3], Jun Niimi [1,4] and Susan E. P. Bastian [1,*]

1 Waite Campus, School of Agriculture, Food & Wine, The University of Adelaide, PMB 1, Glen Osmond, SA 5064, Australia; a1642412@adelaide.edu.au (W.K.); xingchen.wang@adelaide.edu.au (X.W.); richard.muhlack@adelaide.edu.au (R.A.M.); niimi@bio.uni-frankfurt.de (J.N.)
2 The Australian Wine Research Institute, Hartley Grove, Urrbrae, Adelaide, SA 5064, Australia; keren.bindon@awri.com.au
3 Wine Australia, Industry House, Corner Hackney and Botanic Roads, Adelaide, SA 5000, Australia; paul.smith@wineaustralia.com
4 Institute for Molecular Biosciences, Goethe University Frankfurt, 60438 Frankfurt am Main, Germany
* Correspondence: sue.bastian@adelaide.edu.au; Tel.: +61-8-83136647

Received: 26 June 2020; Accepted: 23 July 2020; Published: 31 July 2020

Abstract: Accentuated Cut Edges (ACE) is a recently developed grape must extraction technique, which mechanically breaks grape skins into small fragments but maintains seed integrity. This study was the first to elucidate the effect of ACE on Shiraz wine's basic chemical composition, colour, phenolic compounds, polysaccharides and sensory profiles. A further aim was to investigate any potential influence provided by ACE on the pre-fermentation water addition to must. ACE did not visually affect Shiraz wine colour, but significantly enhanced the concentration of tannin and total phenolics. Wine polysaccharide concentration was mainly increased in response to the maceration time rather than the ACE technique. ACE appeared to increase the earthy/dusty flavour, possibly due to the different precursors released by the greater skin breakage. The pre-fermentation addition of the water diluted the wine aromas, flavours and astringency profiles. However, combining the ACE technique with water addition enhanced the wine textural quality by increasing the intensities of the crucial astringent wine quality sub-qualities, adhesive and graininess. Furthermore, insights into the chemical factors influencing the astringency sensations were provided in this study. This research indicates that wine producers may use ACE with pre-fermentation water dilution to reduce the wine alcohol level but maintain important textural components.

Keywords: skin fragmentation; water addition; tannin; phenolics; polysaccharides; rate-all-that-apply; astringent sub-quality; progressive profiling

1. Introduction

Accentuated Cut Edges (ACE) is a new grape must processing technique that has recently received interest in the Australian and New Zealand wine sectors. The ACE technique, which is employed after conventional grape crushing, is a process whereby grape skins are mechanically cut into smaller fragments (6% of their original size) while maintaining seed integrity [1]. This technique provides more broken skin edges, with the goal of enhancing the extraction of phenolic components from the grape skin earlier during fermentation, while avoiding the extraction of astringent or bitter compounds potentially resulting from seed damage [2]. The development of ACE started from a northern Tasmanian vineyard in Australia working on *Vitis vinifera* cv. Pinot noir grapes [3]. The work was initiated

due to the recognition that wines made from this variety can have poor colour development and low pigment stability [4]. Since a more intense colour in red wines is often associated with higher quality perception by consumers [5], the finding that ACE resulted in the intensification of wine colour was promising for the future production of higher quality wine. Compared with conventional crushing, Pinot noir wines made using the ACE technique had 50% higher wine colour density and 95% higher stable pigment concentration [1]. In addition to colour, the quality of red wine is also associated with a positive mouthfeel (or textural) properties, such as the sensation of astringency, which is known to be influenced by various phenolic components such as tannins [6]. In the study on Pinot noir, wines produced by ACE were three times higher in tannin concentration than those prepared by conventional crushing [1], and had both greater astringency and bitterness intensities [2]. Recent research demonstrated that wines with the same overall astringency intensity may possess subtle mouthfeel texture sub-quality differences e.g., velvety, puckering [7,8]. Whether ACE treatment affects these more nuanced sensations is not known. ACE-treated Pinot noir wine also had a greater intensity of fruity components, notably the aromas of banana, peach, and black currant and the flavour of dark fruit [2].

Currently, Australian wine producers are faced with managing the impacts of a shortened vintage period for many grape cultivars, termed 'vintage compression'. This is thought to be due to the influence of climate change, with warmer growing seasons, a greater number of high temperature days and more days that have smaller diurnal temperature differences, resulting in the grapes harvested earlier and at higher sugar levels [9]. Management techniques to deal with the logistical disadvantages of processing the same tonnage of grapes in the face of vintage compression has increasingly gained importance within the wine industry [10]. In 2017, ACE was studied to address vintage compression, proposing the concept of Pressed Early Accentuated Cut Edges (PEACE) [11]. Based on the preliminary findings from PEACE, a two-day maceration on skins following ACE treatment was shown to be sufficient to extract a larger proportion of anthocyanin and tannin in Pinot noir wines relative to conventional crushing (eight days on un-fragmented skins). Thus, the ACE treatment allows the ferments to be pressed off skins earlier when compared with conventional crushing techniques, thereby highlighting the potential of PEACE to economise on tank space, pump-over logistics and labour requirements under the conditions of a compressed vintage [11].

However, as highlighted previously, ACE studies have thus far focused on Pinot noir, but one of the most planted red wine grape varieties globally, including in Australia, is *Vitis vinifera* cv. Shiraz [12], giving it a higher level of economic importance. Meanwhile, as vintage compression conditions lead to grapes destined for winemaking being harvested with increased sugar levels, the alcohol concentrations of wines made in Australia and elsewhere have also risen [13]. The high level of residual sugar or alcohol concentration in wines influences the sensory perception and hence reduces the perceived wine balance, quality or consumer preference [14]. While opportunities to manipulate wine alcohol through techniques such as earlier harvests, pre-fermentation water addition and reverse osmosis have been studied, these operations might also potentially lead to reduced wine quality [15–17].

Shiraz is economically important, but faces the same compressed vintage challenges. There is potential for ACE to be applied to Shiraz, however, this has not been done in a highly coloured and phenolic red grape variety before. The extent to which ACE can enhance Shiraz wine properties/sensory is unknown. Thus, the aims of the present study were to investigate, in Shiraz wine production, the impact of the ACE technique on wine chemical composition, sensory attributes and in particular, astringency and its sub-qualities. In order to determine the potential improvement provided by ACE over conventional crushing, a combination of both early pressing and water addition to wines were examined. Three treatments were investigated for both ACE and conventional crushing, whereby short skin maceration (three days on skins) was compared with a longer skin maceration time (six days). Furthermore, the longer skin contact treatments (6 days) for both standard and ACE-processed grapes were also prepared with water addition (at the pre-fermentation stage to reduce must sugar to 13.5 Baumé (Bé)). All wine treatments were chemically characterised through a

number of basic wine compositional parameters, most importantly colour, phenolic composition and polysaccharide concentration. In addition, the sensory characteristics of all treatments were profiled by rate-all-that-apply (RATA) using 61 untrained participants, and then astringency and astringent sub-qualities, assessed by modified progressive profiling (PP) using a trained panel.

2. Materials and Methods

2.1. Chemicals

Reagents and reference compounds (≥97% purity) used for the high-performance liquid chromatography (HPLC), methyl cellulose precipitable (MCP) tannin method, and the modified Somers assay were purchased from Sigma-Aldrich (Castle Hill, NSW, Australia). Milli-Q water (Millipore, North Ryde, NSW, Australia) was utilised for the preparation of solutions.

For the winemaking process, potassium metabisulfite (PMS) and diammonium phosphate (DAP) were purchased from Laffort Australia (Woodville North, SA, Australia), while tartaric acid (H_2T) was purchased from Tarac Technologies (Nuriootpa, SA, Australia). Springwater (Woolworths®, Unley, SA, Australia) was used for the preparation of solutions for addition to wine as well as for must dilution, to avoid chlorine impact (potential formation of 2, 4, 6-trichloroanisole).

2.2. Vinification Protocol

Shiraz grapes were sourced from a vineyard (35°13′ S, 138°62′ E) located in the McLaren Vale region of South Australia during the 2019 vintage. The region experiences a temperate-warm Mediterranean climate, and the mean January temperature in 2019 was 31.6 °C, and the average annual rainfall from 2000 to 2019, 518.1 mm [18]. The grapes were machine harvested from 22 year-old vines holding 7.63 tonnes/hectare average yield (1 hectare is 10,000 m^2). A total of 600 kg was subsampled from the machine-harvested grapes. A portion of the grapes (300 kg) underwent a conventional crushing technique (Miller MC250) and was named NOACE treatment. The remaining 300 kg of grapes were crushed firstly by the same conventional approach and then underwent further processing through the Della Toffola Maceration Accelerator (DTMA, Della Toffola, TV, Italy; ACE treatment; minimum grape amount required by the winery). After the homogenisation of the two musts, the initial must conditions were measured by OenoFoss Type 41-01, and were not different to one another, having the following chemical compositions; sugar 14 Bé (1 Bé = 1.8 Brix = 18 g/L fermentable sugar = 1% potential alcohol), pH 3.39, 5.2 g/L titratable acidity (TA), 1.5 g/L malic acid, and 171.2 mg/L yeast assimilable nitrogen (YAN).

Thereafter, both musts were acid-adjusted by the addition of 1 g/L H_2T, 300 mg/L DAP added, followed by yeast inoculation with Enartis Ferm® red fruit (batch L.ES 736051) at a rate of 200 mg/L. As shown in Figure 1, both NOACE and ACE musts were further separated (under constant stirring to maintain the ratio between the skin and juice) into 9 by 25 kg aliquots in 30 L plastic fermenters (Brewcraft, SA, Australia). Water addition treatments were conducted by the direct addition of 500 mL of spring water (i.e., no juice run off was performed) to the NOACE- and ACE-treated musts in triplicate, to reduce the sugar concentration to 13.5 Bé, based on the Australian water addition regulatory limit. The fermentation of all six treatments (Figure 1) was conducted in triplicate, in a 20 °C temperature-controlled room, with manual plunging performed twice daily (at 10 am and 4 pm, with 10 punch downs per plunging). One day after inoculation with yeast, the lactic acid bacteria were co-inoculated by the addition of VP41 (LALLEMAND®, Edwardstown, SA, Australia, batch 314125093016) at a rate of 1.5 mg/L. After either 3 or 6 days of skin contact, the wines were pressed at 1.5 bar for 10 min using a water bag press, transferred to 10 L glass demijohns with airlocks (Ambrosio, Italy) and stored at 18 °C until dry (the total residual sugar and malic acid of all wines were below 2 g/L and 0.4 g/L, respectively). PMS was added to achieve 60 mg/L total Sulphur, then the wines stored in a 0 °C room for one week and racked off "gross lees". Thereafter, the wines were settled for a month at 0 °C and again racked from the "fine lees" before bottling. Wines were bottled in

375 mL dark green bottles covered with carbon dioxide and screw caps, and cellared at 16 °C for a month before being analysed.

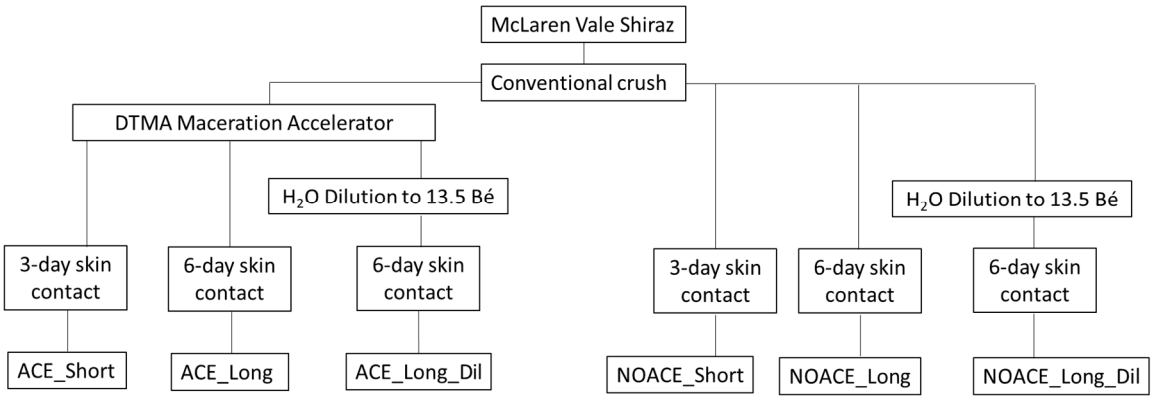

Figure 1. Summary of the treatments conducted on Shiraz musts prepared by the NOACE (conventional crush) or Accentuated Cut Edges (ACE) (conventional crush plus Della Toffola Maceration Accelerator (DTMA)) treatment, with six different treatments performed in triplicate.

2.3. Basic Wine Composition and Wine Colour Measurements

The wine samples were analysed for pH, titratable acidity (TA, as tartaric acid g/L equivalents and a TA measurement pH endpoint of 8.2), volatile acidity (VA, as g/L equivalent to acetic acid), and sulphur dioxide (SO_2, free and total) by the Australian Wine Research Institute's (AWRI) Commercial Services Laboratory (using the Winescan method and the method of sulphur dioxide free and total (the Thermo Fisher Discrete Analyser), respectively). The total residual sugars and malic acid levels were measured by Chemwell® 2910 Automated EIA and Chemistry Analyser (Awareness Technology, Palm City, FL, USA) with the Megazyme K-FRUGL (Chicago, IL, USA) and Vintessential Enzymatic L-Malic Acid (Dromana, VIC, Australia) test kits. The alcohol level of the samples was measured with the Anton Paar Alcolyzer Wine ME and DMA 4500M (North Ryde, NSW, Australia).

The wine colour was measured by both the modified Somers assay [19] and CIELab tristimulus using the Cintra 4040, (GBC Scientific Equipment, Braeside, VIC, Australia), and the results calculated and presented as the chroma and hue angle as described previously [20].

2.4. Phenolic Components and Polysaccharide Analyses in Wines

Total tannin concentration for the treatments was measured by the high-throughput MCP tannin method in technical duplicates, while the total phenolic concentration was determined by the modified Somers assay in technical triplicates [19]. Furthermore, the tannins from wine samples were isolated by solid-phase extraction [21] and analysed by HPLC (Agilent 1100) following phloroglucinolysis [22] to determine the subunit composition, mean degree of polymerisation (mDP), and molecular mass (MM (phloro)) according to the conditions outlined previously [23]. All the terminal monomer subunits had their retention times authenticated using standards before measurement [23]. The tannin molecular mass was also measured by gel permeation chromatography (MM (GPC)) on an Agilent 1200 with the modifications described previously [24]. 20 mg/mL malvidin-3-glucoside in methanol was used as a standard to validate the method; this standard was removed from the freezer, equilibrated to temperature and then diluted 1:5 with *N*,*N*-dimethylformamide prior to analysis.

For the polysaccharide analysis, the wine samples were prepared and hydrolysed as described by Li, et al. [25], but the dialysis step was replaced by a cold, pure ethanol wash [9]. The total wine soluble polysaccharides and the monosaccharide residues following acid hydrolysis were determined by HPLC (Agilent 1100) [26]. The monosaccharides were identified and quantified using commercial standards (Sigma-Aldrich, St. Louis, MO, USA).

2.5. Sensory Evaluations

2.5.1. Wine Descriptive Profiling by Naïve Wine Consumers Using Rate-All-That-Apply (RATA)

RATA is a rapid and flexible method that can profile different food or beverages products using naïve consumers as subjects [27,28]. For the characterisation of wines products, the discrimination and profiling abilities of RATA with naïve consumers have been validated against descriptive analysis using small, highly trained panellists [27]. Thus, a panel of 61 untrained participants (34 female and 27 male, average age 26 years) who had consumed red wine in the last 12 months assessed the Shiraz treatment wines in this study. The RATA assessment was conducted across two sessions (nine wine samples per session, all the samples from the triplicate of winemaking were assessed) under the same conditions as the work of Danner et al. [27] in computerized, individual booths with forced one minute breaks between each sample, and a five minute break after the first four wines. The participants used a seven-point intensity RATA scale (anchored from 1 = "extremely low" to 7 = "extremely high") to evaluate 58 attributes (Table S1, definitions were provided to the consumers) across the sensory modalities of wine colour, aroma, flavour, taste, mouthfeel, and aftertaste.

2.5.2. Astringency Profiles of Wines Assessed by a Trained Sensory Panel Using Modified Progressive Profiling (PP)

Wine astringency is a complex sensation, and is particularly hard and fatiguing for untrained individuals (normal consumers) to assess, comprehend and describe, especially the different sub-qualities of astringency perception [29]. As one study aim was to obtain an advanced understanding of the impact of ACE on the temporal perception of Shiraz wine's texture, the astringency profiles of treatment wine samples in this study were evaluated in more detail by a trained sensory panel (n = 8, 3 male and 5 female, average age 51 years) using the modified PP methodology [30]. The processes of panel recruitment, training, and sample evaluation were conducted in the same manner as our previous work [30]. Seven attributes of wine astringency were evaluated as previously determined [30] including overall astringent intensity (OAI) and 6 sub-qualities (pucker, mouth coat, dry, grippy, adhesive and graininess). The intensity of attributes in each wine were rated consecutively on 15 cm scales with low and high word anchors located at 10 and 90% of the scale, respectively. The entire attribute set were assessed in two rounds, one after the other for a given wine sample. However, the PP evaluation in this study only had 5 time periods (each lasting 10 s; the first with wine in the mouth and then 4 after expectoration, with 20 s gaps between each time period). This was because the panel training had revealed that the astringency sensation had disappeared by the fifth evaluation time period (Figure 2). All wines were presented to panellists in coded black glasses, monadically in randomised order and evaluated in computerised, individual booths. The 18 wines (6 treatments × 3 replicate of winemaking) were evaluated in duplicate across four sessions (two hours, twice weekly commencing at 10 a.m. at the University of Adelaide's Waite campus sensory facility).

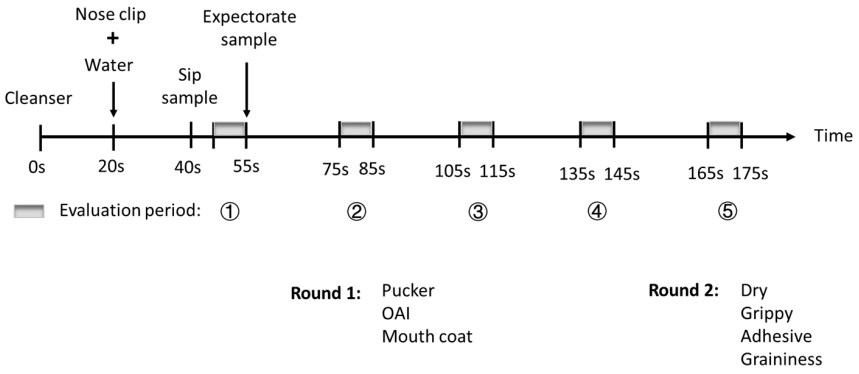

Figure 2. Schematic representation of the modified Progressive Profiling protocol. OAI is overall astringent intensity.

2.6. Data Analyses

The chemical measures were analysed by one-way analysis of variance (ANOVA) at an alpha level (α) of 5% with Fisher's least significant difference post hoc test (LSD) in XLSTAT (ver. 2016; Addinsoft SARL, Paris, France). The data from RATA were analysed by a multivariate ANOVA (at α 10%), with two-way interaction (treatment and replicate of winemaking as fixed factors, and assessor as random factor) using XLSTAT. Significantly different RATA attributes (means) were further analysed with Principal components analysis (PCA). In terms of PP assessment, the data were firstly analysed by univariate ANOVA (at α 5%) for each attribute at every single time period, with a treatment, replicate of winemaking and a replicate of sensory evaluation as fixed factors, and an assessor as a random factor using XLSTAT. Significantly different PP attributes were further analysed by the mixed assessor model canonical variate analysis (MAM-CVA) in RStudio (R ver. 3.5.1, Boston, MA, USA) with the software package CVAS (Version 1.0, written by Caroline Peltier on 3 November 2014). A partial least squares regression (PLS-R) between the significantly different attributes in PP (Y, the variables being predicted) and the significantly different chemical parameters (X, the predictor variables) were performed (stop conditions was automatic, cross-validation method used was Jackknife (LOO), and a confidence interval was 95%) using XLSTAT.

3. Results and Discussion

3.1. Basic Wine Chemical Composition and Colour

The basic wine composition resulting from the winemaking treatments is shown in Table 1. The treatments were significantly differentiated on the chemical parameters of alcohol and acid. The alcohol concentration in the water addition treatments was significantly lower in both the ACE and NOACE groups, as expected. A trend of higher pH and lower TA was found in the water addition treatments. pH is known to influence both wine colour [31] and astringency sensation [32]. The range of difference in pH was less than 0.1, which would only influence the wine colour and astringency perception negligibly, if at all.

Table 1. Basic chemical composition of the Shiraz wines prepared following NOACE and ACE maceration with either 3 days (Short) or 6 days (Long) on skins, or 6 days on skins with pre-fermentation water dilution to 13.5 Bé (Long_Dil).

	Alcohol (% v/v)	Total Residual Sugar (g/L)	pH	TA (g/L)	VA(g/L)	Malic Acid (g/L)	Free SO_2 (mg/L)	Total SO_2 (mg/L)
ACE_Short	[§] 14.83 ± 0.05 a	1.63 ± 0.12	3.54 ± 0.02 ab	6.83 ± 0.06 bc	0.72 ± 0.06	<0.40	29.67 ± 0.57	51.33 ± 2.52
ACE_Long	14.57 ± 0.15 b	1.57 ± 0.21	3.53 ± 0.02 b	6.77 ± 0.06 c	0.70 ± 0.06	<0.40	30.00 ± 1.00	48.33 ± 1.52
ACE_Long_Dil	14.23 ± 0.25 c	1.37 ± 0.12	3.57 ± 0.02 a	6.67 ± 0.21 c	0.70 ± 0.21	<0.40	28.67 ± 1.52	50.33 ± 0.57
NOACE_Short	14.83 ± 0.05 a	1.93 ± 0.15	3.48 ± 0.01 c	7.17 ± 0.06 a	0.73 ± 0.06	<0.40	27.33 ± 1.52	48.67 ± 1.53
NOACE_Long	14.93 ± 0.05 a	1.33 ± 0.23	3.52 ± 0.01 b	6.97 ± 0.06 b	0.71 ± 0.06	<0.40	29.00 ± 2.00	48.00 ± 0.00
NOACE_Long_Dil	14.50 ± 0.00 b	1.47 ± 0.25	3.57 ± 0.01 a	6.70 ± 0.06 c	0.70 ± 0.10	<0.40	31.00 ± 1.00	50.00 ± 1.73
F	8.452	2.914	8.502	6.488	1.492	N/A	1.594	1.827
p	[†] **0.002**	0.061	**0.002**	**0.004**	0.273	N/A	0.243	0.187

[§] Data are the means (± standard deviation) of triplicate fermentations, analysed with one-way analysis of variance at an alpha level of 5% and Fisher's least significant difference test. [†] Bold *p* values represent significant differences between treatments. A post-hoc test was run across wines within each column; values followed by the same letter in a column are not significantly different.

The effect of the ACE treatment on wine colour was firstly examined using the modified Somers method (Table 2). Similar to the previous findings from Pinot noir wines [1], the ACE treatments with longer time on skins had significantly increased wine colour density and stable pigment concentration

(SO_2 resistant pigments). However, the colour enhancement in the Shiraz wines was not as large in magnitude (approx. 17% higher wine colour density and 8% higher stable pigment concentration) relative to that observed in Pinot noir (50% higher wine colour density and 95% higher stable pigment concentration). The difference in the grape varieties may have been the cause, since the Shiraz grapes have inherently more red pigments and a darker colour than Pinot noir, and compounds which may also be more readily extractable [4]. Additionally, the colour effects were measured by CIELab (Figure 3), which is expected to better approximate the colour perceived by the human eye (the modified Somers assay was based on the measurement of spectrophotometric data for several wavelengths rather than the CIELab (a whole range, 375 to 780 nm)) [33]. The chroma, represents the intensity/depth of the wine colour, and the hue angle is identified as orange, yellow, beige, brown, pink or any of the other colours. There was no significant difference in the wine colour by CIELab across the six treatments, with the chroma of all wines being approximately 50 and the hue angle 355 (i.e., a purple to red hue). The results differed to those obtained by the Somers assay and the previous Pinot noir study. The modified Somers assay was more sensitive, however, in the case of this study, the colour differences were most likely not perceivable based on the CIELab measurements.

Table 2. Colour measurements by the modified Somers assay of Shiraz wines prepared following the NOACE and ACE maceration with either 3 days (Short) or 6 days (Long) on skins, or 6 days on skins with pre-fermentation water dilution to 13.5 Bé (Long_Dil).

	§ Wine Color Density (a.u.)	Hue	Total Anthocyanins (mg/L)	SO_2 Resistant Pigments (a.u.)
ACE_Short	† 14.74 ± 0.73 a	0.56 ± 0.00	590 ± 28	2.70 ± 0.10 ab
ACE_Long	14.76 ± 0.31 a	0.56 ± 0.01	607 ± 10	2.68 ± 0.08 ab
ACE_Long_Dil	13.75 ± 0.53 ab	0.56 ± 0.01	608 ± 20	2.56 ± 0.09 bc
NOACE_Short	14.28 ± 0.61 a	0.56 ± 0.00	587 ± 13	2.72 ± 0.06 a
NOACE_Long	12.58 ± 0.43 c	0.58 ± 0.01	557 ± 21	2.48 ± 0.06 c
NOACE_Long_Dil	12.93 ± 0.80 bc	0.58 ± 0.01	573 ± 31	2.45 ± 0.06 c
F	7.261	2.860	2.391	6.225
p	‡ **0.002**	0.063	0.100	**0.005**

§ Superscript represents that a.u. is the absorbance units. † Data are the means (± standard deviation) of triplicate fermentations, analysed with one-way analysis of variance at an alpha level of 5% and Fisher's least significant difference test. ‡ Bold *p* values represent the significant differences between the treatments. A post hoc test was run across the wines within each column; the values followed by the same letter in a column are not significantly different.

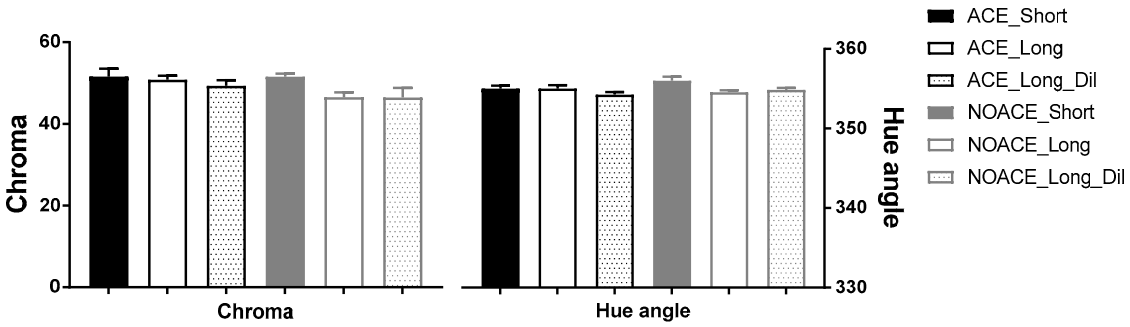

Figure 3. The colour of wines measured by CIELab. Shiraz wines were prepared following NOACE and ACE maceration with either 3 days (Short) or 6 days (Long) on skins, or 6 days on skins with pre-fermentation water dilution to 13.5 Bé (Long_Dil). Results are presented as the chroma and hue angle (mean ± standard deviation of triplicate fermentations).

3.2. Wine Total Phenolics and Total Tannin

3.2.1. ACE Effects

Wine phenolic components are important to wine colour, stability and quality, and they are considered to be primarily responsible for the sensation of astringency in wine [6,34,35]. As shown in Figure 4, with the exception of ACE_Short treatment, the total tannin concentrations in ACE-treated Shiraz wines were significantly higher than all NOACE treatments ($F = 3.72$, $p = 0.036$). Since no oak treatment was applied in this study, the tannins in wines were condensed tannins derived from the grape berries, and are located in the skin hypodermal layers, pulp, and the soft parenchyma of the seed between the cuticle and the hard seed coat [36,37]. Consistent with the previous literature [1,2], more broken skin edges provided by the ACE technique resulted in an increase in tannin extraction in Shiraz wines.

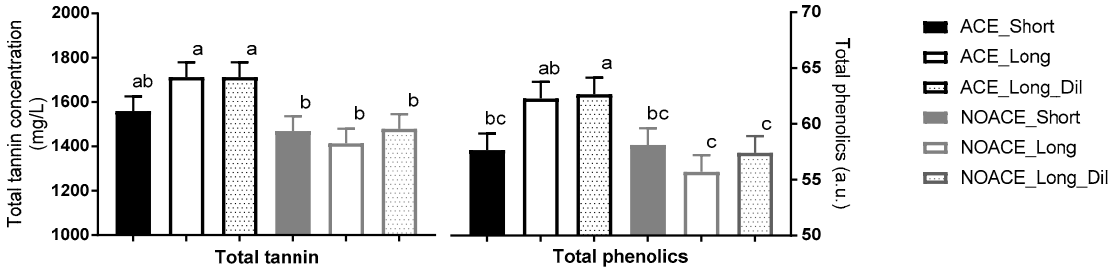

Figure 4. Mean total tannin concentrations and total phenolics (± standard error) of Shiraz wines prepared following NOACE and ACE maceration with either 3 days (Short) or 6 days (Long) on skins, or 6 days on skins with pre-fermentation water dilution to 13.5 Bé (Long_Dil). Different superscript letters above the bars indicate significant differences ($p < 0.05$) between treatments analysed by LSD. The a.u. in the right axis is absorbance units.

3.2.2. Maceration Time and Dilution Impacts

However, the enhancement of tannin extraction in the shorter skin maceration treatment was more obvious in Pinot noir wines [11] compared to the Shiraz in this study. This might due to the DTMA machine being less destructive when cutting Shiraz skins than the original ACE equipment and Pinot noir must processing. In addition, there was no significant difference in the tannin concentration between the long skin maceration and long skin maceration plus dilution treatments. This meant that the small amount of water addition before fermentation could reduce the alcohol level without significantly influencing the total tannin concentration in Shiraz wines. This is contrary to the losses in tannin concentration observed following the dilution of Shiraz in other studies [12,17], nevertheless, the amount of water addition in the current study was much lower. The total phenolics measurement indicated that the combined estimate of wine tannins together with other phenolic components, such as non-polymeric flavonoids and derived pigments, tracked similarly to the tannin concentration ($F = 3.59$, $p = 0.041$). The contents of total anthocyanins were not significantly different across the six treatments, thus the differences observed in total phenolics might mainly be caused by the proanthocyanidins and polymeric pigments (SO_2 resistant pigments).

3.3. Wine Tannin Composition

3.3.1. Maceration Time and Dilution Impacts

The tannin composition of the winemaking treatments was determined and are shown in Table 3. The mass conversion indicates the extent to which the isolated tannin was depolymerised to resolved constituent subunits by the phloroglucinolysis method, which also reflects the confidence for the interpretation of the measured subunit compositions as representative of all tannin in the sample.

Tannin mDP, which represents the average length of tannin polymers, was found to increase in the shorter skin maceration treatments relative to the longer maceration time of 6 days, independently of the treatment at crushing. The shorter skin maceration treatments also had a higher percentage of epigallocatechin subunits, indicating a greater proportion trihydroxylated material extraction from the grapes, likely reflecting a contribution from the grape skins [36,38]. On the contrary, the wines undergoing longer maceration times, including the water addition treatments, had a higher percentage of epicatechin gallate, which mainly originates from the grape seeds [36]. This indicated that when a greater proportion of grape seed tannins was transferred into wines, that this was mainly due to the maceration time, rather than the implementation of the ACE technique. It is important to highlight from the current results that the overall molecular mass (MM) of the tannin population was determined by either the phloroglucinolysis or GPC techniques had different outcomes in the current study. The MM determination by phloroglucinolysis correlated with the mDP measure, and was found to decrease in response to the extended maceration time, in agreement with an increase in seed tannin extraction. On the other hand, the MM measurement from GPC, which more accurately determines the average size of tannins as a function of their hydrodynamic volume rather than by mDP per se, was found to increase with longer maceration times. This was expected, since seed tannins are known to have a larger absolute size, or hydrodynamic volume, independent of the polymer length [23].

Table 3. The tannin composition of Shiraz wines prepared following the NOACE and ACE maceration with either 3 days (Short) or 6 days (Long) on skins, or 6 days on skins with pre-fermentation water dilution to 13.5 Bé (Long_Dil).

	§ MM (Phloro) (g/mol)	† mDP	Epigallocatechin (%)	Epicatechin Gallate (%)	Mass Conversion (%) of Phloroglucinolysis	‡ MM (GPC) (g/mol)
ACE_Short	δ 2893 ± 53 a	9.58 ± 0.17 a	34.6 ± 1.0 a	4.1 ± 0.0 c	40 ± 2	1793 ± 33 b
ACE_Long	2616 ± 15 b	8.64 ± 0.06 b	32.6 ± 0.7 bc	4.9 ± 0.2 a	40 ± 1	1833 ± 32 a
ACE_Long_Dil	2691 ± 82 b	8.89 ± 0.27 b	31.8 ± 1.3 c	4.7 ± 0.2 a	38 ± 2	1811 ± 12 ab
NOACE_Short	2884 ± 46 a	9.55 ± 0.15 a	34.3 ± 0.7 ab	4.1 ± 0.1 c	38 ± 2	1778 ± 23 b
NOACE_Long	2720 ± 105 b	8.99 ± 0.34 b	31.1 ± 1.0 c	4.7 ± 0.1 a	39 ± 3	1787 ± 36 b
NOACE_Long_Dil	2583 ± 114 b	8.55 ± 0.37 b	32.0 ± 1.3 c	4.4 ± 0.0 b	39 ± 4	1673 ± 24 c
F	7.752	7.968	5.595	18.758	N/A	20.966
p	Φ **0.003**	**0.003**	**0.010**	**<0.0001**	N/A	**<0.0001**

§ Tannin molecular mass determined by phloroglucinolysis. † Tannin mean degree of polymerisation determined by phloroglucinolysis. ‡ Tannin molecular mass determined by gel permeation chromatography at 50% elution. δ Data are the means (± standard deviation) of triplicate fermentations, analysed with one-way analysis of variance at an alpha level of 5% and Fisher's least significant difference test. Φ Bold *p* values represent the significant differences between treatments. A post-hoc test was run across the wines within each column; the values followed by the same letter in a column are not significantly different.

3.3.2. ACE Effects

The observations from the tannin profiles could potentially indicate that seed integrity was maintained by ACE, since the amount of extracted tannin increased in response to ACE, but the tannins remained compositionally similar for comparable maceration times. Should ACE have disrupted the seed integrity, a decrease in mDP and an increase in proportional epicatechin gallate would have been expected earlier during maceration. According to the GPC results, the tannins derived from the ACE_Long and ACE_Long_Dil treatments were significantly larger in size than those found in the NOACE wines, suggesting more skin tannin components. Of relevance to the current study, is that larger tannins could potentially result in greater astringency perception, and this will be addressed in greater detail in the sections to follow.

3.4. Wine Polysaccharide Composition

ACE treatment and dilution had little impact on the polysaccharide composition (Table 4), while the total polysaccharide concentrations increased slightly as the maceration was prolonged from 3 to 6 days. In terms of the proportional composition of the individual monosaccharide residues,

recovered following the acid hydrolysis of polysaccharides, fucose residues were significantly different across the treatments, but the levels were very low. At these equivalent levels, even in water, it is difficult to perceive the sweetness of fucose [39]. Significant differences across the treatments were also detected for rhamnose residues and the residues of galactose and arabinose, which are usually attributed to the rhamnogalacturonans (RGs) (e.g., RGII) and polysaccharides rich in arabinose and galactose (PRAGs), respectively; where both classes of polysaccharides are grape-derived. RG II and PRAGs have been shown to be important contributors to the mouthfeel of red wines and are thought to be negatively associated with bitterness and astringency [40,41]. Polysaccharides can also directly contribute to the mouthfeel properties of wines, such as the enhancement of the perception of palate fullness [41,42]. In addition, mannose (expected to be released by yeast as mannoproteins during fermentation and aging) was not significantly different across treatments.

3.5. Sensory Characteristics

3.5.1. Wine Descriptive Profiling by RATA

In the current study, the ACE technique was also studied to determine the outcomes of the sensory profile of Shiraz wines. Samples were firstly evaluated by 61 untrained wine consumers to evaluate the properties of wine colour, aroma, flavour, taste, mouthfeel, and aftertaste. Among the 58 attributes of RATA, eight were significantly discriminated between the wine treatments ($p < 0.1$) by the wine consumers, and are displayed in Table 5. The eight significantly different attributes were further visualized in a PCA plot with the sample loadings (Figure 5). Encouragingly, the winemaking triplicates for each treatment appeared consistent, as a significant treatment × replicate of winemaking sensory difference was not detected. As shown, the average intensities of vanilla were higher in the ACE treatment with short maceration on both the nose and palate. The NOACE maceration with 3 and 6 days on skins had more intense "FL" (floral/perfume/musk) flavour, but the aroma of "FL" was more intense in the ACE_Short treatment wines. These observations are interesting and the profiles of volatile aromatic compounds from wines measured by head space gas chromatography (GC) with mass spectrometry would be useful to examine this further (e.g., Monoterpenoids and C13-Norisoprenoids) [43]. The intensity of sweetness in NOACE (Short and Long) wines were higher than ACE wines, but all the samples in the current study were technically dry wines (total residual sugar were all below 2 g/L). The different perceptions in sweetness were likely to be due to the different matrix effect (such as wine alcohol level and/or possibly release of yeast-derived compounds) across the treatments [44,45]. In addition, the intensity of F_ED (flavour of earthy/dusty) in the ACE treatments were higher than in the NOACE one, especially the sample of ACE_Long. A longer skin contact combined with an increase in skin breakage could account for this observation, whereby more related flavour substances (such as 3-Isopropyl-2-Methoxypyrazine) may have been released into wine [46]. In other words, the ACE technique may have accelerated the release of certain volatile substances or their precursors. However, the intensities of the flavour of herbaceous and red fruits were negatively impacted by the ACE technique, which would be worth analysing in the future by GC, such as detecting 3-sec-Butyl-2-methoxypyrazine and Nerol for the herbaceous character, as well as β-Ionone and Furaneol for the red fruits character [43]. Furthermore, the intensity improvement of dark fruits found in ACE-treated Pinot noir wines [2] was not detected in the current Shiraz wines, which might be caused by the difference in grape varieties. Wines made by Shiraz grapes are commonly associated by the sommeliers with attributes of dark fruits [47], thus, the ACE technique did not significantly affect this character. Last, but not the least, the negative dilution effects (intensity reduction in every significantly different RATA attribute) for the pre-fermentation water addition were clear to see in the RATA evaluation, which was consistent with previous literature [12].

Table 4. Concentrations (mg/L) of total polysaccharides and monosaccharide residues following acid hydrolysis. Shiraz wines prepared following the NOACE and ACE maceration with either 3 days (Short) or 6 days (Long) on skins, or 6 days on skins with pre-fermentation water dilution to 13.5 Bé (Long_Dil).

	Mannose	Rhamnose	Glucuronic Acid	Galacturonic Acid	Glucose	Galactose	Xylose	Arabinose	Fucose	Total Polysaccharides
ACE_Short	[§] 114 ± 4	40 ± 2 b	8 ± 1 b	271 ± 12 c	32 ± 4 c	123 ± 4 bc	7 ± 1	126 ± 6 c	13 ± 1 c	736 ± 28 c
ACE_Long	116 ± 4	49 ± 3 a	10 ± 0 a	307 ± 9 a	50 ± 11 ab	135 ± 2 a	7 ± 2	153 ± 4 a	16 ± 2 ab	842 ± 26 a
ACE_Long_Dil	113 ± 1	49 ± 2 a	11 ± 1 a	293 ± 9 ab	57 ± 4 ab	130 ± 3 ab	8 ± 0	148 ± 2 ab	15 ± 0 ab	824 ± 9 ab
NOACE_Short	116 ± 5	38 ± 1 b	11 ± 1 a	251 ± 9 d	61 ± 2 a	121 ± 5 c	7 ± 1	125 ± 5 c	14 ± 1 bc	744 ± 23 c
NOACE_Long	117 ± 2	46 ± 1 a	11 ± 1 a	283 ± 6 bc	47 ± 12 b	131 ± 4 ab	6 ± 1	145 ± 3 b	16 ± 1 a	802 ± 26 ab
NOACE_Long_Dil	111 ± 9	46 ± 1 a	11 ± 1 a	281 ± 4 bc	50 ± 5 ab	129 ± 6 abc	7 ± 1	144 ± 7 b	17 ± 1 a	795 ± 35 b
F	0 602	15 325	3 947	14 743	5 155	3 898	1 029	19 492	5 621	8 146
p	0 700	[†] **<0.0001**	**0.024**	**<0.0001**	**0.009**	**0.025**	0 443	**<0.0001**	**0.007**	**0.001**

[§] Data are the means (±standard deviation) of triplicate fermentations, analysed with one-way analysis of variance at an alpha level of 5% and Fisher's least significant difference test [†] Bold *p* values represent significant differences between the treatments A post-hoc test was run across the wines within each column; values followed by the same letter in a column are not significantly different

Appendix

215

Table 5. The significantly different attributes across the treatments from rate-all-that-apply (RATA) detected by a multivariate ANOVA (at α 10%).

Attribute	Definition	F	*p*
Aroma			
A_FL	Floral/perfume/musk	2.292	0.044
A_Van	Vanilla	2.112	0.062
Taste			
T_Sw	Sweet	2.201	0.052
Flavour			
F_RF	Red fruits (e.g., raspberry, strawberry, red cherry, and red current...)	2.036	0.071
F_ED	Earthy/dusty	3.210	0.007
F_FL	Floral/perfume/musk	1.999	0.076
F_Her	Herbaceous	1.984	0.079
F_Van	Vanilla	2.144	0.058

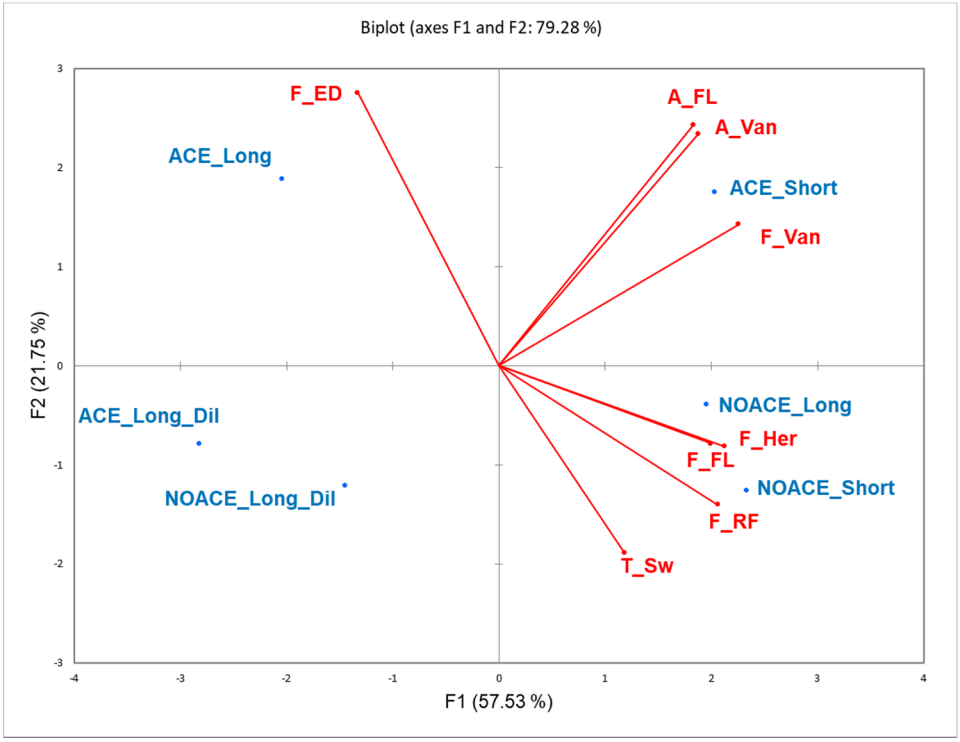

Figure 5. The PCA of six treatments for all the significantly different sensory attributes ($p < 0.1$) from RATA. Shiraz wines prepared following the NOACE and the ACE maceration with either 3 days (Short) or 6 days (Long) on skins, or 6 days on skins with pre-fermentation water dilution to 13.5 Bé (Long_Dil). A_FL and A_Van represent the aroma of floral/perfume/musk and the aroma of vanilla, respectively. T_Sw is the taste of sweetness. In terms of flavours, "RF", "ED", "FL", "Her" and "Van" represent red fruits, earthy/dusty, floral/perfume/musk, herbaceous, and vanilla, respectively.

Wine colour differences were not detected by the consumers, in agreement with the results of the CIELab measurements taken in this study. The differences found in the chemical parameters of the acid and phenolics were not sufficiently large to elicit a sensory perception difference in the current study for either acidity or bitterness. Sixty-one untrained wine consumers did not detect a significant difference in astringency intensity between the six winemaking treatments. However, it is relevant to note that the intensity of astringency alone is insufficient to fully characterize the perception of wine astringency, that is, some wines may have a similar astringency intensity but diverse sub-qualities (textures) [48].

Meanwhile, it is also important to recognise that astringency perception is dynamic [49], in that the progression of both the intensity and sub-qualities varies depending upon the wine matrix [30,50–52]. Hence, a comprehensive astringency profile of each winemaking treatment was further evaluated by a trained sensory panel using PP.

3.5.2. Astringency Profiles of Wines Assessed by PP

The PP technique is a sensory tool for the dynamic and quantitative measurements of astringency intensity and sub-qualities [30,53]. An examination of the PP panel data in this study showed good repeatability performance by the panel, as there were no significant differences between the replicates of sensory evaluation for each attribute at five evaluation periods. Significantly different astringency profiles of the Shiraz wine treatments were perceived by the panel according to the statistical analysis of the perception data ($p < 0.05$). Six treatments significantly differed by intensity for mouth coat ($F = 70.27$, $p < 0.0001$) and adhesive ($F = 21.34$, $p < 0.0001$) at the second evaluation period (20–30 s after expectoration of wine sample). Meanwhile, the intensities of OAI ($F = 27.03$, $p < 0.0001$) and graininess ($F = 85.67$, $p < 0.0001$) were significantly different by treatment at the third evaluation period (50–60 s after expectorating wine). Although a significant influence of the assessor is common in sensory evaluation ($p < 0.0001$ in the current PP), a MAM-CVA was used to reduce the scaling effect caused by the different assessors [54]. For the ease of interpretation, a joint presentation of the wine sample loadings (six wine treatments configuration plot) and the four significantly different PP attributes (sensory attribute configuration plot) are presented in one MAM-CVA plot (Figure 6). The first two canonical variates (CVs) accounted for 97.8% of the total variance ratio. As seen in Figure 6, the first CV was primarily related to the lower graininess and adhesive mouthfeel. The second CV is dominated by a mouth-coating mouthfeel, and to a lesser extent, the overall astringency intensity in the negative direction. The first axis strongly separated the less adhesive and grainy NOACE_Long dilution wines from all the other treatments. As illustrated by the lack of overlap between the confidence intervals, the grainier and more adhesive ACE_Long and ACE_Long dilution wines were clearly different from all NOACE wines. The astringency profiles of ACE_Short, NOACE_Short and NOACE_Long were similar, and clearly indicated that the astringency profiles of Shiraz wine made by conventional crushing were significantly influenced by the pre-fermentative implementation of water. Nevertheless, the use of the ACE technique not only reduced the impact of water addition on the astringency sensation, but also introduced obvious increases in the intensities of the adhesive and graininess textural sub-qualities. The enhancement provided by the ACE technique on the astringency profiles of Shiraz was consistent with what was found for Pinot noir (Sparrow, Holt, et al., 2016). As mentioned in the introduction, the most planted red wine grape variety in Australia is Shiraz, but this noble grape variety is also important for the wine industry globally (as it is grown and produces Shiraz or Syrah wines from for e.g., France, Portugal, Italy, Spain, South Africa, USA and New Zealand). This study confirmed others in Pinot noir revealing that ACE significantly enhanced the concentration of tannin and total phenolics. It also extended these findings in Shiraz wines showing that ACE was able to modify the astringency reduction caused by water dilution through an increased perception of adhesive and graininess sub-quality intensities. These positive influences on the textural quality of Shiraz wines could lead to a more extensive future application of ACE in the wine industry, not only for this but other red wine grape varieties in multiple wine producing countries.

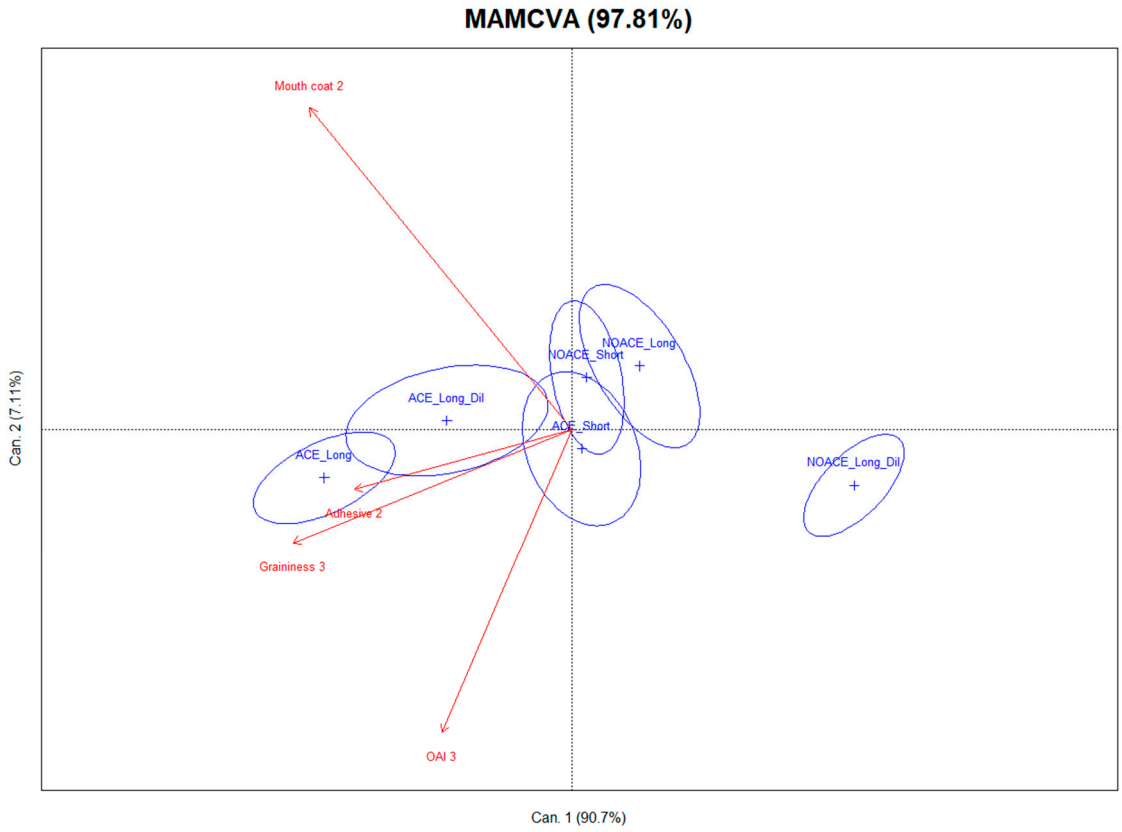

Figure 6. The mixed assessor model canonical variate analysis (MAM-CVA) of six treatments for all significantly different sensory attributes ($p < 0.05$) from five evaluation periods. Shiraz wines prepared following the NOACE and ACE maceration with either 3 days (Short) or 6 days (Long) on skins, or 6 days on skins with pre-fermentation water dilution to 13.5 Bé (Long_Dil). Hotelling Lawley stat = 4.458, F = 6.711 ($p \leq 0.001$). Ellipses indicate the confidence intervals of 90%.

To explore the underlying relationships between the significantly different mean PP sensory and wine chemistry data, the correlations between the discriminated astringency attributes (Y) and significantly different chemical parameters (X) were analysed by PLS-R (details of the first run of the PLS-R model are shown in Table S2 and Figure S1). The model was refined by a re-run of PLS-R using variables that produced variable importance in the projection (VIP) values greater than or close to 1 [55]. In the new model, the optimum number of components/latent variables required was 2, and the cross-validation index Q^2 for two components was 0.829 (and being greater than 0.5 represented the large predictive relevance of the model) [56]. This improved model (Table 6) explained 90.8% of the variation in wine chemical composition (X-variables) and 93.5% of the variation in sensory attributes (Y-variables). To extract the relevant features for the corresponding responses (mouth coat 2, adhesive 2, OAI 3, and graininess 3), the standardized regression coefficients of the selected chemical parameters (MM (GPC), total tannin, total phenolics, galacturonic acid, epicatechin gallate (%), fucose, and total polysaccharides) are displayed, respectively, in Figure 7. The intensity of the overall astringency and three discriminated sub-qualities were all significantly (standardized coefficients were all greater than 0.3) and positively associated with tannin MM (GPC), which confirmed earlier research [30,35]. The total tannin and total phenolics concentrations and the percentage of tannin galloylation also positively contributed to OAI, which was consistent with earlier findings [30,57]. However, this was the first reported observation of the contribution of these three phenolic parameters for astringency sub-qualities. On the contrary, the negative associations of OAI and three sub-qualities with fucose residues (recovered following the acid hydrolysis of polysaccharides) were found. It is difficult to perceive the sweetness of fucose at a low level which was mentioned in Section 3.3 [39], and therefore

suppress the perception of astringency [58]. However, the negative associations might support the idea that the fucose in wines co-operated with other wine matrix components, eliciting a dampening of astringency perception, and this too warrants further investigation. The chemical parameters of galacturonic acid and total polysaccharides did not predominantly influence any astringency sensation, as standardised regression coefficients were <0.1 [59]. However, it should not be neglected that phenolic and polysaccharide composition in wine did not affect astringency perception alone in many cases, and their interactions are also important [25,40,41], but this needs to be meticulously investigated in the future.

Table 6. Fit statistics of the partial least squares regression (two components) analysis between the discriminated astringency attributes (Y) and significantly different chemical parameters (X).

	Mouth Coat 2	Adhesive 2	Overall Astringency Intensity 3	Graininess 3
Cumulative Q^2 quality index	0.721	0.918	0.757	0.924
R^2	0.897	0.971	0.899	0.974
Std. deviation	0.913	0.549	0.964	0.209
Mean-square error	0.334	0.120	0.372	0.017
Root mean squared error of prediction	0.578	0.347	0.610	0.132

Mouth Coat 2 and Adhesive 2 attributes were perceived 20–30 s after the expectoration of the wine samples. Overall Astringency Intensity 3 and Graininess 3 attributes were evaluated 50–60 s after the expectoration of the wine samples.

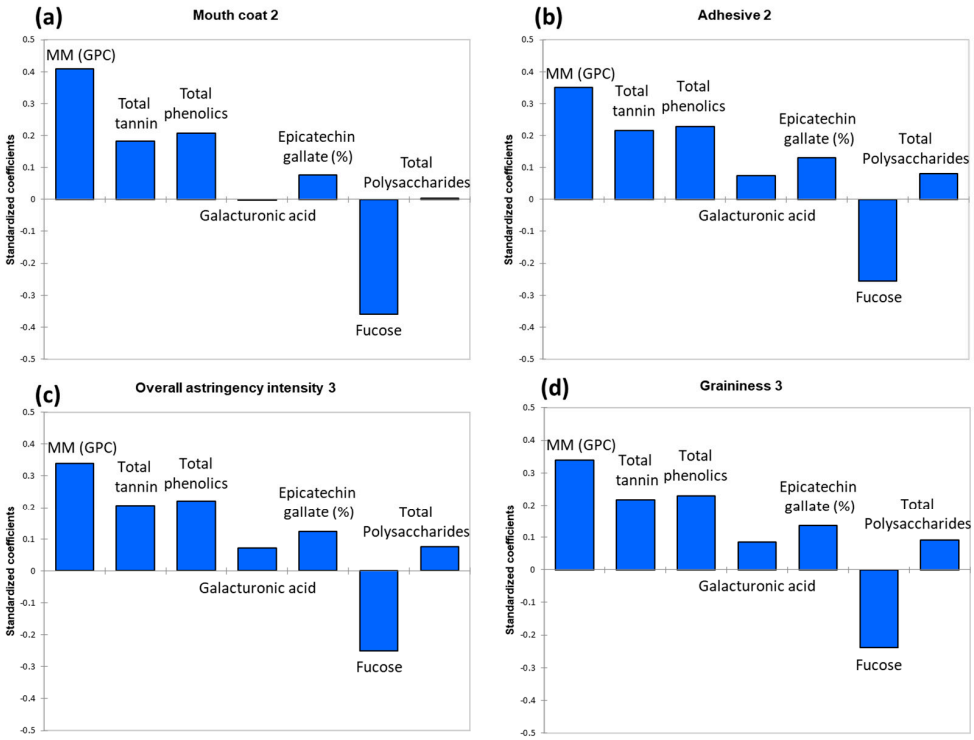

Figure 7. Standardised coefficients of the partial least squares regressions between the significantly different sensory attributes in PP (Y) and the selected (based on the variable importance in the projection) significantly different chemical parameters (X). MM (GPC) is tannin molecular mass determined by gel permeation chromatography at 50% elution. (**a**) Mouth coat 2 (20–30 s after the expectoration of wine sample) (**b**) Adhesive 2 (**c**) Overall astringency intensity 3 (50–60 s after expectorating wine) (**d**) Graininess 3.

4. Conclusions

A new grape must processing technique (ACE) was applied for the first time on Shiraz wines to elucidate the impacts on non-volatile wine chemical compositions and sensory profiles. The ACE technique did not influence the visual colour perception of Shiraz wines, but significantly increased the concentrations of total tannin and phenolics. The polysaccharide concentration in Shiraz wines was mainly influenced by the maceration time rather than ACE technique. In addition, the greater contribution of broken skin edges provided by ACE could accelerate the release of substances related to the flavour of earthy/dusty characters into wine, which should be studied further. The pre-fermentation addition of water had significant dilution effects on the consumer-perceived wine aromas and flavours. Water addition did not reduce the concentrations of tannin or phenolics significantly, but influenced the astringency profile evaluated by a trained panel. However, the ACE technique was able to moderate the perceived astringency reduction caused by dilution through an increased intensity of perception of adhesive and graininess sub-qualities. The differences on astringency sensation could be perceived by the trained panel but not in the consumers' assessment, however, more involved consumers may perceive these subtle changes. The knowledge generated by this study suggests that wine producers could utilise the ACE processing technique, in particular when winemakers need to modify the wine alcohol level by using pre-fermentative water dilution, and minimising the loss of important wine textural attributes. Insights into the compositional factors affecting the astringency sensation (overall intensity and sub-qualities) were provided in this study.

Supplementary Materials: The following are available online at http://www.mdpi.com/2304-8158/9/8/1027/s1, Table S1: List of sensory attributes scored in the rate-all-that-apply (RATA) assessment, Table S2: The model performance for the first run of partial least squares regression, and Figure S1: The plot of the first run of Partial Least Squares regression between the significantly different sensory attributes from PP (in blue) and significantly different chemical parameters (in red).

Author Contributions: W.K., K.A.B., X.W., S.E.P.B. conceived and designed the experiments. W.K. and X.W. performed the experiments. W.K. analysed the data and drafted the manuscript. W.K., X.W., K.A.B., R.A.M., P.A.S., J.N., S.E.P.B. contributed to the data interpretation, as well as reviewed and edited the manuscript. All authors have read and agreed to the published version of the manuscript.

Funding: This study was funded by the University of Adelaide (The Adelaide Graduate Research Scholarship) and Wine Australia (AGW Ph1605, WA Ph1803 and AWR1701). Wine Australia invests in and manages research, development, and extension on behalf of Australia's grape growers and winemakers and the Australian government.

Acknowledgments: We thank Coriole wines (Mark Lloyd and Duncan Lloyd) for the donation of uncrushed grapes and ACE-treated musts, and Richard E. Smart, the developer of the commercialised ACE technique, for guidance and useful discussion. Luke Qi (AWRI) is acknowledged for technical support in winemaking, and the analysis of the composition of wine tannin and polysaccharide. The sensory assessment was approved by the Human Research Ethics Committee of the University of Adelaide (project number: H-2016-084). We are thankful for the assistance of Lukas Danner, Trent Johnson, David Jeffery, Dimitra Capone, Claire Armstrong, Pietro Previtali and all participants of the sensory evaluations.

Conflicts of Interest: The authors declare no conflict of interest.

References

1. Sparrow, A.M.; Smart, R.E.; Dambergs, R.G.; Close, D.C. Skin particle size affects the phenolic attributes of Pinot noir wine: Proof of concept. *Am. J. Enol. Viticult.* **2016**, *67*, 29–37. [CrossRef]
2. Sparrow, A.M.; Holt, H.E.; Pearson, W.; Dambergs, R.G.; Close, D.C. Accentuated cut edges (ace): Effects of skin fragmentation on the composition and sensory attributes of Pinot Noir wines. *Am. J. Enol. Viticult.* **2016**, *67*, 169–178. [CrossRef]
3. Smart, R.; Sparrow, A. New winemaking process conceived in a northern Tasmania pilot winery-the beginnings of ACE. *Wine Vitic. J.* **2016**, *31*, 9.
4. Sacchi, K.L.; Bisson, L.F.; Adams, D.O. A review of the effect of winemaking techniques on phenolic extraction in red wines. *Am. J. Enol. Viticult.* **2005**, *56*, 197–206.

5. Parpinello, G.P.; Versari, A.; Chinnici, F.; Galassi, S. Relationship among sensory descriptors, consumer preference and color parameters of Italian Novello red wines. *Food Res. Int.* **2009**, *42*, 1389–1395. [CrossRef]
6. Harrison, R. Practical interventions that influence the sensory attributes of red wines related to the phenolic composition of grapes: A review. *J. Food Sci. Technol.* **2018**, *53*, 3–18. [CrossRef]
7. Gawel, R.; Iland, P.G.; Francis, I.L. Characterizing the astringency of red wine: A case study. *Food Qual. Prefer.* **2001**, *12*, 83–94. [CrossRef]
8. Ferrer-Gallego, R.; Hernández-Hierro, J.M.; Rivas-Gonzalo, J.C.; Escribano-Bailón, M.T. Sensory evaluation of bitterness and astringency sub-qualities of wine phenolic compounds: Synergistic effect and modulation by aromas. *Food Res. Int.* **2014**, *62*, 1100–1107. [CrossRef]
9. Schelezki, O.J.; Smith, P.A.; Hranilovic, A.; Bindon, K.A.; Jeffery, D.W. Comparison of consecutive harvests versus blending treatments to produce lower alcohol wines from Cabernet Sauvignon grapes: Impact on polysaccharide and tannin content and composition. *Food Chem.* **2018**, *244*, 50–59. [CrossRef]
10. Petrie, P. Quantifying the advancement and compression of vintage. *Aust. N. Z. Grapegrow. Winemak.* **2016**, *5*, 40.
11. Sparrow, A.M.; Smart, R.E. Pinot noir wine processing and quality improved by skin fragmentation. *Catal. Discov. Pract.* **2017**, *1*, 88–98. [CrossRef]
12. Schelezki, O.J.; Antalick, G.; Šuklje, K.; Jeffery, D.W. Pre-fermentation approaches to producing lower alcohol wines from Cabernet Sauvignon and Shiraz: Implications for wine quality based on chemical and sensory analysis. *Food Chem.* **2020**, *309*, 125698. [CrossRef] [PubMed]
13. Schelezki, O.J.; Šuklje, K.; Boss, P.K.; Jeffery, D.W. Comparison of consecutive harvests versus blending treatments to produce lower alcohol wines from Cabernet Sauvignon grapes: Impact on wine volatile composition and sensory properties. *Food Chem.* **2018**, *259*, 196–206. [CrossRef]
14. King, E.S.; Dunn, R.L.; Heymann, H. The influence of alcohol on the sensory perception of red wines. *Food Qual. Prefer.* **2013**, *28*, 235–243. [CrossRef]
15. Longo, R.; Blackman, J.W.; Torley, P.J.; Rogiers, S.Y.; Schmidtke, L.M. Changes in volatile composition and sensory attributes of wines during alcohol content reduction. *J. Sci. Food Agric.* **2017**, *97*, 8–16. [CrossRef] [PubMed]
16. Petrie, P.; Teng, B.; Smith, P.A.; Bindon, K.A. Sugar reduction: Managing high Baume juice using dilution. *Wine Vitic. J.* **2019**, *34*, 36.
17. Teng, B.; Petrie, P.R.; Smith, P.A.; Bindon, K.A. Comparison of water addition and early-harvest strategies to decrease alcohol concentration in *Vitis vinifera* cv. Shiraz wine: Impact on wine phenolics, tannin composition and colour properties. *Aust. J. Grape Wine Res.* **2020**, *26*, 158–171. [CrossRef]
18. Australian Government, Bureau of Meteorology. Available online: http//www.bom.gov.au (accessed on 11 October 2019).
19. Mercurio, M.D.; Dambergs, R.G.; Herderich, M.J.; Smith, P.A. High throughput analysis of red wine and grape phenolics adaptation and validation of methyl cellulose precipitable tannin assay and modified Somers color assay to a rapid 96 well plate format. *J. Agric. Food Chem.* **2007**, *55*, 4651–4657. [CrossRef]
20. Kang, W.; Niimi, J.; Bastian, S.E.P. Reduction of red wine astringency perception using vegetable protein fining agents. *Am. J. Enol. Viticult.* **2018**, *69*, 22–31. [CrossRef]
21. Kassara, S.; Kennedy, J.A. Relationship between red wine grade and phenolics. 2. Tannin composition and size. *J. Agric. Food Chem.* **2011**, *59*, 8409–8412. [CrossRef]
22. Kennedy, J.A.; Jones, G.P. Analysis of proanthocyanidin cleavage products following acid-catalysis in the presence of excess phloroglucinol. *J. Agric. Food Chem.* **2001**, *49*, 1740–1746. [CrossRef] [PubMed]
23. Kennedy, J.A.; Taylor, A.W. Analysis of proanthocyanidins by high-performance gel permeation chromatography. *J. Chromatogr. A* **2003**, *995*, 99–107. [CrossRef]
24. Bindon, K.A.; Kennedy, J.A. Ripening-induced changes in grape skin proanthocyanidins modify their interaction with cell walls. *J. Agric. Food Chem.* **2011**, *59*, 2696–2707. [CrossRef] [PubMed]
25. Li, S.; Bindon, K.; Bastian, S.E.; Jiranek, V.; Wilkinson, K.L. Use of winemaking supplements to modify the composition and sensory properties of shiraz wine. *J. Agric. Food Chem.* **2017**, *65*, 1353–1364. [CrossRef]
26. Ruiz-Garcia, Y.; Smith, P.A.; Bindon, K.A. Selective extraction of polysaccharide affects the adsorption of proanthocyanidin by grape cell walls. *Carbohydr. Polym.* **2014**, *114*, 102–114. [CrossRef]
27. Danner, L.; Crump, A.M.; Croker, A.; Gambetta, J.M.; Johnson, T.E.; Bastian, S.E.P. Comparison of rate-all-that-apply (RATA) and descriptive analysis (DA) for the sensory profiling of wine. *Am. J. Enol. Viticult.* **2018**, *69*, 12–21. [CrossRef]

28. Oppermann, A.; de Graaf, C.; Scholten, E.; Stieger, M.; Piqueras-Fiszman, B. Comparison of rate-all-that-apply (RATA) and descriptive sensory analysis (DA) of model double emulsions with subtle perceptual differences. *Food Qual. Prefer.* **2017**, *56*, 55–68. [CrossRef]
29. Vidal, L.; Giménez, A.; Medina, K.; Boido, E.; Ares, G. How do consumers describe wine astringency? *Food Res. Int.* **2015**, *78*, 321–326. [CrossRef]
30. Kang, W.; Niimi, J.; Muhlack, R.A.; Smith, P.A.; Bastian, S.E. Dynamic characterization of wine astringency profiles using modified progressive profiling. *Food Res. Int.* **2019**, *120*, 244–254. [CrossRef]
31. Somers, T.C.; Evans, M.E. Spectral evaluation of young red wines: Anthocyanin equilibria, total phenolics, free and molecular SO_2, "chemical age". *J. Sci. I Food Agric.* **1977**, *28*, 279–287. [CrossRef]
32. Payne, C.; Bowyer, P.K.; Herderich, M.; Bastian, S.E.P. Interaction of astringent grape seed procyanidins with oral epithelial cells. *Food Chem.* **2009**, *115*, 551–557. [CrossRef]
33. McGuire, R.G. Reporting of objective color measurements. *HortScience* **1992**, *27*, 1254–1255. [CrossRef]
34. Sun, B.; Sá, M.d.; Leandro, C.a.o.; Caldeira, I.; Duarte, F.L.; Spranger, I. Reactivity of polymeric proanthocyanidins toward salivary proteins and their contribution to young red wine astringency. *J. Agric. Food Chem.* **2013**, *61*, 939–946. [CrossRef]
35. McRae, J.M.; Schulkin, A.; Kassara, S.; Holt, H.E.; Smith, P.A. Sensory properties of wine tannin fractions: Implications for in-mouth sensory properties. *J. Agric. Food Chem.* **2013**, *61*, 719–727. [CrossRef] [PubMed]
36. Adams, D.O. Phenolics and ripening in grape berries. *Am. J. Enol. Viticult.* **2006**, *57*, 249–256.
37. Bindon, K.A.; Kassara, S.; Smith, P.A. Towards a model of grape tannin extraction under wine-like conditions: The role of suspended mesocarp material and anthocyanin concentration. *Aust. J. Grape Wine Res.* **2017**, *23*, 22–32. [CrossRef]
38. Bindon, K.A.; Smith, P.A.; Holt, H.; Kennedy, J.A. Interaction between grape-derived proanthocyanidins and cell wall material. 2. Implications for vinification. *J. Agric. Food Chem.* **2010**, *58*, 10736–10746. [CrossRef]
39. Moskowitz, H.R. The sweetness and pleasantness of sugars. *Am. J. Psychol* **1971**, *84*, 387–405. [CrossRef]
40. Quijada-Morín, N.; Williams, P.; Rivas-Gonzalo, J.C.; Doco, T.; Escribano-Bailón, M.T. Polyphenolic, polysaccharide and oligosaccharide composition of Tempranillo red wines and their relationship with the perceived astringency. *Food Chem.* **2014**, *154*, 44–51. [CrossRef]
41. Chong, H.H.; Cleary, M.T.; Dokoozlian, N.; Ford, C.M.; Fincher, G.B. Soluble cell wall carbohydrates and their relationship with sensory attributes in Cabernet Sauvignon wine. *Food Chem.* **2019**, *298*, 124745. [CrossRef]
42. Vidal, S.; Francis, L.; Noble, A.; Kwiatkowski, M.; Cheynier, V.; Waters, E. Taste and mouth-feel properties of different types of tannin-like polyphenolic compounds and anthocyanins in wine. *Anal. Chim. Acta* **2004**, *513*, 57–65. [CrossRef]
43. Unterkofler, J.; Muhlack, R.A.; Jeffery, D.W. Processes and purposes of extraction of grape components during winemaking: Current state and perspectives. *Appl. Microbiol. Biotechnol.* **2020**, *104*, 1–19. [CrossRef] [PubMed]
44. Cretin, B.N.; Dubourdieu, D.; Marchal, A. Influence of ethanol content on sweetness and bitterness perception in dry wines. *LWT* **2018**, *87*, 61–66. [CrossRef]
45. Hufnagel, J.C.; Hofmann, T. Quantitative reconstruction of the nonvolatile sensometabolome of a red wine. *J. Agric. Food Chem.* **2008**, *56*, 9190–9199. [CrossRef] [PubMed]
46. Waterhouse, A.L.; Sacks, G.L.; Jeffery, D.W. *Understanding Wine Chemistry*; John Wiley & Sons: Chichester, West Sussex, UK, 2016.
47. Pearson, W.; Schmidtke, L.; Francis, L.; Blackman, J. Sensory analysis: Provenance, preference and pivot: Exploring premium Shiraz with international sommeliers and Australian winemakers using a new rapid sensory method. *Wine Vitic. J.* **2018**, *33*, 35.
48. Bajec, M.R.; Pickering, G.J. Astringency: Mechanisms and perception. *Crit. Rev. Food Sci. Nutr.* **2008**, *48*, 858–875. [CrossRef]
49. Guinard, J.-X.; Pangborn, R.M.; Lewis, M.J. The time-course of astringency in wine upon repeated ingestion. *Am. J. Enol. Viticult.* **1986**, *37*, 184–189.
50. Vidal, L.; Antúnez, L.; Giménez, A.; Medina, K.; Boido, E.; Ares, G. Dynamic characterization of red wine astringency: Case study with Uruguayan Tannat wines. *Food Res. Int.* **2016**, *82*, 128–135. [CrossRef]
51. Vidal, L.; Antúnez, L.; Giménez, A.; Medina, K.; Boido, E.; Ares, G. Sensory characterization of the astringency of commercial Uruguayan Tannat wines. *Food Res. Int.* **2017**, *102*, 425–434. [CrossRef]
52. Kemp, B.; Trussler, S.; Willwerth, J.; Inglis, D. Applying temporal check-all-that-apply (TCATA) to mouthfeel and texture properties of red wines. *J. Sens.* **2019**, *34*, e12503. [CrossRef]

53. Jack, F.R.; Piggott, J.R.; Paterson, A. Analysis of textural changes in hard cheese during mastication by progressive profiling. *J. Food Sci.* **1994**, *59*, 539–543. [CrossRef]
54. Peltier, C.; Visalli, M.; Schlich, P. Enhancing canonical variate analysis by taking the scaling effect into account. *Food Qual. Prefer.* **2018**, *64*, 88–93. [CrossRef]
55. Lattey, K.A.; Bramley, B.; Francis, I. Consumer acceptability, sensory properties and expert quality judgements of Australian Cabernet Sauvignon and Shiraz wines. *Aust. J. Grape Wine Res.* **2010**, *16*, 189–202. [CrossRef]
56. Cramer, R.D. Partial least squares (PLS): Its strengths and limitations. *Perspect. Drug Discov. Des.* **1993**, *1*, 269–278. [CrossRef]
57. Bindon, K.A.; Kassara, S.; Solomon, M.; Bartel, C.; Smith, P.A.; Barker, A.; Curtin, C. Commercial *Saccharomyces cerevisiae* yeast strains significantly impact Shiraz tannin and polysaccharide composition with implications for wine colour and astringency. *Biomolecules* **2019**, *9*, 466. [CrossRef]
58. Courregelongue, S.; Schlich, P.; Noble, A.C. Using repeated ingestion to determine the effect of sweetness, viscosity and oiliness on temporal perception of soymilk astringency. *Food Qual. Prefer.* **1999**, *10*, 273–279. [CrossRef]
59. Nguyen, A.N.; Johnson, T.E.; Jeffery, D.W.; Capone, D.L.; Danner, L.; Bastian, S.E. Sensory and chemical drivers of wine consumers' preference for a new Shiraz wine product containing Ganoderma lucidum extract as a novel ingredient. *Foods* **2020**, *9*, 224. [CrossRef]